From Biomass to Materials: Functionalized Lignin as a Building Block for More Sustainable Polymers

Zur Erlangung des akademischen Grades einer

DOKTORIN DER NATURWISSENSCHAFTEN

(Dr. rer. nat.)

von der KIT-Fakultät für Chemie und Biowissenschaften
des Karlsruher Instituts für Technologie (KIT)

genehmigte

DISSERTATION

von

M. Sc. Celeste Libretti

aus Fano

1. Referent: Prof. Dr. Michael A. R. Meier
2. Referent: Prof. Dr. Patrick Théato

Tag der mündlichen Prüfung: 20.04.2026

A tutte le persone che hanno contribuito, in modi diversi, a questo percorso.

„Our greatest weakness lies in giving up. The most certain way to succeed is always to try just one more time.”

Thomas A. Edison

Declaration of Authorship

Die vorliegende Arbeit wurde von März 2023 bis Februar 2026 unter Anleitung von Prof. Dr. Michael A. R. Meier am Institut für Organische Chemie (IOC) des Karlsruhe Instituts für Technologie (KIT) angefertigt.

Erklärung

Hiermit versichere ich, dass ich die Arbeit selbstständig angefertigt, nur die angegebenen Quellen und Hilfsmittel benutzt und mich keiner unzulässigen Hilfe Dritter bedient habe. Insbesondere habe ich wörtlich oder sinngemäß aus anderen Werken übernommene Inhalte als solche kenntlich gemacht. Die Satzung des Karlsruher Instituts für Technologie (KIT) zur Sicherung guter wissenschaftlicher Praxis habe ich beachtet. Des Weiteren erkläre ich, dass ich mich derzeit in keinem laufenden Promotionsverfahren befinde und auch keine vorausgegangenen Promotionsversuche unternommen habe. Die elektronische Version der Arbeit stimmt mit der schriftlichen Version überein und die Primärdaten sind gemäß Abs. A (6) der Regeln zur Sicherung guter wissenschaftlicher Praxis beim Institut abgegeben und archiviert.

Karlsruhe, den 21.02.2026

_____

Celeste Libretti

Abstract

The development of bio-based materials is crucial to reduce dependence on fossil resources and to support the transition towards more sustainable polymer production. As one of the most abundant renewable sources of aromatic structures, lignin represents a highly promising renewable feedstock for valorization, both as a precursor for high-value chemicals and as a macromonomer for lignin-based polymers. This thesis presents three complementary strategies for the implementation of lignin as a macromonomer in the design of more sustainable thermosetting materials.

Initially, lignin was modified using dimethyl carbonate (DMC) to enable the synthesis of lignin-based polycarbonates with potential for chemical recyclability *via* methanolysis. Several synthetic routes were investigated and compared, including a two-step approach involving intermediate functionalization followed by self-condensation, and an additional strategy employing an external diol co-monomer.

The second part describes an innovative methodology for the preparation of partially lignin-based, fully bio-based non-isocyanate polyurethane (NIPU) thermosets. Lignin was functionalized bearing cyclic carbonate groups, enabling it to act as a crosslinker for NIPUs, acting as a safer alternative to conventional and toxic isocyanates used in polyurethane (PU) production. In parallel, a bio-based polyamine derived from high oleic sunflower oil was synthesized *via* thiol–ene chemistry. The process was optimized in both batch and continuous flow, and the resulting polyamine was employed as the amine component, together with cyclic carbonate-functionalized lignin and a sugar-based co-component, to achieve fully bio-based NIPU thermosets. Comprehensive characterization confirmed successful curing and revealed promising thermal and surface properties, supporting their potential as greener alternatives to conventional polyurethanes.

Lastly, lignin was functionalized with two cyclic anhydrides (itaconic and succinic anhydride) to produce lignin-based polycarboxylic acids, which can serve as crosslinkers in diverse thermosetting systems, including epoxy and Passerini resins, together with an additional difunctional renewable diacid, Pripol™ 1009, which was utilized to tune the lignin content. The synthesis of the lignin macromonomers was optimized, and multiple strategies for solvent and precipitation-medium recovery were developed to reduce the environmental impact and to lower the E-factor. Subsequently, detailed characterization of the resulting thermosets demonstrated that lignin incorporation can yield epoxy networks with tunable lignin content, high flexibility, and degradability under alkaline conditions. In addition, Passerini-based materials showed high thermal stability, tunable gel content and glass transition temperature (T_g) correlating with lignin content. Moreover, for one lignin derivative, the reactivity of the installed Michael system was also tested for thermoset preparation as a proof of concept, further highlighting the versatility of these derivatives.

Overall, this work demonstrates that lignin can be successfully implemented as a versatile macromonomer for the production of polymer networks while increasing renewable content and enabling more sustainable end-of-life options. These findings highlight the potential of lignin as a key component in the development of environmentally friendlier polymeric materials.

Zusammenfassung

Die Entwicklung biobasierter Materialien ist entscheidend um die Abhängigkeit von fossilen Ressourcen zu verringern und den Übergang zu einer nachhaltigeren Polymerproduktion zu unterstützen. Als eine der reichhaltigsten nachwachsenden Quellen aromatischer Verbindungen stellt Lignin einen äußerst vielversprechenden erneuerbaren Rohstoff für die Valorisierung dar – sowohl als Ausgangsstoff für hochwertige Chemikalien als auch als Makromonomer für ligninbasierte Polymere. Diese Dissertation präsentiert drei komplementäre Strategien zur Implementierung von Lignin als Makromonomer für die Entwicklung nachhaltigerer duroplastischer Materialien.

Zunächst wurde Lignin mit Dimethylcarbonat (DMC) modifiziert, um die Synthese ligninbasierter Polycarbonate mit Potenzial für eine chemische Rezyklierbarkeit mittels Methanolyse zu ermöglichen. Mehrere Syntheserouten wurden untersucht und miteinander verglichen, darunter ein zweistufiger Ansatz über eine Zwischenfunktionalisierung mit anschließender Selbstkondensation sowie eine zusätzliche Strategie unter Einsatz eines externen Diol-Co-Monomers.

Der zweite Teil beschreibt eine innovative Methodik zur Herstellung teilweise ligninbasierter, vollständig biobasierter nicht-isocyanatbasierter Polyurethan-(NIPU)-Duroplaste. Lignin wurde mit cyclischen Carbonatgruppen funktionalisiert, wodurch es als Vernetzer für NIPUs eingesetzt werden kann und eine sicherere Alternative zu konventionellen und toxischen Isocyanaten darstellt, die üblicherweise in der Polyurethan-(PU)-Herstellung verwendet werden. Parallel dazu wurde ein biobasiertes Polyamin aus High-Oleic-Sonnenblumenöl mittels Thiol-En-Chemie synthetisiert. Der Prozess wurde sowohl im Batch- als auch im kontinuierlichen Flow-Verfahren optimiert, und das erhaltene Polyamin wurde als Aminkomponente zusammen mit cyclisch-carbonatfunktionalisiertem Lignin und einer zuckerbasierten Co-Komponente eingesetzt, um vollständig biobasierte NIPU-Duroplaste zu erhalten. Eine

umfassende Charakterisierung bestätigte eine erfolgreiche Aushärtung und zeigte vielversprechende thermische sowie oberflächenbezogene Eigenschaften, welche das Potenzial dieser Materialien als umweltfreundlichere Alternative zu konventionellen Polyurethanen unterstreichen.

Abschließend wurde Lignin mit zwei cyclischen Anhydriden (Itaconsäureanhydrid und Bernsteinsäureanhydrid) funktionalisiert, um ligninbasierte Polycarbonsäuren zu erzeugen, die als Vernetzer in unterschiedlichen duroplastischen Systemen eingesetzt werden können, darunter Epoxid- und Passerini-Harze. Zur Einstellung des Ligningehalts wurde zusätzlich eine difunktionelle erneuerbare Dicarbonsäure, Pripol™ 1009, eingesetzt. Die Synthese der Lignin-Makromonomere wurde optimiert und mehrere Strategien zur Rückgewinnung des Lösungsmittels, sowie des Fällungsmediums entwickelt, um die Umweltbelastung zu reduzieren und den E-Faktor zu senken. Anschließend zeigte eine detaillierte Charakterisierung der resultierenden Duroplaste, dass die Integration von Lignin Epoxidnetzwerke mit einstellbarem Ligningehalt, hoher Flexibilität und Abbaubarkeit unter alkalischen Bedingungen ermöglichen kann. Darüber hinaus wiesen Passerini-basierte Materialien eine höhe thermische Stabilität sowie einen einstellbaren Gelgehalt und eine einstellbare Glasübergangstemperatur (T_g) auf, welche mit dem Ligningehalt korrelieren. Zudem wurde für ein Ligninderivat die Reaktivität des eingeführten Michael-Systems als Proof-of-Concept für die Herstellung von Duroplasten untersucht, wodurch die Vielseitigkeit dieser Derivate zusätzlich hervorgehoben wird.

Insgesamt zeigt diese Arbeit, dass Lignin erfolgreich als vielseitiges Makromonomer zur Herstellung polymerer Netzwerke eingesetzt werden kann, wobei der Anteil erneuerbarer Rohstoffe erhöht und gleichzeitig nachhaltigere End-of-Life-Optionen ermöglicht werden. Die vorliegenden Ergebnisse verdeutlichen das Potenzial von Lignin als Schlüsselkomponente für die Entwicklung umweltfreundlicherer polymerer Materialien.

Table of Contents

Declaration of Authorship ..... **vii**

Erklärung vii

Abstract ..... **ix**

Zusammenfassung ..... **xi**

Table of Contents ..... **xiii**

Acknowledgments ..... **xvii**

1 Preface **1**

2 Theoretical Background **5**

2.1 Green Chemistry 5

2.1.1 Green Chemistry Metrics 9

2.1.2 Multicomponent Reactions 14

2.1.3 Click Chemistry 20

2.2 Renewable Feedstocks 24

2.2.1 Lignin 26

3 Aim **69**

4 Results and Discussion **70**

4.1 Lignin Carbonates 71

4.1.1 Abstract 71

4.1.2 Introduction 72

4.1.3 First Approach with DMC as Limiting Reagent 74

4.1.4 Second Approach – Intermediate Route 86

4.1.5 Conclusions and Outlook 103

4.2 Lignin-NIPUs *via* HOSO-derived Polyamine 104
4.2.1 Abstract 105
4.2.2 Introduction 106
4.2.3 Synthesis of HOSO-derived PA in Batch 109
4.2.4 Synthesis of HOSO-derived PA in Flow 113
4.2.5 Lignin Functionalization with Cyclic Carbonates 115
4.2.6 Thermosets NIPUs 127
4.2.7 Conclusions and Outlook 138
4.3 Functionalization of Lignin with Cyclic Anhydrides 139
4.3.1 Abstract 140
4.3.2 Introduction 141
4.3.3 Lignin Functionalization with Itaconic Anhydride 144
4.3.4 Environmental Factor, Recyclability of the Solvent, and the Precipitation Medium 154
4.3.5 Thermosets 157
4.3.6 Conclusions and Outlook 192
5 Conclusions 193
6 Experimental Section 196
6.1 Solvents and Reagents 196
6.2 Instrumentation and Laboratory Equipment 199
6.3 Organosolv Lignin Characterization 207
6.3.1 Theoretical Yield Calculations for Lignin Modification 209
6.4 Experimental Procedures for Chapter 4.1 – Lignin Carbonates 210
6.4.1 First Approach-DMC as Limiting Reagent 210

6.4.2 Second Approach—Intermediate Route 211
6.5 Experimental Procedure for Chapter 4.2 – Lignin-NIPUs *via* HOSO-derived Polyamine 218
6.5.1 UV-systems and Reaction Setups 218
6.5.2 Triglyceride Modification 221
6.5.3 Lignin Modification 232
6.5.4 Thermosets 241
6.6 Experimental Procedures for Chapter 4.3 – Functionalization of Lignin with Cyclic Anhydrides 245
6.6.1 Lignin Functionalization 245
6.6.2 E-factor Calculations and Recovered Solvent Characterization 260
6.6.3 General Passerini Thermosets Formulation 263
6.6.4 Epoxy Thermosets 284
6.6.5 Thia-Michael Thermosets 295
7 Appendix 296
7.1 Calculations of the E-factor Values of Chapter 2.2.1 296
7.2 E-Factor Calculations for Amino Group Functionalized Lignin ..297
7.3 E-Factor Calculations for Epoxide Functionalized Lignin 302
7.4 E-Factor Calculations for Carboxylic Acid Functionalized Lignin 315
7.5 E-Factor Calculations for Ester Group Functionalized Lignin 316
7.6 E-Factor Calculations for Multiple Bond Functionalized Lignin..330
7.7 E-Factor Calculations for Hydroxyl Group Functionalized Lignin 335
8 Publication List 340

9 Conference Contributions 341

10 CV 342

11 Abbreviation List 343

12 Bibliography 346

Acknowledgments

What a bittersweet moment! I remember like yesterday the day that I started, and it seems almost not true that all this time has already passed.

Zunächst möchte ich meinem Chef, **Mike**, danken. Als ich nach Deutschland zog, hatte ich nicht die Absicht, zu promovieren. Aber schon nach wenigen Monaten meines Forschungsaufenthalts in deiner Gruppe war ich überzeugt. Ich kann gar nicht in Worte fassen, wie sehr ich unter deiner Anleitung sowohl persönlich als auch wissenschaftlich gewachsen bin. Ich möchte dir ganz besonders für deine Verfügbarkeit, deine Freundlichkeit und die absolute Freiheit danken, die du mir bei meiner Forschung gewährt hast. Ich hätte mir keinen besseren Betreuer wünschen können.

AKM, I would like to express my most sincere gratitude for all of these years of grind, laughter, fun and growth. The group changed a lot since the day I arrived, but certainly the warmth and the welcoming atmosphere left unaffected. In particular, I would like to thank the first person that I met, **Anja**. During these years we became so close and I treasure our friendship so much. You always put me in a better mood and cheer me up, and I am so grateful to have you as a friend. Looking forward to more adventures with you! During these years I met so many special souls through the AKM: **Clara**, you are the sunshine in human form. Your kindness and generosity made such a big difference in my days, thank you for being like you are. **Henni**, **Leon** and **Sandra**: my most trusted friends of the *SpasTisch*. Thank you for always making me laugh even on the days when I only wanted to cry. It was a pleasure to have you around me every day. **Qianyu**, thank you for being so funny! Looking forward to some more evenings together. **Pete**, thank you for your help and for all the memories. **Francesca**, è stato un onore collaborare con te. **Mundi**, grazie per le nostre gite in moto e tutti gli spritz! A special thanks goes to my most trusted army: **Sophia**, grazie per le lunghe ore in lab, sei stata la migliore Azubi che potessi avere (e con la quale ho potuto fare

tanto gossip); **Gianni**, thank you for working so tirelessly with me and fighting with lignin. With you, the lab work was more fun! Finally, **Aaron**, the best HiWi I could ever imagine, just thank you! Other members of the AK that I would like to thank, to which I am extremely grateful: **Luca (Holzi)**, **Simon**, **Svenja**, **Andreas**, **Luis**, **Timo**, **Dani**, **Jow**, **Roman**, **Bohni**, **Michi**, **Nichollas, Luca N.**. I would also like to thank **Pinar**, for her support with the bureaucracy and her patience.

A special thanks goes to all the proofreaders of this thesis: **Hendrick**, **Qianyu**, **Sandra**, **Luca Holzi**, **Simon**, **Leon**, **Anja**, **Fabian**. Without you this thesis would certainly not look so good (and probably would still be full of typos).

Un ringraziamento speciale va ai miei due cuori **Roberta** e **Federico**. Grazie per avermi accolta a Karlsruhe e fatto sentire a casa. Mi mancano le nostre serate di *C'è Posta* e i nostri pomeriggi alle terme.

A big big thanks goes to **Mats**, my co-supervisor in Stockholm. Thank you for making me feel so welcome and for your endless curiosity about lignin. It was a pleasure to stay in your group for three months, thanks to **all the Coating Division**! I would also like to thank another person that made my stay in Stockholm so wonderful: **Jennifer**, I already miss your house and sharing my life with you. You have been so kind and lovely, and I can't wait to visit you in Stockholm again. Moreover, I would like to thank the Karlsruhe House of Young Scientists (**KHYS**) for financing the research stay abroad to KTH in Stockholm.

Außerdem, möchte ich mich meine zweite-Familie hier in Deutschland bedanken: **Kathrin** und **Michael**, vielen lieben Dank, dass ihr mich in eure Familie aufgenommen habt und für eure Liebe. Ich bin sehr glücklich, euch zu haben. **Julia & Alina**, Danke, dass ihr so liebe Menschen seid. Ich bin so dankbar, euch beide in meinem Leben zu haben. **Benny**, ich könnte mir keinen besseren Schwager wünschen.

Sari & **Lari**: le mie due sorelle adottive. Grazie per tutte le videochiamate, per esserci sempre, siete davvero le mie migliori amiche. Mi mancate così tanto!

Fabian, thank you for being my rock, every day. You make the days feel lighter and always make me smile even on those 48 h days. Thank you for being my sunshine and my better half. You make me feel at home, even if home is 910 km away.

Babbo, grazie per avermi portato fino a Karlsruhe nel lontano 2022, quando ancora pensavo che sarei tornata in Italia. Grazie per esserci, per le telefonate e per tirarmi su il morale, sempre. **Mamma**, non sarei qui senza di te. Grazie per tutto quello che fai. Sono così grata ad entrambi voi per il supporto, l'amore e la forza che mi date. **Federica**, grazie per essere la mia spalla e la migliore sorella che potessi chiedere. Mi manca tanto averti con me ogni giorno. Ti auguro solo il meglio. **Elia**, il mio piccolo uomo, grazie per essere un fratello così speciale. Mi manchi!

Nonni, mi mancate sempre così tanto. Grazie per le lunghe telefonate, per cucinarmi sempre qualcosa di buono quando torno e per tutto l'amore che mi fate sentire, sempre. Grazie per avermi trasmesso dei valori così importanti e per avermi fatto diventare la persona che sono ora.

I hope I did not forget anybody! So many people contributed to this time, and I am so grateful to every one of you.

Lastly, I would like to thank **myself**, for all the hard work that I put in, the endless hours in the lab, the fights against lignin and for not quitting.

I hope that after reading this thesis, you will find lignin fascinating as much as I do.

Ad maiora semper

1 Preface

Climate change remains one of the most complex challenges of our time, requiring action from society. Its origins and its resolution are rooted in a collective societal effort, in which governments and nations, as well as individual citizens, are called as major actors to take responsibility for safeguarding our shared future and that of generations to come.

The latest International Panel of Climate Change (IPCC, 6th Assessment Report presentation)[1] opens with a significant statement:

> *"Pace and scale of climate action are insufficient to tackle climate change."*

Climate change is measured by tracking the long-term changes such as the global average temperature and Greenhouse Gases (GHGs) emissions. The latest data (2011-2020) describe a global warming of + 1.1 °C (compared to the 1850-1900). Higher concentrations of GHGs, especially related to human-activities, led to global warming, with CO_2 and CH_4 as the most impactful gases. In the latest years, emissions have tremendously increased, and will continue to increase, impacting every aspect of human life. It is clear that common consequences of global warming (floods, heavy precipitations, tropical cyclones, heatwaves) are anthropogenic and impact several areas of our planet (including ocean, atmosphere, cryosphere and biosphere). According to the 2025 *Emissions Gap Report* published by the United Nations Environment Programme (UNEP), the mitigation pathway required to meet international temperature targets is substantially more stringent than previously assumed. To remain below 2 °C and 1.5 °C of global warming, global annual greenhouse gas emissions must be reduced by approximately 35% and 55%, respectively, relative to 2019 levels, by 2035.[2] The Director of UNEP's Climate Change Division, Martin Krause, further notes that current national commitments are projected to reduce emissions by only 12–15% by 2035, making the 2 °C pathway increasingly

unlikely.[3] Under existing policies, global mean temperature is projected to increase by approximately 2.8 °C by the end of the century.[2] Together, these figures highlight the urgent need for rapid and sustained policy action to close the emissions gap.

In an article published in 1999,[4] Mann, Bradley and Hughes used a multiproxy network (tree rings, corals, ice cores, documentary records, etc.) to reconstruct the annual Northern Hemisphere mean temperatures from the year 1000 until the late 20th century. The resulting reconstruction displayed relatively low variability and a slight long-term cooling trend from around the year 1000 until the late 19th century, followed by a sharp increase during the 20th century, when reconstructed temperatures, later supported by instrumental records, rose rapidly and exceeded pre-industrial levels. Owing to the distinctive shape of this curve, climatologist Jerry Mahlman coined the term “hockey stick graph” to describe the reconstruction. The study subsequently became the subject of intense scrutiny and controversy and a focal point for climate change sceptics, who questioned the methodology and disputed the robustness of the reconstruction.
Nevertheless, numerous independent studies and subsequent assessments evaluated the methods and findings of Mann, Bradley, and Hughes and consistently reached the same conclusion: the pronounced warming observed in the 20th century is anomalous in the context of the previous millennium.[5–7]

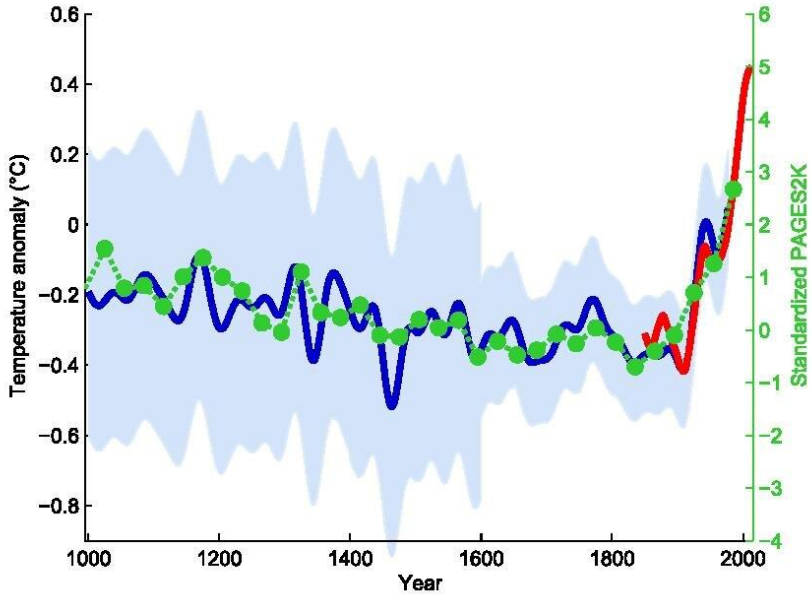

Figure 1.1 – In blue is the original hockey stick of Mann, Bradley and Hughes (1999)[4] with its uncertainty range (light blue). Green dots show the 30-year average of the new PAGES 2k reconstruction. The red curve shows the global mean temperature, according to HadCRUT4 data from 1850 onwards. Source: Klaus Bittermann, T comp 61–90, Wikimedia Commons, licensed under Creative Commons Attribution-ShareAlike 4.0 International (CC BY-SA 4.0) — reproduced unchanged.

Despite measurable progress made, inadequate adaptation gaps remain. As the AR6 states, many current initiatives focus primarily on short-term risk reduction, addressing immediate impacts rather than enabling long-term transformational adjustments. It is also outlined that these limitations are often intensified by insufficient financial resources and by the absence of robust political frameworks and economic incentives.

An important issue that emerged from the report is that public and private investments in fossil fuels continue to exceed those allocated to climate mitigation and adaptation. These imbalances hinder the transition toward building a resilient, low-carbon economy.

At the European level, recent regulatory developments aim to address these shortcomings. To name some: The European Climate Law, the Fit for 55 package, the EU Taxonomy, and the Sustainable Finance Disclosure Regulation (SFDR) are designed to align financial markets with climate objectives, redirect capital toward sustainable activities, and reinforce long-term climate ambition

toward 2030 and beyond. In parallel, instruments such as the Social Climate Fund and an increased attention to adaptation within EU climate strategies highlight a growing recognition of social equity and resilience needs. However, the effectiveness of these measures will depend on their swift and coherent implementation, alongside the increase of dedicated financing adaptation and the systematic phaseout of fossil fuel subsidies.

In this context, approximately 99 % of global plastic production still relies on fossil-based feedstocks. The plastics sector is estimated to account for roughly 4 % of global greenhouse gas emissions, considering emissions associated with fossil fuel extraction and transport, refining, polymer manufacturing, and end-of-life treatment. However, this value may be underestimated due to limited data availability across the full life cycle of plastic products.[8,9] Moreover, plastics are not only associated with substantial emissions, but also with major environmental challenges, including waste accumulation, pollution, and degradation into microplastics, which can impact ecosystems and living organisms.[10] Therefore, a transition toward renewable alternatives to fossil-based polymers, together with the development of more effective recycling strategies, is urgently required.

Within this broader transition framework, the present doctoral thesis offers a focused yet substantive contribution, by examining the use of renewable resources (in particular lignin) and green chemistry principles for the development of more environmentally sustainable polymeric materials.

2 Theoretical Background

2.1 Green Chemistry

In regards of the transition toward a world being less dependent on fossil-fuels and a collective effort to achieve a more sustainable future, it is essential to understand two main concepts: *Sustainability* and *Green Chemistry*.

Sustainability itself may seem like a simple concept, however there are various facets to it that need to be explained. The most famous and cited definition of sustainability was introduced in 1987 by the UN World Commission on Environment and Development as:[11]

> *"Meeting the needs of the present without compromising the ability of future generations to meet their own needs."*

Within the concept of Sustainability, the intricate equilibrium between nature, economy, and society cannot be neglected. It thus integrates these aspects through a dynamic and inter-connected system that builds a long-term fusion between environmental sustainability (managing natural resources, keeping biodiversity, and protecting nature) with societal sustainability (equity, health, and human well-being) and economic sustainability (long-term growth and profit without negatively impacting other aspects).[12] Since 2015, the UN's *Sustainable Development goals* (SDGs) have served as global objectives and a positive call to action aimed to end poverty, protecting the planet, and ensuring prosperity for each individual.[13] The SDGs are a perfect example that highlights the connection between the economic, environmental, and societal aspects of *Sustainability*.

Figure 2.1.1 – Left: the three core-aspects of sustainability and sustainable development; right: the UN's Sustainable Development goals. *Picture drawn by the author, readapted from Ref. [13].*

During the 1960s, the need for greater awareness to chemical substances and chemical processes began to emerge, notably with the publication of a seminal book by marine biologist **Rachel Carson**. *Silent Spring* exposed the devastating effects of pesticides—particularly 1,1,1-trichloro-2,2-bis(4-chlorophenyl)ethane **(DDT)**—highlighting their environmental persistence, bioaccumulation, and harmful impacts on wildlife and human health.[14]

Originally developed for the effective control of mosquitoes, the primary vectors of malaria, DDT later saw widespread application in agriculture with limited prior assessment of its long-term consequences for human health and ecosystems. In one of the book's most striking chapters, *A Fable for Tomorrow*, Carson depicts a fictional town in which "spring has been silenced": birds no longer fly, bees disappear and fail to pollinate trees, and a pervasive shadow of death hangs over the landscape. The book helped catalyze a wave of environmental movements and sharpened public awareness of the chemical industry and its products. This growing concern contributed, in the early 1970s, to the establishment of the U.S. Environmental Protection Agency (EPA) and, only two years later, to the ban of DDT.[15]

During the same period, a series of significant environmental disasters further intensified the ongoing transformation in the relationship between the scientific community and governmental authorities. Notable examples include the *Love Canal* disaster, in which approximately 21 kt of toxic chemical waste were disposed of over a ten-year period by the Hooker Chemical Company,[16] as well as the *Seveso* disaster in Italy in 1976, which resulted in the release of exceptionally high concentrations of 2,3,7,8-tetrachlorodibenzo-*p*-dioxin (TCDD) into the environment.[17]

Those events unquestionably led to the implementation of stricter environmental regulations, simultaneously catalyzing a broader re-evaluation within the scientific community. Progressively, attention shifted toward preventing environmental and public-health risks, rather than bearing the far greater social, economic, and environmental costs of remediation after damage had occurred.

With the *Pollution Prevention Act* of 1990, the conception and design of new processes and products moved from an “end of pipe” approach to a more circular approach. The policy declared that pollution should be eliminated (or prevented) within the design phase, instead of focusing on the treatment and disposal phase.

A few years later, Paul Anastas and John Warner established the *12 principles of Green Chemistry* as a guide to serve further development of green chemistry practices.[18] The principles cover concepts based on several pathways to lower environmental and health impacts, and they indicate priorities for both industrial chemistry practices and research. In **Figure 2.1.2**, the principles are illustrated.

In that period, there were other milestones in the history of green chemistry, such as the establishment of *The Presidential Green Chemistry Challenge Awards* that commenced in 1996, and the institution of the journal *Green Chemistry* in 1999.

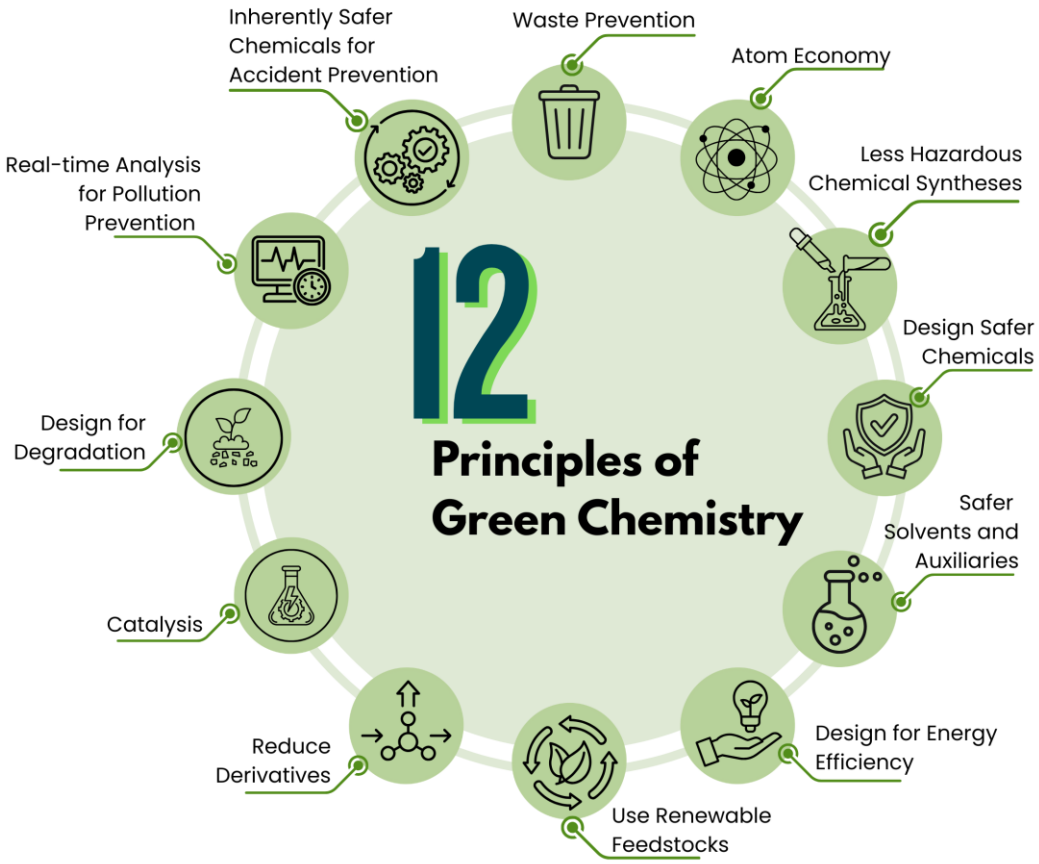

Figure 2.1.2 – The 12 Principles of Green Chemistry. *Picture drawn by the author based on the original Ref. [18].*

As leading example, the Small Business Award of the Presidential Green Chemistry Challenge in 2011 went to BioAmber Inc. for the production of bio-based succinic acid. Succinic acid, an important building block used in the chemical industry, was conventionally produced from petroleum-based resources (butane).[19] BioAmber developed the technology to produce bio-based succinic acid by bacterial fermentation of glucose, reducing energy consumption by 60 % compared to its petrochemical equivalent while consuming CO_2, rather than generating it. However, in 2018 the company filed for bankruptcy due to declining oil prices, emphasizing that technological viability and greener environmental intent alone are insufficient in the absence of market conditions and financial frameworks that adequately value sustainability.[20,21]

2.1.1 Green Chemistry Metrics

Contextually to the 12 Principles, new metrics to evaluate the sustainability and efficiency of chemical processes started to develop. In 1991, Barry Trost introduced for the first time the concept of *Atom Economy* (AE).[22] This metric is intended to provide an initial indicator to assess whether a reaction can be considered greener by design. In particular, the most basic definition of AE is the ratio between the molar mass of the desired product (or products) and the molar mass of all reactants, often expressed as a percentage, according to **Eq. 1**.

$$AE = \frac{M_{w,desired\ product}}{\sum_i M_{wi,starting\ materials}} \cdot 100\% \qquad \text{Eq. 1}$$

In the case of an ideal reaction, where all the reactants convert into the desired product without unwanted side products, the AE would correspond to 100 %. AE is an important metric to look at while planning a new synthetic protocol. Examples of reactions with high AE are, for instance, addition reactions such as Diels Alder reactions or catalytic hydrogenations.[23] AE is a useful metric, however does not take into account solvents and auxiliaries employed during the synthesis. It does furthermore not consider yield or stoichiometric imbalance.

Another valuable metric was introduced in 1992 by R. A. Sheldon,[24] the *Environmental factor*, or simply E-factor. This metric is defined as the amount of waste produced for a given process, considering everything but the desired product as waste. It is calculated following **Eq. 2**, and includes solvent losses, auxiliaries, yield and reagents.

$$E - factor = \frac{\sum m_{starting\ materials} - m_{product}}{m_{product}} \qquad \text{Eq. 2}$$

An ideal E-factor is *zero*, as a higher the E-factor is related to more waste generated.[25] However, the E-factor does not take into account *which* type of waste is generated, therefore, ideally prior investigation into the toxicity or hazardousness of the process is needed. According to the original work of Sheldon,[24] water is generally excluded from E-factor calculations, as it can lead to exceptionally high E-factors, making comparisons more difficult. Later work defined a simple E-factor (**sEF**) avoiding the inclusions of solvents and water in the calculations, and a complex E-factor (**cEF**), that includes both but no recycling steps.[26,27] **Eq. 3** and **Eq. 4** describe their calculations:

$$sEF = \frac{\sum m_{raw\ materials} + \sum m_{reagents} - m_{product}}{m_{product}} \quad \text{Eq. 3}$$

$$cEF = \frac{\sum m_{raw\ materials} + \sum m_{reagents} + \sum m_{solvents} + \sum m_{water} - m_{product}}{m_{product}} \quad \text{Eq. 4}$$

The sEF, with the relative approximations, should be regarded as an early assessment metric when developing a new synthesis method, but with some important advantages compared to the AE. cEF, on the other hand, does not take into account any recovery practice that can be applied to the solvents or to the water waste. Therefore, when recyclability measures are applied, the real E-factor will fall between sEF and cEF.

In **Table 2.1.1**, the E-factors of the main areas of the chemical industry are highlighted. Fine chemicals and pharmaceuticals present higher E-factor values compared to oil refining and bulk chemical sectors, due to the complex or multi-step syntheses.

Table 2.1.1 – Overview of the E-factors for the main sectors of the chemical industry, adapted from Sheldon.[28]

Industry segment	Product ($t \cdot a^{-1}$)	E-factors (kg waste/kg products)
Oil refining	10^6–10^8	<0.1
Bulk chemicals	10^4–10^6	<1–5
Fine chemicals	10^2–10^4	5–50
Pharmaceuticals	10–10^3	25–100

Other worth-mentioning metrics include for instance the Process Mass Intensity (PMI). PMI is a mass-based metric defined as the total mass of starting materials needed (including solvents, raw materials, reagents, and catalysts) to produce a specific mass of final product, as described in **Eq. 5**. Due to its definition, the value is equivalent to the E-factor value+1.

$$PMI = \frac{m_{materials}}{m_{product}} = E - factor + 1 \qquad \text{Eq. 5}$$

PMI is broadly adopted in the pharmaceutical industry for its ease applicability and clear data.[29]

For a more detailed analysis, a far more precise analysis of a process can be achieved *via* Life-Cycle-Assessment (LCA). LCA is a comprehensive approach that identifies and quantifies the environmental and human health impacts of a product or system throughout its life cycle.

The life of the product is therefore understood as a set of activities and processes, that require a certain amount of material and energy. Each stage undergoes a series of transformations, and results in the release of various emissions. LCA applies standardized scientific models to describe the cause-effect chain linking human activity to the impact on the ecosystem.

Recognized procedures for conducting LCA studies are provided in the *ISO 14000* series (a set of international standards for environmental

management systems) that provides reference standards for impact assessment, labeling, and environmental communication.[30]

An LCA study is normally articulated in four stages,[31,32] the *goal and scope definition* phase, which includes a description of the intent of the study and which parameters are part of the analysis; the *life cycle inventory* (LCI), in which the data and information necessary for the study are collected; *the life cycle impact assessment* (LCIA) phase, in which the material and energy flow inventory is transformed into a potential environmental impact; lastly the *interpretation of the results* supports actions and planning strategies that can reduce the environmental impact of the system under consideration.

When establishing the scope of an LCA study, there are generally three approaches which define the boundaries of systems relating to the anthropogenic resource cycle. These approaches are:[33,34]

- *Cradle to grave*: Refers to the entire life cycle of a product system, from the extraction of raw materials to final disposal.
- *Cradle to gate*: Limits the LCA study to the stages from the extraction of raw materials to the production of the material, product, or service. The phases of use and end-of-life management are excluded.
- *Cradle to cradle*: This concept is based on the idea that materials should be designed for continuous circulation in closed loops, thereby eliminating the notion of waste and promoting regenerative systems.[35]

The *Cradle to cradle* concept was introduced in the early 2000s by William McDonough and Michael Braungart[36] as a variant of the *Cradle to grave* approach that emphasizes material recycling and energy recovery as alternative strategies for disposal.

Within the *Cradle to cradle* framework, material flows are divided into two distinct cycles: the biological cycle and the technological cycle. Materials in the biological

cycle are designed to safely return to the biosphere after use, where they can biodegrade and contribute to natural systems without causing harm. In contrast, materials in the technological cycle are intended to remain in closed industrial loops through reuse, repair, remanufacturing, or recycling, thereby retaining their material value over multiple life cycles. A schematic overview of the concept with the two cycles is reported in **Figure 2.1.3**.

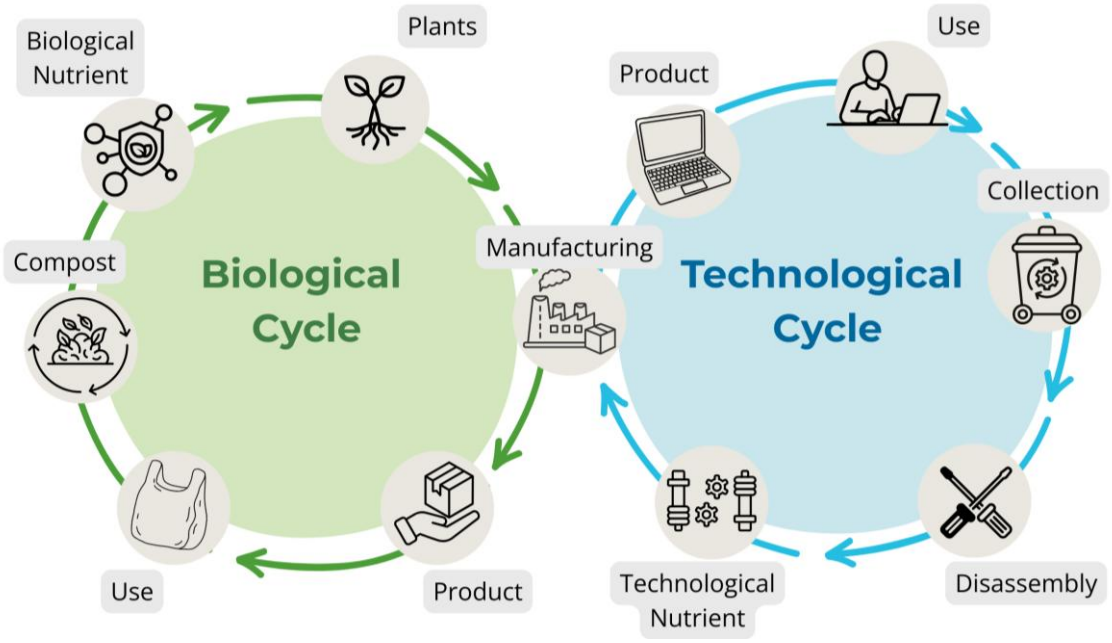

Figure 2.1.3 – Schematic representation of the *Cradle to cradle* concept, illustrating the biological and technological material cycles. The scheme was drawn by the author based on the *Cradle to cradle* design framework originally proposed by McDonough and Braungart.[36]

While LCA provides robust insights for industrial-scale and well-developed processes, its implementation during early-stage research is frequently constrained by high data requirements, uncertainty, and cost, limiting its applicability for initial process evaluation.

2.1.2 Multicomponent Reactions

According to the principles of *Green Chemistry*, minimizing waste, improving process efficiency, and reducing the number of derivatization steps are key objectives to achieve a more sustainable synthesis. In this context, multicomponent reactions (MCRs) represent an attractive class of transformations, as they enable the selective combination of three or more starting materials into a single product, typically in a one-pot and one-step process.[37] MCRs are therefore often associated with high atom economy, reduced solvent and energy consumption, and improved overall synthetic efficiency, making them advantageous compared to traditional multistep synthetic routes in regards of sustainability.[38] Historically, the first example of a MCR was reported in 1850 with the *Strecker* reaction, where an aldehyde, ammonia, and hydrogen cyanide combine together to give an α-amino nitrile, which is subsequently hydrolyzed to an amino acid.[39] Another significant representative is the *Biginelli* reaction. This three-component reaction between an aldehyde, urea, and a 1,3-dione affords the straightforward synthesis of 3,4-dihydro-2(*H*)-pyrimidinones (DHPM),[40] which have aroused particular interest in medicinal chemistry due to their interesting pharmacological properties.[41,42]

Another noteworthy example is the *Mannich* reaction, which is also discussed in **paragraph 2.2.1.4.1** in relation to lignin modification. This reaction involves the condensation of three components, typically under acidic conditions: an enolizable ketone/aldehyde, a non-enolizable aldehyde, and an amine component (primary / secondary amine or ammonia).[43] *Hantzsch* developed multicomponent reactions for pyrrole and especially for dihydropyridines, with the latter yielding their respective pyridines after oxidation.[44]

Among the different classes of MCRs, isocyanide-based reactions, such as the *Passerini* and *Ugi* reactions, have attracted significant attention in macromolecular and polymer chemistry. The Passerini reaction involves the coupling of a carboxylic acid, an aldehyde or ketone, and an isocyanide to form

an α-acyloxy amide, while the Ugi four-multicomponent reaction (4-MCR) proceeds analogously with the additional incorporation of an amine, yielding α-aminoacyl amides.[45] Notably, the Passerini reaction shows 100% atom economy due to the absence of stoichiometric by-products, in contrast to many other MCRs where water is typically formed. Owing to its mild conditions, broad functional group tolerance, and efficiency, the Passerini reaction has emerged as a particularly powerful tool for polymer synthesis and macromolecular design.[46–49] An overview of the multicomponent reactions discussed in this section is reported in **Scheme 2.1.1**, as well as their AE values.

Scheme 2.1.1 – Overview of the above-mentioned MCRs with the necessary components. For AE calculations, all non-specified substituents were assumed to be methyl groups.

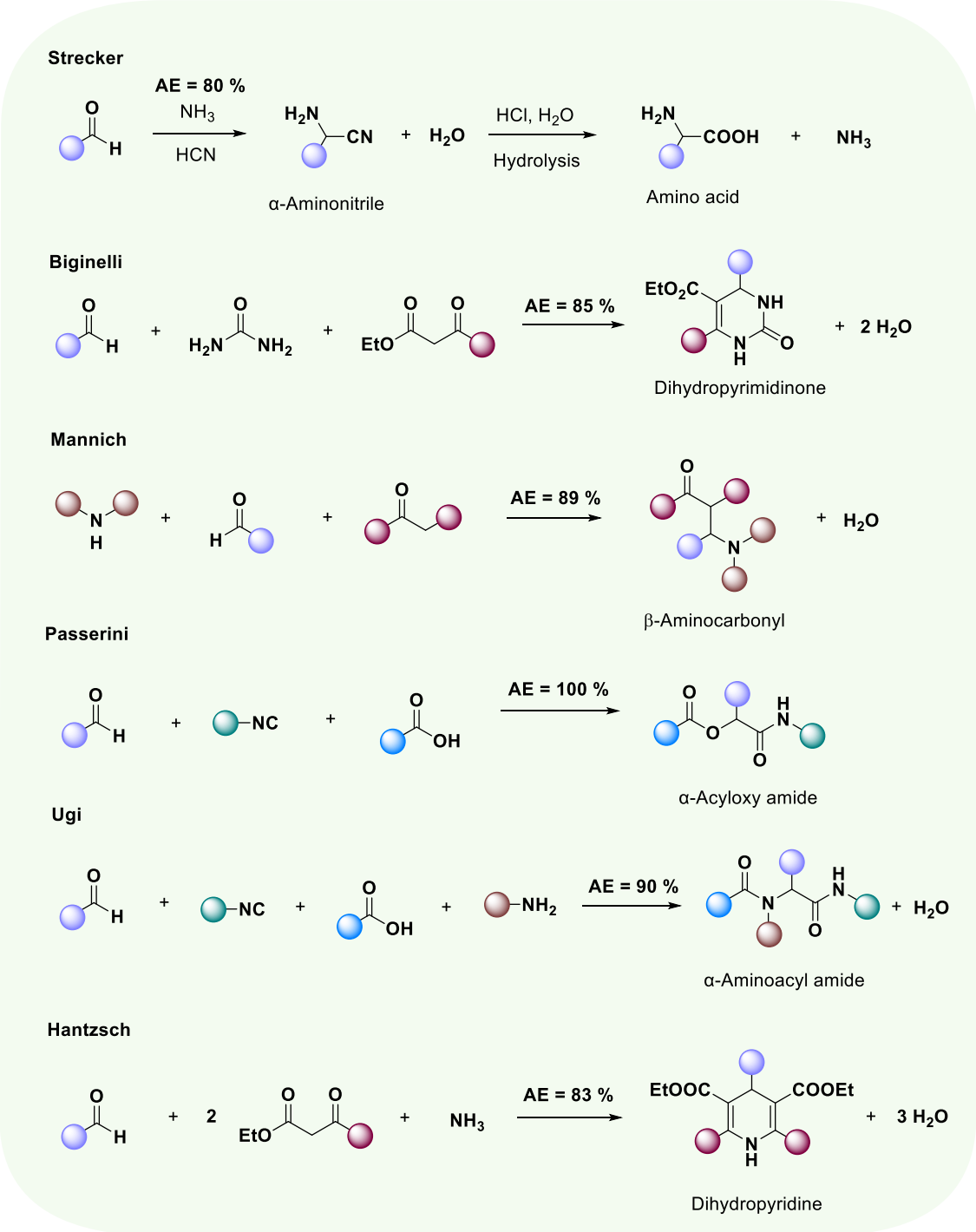

To further emphasize the applicability of the Passerini reaction in polymer chemistry, its ability to proceed under mild conditions, often at room temperature

and without the need for a catalyst, makes it an operationally simple yet powerful tool for the synthesis of complex macromolecular architectures with tunable properties. Several strategies have been reported for Passerini-based polymer synthesis, including multicomponent polyaddition using bifunctional monomers, as well as post-polymerization modification through Passerini grafting.[49,50] In the case of multicomponent polyaddition, bifunctional monomers can be employed either as AA+BB type, or AB-type monomers. For AA + BB approaches, three different monomer combinations are possible, as depicted in **Scheme 2.1.2**. By selecting the functional groups of each component, the resulting polymers can be tailored in terms of backbone structure and side-chain functionality, enabling access to a wide range of poly(ester-amide)-type materials.[49]

In a notable work from Meier *et al*. several strategies for the synthesis of polymers *via* Passerini chemistry were outlined.[51] In one approach, monomers bearing terminal double bonds were prepared through the Passerini reaction and subsequently polymerized *via* acyclic diene metathesis (ADMET). Alternatively, the authors demonstrated the direct Passerini polyaddition of dialdehydes and diacids with various isocyanides, providing an efficient route to poly(ester-amide)-type materials. In addition, Li and Du *et al*. report of a new library of poly(ester-amide)s *via* Passerini multicomponent polymerization with a diacid, difunctional isocyanide, and different electron-deficient ketones, generating tertiary ester linkages in the polymer chains.[52] The resulting polymers exhibited tunable properties depending on the ketone species.

As mentioned previously, polymers can also be obtained using AB-type monomers. In this strategy, a difunctional monomer bearing both aldehyde and carboxylic acid functionalities is polymerized through the Passerini three-component reaction in the presence of monofunctional isocyanides. This enables the synthesis of polyester-type backbones while introducing tunable amide-containing side chains depending on the isocyanide structure (**Scheme 2.1.2**). Meier and co-workers reported an AB-type monomer prepared *via* thiol–ene addition between 10-undecenal and 3-mercaptopropionic acid, which was

subsequently polymerized successfully, yielding polymers with molecular weights up to 34.6 kDa.[48]

Scheme 2.1.2 – Examples of polymerization possibilities from AA+BB-type or AB-type monomers. Scheme is readapted and modified with permission from ref. [49].

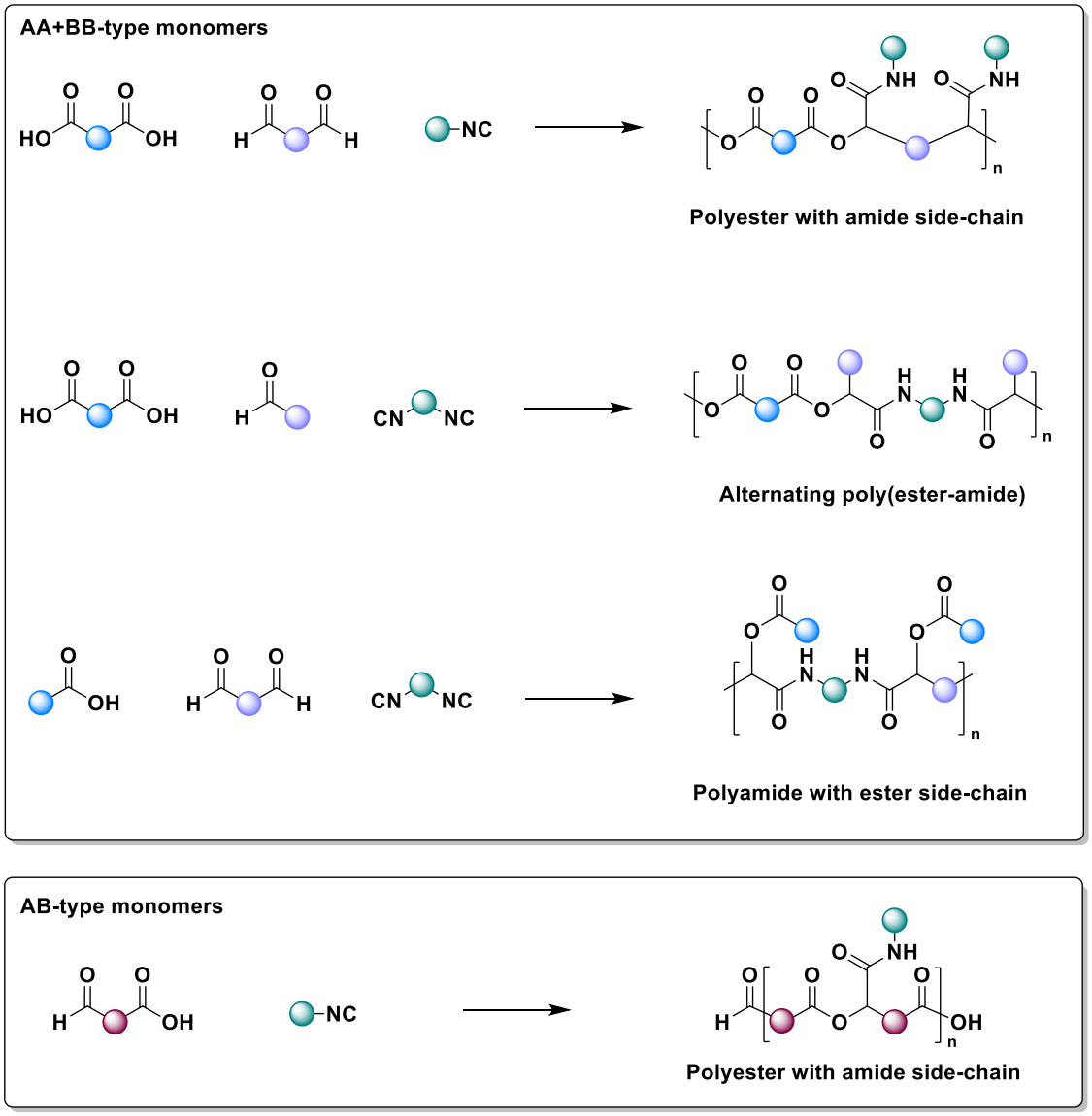

Passerini chemistry has also been exploited in polymer science as a post-polymerization modification strategy to tune material properties. In particular, Meier and Montero de Espinosa *et al*. reported the preparation of poly(ethylene-co-butylene) (PEBs) with Passerini modified end-groups, in order to display

different amide derivatives as end groups and study their phase segregation behavior.[53] Another interesting example from Fleury and Charlot *et al.* involves the modification of the carboxylic acid groups of carboxymethyl cellulose (CMC) *via* Passerini through different aldehydes and isocyanides, leading to a wide scope of CMC-Passerini derivatives.[54] Moreover, Meier *et al*. presented the a MCR-post-functionalization of cellulose succinates *via* Passerini 3-MCR and Ugi 4-MCR.[55]

In addition Tunca and Durmaz *et al*., describe an elegant sequence modification of an electron-deficient polyester *via* Huisgen 1,3-dipolar cycloaddition to introduce a pendant carboxylic acid functionality, followed by a Passerini modification reaction using different aldehydes and isocyanides.[56]

Collectively, these studies highlight the versatility and broad applicability of Passerini-based MCRs for the functionalization of polymeric substrates. In this doctoral thesis, Passerini chemistry will be exploited for the synthesis of Passerini-based thermosets, as discussed in **Section 4.3.5.1**.

2.1.3 Click Chemistry

Click chemistry was introduced by Sharpless and co-workers in 2001 as a concept describing a class of highly efficient and reliable chemical transformations.[57] In their seminal work, a set of defining criteria was proposed, including modularity, broad substrate scope, high yields, stereospecificity, and the formation of only benign or easily removable by-products. In addition, click reactions are characterized by operational simplicity, the use of readily available starting materials, mild reaction conditions, and minimal purification requirements, often employing solvent-free or environmentally benign solvents.[58]

Owing to these features, click chemistry has become a powerful and widely adopted toolbox in polymer and materials science. Several reactions fulfill the click chemistry criteria, including CuAAC (Cu-catalyzed azide–alkyne cycloadditions),[59] Diels–Alder reactions,[60] and thiol-based coupling reactions.[61,62] Among these, thiol–ene and thia–Michael reactions have emerged as particularly attractive for macromolecular synthesis and network formation due to their high efficiency and compatibility with complex, multifunctional substrates.

2.1.3.1 Thia-Michael Reaction

The thia–Michael addition reaction refers to the hydrothiolation of an electron deficient C=C double bond and can be considered a specific type of nucleophilic 1,4-addition in which a thiol acts as the nucleophile. This reaction is well established and is widely regarded as a click-like transformation due to its broad substrate scope, mild reaction conditions, operational simplicity, high selectivity, and ability to proceed efficiently even under solvent-free conditions.[63]

The reaction between the thiol and the activated C=C bond can be facilitated by catalytic amounts of base, which deprotonate the thiol to generate the corresponding thiolate anion and conjugate acid, initiating the reaction (**Scheme 2.1.3**). This process can also be catalyzed by strong nucleophiles, which ultimately lead to the formation of the same reactive thiolate species.[63] Reaction

rates are often faster for nucleophile-catalyzed thia–Michael additions.[64] Several factors influence the reaction rate and the selectivity, such as solvent, pH, nature of the electron withdrawing groups and the one of the thiols.[65] Common Michael-acceptors are, for instance, α,β-unsaturated carbonyl compounds,[66] maleimides,[67] or vinyl sulfones.[68] It is important to note that the classification of the thia–Michael addition as a click reaction depends strongly on the choice of Michael acceptor, thiol, and reaction conditions. For instance, highly activated acceptors such as maleimides and acrylates typically show rapid kinetics and high conversion under mild conditions, consistent with click chemistry,[69,70] whereas less activated acceptors (e.g., certain acrylamides) require stronger bases or longer times and may not inherently exhibit ideal *click* characteristics.[71]

Scheme 2.1.3 – Schematic representation of the nucleophilic or base initiated thia–Michael reaction, as well as the formation of the thiol-Michael adduct and the regeneration of the thiolate anion. The anionic intermediate is resonance-stabilized by the electron-withdrawing group (EWG).

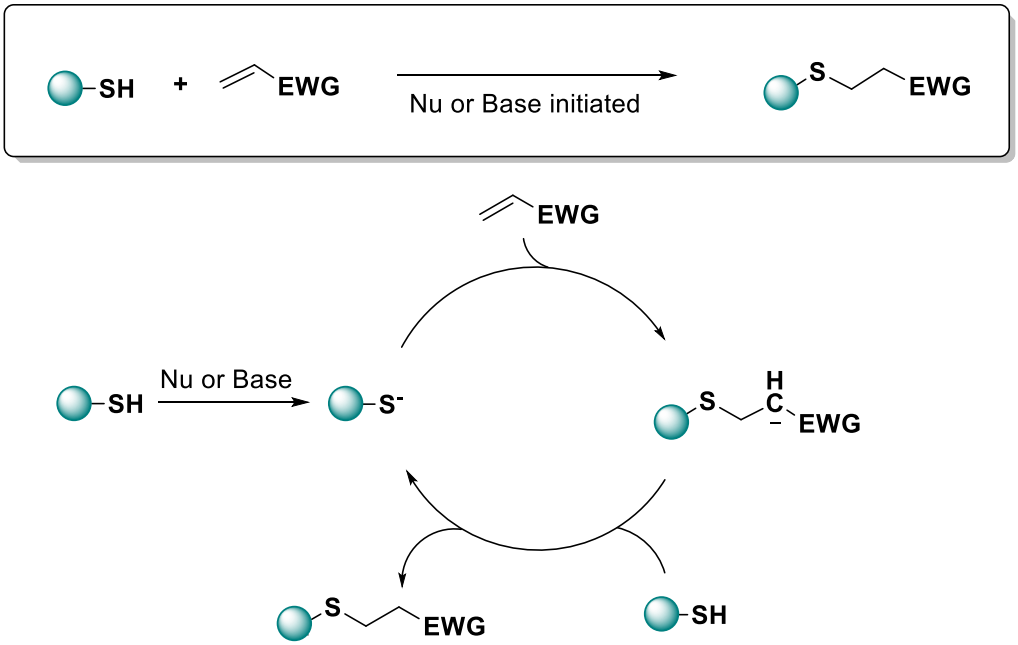

Notably, it has been demonstrated that the dynamic behavior of thia–Michael linkages can be activated, and in some cases tailored, through the structure of the Michael acceptor and the alkene substituents, as well as by external stimuli.[72,73] It was observed that under elevated temperatures or elevated pH,

thiol-Michael adducts can undergo dynamic covalent exchange. Moreover, by fine tuning the type of acceptor, this dynamicity could be achieved under catalyst-free and room temperature conditions.[74]

Thia–Michael addition will be used in **Section 4.3.5.3** in relation to lignin-based thermoset formation.

2.1.3.2 Thiol-Ene Reaction

The thiol–ene reaction generally proceeds through a radical-mediated mechanism. While it is conceptually related to thia–Michael addition in terms of overall hydrothiolation, thiol–ene coupling does not necessarily require an electron-deficient alkene and can be applied to a broader range of C=C bonds.[75–77] The reaction is most commonly initiated photochemically, generating thiyl radicals, although thermal initiation is also possible. Propagation occurs *via* anti-Markovnikov addition of the thiyl radical to the alkene, forming a carbon-centered radical intermediate. Subsequent hydrogen atom abstraction from another thiol molecule yields the thioether product and regenerates the thiyl radical, enabling the radical chain reaction (**Scheme 2.1.4**). Thiol–ene reactivity generally decreases as the electron density of the C=C bond decreases.[78] Reactivity is also affected by the substitution of the alkene species, due to steric hindrance and competing cis–trans isomerization, as thiyl radical addition to the double bond can be reversible.[76,79]

Scheme 2.1.4 – Schematic representation of the thiol–ene reaction following a radical pathway.

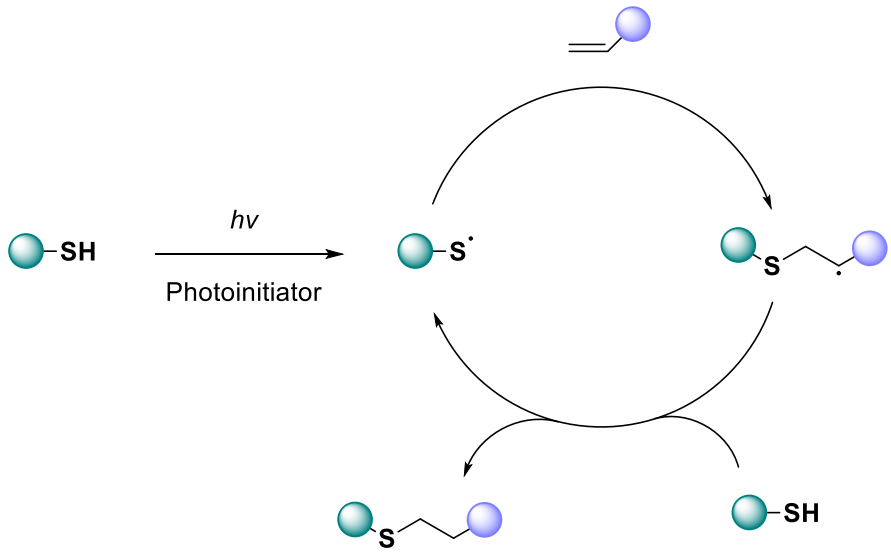

Thiol–ene reactions will be utilized in **Sections 4.2.3 and 4.2.4** to synthesize a renewable vegetable oil-based polyamine for lignin-based thermosets.

2.2 Renewable Feedstocks

The term “renewable feedstocks” refers to a class of resources that replenish themselves naturally within a shorter time than their use phase, making them sustainable for continuous use. Renewable feedstocks for polymer chemistry include lignocellulosic biomass, starch, chitin, vegetable oils and fats, terpenes, waste and by-products (organic waste, food-industry residues, and forestry by-products),[80] and CO_2. In this context, they can be divided into *first-generation* resources, such as starch, corn, and sugarcane, which rely on food-grade feedstocks, and *second-generation* resources, which rely on non-food-based materials, such as wood, cellulose, straw, and agricultural residues.[81] In recent years, a clear shift toward second-generation feedstocks has been observed to mitigate food–fuel competition and land-use concerns.[82] Moreover, replacing fossil carbon with renewable carbon (derived from both biomass and CO_2) can significantly lower life-cycle greenhouse gas emissions, particularly when biomass valorization is combined with CO_2-utilization routes within polymer supply chains.[83]

According to a report by Plasticseurope 2025,[84] global biobased plastics production capacity currently accounts for approximately 0.6% of the 431 million tonnes of plastics produced annually. When circular plastics, including mechanically and chemically recycled materials, are considered, this share increases to 10.2%. In Europe, of the total 54.6 million tonnes of plastics produced, 1.1% are biobased. These figures indicate that significant efforts are still required to enable the transition from fossil-based to renewable and circular polymer production. Among bio-based polymers, two main categories can be distinguished: natural bio-based polymers, which occur naturally (e.g., starch, chitin, nucleic acids, and lignin), and bio-based polymers analogous to conventional polymers.[85] The latter can be obtained through the chemical modification of natural biobased polymers,[86] the synthesis of biobased monomers followed by polymerization (e.g., poly(lactic acid) and polybutylene

succinate),[87,88] or *via* microbial fermentation processes, such as the production of polyhydroxyalkanoates.[89] Among second-generation renewable feedstocks, lignocellulosic biomass has attracted particular attention due to its abundance, non-food nature, and rich chemical functionality. Wood, as one of the most widely available lignocellulosic resources, represents a key feedstock for sustainable polymer development. The structure of wood and plants in general can be ascribed to four main natural biobased polymers: cellulose, hemicellulose, lignin, and pectin.[90] For wood and other lignified tissues, typical mass fractions are roughly 35–55% cellulose, 20–35% hemicellulose, and 15–36% lignin, along with smaller amounts of pectin and other components.[91] In the cell wall, stiff cellulose microfibrils are embedded in and interconnected by a branched hemicellulose matrix, while lignin fills the spaces between these polysaccharides, providing additional rigidity and mechanical strength to the plant tissue.[92] In **Figure 2.2.1**, an overview of the plant cell walls and its main component is depicted.

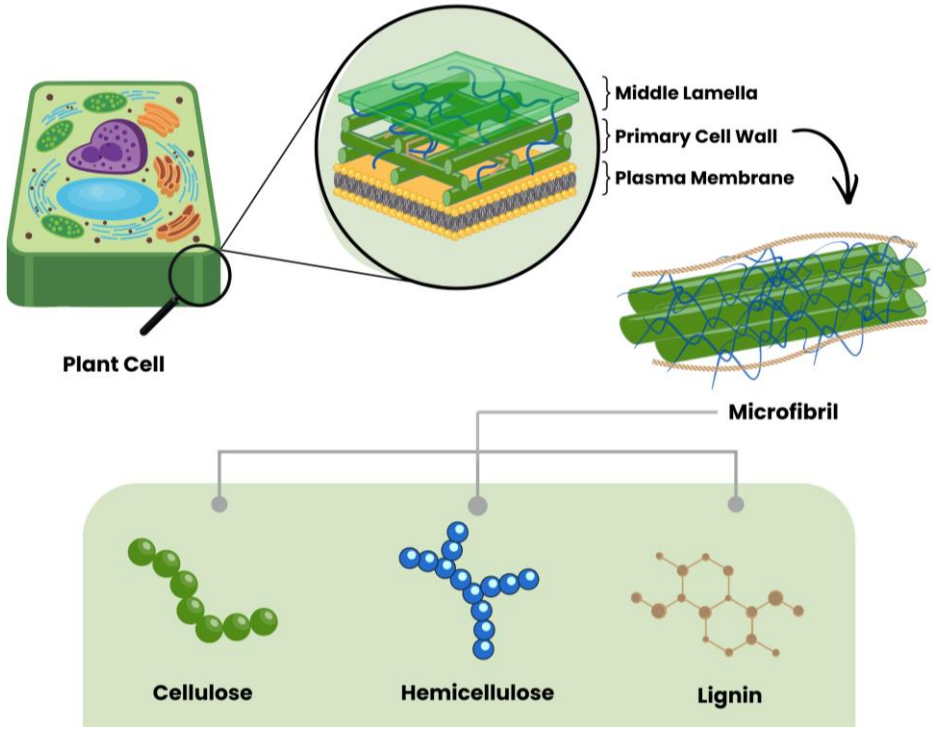

Figure 2.2.1 – Overview of the structure of the plant cell wall and its main components, cellulose, hemicellulose and lignin, for woody biomass. *Picture drawn by the author.*

2.2.1 Lignin

This chapter is based on a published literature review by the author of this thesis:[93]

C. Libretti; L. Santos Correa; M. A. R. Meier. From waste to resource: advancements in sustainable lignin modification. *Green Chem.*, **2024**, *26*, 4358-4386.

L. Santos Correa contributed to the conceptualization and drafting of the work and provided valuable scientific input during discussions.

Detailed E-factor calculations for the protocols discussed in this chapter are reported in **Appendix 7** and were previously published in ref. [93]

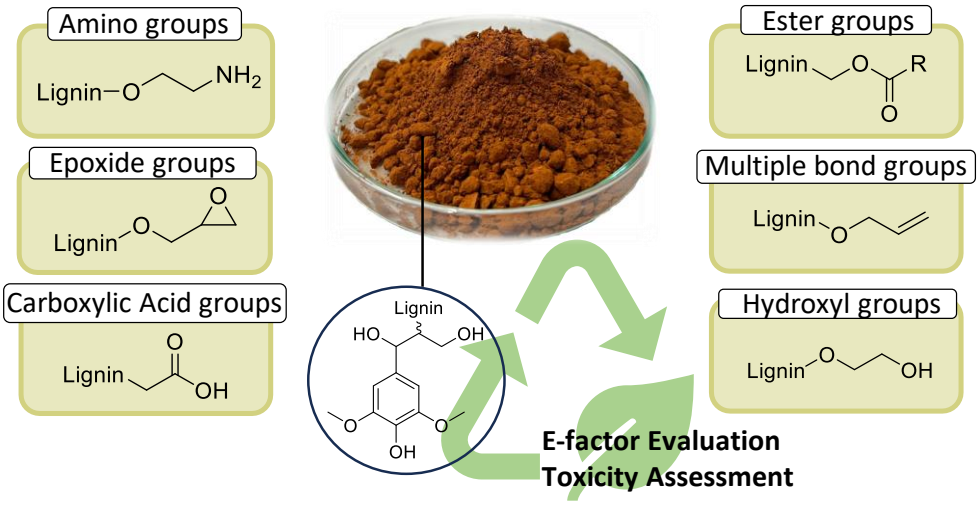

2.2.1.1 Chemical Structure of Lignin

Besides its intrinsic heterogeneity, the basic chemical structure of lignin is characterized by three phenylpropane units: *p*-hydroxyphenyl (H), guaiacyl (G), and syringyl units (S), derived, respectively, from *p*-coumaryl alcohol, coniferyl alcohol, and sinapyl alcohol, which can vary considerably in their ratio depending on the lignin source.[94] In **Figure 2.2.2**, a model representation of the structure of lignin is presented, alongside the common interunit linkages and their typical occurrence in hardwood and softwood lignin, which are listed in **Table 2.2.1**. Among the various linkages, the β-O-4 is the most common and the most affected during depolymerization processes.[95] In fact, C-O bonds usually have a lower bond dissociation energy than C-C bonds,[96] rendering them easier to cleave.

Table 2.2.1 – Typical interunit linkages of different lignins and their natural occurrence; structures of interunit linkages are shown in **Figure 2.2.2**. HW: hardwood; SW: softwood.

		Natural occurrence (%)[97,98]	
Letter	**Interunit linkage**	**HW**	**SW**
A	β-O-4	60	46
B	β-5	6	11
C	β-β	3	2
D	5-5	5	10
E	Dibenzodioxocin	5-7	0-2
F	β-1	7	7
G	4-O-5	7	4
H	α-O-4	7	7

HW: hardwood; SW: Softwood

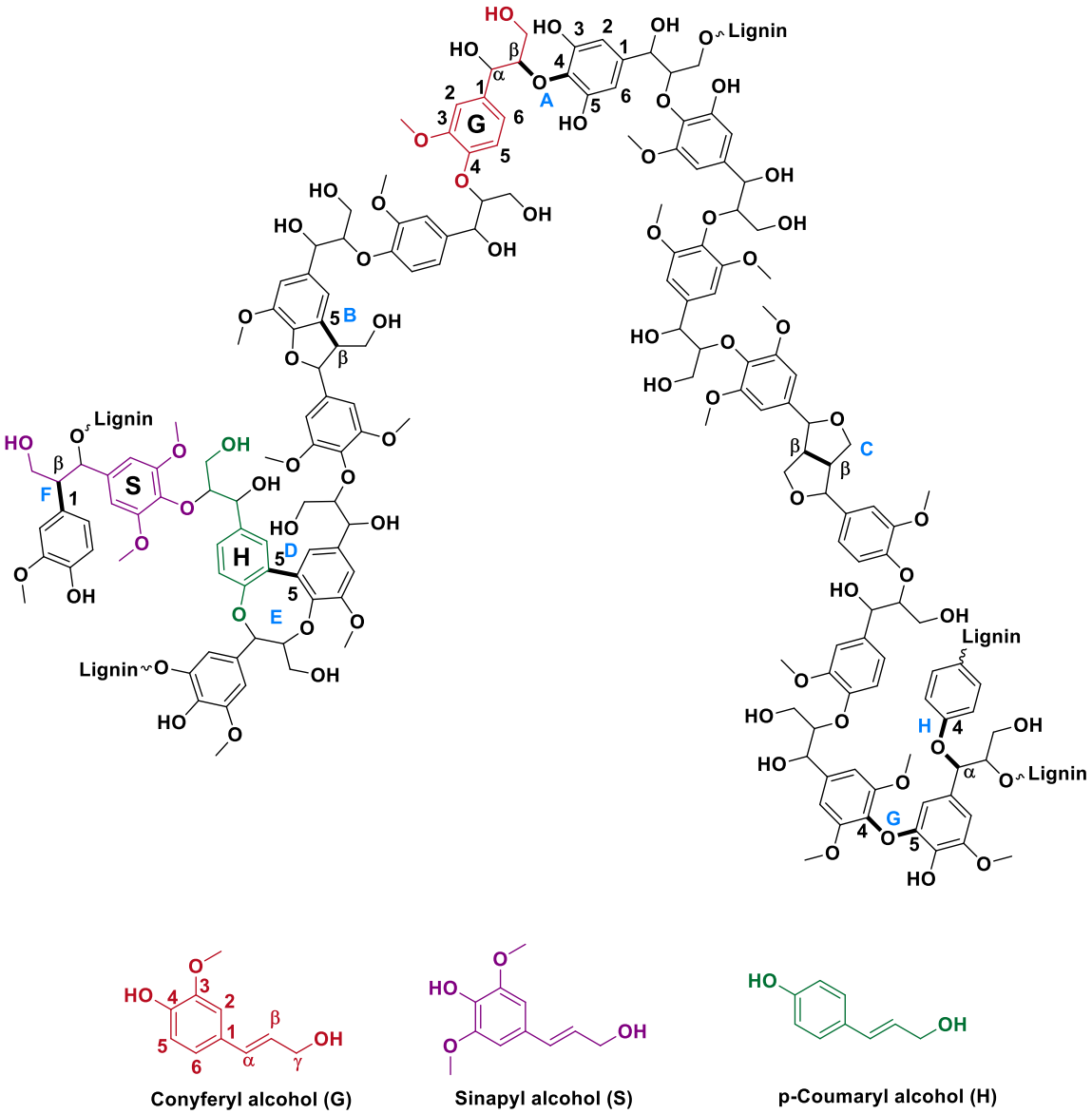

Figure 2.2.2 - Model representation of the chemical structure of lignin (readapted from ref. [95]), structures A-H are specified in **Table 2.2.1**.[93]

2.2.1.2 Lignin Isolation Methods

A variety of processes have been developed for lignin production and biomass separation of cellulose/hemicellulose/lignin fractions. A schematic representation of the commercially developed and emerging processes is presented in **Figure 2.2.3**.

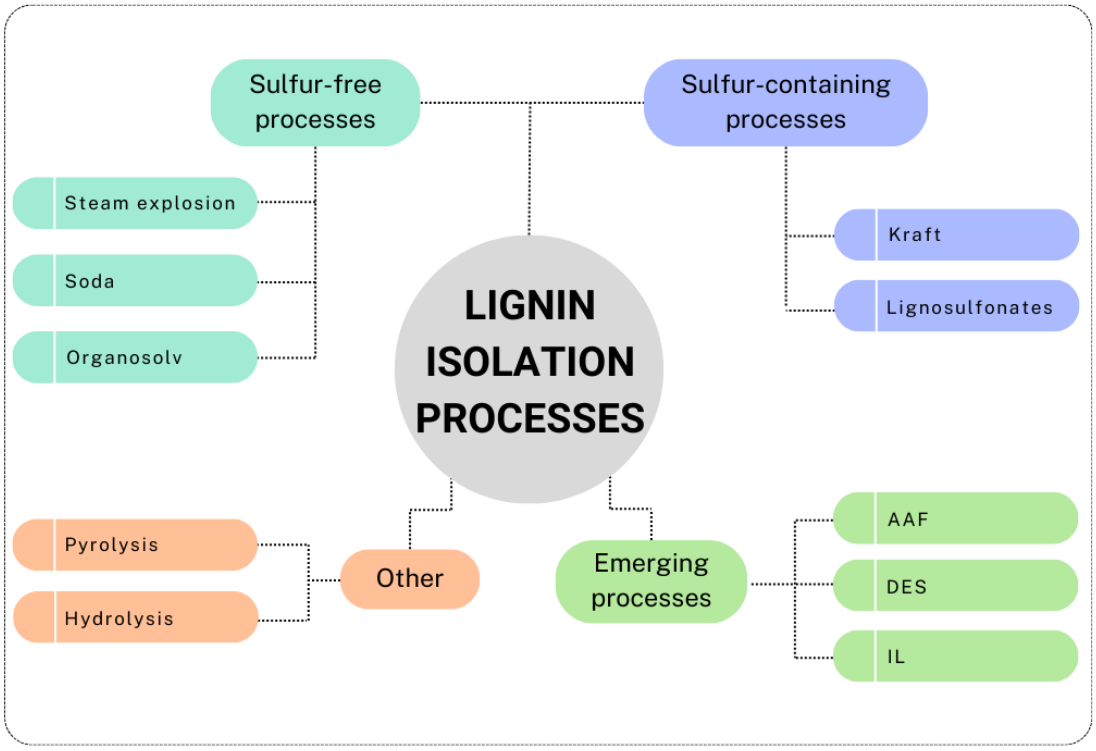

Figure 2.2.3 – Schematic representation of commercially developed and emerging processes for lignin isolation (readapted from ref. [99]).[93]

Sulfur-containing processes, i.e., Kraft and Lignosulfonates (or Sulfite) processes, account for the main annual lignin production. Recently, a decline in the lignosulfonate production process has been observed, thereby facilitating the growth of kraft processes as predominant methods for lignin production.[100] The Kraft process, which is the most used process by the pulp and paper industry, applies a hot mixture of water, sodium hydroxide (NaOH) and sodium sulfide (Na_2S). This medium, also called “white liquor”, allows the breaking of the linkages between lignin and cellulose, its depolymerization and, to a lesser extent, its derivatization (for instance with thiol functional groups).[101] In this

process, ~90% of lignin is separated from the cellulosic fibers, and the lower molecular weight fragments are soluble in the basic medium, which assumes a dark coloration (hence the name “black-liquor”). The separation is achieved by acidification of the medium, which causes the lignin to agglomerate and precipitate, permitting the subsequent filtration.[102] Kraft lignin contains usually about 2−3 wt% of sulfur, while the Lignosulfonate lignin usually has a higher sulfur content, between 5−9 wt%.[101] In the Sulfite process, the pulp is treated with sulfur dioxide (SO_2), which forms a variety of sulfite (SO_3^{2-}) /bisulfite (HSO_3^-) salts, depending on the type of bases used, at 130−180 °C.[103] The isolated lignin can eventually be sulfonated by replacing a hydroxyl group with a sulfonate group.[104] The Lignosulfonate lignin is water-soluble and can be separated from the rest of the biomass. On the other hand, the *Soda Process* has seen extensive pilot trials.[101] This process, despite being remarkably similar to the Kraft process, does not involve sulfur, since it employs just an alkaline medium, such as sodium or potassium hydroxide (KOH). This process causes hydrolytic cleavage of the lignin structure into smaller fragments, leaving a type of lignin relatively chemically unaltered compared to other types of lignins.[105] Environmental concerns associated with traditional pulping processes (Kraft and Sulfite in particular) have been discussed. Indeed, these processes have been tied to significant emissions and negative impact on the environment.[106] Major pollution sources are associated with air emissions and liquid effluents, *i.e.*, wastewater high in BOD (biochemical oxygen demand) and COD (chemical oxygen demand).[107] Discussing in detail and comparing the various processes in terms of sustainability would require the use of other instruments, such as LCAs (life cycle assessments), and it is beyond the scope of this thesis. Still, in this paragraph are delineated recent advancements in LCB delignification processes toward more sustainable solutions.

Other types of sulfur-free isolation procedures, namely the *Organosolv* and the *Steam explosion* processes, involve the use of organic solvents for the former and high-pressure steam for the latter. In the Organosolv process, biomass is

mixed with organic solvents, such as methanol, ethanol, acetone, *etc*., whereby the solubility of lignin during the process depends on the organic solvent used.[108] To be financially competitive and more sustainable, due to the higher costs of solvents, the process must contemplate a recycling phase of the solvents used, i.e. *via* distillation.[109–111] Furthermore, this process yields a sulfur-free lignin, typically characterized by lower molecular weights compared to *Kraft* lignin.[112] *Organosolv* pulping was the isolation method for the lignin employed in this doctoral thesis.

Interestingly, a study from 2021 analyzed the GWP (global warming potential) of an Organosolv process from spruce bark, leading to 0.23 kg CO_2 eq./kg lignin using ethanol, while using bioethanol from wood the GWP could be more than halved to 0.11 kg CO_2 eq./kg lignin.[113] These results are considerably lower compared to Kraft lignin with a GWP of 0.6 kg CO_2 eq./kg lignin.[114]

In contrast, during the Steam explosion process, biomass is treated with hot steam at high temperatures and pressures. Then, the pressure is released rapidly and the steam present in the biomass expands, causing fibers to break down.[99] This process is considered to be one of the most efficient and cost-effective, although it is important to note that it is often used as pretreatment of lignocellulosic biomass before other processes are applied,[115] and there is a large heterogeneity of the lignin obtained.[99] Hydrolysis lignin, on the other hand, is usually a by-product of bio-ethanol production from cellulose hydrolysis.[99,116] The process aims to hydrolyze cellulose and hemicellulose in order to obtain fermentable sugars, while lignin is a solid by-product. Hydrolysis lignin presents a different structure compared to Kraft lignin, it is reported to have more condensed and cross-linked structures, making it more difficult to depolymerize.[116,117] Pyrolysis methods convert lignocellulosic biomass to bio-oil, char and gases (H_2, CO, CO_2, CH_4), in absence of oxygen.[118] Numerous concomitant reactions take place during pyrolysis, such as a major degradation of the lignin structure, resulting in phenolic compounds and char formation.[118] The yield of the liquid fraction can be enhanced by optimization of the process

temperature.[119] Pyrolytic lignin (PL) is subsequently obtained through a straightforward phase separation of such fraction, due to water addition. The fragments and oligomers of PL precipitate and can be separated from the pyrolytic-sugar fraction.[120] Being a by-product of the pyrolysis processes, pyrolytic lignin has lower molecular weight and an increased number of hydroxyl groups compared to other types of lignin[119] and represents a promising precursor for aromatic and phenolic monomers.

Among the emerging methods for lignin isolation, the Aldehyde-Assisted Fractionation (AAF) is making its way as a powerful process to retrieve uncondensed lignin. This aldehyde-aided treatment generates a type of lignin easier to depolymerize, avoiding undesired condensation pathways that lead to C-C coupling. The most problematic pathway leading to condensation involves the elimination of benzylic alcohol, producing a relatively stable benzylic carbocation, which undergoes electrophilic aromatic substitution with guaiacyl or syringyl units.[121] This significantly alters the possibility of selectively cleaving these C-C bonds, and therefore the depolymerization.[122] In the presence of an aldehyde (usually formaldehyde or propionaldehyde are used), the 1,3-diols of the β-O-4 linkages form an acetal that avoids benzylic alcohol elimination (**Scheme 2.2.1**).[122] AAF oligomers were tested in comparison to Kraft lignin oligomers, demonstrating their superior properties (enhanced solubility, lighter colors, better structural composition).[123]

Scheme 2.2.1 – General scheme for condensation and repolymerization pathway (top) in traditional lignin fractionation and aldehyde-assisted fractionation with formaldehyde or propionaldehyde (bottom); readapted from ref. [99,124].[93]

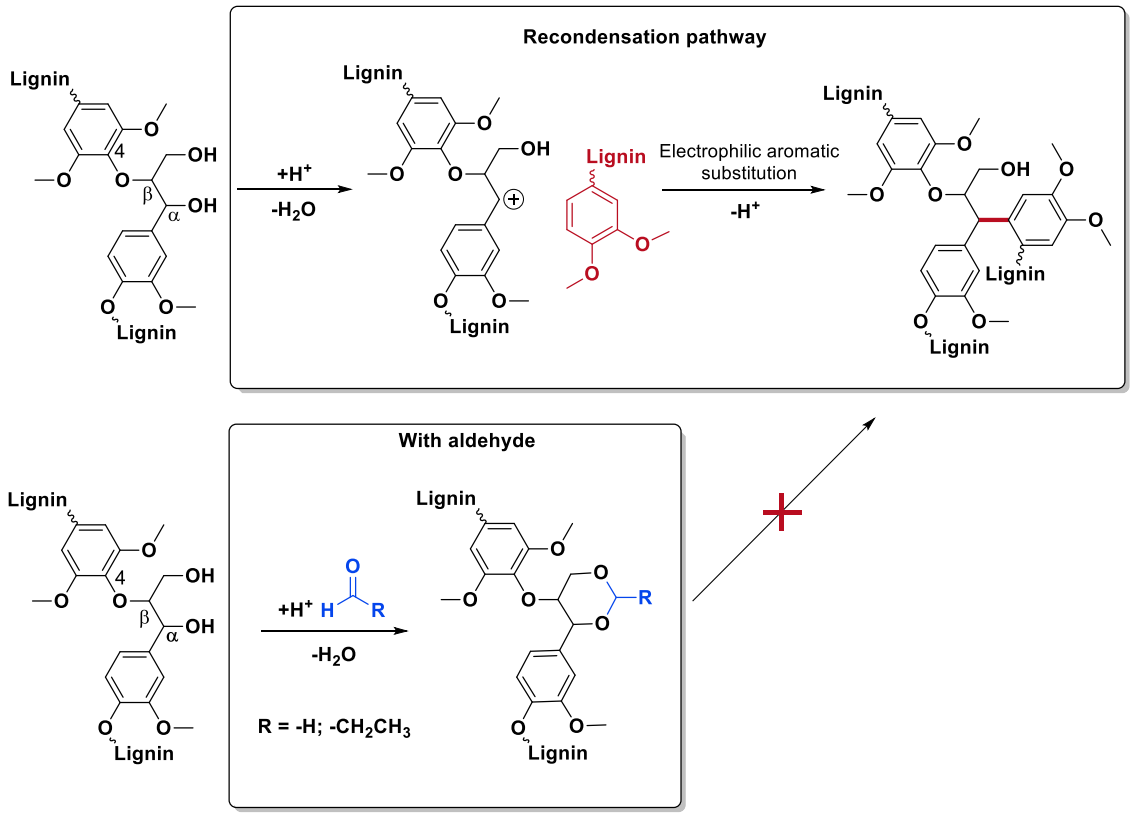

Furthermore, ionic liquids (ILs) have recently gained attention as a promising method for biomass delignification.[125] The *Ionosolv* process presents various analogies with the Organosolv process, however, the cost of ILs is one of the main difficulties that prevents their application in industry. Recently, the use of protic ionic liquids (PIL) seems to have solved cost-related problems.[125,126] A study from 2022 showed a recovery of 70% lignin *via* an Ionosolv process at 135 °C.[126] It was also noted that increasing the time of the treatment influenced the properties of lignin, especially its thermal stability due to increased recondensation processes.[127]

Deep eutectic solvents (DESs) are another class of solvents recently applied for lignin extraction. They are generally composed of both a hydrogen bond acceptor and a donor, at specific molar ratios. DESs have gathered significant attention in recent years as an alternative to traditional ionic liquids owing to their numerous

advantages, such as lower costs, biodegradability and easier preparation processes compared to ILs.[128] They have recently been recognized as a class of safe and environmentally friendlier media, capable of extracting lignin with high efficiency and selectivity, and minimizing waste generation.[129]

DESs are often labeled as non-toxic, however, the intrinsic diversity within the class of DES compounds highlights the variability in their overall toxicity and individual properties, emphasizing the need for case-specific evaluations. Despite these challenges, the advantages of DESs persist, for instance they exhibited remarkable delignification efficiencies of different lignocellulosic biomass materials.[130] Additionally, DES can be recovered and re-used post-lignin fractionation. A recent publication developed tunable DES systems for lignin isolation that allowed stabilization of reactive intermediates and therefore less recondensation reactions, improving aromatic monomer yield after depolymerization.[131]

At the current state, ~98% of lignin is used for heat generation and only 2% finds useful applications in various industry fields,[120,132] or is often depolymerized to obtain high-value-added chemicals. The various isolation methods briefly discussed above must be taken into consideration when considering the destiny of the lignin: if the final aim is lignin depolymerization for monomer production, less condensed structures are preferred. This also needs to be taken into consideration when the final goal is to modify the functional groups of lignin to produce a final material with a certain set of features. Lignin properties can vary among different isolation methods as well as biomass type and source.[133,134] Not only the isolation method can influence the chemical structure, but also the type of biomass from which lignin is extracted, such as hardwood, softwood, or grass.[135]

This paragraph highlights the intricate relationship between isolation techniques and chemical properties of the respective lignins. Nonetheless, evaluation of sustainability through comparison of the distinct processes is difficult due to the

lack of data available. For instance, LCAs for established processes such as Kraft and Organosolv are readily available in the literature, while for newer processes this presents challenges due to a scarcity of data.

2.2.1.3 E-factors calculations

The E-factor was chosen as green metric for the evaluation of sustainability, for its clarity and ease of application to different methodologies, together with a careful evaluation of toxicity and hazardousness of the used substances. This chapter thus provides an overview of lignin modifications and application possibilities and, importantly, quantitatively compares all discussed literature procedures in terms of sustainability. In this context, only synthetic E-factors are reported. In line with the original definition proposed by Sheldon,[51] these parameters do not account for water. In the field of lignin modification, the work-up of reactions is usually performed *via* precipitation in an aqueous medium and subsequent filtration of the lignin derivatives. The exact volume of the water used for the work-up is not always given, leading to incomparable data. Therefore, when comparing E-factors for lignin modification protocols, the water is usually excluded.

The E-factors discussed herein are classified as simple E-factors (E_{simple}), which exclude solvents used during synthesis, and complex E-factors ($E_{complex}$), which include synthetic solvents in the calculation in order to highlight their contribution to the overall waste generation.

Comprehensive overview of the values for each modification and details on the calculations for the E-factors can be found in the **Appendix 7**.

2.2.1.4 Lignin Modification

2.2.1.4.1 Amination of Lignin

Amination of lignin enables the insertion of reactive sites onto lignin, leading to applications in the field of fertilizers,[136] as well as curing agents for epoxy resins. Introduction of nitrogen to lignin can be achieved *via* ammonoxidation,[137,138] although it typically leads to nitriles and a mixture of N-containing functional groups, rather than amino groups. Introducing primary amino groups onto lignin could be a useful contribution to the field of biobased amines, especially toward non-isocyanate polyurethane applications or for epoxy resins. In addition, amine groups are ionizable, possibly contributing to other promising applications, *e.g.*, as polycationic materials[139] or for water purification systems.[140,141]

Different protocols can be found in the literature to introduce amino groups onto lignin, but the most common is the Mannich reaction, a multicomponent reaction involving the utilization of formaldehyde, an amine and in this case phenolic groups of lignin, as shown in **Scheme 2.2.2**.

Scheme 2.2.2 - General reaction scheme for lignin amination *via* the Mannich reaction.[93]

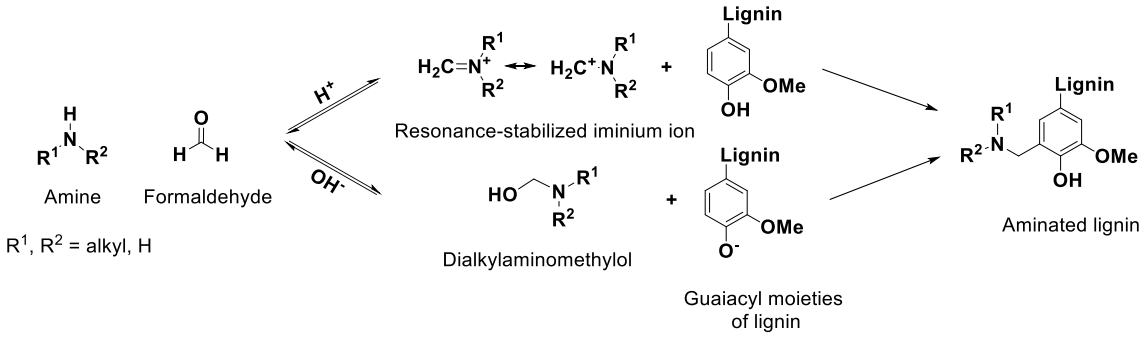

Depending on the reaction conditions, i.e. the pH, the active species involved in the reaction are phenolic lignin and iminium ion as electrophile, or phenolate and *N*,*N*-dialkylaminomethylol (under acidic or basic conditions, respectively). Amine substitution takes place selectively at the *ortho* position of non-etherified

phenolic hydroxyl groups,[142] leading to one amino group for guaiacyl units (G) and two for *p*-hydroxy phenyl (H) units.

The work of She *et al.*[143] discloses an effective amination of lignin with dimethylamine, ethylenediamine or diethylenetriamine. Nitrogen contents up to 10.18 % are reported and the nitrogen release behavior was investigated, an important metric for fertilizing purposes. This procedure involves the utilization of a sodium hydroxide (NaOH) solution to dissolve phenolated lignin. Phenolation pretreatment is usually conducted prior to Mannich amination,[143–146] in order to enhance lignin reactivity. Typical conditions consist of treatment of lignin with phenol under acidic conditions at relatively high temperatures (90 −170 °C).[145] In this work, phenolation increased the number of active sites from 2.91 mmol/g up to 8.26 mmol/g if a weight ratio of lignin/phenol of 1:6 was used. Notably, a ratio of 1:1 sufficed to effectively double the quantity of reactive sites. Nevertheless, in the pursuit of more environmentally-friendly procedures, phenolation pretreatment should be avoided as it is an extra step that generates waste and phenol is highly toxic and fossil resource derived. The simple E-factor calculated for the subsequent Mannich amination procedure is 4.15. A comparable methodology was adopted from Li *et al.*,[144] where softwood kraft lignin was aminated in a similar fashion. In this case, both pristine and phenolated lignin were aminated *via* Mannich reaction under acidic conditions in the presence of dimethylamine (DMA) and formaldehyde. Phenolated lignin (1:6 weight ratio lignin/phenol) presented an improved total nitrogen content of 4.8%, compared to 2.5% reached for the amination of unmodified lignin. Both aminated lignins exhibited high zeta potentials (27.2-31.6 mV) and large charge densities (1.2-1.6 $\times$ 10^{-7} equiv./mL), indicating useful colloidal properties. This procedure shows a E_{simple} of 5.51, higher than the previous one, moreover the procedure involves the use of dioxane as solvent, which raises concerns for its toxicity.[147] Jameel *et al.*[142] employed a fairly similar procedure, but used a lower amount of both the amine and formaldehyde compared to Li *et al.*, lowering E_{simple} to 2.98. However, also in this procedure dioxane was used as solvent, leading to toxicity concerns and increasing $E_{complex}$ to 13.74 with a solvent contribution of 78% (**Table 7.2.1**).

An interesting example from Biesalski *et al.*[148] reached the lowest E_{simple} of 1.91 using 1,3-propylenediamine. The authors used a lower amount of amine for the functionalization of lignin compared to other procedures (15.5 mmol amine/g lignin), thereby lowering the E-factor. In this case, no phenolation pretreatment was performed, but the lignin was directly dissolved in NaOH solution (this explains the increased $E_{complex}$ up to 26.59). The amount of amine moieties introduced varied from 1.2 to 2.0 mmol g^{-1}, with the lowest value obtained for ammonia. Intramolecular crosslinking occurred at a higher extent with ammonia functionalization, generating benzoxazine species, leaving less reactive positions for further ammonia introduction (**Scheme 2.2.3**).[148–150] Aminated lignins were then used for epoxy resin synthesis.

Scheme 2.2.3 - Benzoxazine formation and cross-linking products during lignin amination *via* Mannich reaction, readapted from ref. [148].[93]

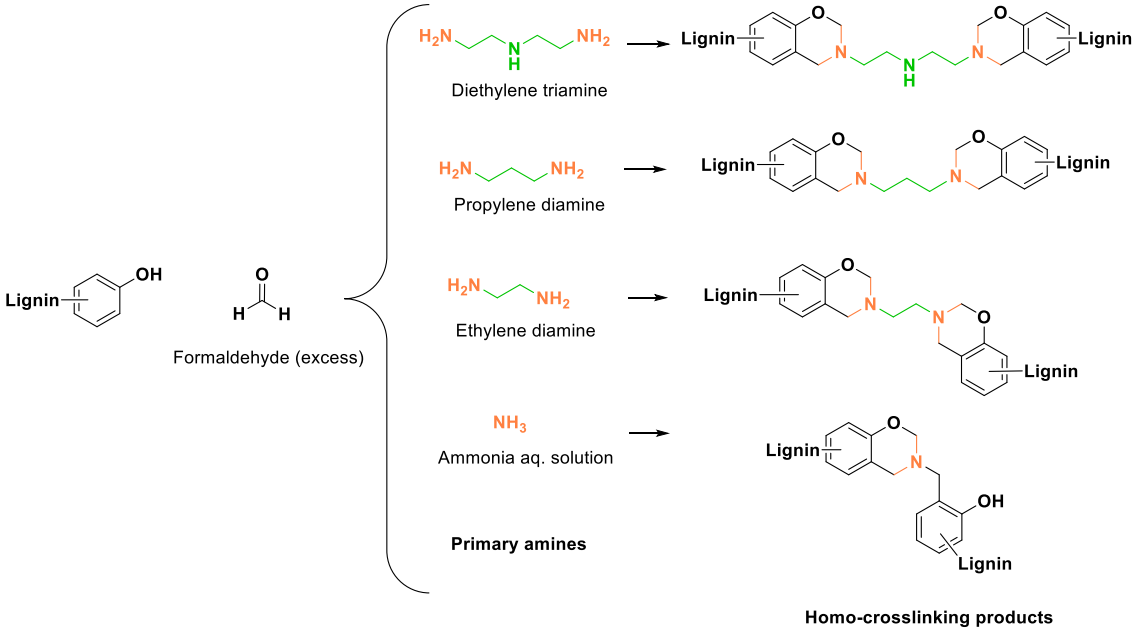

The main issue concerning the amination *via* Mannich reaction remains the toxicity of formaldehyde,[151,152] but this can be put into perspective considering that the simple one-step multi-component reaction is usually accompanied by low E-factors. Moreover, the use of paraformaldehyde, which is still toxic, but considerably less than formaldehyde, might further improve this procedure.

Amination procedures that do not require the use of formaldehyde are also reported in the literature. In the work from Y. S. Kim *et al.,*[153] lignin was aminated with 2-chloroethylamine hydrochloride in water (**Scheme 2.2.4**). However, in this case the E-factor, both simple and complex, increased dramatically compared to the Mannich amination (12.27 and 142, respectively, with 91% of solvent contribution to the E-factor), confirming that nucleophilic substitution reactions of haloalkanes should be avoided due to the generation of large amounts of waste. Moreover, hazardousness is an issue due to the 2-chloroethylamine hydrochloride.[154]

Scheme 2.2.4 - Reaction scheme for lignin amination using 2-chloroethylaminehydrochloride; readapted from ref. [153].[93]

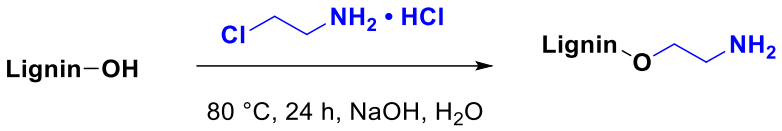

Another formaldehyde-free protocol for potential lignin amination exploits the concept of hydrogen borrowing in order to insert tertiary amino-groups onto lignin model compounds, namely 3-(4-hydroxyphenyl)-1-propanol and dihydroconiferyl alcohol.[155] Hydrogen borrowing (HB) involves the direct amination of an alcohol, consisting of a first dehydrogenation step, forming a carbonyl compound from the respective alcohol, followed by condensation of the carbonyl with an amine and a subsequent imine-to-amine reduction step, consuming the hydrogen generated in the first oxidation step.[155,156] The authors report good to excellent conversion of the model compounds (86-98%) in the presence of dimethylamine as functionalizing agent and a Cu-ZrO_2 catalyst, as well as no amination of the phenolic moiety. Despite that this protocol was not yet conducted on pristine lignin, it is noteworthy due to the excellent atom economy of the procedure and high conversions, paving the way for further research on lignin amination.

A recent work from Renneckar *et al.*[157] reports an interesting solventless amination of softwood kraft lignin *via* 2-oxazolidinone (OZD, see **Scheme 2.2.5**). This compound exhibits a non-hazardous nature, according to its Safety Data

Sheet (SDS).[158] Furthermore, recent progresses, as outlined in a comprehensive review,[159] have highlighted the potential for sustainable production methods of OZDs. The synthesis processes of OZDs involve CO_2 as a feedstock, *i.e.*, *via* dehydration condensation of β-aminoalcohols, or *via* cycloaddition reaction of aziridines with CO_2. Comparing the two methods, it should be noted that aziridines are typically highly toxic, aziridine itself is rated CMR. Lignin functionalization with OZD proceeds *via* nucleophilic attack of deprotonated ArOH or COOH groups to the methylene carbon adjacent to the oxygen of OZD, resulting in a carbamate ion intermediate (**Scheme 2.2.5**, B), which subsequently releases CO_2 to form a primary amino group (**Scheme 2.2.5**, C). A side reaction can occur between carbamate ions and the newly inserted primary amino groups, leading to urea linkage formation (**Scheme 2.2.5**, D) and thus oligomerization or cross-linking of lignin.

The protocol reported by the authors presents a facile synthesis procedure, using only OZD both as reagent and solvent and NaOH in catalytic amount. The calculated E_{simple} for the optimized conditions (150 °C, 2 h, molar ratio of OZD/sum of (ArOH+COOH) = 6) is 3.10, with lignin presenting a nitrogen content of 5.24 %. An overview of the discussed protocols for lignin amination procedures with their corresponding E-factors can be found in **Table 7.2.1.**

Scheme 2.2.5 - Reaction scheme for lignin amination via 2-oxazolidinone (OZD). A) nucleophilic attack of deprotonated ArOH or COOH groups of lignin to OZD; B) formation of carbamate ion intermediate; C) CO_2 release and formation of primary amino groups, which react in a side reaction with carbamate ions to form urea linkages, D); readapted from ref. [157].[93]

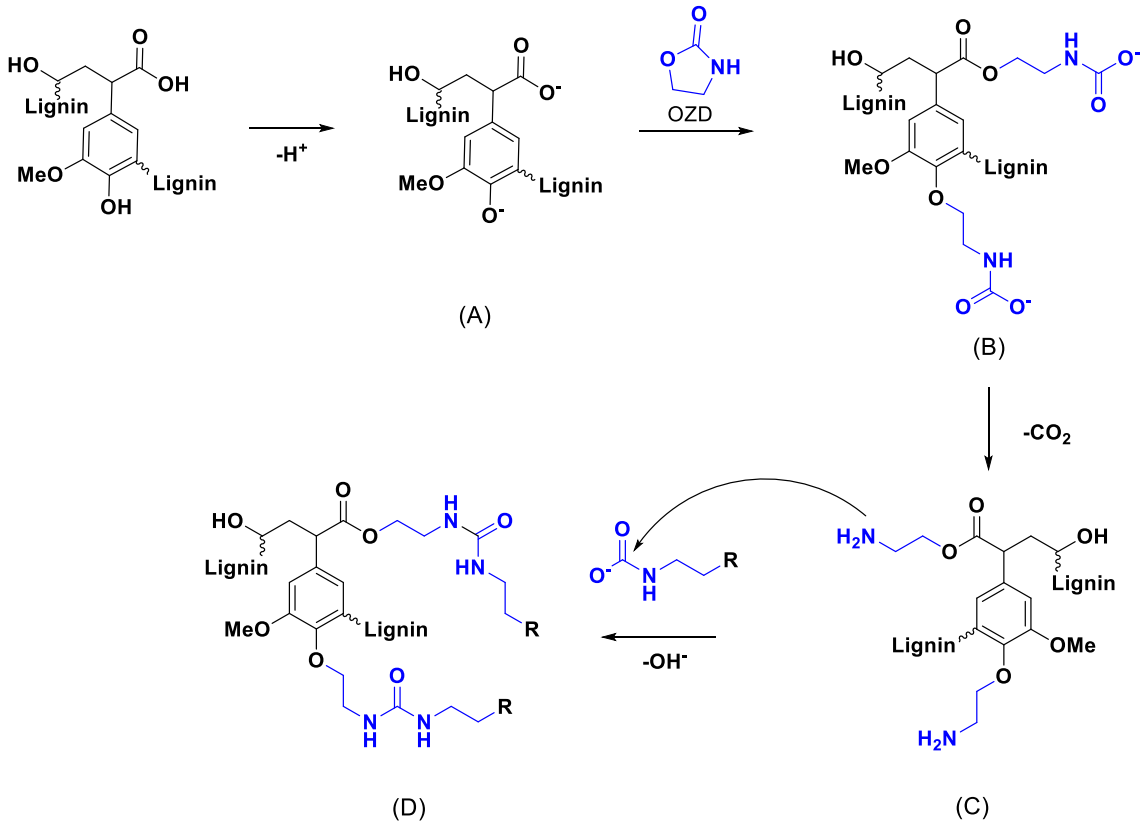

2.2.1.4.2 Epoxide functionalized lignin

Lignin-based polyepoxides are mostly used as cross-linkers for the introduction of hard segments into epoxy resins. For instance, multiple literature reports demonstrated that bisphenol A (BPA) can be partially substituted by lignin to improve material properties.[160–162] A substitution of up to 30 wt% of bisphenol-A diglycidyl ether (BPADGE) with lignin-based epoxides is possible without negative effects on the properties of the resulting material. Instead, incorporation of lignin units into epoxy resins turned out to be beneficial for material properties, such as glass transition temperature and Young's modulus.

The addition of epoxide groups to lignin is usually achieved by reaction with epichlorohydrin, a potentially renewable,[163,164] yet highly harmful and toxic chemical.[165,166] Depending on the report, E-factors for reactions of lignin with epichlorohydrin vary between 4 and 16, if epichlorohydrin is used as reagent and solvent (**Table 7.3.1**).[160–162,167,168] In 2017, BPA based epoxy resins with varying content of epoxidized lignin and isophorone diamine as hardener were reported ($E_{complex}$: 6.35, **Scheme 2.2.6**).[160] In the used epoxy formulation, BPADGE was substituted gradually by glycidylated organosolv lignin to investigate the properties of the resulting material depending on the lignin content. 33 wt% of lignin-based epoxide was incorporated into the final epoxy resin, while maintaining good thermal and mechanical properties compared to the epoxy resin containing 100% BPADGE.[160] In another study, Sun *et al.* synthesized different lignin epoxides with varying epoxide content from lignin functionalization with epichlorohydrin and cured them with BPADGE and Jeffamine D400 as curing agent ($E_{complex}$: 57.0, **Scheme 2.2.6**). The incorporation of 10 wt% of epoxidized lignin (based on BPADGE mass) significantly improved the stiffness of the resulting material and its tensile strength (from 6.2 MPa without lignin to 10.9 MPa with lignin).[162]

The use of bisphenol A in epoxy resin formulations is ubiquitous in literature due to the excellent mechanical properties of the final materials.[169,170] However, to

further improve sustainability, the use of toxic substances such as bisphenol A should be fully omitted.[171–173] For instance, Zhang *et al.* synthesized a fatty acid based cyclic anhydride from eleostearic acid methyl ester and maleic anhydride *via* Diels-Alder reaction and cured it with glycidylated lignin ($E_{complex}$: 16.2) to manufacture a bisphenol A-free epoxy resin that can be used as asphalt binder.[168] The thermal properties of the resulting material were comparable to the properties of the corresponding bisphenol A-based epoxy resin. In another report, Lawoko *et al.* fractionated Kraft Lignin *via* extraction with organic solvents into four different molecular weight fractions.[174] Bisphenol A-free epoxy resins were synthesized through curing of all glycidylated fractions with Jeffamine D2000. The investigation showed that mechanical properties of the resulting materials strongly depended on the molecular weight of the used lignin fraction.

Scheme 2.2.6 - Synthesis of epoxy resins from glycidylated lignin, bisphenol-A diglycidyl ether (BADGE) and diamine hardener (readapted from refs. [160–162]).[93]

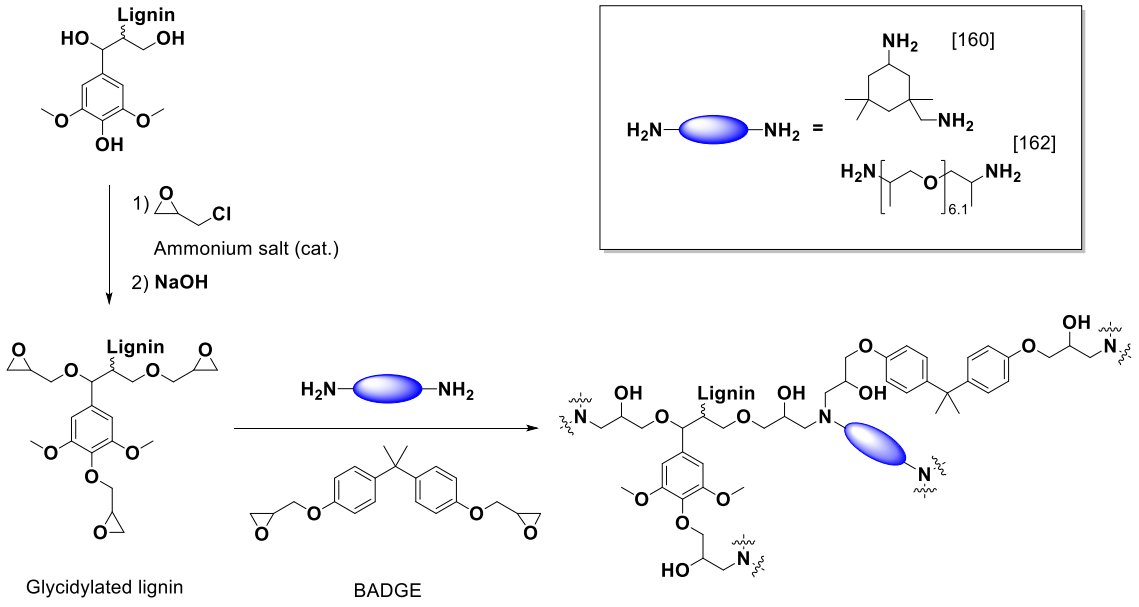

Although improving the sustainability of epoxy resins by substitution of bisphenol A based epoxides, most studies still use the carcinogenic substance epichlorohydrin as reagent to introduce epoxy groups.[165] Daugaard *et al.* reported an epichlorohydrin free procedure for the synthesis of lignin epoxides from Kraft lignin and rapeseed oil (**Scheme 2.2.7**).[175] The used rapeseed oil fatty acid mixture was first epoxidized with hydrogen peroxide ($E_{complex}$: 4.78) and then

esterified with lignin by means of a Steglich esterification ($E_{complex}$: 22.7).[176,177] Curing of the synthesized lignin epoxide and commercially available curing agent Ancamide® 3030 resulted in an epoxy resin with a Young's modulus of 103 MPa. The rather low Young's modulus was attributed to the high flexibility provided by long fatty acid chains and the low cross-linking density. Substitution of up to 30 wt% of lignin epoxide by low molecular weight furan-2,5-dicarboxylic acid diglycidyl ester (FDCADGE) significantly increased the cross-linking density and the Young's modulus to 440 MPa. The addition of an aromatic bisepoxide to the formulation therefore improved the stiffness of the material. However, this specific example is not an improvement in terms of sustainability, as hazardous substances such as oxalyl chloride and glycidol were used for the synthesis of FDCADGE. While toxic epichlorohydrin was omitted in the synthesis, the applied Steglich esterification used stoichiometric coupling reagents such as allergenic *N*,*N*'-dicyclohexylcarbodiimide (DCC)[178] to allow mild esterification conditions that are necessary to tolerate sensitive groups such as epoxides. The use of DCC further results in large amounts of waste, as evidenced by the high E-factor ($E_{sequence}$: 38.0). hence, epoxide groups should potentially be introduced into the lignin scaffold as last synthetic step to circumvent this issue and further improve sustainability.

Indeed, Avérous *et al.* esterified organosolv lignin with oleyl chloride and epoxidized the double bonds afterwards with peracetic acid to synthesize a similar fatty acid based lignin epoxide ($E_{sequence}$: 14.2, **Scheme 2.2.7**).[179] Ring-opening of the epoxide groups was then performed with methanol to obtain a polyol for the synthesis of partly biobased polyurethanes (PUs). The initially sterically hindered alcohol groups of the used lignin were thus extended by fatty acid ester chains to be more available for further reactions.

Scheme 2.2.7 - Fatty acid-derived lignin epoxides synthesized *via* Steglich esterification of lignin with epoxidized fatty acids,[175] or *via* epoxidation of lignin previously esterified with oleyl chloride;[179] readapted from refs. [175,179].[93]

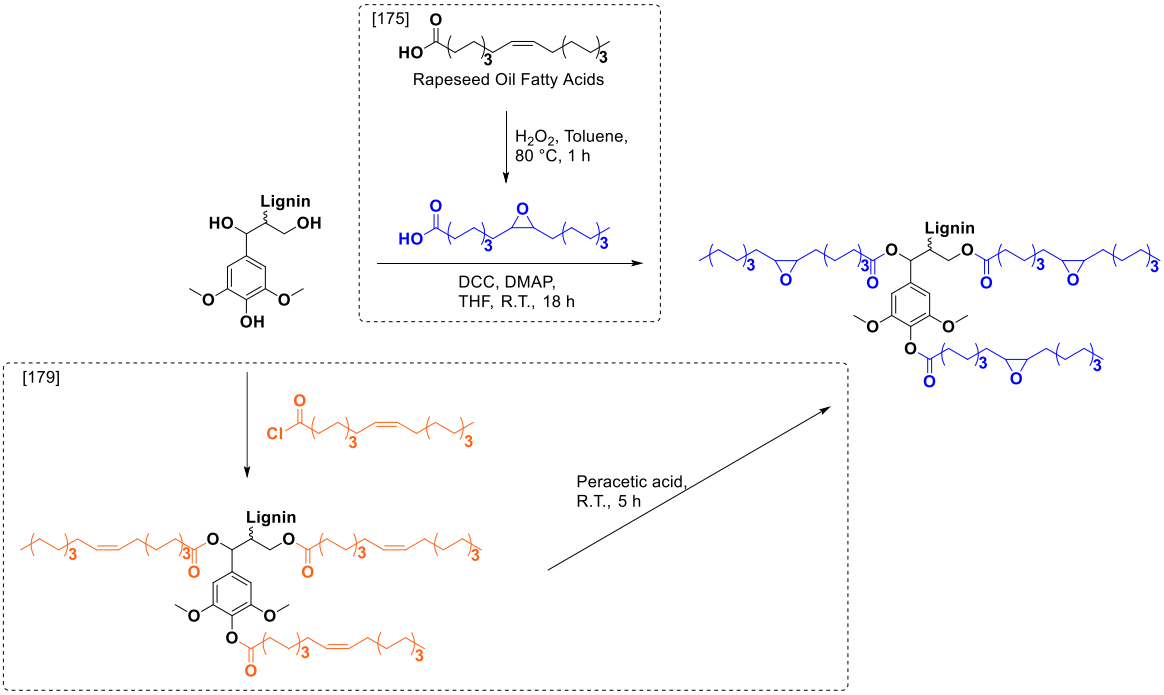

Finally, polyurethane networks were obtained through curing of the oleic acid-based lignin polyol with diisocyanates to synthesize a variety of PUs with adjustable glass transition temperatures between −6 °C and −42 °C and Young's moduli between 0.2 MPa and 2.8 MPa. Although the reaction sequence of esterification and epoxidation represents a promising and potentially more sustainable way to introduce epoxide groups to lignin, here the esterification procedure ($E_{complex}$: 0.57) cannot be considered sustainable due to the use of carboxylic acid chlorides that were synthesized from hazardous oxalyl chloride ($E_{complex}$: 7.13). The subsequent oxidation using overstoichiometric amounts of peracetic acid and hazardous dichloromethane as solvent ($E_{complex}$: 7.39, solvent contribution of 97%) can most likely be improved by catalytic epoxidation with hydrogen peroxide to reduce the amount of waste generated.[180,181]

Esterification of lignin with oleyl chloride was improved by the group of Renneckar *et al.,* who developed an acyl chloride free procedure for the esterification of hydroxyethylated lignin with propionic acid (C_3), valeric acid (C_5), octanoic acid

(C_8), and oleic acid (C_{18}, **Scheme 2.2.8**).[182] Initial studies with propionic acid at 120 °C showed a high esterification selectivity toward aliphatic alcohol groups of unmodified lignin, while aromatic alcohol groups remained unmodified.

Scheme 2.2.8 – Hydroxyethylation of organosolv lignin and subsequent esterification with oleic acid; readapted from ref. [182].[93]

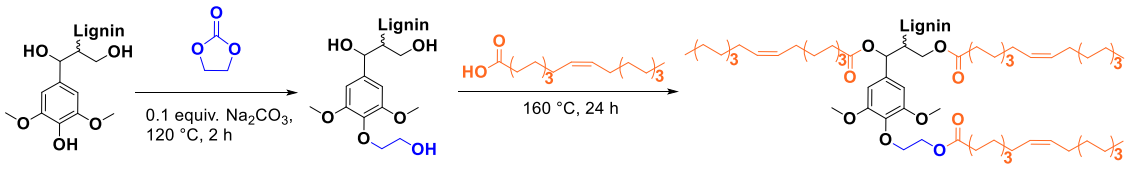

Hence, Renneckar *et al*. implemented a hydroxyethylation step with ethylene carbonate prior to esterification to transform present aromatic alcohol groups into hydroxyethyl ethers ($E_{complex}$: 2.19). By this procedure, a more uniform chemical functionality was achieved, as the resulting lignin sample contained 91% aliphatic alcohol groups instead of initially present 33% aliphatic alcohol groups. In this procedure, ethylene carbonate serves as hydroxyethylation substitute for ethylene oxide, a highly volatile and dangerous compound.[183,184] Hydroxyethylated lignin was then esterified at 160 °C with oleic acid as solvent and reagent to achieve a degree of substitution of 77% ($E_{complex}$: 2.15, $E_{sequence}$: 5.80). The more sustainably esterified lignin could potentially be epoxidized to synthesize an epoxidized lignin sample, but this was not reported.

A different approach by Vásquez-Garay *et al*. describes the synthesis of glycidylated lignin without the use of epichlorohydrin (**Scheme 2.2.9**).[185] After introduction of allyl ether groups to the lignin scaffold, epoxidation was achieved chemo-enzymatically with immobilized candida antarctica lipase B as catalyst. The Lipase generates percaprylic acid from caprylic acid and hydrogen peroxide *in situ*, which in turn epoxidizes allyl groups connected to lignin. The catalytic system achieved conversions of up to 90% for organosolv lignin (E_{simple}: 1.45). However, due to high dilution in toluene and overstoichiometric amounts of caprylic acid and hydrogen peroxide, this specific procedure cannot be

considered sustainable, showing an $E_{complex}$ of 51.5, with solvent contribution of 97%. Moreover, the applied allylation procedure uses highly toxic allyl bromide and is therefore not a suitable alternative for epichlorohydrin using procedures ($E_{complex}$: 31.4).[186] Combination of a more sustainable procedure for the addition of allyl ether groups to lignin with a subsequent epoxidation represents a promising path to synthesize lignin epoxides that are conventionally produced from epichlorohydrin.

Scheme 2.2.9 - Chemoenzymatic epoxidation of allylated lignin with hydrogen peroxide as oxidant; readapted from ref. [185].[93]

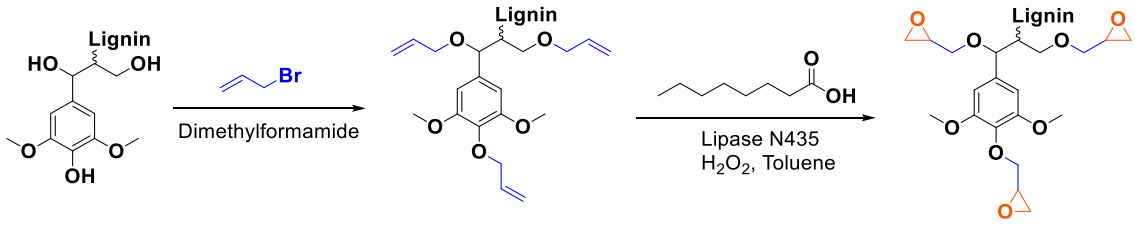

In summary, literature about sustainable epoxidation procedures of lignin is scarce, since most epoxy resin research focuses on the properties of the resulting material instead of the sustainable production of its epoxy component. However, a combination of several literature reports can lead to the development of more sustainable reaction sequences for the synthesis of lignin epoxides. Furthermore, it is of utmost importance to substitute conventional fossil based and toxic chemicals such as bisphenol A and epichlorohydrin by renewable and more benign chemicals.

2.2.1.4.3 Carboxylic acid functionalized lignin

Lignin molecules bearing multiple carboxylic acid functionalities are used as hardeners for epoxy resins and for the synthesis of cross-linked polyesters. The number of distinct procedures to synthesize lignin carboxylic acids remains low as most modifications are performed with cyclic anhydrides. Hirose *et al.* were the first to introduce the use of succinic anhydride (SAn) to synthesize lignin-based ester-carboxylic acid derivatives (**Scheme 2.2.10**).[187–189] In their first report, Hirose *et al*. reacted alcoholysis lignin (AL) with ethylene glycol (EG) and succinic anhydride to synthesize a mixture of polycarboxylic acid derivatives (so-called alcoholysis lignin ethylene glycol polyacid, ALEGPA).[187] A second polyacid containing only ethylene glycol and succinic anhydride (EGPA) was synthesized and the two polyacids were mixed in different weight ratios (from 0% ALEGPA to 100%). Epoxy resins were then synthesized by curing of the carboxylic acid mixtures with ethylene glycol diglycidyl ether (EGDGE, **Scheme 2.2.10**). The glass transition temperature (T_g) of the materials increased from −20 °C to −10 °C with an increasing content of lignin and therefore with an increasing cross-linking density. In another report, the group of Hirose mixed ALEGPA with either succinic acid (C_4), adipic acid (C_6), or sebacic acid (C_{10}) in different weight ratios and then cured the mixtures with EGDGE to synthesize epoxy resins (**Scheme 2.2.10**).[188] T_g decreased with increasing chain length of the used dicarboxylic acid (DCA), since the distance between network points increased. By variation of the lignin content and dicarboxylic acid component, the T_g of the epoxy resins was adjustable in a range from −40 °C to −10 °C.[188] Furthermore, Hirose *et al.* showed that ethylene glycol can be substituted by glycerol in the polyacid mixture to further increase the cross-linking density and expand the T_g range to +10 °C.[189] However, due to the high dilution of lignin in all epoxy resins (below 9 wt%, see **Appendix paragraph 7.4**), the majority of the respective resins consists of long and flexible aliphatic ester chains, which mainly impact the properties of the materials (*e.g.*, T_g below room temperature for all resins).[187–189]

Scheme 2.2.10 - Synthesis of polycarboxylic acid mixtures from lignin, ethylene glycol, and succinic anhydride and subsequent epoxy resin synthesis; readapted from ref. [187–189].[93]
Note: Functionalization of ArOH is not depicted, as other reports observed low conversions.[190,191]

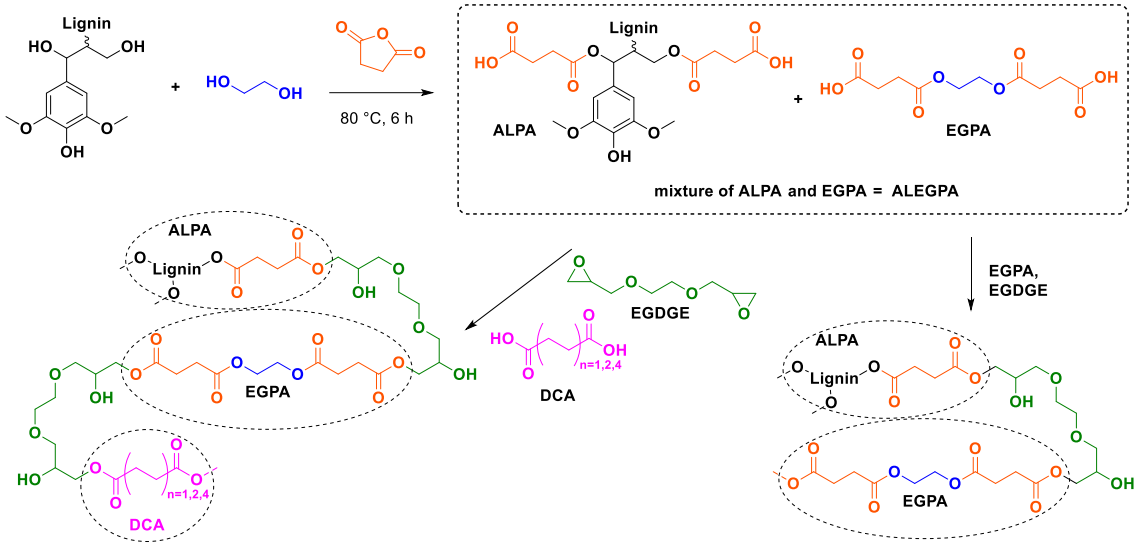

Griffini *et al.* used succinic anhydride for the synthesis of lignin-based carboxylic acids as well.[191] Kraft lignin was functionalized in tetrahydrofuran with varying equivalents of succinic anhydride to find a maximum ratio of SAn/lignin that ensured a full conversion without unreacted anhydride being left in the product. A high selectivity for the esterification reaction of aliphatic alcohol groups was observed *via* ^{31}P NMR spectroscopy, while aromatic alcohols remained almost unfunctionalized. Hence, it was possible to incorporate a maximum of 20 wt% of succinic anhydride (0.35 equiv.) into the SAn/lignin adduct.[191] The synthesized adduct was then dissolved in an organic solvent and applied onto surfaces as coating. After evaporation of solvent, the samples were thermally treated at 200 °C to allow self-esterification reactions between residual aromatic alcohol groups and carboxylic acid moieties. The high lignin derived polyester coating exhibited good solvent resistance, a T_g of 138 °C, and was applicable as adhesive on wood and glass surfaces.[191] Another example for the use of succinylated lignin is as co-hardener for bisphenol A-based epoxy resins. Incorporation of up to 10 wt% lignin had a reinforcing effect on the epoxy resins.[192,193] Other cyclic anhydrides, like maleic anhydride,[190,194,195] Aradur 917,[196] and methylhexahydrophthalic anhydride[197] were used as well for the synthesis of carboxylic acid functionalized lignins.

Considering the amount of waste produced, cyclic anhydrides are sustainable functionalization agents, since no byproducts are formed during the addition reaction itself. The only waste formed during modification originates from solvents, catalysts, or excess anhydride (E-factors were not calculated due to missing information in reported procedures). Maleic and succinic anhydride are industrially produced from fossil resources by catalytic oxidation of benzene or *n*-butane.[198,199] However, both anhydrides are potentially biobased as they can be produced from succinic acid, which in turn can be obtained by fermentation of sugars.[200,201] The synthesis of lignin polycarboxylic acids from cyclic anhydrides therefore represents a promising field for the production of renewable polymers. In light of these considerations, cyclic anhydrides, namely itaconic and succinic anhydrides, are reported in **Chapter 4.3** for lignin functionalization.

Luterbacher *et al*. attached carboxylic acid moieties to lignin through aldehyde-assisted fractionation (AAF) with glyoxylic acid (**Scheme 2.2.11**).[124] Addition of glyoxylic acid functionalized lignin (GA-lignin) to an emulsion of mineral oil and water significantly prolonged the stability of the emulsion from 7 days to 180 days without any visible phase separation and therefore allowed its use in cosmetic applications such as creams and lotions.[124] In another study, GA-lignin was used for the synthesis of epoxy resins that contained up to 70 wt% of lignin, by curing with polyethylene glycol diglycidyl ether (PEGDGE, **Scheme 2.2.11**).[202] All epoxy films possessed excellent UV barrier properties while maintaining good visible light transparency and are therefore promising materials for food packaging applications.[202] The reported procedures for AAF with glyoxylic acid and epoxy resin synthesis are considered unsafe due to the use of possibly carcinogenic 1,4-dioxane as solvent.[147] In other procedures, more sustainable 2-methyltetrahydrofuran was used as solvent for AAF with isobutyraldehyde and propionaldehyde.[123,203,204] Glyoxylic acid can potentially be produced through electrochemical conversion of carbon dioxide to further improve the sustainability of this functionalization.[205,206] In general, AAF is a versatile method that extracts

lignin from wood in a single step with an aldehyde of choice to introduce new functional groups.[203,207]

Scheme 2.2.11 – Aldehyde-assisted fractionation of lignin with glyoxylic acid and subsequent epoxy resin synthesis; readapted from ref. [124,202].[93]

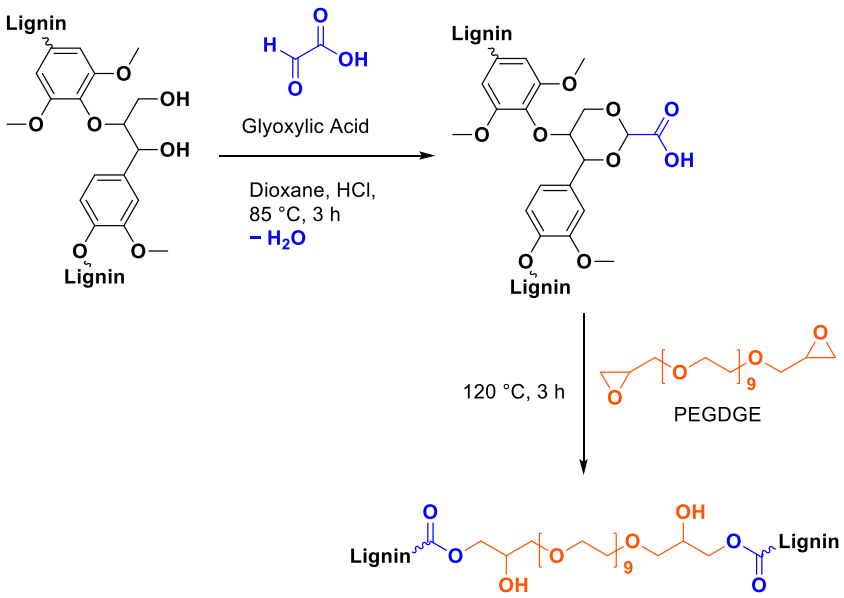

2.2.1.4.4 Ester group functionalized lignin

Lignin esters exhibit more flexibility and a reduced T_g in contrast to pristine lignin, rendering them suitable for thermoplastic applications on their own or in blends.[208,209] Esterification of lignin is easily achieved by reaction with highly reactive electrophiles, such as anhydrides or acyl chlorides, resulting in a complete functionalization of all alcohol groups, but also waste associated with byproducts, the use of bases, and the necessary synthesis of the mentioned electrophiles (**Scheme 2.2.12**). Koivu *et al*. reacted softwood kraft lignin with acetyl (C_2), octanoyl (C_8), lauroyl (C_{12}), or palmitoyl (C_{16}) chloride to prepare lignin esters of different aliphatic chain lengths ($E_{complex}$: 6.65−8.07, **Table 7.5.1**).[210] The initial T_g of lignin of 145 °C decreased for all esters with an increasing degree of substitution to a minimum of 45 °C for the fully functionalized C_{16} ester. Moreover, a remarkable decrease of T_g was observed for lignin functionalized with longer chain esters (T_g = 121 °C for C_2 and 50 °C for C_8, both with DS = 100%). Finally, Koivu *et al*. used the C_{16} ester sample to manufacture a polyethylene blend *via* melt extrusion.[210] The group of Dubois used biobased 10-undecenoyl chloride (C_{11})[211] and oleoyl chloride (C_{18}) for the esterification of soda lignin ($E_{complex}$: 0.10).[212] UV-blocking films were manufactured by compression molding of biodegradable poly(butylene adipate-*co*-terephthalate) (PBAT) blended with the synthesized lignin esters. Incorporation of 10 wt% of lignin ester into the PBAT matrix resulted in excellent UV protection in the irradiation range from 280 nm to 400 nm without negative effects on material properties.[212] Another commonly used functionalization agent for esterification are linear anhydrides (cyclic anhydrides have been discussed previously, see **paragraph 2.2.1.4.3**). In 2005, Thielemans and Wool synthesized various lignin esters from anhydrides to investigate their solubility depending on the chain length in nonpolar solvents such as styrene.[194] Lignin esterification was performed solventless in acetic anhydride (C_2), propionic anhydride (C_3), butyric anhydride (C_4) and methacrylic anhydride with 1-methylimidazole as catalyst to achieve full functionalization for all modifications (**Scheme 2.2.12**,

$E_{complex}$: 2.05). Lignin butyrate and butyrate/methacrylate were found to be soluble in styrene and can therefore potentially be incorporated into unsaturated polyester composites.[194,213] Luo *et al*. used crotonic anhydride to add polymerizable double bonds to lignin for thermosetting applications ($E_{complex}$: 1.75).[214] To investigate whether the introduced crotonyl groups improve the radical polymerization, lignin crotonate and lignin butyrate (as reference sample without double bonds) were cured at 175 °C. Thermally initiated cross-linking was observable through increased viscosity and T_g of lignin crotonate after heating. In contrast, lignin butyrate ($E_{complex}$: 1.59) showed no difference in properties after curing.[214] Esterification procedures using acyl chlorides and acid anhydrides achieve full functionalization for almost every procedure and exhibit good E-factors with solventless conditions ($E_{complex}$: 1.59−8.07, **Table 7.5.1**).[212,214,215] However, additional waste will be generated if acyl chlorides are used, since the byproduct hydrogen chloride requires neutralization with stoichiometric amounts of bases. Moreover, the discussed procedures using anhydrides are hazardous due to the use of toxic 1-methylimidazole as catalyst.[216,217]

Scheme 2.2.12 - Esterification of lignin with acyl chlorides (**left**) and anhydrides (**right**); readapted from ref. [194,210,212,214].[93]

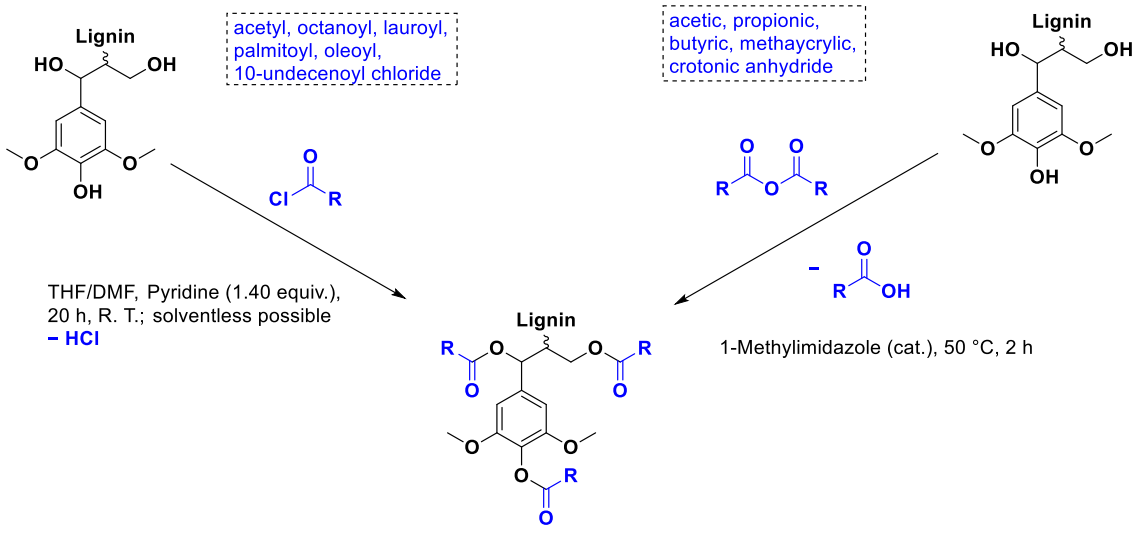

To allow comparison with other esterification procedures, acyl chloride and anhydride containing procedures must be considered as sequences starting from

the corresponding carboxylic acids. Chlorination of carboxylic acids is usually achieved by reaction with hazardous oxalyl chloride, which itself is produced from ethylene carbonate and toxic chlorine ($E_{complex}$: 2.01−7.13).[179,212,218,219] Acetic anhydride is industrially produced from acetic acid by thermal dehydration into ketene at 700 °C and subsequent reaction of ketene with acetic acid (ketene process).[220] Propionic anhydride is similarly produced from propionic acid.[221] higher homologues of acid anhydrides are prepared from the corresponding carboxylic acid by reaction with its acyl chloride derivative or more sustainably by reaction with its mixed anhydride of acetic acid.[220,222] The use of anhydrides is therefore preferred over acyl chlorides, since no toxic substances are needed for their production. However, it should be noted that only procedures for up to C_6 anhydrides are reported for lignin esterification.[223] Considering the amount of waste generated during esterification, the use of carboxylic acids as functionalization agent is theoretically more sustainable than with acyl chlorides or anhydrides, since the condensation byproduct water (18.0 g mol^{-1}) has a lower molecular weight than the respective condensation byproducts hydrogen chloride (36.5 g mol^{-1}) and carboxylic acids (acetic: 60.1 g mol^{-1}, propionic: 74.1 g mol^{-1}). Esterification of lignin with pure carboxylic acids is however scarcely found in literature and usually results in low degrees of substitution. As already mentioned in the epoxide section (**2.2.1.4.2**), Renneckar *et al*. esterified kraft lignin with propionic acid at 120 °C and removed the byproduct water by evaporation thus shifting the equilibrium toward the product side ($E_{complex}$: 9.93, **Scheme 2.2.13a**).[224] A degree of substitution higher than 80% was observed for aliphatic alcohol groups, proving that esterification with carboxylic acids as reagent is a viable method for lignin functionalization. However, aromatic alcohol groups stayed almost unfunctionalized with this method, as expected, resulting in a low overall degree of substitution. Renneckar *et al*. therefore implemented a hydroxyethylation step prior to esterification to convert aromatic alcohol groups through selective functionalization (**Scheme 2.2.13b**).[224]

Scheme 2.2.13 – Esterification of lignin with carboxylic acids; readapted from ref. [224,225].[93]

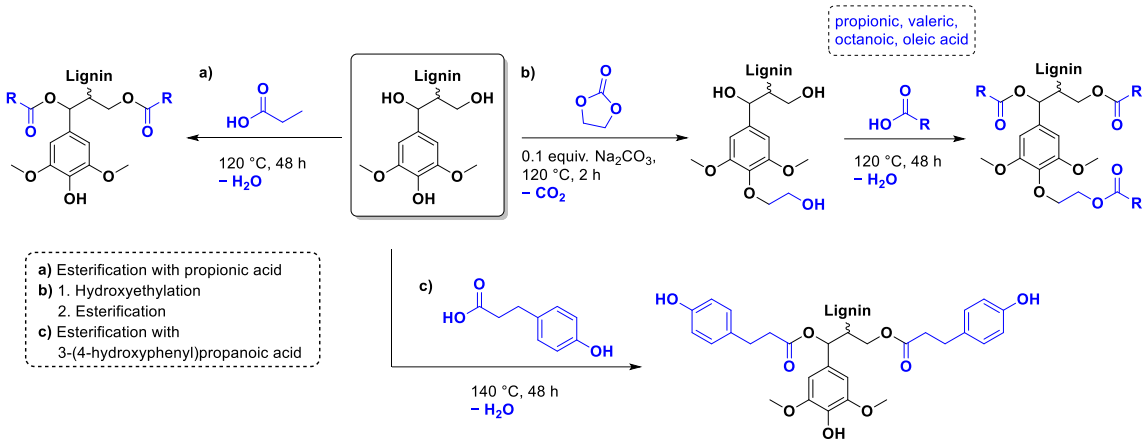

Optimized reaction conditions used ethylene carbonate as reagent and solvent and efficiently converted 90% of aromatic alcohol groups into hydroxyethyl ethers ($E_{complex}$: 2.19).[182] hydroxyethylated lignin had an increased thermal stability and a lower T_g than unmodified lignin. Finally, hydroxyethylated lignin was functionalized with propionic acid (C_3), valeric acid (C_5), octanoic acid (C_8), or oleic acid (C_{18}) to achieve degrees of substitution of 87%, 79%, 81%, and 77%, respectively.[182] Recycling of excess carboxylic acids used as solvent for the reaction was possible by distillation to further reduce the amount of waste generated ($E_{complex}$: 0.99−2.15).[182] Moreover, for the esterification procedure with propionic acid, a one-pot procedure was developed that allows precipitation of different molecular weight fractions with low dispersities and high degrees of esterification (DS ≥ 85%).[226] Intriguingly, Verge *et al*. utilized the reduced reactivity of phenols toward esterification and reacted soda lignin with 3-(4-hydroxyphenyl)propanoic acid ($E_{complex}$: 1.19, **Scheme 2.2.13c**).[225] Reaction conditions similar to the esterification procedure by Renneckar *et al*. were applied to prevent esterification of aromatic alcohols.[182,224] After reaction at 140 °C, a large decrease of aliphatic alcohol groups and a simultaneous increase in *p*-hydroxyphenyl alcohols was observed *via* ^{31}P NMR spectroscopy, while the number of substituted phenols (e.g., syringyl) did not change. Aliphatic alcohols were thus efficiently transformed into esters with hydroxyphenyl moieties to establish a more uniform functionality of aromatic alcohols, while carboxylic acids

stayed unfunctionalized.[225] Furthermore, this procedure resembles a benign and more sustainable alternative to phenolation pretreatment, which is often applied prior to amination reactions (see above), which uses toxic phenol to add more aromatic alcohol groups to lignin.[227] Esterification of aliphatic alcohol groups of lignin with pure carboxylic acids is efficient and can be conducted in solvent- and catalyst-free systems. The presented procedures exhibit low E-factors ($E_{complex}$: 1.19−2.15) and use more benign chemicals than procedures involving acyl chlorides and anhydrides.

2.2.1.4.5 Multiple bond functionalized lignin

The insertion of multiple bonds onto lignin (i.e., double or triple bonds) unlocks various possibilities for the use of lignin as macromonomer (**Table 7.6.1**). In 2017,[228] the functionalization of hydroxyl groups of lignin *via* typical Steglich esterification conditions, namely DCC mediated esterification with 4-pentenoic acid in the presence of 4-(dimethylamino)pyridine (DMAP), in dimethylformamide (DMF) as solvent was reported. The thus obtained double bond containing lignin was subsequently reacted with polyethyleneglycol (PEG)-thiol (and other thiols) to produce poly(lignin-co-PEG). It was unfortunately not possible to calculate any E-factor for this procedure, due to a lack of necessary data. However, major concerns are related to some compounds used for the functionalization, *i.e.*, DCC and DMAP are classified as toxic substances[178,229] and DMF is also considered a harmful substance.[230] Insertion of triple bonds to lignin is also reported in the literature, mostly for subsequent azide-alkyne click reaction purposes. For instance, lignin-alkyne synthesis is reported *via* esterification with 5-hexynoic acid (in the presence of pivalic anhydride and DMAP in THF)[231] or *via* functionalization with propargyl bromide.[232] Both procedure involve toxic chemicals[229,233–235] and an imperative shift toward more environmentally benign and sustainable methodologies is necessary.

A recent protocol, published in 2023 by Renneckar *et al.*,[236] provides a simple esterification protocol to introduce vinyl esters onto lignin. Advantages of the procedure are its solventless and catalyst-free conditions. However, despite these favorable features, the protocol consists of a two-step modification, first hydroxyethylation with ethylene carbonate, followed by esterification with acrylic acid (**Scheme 2.2.14**). Multi-step procedures should be avoided, as already mentioned previously concerning phenolation pretreatment. Moreover, acrylic acid raises concerns due to its toxicity.[237] The authors report a degree of substitution (DS) of 40.7% of the aliphatic hydroxyl groups using optimized conditions for the esterification. The calculated E_{simple} for this procedure are 4.80 and 3.07 for the first and second step, respectively, leading to a $E_{sequence}$ of 7.76 for the two-step procedure.

Scheme 2.2.14 - Introduction of vinyl moieties to lignin via esterification with acrylic acid; readapted from ref. [236].[93]

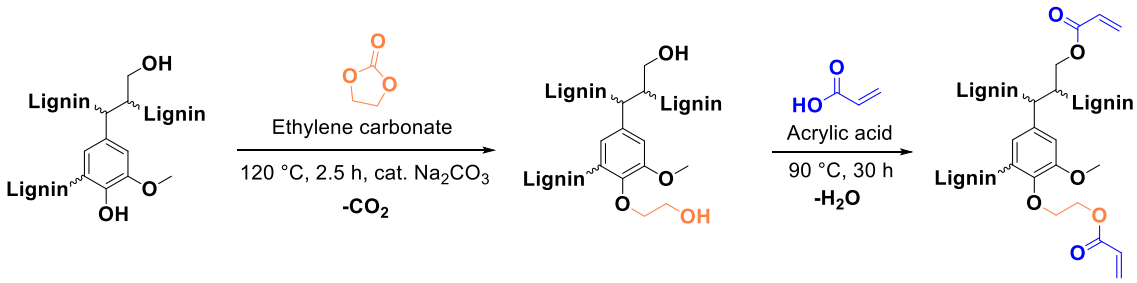

A selective allylation of the phenolic hydroxyl groups of lignin is reported by C. Gioia and M. Lawoko *et al.*[238] by reacting them with allyl chloride. This procedure, despite being useful for tailor-made functionalization of lignin, involves the use of toxic allyl chloride,[239] therefore better alternatives should be employed when selectivity is not necessary. Alternatively, and far less toxic, allyl methyl carbonate was successfully applied for the selective allylation of organosolv lignin in a water/ethyl acetate mixture.[240] The procedure relies on a palladium nanoparticle catalyzed Tsuji-Trost allylation, very high turnover numbers of up to 500.000 were reported for model compounds. Generally, organic carbonates are a class of compounds that has received increased interest in recent years, especially in the field of lignin modification. They are widely recognized as greener reagents and benign alternatives to common organic solvents and/or reagents.[241] For instance, in 2015, methylation of softwood kraft lignin was achieved *via* reaction with dimethyl carbonate (DMC),[242] a greener alternative to toxic and carcinogenic methylating agents commonly used, such as dimethylsulfate,[243,244] methyl iodide,[245] or trimethyl phosphate.[246] In this context, introduction of double bonds onto lignin can be achieved both *via* utilization of non-cyclic and cyclic organic carbonates. The work of Meier and Over[247] reports a solvent-free allylation procedure of organosolv lignin *via* functionalization with diallyl carbonate (DAC) in the presence of tetrabutyl ammonium bromide (TBAB) as phase transfer catalyst (**Scheme 2.2.15**). With optimized conditions (120 °C, 5 h, 1 equiv. TBAB, 10 eq. DAC) 100% and 79% conversion of aromatic and aliphatic hydroxyl groups was achieved, respectively. The authors also report

recycling attempts for TBAB and DAC, resulting in 97% recovery of TBAB and 59-62% recovery of DAC, *via* extraction and distillation, respectively. The lowest calculated E_{simple} for this procedure is 5.42, considering the recovery of DAC, and 9.43 in the case of recovery of TBAB. These relatively high E-factors are ascribed to the high equivalents of DAC used (10, with respect to the total of OH groups). However, Meier *et al.*, reported that the equivalents of DAC could be decreased to 3, obtaining similar conversions. Indeed, this was further demonstrated by the same group in a subsequent work[248] and later by Johansson *et al*.[249] In both cases, 3 equiv. of DAC (with respect to the total of OH groups) were employed to functionalize lignin, and in both procedures TBAB was recycled, with 92% and 88±3% recovery, respectively (E_{simple}: 1.87 and 2.09, respectively, considering recovery of TBAB). This further demonstrates the intrinsic sustainability of this procedure. Moreover, DAC can be synthesized from sustainable DMC in the presence of allyl alcohol.[250,251] However, allyl alcohol still presents difficulties correlated to its toxicity[252] and production methods,[253] even if recent progress has been made to produce it more sustainably *via* deoxydehydration of glycerol.[254,255]

Scheme 2.2.15 - General reaction scheme of the allylation of lignin using diallyl carbonate; readapted from ref. [247].[93]

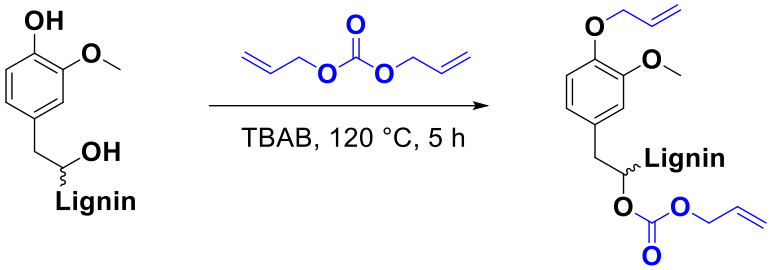

Functionalization of lignin using cyclic carbonates is also widely reported, leading to insertion of different functional groups, depending on the cyclic carbonate used.[224,256–259] Concerning the introduction of double bonds, an interesting procedure is reported by Avérous *et al.*, where lignin is functionalized with different organic cyclic carbonates, in particular with vinyl ethylene carbonate (VEC).[257] VEC is used both as solvent and reagent, in excess (10 equiv. with respect to the reactive groups), in the presence of potassium carbonate (K_2CO_3)

in catalytic amounts (0.1 equiv. with respect to the reactive groups). Despite the toxicity of VEC,[260] which needs to be taken into consideration, advantages of this procedure are the use of the economic and benign K_2CO_3 catalyst, as well as its solvent-free character. Full conversion of phenolic hydroxyl groups was reached in 1 hour at 150 °C (E_{simple}: 6.01). Further investigation should be considered in order to assess if VEC equivalents can be reduced, maintaining the same conversions. A scheme of the reaction between a general cyclic carbonate and different hydroxyl groups of lignin can be found in **Scheme 2.2.16**, and a more detailed discussion on this topic will be provided in a later section.

2.2.1.4.6 Hydroxyl group functionalized lignin

Lignin-based polyols (LBPs) have attracted growing interest in the field of polymeric materials, due to the introduction of lignin as a renewable feedstock for the production of biobased polyols. Lignin itself presents a variety of hydroxyl groups in its structure, as already described previously. However, due to the different nature of lignin's hydroxyl groups and its intrinsic heterogeneity, it is difficult to achieve homogeneous reactivities, and often this is a drawback in order to obtain reproducible results. This problem can be addressed by rendering the chemical structure of lignin more homogeneous, i.e., converting phenolic hydroxyl groups into less sterically-hindered and predominantly aliphatic ones. LBPs have seen extensive research as substitutes for conventional polyols in polyurethane (PU) synthesis, which are commonly synthesized from diisocyanates and polyols. Generally, the traditional way to produce LBPs, first introduced in the 1980s by Glasser *et al*.,[261] is oxyalkylation in the presence of alkylene oxides. Several works explored lignin oxypropylation with propylene oxide (PO),[262–264] as well as other alkylene oxides,[265] and the behavior of the obtained LBPs was investigated for PU rigid foam application. In the work of Ragauskas and Li,[262] for instance, a lignin polyol was obtained from oxypropylation with PO, and mixed in different percentages with two other polyols and reacted with polymeric methylene diphenyl diisocyanate (MDI). The percentage of lignin polyols in the mixture ranged from 0% to 100%. Interestingly, as the weight percentage of lignin polyols increased, a corresponding improvement in compressive strength and modulus of the PUs was observed. Specifically, when using 100 wt% of lignin polyols, the foam exhibited a 44% increase in compressive strength and a 135% increase in modulus compared to the control foam, which contained 0 wt% lignin polyols. Usually, oxypropylations with PO are conducted in the presence of a base *via* anionic ring-opening polymerization (AROP),[264] leading to grafting of oligomeric chains of polypropylene glycol onto lignin, and generating the correspondent homopolymer,[266] that can either be removed *via* solvent extraction[257,262] or can be left in the reaction mixture as bifunctional co-polyol.[262]

Moreover, oxypropylation reactions are typically conducted at high temperatures (around 150 °C), far above the boiling point of PO (34 °C). Therefore, high pressure is required, raising the overall energy consumption and necessitating specialized equipment, such as pressure reactors.[264] Another work[265] partially circumvented some issues by synthesizing a family of LBPs *via* cationic ring-opening polymerization (CROP) with different oxiranes in the presence of boron trifluoride (BF_3) as Lewis acid catalyst and THF as solvent and co-monomer. The reaction conditions were mild (room temperature and atmospheric pressure), decreasing the energy consumption compared to the AROP method. Notably, the formation of the homopolymer side product was minimized to 5 wt%, a significant reduction compared to maximum values up to 70 wt% reported for the AROP method.[264] Oxyalkylation is a useful tool that permits the synthesis of LBPs in a straightforward manner, however, it suffers from numerous drawbacks, and more sustainable ways to produce LBPs have been the subject of recent research advancements. PO, as well as other alkylene oxides, is a highly toxic and harmful substance with several concerns correlated also to its difficult handling, flammability, and explosivity.[267,268] An alternative method was investigated by Avérous *et al.* in 2016,[269] performing oxypropylation on condensed tannins, the second most abundant source of renewable aromatic structures, with propylene carbonate (PC). In particular, PC was utilized as a replacement for PO in tannin functionalization and optimization of the reaction conditions was carried out. Cyclic carbonates (such as propylene carbonate and ethylene carbonate) are a well-known class of organic reagents and solvents of high boiling point, and in most cases represent a sustainable alternative to traditional toxic reactants.[270] The different reactivity of lignin moieties with a general cyclic carbonate is depicted in **Scheme 2.2.16**.

Scheme 2.2.16 – Reactions of a general cyclic carbonate with different functional groups of lignin.[93]

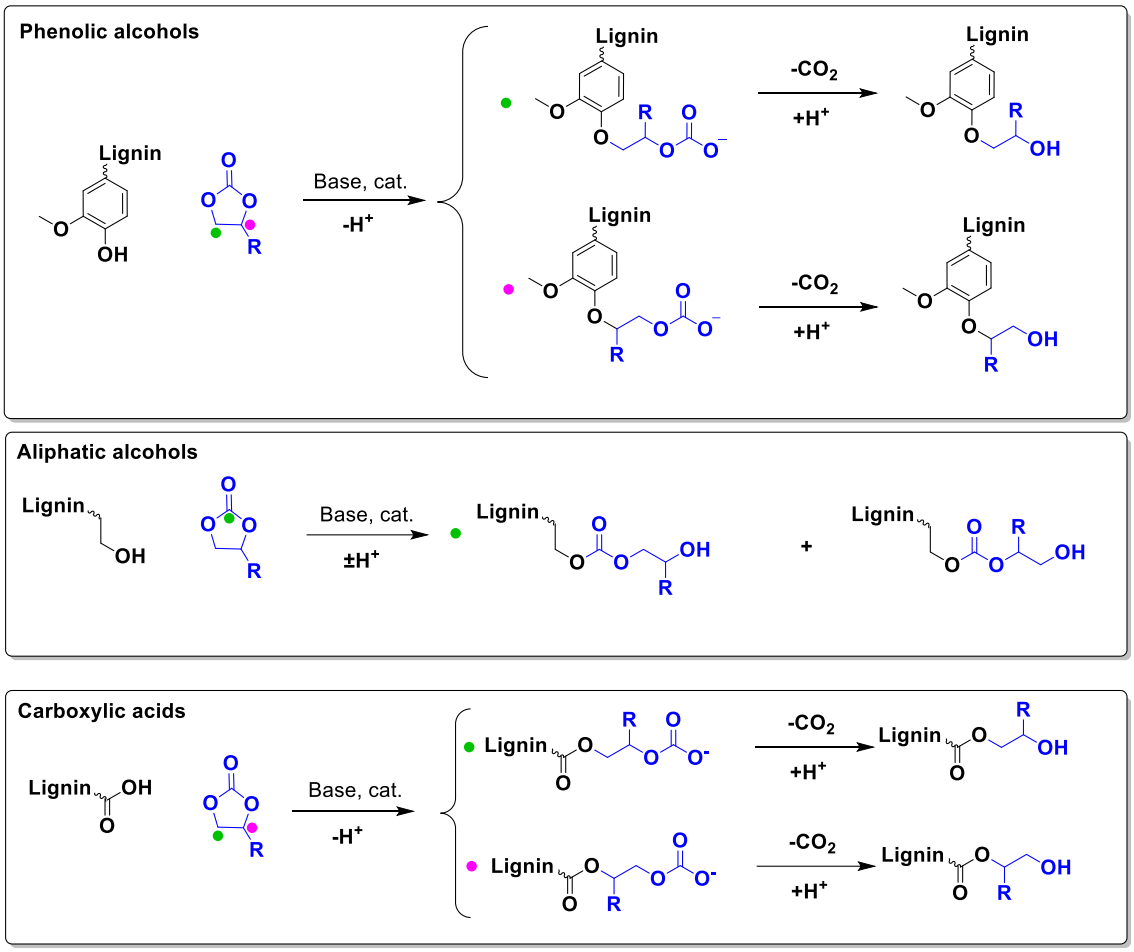

Usually harder nucleophiles, such as aliphatic alcohols, tend to react preferably at the carbonyl of the cyclic carbonate, leading to carbonate linkages. Phenolic alcohols and carboxylic acids, i.e. softer nucleophiles, preferably attack one of the two alkylene carbons with concomitant release of CO_2, generating ether linkages. This difference in reactivity can further be tuned by varying the reaction conditions. For instance, it was observed that for high reaction temperatures (>170 °C), basic catalysts, and lower reaction times, etherification is favored over carbonate linkages.[256,258] Oxyalkylation of organosolv lignin with PC was studied and optimized by the work of Lehnen *et al.* in 2017.[258] In this work, the influence of parameters such as reaction temperature, time, and equivalents of catalyst and PC was studied. The solvent-free procedure led to a maximum chain length of grafted propyl units of 4.6 utilizing the optimized conditions, in the presence of

catalytic amount of 1,8-diazabicyclo(5.4.0)undec-7-ene (DBU). A later publication of the same group[256] applied the optimized conditions for PC to other cyclic carbonates, namely ethylene carbonate (EC), propylene carbonate (PC), butylene carbonate (BC) and glycerol carbonate (GC), generating a family of LBPs (**Scheme 2.2.17**). Moreover, the influence of pulping process and lignin source was examined, unveiling the higher reactivity for the two kraft lignins tested, due to their higher number of aromatic hydroxyl groups, compared to the other types of lignins investigated (organosolv and soda lignin), proving once again the importance of the isolation method on the chemical structure of lignin. Calculated E_{simple} for this procedure are in the range 3.59 – 4.19 (**Table 7.7.1**).

Another study from Avérous *et al.*[257] compared reactivities of four different cyclic carbonates, namely EC, PC, GC and vinyl ethylene carbonate (VEC). In this procedure, the toxic and expensive organobase DBU was substituted by the more benign and cheaper inorganic catalyst, potassium carbonate (E_{simple}: 4.94 - 6.02). The equivalents of the cyclic carbonate and catalyst remain the same for both procedures (10 and 0.1 equiv., respectively, relative to the sum of reactive sites of lignin). Consequently, the lower E-factors for the procedure of Lehnen *et al.* (E_{simple}: 3.59 – 4.19) are attributed to the fact that they were calculated based on theoretical yield, therefore they reflect the lowest possible values obtainable with this procedure (see **Appendix 7** for details).

Scheme 2.2.17 - Lignin hydroxyalkylation with different cyclic carbonates: butylene carbonate (red), ethylene carbonate (blue), propylene carbonate (green) and glycerol carbonate (orange), readapted from ref. [256].[93]

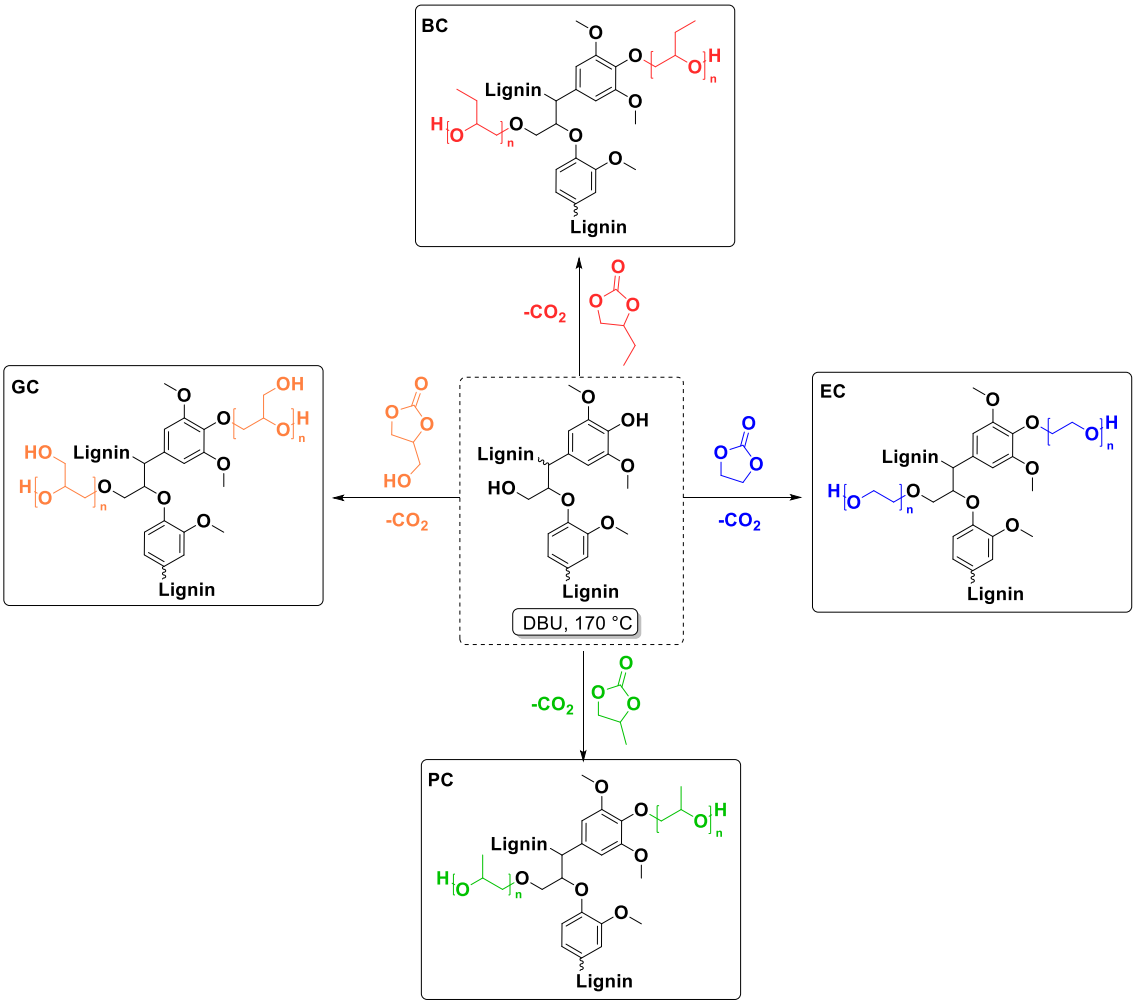

The same group later applied the concept of lignin functionalization with ethylene carbonate for PU foam production.[259] In particular, they developed a new method for lignin-based liquid polyol synthesis in PEG as solvent. The LBPs were prepared in a single-step and purification-free manner, mixing different ratios of lignin with PEGs of different chain lengths, and subsequently reacted with EC. The lignin content in the polyols was varied between 20 and 30 wt%. The process was scaled up to 200 g batches, obtaining four LBPs that were used in the preparation of rigid PU foams, varying the substitution of a standard polyether polyol with LBPs up to 100 wt%. Since the preparation of LBPs does not require, in this case, any work-up or purification procedure (they can be directly employed

for foams preparation) the E-factor for this procedure is equal to 0, because no waste is generated.

Turning to a different aspect, an interesting procedure was reported by the group of Lehnen *et al.*,[271] where lignin was first functionalized with glycerol carbonate (GC), following a previous procedure.[256] Afterwards, the newly inserted 1,2-diols were reacted with dimethyl carbonate (DMC) to produce cyclic carbonate functionalized lignin (**Scheme 2.2.18**, (271)). Cyclic carbonate moieties can be obtained *via* carbonation of epoxides with CO_2. However, for lignin, epoxide groups are typically introduced *via* epoxidation with toxic epichlorohydrin.[272–274] However, in this work, a more sustainable route was followed. Under optimized conditions, a lignin containing 1.54 mmol g^{-1} carbonate functionalities was obtained. Potassium carbonate was utilized as catalyst for the transesterification reaction (0.4 equiv.), together with 5 equiv. of DMC in DMSO as solvent. Furthermore, the catalyst K_2CO_3 could be quantitatively recovered (97-99%) and reused for subsequent syntheses with comparable results to commercial K_2CO_3, lowering the E_{simple} for the transesterification step from 5.04 to 4.78 due to this recycling.

Cyclic carbonate functionalized lignin can be used as a lignin-based prepolymer for non-isocyanate polyurethane (NIPU) applications. NIPUs have arisen as sustainable alternative to the use of toxic isocyanates (and their precursor, phosgene) for PUs synthesis. They are often synthesized from polyamines in the presence of (poly)cyclic carbonates. In this context, an interesting work from 2020[275] follows the path reported by Lehnen *et al.*[271] to produce cyclic-carbonate (CC) functionalized lignin, which was then used, together with Priamine™, a fatty - acid based diamine, to obtain NIPU foams from renewable resources (**Scheme 2.2.18**, (275)).

Scheme 2.2.18 - Lignin hydroxyalkylation with glycerol carbonate and subsequent transesterification with dimethyl carbonate, to produce cyclic carbonate functionalized lignin,[271] that is subsequently reacted with Priamine™ to yield lignin-based NIPU;[275] readapted from ref. [271,275].[93]

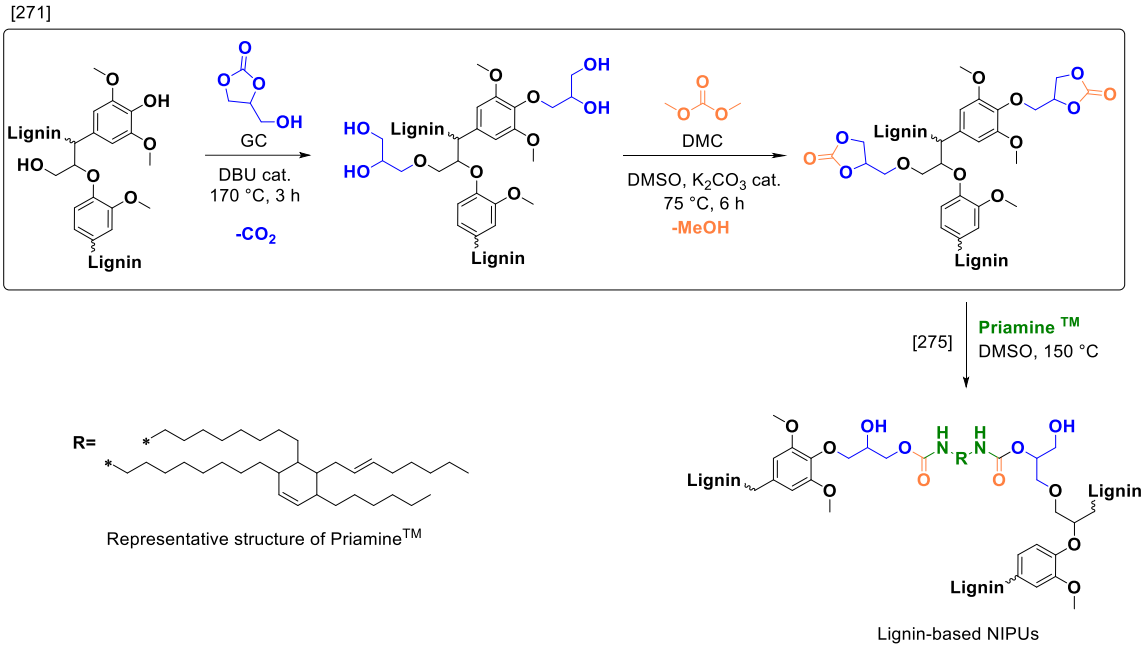

The cross-linked polymers were tested in dog-bone shaped samples for mechanical properties, showing a decrease in ultimate-tensile strength and modulus with decreasing ratio CC:NH_2 from 1:1 to 1:2, confirming that a lower cross-linking density contributes to more flexible materials. Interestingly, the samples also showed shape-memory capability, thanks to the simultaneous presence of both hard and soft segments. In addition, the authors produced lignin-based NIPU foams in the presence of the chemical blowing agent poly(methylhydrosiloxane) (PMHS). Foams were tested for their density, porosity and compressive strength at 10% strain, revealing once again that a higher crosslinking density leads to an increase in compressive strength. Moreover, SEM measurements showed that cell diameters doubled from ratio 1:1 compared to 1:2, revealing a more open structure with decreasing crosslinking density.

Recently, the same group demonstrated that lignin-based NIPU foams can be chemically recycled, with subsequent reutilization of lignin in a second generation of polymers.[276] Ethylene glycol (EG) assisted hydroglycolysis, i.e., alkaline hydrolysis aided by the addition of EG, showed 93% mass recovery of

the waste NIPU foams. Moreover, recycled NIPU foams were re-synthesized using 100% recovered lignin, showing very similar properties to virgin foams. LCA analysis of the process was also reported, leading to a GWP value for the first generation of foams of 1.89 kgCO_2eq.

Finally, more sustainable ways have been developed for the synthesis of LBPs, involving the utilization of organic cyclic carbonates. The corresponding polyols have been tested for PU rigid foam application, and more recently, for NIPU synthesis. Moreover, hydroxyethylation of lignin with ethylene carbonate is widely reported as a pretreatment in order to achieve homogeneous reactivity of the lignin macromonomer structure.

3 Aim

In light of the considerations discussed in the previous chapters, a transition toward renewable and more sustainable materials is essential. Lignin represents a promising renewable feedstock due to its abundance, biodegradability, and intrinsic functional properties such as UV absorption and antimicrobial activity. However, its application in polymer chemistry remains limited by structural heterogeneity, variability arising from different sources and isolation methods, and by the frequent use of toxic reagents or precursors reported in lignin modification protocols.

The overall aim of this doctoral work is to design and synthesize novel lignin-based polymeric materials, with particular focus on thermosets, and to systematically characterize their chemical and physical properties.

In accordance with the principles of green chemistry, this work seeks to employ more sustainable synthetic strategies, including the use of multicomponent reactions, the reduction or elimination of solvents, and the avoidance of toxic chemicals and precursors. Within this framework, lignin is utilized as a macromonomer and its structure is modified through the introduction of different crosslinkers and functionalizing agents. These modifications enable the tuning of material properties, as detailed and discussed in the following chapters.

4 Results and Discussion

This section discusses the modification of lignin for its use as a macromonomer in polymer materials, following three complementary strategies.

In the first part, **Chapter 4.1**, lignin is employed as a macromonomer for the synthesis of lignin-derived polycarbonates using dimethyl carbonate as reagent. Different synthetic approaches are explored and critically discussed in relation to their efficiency and the resulting material structures.

The second part, **Chapter 4.2**, focuses on a two-step lignin modification aimed at introducing cyclic carbonate functionalities, enabling its subsequent use as a macromonomer in fully bio-based non-isocyanate polyurethanes (NIPUs). These materials are synthesized in combination with other renewable monomers, and their properties are thoroughly characterized. In addition, the synthesis of a renewable polyamine used in this system is described.

In the third part, **Chapter 4.3**, lignin is functionalized using renewable itaconic anhydride, providing a novel lignin derivative that is comprehensively characterized. This macromonomer is investigated in several thermoset applications, including Passerini-based thermosets, epoxy resins, and thia-Michael networks. Among these systems, epoxy resins are discussed in greater detail. Finally, an analogous macromonomer obtained through modification with saturated succinic anhydride is synthesized using a similar approach and employed for a comparative evaluation of the resulting material properties.

4.1 Lignin Carbonates

The work presented in this chapter has not been previously published. All experiments, optimization studies, data analyses, and interpretation of the results were carried out independently by the author of this thesis.

4.1.1 Abstract

This chapter investigates the use of dimethyl carbonate (DMC) as a benign reagent for the preparation of lignin-based polycarbonates with potential chemical recyclability. DMC enables the formation of carbonate linkages between lignin macromonomers, while simultaneously inducing methylation of phenolic hydroxyl groups under suitable conditions. The resulting carbonate bonds can undergo methanolysis, allowing depolymerization and recovery of a lignin-derived structure, albeit with partial chemical modification. Nevertheless, aliphatic hydroxyl groups remain available for re-crosslinking in this strategy, supporting the concept of a reversible lignin modification cycle. This work explores the potential of carbonate-linked lignin systems as a step toward circular lignin-based polymer materials.

4.1.2 Introduction

Recent advances in lignin chemistry have demonstrated that tailored functionalization can enhance its reactivity,[93] compatibility,[277,278] and processability,[279] enabling access to a wide range of polymeric materials. However, many lignin-derived polymers reported to date are based on reactions that often lead to thermally and chemically stable networks.[174,280,281] While such systems often show excellent mechanical performance,[282,283] their lack of recyclability limits their contribution to a circular materials economy. In this context, organic carbonates provide a promising route for chemical recyclability. Dimethyl carbonate (DMC), for instance, is a benign, non-toxic reagent capable of reacting with lignin hydroxyl groups to install carbonate functionalities. When used in high excess, DMC functionalizes the lignin structure, yielding carbonated moieties for aliphatic hydroxyl groups and methylated derivatives for phenolic hydroxyl groups, whereas in more controlled amounts, DMC can act as a difunctional carbonate linker between lignin fragments. This approach would enable the formation of lignin-based polycarbonate materials in which the lignin macromonomer is connected through carbonate bridges.

The utilization of lignin for the production of polycarbonates remains scarcely explored. Several reports focus on the usage of lignin-based monomers, particularly phenolic diols, which have been investigated as partial or full substitutes for BPA in conventional polycarbonate chemistry.[284–288] In contrast, the direct use of lignin as a macromonomer in polycarbonate systems is still largely unexplored. A very recent study reports the synthesis of lignin-based polycarbonate polyols *via* transesterification with DMC.[289] In this approach, a mixture of lignin and polyethylene glycol (PEG) containing 30 wt% lignin, was first oxyalkylated with propylene carbonate (PC), introducing hydroxypropyl grafted moieties and PEG-chains onto the lignin backbone, as well as the PEG adduct after its reaction with PC. Subsequent transesterification with DMC yielded lignin-based polycarbonate polyols, which were then employed to partially substitute fossil-based polyols in flexible PU foams. Although PEG is typically petroleum-

based, commercially available biobased alternatives can be used as substitutes.[290]

A key advantage of carbonate linkages is their chemical reversibility. In the presence of methanol (MeOH), the carbonate moieties undergo methanolysis, regenerating a lignin structure together with DMC (**Scheme 4.1.1**). Importantly, under these conditions, methylation of phenolic hydroxyl groups cannot be excluded. These methylated derivatives would be hardly cleavable under methanolysis conditions and would therefore remain in the lignin structure after the recycling process. This would certainly influence the properties of the final retrieved material, but should not hinder a possible re-crosslinking *via* DMC through aliphatic hydroxyl groups. This closed-loop depolymerization establishes a reversible lignin modification cycle, positioning lignin polycarbonates as an example of macromolecular systems that can be assembled and disassembled under potentially mild conditions.

Scheme 4.1.1 – Illustrative scheme of the desired synthesis of lignin-derived polycarbonates from OL, focusing on the circularity of the project *via* the cycle of functionalization – recycling. Phenolic *O*-methylation side reactions are not shown in this simplified scheme.

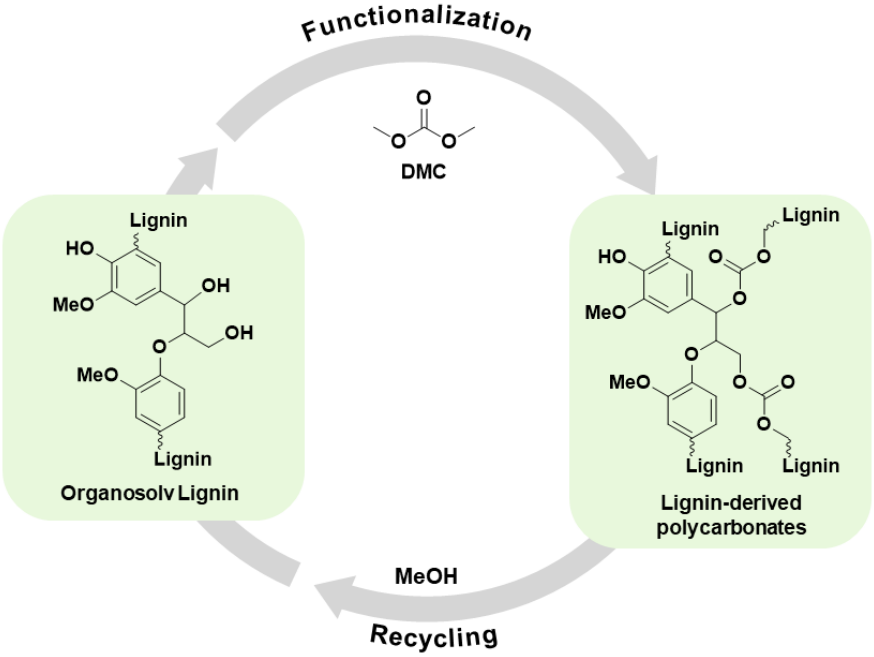

This chapter explores the synthesis and characterization of lignin-based polycarbonates prepared through DMC-mediated coupling and highlights the potential of lignin as a truly circular macromonomer for future polymer materials.

4.1.3 First Approach with DMC as Limiting Reagent

4.1.3.1 Reactivity of DMC with Lignin

It is well established in the literature that DMC represents a significantly more environmentally benign alternative to traditional reagents such as methyl halides, dimethyl sulfate, and phosgene.[291] It can serve both as a methylating agent (in place of methyl halides or dimethyl sulfate) and as a carbonylating agent (in place of phosgene), thereby substantially reducing operator exposure risks and minimizing waste-treatment challenges. In addition to being of low toxicity, DMC offers a greener and more sustainable option compared to conventional reagents, and its reactivity can be readily tuned by adjusting reaction conditions and parameters.[292] In particular, in the presence of a nucleophile, DMC can react *via* two different pathways, illustrated in **Scheme 4.1.2**. In the first pathway, $B_{AL}2$ (bimolecular, base-catalyzed, alkyl cleavage, nucleophilic substitution), the nucleophile attacks the methyl groups of DMC, leading to the formation of the methylated adduct, methanol, and CO_2, the latter leaving the reaction as a gas and thus leading to the irreversibility of this process. In the second pathway, instead, the nucleophile attacks the carbonyl carbon of DMC, leading to the carboxymethylated adduct *via* $B_{AC}2$ (bimolecular, base-catalyzed cleavage, nucleophilic acyl substitution). These two pathways can be influenced by temperature and type of nucleophiles. It was generally observed that at reflux (T = 90 °C) and atmospheric pressure, DMC acts predominantly as carboxymethylating agent, following $B_{AC}2$ pathway, while for higher temperatures (under pressure and over its boiling point) it acts as a methylating agent *via* $B_{AL}2$ pathway.[292,293] More importantly, the nature of the nucleophile strongly influences the reactivity. DMC possesses two electrophilic sites and the selectivity toward either one or the other can be explained by the Hard–Soft

Acid–Base Theory (HSAB Theory), introduced by Pearson.[294] For instance, it is reported that hard nucleophiles, such as alkoxides, react preferably *via* the $B_{AC}2$ mechanism, while softer phenolate anions (or thiolates) preferentially react *via* the $B_{AL}2$ mechanism.[295]

Scheme 4.1.2 – Typical pathways for DMC reactivity with nucleophiles, *via* methylation or carboxymethylation, with a generic nucleophile (Nu).

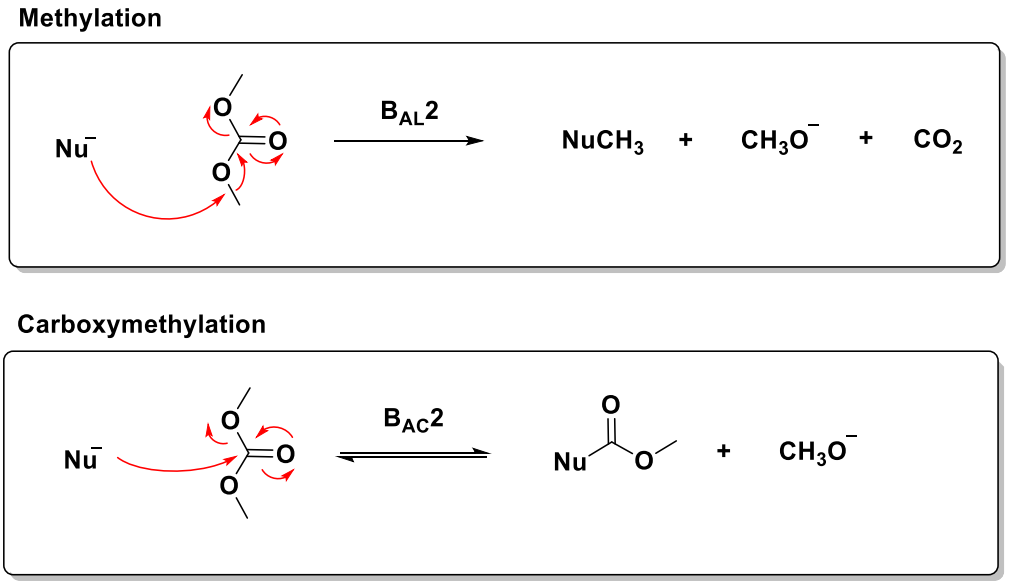

Lignin presents a multitude of different functional groups that can react with DMC according to different mechanisms. In **Scheme 4.1.3** the general expected reaction pathways between lignin and DMC are delineated.

Scheme 4.1.3 – Main reaction pathways between lignin main functional groups and DMC.

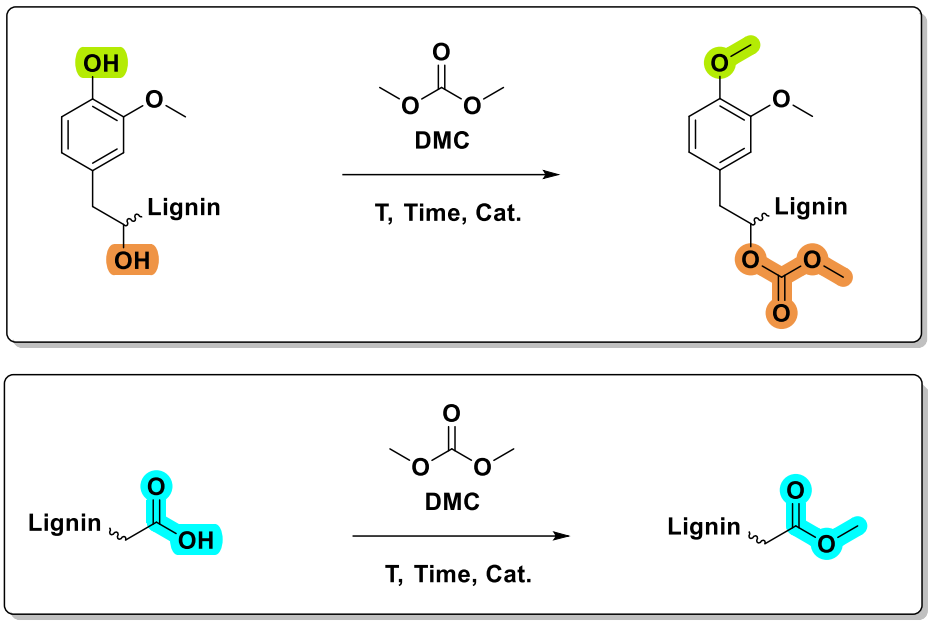

4.1.3.2 Influence of Reaction Time

The employed *Organosolv* beech wood lignin (OL) used in this doctoral thesis was kindly donated by the Fraunhofer Center for Chemical-Biotechnological Processes, CBP. OL was isolated *via* organosolv pulping in an ethanol-water mixture and used without any further treatment, unless stated otherwise. Characterization of OL was performed *via* SEC (both in THF and DMAc as solvents), IR, ^{1}H NMR, ^{13}C NMR, TGA, DSC, and ^{31}P NMR. The data are reported in **Chapter 6.3**. Quantitative determination of -OH group content and distribution in OL and its derivatives was performed *via* ^{31}P NMR by quantitatively reacting the free hydroxyl groups with 2-chloro-4,4,5,5-tetramethyl-1,3-2-dioxaphospholane (TMDP) to yield phosphite esters, according to the original procedure of Argyropoulos *et al*.[296] The phosphitylated products can be detected quantitatively, with the assistance of a phosphitylated internal standard, *endo-N*-hydroxy-5-norbornene-2,3-dicarboximide (NHND), *via* ^{31}P NMR spectroscopy. By integration of the signals, it is possible to obtain quantitative values of different hydroxyl group types, according to the calculations reported from Argyropoulos *et al*.[297], as described in the experimental section (**Chapter 6.2**).

Initial efforts were devoted to finding optimal conditions for the carboxymethylation reaction that could lead to crosslinking. Literature reports that the reactivity of DMC toward hydroxyl groups depends strongly on substrate and reaction conditions. In model systems resembling lignin, aliphatic hydroxyls usually require basic catalysts and high temperatures to quantitatively undergo transesterification with DMC.[298] A low reactivity, and therefore no full conversion of the aliphatic groups, was expected. Consequently, the equivalents of DMC were initially kept stoichiometric to the total amount of -OH groups of lignin and the influence of several parameters was investigated, starting with the reaction time. Due to the low amount of DMC employed, an additional solvent was needed for the reaction. Briefly, OL was dissolved in dry DMSO in a 5 wt% concentration and was allowed to react with DMC in the presence of DBU as base, at 90 °C. In **Table 4.1.1** an overview of the conditions tested is described.

A first assessment to detect the successful outcome of the reaction was done *via* IR spectroscopy, and for selected samples, ^{31}P NMR was also conducted.

To identify the optimal reaction time, in the first experiment, several aliquots were collected after 24, 48, and 72 h at 90 °C, to investigate the outcome of the reaction over time. As shown in **Figure 4.1.1**, the IR spectra of different aliquots over time do not show significant changes among each other, showing that the conversion of the reaction was not significantly altered by the reaction time. In case of successful carbonate linkage introduction, an increase in the carbonyl stretching vibration area (1800–1700 cm^{-1}) is expected. Moreover, a modest increase in the C-H stretching vibration area (2900–2800 cm^{-1}), that indicates concomitant methylation of phenolic -OH and/or reaction of aliphatic - OH groups with only one side of DMC, leading to carboxymethylated structures, would probably be observed as well.

For the first two samples (24 h and 48 h, Entries 1 and 2 **Table 4.1.1**), however, the ^{31}P NMR results do not fully align with these observations. The reduction in aliphatic hydroxyl groups determined by ^{31}P NMR is significantly higher than suggested by the IR spectra (a visual representation of the hydroxyl group distribution is shown in **Figure 4.1.2**). Although, in this case, IR spectroscopy is mainly used to provide qualitative information, such a high decrease in aliphatic -OH groups shown by ^{31}P NMR (from 2.42 $mmol \cdot g^{-1}$ aliphatic -OH in the starting material (OL) to 1.00 $mmol \cdot g^{-1}$ after 48 h of reaction) should result in a noticeably stronger carbonyl stretching vibration signal, which was not observed. To clarify this discrepancy, additional experiments were conducted, as described in the following paragraphs.

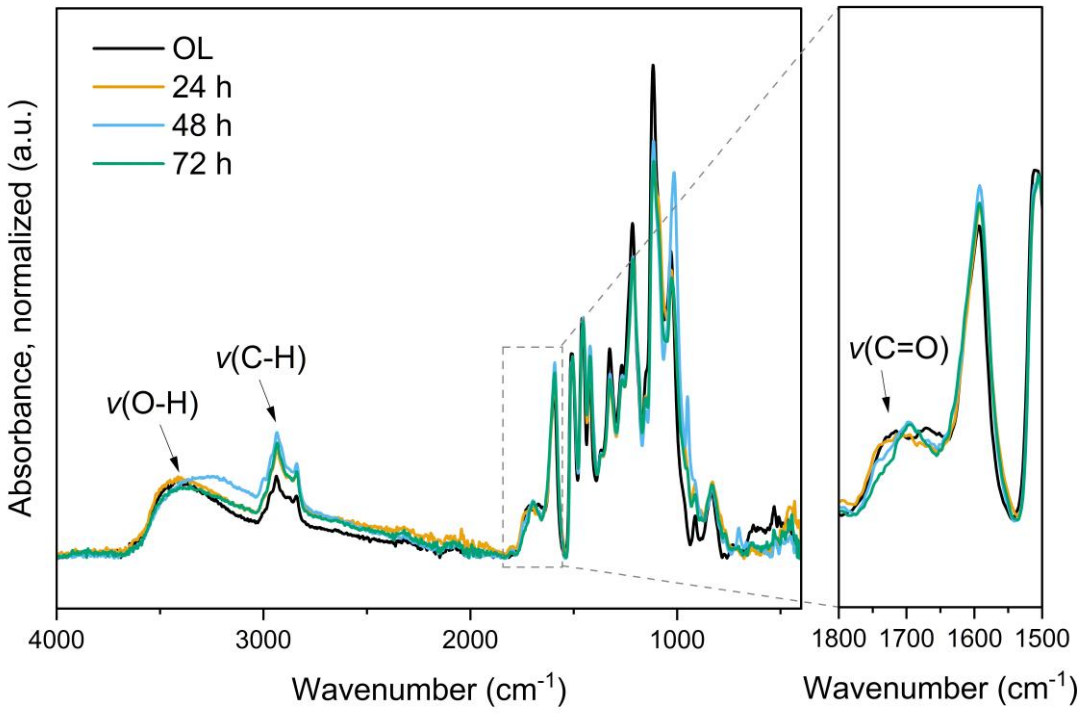

Figure 4.1.1 – IR spectrum overlay of the starting material (OL, black) and the aliquot of the reaction with stoichiometric amounts of DMC after 24 h (orange), 48 h (blue) and 72 h (green). IR spectra are normalized to the 1504 cm^{-1} aromatic C=C stretching vibration of lignin, which is not expected to change after the modification.

Table 4.1.1 – Main reaction parameters for the initial screening of reaction time investigated.

Entry	Time (h)	$OH_{Aliphatic}$ ($mmol \cdot g^{-1}$)[a]	$OH_{Aromatic}$ ($mmol \cdot g^{-1}$)[a]	OH_{Total} ($mmol \cdot g^{-1}$)[a]
OL	-	2.42	1.83	4.35
1	24	1.56	1.70	3.26
2	48	1.00	1.38	2.43
3	72	-[b]	-[b]	-[b]

General conditions: dried OL (5 wt% in DMSO, anhydrous), 1 equiv. of DBU and 1 equiv. of DMC (both respectively to the total amount of -OH groups of lignin, calculated from ^{31}P NMR) are added into a crimp vial. The solution is stirred at 90°C. [a]: Determined from ^{31}P NMR. [b]: not performed.

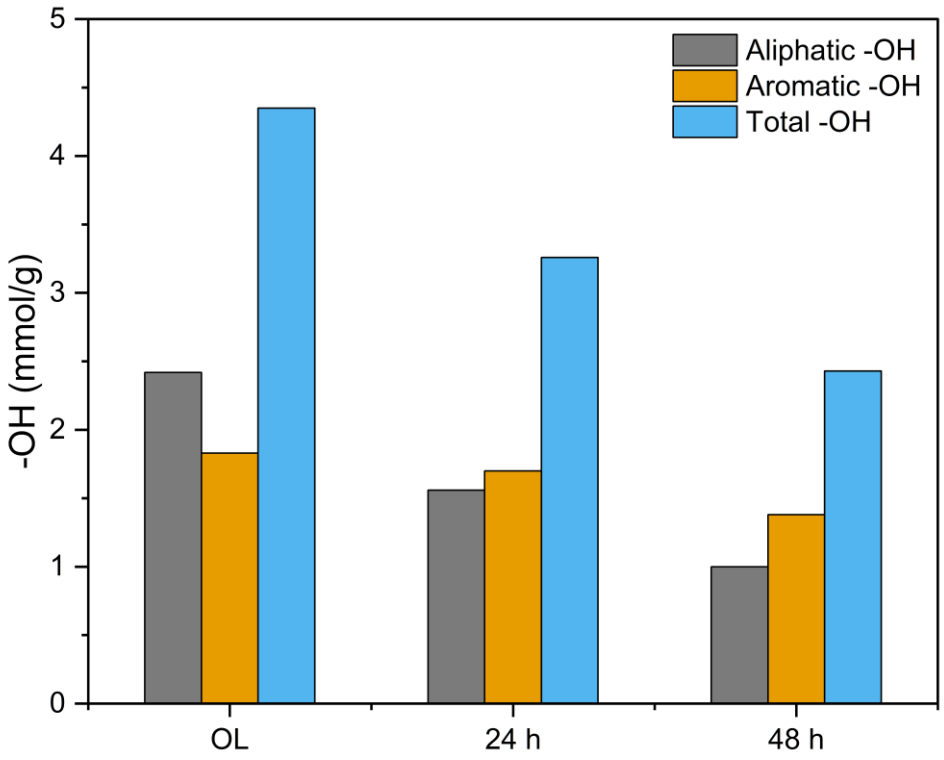

Figure 4.1.2 – Column bar graph showing the -OH distribution for the starting material (OL), and the hydroxyl groups profile distribution for the aliquots after the reaction with stoichiometric amounts of DMC after 24 and 48 h.

4.1.3.3 Influence of the Catalyst

To gain further insights into the reaction conditions, the type of base was also tested as a parameter that could influence the conversion for this reaction. Typically, organobases such as 1,8-diazabicyclo(5.4.0)undec-7-ene (DBU) or 1,5,7-triazabicyclo(4.4.0)dec-5-ene (TBD), are known to promote transesterification[299,300] and alkylation of substituted phenols with dialkyl carbonates.[301] In particular, TBD has been described as a dual catalyst in the aminolysis of five-membered cyclic carbonates, activating simultaneously *via* hydrogen bonding both the cyclic carbonate and the amine.[302] Although this catalytic behavior has been primarily discussed for amines, a similar activation principle can reasonably be extended to alcohols. Tetrabutylammonium bromide (TBAB) was instead chosen as a phase transfer catalyst. It has been shown that TBAB was very effective in the alkylation of phenols[303] and lignin phenolic -OH[247] with dialkyl carbonates. In this context, it was worth investigating whether this catalytic efficiency could be extended to the carboxymethylation pathway as well and whether TBAB could also promote reactions involving aliphatic hydroxyl groups, thereby enabling access to both reaction pathways. The postulated mechanism for the methylation of phenol with DMC is shown in **Scheme 4.1.4**, as previously reported from Thiébaud *et al*.[303] where TBAB forms a complex with the phenolate, which in turn attacks the DMC molecule in a $B_{AL}2$ fashion. It should be noted that this mechanism was proposed based on experiments conducted at elevated temperatures (130 °C), and no experimental data were reported for lower reaction temperatures. Therefore, deviations from this mechanistic pathway cannot be excluded under the reaction conditions employed in the present study.

Scheme 4.1.4 – Plausible mechanism for alkylation of phenols in the presence of TBAB, readapted with permission from Thiébaud *et al*.[303]

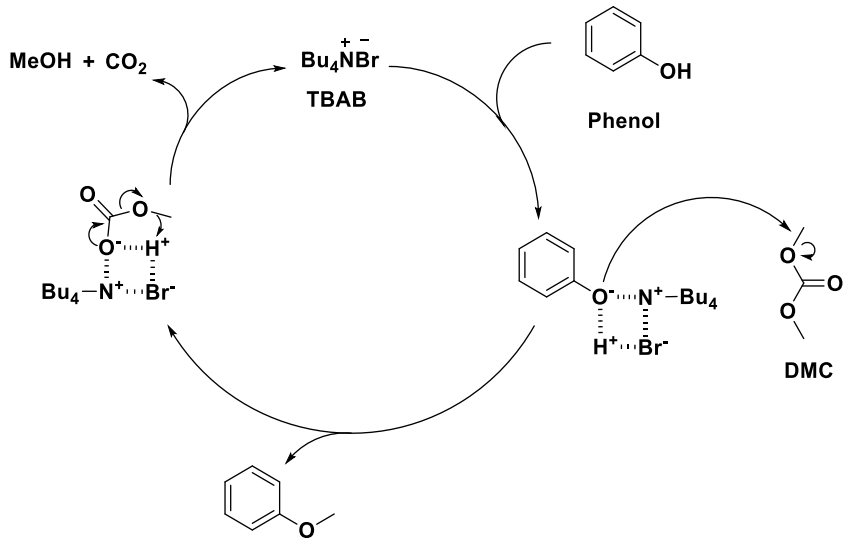

Briefly, the reaction time was fixed at 24 h. OL was dissolved in dry DMSO in a 5 wt% concentration and was allowed to react with DMC in the presence of 1 equiv. of either TBAB, TBD or DBU at 90 °C. The IR spectra of the reactions performed with different bases show only minor variations and no significant improvement in conversion could be identified (**Figure 4.1.3**). A slight increase in the carbonyl stretching region was observed after the reaction with TBD, suggesting a possible higher conversion relative to the other bases. However, this observation could not be verified by ^{31}P NMR spectroscopy due to insufficient sample quantity (**Table 4.1.2, Entry 5**). For the other two cases, i.e. TBAB and DBU, it was possible to observe that despite no significant changes being detected through IR spectroscopy, the ^{31}P NMR results show a general decrease in the hydroxyl group content, for both aliphatic and aromatic ones. In the case of TBAB, however, this decrease was rather low, and this could be associated with a very low conversion of the hydroxyl groups toward the carboxymethylated/carbonated and methylated structures, for aliphatic and aromatic, respectively (**Table 4.1.2**, **Entry 4**). When DBU was employed as a base, on the other hand, the decrease in the aliphatic -OH groups content was higher, as observed and discussed in the previous paragraph, and did not align with the IR results. (**Figure 4.1.3**).

Table 4.1.2 – Main reaction parameters for the reaction between lignin and DMC with different bases.

Entry	Time (h)	Base	$OH_{Aliphatic}$ (mmol·g^{-1})[a]	$OH_{Aromatic}$ (mmol·g^{-1})[a]	OH_{Total} (mmol·g^{-1})[a]
OL	-	-	2.42	1.83	4.35
4	24	TBAB	2.14	1.70	3.85
5	24	TBD	N.a.	N.a.	N.a.
6	24	DBU	1.56	1.70	3.26

General conditions: dried OL (5 wt% in DMSO, anhydrous), 1 equiv. of base and 1 equiv. of DMC (both respectively to the total amount of -OH groups of lignin, calculated from ^{31}P NMR) are added into a crimp vial. The solution is stirred at 90°C. [a]: Determined from ^{31}P NMR. N.a.: not enough sample available to perform further analyses.

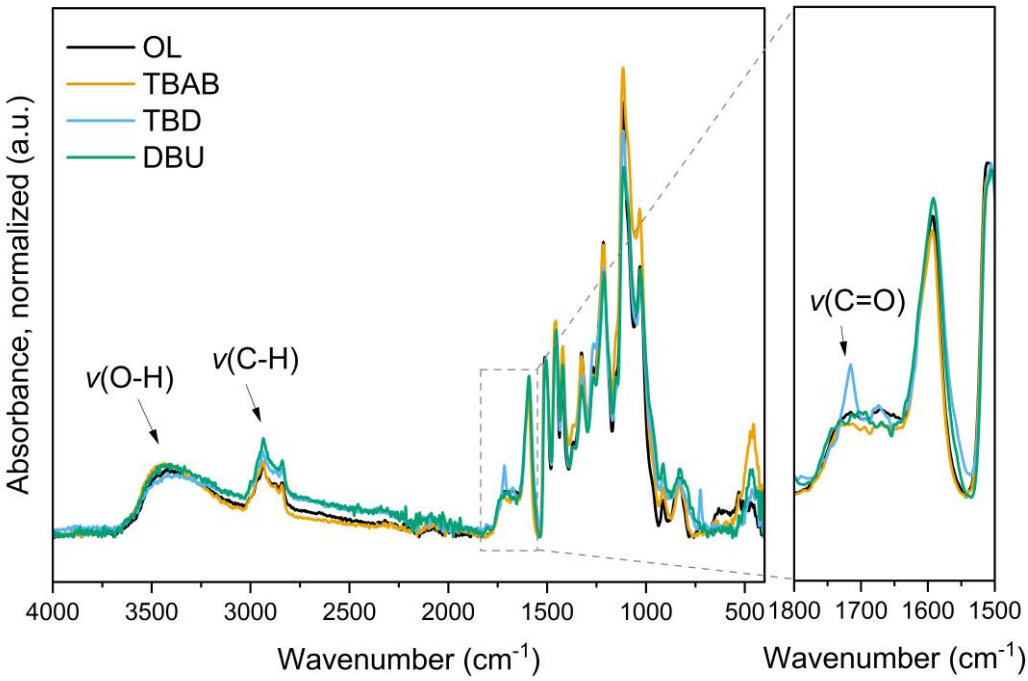

Figure 4.1.3 – IR spectrum after 24 h for different bases. IR spectrum overlay of the starting material (OL, black) and the reaction with stoichiometric amounts of DMC with TBAB (orange), TBD (blue) and DBU (green). IR spectra are normalized to the 1504 cm^{-1} aromatic C=C stretching vibration of lignin, which is not expected to change after the modification.

4.1.3.4 Influence of the Solvent

Given the inconsistencies observed between the analytical techniques in assessing the extent of the reaction, a more detailed examination was necessary. For this purpose, a series of control experiments was carried out in the absence of DMC to determine the influence of the solvent on the lignin structure and rule out possible side reactions. Specifically, two solvents, DMSO—which was the solvent of choice for the previous experiments— and DMAc, were tested in the presence of OL, in a 5 wt% concentration, and 1 equiv. of DBU. As can be depicted from **Table 4.1.3** and **Figure 4.1.4**, the solvent has a pronounced effect on the lignin structure, particularly with respect to the distribution of hydroxyl groups. Notably, even in the absence of DMC as a functionalizing agent, a reduction in the total -OH content is observed when the reaction is conducted in DMSO. In the literature, a possible side reaction between DMSO and the -OH groups of lignin is described.[242] In particular, Argyropoulos *et al*.[242] postulate a reaction between DMSO and the aliphatic -OH of lignin in the presence of a base, thereby leading to decreased amounts.[304] This could lead to the reduction in the aliphatic -OH groups of lignin, as observed in the conducted experiments.

Table 4.1.3 – Hydroxyl groups distribution for the starting material (OL) and the two control reactions in the absence of DMC.

Sample	$OH_{Aliphatic}$ (mmol·g^{-1})[a]	$OH_{Aromatic}$ (mmol·g^{-1})[a]	COOH (mmol·g^{-1})[a]	OH_{Total} (mmol·g^{-1})[a]
OL	2.42	1.83	0.10	4.35
DMSO	1.37	1.54	0.08	3.01
DMAc	2.37	1.86	0.12	4.35

General conditions: In dry DMSO or DMAc, OL (5 wt%) and 1 equiv. of DBU (respectively to the total amount of -OH groups of lignin, calculated from ^{31}P NMR) are added into a crimp vial. The solution is stirred at 90 °C for 24 h. [a]: Determined from ^{31}P NMR.

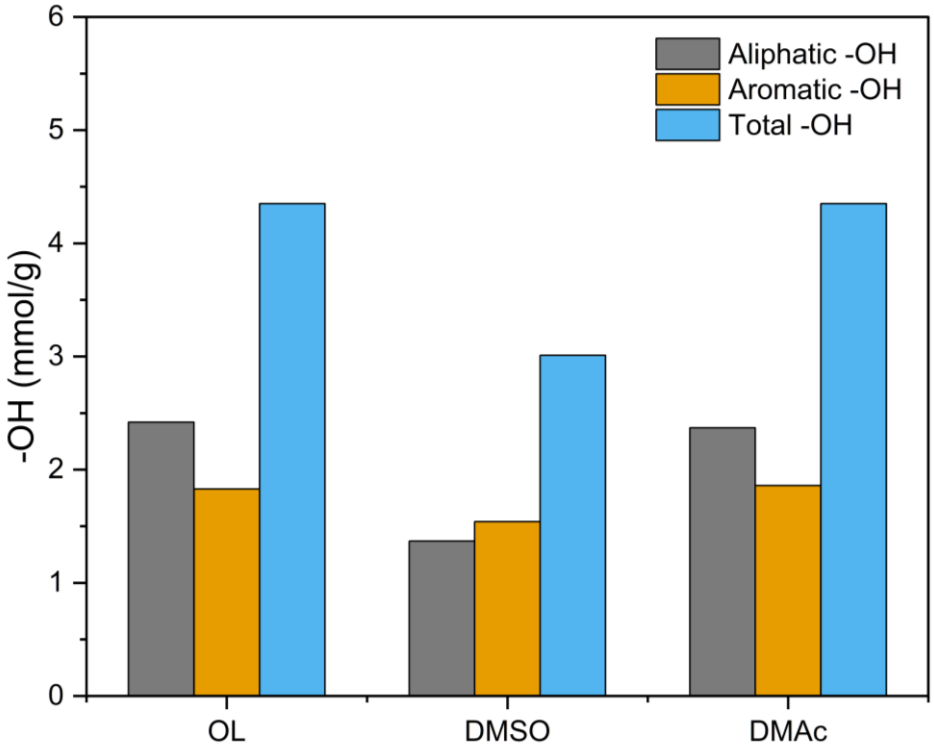

Figure 4.1.4 – Column bar graph showing the -OH distribution for the starting material (OL), and the hydroxyl groups profile distribution for the control reactions conducted in DMSO and DMAc. A clear decrease in the -OH content can be observed when DMSO is used as a solvent.

When DMAc was used as solvent instead, no decrease in the -OH content was registered, and the slight variations between the measured values fall within the experimental error of the procedure.

4.1.4 Second Approach – Intermediate Route

The first approach described in **Chapter 4.1.3**, which required the use of an additional solvent due to the low equivalents of DMC, was ultimately discarded due to the occurrence of side reactions between OL and DMSO. DMAc was not initially selected as a solvent of choice owing to concerns regarding its toxicity and its limited compliance with green chemistry principles. Consequently, a new strategy was developed to obtain the same target material without relying on an organic solvent. In this alternative approach, lignin is first reacted with an excess of DMC to quantitatively methylate the aromatic hydroxyl groups and partially carboxyalkylate the aliphatic ones. Owing to their lower reactivity, the aliphatic -OH groups are likely not fully converted under these conditions. This results in an **intermediate**—referred to as “pre-functionalized lignin”—that contains residual aliphatic hydroxyl groups alongside newly introduced carbonate functionalities. This intermediate is then allowed to undergo self-condensation to form lignin-derived polycarbonates. This pathway, without additional solvents, avoids the limitations encountered in the initial approach, while potentially still enabling chemical recycling of the final material through methanolysis, although the recovered lignin is expected to contain a higher degree of methylation compared to the original strategy, due to the higher excess of DMC. For clarity, an overview of the presented approach is presented in **Scheme 4.1.5**.

Scheme 4.1.5 – Overview of the second approach that involves two steps: pre-functionalization and self-condensation.

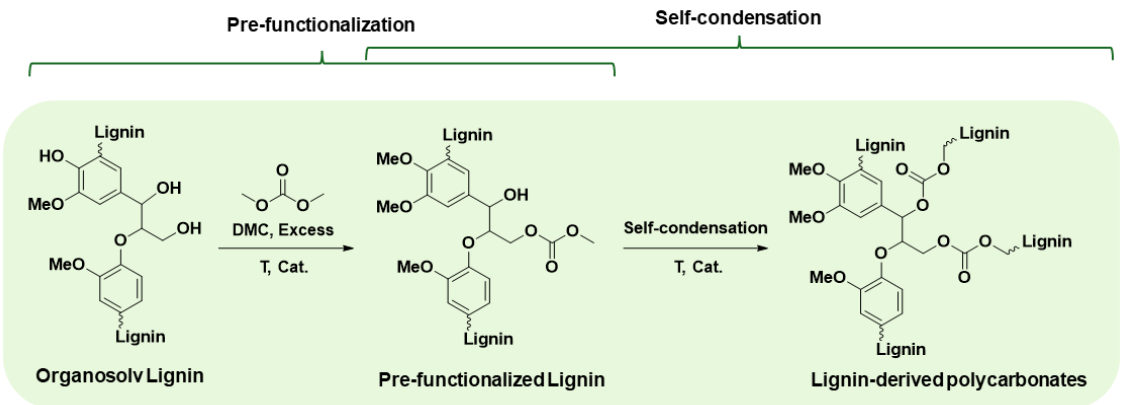

4.1.4.1 Pre-functionalized Lignin Optimization

The reaction between OL and an excess of DMC to give the intermediate was first investigated. For the pre-functionalization step, 10 equivalents of DMC were employed, as this large excess enables the reaction to be conducted without additional solvent. The intermediate (**LC-1**) was synthesized with DMC acting both as reactant and solvent at 90 °C in the presence of TBAB, with a reaction time of 5 h. These initial parameters were employed according to previously reported literature procedures of functionalization of lignin with dialkyl carbonates.[247,304]

The reaction conditions, as well as the most significant analytical data, are summarized in **Table 4.1.4**.

Table 4.1.4 – Overview of the reaction conditions and corresponding analytical data for the synthesis of the pre-functionalized lignin intermediate LC-1.

Sample	$OH_{Aliphatic}$ (mmol·g^{-1})[a]	$OH_{Aromatic}$ (mmol·g^{-1})[a]	COOH (mmol·g^{-1})[a]	OH_{Total} (mmol·g^{-1})[a]	M_n (g·mol^{-1})[b]	$Đ$
OL	2.42	1.83	0.1	4.35	800	1.6
LC-1	1.56	0.19	0	1.75	1300	2.1

General conditions: dried OL, 1 equiv. of TBAB and 10 equiv. of DMC (respectively to the total amount of -OH groups of lignin, calculated from ^{31}P NMR) are added into a crimp vial. The solution is stirred at 90 °C for 5 h. [a]: Determined from ^{31}P NMR. [b]: SEC-THF.

The reaction proceeded efficiently, yielding a decrease of 90 % of aromatic hydroxyl groups and 35 % of aliphatic hydroxyl groups. As expected after functionalization, the molecular weight of the product increased relative to the starting material OL. As an initial proof of concept, three self-condensation experiments were carried out. The first objective was to determine whether bulk conditions could be applied for the self-condensation step. To this end, a DSC analysis was performed on the intermediate to assess the presence of a melting transition. However, the DSC thermogram of **LC-1** (**Figure 4.1.5**) showed no detectable melting point and only a decrease in the glass transition temperature compared to the original lignin, as expected following the introduction of

carboxymethylated and methylated moieties. Bulk processing was therefore deemed unfeasible, and a minimal amount of DMAc was employed as solvent for the self-condensation reactions, since DMSO had previously shown issues related to side reactions.

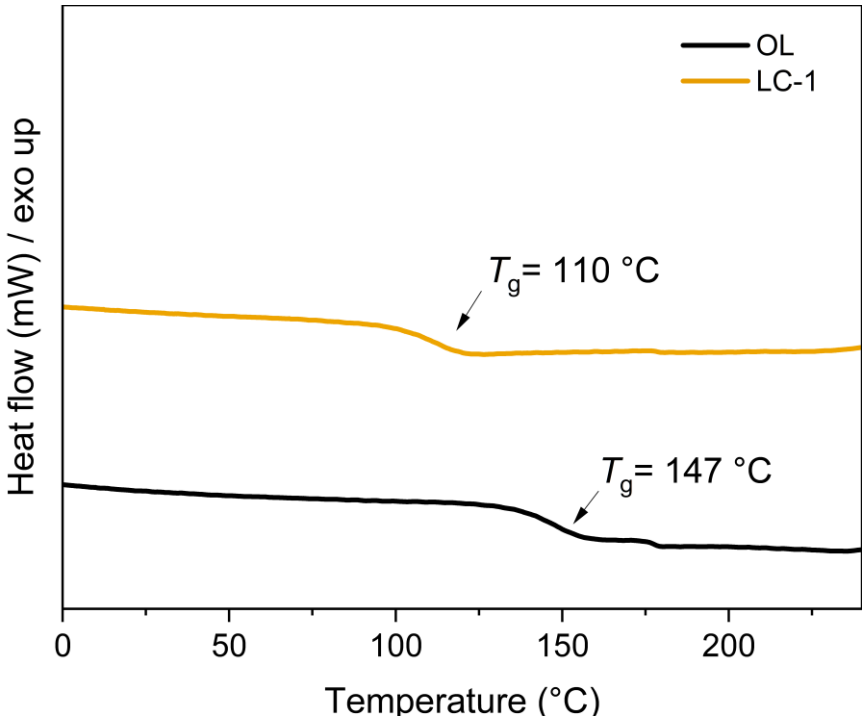

Figure 4.1.5 - DSC traces of OL (black) and LC-1 (orange) showing only the glass transition.

At this stage, various conditions were evaluated for the self-condensation reaction (**LC-1A**, **LC-1B**, **LC-1C**, **Table 4.1.5**). TBD was selected as the catalyst and tested both in stoichiometric amounts and with 0.2 equivalents, while reaction times of 5 h and 24 h were investigated. In all cases, the temperature was maintained at 90 °C, as this had previously been described as the optimal temperature for the carboxymethylation step.

Table 4.1.5 – Summary of the reaction parameters screened for the self-condensation reactions, starting from the intermediate LC-1.

Sample	Time (h)	TBD (equiv.)	$OH_{Aliphatic}$ (mmol·g^{-1})[a]	$OH_{Aromatic}$ (mmol·g^{-1})[a]	M_n (g·mol^{-1})[b]	Đ
LC-1	-		1.56	0.19	1300	2.1
LC-1A	24	1	1.58	0.36	900	1.9
LC-1B	5	1	1.67	0.35	800	2.0
LC-1C	5	0.2	1.67	0.28	1000	2.2

General conditions for the self-condensation: 150 mg dried LC-1, TBD and 1 mL of DMAc (anhydrous) are added into a crimp vial. The solution is stirred at 90 °C for 5 or 24 h. [a]: Determined from ^{31}P NMR. [b]: SEC-THF.

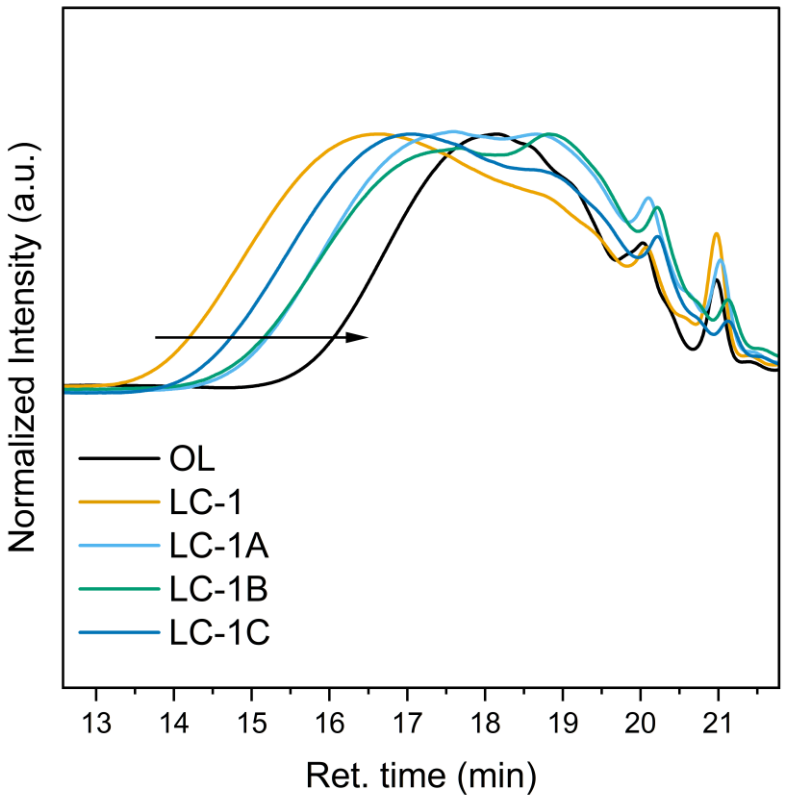

Figure 4.1.6 – SEC traces of the starting material (OL, black), the intermediate LC-1 (orange) and the self-condensation tests (LC-1X).

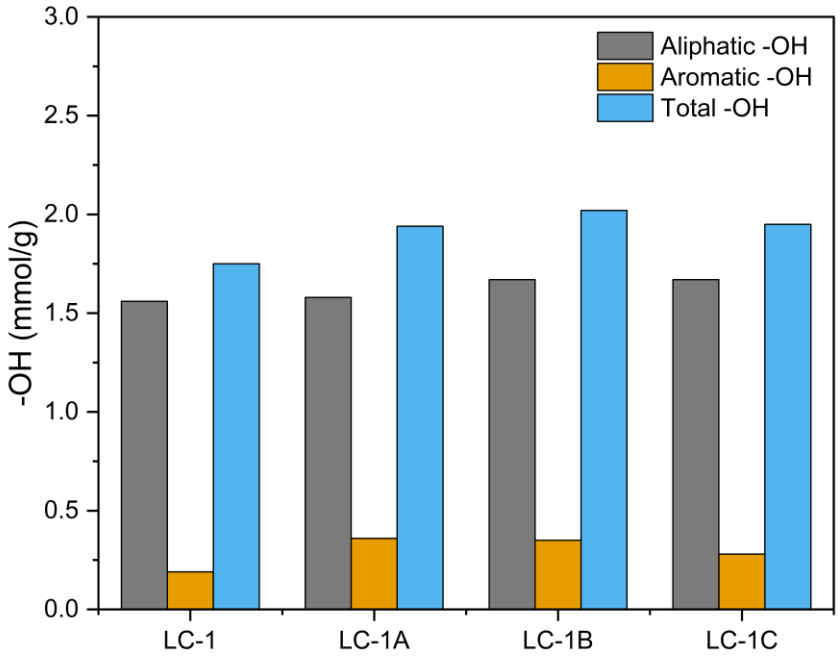

Figure 4.1.7 – Column bar graph showing the -OH distribution for the starting material (intermediate LC-1) and the self-condensation tests (LC-1X).

As evidenced by the SEC and ^{31}P NMR data (**Figure 4.1.6** and **Figure 4.1.7**), none of the tested conditions yielded the expected outcome. If condensation between the residual aliphatic hydroxyl groups and the carbonate functionalities had taken place, a decrease in the aliphatic OH content accompanied by an increase in molecular weight—reflecting oligomerization or crosslinking—would be expected. Instead, the results indicate defuntionalization, manifested by an increase in hydroxyl group content and a reduction in molecular weight.

Before proceeding further, additional optimization of the intermediate synthesis was carried out. Increasing the degree of carboxymethylation, to a certain extent, was expected to enhance the probability of polymerization. To evaluate this effect, four different sets of reaction conditions for the intermediate synthesis were examined, as summarized in **Table 4.1.6**.

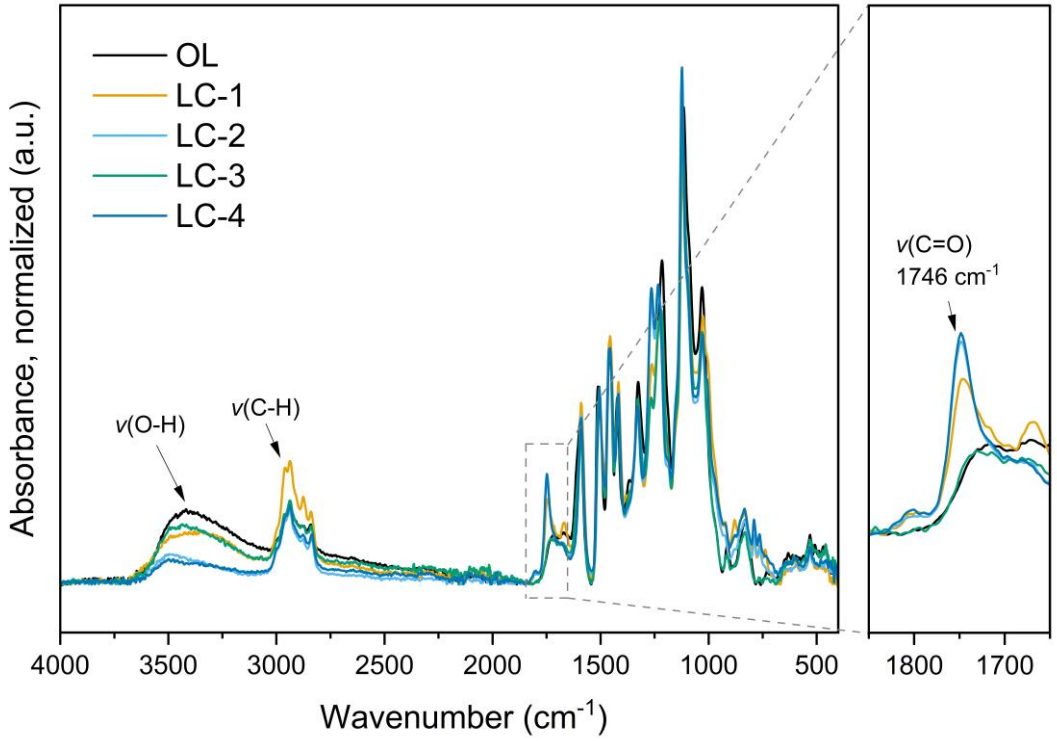

Figure 4.1.8 – IR spectra of the starting material (OL, black) and the intermediate (LC-X) during the optimization. IR spectra are normalized to the 1504 cm^{-1} aromatic C=C stretching vibration of lignin, which is not expected to change after the modification.

Typical signals associated with a successful functionalization are the increased absorbance of the carbonyl stretching band at 1746 cm^{-1} and a more intense aliphatic C–H stretching region, consistent with the introduction of methyl and carboxymethyl groups, as depicted in **Figure 4.1.8**. In comparison to the starting material, the IR spectra also show a decrease in the O–H stretching vibrations, which becomes more pronounced at higher conversions. Based on the ^{31}P NMR and SEC results (**Figure 4.1.9**), extending the reaction time from 5 to 15 h while maintaining a stoichiometric amount of TBAB (entries **LC-1** and **LC-4**, **Table 4.1.6**) did not lead to a significant improvement in the conversion. However, the amount of TBAB appears to have the strongest influence. In fact, **LC-2** (2 equivalents of TBAB, **Table 4.1.6**) showed the highest degree of functionalization, whereas **LC-3** (0.5 equivalents of TBAB, **Table 4.1.6**) exhibited the lowest.

Table 4.1.6 – Overview of the investigated parameter and relative analytical data for the optimization of the intermediate synthesis.

Sample	Time (h)	TBAB (Equiv.)	$OH_{Aliphatic}$ (mmol·g^{-1})[a]	$OH_{Aromatic}$ (mmol·g^{-1})[a]	OH_{Total} (mmol·g^{-1})[a]	M_n (g·mol^{-1})[b]	$Đ$
OL	-	-	2.42	1.83	4.35	800	1.6
LC-1	5	1	1.56	0.19	1.75	1300	2.1
LC-2	5	2	1.26	0	1.26	1500	2.3
LC-3	5	0.5	2.14	1.15	3.30	1000	1.7
LC-4	15	1	1.42	0	1.42	1500	2.7

General conditions: 500 mg dried OL, TBAB and 10 equiv. of DMC (respectively to the total amount of -OH groups of lignin, calculated from ^{31}P NMR) are added into a crimp vial. The solution is stirred at 90 °C for 5 or 15 h. [a]: Determined from ^{31}P NMR. [b]: SEC-THF.

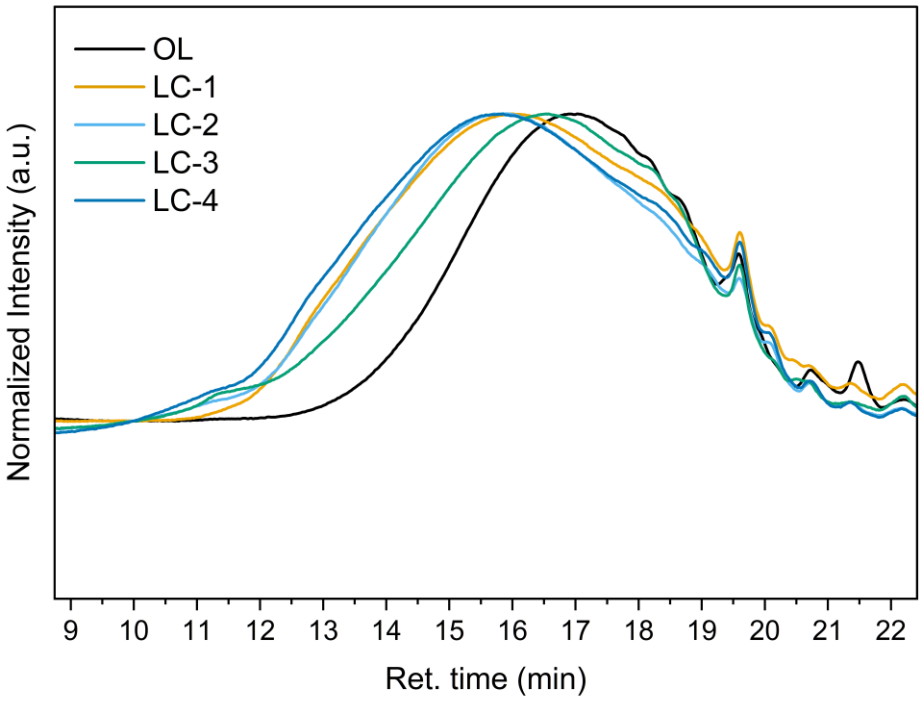

Figure 4.1.9 – SEC traces of the starting material (OL, black) and the optimization of the intermediate synthesis (LC-X).

Thus, the **LC-2** conditions—showing the highest functionalization—were adopted, and a larger scale batch (2 g) was prepared for the self-condensation experiments. In **Table 4.1.7,** a summary of the analytical data for this sample (LC-5) is provided.

Table 4.1.7 – Summary of the analytical data of the 2 g batch of the intermediate synthesized.

Sample	$OH_{Aliphatic}$ (mmol·g^{-1})[a]	$OH_{Aromatic}$ (mmol·g^{-1})[a]	OH_{Total} (mmol·g^{-1})[a]	M_n (g·mol^{-1})[b]	$Đ$
LC-5	1.051	0	1.051	1700	3.0

[a]: Determined from ^{31}P NMR. [b]: SEC-THF.

4.1.4.1.1 Recycling TBAB:

To improve the sustainability of this protocol, in accordance with the principles of green chemistry, the phase-transfer catalyst TBAB was recycled according to the previously reported procedure from Meier *et al*.[247] In particular, the aqueous phase collected after lignin precipitation and filtration were evaporated under reduced pressure (80 mbar, 60 °C) to recover TBAB as a viscous yellowish liquid, that crystalized after cooling (91 % recovery). The purity of recovered TBAB was verified *via* ^{1}H NMR (**Figure 4.1.10**), resulting in an identical spectrum for commercial and recycled TBAB.

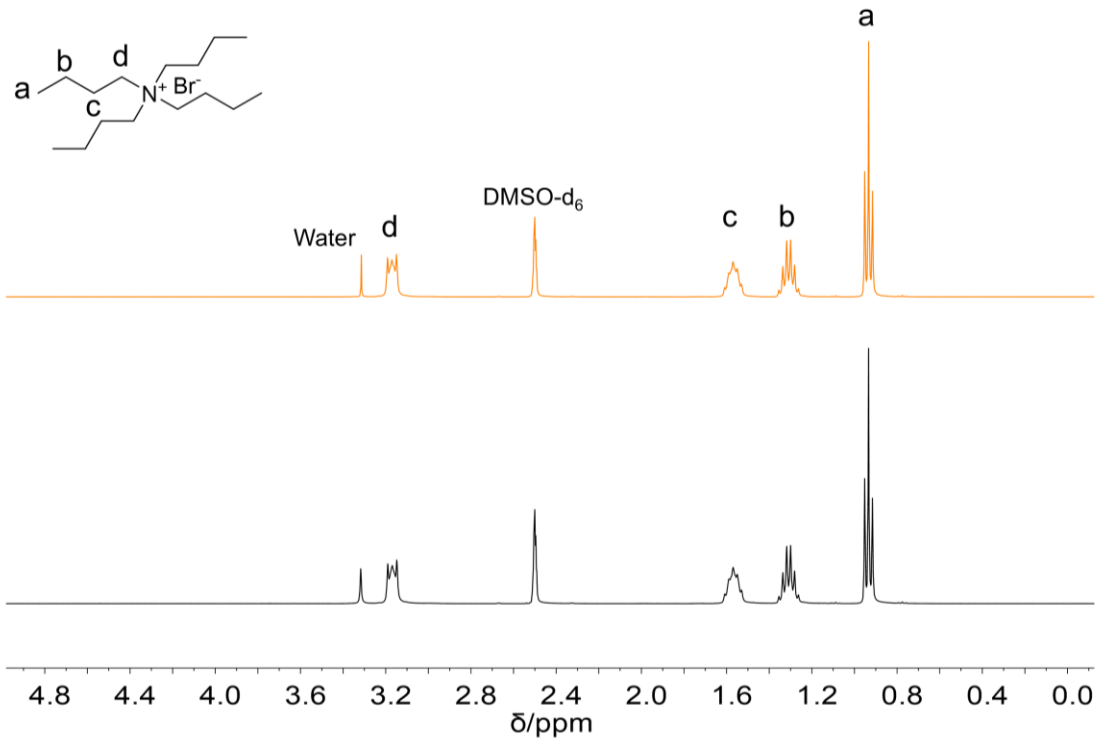

Figure 4.1.10 – ^{1}H NMR spectrum of commercial TBAB (top), and recycled TBAB (bottom), in DMSO-d_6.

4.1.4.2 Self-condensation Optimization

4.1.4.2.1 Catalyst Screening

According to the previous tests (**Figure 4.1.6** and **Table 4.1.5**, **LC-1A–C**), although depolymerization and/or defunctionalization occurred under all conditions, the lowest extent of depolymerization was observed when using 0.20 equiv. of TBD. Based on this result, a catalyst screening was performed for the self-condensation reaction, keeping the catalyst loading fixed at 0.20 equiv.

Table 4.1.8 – Overview of the catalyst screening conditions and analytics for the self-condensation reactions.

Sample	Cat.	Cat. (Equiv.)	$OH_{Aliphatic}$ ($mmol \cdot g^{-1}$)[a]	$OH_{Aromatic}$ ($mmol \cdot g^{-1}$)[a]	OH_{Total} ($mmol \cdot g^{-1}$)[a]	M_n ($g \cdot mol^{-1}$)[b]	$Đ$
LC-5	-		1.051	0	1.051	1700	3.0
LC-5A	TBD	0.20	1.40	0.06	1.46	1300	2.3
LC-5B	DBU	0.20	0.94	0	0.96	1700	3.2
LC-5C	Cs_2CO_3	0.20	1.40	0	1.40	1500	2.6
LC-5D	K_2CO_3	0.20	1.12	0	1.12	1600	2.8
LC-5E	Thiourea	0.20	0.90	0	0.90	1700	3.0
LC-5F	No catalyst	-	1.05	0	1.05	1700	3.2

General conditions: 150 mg of dried LC-5, 1 mL of DMAc (anhydrous) and 0.20 equiv. of catalyst (respectively to the total amount of -OH groups of lignin, calculated from ^{31}P NMR) are added into a crimp vial. The solution is stirred at 90 °C for 5 h. [a]: Determined from ^{31}P NMR. [b]: SEC-THF.

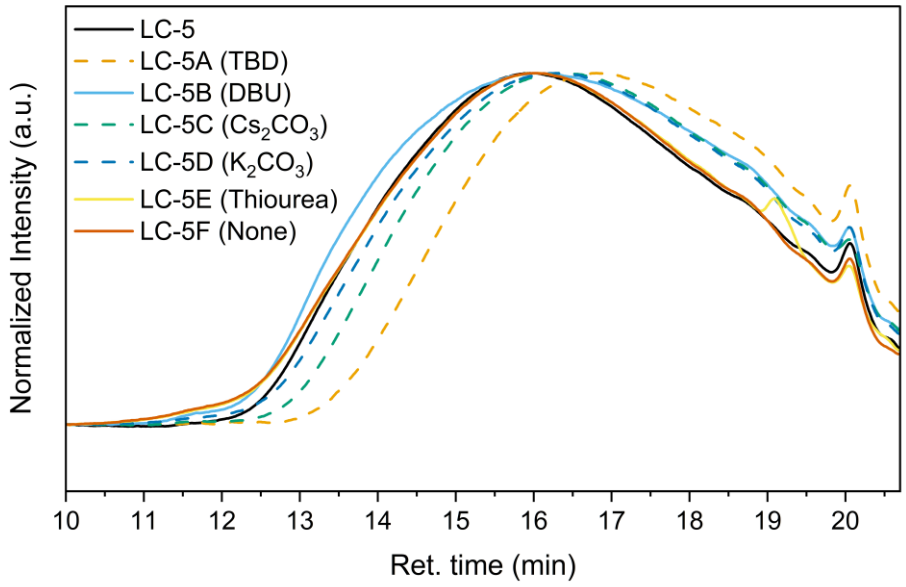

Figure 4.1.11 – SEC traces of the tested catalyst screening, as well as the starting material (intermediate LC-5, black). The dashed lines indicate depolymerization.

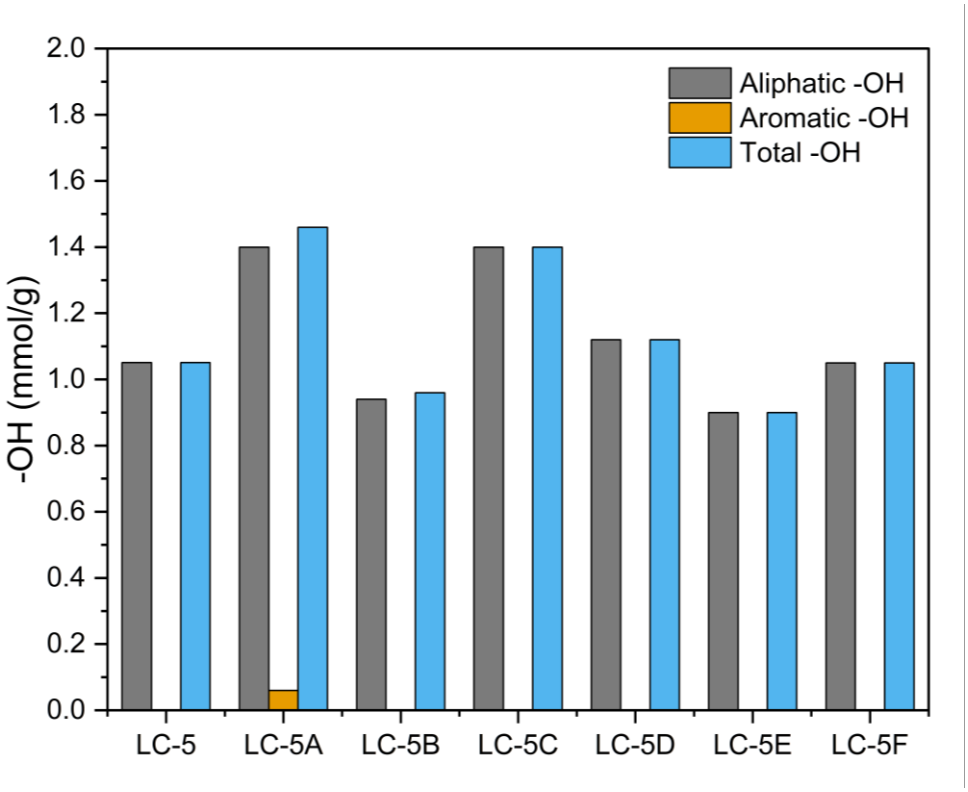

Figure 4.1.12 – Column bar graph showing the -OH distribution for the starting material (intermediate LC-5) and the self-condensation tests (LC-5X).

The SEC and ^{31}P NMR data (**Figure 4.1.11** and **Figure 4.1.12**) indicate that defunctionalization occurred in most cases. When no catalyst was used, or when thiourea (Schreiner′s thiourea catalyst) was employed, the SEC trace closely resembled that of the starting material. The ^{31}P NMR data confirm that no reaction occurred in the absence of a catalyst, whereas the use of thiourea resulted in a slight decrease in hydroxyl group content, as observed in the case of DBU, suggesting partial reaction. While both DBU and thiourea resulted in comparable dispersity and M_n values, the use of DBU as a catalyst resulted in a small high molecular weight shoulder in the SEC trace, together with a reduction in hydroxyl group content and also lower molecular weight species. On this basis, DBU was considered the most favorable catalyst and was selected for subsequent experiments.

4.1.4.2.2 Solvent and Reaction Time Screening

The catalyst screening was initially conducted over a 5 h reaction time; therefore, it was important to assess the effect of longer reaction times. Another concern remained related to the use of DMAc as a solvent, encouraging the investigation of alternative solvents. Solubility tests of the intermediate revealed that Cyrene™ effectively dissolved it, making it a suitable candidate for subsequent reactions. (**Figure 4.1.13**). Therefore, Cyrene™ was selected as a potentially suitable solvent for the self-condensation step.

Figure 4.1.13 –Solubility tests of the intermediate (20 mg), with 0.4 mL of solvent (from left to right: Cyrene™, Ethyl acetate, 2-MeTHF, after vortexing for 5 minutes and gently heating).

At this stage, a series of experiments was designed to monitor the self-condensation reaction over time, using DBU as the catalyst in both DMAc and Cyrene™ as solvents. The same conditions applied in the catalyst screening (0.20 equiv. of DBU, in respect to the total amount of -OH groups of lignin, 90 °C) were maintained, and aliquots were collected from each solvent after 3, 24, and 48 h (detailed procedure is reported in the Exp. Section, **paragraph 6.4.2.3**). These samples were analyzed by SEC to follow the evolution of the molecular weight during the reaction. However, as can be seen in **Figure 4.1.14** and **Table 4.1.9**, in both cases the molecular weight remained constant or decreased over time. Defunctionalization appeared to be slightly more pronounced when the reaction was carried out in DMAc. Nevertheless, this approach was discarded, as

the lignin hydroxyl groups exhibited insufficient reactivity to achieve the desired product.

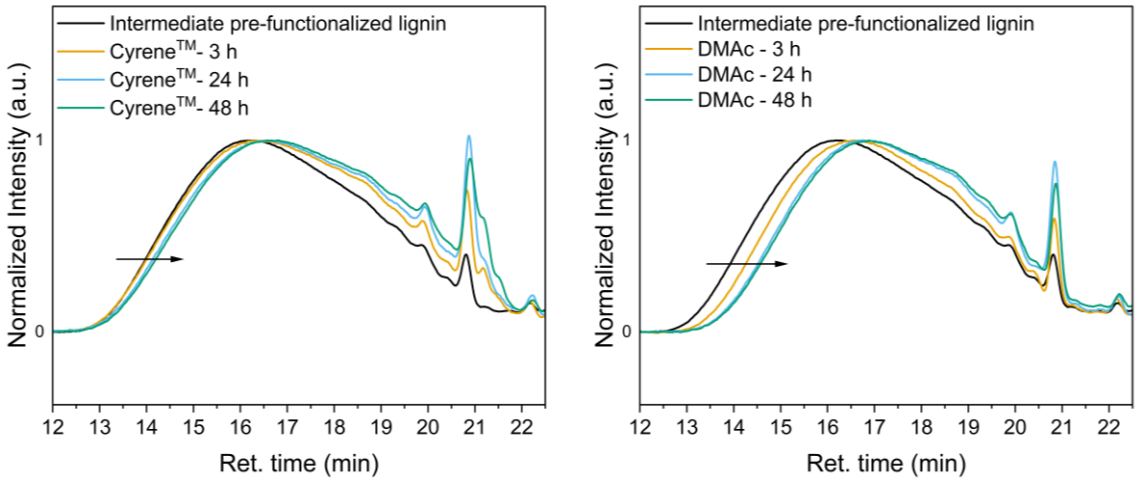

Figure 4.1.14 – SEC traces of the self-condensation aliquots performed in Cyrene™ and DMAc after 3, 24 and 48 h.

Table 4.1.9 – SEC data for the self-condensation screening with DBU as catalyst and longer reaction times, employing Cyrene™ and DMAc as solvents.

Solvent	Time Aliquot (h)	M_n (g·mol^{-1})[b]	$Đ$
Intermediate pre-functionalized lignin[a]	-	1100	3.1
Cyrene™	3	700	4.5
Cyrene™	24	700	4.3
Cyrene™	48	700	4.3
DMAc	3	600	4.5
DMAc	24	700	3.8
DMAc	48	600	3.9

[a]: Due to depletion of the initial starting material (LC-5), a second batch of the same material was synthesized and used for the experiments in chapter **4.1.4.2.2** and **4.1.4.2.3**. This batch displayed a different initial M_n, which is reflected in the corresponding SEC data. [b]: SEC-THF.

4.1.4.2.3 Condensation with 1,12-Dodecanediol

As a final proof of concept, an external diol (1,12-dodecanediol) was employed to promote the condensation, as can be seen in **Scheme 4.1.6**. For this purpose, the exact amount of carbonate moieties present in the intermediate had to be quantified, which was achieved through quantitative ^{13}C NMR analysis (**Figure 4.1.15**, procedure details can be found in **Chapter 6.2**).

Scheme 4.1.6 – Overall scheme for self-condensation in the presence of the external diol 1,12-dodecanediol.

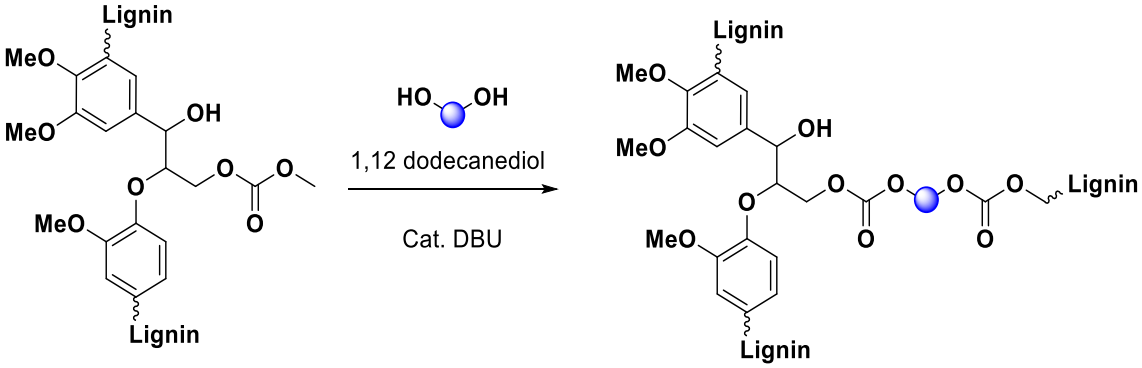

Pre-functionalized Lignin **Cross-linked lignin**

The ^{13}C NMR spectrum shows the appearance of a new signal at 156 ppm, attributed to the carbonyl carbon of the carbonate moieties introduced upon reaction with DMC. From this signal's integral ratio, it was possible to calculate a value of 0.28 $mmol \cdot g^{-1}$ of carbonyl groups, which was used as the reference value for determining the stoichiometric amount of 1,12-dodecanediol required for the subsequent condensation experiments. Additional evidence for successful functionalization is provided by the signals associated with methoxy groups and with the **S** (syringyl) and **G** (guaiacyl) units in their etherified and non-etherified forms (*e.* and *n.e.* in **Figure 4.1.15**, respectively). As shown in the spectrum, the intensity of the resonance corresponding to the non-etherified structures

decreases evidently, indicating that etherification is occurring to a significant extent.

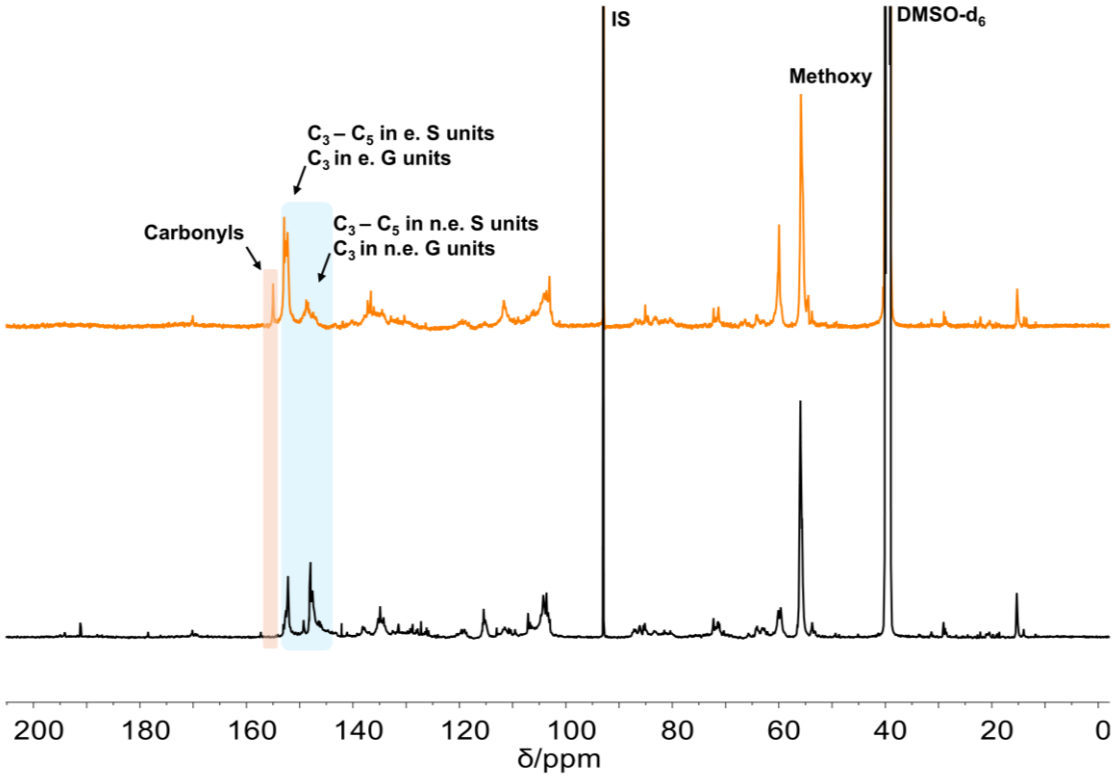

Figure 4.1.15 – ^{13}C NMR overlay in DMSO-d_6 between the starting material OL (black) and the intermediate pre-functionalized lignin (orange). Highlighted in orange is the carbonyl signal used for the carbonyl quantification. **IS**: Internal standard 1,3,5-trioxane.

A stoichiometric amount of hydroxyl groups from 1,12-dodecanediol relative to the carbonate groups was required to prevent over-functionalization of lignin and to ensure that polymerization and eventually cross-linking occurred selectively between the chains. The reaction was performed at 90 °C, in the presence of 0.2 equiv. of DBU (relative to the carbonate moieties), with DMAc as a solvent (for detailed procedure, see the Exp. Section, **paragraph 6.4.2.4**). The reaction progress was monitored by SEC. As shown in **Figure 4.1.16**, even after extended reaction times, no significant increase in molecular weight was detected. Instead, a slight shift toward lower molecular weights was observed, indicating that dpolymerization and/or defunctionalization predominates over condensation under these conditions.

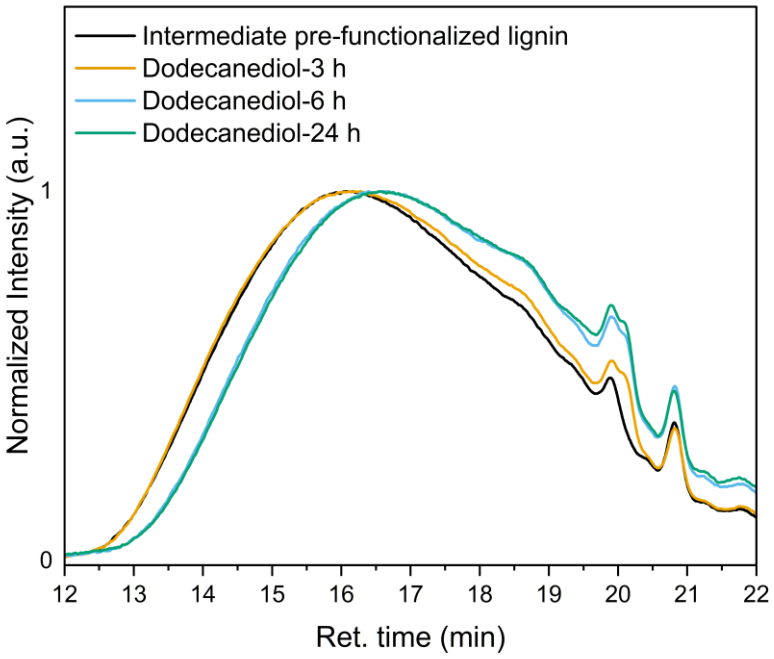

Figure 4.1.16 – SEC traces of the condensation of the intermediate with 1,12-dodecanediol in DMAc.

Table 4.1.10 – SEC data for the self-condensation screening with 1,12-dodecanediol in DMAc as solvent and DBU as catalyst.

Solvent	Time Aliquot (h)	M_n (g·mol^{-1})[b]	$Đ$
Intermediate pre-functionalized lignin[a]	-	1100	3.1
DMAc-dodecanediol	3	1100	3.5
DMAc-dodecanediol	24	1000	3.1
DMAc-dodecanediol	48	1000	3.3

[a]: Due to depletion of the initial starting material (LC-5), a second batch of the same material was synthesized and used for the experiments in chapter **4.1.4.2.2** and **4.1.4.2.3**. This batch displayed a different initial M_n, which is reflected in the corresponding SEC data. [b]: SEC-THF.

4.1.5 Conclusions and Outlook

Overall, despite extensive optimization efforts, none of the investigated self-condensation strategies yielded the desired lignin-derived polycarbonates. All tested conditions—variations in catalyst, reaction time, solvent, or the use of an external diol—consistently resulted in partial or pronounced depolymerization rather than polymerization or cross-linking. These results indicate that neither the reactivity of the remaining aliphatic –OH groups in the intermediate, nor the carboxymethyl functionalities with an external diol are sufficient to promote effective condensation under the conditions explored. On a side note, the initial functionalization of lignin with DMC to yield the intermediate “Pre-functionalized Lignin” was a successful step within the workflow, yielding a complete methylation of the aromatic hydroxyl groups and partial reactivity of the aliphatic hydroxyl groups. Because of the reactivity limitations observed in this work, this project was discontinued due to time constraints and the results described above, indicating that the idea behind this approach is practicably not feasible. Nevertheless, the results obtained do not preclude future investigations, for instance the use of the pre-functionalized lignin for other polymerization approaches.

4.2 Lignin-NIPUs *via* HOSO-derived Polyamine

This chapter is partially based on the publication:[305]

F. C. Destaso; C. Libretti; C. Le Coz; E. Grau; H. Cramail and M. A. R. Meier Optimized synthesis of a high oleic sunflower oil-derived polyamine and its lignin-based NIPUs. *Green Chem.*, **2025**, *27*, 1440-1450.

Additional experimental procedures, optimization studies, and analyses not included in the publication were carried out as part of the doctoral research and are discussed in detail in the present chapter.
The co-author, F. C. Destaso, contributed to the conceptualization of the project, investigation of the reaction conditions for the synthesis of HOSO-PA in batch, to the interpretation of the corresponding data, and to the optimization and upscaling of the HOSO-PA synthesis under continuous-flow conditions, formal analysis, and writing of the original draft.

C. Le Coz performed the DMA analyses and provided valuable input.

Regarding the synthesis of HOSO-PA in batch, only the experiments solely conducted by the author of the thesis are reported in this chapter. Regarding the synthesis of HOSO-PA in flow, the experiments were conducted together with Dr. F. C. Destaso within the framework of the collaborative project.

All additional experiments, data interpretation, and the extended discussion were conducted within the scope of this thesis.

4.2.1 Abstract

In the continuing effort toward reducing reliance on fossil resources, the transition to biobased materials is of utmost importance, together with the adoption of more sustainable and safe production processes. This work focuses on the implementation of renewable resources and greener protocols for the synthesis of a bio-based amino crosslinker and its subsequent use in non-isocyanate polyurethane (NIPU) synthesis. NIPUs are a new class of materials, analogous to isocyanate-derived polyurethanes (PUs), that avoid hazardous chemicals in their production process, such as phosgene and isocyanates, which raise high concern in the PU manufacturing processes. Vegetable oils and lignin are two abundant renewable feedstocks largely investigated during the last decade. In this paper, the synthesis of a high oleic sunflower oil (**HOSO**) derived polyamine (**PA**) *via* thiol-ene photoreaction in batch and in flow is studied. Additionally, cyclic carbonate functionalized lignin (**CCLF**) was synthesized and reacted with **PA** to create fully bio-based NIPU networks with different lignin contents. The curing behavior as well as the characterization of the obtained thermosets are described.

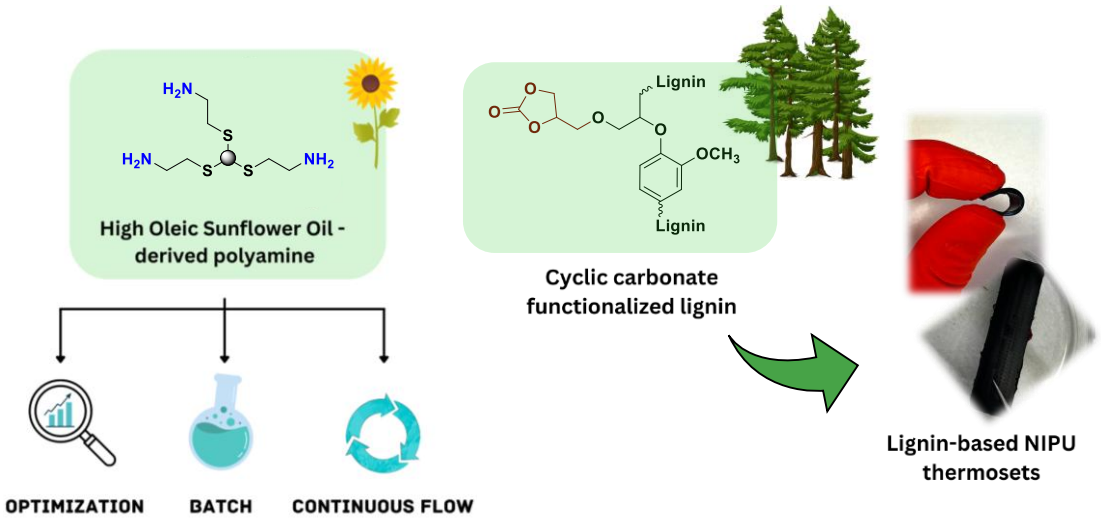

4.2.2 Introduction

With a global market production of 25 million tons,[306] polyurethanes (PU) are a class of polymers useful for many applications, such as coatings, adhesives, foams, sealants, elastomers, and more.[307,308] Among their relevance in everyday human life, PU production faces significant obstacles, mainly due to the use of isocyanates. Isocyanates are known to be irritant and sensitizing agents.[309,310] Even worse, their production relies on the use of phosgene, a highly toxic gas. Both their precursor, phosgene, and isocyanates themselves present several concerns correlated to toxicity[311] and carcinogenicity.[312] Moreover, the most commonly used diisocyanates (toluene diisocyanate, TDI, $LD_{50\ oral\ rat}$ = 5130 mg/kg and methylenediphenyl diisocyanate, MDI, $LD_{50,oral,rat}$ = 4130 mg/kg)[313] have been restricted in their use by REACH regulations.[314,315] The most updated REACH regulation limits the presence of isocyanates in formulations to a maximum of 0.1% by weight.[316] For all these reasons, current research efforts in the area of PUs concern the development of isocyanate-free routes to isocyanate-derived PU replacements to generate a new class of materials named non-isocyanate polyurethanes (NIPUs).[313,317] Common pathways may involve, for instance, transurethanization reactions or aminolysis of cyclic carbonates, generating, respectively, polyurethanes and polyhydroxyurethanes (PHU). In a world increasingly driven by the need for more sustainable solutions, shifting toward greener protocols that adhere to the principles of *Green Chemistry* is imperative.[18] This involves, for instance, the utilization and valorization of renewable resources to increase the bio-content of materials and reduce waste. Numerous studies concerning the development of bio-based NIPUs using various renewable feedstocks, such as terpenes, biomass or oleochemicals, can be found in the literature.[318–323]

Lignin, accounting for up to 40 wt.% of the biomass content,[103] is the most abundant renewable source of aromatic compounds. However, lignin is usually treated as a low-value by-product of the pulp and paper industry, and is often

thermally utilized as biofuel.[103,324] The utilization of lignin as an attractive macromonomer in NIPU formulations is yet scarcely researched. A study from 2017 reports the use of cyclic carbonate-functionalized lignin as a cross-linker in different PHU formulations in the presence of 1,12-diaminododecane and poly(ethylene glycol) bis-cyclic carbonate as a chain extender.[325] However, the protocol employs an epichlorohydrin ($LD_{50,oral,rat}$ = 175 mg/kg) route followed by CO_2 insertion for the synthesis of the lignin monomer. Additionally, the final materials were too brittle for mechanical characterization. More recently, several works describe the development of more sustainable protocols based on a two-step modification with organic carbonates; the thereof derived PHUs were characterized in detail.[271,276,326]

While bio-based cyclic carbonate monomers are well-researched, bio-based polyamines are still required as important building blocks to achieve fully bio-based NIPUs. Such renewable polyamines are far less frequently described.

With a global annual production of 210.3 MMT (million metric tons), vegetable oils are an important class of renewable feedstock.[327] Their abundance and structural variety render them suitable sources for the synthesis of many different bio-based monomers and polymers.[328] The key characteristic of triglycerides is the presence of one or multiple unsaturations, facilitating easy functionalization or cleavage of the structure.[329–331] In the field of NIPUs, different examples of polycyclic carbonate monomers obtained from triglycerides are reported.[332,333] Moreover, the presence of double bonds in triglycerides allowed the introduction of primary amine moieties *via* thiol-ene chemistry.[77] Following this approach, a variety of (bio)polyols were synthesized employing mercapto alcohols. Furthermore, Meier *et al.* reported the first procedure to achieve a difunctional amine from limonene *via* thiol-ene reaction with cysteamine hydrochloride as the sulfur-containing molecule bearing a primary amine moiety. Following this work, the application of this route was extended to vegetable oils, such as grapeseed oil and canola oil, more recently by others.[16, 35] Here, a bio-based polyamine derived from high oleic sunflower oil was synthesized *via* thiol-ene chemistry.

Reaction conditions were thoroughly investigated and optimized, testing two different reaction systems in batch and continuous flow. Subsequently, the polyamine was utilized in the formulation of fully biobased PHUs, together with cyclic carbonate functionalized lignin and erythritol bis-cyclic carbonate, obtaining flexible materials with tunable lignin content.

4.2.3 Synthesis of HOSO-derived PA in Batch

High oleic sunflower oil was chosen to be modified with cysteamine due to its quite homogeneous fatty acid composition (≥ 85% oleic acid, for complete characterization of the oil see Experimental Section, **Paragraph 6.5.2**) to yield a renewable polyamine (**PA**).

Scheme 4.2.1 – General reaction scheme for the synthesis of **PA**. On the bottom left (box inset) of the scheme, a simplified structure of **PA** is provided and will be used throughout this chapter for clarity.

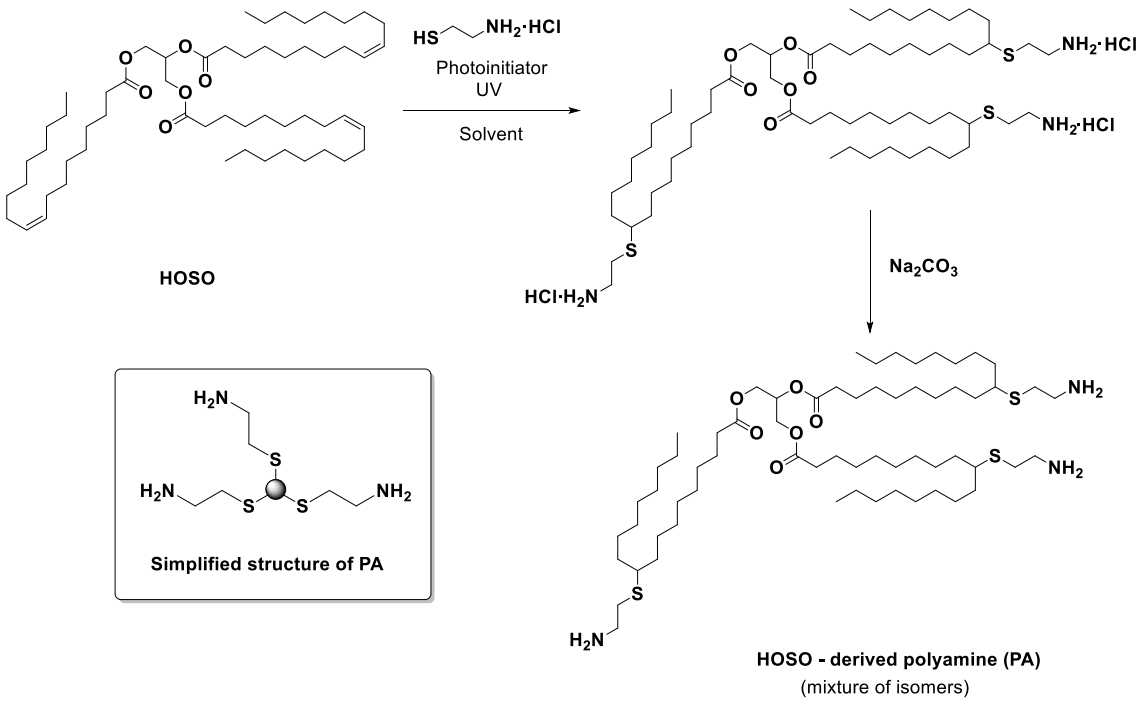

To understand and optimize the reaction, the solvent and photoinitiator concentration, wavelength and light intensity were investigated. First, 2,2-dimethoxy-2-phenyl-acetophenone (**DMPA**) was chosen, as it is a widely used benzoin ether photoinitiator. Because the oil and the cysteamine hydrochloride salt (**CAHC**) were not soluble in the same medium, a solvent mixture of dichloromethane and ethanol was initially tested. However, also with this combination the mixture never fully homogenized due to the excess of the cysteamine salt used. In order to find a more suitable solvent mixture, initial investigations were conducted by repeating a literature known procedure from

Stemmelen *et al*.,[335] where a solvent mixture of 1,4-dioxane:ethanol (7:3) was employed. However, in order to comply with the principles of *Green Chemistry* to avoid unsafe chemicals, dioxane was replaced in the solvent mixture by isopropanol, as reported by Rios *et al.*[320] Initially, this solvent mixture was tested in a LED setup with 365 nm. LEDs have the advantage of not producing notable amounts of heat and therefore the distance between light and the sample can be reduced. A considerable advantage of LEDs is their lowered energy consumption.

Table 4.2.1 – Overview of conditions tested for **PA** synthesis in batch utilizing UV irradiation. A UV lamp (45 W or 45 W+12 W) and 365 nm LED system (2 W) were used (setup UV systems: see Experimental Section **6.5.1**). DMPA was used as photoinitiator, 0.1 equiv. per double bond of the oil were used.

Entry	Solvent mixture	DMPA (equiv./db)	UV system	Addition of CAHC	Scale (g)	Conversion after 48 h (%)
1	iPrOH:EtOH	0.1	2	One step	2	71
2	iPrOH:EtOH	0.1	1	One step	1	63
3	iPrOH	0.1	1	One step	1	84
4	iPrOH	0.1	3	Stepwise	1	98
5	iPrOH	0.1*	1	One step	1	85

General conditions: Concentration of the HOSO is kept 0.22 g/mL for all entries. Temperature is r.t. and 3 equiv. per double bond of CAHC were employed in all entries. *: Stepwise addition of DMPA.

In this first experiment, the conversion (calculated from the integral of the double bond, for details see Experimental Section, **Paragraph 6.5.2.5**) reached 71 % after 48 h (**Table 4.2.1**, Entry 1). Changing the UV irradiation system to a UV lamp with 365 nm and lowering the reaction scale did not improve the conversion, that reached only 63 % (**Table 4.2.1**, Entry 2). However, by changing the solvent mixture to only isopropanol (iPrOH) under the same reaction conditions, the

conversion improved from 63 to 84 % (**Table 4.2.1**, Entry 2 and 3, respectively). Finally, by adding another source of irradiation at the same wavelength of 365 nm (12 W) to the flask and implementing a stepwise addition of **CAHC** method, a conversion of 97 % after 24 h was observed (**Table 4.2.1**, Entry 4). A stepwise addition can be beneficial from a point of view of turbidity of the reaction mixture. **CAHC** only partially solubilizes in the reaction medium. A high turbidity of the reaction mixture is disadvantageous for homogeneous and effective light penetration, which is a crucial factor for photoreactions.

As a last parameter, a multistep addition of the photoinitiator was also tested. Keeping a single step addition of **CAHC**, the photoinitiator **DMPA** was added to the reaction mixture in two aliquots, with a 2 h difference between them. This, however, did not improve the conversion compared to the same reaction conditions with a single addition of **DMPA** (**Table 4.2.1**, Entry 5 and 3, respectively). In **Figure 4.2.1** an overview of the most important conditions tested is presented.

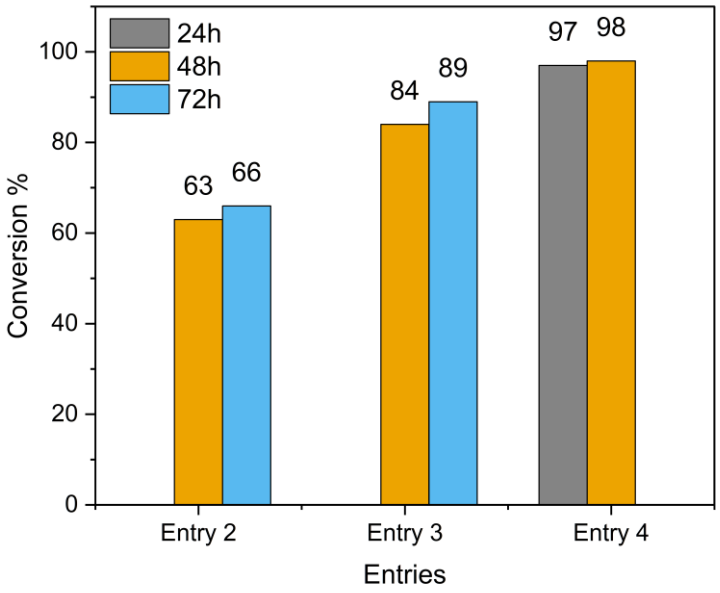

Figure 4.2.1 − Overview of the different experiments conducted to investigate the influence of CAHC addition on the synthesis of PA. **Entry 2**: single step addition of CAHC, in EtOH:iPrOH 1:1; **Entry 3**: single step addition of CAHC in iPrOH; **Entry 4**: Stepwise addition of CAHC (half of the calculated total amount at the starting time, then a quarter of the total amount after 1.5 h, the remaining quarter after 4 h) in iPrOH. DMPA was used as photoinitiator for each entry. For all entries the scale of the reaction corresponds to 1 g of oil. Concentration is 0.22 g/mL for each entry.[336]

4.2.4 Synthesis of HOSO-derived PA in Flow

As a further promising path to scale up the production of the desired polyamines, the reaction depicted in **Scheme 4.2.1** was also investigated using a flow reactor equipped with a 365 nm UV lamp (see Experimental Section, **Figure 6.5.4**). Due to the long reaction time necessary to achieve complete conversion, the mixture was run in a closed loop system, and aliquots were collected to monitor the process. Isopropanol was selected as a solvent due to its good performance in bulk reactions and different flow rate values were screened. It was noticed, as could be expected in the used closed loop setup, that increasing the flow rate led to improved conversion at the same reaction time. The best outcome was achieved with 9 mL/min with a conversion of 99 % after 6 h (**Table 4.2.2**). For a better comparison of the different flow rates, conversions after 3 h are summarized in **Figure 4.2.2**. Thus, at high flow rates, higher conversions can be achieved, at the same increased scale of 2 g. In summary of all reported optimization reactions, PA can now be prepared in larger scales at shorter reaction times and by using less environmentally problematic solvents.

Table 4.2.2 – Overview of the different flow rates tested for the synthesis of PA via continuous flow chemistry. DMPA was used as photoinitiator for each entry, all experiments were carried out under 365 nm irradiation. For all entries, the scale of the reaction corresponds to 2 g of oil. Concentration is 0.14 g/mL for each entry.

	Time (h)	Flow rate (mL/min)	Conversion[a] (%)
Entry 1	6	0.5	87
Entry 2	3[b]	1	88
Entry 3	6	2	97
Entry 4	6	9	99

[a]: determined from ^{1}H NMR from the integral ratio of the double bond protons.

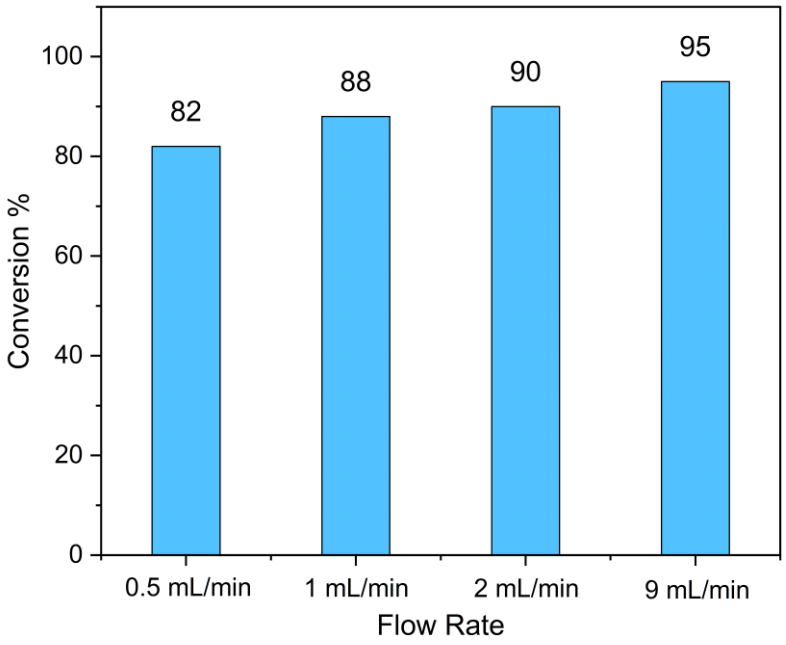

Figure 4.2.2 – Conversions of double bonds of HOSO *via* thiol-ene reaction in flow at different flow rates after 3 h. To evaluate the conversion, a 100 µL sample was taken at different reaction times and ^{1}H NMR was recorded. Reactions in isopropanol with a flow rate 0.5 mL/min, 1 mL/min, 2 mL/min and 9 mL/min were performed.

4.2.5 Lignin Functionalization with Cyclic Carbonates

Lignin functionalization was performed following a two-step modification with organic carbonates as benign reactants and solvents. The procedure was adapted and modified from Lehnen *et al*.[271] Briefly, a two-step procedure was employed. First, glycerol carbonate (**GC**) was utilized to introduce further 1,2-diol moieties to the structure of lignin. Subsequently, these 1,2-diols underwent ring closure to 5-membered cyclic carbonates by further treatment with DMC, as shown in **Scheme 4.2.6**. The first step of the modification is solventless, as glycerol carbonate acts both as reactant and solvent, the second step was further optimized proving that a solventless procedure is also possible, achieving similar results compared to the one using solvent. In the first step of the synthesis, several side reactions are possible depending on the type of hydroxyl groups reacting. A more detailed discussion highlighting different reactivities is reported herein.

It is known that the reaction between the hydroxyl groups of and organic carbonates can take place at both the electrophilic sites of the carbonyl and the alkyl carbons of an organic carbonate, generating, carbonyl and ether linkages, respectively (see **Scheme 4.2.2**).[93,258,337] Regarding cyclic carbonates, several studies have been conducted in order to gain insights on the different reactivities. For instance, in the work of Lehnen *et al*.[256,258] oxyalkylation of beech wood organosolv lignin with propylene carbonate was investigated, showing that the formation of carbonate linkages is favored by longer reaction times, higher catalyst amounts and equivalents of propylene carbonate used. Under their optimized conditions, only 0.3 % of the total propyl units were grafted *via* carbonate linkages.

Scheme 4.2.2– General scheme illustrating different reactivities for hydroxyl groups of lignin and a general structure of a cyclic carbonate.

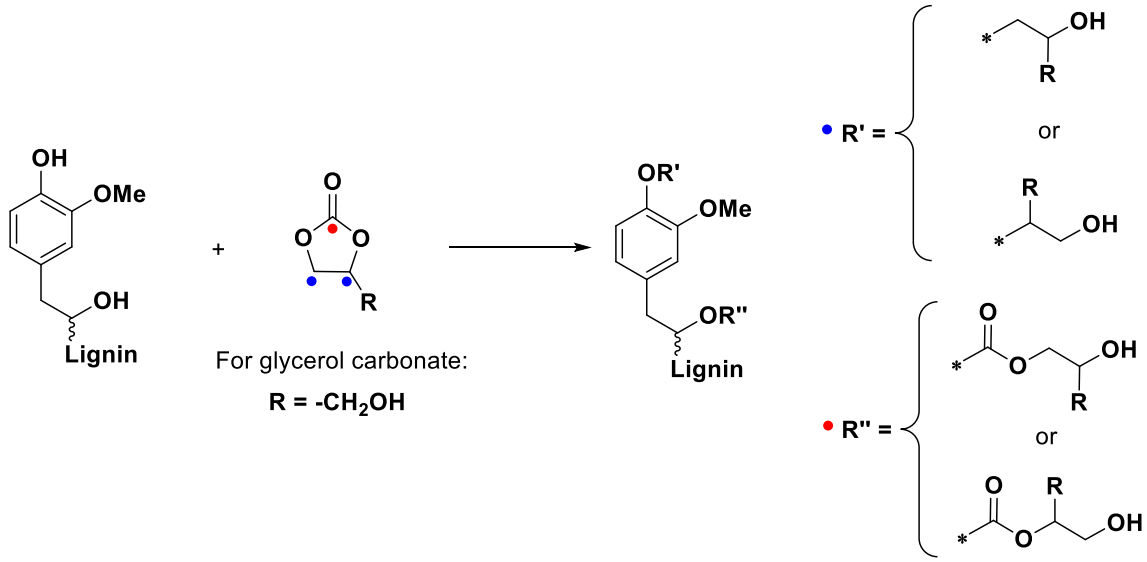

In another study from Avérous *et al.*,[337] oxyalkylation of lignin was investigated with four different cyclic carbonates. Among them, **GC** was tested as well. According to their IR data, for all other derivatives a new peak between 1728 and 1743 cm^{-1} is forming, corresponding to the C=O stretching band of linear carbonate linkages. Interestingly, in the case of oxyalkylation with **GC**, this peak was shifted to higher wavenumbers (1786 cm^{-1} for Avérous *et al.*;[337] 1789 cm^{-1} in this work) in the range of cyclic carbonates, suggesting a competing reaction between the formed 1,2-diols and **GC**, as can be seen in **Scheme 4.2.3**.

Scheme 4.2.3 – Side reaction between newly inserted 1,2-diols and excess glycerol carbonate, leading to cyclic carbonate structures and generating glycerol as by-product, as reported from Duval and Avérous and Lehnen *et al.*[256,337]

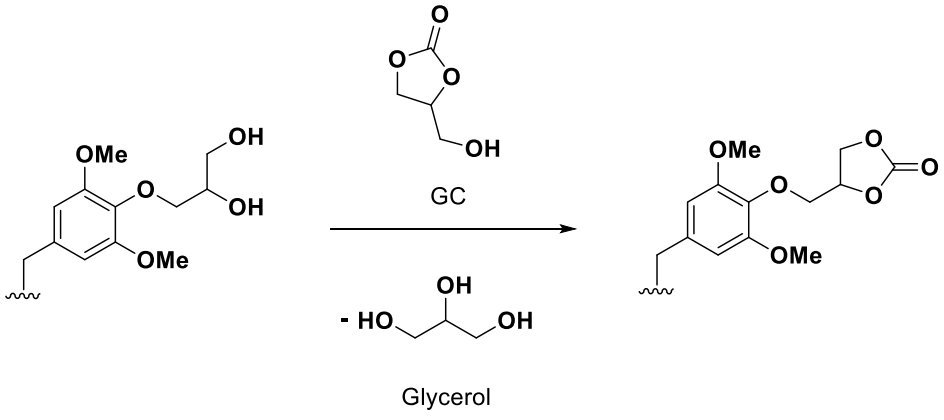

This was further confirmed in the same study *via* hydrolysis of the aforementioned carbonates. Complete hydrolysis was confirmed *via* IR spectroscopy, while it was possible to distinguish that 1,2-diols structures substantially increased after hydrolysis, while the content of 1,3 diols was unaltered *via* ^{31}P NMR spectroscopy, confirming the presence of five-membered cyclic carbonate structures prior to hydrolysis. These results were also in accordance with the findings from Lehnen *et al.*,[256] where cyclic carbonates structures could also be observed after oxyalkylation with **GC**.

Based on these considerations, it can be assumed that the etherification pathway will be the preferred one in the reaction with **GC** and some cyclic carbonate structures will already be present after the first step of the modification. However, since this reaction does not reach completion (a high amount of hydroxyl groups is still present, as can be observed from ^{31}P NMR), the second step of the modification is necessary to achieve a high degree of functionalization with cyclic carbonate structures.

4.2.5.1 Hydroxyalkylation of Lignin

The first step of the synthesis was the hydroxyalkylation of **OL** with **GC**, in order to obtain Hydroxyalkylated Lignin (**HAL**).

Scheme 4.2.4 – General reaction scheme for the synthesis of Hydroxyalkylated Lignin. Only isomers of the etherification pathway with GC are shown, leading to 1,2-diols and 1,3-diols structures. For a comprehensive overview of all the possible structures, see **Scheme 4.2.2** and **Scheme 4.2.3**.

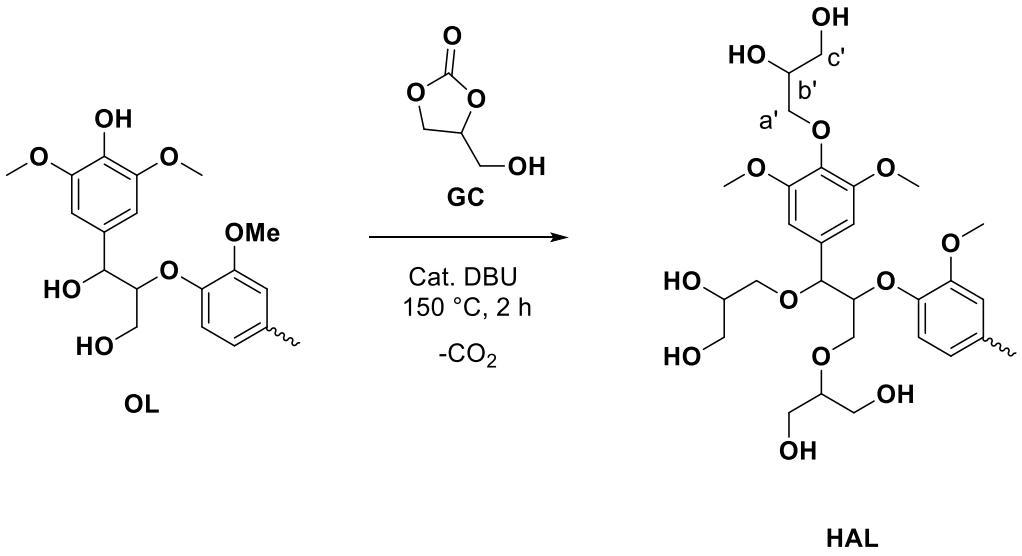

Several literature examples have already researched the reaction between lignin or tannins with cyclic carbonates, especially as potential replacement for alkylene oxide for the synthesis of lignin-based polyols.[93,258,269]

To adapt literature protocols to the available lignin source and identify suitable reaction conditions, an initial screening of the oxyalkylation of lignin with **GC** was carried out. The reaction time was fixed at 2 h, as a preliminary experiment conducted for 3 h resulted in a product that remained fully soluble in the acidic aqueous medium used during the precipitation work-up. Because temperature is known to play a decisive role in oxyalkylation reactions, a series of three experiments was performed to determine the optimal temperature (**Table 4.2.3**).

Table 4.2.3 – Optimization experiments for the oxyalkylation of OL with GC under different temperatures.

Sample	T (°C)	$OH_{Aliphatic}$ (mmol·g^{-1})[a]	$OH_{Aromatic}$ (mmol·g^{-1})[a]	COOH (mmol·g^{-1})[a]	OH_{Total} (mmol·g^{-1})[a]
OL	-	2.42	1.83	0.1	4.35
HAL-1	170	-[b]	-[b]	-[b]	-[b]
HAL-2	160	-[c]	-[c]	-[c]	-[c]
HAL-3	150	4.35	0	0	4.35

General conditions: 1 g of OL (previously dried) are dissolved in 10 equiv. of GC and 0.1 equiv. DBU is added (equiv. are in respect to the -OH groups of OL). The reaction mixture is allowed to react for 2 hours at the desired temperature under Ar flow.[a]: Calculated from ^{31}P NMR. [b]: Not soluble in the $CDCl_3$:Py solvent mixture used for ^{31}P NMR. [c]:Only partially soluble in the $CDCl_3$:Py solvent mixture used for ^{31}P NMR.

An initial reaction temperature of 170 °C (**HAL-1**) yielded a highly viscous material that was difficult to handle and process during the work-up. In addition, part of the product was completely insoluble in DMSO, suggesting the occurrence of undesired crosslinking. In contrast, reducing the temperature to 160 °C (**HAL-2**) improved the work-up and the entire product could be isolated. However, in both cases partial or complete insolubility in the solvent mixture required for ^{31}P NMR analysis was observed, preventing quantification by this method. This behavior is most likely attributable to the high degree of functionalization and resulting increase in aliphatic hydroxyl content, which could negatively impact solubility. Further lowering the reaction temperature to 150 °C (**HAL-3**) finally produced a material that was fully soluble and could be characterized by both IR and ^{31}P NMR spectroscopy. Under these conditions, a quantitative conversion of aromatic hydroxy and carboxylic acid groups into aliphatic hydroxyl groups was achieved.

As can be depicted from IR spectroscopy of the experiments (**Figure 4.2.3**), typical signals associated with a successful reaction can be clearly identified. An increase in the broad O–H stretching vibration (3000–3500 cm^{-1}) is observed, consistent with the formation of newly introduced 1,2- and 1,3-diol structures within the lignin backbone. This is accompanied by an enhanced C–H stretching

signal of methylene groups (2800–3000 cm^{-1}) and an increase in the band intensity in the C–O stretching region characteristic of ether linkages (1000–1100 cm^{-1}). Interestingly, a C=O stretching vibration band appeared at 1790 cm^{-1}, suggesting the presence of cyclic carbonate structures. These structures form due to the side reaction between the newly formed 1,2 diols and excess of **GC** (see **Scheme 4.2.3**), as already reported from Lehnen *et al.*[256] and Duval and Avérous.[337] This is also confirmed by ^{13}C NMR analysis, that shows a carbonyl peak ("d") forming after hydroxyalkylation (**Figure 4.2.6**). Furthermore, although the formation of linear carbonate structures cannot be fully excluded under these conditions, it is expected to be restrained due to the reasons mentioned above (**paragraph 4.2.5**).

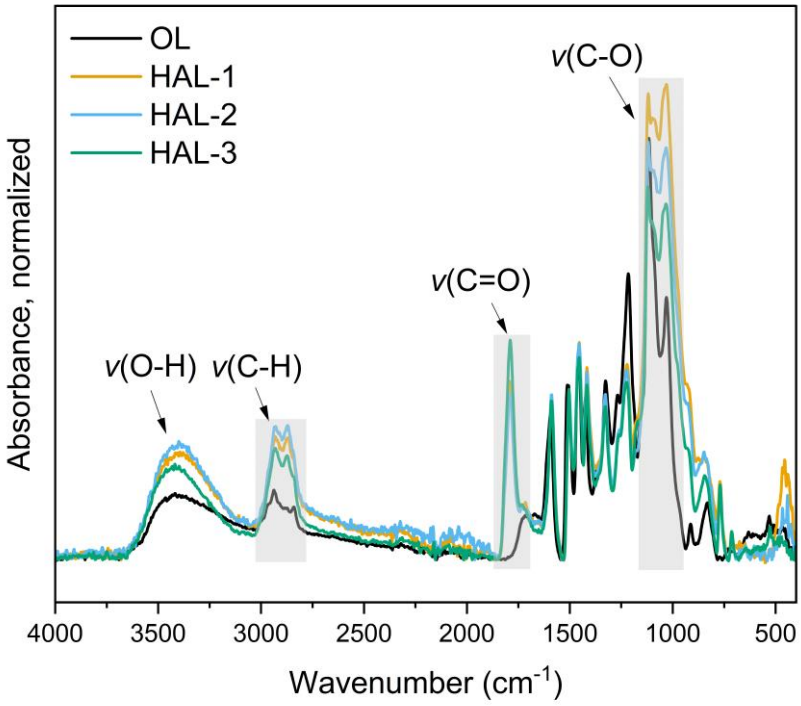

Figure 4.2.3 – IR spectra overlay of the starting material (OL, black) and the experiments HAL-1 (orange), HAL-2 (blue) and HAL-3 (green). Spectra were normalized for the aromatic C=C stretching vibration at 1504 cm^{-1}.

The conditions of **HAL-3** were deemed satisfactory and were selected for a scale-up in a 10 g batch of **HAL**, in order to proceed with the second step of the functionalization.

4.2.5.2 Cyclocarbonation of Lignin

For the second step of the synthesis, involving the formation of five-membered cyclic carbonate structures on lignin (cyclic carbonate-functionalized lignin, **CCFL**), several conditions were tested in order to identify the best conditions.

Scheme 4.2.5 – General reaction scheme for the synthesis of cyclic carbonate functionalized lignin. The main reaction leading to the formation of cyclic carbonate structures is shown, as well as the formation of linear carbonates due to the reaction of hydroxyl groups with only one side of DMC. Both possible isomers deriving from etherification with GC are shown (forming 1,2-diols and 1,3-diols).

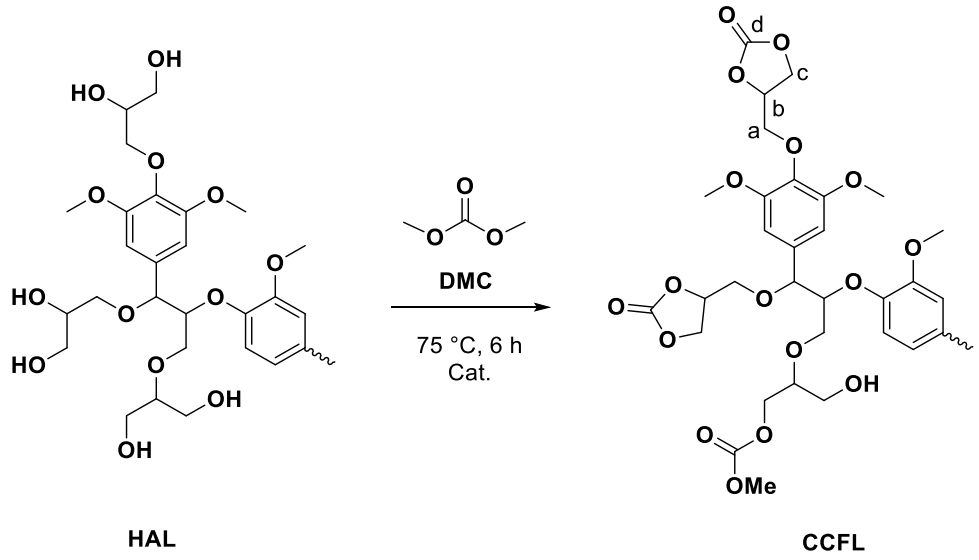

Initially, the inorganic base K_2CO_3 was selected as catalyst (0.4 equiv.) together with 5 equiv. of DMC, in DMSO as solvent. In this initial screening phase, the reaction was evaluated by ^{31}P NMR spectroscopy in order to identify the most suitable reaction conditions. As shown in Entries 1 and 2 (**Table 4.2.4**), increasing the reaction temperature from 75 °C to 90 °C did not significantly influence the conversion; the reduction in hydroxyl-group content remained comparable (26 % and 22 %, respectively). In line with the considerations discussed in **paragraph 4.1.3.4**, where DMSO as solvent proved to strongly influence the -OH groups distribution, a control experiment in the absence of DMC was also performed, with DMSO as solvent, to check the influence of the solvent on lignin (**Table 4.2.4**, Entry 3). In this case, no change in the hydroxyl-group distribution was observed, in contrast to the decrease observed in the previous chapter (**paragraph 4.1.3.4**). A plausible explanation is the substantially higher lignin concentration employed

in this system compared to the conditions examined previously (0.4 g lignin·mL $DMSO^{-1}$ in this system *vs*. 0.05 g lignin·mL $DMSO^{-1}$ in the previous experiments, see **Chapter 4.1**), together with the use of a different catalyst (K_2CO_3 here, instead of DBU previously) and a lower temperature (75 °C here, instead of 90 °C previously). Nevertheless, changing the solvent from DMSO to DMAc proved beneficial for the reaction (Entry 1 and 4, **Table 4.2.4**).

Table 4.2.4 – Optimization parameters for the reaction between HAL and DMC, in order to yield CCFL.

Entry	Solvent	T (°C)	Time (h)	Catalyst	Reagent	Reduction in - OH groups (%)
CCFL-1	DMSO	75	6	K_2CO_3	DMC	26
CCFL-2	DMSO	90	6	K_2CO_3	DMC	22
CCFL-3[a]	DMSO	75	6	K_2CO_3	-	2
CCFL-4	DMAc	75	6	K_2CO_3	DMC	35
CCFL-5	DMAc	75	6	TBD	DMC	47
CCFL-6[b,c]	-	75	6	TBD	DMC	-
CCFL-7[c]	-	75	6	DBU	DMC	64
CCFL-8[d]	DMAc	75	6	TBD	DMC	65

General conditions: 0.2 g of HAL is dissolved in a solvent (dry, anhydrous) in a concentration of 0.4 g/mL. Subsequently, 5 equiv. of DMC (anhydrous, related to the -OH group content), as well as the catalyst (0.4 equiv.) are added. The reaction mixture is stirred under Ar atmosphere for the desired time and temperature. [a]: control reaction in absence of DMC. [b]: heterogeneous reaction mixture, no stirring possible. [c]: Performed on a 1 g scale in bulk. [d]: scale-up on a 6 g scale.

Moreover, in DMAc, TBD performed better than K_2CO_3, resulting in a 47 % reduction of hydroxyl groups compared to 35 % (Entries 5 and 4, respectively, **Table 4.2.4**). In line with the principles of *Green Chemistry*, solvent-free (bulk) conditions were also evaluated. TBD was initially retained as the catalyst due to its favorable performance in solution; however, in the absence of solvent the reaction mixture became highly heterogeneous and insoluble in DMC, rendering these conditions unsuitable (Entry 6, **Table 4.2.4**). When TBD was replaced with DBU under bulk conditions, a significantly higher reduction in hydroxyl groups (64 %) was achieved (Entry 7, **Table 4.2.4**). Finally, the reaction was successfully scaled up to a 6 g batch (Entry 8, **Table 4.2.4**), while maintaining a similar level of conversion (65 % reduction in hydroxyl groups). While bulk conditions were effective at a smaller scale, scale-up was performed under solvent-based conditions to ensure reaction homogeneity and adequate solubility.

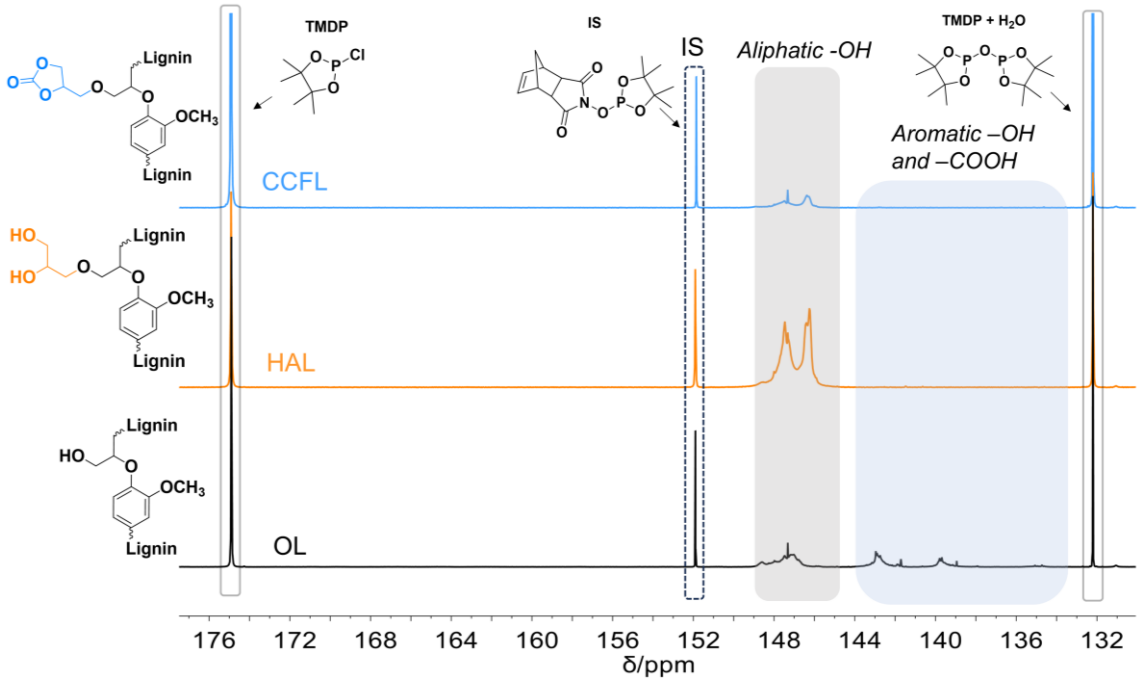

Figure 4.2.4 – Overlay of ^{31}P NMR spectra for OL (black), HAL (orange) and CCFL (blue). After hydroxyalkylation, a complete conversion of aromatic hydroxyl and carboxylic acid groups is observed, as well as a concomitant increase of aliphatic hydroxyl groups.

As depicted from **Figure 4.2.4**, it is possible to follow visually and quantitatively the changes in the -OH distribution after each modification. In particular, after the first step of the modification with **GC**, full conversion was observed for aromatic and carboxylic acid groups, to aliphatic ones. In particular, for **HAL**, two signals are visible, due to the primary and secondary alcohols formed at the end of the grafted chain.[256] After subsequent reaction with dimethyl carbonate, a strong decrease in aliphatic hydroxyl groups is observed, as a consequence of cyclic carbonate moieties formation.

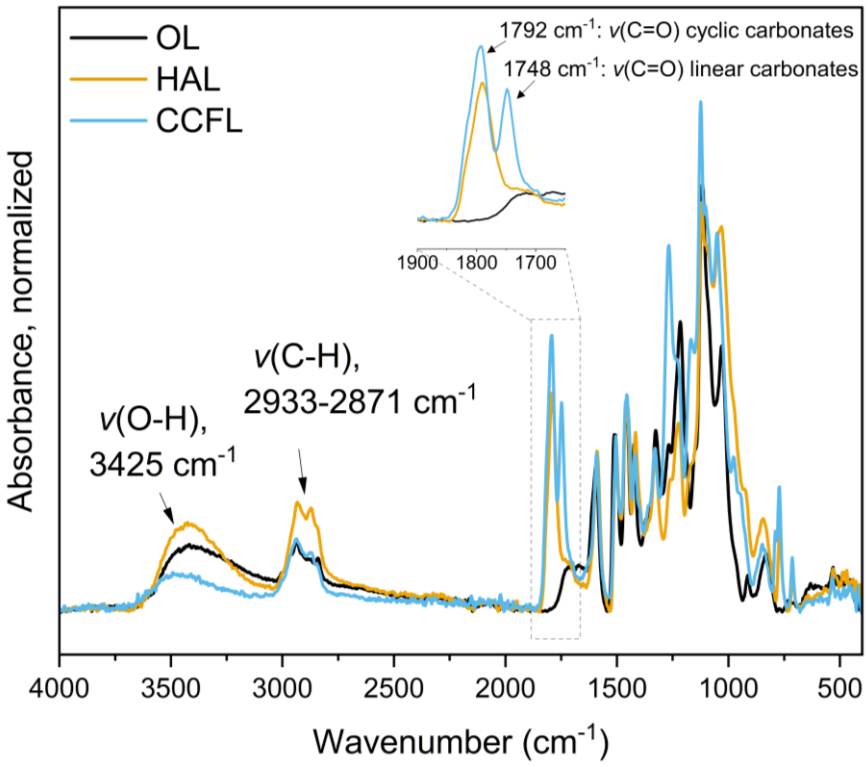

Figure 4.2.5 – Overlay of IR spectra for OL (black), HAL (orange) and CCFL (blue); all spectra are normalized to the signal at 1504 cm^{-1}, ascribed to the C=C aromatic stretching vibration that is not affected during the modifications.

After reaction with DMC, the signal of cyclic carbonate stretching vibration increases further, and a new signal appears at 1748 cm^{-1} (**Figure 4.2.5**), due to the formation of linear carbonates between alcohols and one functionality of DMC, as depicted in **Scheme 4.2.5**.

From quantitative ^{13}C NMR (**Figure 4.2.6**), it was possible to gain further insights into the reaction outcome. The increasing signal ascribed to the carbonyl of cyclic carbonates structures (d) is already present after hydroxyalkylation step, due to the side reaction shown in **Scheme 4.2.3**. Additionally, the signal attributed to the C_3-C_5 of etherified syringyl and guaiacyl units increases, while the signal for the C_3-C_5 of non-etherified syringyl and guaiacyl units decreases, providing further confirmation of a successful reaction (both highlighted in gray).

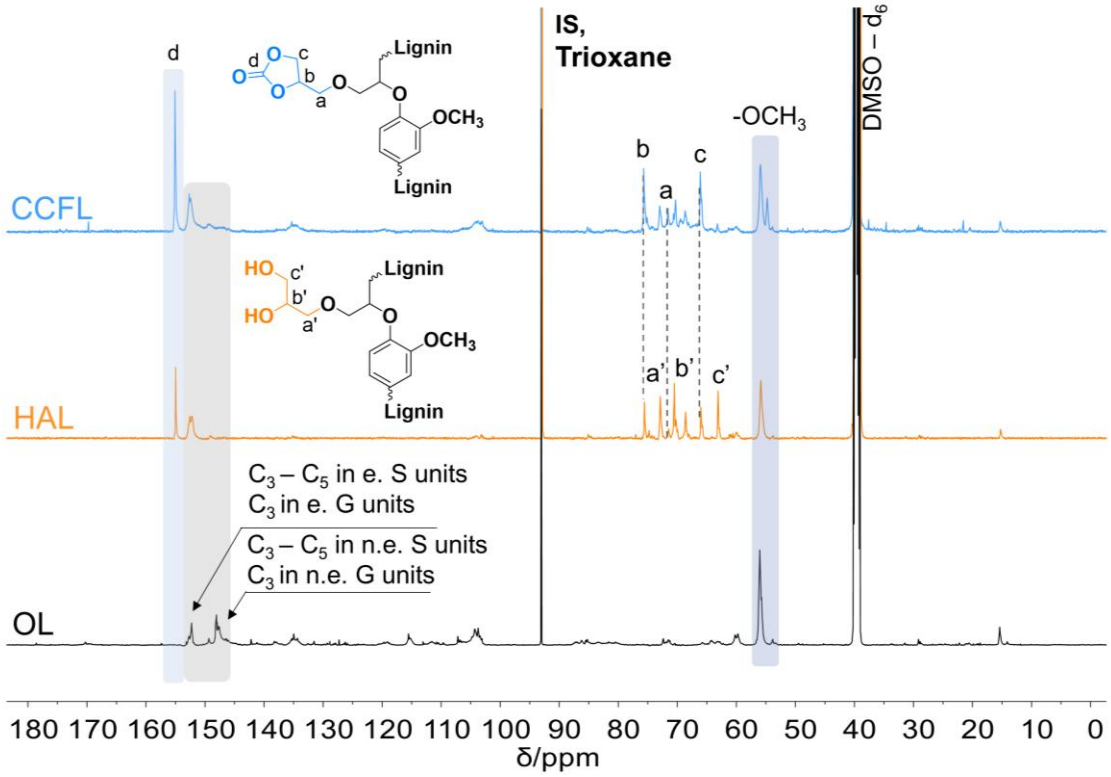

Figure 4.2.6 – Overlay of ^{13}C NMR spectra for OL (bottom), HAL (middle) and CCFL (top). Peak assignment was performed based on literature values.[271]

In **Table 4.2.5**, an overview of the analytical data of the starting material **OL**, as well as **HAL** and **CCFL** is presented.

Table 4.2.5 – Overview of the analytical data for the starting material OL, HAL and CCFL.

Entry	$OH_{Aliphatic}$ (mmol·g^{-1})[a]	OH_{Total} (mmol·g^{-1})[a]	M_n (g·mol^{-1})[b]	$Đ$[b]	Carbonyl content (mmol·g^{-1})[c]
OL	2.42	4.35	5000	2.6	-
HAL	4.66	4.66	13800	4.8	0.34
CCFL	1.64	1.64	12600	3.9	0.91

[a]: determined from ^{31}P NMR. [b]: SEC-DMAc. [c]: Determined *via* quantitative ^{13}C NMR.

4.2.6 Thermosets NIPUs

PA was employed as a crosslinking agent for the formation of non-isocyanate polyurethane (NIPU) networks together with cyclic carbonate functionalized lignin (**CCFL**) and erythritol-bis cyclic carbonate (**EBC**), to afford renewable thermosets as shown in **Scheme 4.2.6**.

Scheme 4.2.6 – General reaction scheme for lignin functionalization to achieve CCFL, and subsequent reaction with EBC and crosslinker PA to form NIPU networks. For simplicity, only the main reactions are shown.

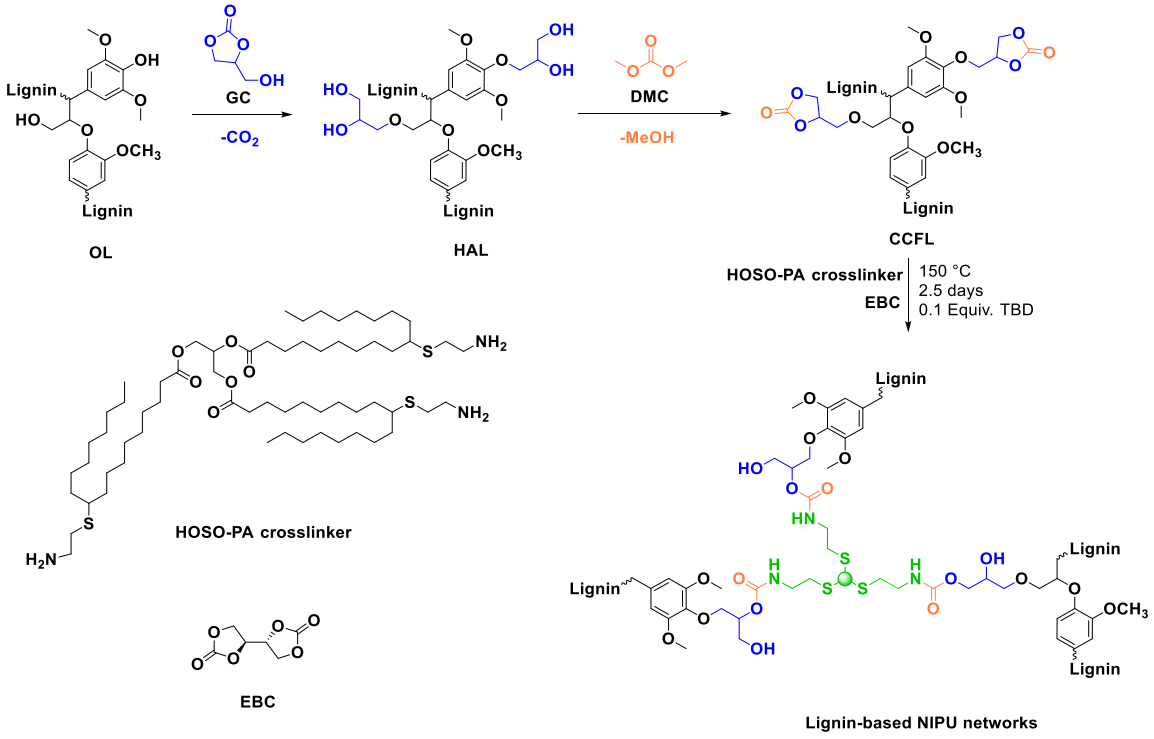

Having both monomers in hand, the curing behavior of the lignin-NIPU thermosets (**Scheme 4.2.6**) was followed by IR spectroscopy. Initially, thermosets with only cyclic carbonate functionalized lignin (**CCFL**, 0.89 mmol·g^{-1} carbonate moieties) and **PA** were synthesized, with a CC:NH_2 ratio of 1:1 and 1:1.5. For both formulations, the samples resulted in a very brittle material after curing, breaking instantly when recording IR spectra (**Figure 4.2.7**).

Figure 4.2.7 – Picture of a first batch of thermosets without erythritol bis-cyclic carbonate as third component, with CC:NH_2 ratio of 1:1 (left) and 1:1.5 (right). The material was brittle and broke during IR measurements. *Picture taken by the author*.

Therefore, a third bifunctional component was added to the thermoset formulation to achieve more flexible materials, decreasing the crosslinking density inherently brought by the lignin macromolecular structure. Thus, erythritol bis-cyclic carbonate (**EBC**) was synthesized following a more sustainable procedure developed by Meier *et al.*[338] starting from erythritol, a naturally occurring polyalcohol present in fruit and used as sweetener. Initial experiments were conducted with **PA** and **EBC** only. However, without the contribution of lignin, a network was not successfully formed, resulting in materials lacking structural integrity and exhibiting very high viscosity, making them difficult to handle. This outcome reinforces the fact that the optimal formulation for the thermosets relies on the contribution of all three components (**CCFL**, **EBC** and **PA**) to form a PHU network efficiently. Considering the chemical nature of the three components, their combination can overcome the typical brittleness of lignin-containing materials.

Due to the solid nature of lignin and **EBC**, a minimal amount of DMSO was employed to aid the mixing of the monomers. The viscous-liquid nature of **PA** also contributed an efficient and homogeneous mixing of all the components. Different thermoset compositions were prepared, an overview is reported in **Table 4.2.6**.

Table 4.2.6 – Overview of the molar and weight composition for the synthesized thermosets, with different lignin content.

Entry	Cyclic carbonate component (Equiv.)			Amine component	Catalyst	Lignin content (mol%)[a]	Lignin content (wt%)[b]
	EBC	CCFL	Total equiv.	PA (Equiv.)	TBD (Equiv.)		
1	0.85	0.15	1	1	0.1	15	**26**
2	0.75	0.25	1	1	0.1	25	**38**
3	0.50	0.50	1	1	0.1	50	**56**
4	0.25	0.75	1	1	0.1	75	**67**

[a]: molar content of **CCFL** (in percent) with respect to the total moles of cyclic carbonate component. [b]: weight content of lignin (in percent) with respect to the total weight of all components, not considering the weight of the solvent.

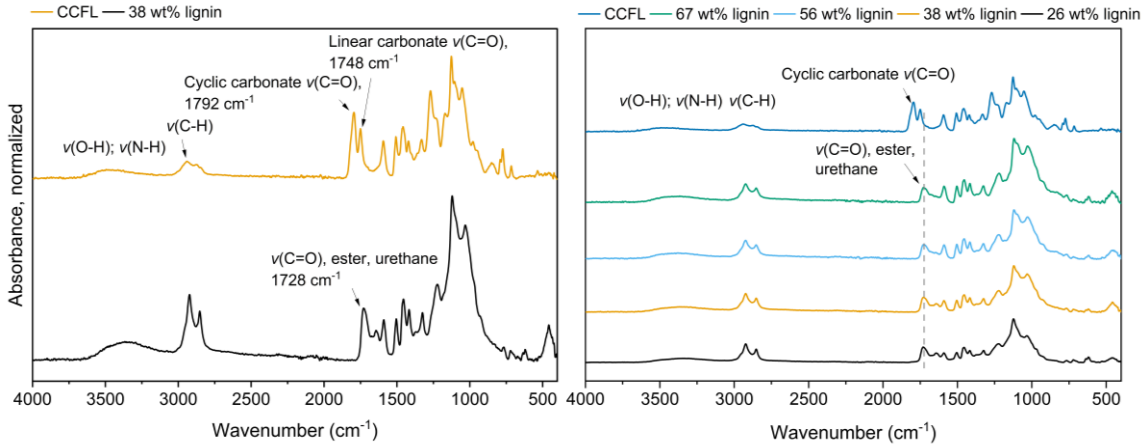

Figure 4.2.8 – Left: overlayed IR spectra of CCFL (orange, top) and the thermoset with 38 wt% lignin content (**Table 4.2.6**, entry 2, black, bottom). Right: overlay of IR spectra of CCFL (blue, top) and the thermosets with different lignin compositions (see **Table 4.2.6**). Relevant signal changes are highlighted.

Initially, a 38 wt% lignin formulation with **EBC**, **CCFL** and **PA** was prepared. Its curing behavior was followed in time at 150 °C *via* IR spectroscopy, revealing an optimal curing time of 2.5 days, as after this time the signal ascribed to the cyclic carbonate *ν*(C=O) at 1792 cm^{-1} was no longer observed. Next, applying these conditions, four different lignin weight percentages were tested, 26, 38, 56 and

67 wt% (see **Table 4.2.6**). IR spectroscopy of the cured thermosets is shown in **Figure 4.2.8**. Comparing the IR spectrum of **CCFL** (**Figure 4.2.8**, left, top) with the fully-cured thermoset with 38 wt.% lignin (**Figure 4.2.8**, left, bottom), different signals show the successful formation of the PHU thermosetting network. In particular, a strong increase in the stretching vibration signal ascribed to C-H bonds (2760 – 3000 cm^{-1}) relates to the incorporation of the aliphatic fatty acid chains into the structure of the thermoset. Also, *v*(O-H) and *v*(N-H) stretching vibration signals (3100 – 3600 cm^{-1}) increased as a consequence of the formation of hydroxyl groups due to ring opening of cyclic carbonate and urethane moiety formation, respectively. The disappearance of the cyclic carbonate *v*(C=O) signal (1792 cm^{-1}) confirms the effective curing of the material, while a new signal at 1728 cm^{-1} is associated with the *v*(C=O) of both ester and urethane moieties overlapping with each other. In **Figure 4.2.8**, right, an overlay of all IR spectra of the thermosets with different lignin compositions is shown. The absence of the cyclic carbonate *v*(C=O) stretching absorbance reveals an effective reaction in all compositions.

4.2.6.1 Gel Content and Swelling Properties

Gel content and swelling behavior of the thermosets were investigated according to the procedure described in the supporting information and are reported in **Table 4.2.7**. Typically, these tests provide valuable insights into the material's crosslinking density: the higher the gel content of the material, the higher the crosslinking degree. The soluble fraction typically consists of low molecular weight impurities, unreacted starting materials, or products of low crosslinking density. Here, the presence of soluble oligomeric structures can be excluded as indicated by SEC analysis (see **Figure 4.2.9**).

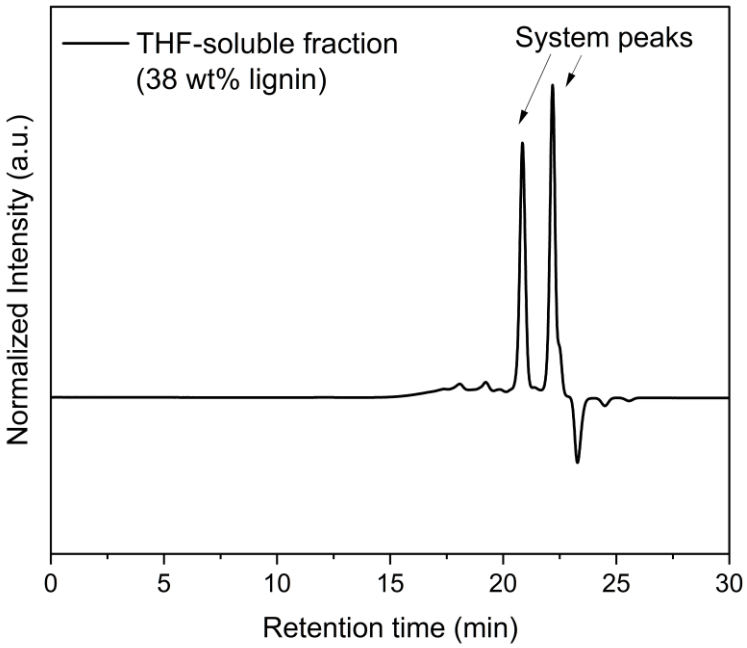

Figure 4.2.9 – SEC plot of the soluble fraction of the thermoset containing 38 wt% lignin after gel content determination.

A clear trend can be identified in both parameters related to lignin content of the PHUs. As the lignin content increases, the swelling percentage decreases, while the gel content exhibits the opposite trend. For the lowest lignin content (26 wt%), the crosslinking density is the lowest among all compositions. This is because **EBC**, which does not contribute to cross-linking, accounts for the majority of cyclic carbonate moieties. As the lignin percentage increased, the crosslinking density also increased. Consequently, the gel content rises, reaching a maximum of 98 % for 67 wt% lignin, and the swelling decreased to 41% for the highest lignin composition. Generally, the results show a satisfactory gel content in all compositions, demonstrating the efficient formation of a network.

4.2.6.2 Thermal Properties of the Thermosets

The thermal properties of the thermosets were also investigated. Initially, thermal stability was analyzed by TGA (**Figure 4.2.10**, right). All thermosets showed a higher thermal stability compared to the precursor **CCFL**.

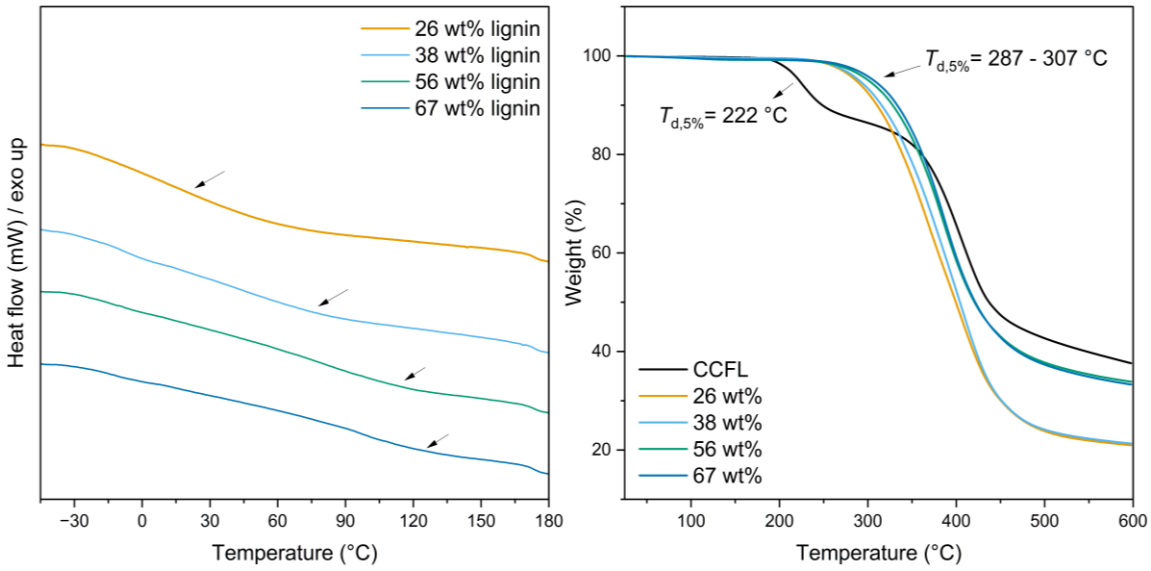

Figure 4.2.10 – Left: DSC thermograms of thermosets with different lignin weight percentages (compare **Table 4.2.6**), right: TGA decomposition curves for the **CCFL** (black) and the thermosets with different lignin weight percentages.

Moreover, they all showed a single-step decomposition curve, corresponding to the degradation of the thermoset structure. In contrast, **CCFL** showed a two-step decomposition curve, where the first step could be ascribed to the cyclic carbonate moieties and the second one to the aromatic structure of lignin. Increased lignin content contributed to improved thermal stability ($T_{d,5\%}$ = 287 °C, $T_{d,50\%}$ = 400 °C for 26 wt% lignin; $T_{d,5\%}$ = 307 °C, $T_{d,50\%}$ = 422 °C for 67 wt% lignin), because a higher amount of lignin increases the cross-linking density. Furthermore, lignin is generally known to enhance thermal stability.[339,340] A trend in the char residue percentage (see **Table 4.2.7**) was observed, where the residue percentage increased with a higher lignin content (from 21.0 to 33.3 %), as lignin contributes to a higher char content.[341]

DSC thermograms of the different thermosets were also recorded to identify the possible presence of a T_g. **Figure 4.2.10**, left, shows the thermograms in a temperature range -30 to 180 °C. Assignment of a clear T_g value was not possible, as the range was too broad to identify it. This is probably a result of the complex and heterogenous networks formed. An increase in the heating rate from 10 to 30 K min^{-1} did not improve the quality of the thermograms. Nevertheless, a T_g is certainly present, as evidenced by the material's behavior when heated. Upon heating, in fact, the material's elasticity changed, making the thermosets appear more flexible, changing back to a more brittle state when cooled back to room temperature (r.t.). The only thermoset that remained very flexible at r.t. is the one with a 26 wt% lignin composition, which has a T_g range near r.t., as indicated by the thermogram.

Table 4.2.7 – Overview of the characterization data for thermosets with different lignin weight percentages.

wt% lignin	T_g (°C)[a]	$T_{d,5\%}$ (°C)	$T_{d,50\%}$ (°C)	Residue (%)	WCA (°)	Swelling (%)	Gel content (%)	Aspect
26	-30 − 60	287	400	21.0	81.13	96	79	Very flexible
38	20 − 80	290	404	21.3	87.99	48	87	Flexible
56	80 − 120	301	421	33.9	101.02	44	93	Fragile
67	90 − 130	307	422	33.3	95.66	41	98	Fragile

[a]: T_g ranges obtained from the DSC thermograms, precise assignation is not possible.

4.2.6.3 DMA Analysis

Amongst the different thermoset compositions that were not fragile (see **Table 4.2.7**), the one with the highest lignin content (38 wt%) was selected for DMA analysis. A representative curve of the storage modulus E' and the tan δ curve is shown in **Figure 4.2.11** and the results are reported in **Table 4.2.8**. The material presents a storage modulus below T_g ranging from 1970 MPa at - 30 °C to 1220 MPa at 25 °C (average values, see **Table 4.2.8**), which dropped reaching a minimum around a temperature of 150 °C ($E'_{150°C}$ = 5.72 ± 2.41 MPa). The glass transition (or α relaxation temperature, T_α) causes a large change in the material's elasticity, resulting in a decrease of the storage modulus and a peak in the tan(δ) curve. Lignin's aromatic backbone structure and crosslinking density are the main influencing factors for this change in the thermosets.

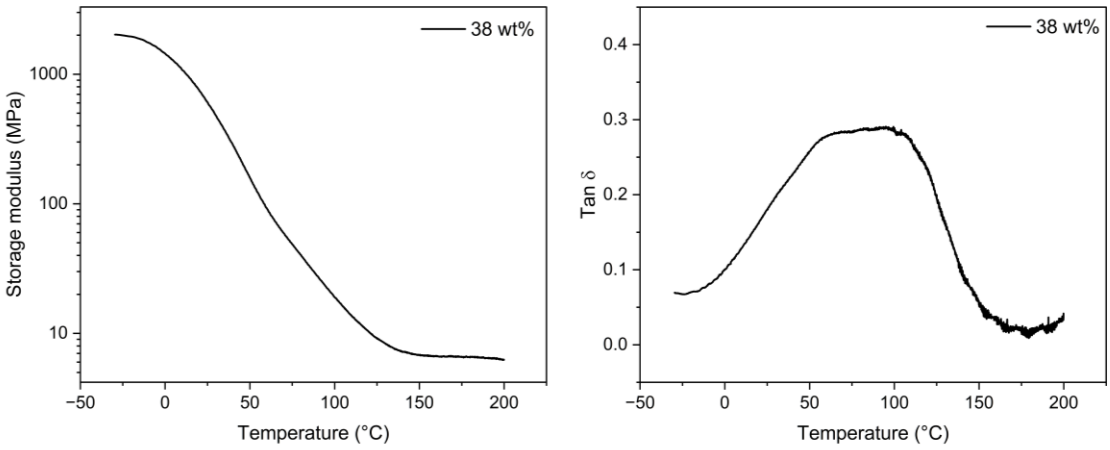

Figure 4.2.11 – Left: representative curve of the storage modulus (E') curve against temperature for the 38 wt% lignin content thermoset. Right: representative curve of the tan (δ) curve against temperature for the 38 wt% lignin content thermoset.

The glass transition can be measured from the onset of the storage modulus or the temperature at the maximum of the tan(δ) peak. The first method usually gives the lowest value of T_g and it is often a good indicator of when the mechanical strength of the material starts to fail. This value may be useful to consider for possible applications. For the composition with 38 wt% lignin

content, a maximum T_g of 97.3 °C was reached (peak tan(δ)), average value of three measurements, see **Table 4.2.8**), showing a value aligning with literature reported results for lignin-based NIPUs.[326]

Table 4.2.8 – DMA analysis results for the 38 wt% lignin content thermoset.

wt% lignin	$E'_{-30°C}$ (MPa)[a]	$E'_{25°C}$ (MPa)[a]	$E'_{150°C}$ (MPa)[a]	T_g Onset E' (°C)[a]	T_g Max tan δ (°C)[a]
38	1970 ± 386	1220 ± 223	5.72 ± 2.41	55.2 ± 2.4	97.3 ± 4.1

[a]: Measurements performed in triplicate. Overview of the triplicates is provided in the Experimental Section, **Paragraph 6.5.4.3**.

4.2.6.4 Water Contact Angle (WCA) Measurements

Hydrophobicity and wettability of the thermosets were investigated *via* static single-drop water contact angle (WCA) measurements. Usually, to be considered hydrophobic, a material should present a WCA higher than 90°. A material is considered superhydrophobic when the WCA is higher than 150°.[342] Due to its complex structure, rich in carbon and aromatics, lignin usually presents a more hydrophobic behavior compared to other bioderived polymers, *i.e.* cellulose or hemicellulose.[343] However, hydrophobic/hydrophilic behavior is strongly influenced by the type of functional groups present in the structure. The measurements of the different thermoset compositions reveal a gradual increase in hydrophobicity in concomitance with increasing the lignin content (see **Figure 4.2.12**), especially when higher than 38 wt%. This trend suggests that the hydrophobic nature of the modified lignin contributes to the final wettability of the material, considering that the molar amount of the **PA** is the same in every composition. Although the average value of the WCA for the 67 wt% formulation appears to be lower than the value for the 56 wt% formulation, the two resins behave quite similar within error margins.

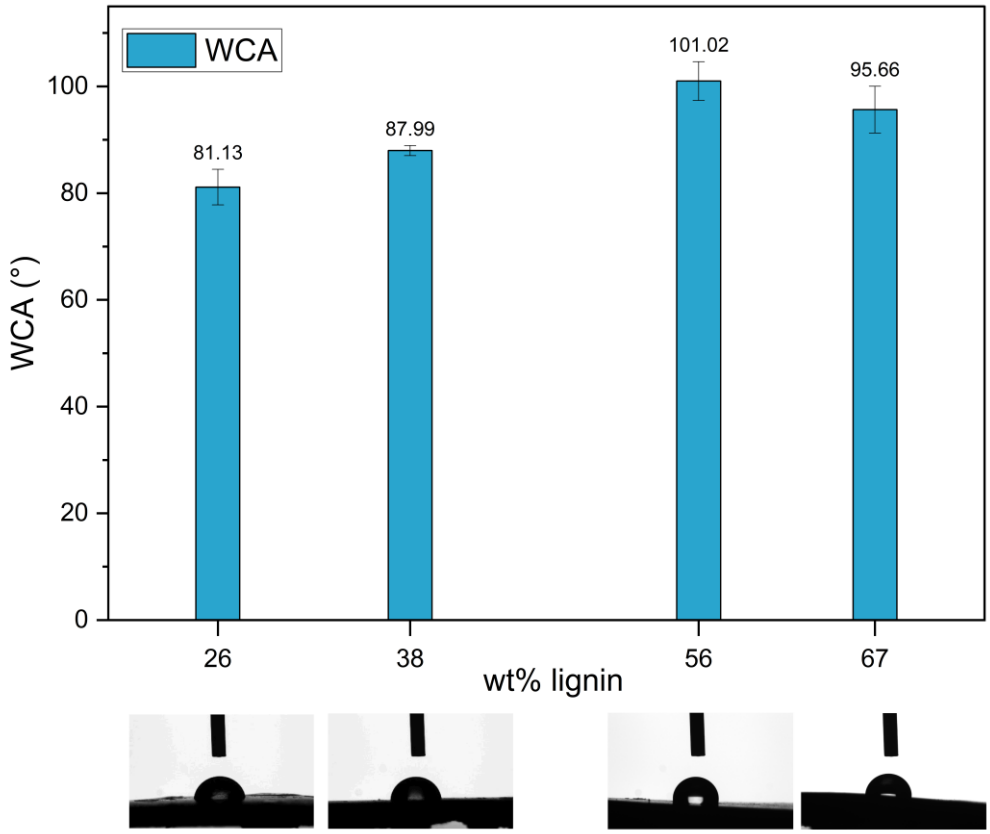

Figure 4.2.12 – Water contact angle measurements for thermosets with different lignin composition. Measurements were performed 5 times per sample to ensure reproducibility and average values are reported, as well as measurement errors.

To compare with literature data, a study showed that the inherently hydrophilic behavior of linear PHU coatings (due to the pendant hydroxyl groups) can be influenced by varying the chain length of the diamine.[344] However, contact angle measurements were still below 90° for all the formulation tested. Detrembleur *et al.*[345] on the other hand investigated the wettability for crosslinked PHUs obtained from cyclocarbonated soybean oil and different diamines revealing a high WCA of 103° for the formulation obtained with m-xylylenediamine (MXDA). This suggests a higher hydrophobicity for aromatic structures, compared to cycloaliphatic (isophorone diamine, 99°) and aliphatic (hexamethylenediamine, 95°) ones.

4.2.7 Conclusions and Outlook

This work represents the synthesis of a high oleic sunflower oil-based amino crosslinker *via* thiol-ene chemistry and its subsequent use in the production of lignin-based non-isocyanate polyurethanes (NIPUs). Although bio-based amines are a crucial component in NIPU formulations, they are rarely documented in the literature. The crosslinker structure was characterized in detail and reaction conditions were investigated both in batch and under continuous flow processes, resulting in a conversion of 99 % obtained in 6 hours and in a 2 grams scale, demonstrating the feasibility of scaling up the reaction. Furthermore, the oil-based amino crosslinker was employed for the synthesis of fully bio-based NIPUs together with cyclic carbonate functionalized lignin and erythritol bis-cyclic carbonate. The lignin content of the resulting thermosets was varied between 26 and 67 wt%, showing how lignin influences the properties of the final materials. IR spectroscopy confirmed the successful and complete curing in all formulations, which was further validated by high gel content values that increased proportionally with lignin content. Formulations up to 38 wt% of lignin were still flexible at room temperature conditions, whereas higher lignin contents resulted in fragile materials with poor mechanical performance. All formulations exhibited thermal stability up to 250 °C, with the 38 wt% lignin formulation showing a T_g of 97.3 °C, as determined by DMA analysis, indicating suitability for applications requiring both high thermal resistance and elevated T_g. The wettability of the materials was also examined, showing an increase in hydrophobicity with higher lignin content. In summary, this work highlights the potential of the bio-based amino crosslinker in the formulation of sustainable NIPUs and underscores the significant role of lignin content in tailoring the mechanical, thermal, and surface properties of the resulting materials.

4.3 Functionalization of Lignin with Cyclic Anhydrides

This chapter is partially based on publication:[346]

C. Libretti; G. G. Rizzo; S. Abou El Mirate; M. Johansson and M. A. R. Meier Biobased Epoxy Resins from Itaconic Anhydride–Functionalized Lignin: Insights and Comparison with Succinic Analogues. *RSC Sustainability*, **2026**, Accepted Manuscript.

The work presented here follows the structure and main findings of the accepted manuscript. Text, figures, and data are reproduced from this article and were partially edited and extended with permission from the Royal Society of Chemistry.

Additional experimental procedures, optimization studies and analyses not included in the manuscript were carried out as part of the doctoral research and are discussed in detail in the present chapter.

G.G. Rizzo and S. Abou El Mirate synthesized parts of the starting materials as well as parts of the thermosets library under co-supervision of the author (for details see Experimental Section, **Chapter 6.6**).
Moreover, part of the synthetic work involved in optimizing the lignin functionalization reaction was carried out by Aaron Seider in his role as a student research assistant, under the author's co-supervision.

All additional experiments, data interpretation, and the extended discussion were conducted within the scope of this thesis.

4.3.1 Abstract

Lignin, the most abundant renewable aromatic polymer, remains underutilized despite its potential as a sustainable feedstock for polymeric materials. In this work, lignin was functionalized with itaconic and succinic anhydrides to introduce carboxylic acid groups, enabling its use as a polyfunctional macromonomer. The influence of temperature, reaction time, reagent stoichiometry, and catalysts on the functionalization efficiency was systematically investigated. The lignin derivatives were furthermore utilized as crosslinkers for Passerini-three multicomponent reaction (3-MCR) thermosets, together with 1,6- or 1,12-diisocyanides, and nonanal. The lignin content was tuned producing lower and higher lignin content thermosets. Thermal properties of the resulting materials were analyzed and compared to succinic anhydride lignin derivatives, and their gel content was optimized investigating several parameters.

The itaconate lignin derivatives were incorporated correspondingly as crosslinkers into fully biobased epoxy resins formulated with epoxidized soybean oil and Pripol™ 1009, and their mechanical and thermal properties, as well as insights into the curing, were investigated in detail. Elastic moduli ranged from 4.87 to 1.24 MPa. The glass transition temperature (between -36 and -23 °C) was found to be primarily influenced by the aliphatic matrix, while the lignin content and the resulting network architecture strongly affected the mechanical properties of the materials. Comparative studies with succinic anhydride modified lignin highlighted the role of unsaturation due to itaconic acid in the network, especially for mechanical properties. Finally, degradation studies demonstrated depolymerization under alkaline hydrolysis, suggesting potential for designing easily cleavable thermoset systems. This work contributes to the development of greener epoxy networks and highlights lignin's versatility as a reactive renewable building block for sustainable polymer chemistry. Finally, a proof of concept for the synthesis of thermosets based on thia-Michael reactions using lignin itaconate derivatives is presented.

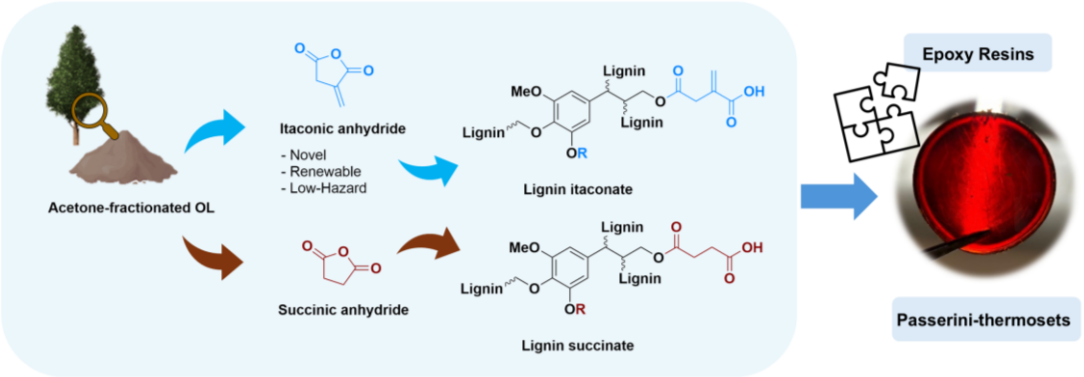

4.3.2 Introduction

Lignin offers a wide variety of functional groups, mainly hydroxyl (aliphatic and aromatic) and carboxylic acid groups, available for further modification. In particular, lignin can be used in the development of several resin types, offering a more sustainable alternative to petroleum-based products, such as in phenol-formaldehyde resins (PFs),[347,348] polyurethanes (PUs),[349,350] or non-isocyanate polyurethanes (NIPUs)[305,325,326] as well as epoxy resins.[351,352]

Among these materials, epoxy resins have attracted considerable attention, thanks to their excellent mechanical and thermal properties, broadening their range of application and expanding their global market.[353] However, inherent challenges associated with lignin epoxidation using ECH, as well as the reliance on petroleum-derived BADGE (bisphenol-A diglycidyl ether, a bisphenol-A derivative), and the toxicity concerns linked to fossil-based (as well as renewable)[354] amine hardeners, still remain.[355]

Lately, several renewable epoxy resin examples have been reported in the literature, based on renewable feedstocks such as plant oils[356,357] or cashew nut shell liquid (CNSL),[358] as well as biobased platform chemicals, such as levulinic acid, furfuryl amine,[359] syringaldehyde,[360] or vanillin.[361] However, even for these more sustainable alternatives, the introduction of epoxy groups still relied heavily on ECH chemistry, and despite the commercialization of glycerol-to-epichlorohydrin (GTE) plants, ECH still presents concerns related to its handling, toxicity and CMR rating.[362]

An additional sustainability challenge is related to the employment of typical amine hardeners presenting toxicity issues.[363,364] In this regard, other well-known crosslinkers for epoxy resins, namely anhydride[365] and carboxylic acid[366] curing agents, would be a less hazardous and potentially more sustainable approach. Interesting approaches for the introduction of carboxylic acid moieties onto lignin have recently been reported through carboxymethylation[367] or oxidative carboxylation with acetic acid and hydrogen peroxide.[368]

Several studies have reported the functionalization of lignin with cyclic anhydrides to obtain polycarboxylic acid–functionalized lignin, which can be directly employed as a crosslinker in various resin systems. For instance, Zhen *et al.*[369] reported fully bio-based epoxy resins from epoxidized soybean oil (**ESBO**) and tung oil anhydride-modified lignin, whereas Ma *et al.*[370] presented a multicarboxyl lignin hardener from glycidol and maleic anhydride, which was used to achieve bio-based epoxy resins, aided by citric acid and **ESBO**. Other examples involve modification of lignin with succinic acid,[371] succinic anhydride,[187,188,372] as well as maleic anhydride to achieve thermosets *via* thiol- and amine-based Michael additions.[373]

Epoxidation of unsaturated vegetable oils is commonly achieved through peracid-mediated reactions (often generated in situ) *via* chemical or chemo-enzymatic routes.[47] ESBO was selected as renewable epoxy crosslinker to furthermore address the toxicity concerns associated with conventional ECH-based epoxy resins, as outlined above.

ESBO-based epoxies are known to exhibit lower mechanical performance than conventional fossil-based glycidyl ether–based systems (e.g., BADGE). Within this framework, lignin is introduced as a rigid, multifunctional macromolecular component to partially compensate for the intrinsic flexibility of ESBO.

Thorough literature research revealed that lignin modification with itaconic anhydride (**IAn**) has not yet been reported. **IAn**, compared to the structurally related maleic anhydride, is renewable (maleic anhydride production still relies

on *n*-butane)[374] and less harmful.[375–377] **IAn** derives from the dehydration of itaconic acid, a well-known bio-based platform chemical produced *via* fermentation, and first reported in 1837 by thermal decomposition of citric acid.[378,379] This chapter presents detailed investigations of the functionalization reaction of lignin with itaconic anhydride. Reaction conditions were thoroughly optimized, and the resulting itaconate-functionalized lignin carefully characterized. **IAn** was then employed for the synthesis of fully renewable epoxy resins, in combination with **ESBO** and **Pripol™ 1009**, a dimeric diacid with a monocyclic core unit, obtained from Diels-Alder reaction of unsaturated long chain fatty acids.[380,381]

Lignin was likewise functionalized with succinic anhydride under the same reaction conditions. The resulting derivatives were subsequently employed in analogous experiments to obtain epoxy resins, allowing a direct comparison of the two anhydride-modified lignins in epoxy resin applications. Moreover, the application of these derivatives was also investigated in Passerini 3-MCR thermosets, focusing on the optimization of gel content and the evaluation of their thermal properties. Passerini reactions are typically achieved *via* a one-pot reaction between a carboxylic acid, an aldehyde, and an isocyanide. Several studies have reported Passerini reactions employing renewable resources, for instance succinylated or carboxymethyl cellulose,[382,383] as well as more recent work utilizing a triacid derived from HOSO.[384] However, no reports have yet described the application of this chemistry to lignin derived monomers. In this context, lignin derivatives bearing itaconate or succinate carboxylic acid groups were employed as crosslinkers, in combination with diisocyanides (C_6 or C_{12}) and nonanal as the aldehyde component. A low lignin content (35 mol%) was compared to a higher content (100 mol%) for both derivatives, and when required, the remaining −COOH groups were partially replaced with **Pripol™** to achieve tunable material properties.

4.3.3 Lignin Functionalization with Itaconic Anhydride

The functionalization of lignin with itaconic anhydride was optimized by systematically varying the reaction conditions such as temperature, reaction time, and reagent stoichiometry, in an initial 0.5 g reaction scale. The progress and outcome of the functionalization were monitored by ^{31}P NMR and IR spectroscopy, as well as SEC. Typically, the extent of the esterification is associated with an increased amount of carboxylic acid (−COOH) and ester (−COOR) groups, as illustrated in **Scheme 4.3.1**. Moreover, an increase in molecular weight is expected.

Scheme 4.3.1 – General reaction scheme of the functionalization of lignin with itaconic anhydride; a representative structure of lignin and lignin itaconate are shown.

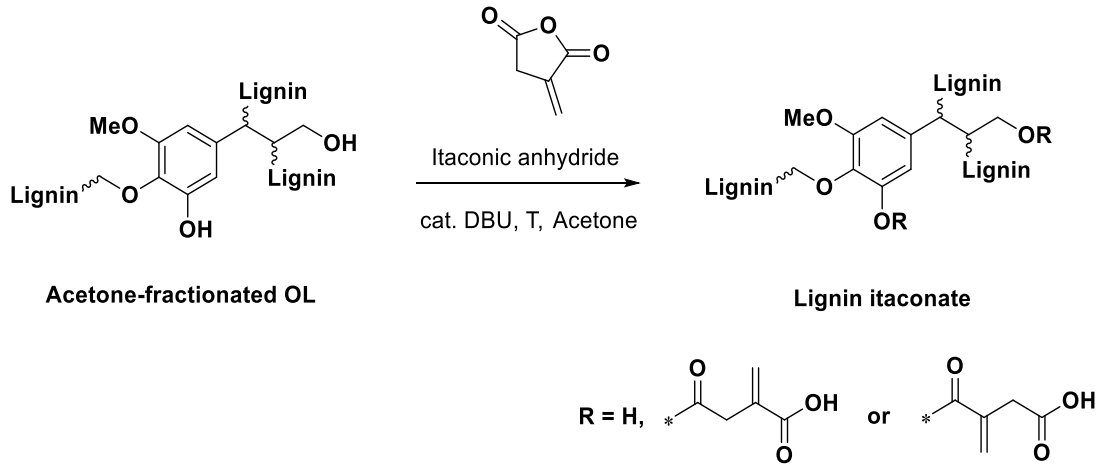

At the initial stage, the reaction was tested under bulk conditions in an effort to minimize solvent use and align with the principles of green chemistry. However, these conditions proved impractical, as achieving a homogeneous mixture between the molten anhydride and lignin required a very large excess of **IAn**. Even with a large excess (10 equiv.), a proper dispersion of the lignin could not be achieved, as the mixture remained inhomogeneous. The use of a reaction solvent—despite introducing an additional component—was considered more practical, especially if the solvent could be easily recovered by distillation. For this reason, Organosolv lignin (**OL**) was fractionated in acetone

prior to the functionalization step and characterized in detail (see Experimental Section, **Paragraph 6.6.1.2**). Acetone was chosen as the reaction solvent for its ability to solubilize all the components and being easily recoverable. Additionally, acetone does not raise major concerns from a health and environmental impact point of view, as depicted by the GSK's solvent selection guide.[385] Moreover, solvent recovery was also included in our work, as will be discussed later.

The performance of four different base catalysts was investigated. Organic superbases are known to catalyze transesterification reactions,[299,300] therefore three different superbases, namely DBU, TBD, and 1,1,3,3-tetramethylguanidine (TMG) were tested, as well as the heterogeneous inorganic base K_2CO_3. DBU and TMG showed comparable performance, with DBU showing slightly higher catalytic activity (0.96 $mmol \cdot g^{-1}$ of −COOH installed, vs. 0.92 $mmol \cdot g^{-1}$ of −COOH with TMG as catalyst), as shown in **Table 4.3.1**, **entries 1 – 4** and **Figure 4.3.1**. TBD and K_2CO_3 were less active. In addition to the environmental impact, it is important to compare the two catalysts in terms of toxicity (DBU: acute toxicity cat.3, $LD50_{oral,\ rat}$ = 215 – 681 mg/kg, TMG: acute toxicity cat. 4 $LD50_{oral,\ rat}$ = 835 mg/kg).[386,387] Thus, TMG can be categorized less toxic than DBU. The experimental data further show similar conversion of TMG and DBU (50 % and 54 % conversion of aliphatic hydroxyl groups for TMG and DBU, respectively). To ensure consistency and direct comparability across the optimization study, DBU was retained as the primary catalyst using a fixed set of reaction conditions (1.4 IAn equiv., 45 °C, 24 h and 6 mol% cat. loading), while individual parameters were systematically varied, despite the lower toxicity of TMG. Nevertheless, the reaction was subsequently upscaled with both catalysts, confirming that TMG performs comparably and demonstrating that the reaction proceeds efficiently in either case (Experimental Section, **paragraphs 6.6.1.4, 6.6.1.5, 6.6.1.7**).

Table 4.3.1 – Effect of different parameters on the reaction between lignin and itaconic anhydride. **Conditions:** 0.5 g of dried, acetone fractionated lignin (**OL acetone 1**) was dissolved in 5 mL of dry acetone. The vessel was flushed with Argon and heated to the desired temperature. Equivalents of functionalizing agent, catalyst, catalyst amount and time were tested. r.t.: room temperature.

Entry	IAn (Equiv.)	T (°C)	Cat.	Cat. (mol %)	Time (h)	OH_{Aliph} (mmol·g^{-1}) (%)[c]	OH_{Arom} (mmol·g^{-1}) (%)[c]	COOH (mmol·g^{-1})[c]	M_n (g·mol^{-1})[d]	$Đ$[d]
Catalyst Influence										
1	1.4	45	***DBU***	6	24	1.01 (*54*)	1.76 (*23*)	0.96	3800	16
2	1.4	45	***TBD***	6	24	1.34 (*41*)	1.56 (*30*)	0.73	3700	4.9
3	1.4	45	***K_2CO_3***	6	24	1.26 (*44*)	1.62 (*28*)	0.78	3800	4.9
4	1.4	45	***TMG***	6	24	1.11 (*50*)	1.53 (*31*)	0.92	4200	8.1
Catalyst Amount										
5	1.4	45	DBU	***6***	24	1.01 (*54*)	1.76 (*23*)	0.96	3800	16
6[a]	1.4	45	DBU	***12***	24	0.93 (*57*)	1.59 (*29*)	0.97	3800	6.4
7[b]	1.4	45	DBU	***100***	24	*Insoluble Fraction Formation*				
Time										
8	1.4	45	DBU	6	***3***	1.45 (*37*)	1.62 (*28*)	0.69	3500	3.8
9	1.4	45	DBU	6	***16***	1.32 (*41*)	1.91(*17*)	0.88	4100	9.2
10	1.4	45	DBU	6	***24***	1.01 (*54*)	1.76 (*23*)	0.96	3800	16
Temperature										
11	2.1	***r.t.***	DBU	6	16	1.21 (*46*)	1.40 (*36*)	0.92	3700	4.1
12	2.1	***45***	DBU	6	16	0.69 (*67*)	1.37 (*38*)	1.07	4000	20
13[a]	2.1	***66***	DBU	6	16	0.5 (*76*)	1.18 (*45*)	1.27	5600	15
IAn Equivalents										
14	***0.7***	45	DBU	6	16	1.60 (*31*)	2.28 (*5*)	0.51	3200	4.1
15	***1.4***	45	DBU	6	16	1.32 (*41*)	1.91 (*17*)	0.88	4100	9.2
16	***2.1***	45	DBU	6	16	0.69 (*67*)	1.37 (*38*)	1.07	4000	20
17	***4.2***	45	DBU	6	16	0.66 (*69*)	1.17 (*46*)	1.45	4000	5.9

[a]: Partial formation of insoluble fraction. Only soluble fraction was analyzed. [b]: Complete insoluble fraction formation, no analysis possible. [c]: Data calculated from ^{31}P NMR. Conversion (%) is

standardized for the increase in molecular weight of the educt compared to the starting material (details on the calculations are reported in **paragraph 6.6.1.1**). [d]: SEC-DMAc.

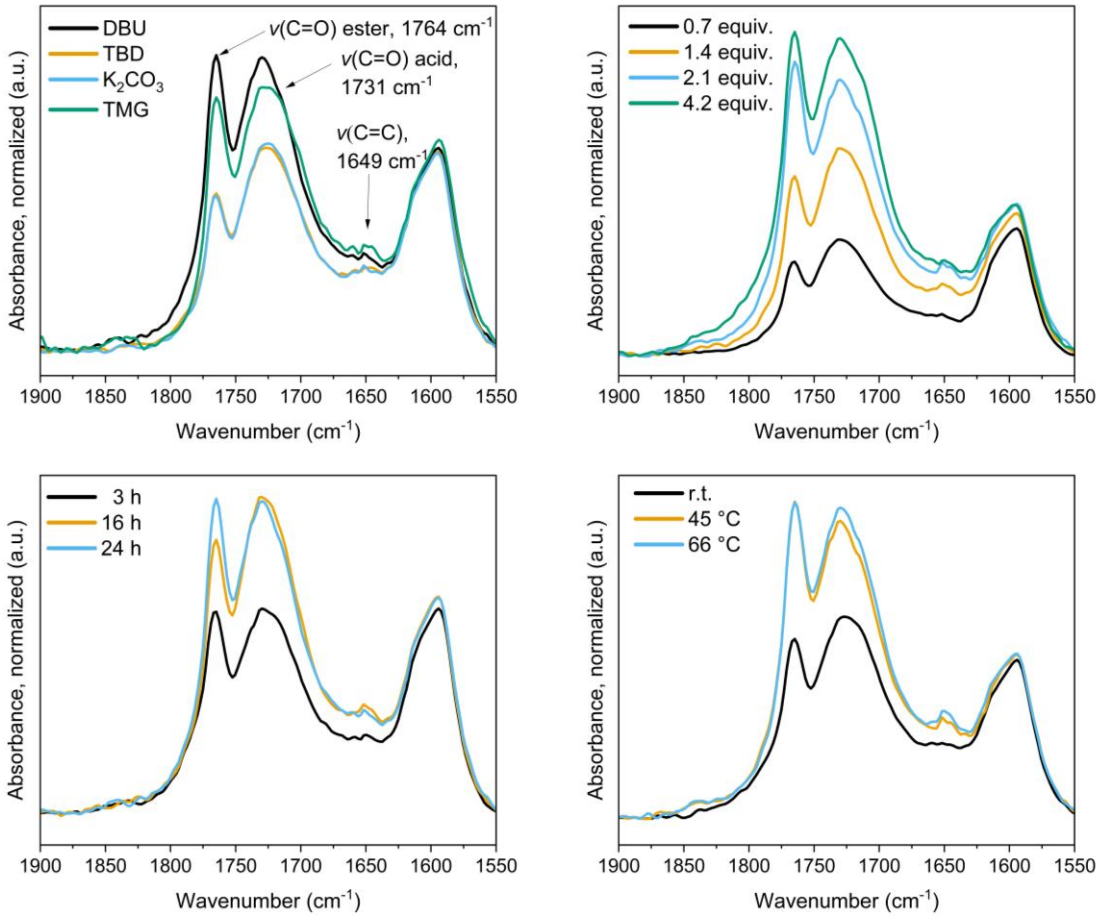

Figure 4.3.1 – Overlay of the IR spectroscopy reaction monitoring in the region of 1900 – 1550 cm^{-1} with different parameters tested. All IR spectra are normalized to the signal at 1504 cm^{-1} for the lignin C_{ar}=C_{ar} stretching vibrations.

Different catalyst amounts were also tested and compared to uncatalyzed conditions. Initially, under the same reaction conditions, the addition of 6, 12, and 100 mol% of DBU was investigated (**Table 4.3.1**, **entries 5 – 7**). A catalyst amount of 6 mol% was beneficial to obtain functionalization with IAn, however, increasing the amount of catalyst above 6 mol% led to a rather high amount of insoluble fraction formation during the reaction, probably due to side reactions (*i.e.,* crosslinking *via* Oxa-Michael addition or salt formation between the excess superbase and the newly formed −COOH groups) that prevented a reliable investigation on the extent of the reaction. For 12 mol% of DBU, only the soluble fraction could be analyzed, while for 100 mol% DBU the reaction mixture turned

completely insoluble after a few minutes, as already observed in the work from Olsén *et al.*[388] in their functionalization of lignin with maleic anhydride with 4−dimethylaminopyridine (DMAP) as catalyst. In contrast, the reaction performed in the absence of catalyst exhibited minimal conversion, as indicated by IR spectroscopy results (**Figure 4.3.2**), highlighting the essential function of the latter.

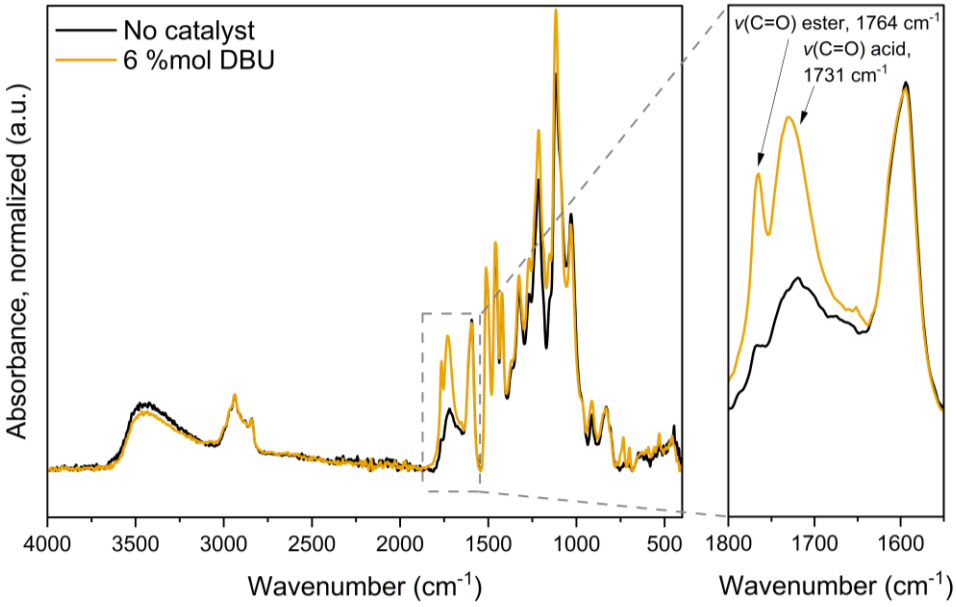

Figure 4.3.2 – IR overlay showing the beneficial catalyst effect on the conversion of the reaction, comparing a reaction without any catalyst (black) and a reaction with 6 mol% DBU (orange), under otherwise same reaction conditions. On the right, a zoom in the region 1800 – 1550 cm^{-1} shows the characteristic signals ascribed to the functionalization. All IR spectra are normalized to the signal at 1504 cm^{-1} for the lignin aromatic C=C stretching vibrations.

Following functionalization, all samples exhibited higher M_n values relative to the starting material (OL acetone (1); M_n: 2900, M_w: 7800, $Đ$: 2.7) as well as an increase in dispersity. These observations are consistent with the findings of Olsén *et al.*[388], where the increased dispersity after functionalization was mitigated by fractionation. In our case, however, this step was deliberately omitted to avoid additional solvent usage. The effect of functionalization on molecular weight and thermal properties depends on the nature of the introduced moieties: the addition of the more rigid itaconate groups increases molecular weight and restricts chain mobility, as demonstrated from

the higher T_g values (140 °C) compared to the starting material acetone-fractionated lignin (T_g = 125 °C).

Increasing the reaction time was found to be beneficial for a higher extent of functionalization. Reaction times of 3, 16, and 24 h were investigated as time intervals for the transesterification reaction. While longer reaction times consistently led to higher −COOH contents, the increase in mmol·g^{-1} of functionalities between 16 h (0.88 mmol −COOH·g^{-1}) and 24 h (0.96 mmol −COOH·g^{-1}) indicated that further extension yielded only marginal benefit. In addition, excessively long reaction times are less attractive from a process efficiency perspective. Thus, 24 h was selected as an upper practical limit (**Table 4.3.1, entries 8 – 10**).

The influence of the reaction temperature was investigated at r.t., 45 °C and 66 °C, respectively (**Table 4.3.1**, **entries 11** – **13**). The results indicate an increase in the carboxylic acid group functionalities with increasing temperature. Nonetheless, the reaction conducted at 66 °C led to a high amount of insoluble solid fraction formation, that prevented an accurate quantification on the outcome of the reaction. Moreover, these conditions (10 °C above the boiling point of acetone) would render more impractical the scaling up of the reaction. Therefore, 45 °C was chosen as the optimal temperature. By varying the equivalents of IAn from 0.7 to 4.2, the amount of installed −COOH groups in the esterified lignin and the molecular weight increased considerably (**Table 4.3.1, entries 14** – **17**), confirmed by IR spectroscopy (**Figure 4.3.1**). Signals associated with successful conversion can be ascribed to the rising C=O stretching vibrations of both the ester (1764 cm^{-1}, forming between lignin backbone and anhydride) and the free carboxylic acid (1730 cm^{-1}). Additionally, the intensity of the emerging signal at 1649 cm^{-1}, attributed to the C=C stretching vibration of the Michael system, increased with proceeding degree of functionalization.

As general trends, longer reaction times and higher equivalents of IAn were found to enhance the overall reaction conversion. Increased temperatures

promoted higher reactivity with the drawback of promoting the formation of side reactions, indicated by solidification. Therefore, 45 °C was identified as compromise between conversion and selectivity. Across all samples, the aliphatic hydroxyl groups displayed higher reactivity than the phenolic −OH groups, with a maximum conversion reached of 46 % observed for the aromatic −OH groups, as indicated by ^{31}P NMR results.

Literature reports that the exo-double bond of IAn can undergo isomerization to the thermodynamically more stable citraconic anhydride (ClAn).[389,390] In order to investigate the stability of the double bond in the IAn structure, different screenings were carried out in the absence of lignin. Initially, IAn and DBU were mixed in acetone and heated to 45 °C to replicate the reaction conditions, and aliquots were taken over time and analyzed *via* NMR spectroscopy. Corresponding data suggest that the isomerization of the double bond takes place almost immediately, reaching close to complete isomerization of the double bond after 10 minutes (**Figure 4.3.3**).

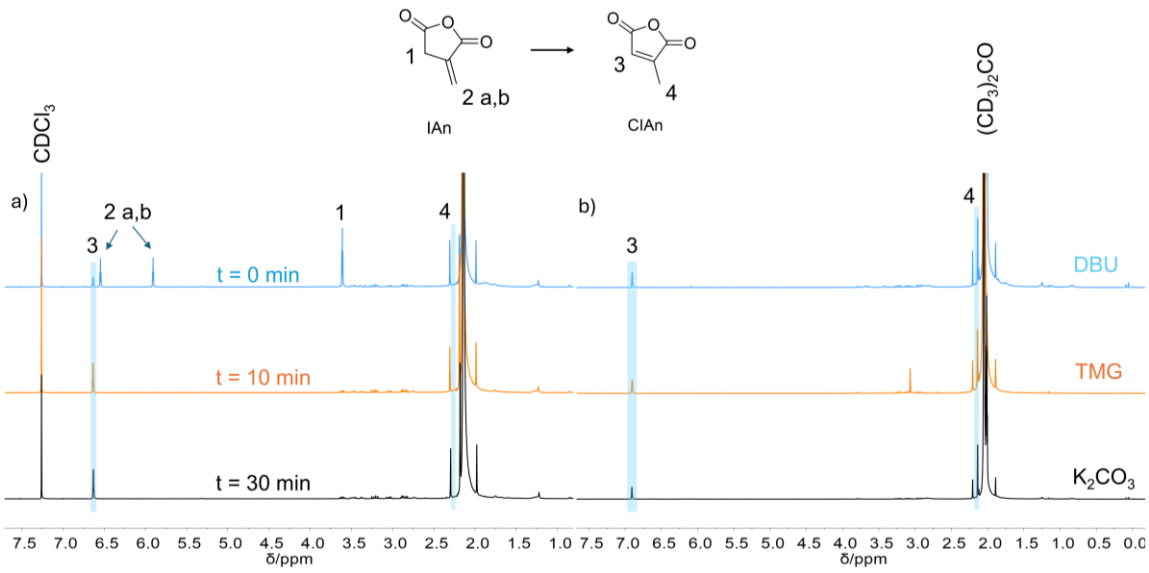

Figure 4.3.3 – a) ^{1}H NMR ($CDCl_3$) of the screening for isomerization of itaconic anhydride (conditions: 0.4 g of IAn, 5 mL dry acetone, 22.2 µL DBU, 45 °C); b) ^{1}H NMR (acetone-d_6) of the screening for isomerization of itaconic anhydride after 30 minutes with different bases.

This is in accordance with literature findings, where the isomerization is favored in the presence of tertiary amines.[59] For comparison, K_2CO_3 and TMG were also tested and exhibited comparable isomerization results to DBU (**Figure 4.3.3**).

These findings suggest that IAn predominantly isomerizes during the reaction and CIAn is most likely the functionalizing agent reacting with lignin, as depicted in **Scheme 4.3.2**. Therefore, while the products are referred to as Lignin Itaconates (**LI**) throughout this work for consistency, the structure likely corresponds predominantly to lignin citraconates. Despite this isomerization, carboxylic acid groups remain incorporated into the modified lignin structure, facilitating the resulting macromonomer to be applied in thermoset systems that rely on −COOH reactivity. Furthermore, the introduced Michael system is still retained, although its reactivity may be reduced compared to the non-isomerized case, as literature postulates.[391,392]

Scheme 4.3.2 – General reaction scheme of isomerized itaconic anhydride (CIAn) and a representative structure of lignin.

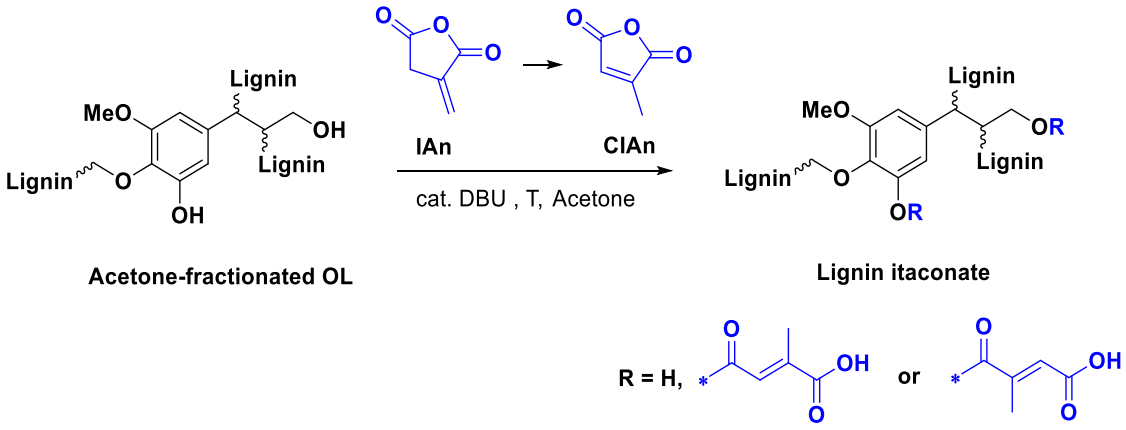

To enable the use of **LI** in thermoset applications, a larger-scale synthesis (15 g) was conducted with optimized reaction conditions. A complete characterization of the product, also for the TMG-catalyzed upscaled reaction, can be found in the Experimental Section, **paragraph 6.6.1.5**, demonstrating that the scale-up effectively works with both catalysts (DBU and TMG). **Figure 4.3.4** presents the IR spectrum of the upscaled reaction product, confirming the successful functionalization through the characteristic signals associated with the insertion of the citraconate moieties. The corresponding ^{31}P NMR spectrum further

supports this assumption, indicating a pronounced increase in the −COOH region relative to the starting material. In particular, the upscaling conditions led to a −COOH value of (1.39 ± 0.02) mmol·g^{-1}.

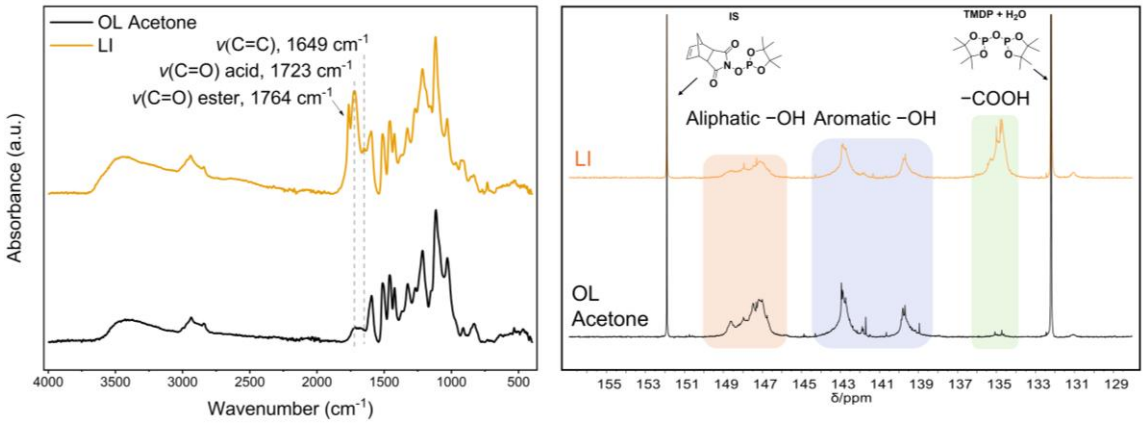

Figure 4.3.4 – Left: representative IR spectra of acetone-fractionated OL (OL Acetone, starting material) and LI. Right: ^{31}P NMR highlighting the change in the characteristic signals for aliphatic hydroxyl (orange), aromatic hydroxyl (green) and carboxylic acid groups (pink).

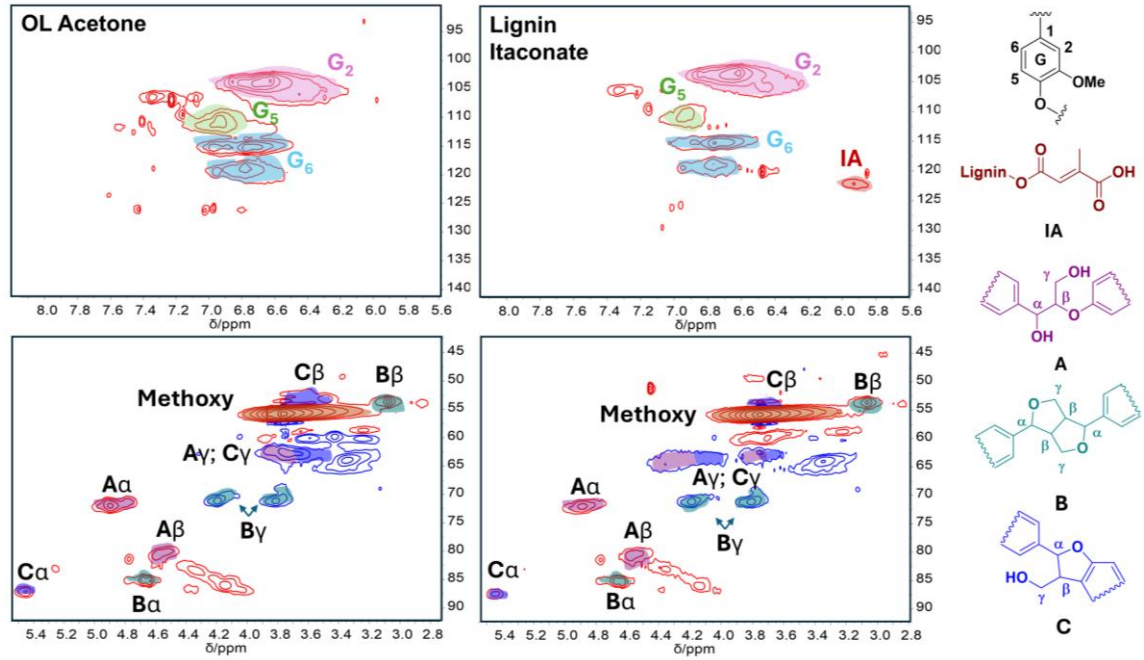

Figure 4.3.5 – HSQC traces of acetone fractionated lignin (OL acetone (2)) and itaconic functionalized lignin.

From HSQC analysis (**Figure 4.3.5**) of both the fractionated lignin in acetone (OL Acetone) and the **LI**, structural understandings can be gathered. Signals ascribed

to pinoresinol (**structure B**) remain unchanged after modification. A shift on the signals of structures such as β-O-4' (**A**) and phenylcoumaran (**C**) from δC/δH 61–65/3.5–3.9 ppm to δC/δH 62–65/4–4.44 ppm can be observed after modification of the primary hydroxyl groups. To the best of our efforts, it was not possible to precisely differentiate between the signals of A_{γ} and C_{γ}. Nevertheless, a shift of the signals is clearly visible, confirming the successful functionalization. However, the signal ascribed to A_{α} did not shift, showing that the reactivity of the modification was not very high with secondary hydroxyl groups (as also demonstrated *via* ^{31}P NMR, aliphatic −OH are still present after modification, with (0.90 ± 0.004) mmol·g^{-1}). In the aromatic region, a new signal appears (IA, δC/δH 122/5.92 ppm), ascribed to the proton of the double bond of the IA moiety (isomerized, indicated as IA structure in **Figure 4.3.5**). Complete HSQC analysis is available in the Experimental Section (**6.6.1**).

4.3.4 Environmental Factor, Recyclability of the Solvent, and the Precipitation Medium

As highlighted recently, the modification of lignin with cyclic anhydrides remains one of the most promising pathways for developing low environmental-factor (E-factor) protocols to access carboxylic acid functionalized lignin.[93] Indeed, the waste streams generated are typically associated with catalysts, solvents, and excess reactants. In this context, bulk conditions and minimal amount of catalyst would be beneficial to lower the overall E-factor of the procedure. As mentioned above, bulk conditions were not feasible with IAn, due to the high excess of reactant required to achieve an adequate mixing with lignin. In order to enhance the overall sustainability of the functionalization process, efforts were thus directed toward solvent recovery (**Table 4.3.2**). Due to the large volume of water required for precipitation during workup, the distillation proved challenging, ultimately leading to a recovery rate of 75% of the initially used acetone (characterization of the recovered solvent is provided in the Experimental section (**Figure 6.6.10**). As a proof of concept, the recovered acetone was dried over molecular sieves for 72 h and subsequently employed in a new functionalization reaction. However, the conversion of the aliphatic groups was lower in comparison to using fresh anhydrous acetone, likely due to residual water presence (**Table 4.3.2**, Entry 1-fresh solvent; Entry 2-recovered solvent).

Table 4.3.2 – Data comparison of the −OH group distribution in the modification of lignin with IAn utilizing fresh solvent (entry 1) and recovered solvent (entry 2). Conditions: 0.50 g of dry OL acetone and 1.40 equiv. of IAn (based on lignin −OH value) were dissolved in dry acetone. DBU (6 mol%) was added, and the reaction mixture was stirred at 45 °C for 24 h.

Entry	OH_{Total} (mmol·g^{-1})[a]	$OH_{Aliphatic}$ (mmol·g^{-1})[a]	$OH_{Aromatic}$ (mmol·g^{-1})[a]	COOH (mmol·g^{-1})[a]	X_{Aliph} (%)[b]	X_{Arom} (%)[b]
1	3.71	1.01	1.76	0.96	54	23
2	3.52	1.44	1.48	0.56	31	23

[a]: Determined from ^{31}P NMR. [b]: Conversion (%) is standardized for the increase in molecular weight of the product compared to the starting material (see **paragraph 6.6.1.1**).

The precipitation medium used for the esterification reaction with the recovered acetone was reused multiple times for additional reactions, demonstrating its reusability. During the experiments, denoted as reutilization of precipitation medium (**LI**-RPM#), the differences in the conversion were monitored *via* IR spectroscopy. Prior to each reuse, the medium was filtered to remove any residual solids. **LI**-RPM1 and **LI**-RPM2 exhibited an almost identical spectrum, while a slight decrease begins with **LI**-RPM3, followed by a more noticeable decline in **LI**-RPM4 (**Figure 4.3.6**). These results suggest that the precipitation medium can be reused effectively at least three times without compromising precipitation efficiency, thereby contributing positively to the sustainability of the process.

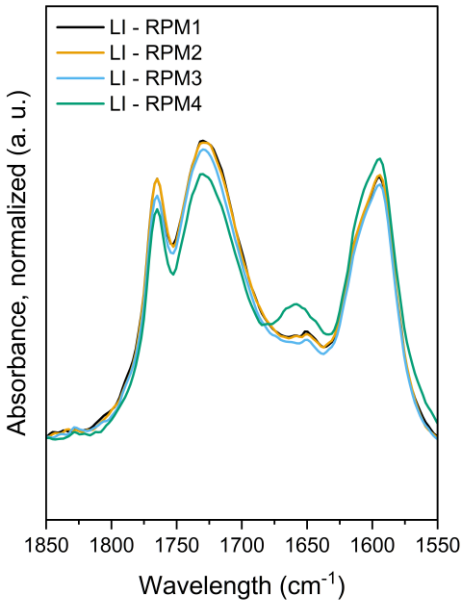

Figure 4.3.6 – Zoom in the region 1850 – 1550 cm^{-1} of the IR spectrum of lignin itaconates obtained reutilizing several times the same precipitation medium. The nomenclature corresponds to LI and the number of Reutilizations of Precipitation Medium (RPM#). Spectra were normalized for the aromatic C=C stretching vibration at 1504 cm^{-1}.

Synthetic E-factor values were estimated using a simplified approach to highlight solvent impact to the total amount of waste, without considering the fractionation pretreatment and the workup. A detailed discussion of the calculation assumptions and limitations is provided in the Experimental Section, **paragraph 6.6.2.1**. By implementing a simple recycling procedure of the solvent *via* distillation, it was possible to lower the total E-factor for the procedure from 6.9 to

2.7. In **chapter 2.2.1.4**,[93] several lignin modification strategies were reported, together with a comparative discussion of their E-factors. Comparing the E-factor of the lignin modification with itaconic anhydride described herein to conventional ECH-based routes, the present approach results in substantially lower values (typically between 4 and 16 for ECH-based systems).[93] Even alternative ECH-free routes reported in the literature, such as those involving epoxidation of fatty acid mixtures followed by esterification with lignin, were associated with considerably higher E-factors (E-factor: 38 for the overall sequence).[175] Also the esterification of Organosolv lignin with oleyl chloride followed by epoxidation of the unsaturated bonds using peracetic acid resulted in a relatively high E-factor (E-factor: 14.2 for the entire sequence).[179]

4.3.5 Thermosets

The optimal conditions established for the scale-up of lignin functionalization with itaconic anhydride were subsequently applied to its modification with succinic anhydride (SAn). SAn was selected as a saturated and unbranched analogue of IAn, allowing a direct comparison of reactivity and final material properties. This yielded a lignin succinate derivative (**LS**) with a −COOH content of 1.79 mmol·g^{-1} (**Scheme 4.3.3**, a complete characterization of this product is provided in the Experimental Section, **paragraph 6.6.1.7**).

Scheme 4.3.3 – Reaction scheme for the modification of acetone-fractionated OL with SAn.

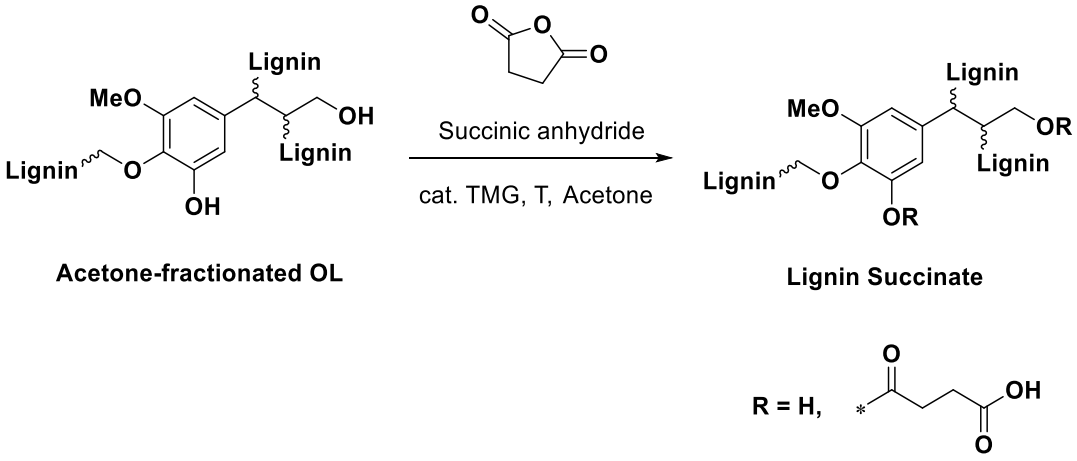

Acetone-fractionated OL

Lignin Succinate

4.3.5.1 Passerini Thermosets

As a first application, the carboxylic acid-functionalized **LI** was employed as crosslinker for Passerini 3MCR-based thermosets.

Scheme 4.3.4 – General scheme of the Passerini thermosets with LI as crosslinker. The representative thermoset structure proposed is simplified by showing only two functionalities for lignin.

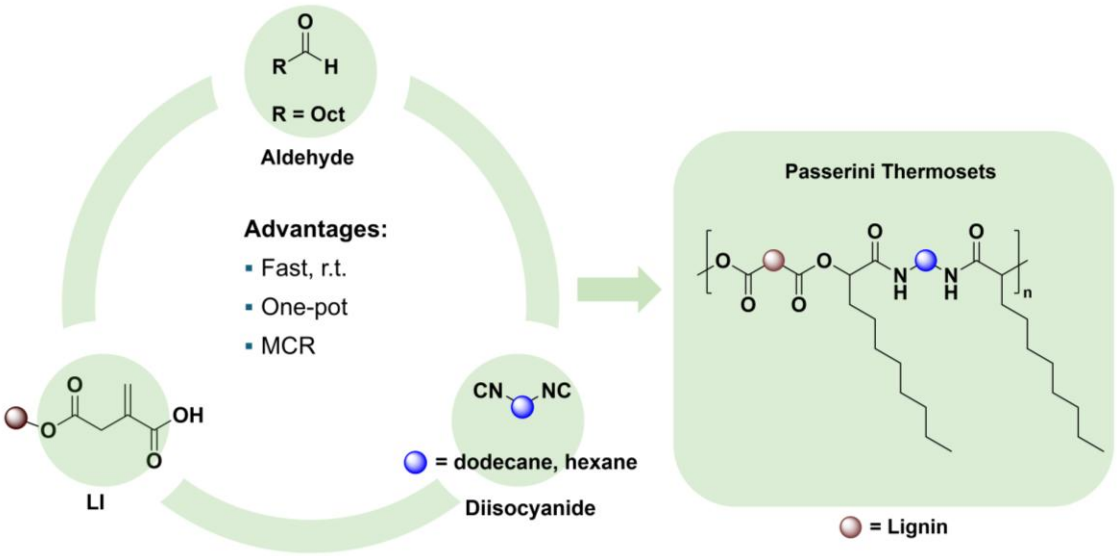

The Passerini reaction involves three main functional groups, namely carboxylic acids, isocyanides and aldehyde groups.[393] Together with **LI**, 1,6 or 1,12-bis isocyanides and nonanal were employed as components. To aid with flexibility and to overcome the typical brittleness associated with lignin derived thermosets, in some cases, **Pripol™ 1009** or other low molecular weight difunctional carboxylic acids were used as diluents. Initially, a suitable solvent needed to be selected, due to the solid nature of lignin (and in some cases, of other components as well). THF efficiently solubilized all the components, however, due to its major concerns regarding its fossil-based origin and potential hazards, greener alternatives were investigated. 2-MeTHF was discarded, as it could not fully solubilize **LI**. Acetone, which was already employed in the lignin functionalization, was tested because of its ability to solubilize all the components effectively. The curing procedure was conducted utilizing a minimal amount of solvent, starting the curing at room temperature, followed by a heated

post-curing in an oven. Details can be found in the Experimental Section, **paragraph 6.6.3**. The successful reaction outcome and curing could be easily confirmed *via* IR spectroscopy (**Figure 4.3.7**). The characteristic aldehyde carbonyl stretching vibration at 1723 cm^{-1} and the corresponding C(O)-H stretching vibration at 2700 cm^{-1}, as well as the isocyanide stretching vibration at 2150 cm^{-1}, are no longer visible in the spectra of the cured thermoset. Additionally, the signal corresponding to the carbonyl group of the free carboxylic acid in lignin itaconate, previously observed at 1720 cm^{-1}, shifted to 1740 cm^{-1}. This new peak, labeled $\nu(C{=}O_{ester\ thermoset})$, corresponds to the ester bond formed between the carboxylic acid of lignin itaconate and the aldehyde in the *Passerini* product, accounting for the disappearance of the free carboxylic acid signal. The ester bond stretching between the lignin structure and itaconic moieties, observed at $\nu(C{=}O_{ester\ lignin})$ = 1760 cm^{-1}, remained unchanged, indicating the stability of this bond. Furthermore, a new peak arose at 1650 cm^{-1}, attributed to the formation of an amide group, supported by another new signal at ν(N-H) = 3300 cm^{-1}. Finally, new signals in the range of ν(C-H, aliphatic) = 2800–3000 cm^{-1} indicate the incorporation of aliphatic chains.

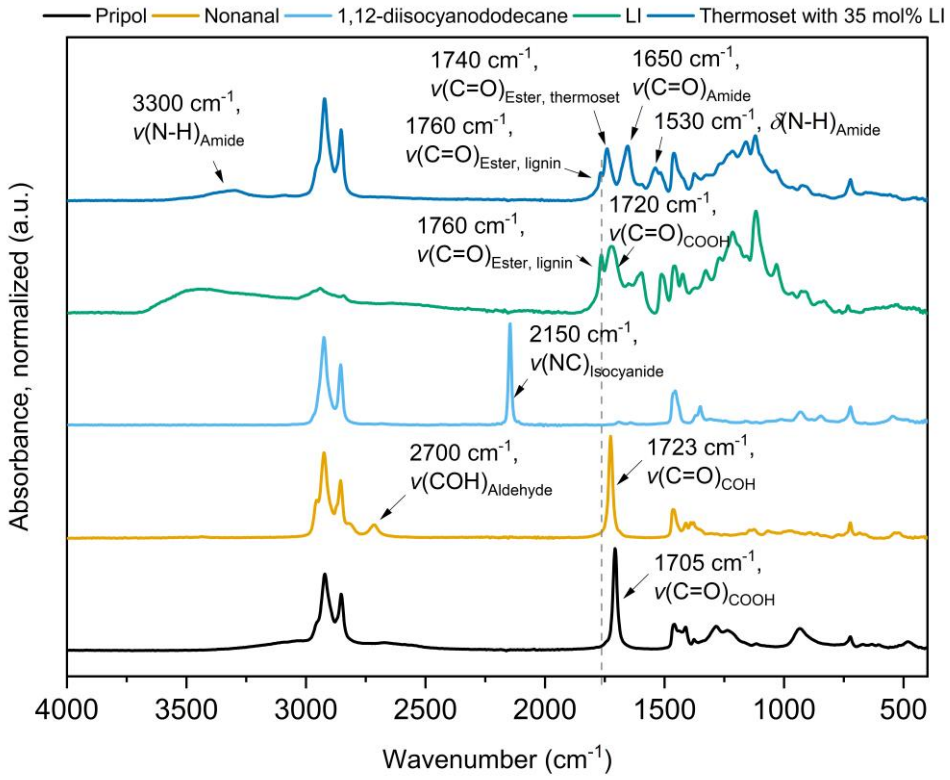

Figure 4.3.7 – IR spectra overlay of the components of the Passerini reaction and the final thermoset with 35 mol% of LI.

It is known that, in addition to aldehydes, ketones may also participate in the Passerini 3-MCR, albeit at significantly reduced reaction rates. Therefore, the influence of the chosen solvent (acetone) in the Passerini thermosets system and its potential involvement in the curing process was initially investigated. As proof of concept, the curing of a **blank** experiment with acetone as solvent, **Pripol™**, **LI**, and isocyanide (without the aldehyde component) was followed *via* IR spectroscopy. In parallel, a **control** experiment was performed in the absence of both aldehyde and isocyanide (only acetone, **Pripol™**, and **LI**) to establish the baseline behavior of the matrix in acetone under the employed curing conditions. After 24 h of curing, IR spectra were taken, showing that the isocyanide peak is still visible. Moreover, the thermosets did not look solid, but rather appeared as a viscous mixture of the starting materials (**Figure 4.3.8**).

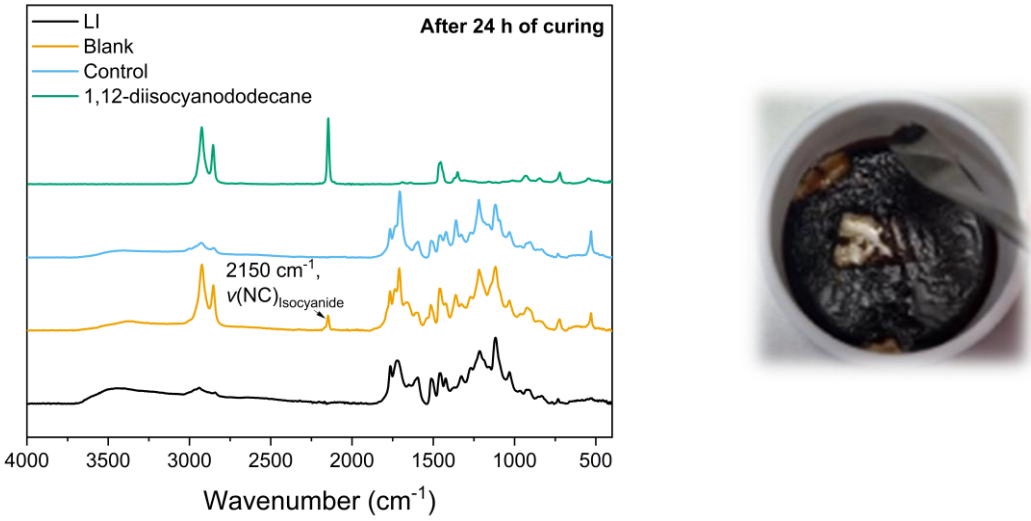

Figure 4.3.8 – Left: IR spectra overlay of the starting materials LI and 1,12-bis(isocyano)dodecane, and blank and control experiments. Right: picture of the "blank" thermoset after 24 h of curing. *Picture taken by the author*.

To gain further mechanistic insight, the influence of the solvent was additionally examined through a model Passerini reaction involving mesaconic acid (the isomeric analogous of itaconic acid), nonanal, and *n*-dodecyl isocyanide, performed both in acetone and in THF under otherwise identical conditions.

In acetone, the formation of a white precipitate was observed after approximately 1 h, which was isolated and identified as the expected Passerini product. The reaction was then repeated in THF and worked up following the same protocol, after which the isolated products obtained from both solvents were directly compared.

Detailed spectroscopic and analytical characterization (reported in the Experimental Section, **paragraph 6.6.3.1.2**) revealed identical spectra and analytical data, confirming that the same Passerini product is formed irrespective of the solvent employed, demonstrating that acetone does not substantially interfere with the reaction pathway or product structure.

In addition, two thermosets were synthesized and cured under identical conditions, using either acetone or THF as solvent. The resulting gel contents were 88 % and 82 %, respectively, indicating comparable network formation in both systems.

While a slow and partial participation of acetone in the Passerini 3-MCR cannot be fully excluded, these results suggest that, in the presence of the aldehyde component, the aldehyde-based Passerini pathway is kinetically favored and thus strongly dominates the curing process. Consequently, acetone primarily acts as a solvent under the investigated conditions.

As mentioned before, an initial gel content of 88 % was obtained for a thermoset with 1,6-bis(isocyano)hexane as diisocyanide component and 100 mol% of **LI**. The thermoset obtained was a glassy, homogenous material, however quite brittle. In order to improve the mechanical properties of the materials, other additional carboxylic acids components were tested, such as **Pripol™**, azelaic acid and citric acid. In particular, **Pripol™** gave the best materials in terms of flexibility and toughness of the samples, while for the other two di/tri-acids the materials remained quite brittle. In terms of gel content, the thermoset with 35 mol% **LI** and azelaic acid, citric acid, or **Pripol™**, gave gel contents of 70 %, 69 % and 58 %, respectively (**Figure 4.3.9**, black graph). These values were not deemed as satisfactory, therefore other parameters were varied in order to achieve a higher crosslinking density. It was found that the **LI** content plays a significant role in the gel content. In particular, when going from 35 mol% to 100 mol%, the gel contents increased from 58 to 88 %, respectively, when 1,6-bis(isocyano)hexane was used as the isocyanide component. The same trend was observed when 1,12-bis(isocyano)dodecane was used, with slightly lower gel contents increasing from 51 to 81 % for 35 and 100 mol%, respectively (**Figure 4.3.9**, orange graph).

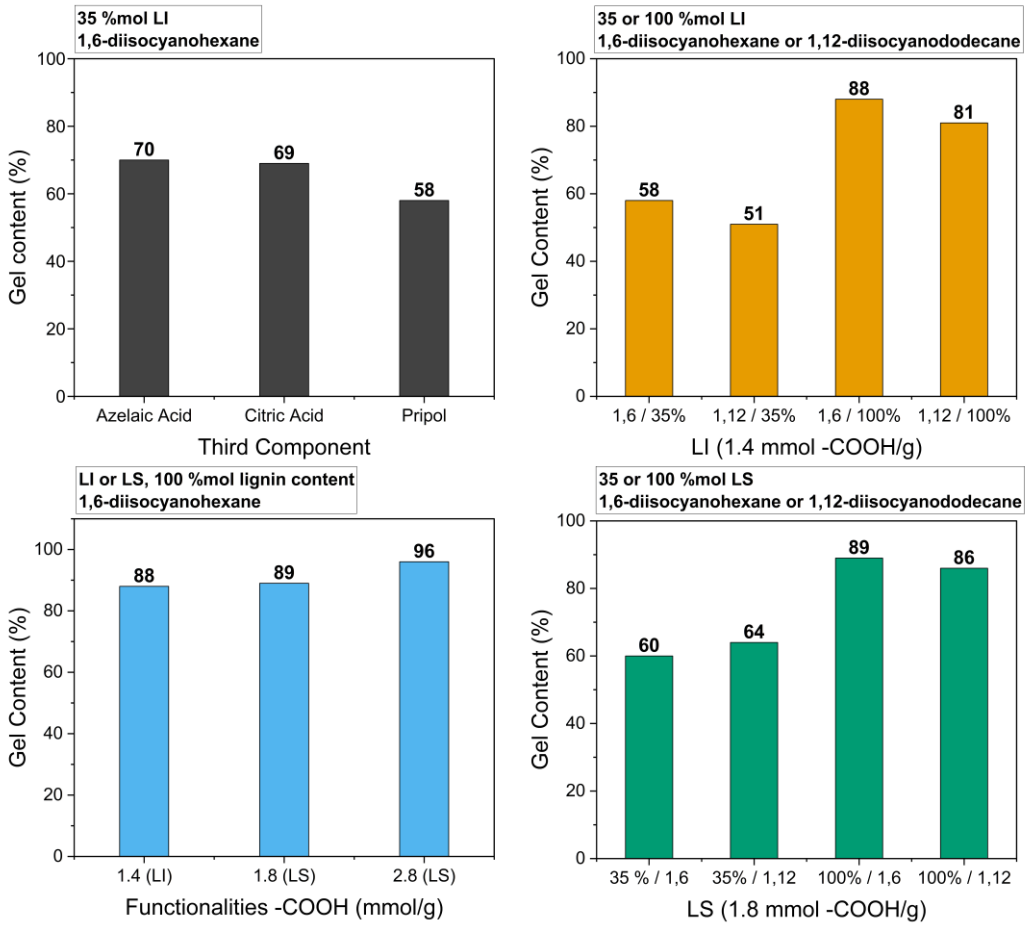

Figure 4.3.9 – Overview of the gel contents of the Passerini thermosets systems. In the black column bar graph, the influence of the third component is investigated. In the orange graph, LI is used in different amounts and both di-isocyanides are employed. In the blue graph, is investigated how the number of functionalities in the lignin impact the gel content. Finally, in the green box, different amounts of LS and both di-isocyanides are employed.

This is easily explained due to the higher crosslinking density provided by **LI** to the network if compared to **Pripol™**. However, thermosets with 100 mol% lignin content were brittle, and possessed poor mechanical properties. The thermosets with 35 mol% **LI** and **Pripol™** were instead flexible and tough. A visual representation is shown in **Figure 4.3.10**.

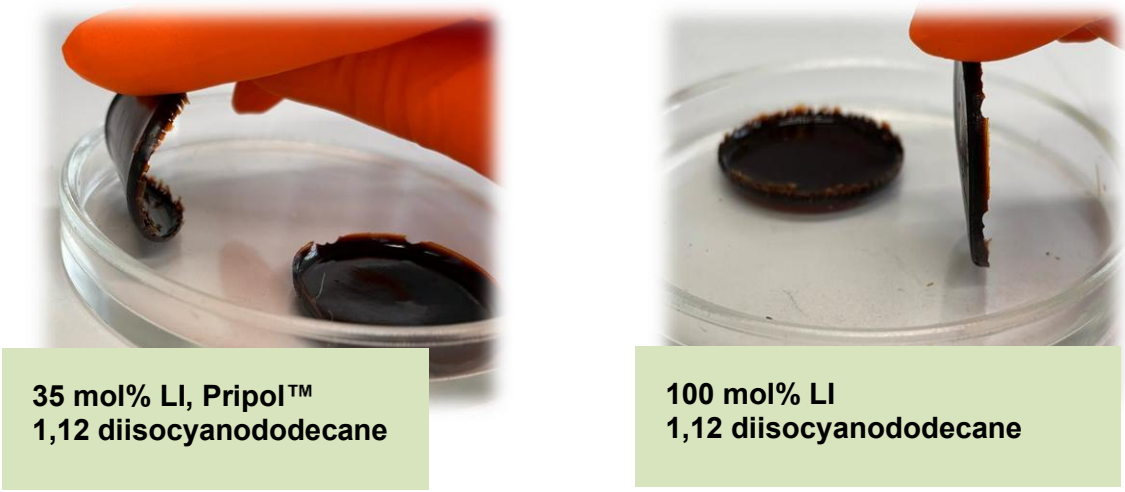

Figure 4.3.10 – Left: Passerini thermoset with 35 mol% LI and Pripol™, appearing flexible. Right: Passerini thermoset with 100 mol% LI, appearing brittle and not bendable. *Pictures taken by the author*.

Another important parameter to consider is the functional group distribution of the lignin component. In fact, when **LI** was used, bearing 1.4 mmol·g^{-1} of -COOH groups, only 88 % gel content was obtained with 1,6-bis(isocyano)hexane as diisocyanide component, while when **LS** was used, the gel content improved greatly, reaching a maximum of 96 % when **LS** with the highest number of functionalities was used (2.8 mmol·g^{-1} -COOH). On the other hand, when **LI** (1.4 mmol·g^{-1} -COOH) and **LS** (1.8 mmol·g^{-1} -COOH) batches with a more comparable carboxylic acid contents were used, similar gel contents were obtained (88 and 89 %, respectively, **Figure 4.3.9**, blue graph).

When **LS** with 1.8 mmol·g^{-1} -COOH was used in combination with 1,6 or 1,12-bis isocyanides and different lignin content, a similar trend was observed to what was previously found for **LI**. For lower lignin content (35 mol%), the gel content remains low, regardless of the diisocyanide chain length (a slight increase from 60 % to 64 % is observed when passing from 1,6 to 1,12; contrary to what observed for **LI**, where the gel content decreased from 58 % to 51 %, when passing from 1,6 to 1,12). For higher lignin contents (100 mol%) the gel content increased as well, as previously observed (**Figure 4.3.9**, green graph).

In general, with **LS** as lignin type, slightly higher gel content compared to **LI** were observed, this can be attributed to a higher amount of functionalities.

In order to improve the gel content without sacrificing the mechanical properties of the thermosets, several other approaches were tested. Initially, 2,5-furandicarboxylic acid (FDCA) was investigated as potential candidate to substitute **Pripol™** (or to use in combination). However, this approach was discarded because of solubility issues of FDCA in the thermoset mixture. Another approach involved partially substituting the aldehyde component (nonanal, monofunctional) with a difunctional aldehyde (decandial, difunctional). For this purpose, 20 % of the total -CHO groups were substituted with decandial, maintaining nonanal for the remaining 80 %. The remaining components were 1,6-bis(isocyano)hexane, 35 mol% -COOH **LI** and 65 mol% -COOH covered by **Pripol™**. This approach, however, was unsuccessful, because despite the thermoset looking stiffer in comparison to those without decandial under the same conditions, the gel content was still 62 %. Another approach involved introducing more functionalities in the carboxylic acid component, without increasing the lignin content. For this reason, a mixture of **Pripol™** and citric acid (50:50) was used in a thermoset with 35 mol% **LI** and 1,6-bis(isocyano)hexane. However, the gel content was 65 %. Extensive experimentation and optimization were undertaken to achieve a suitable balance between gel content and mechanical properties, however no satisfactory compromise could be identified within the conditions investigated. In addition, the structure of **Pripol™**—characterized by a long aliphatic chain and a bulky architecture—likely contributes to a reduced crosslinking density, as discussed in a later section. Moreover, a higher number of functionalities in the lignin structure would be beneficial for higher gel contents.

4.3.5.1.1 Thermal Characterization

The thermal properties of the developed thermosets were investigated in order to observe possible trends correlating the lignin type and content and the diisocyanide chain and the decomposition temperatures with the T_g. Indeed, a clear trend can be identified for the T_g: for lower lignin contents (35 mol%), independently from the lignin type (**LI** or **LS**) or the diisocyanide length, the T_g is well below r.t. for all cases, ranging from a minimum of – 27 °C to a maximum of – 20 °C, confirming their marked flexibility. When transitioning to higher lignin contents (100 mol%), several differences can be noticed. The diisocyanide chain length does not have a significant impact on the T_g, with only small differences when switching from C_6 to C_{12} chain length. Lignin type plays a crucial role here, accounting for the totality of -COOH groups. With **LI**, the T_g values are 100 and 98 °C, for 1,6 and 1,12-diisocyanides, respectively. For **LS** instead, the values are lower, namely 79 and 71 °C, for 1,6 and 1,12-bis isocyanides, respectively. This can be attributed to the T_g of the starting material **LS** (104 °C) being much lower than the one of **LI** (140 °C), the latter representing a more rigid structure. DSC and TGA traces are provided in the Experimental Section, **paragraph 6.6.3**.

Table 4.3.3 – Overview of the thermal properties analyzed *via* DSC and TGA of the Passerini thermosets, with different lignin contents and diisocyanide length. [a]: starting materials, LI and LS.

Lignin Type	Bis-Isocyanide	Lignin (mol%)	$T_{d,5\%}$ (°C)	$T_{d,50\%}$ (°C)	Residues (%)	T_g (°C)
LI	1,6	35	295	438	16	-25
LI	1,6	100	251	417	30	100
LI	1,12	35	282	440	11	-27
LI	1,12	100	247	418	26	98
LS	1,6	35	300	430	11	-22
LS	1,6	100	225	392	25	79
LS	1,12	35	302	435	10	-20
LS	1,12	100	232	399	23	71
LI[a]	-	-	213	441	36	140
LS[a]	-	-	230	423	35	104

The thermal decomposition of the thermosets presents a single-step degradation curve with a clear trend of decreasing thermal stability with increased lignin content. This observation could be recognized for both lignin types, where, for instance, the $T_{d,5\%}$ decreases from 295 to 251 °C in the case of 1,6-bis(isocyano)hexane and from 282 to 247 °C for the 1,12-bis(isocyano)dodecane. A similar trend is observed when **LS** was used as lignin crosslinker. This is attributed to the lower thermal stability of the starting materials (213 °C for **LI** and 230 °C for **LS**, $T_{d,5\%}$) compared to the one of the cured thermosets.

4.3.5.1.2 Conclusions and Outlook

In this first part of the project, the suitability of the newly synthesized macromonomer **LI** as crosslinker was investigated in a Passerini-3MCR system. Several conditions such as the influence of the third component, solvent, lignin content and lignin type, as well as the number of functionalities were investigated. However, under the investigated conditions, no set of parameters was identified that could simultaneously yield materials with satisfactory mechanical properties and a high crosslinking density, which is a key requirement for thermoset materials. Consequently, despite the fact that several alternative approaches remain open for future investigation, this part of the project was concluded at this stage. Further outlooks could involve, for instance, the utilization of trifunctional isocyanides or a pretreatment of lignin with ethylene carbonate (known as *hydroethylation*) that could increase the reactivity of lignin with the cyclic anhydrides leading to a higher number of functionalities, that were proven to be beneficial for the crosslinking density.

4.3.5.2 Epoxy Resins

With both **LI** and **LS** synthesized and characterized, their performance in the development of fully biobased epoxy resin systems was investigated as well. Initial efforts were dedicated to finding the optimal formulation for the thermosets, consisting of **LI** or **LS** as the lignin component, **Pripol™ 1009** as diluent and **ESBO** (Epoxidized Soybean Oil) as epoxy component. A representative scheme of the reaction is shown in **Scheme 4.3.5**.

Scheme 4.3.5 – General reaction scheme of the epoxy resin formation. The starting materials (lignin types LI or LS, Pripol™, and ESBO) as well as the final resins are shown with representative structures. LI is chosen as default representative structure, but the isomerized structure (citraconate) is likely also present, as depicted in **Scheme 4.3.2**.

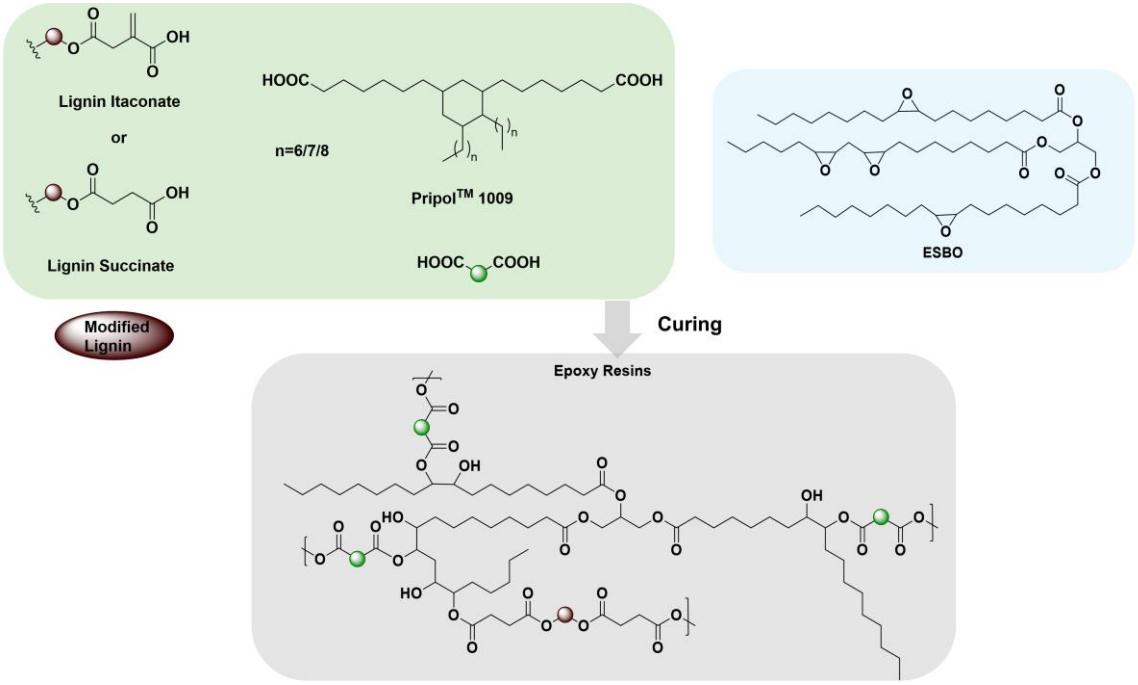

The stoichiometric ratio of COOH:Epoxy was chosen to be 1:1.2, which was previously reported to deliver the best performance in terms of mechanical properties and crosslinking density.[394–397] Different mol% of lignin component were tested, namely 5, 10, 15, 25 and 35 mol% (with respect to the total amount of −COOH groups, the rest to achieve the desired functional group equivalents was covered by **Pripol™** (for detailed calculations see Exp. Section, **Table**

6.6.7). Higher lignin percentages were not investigated due to the brittleness of the materials, being the 35 mol% lignin thermoset already quite brittle. Due to the presence of lignin, the resin mixtures required the use of a solvent to dissolve all the components prior to curing. Initially, acetone was selected as the solvent for resin preparation due to its ease of removal and ability to fully dissolve the carboxylic acid-functionalized lignin. However, in preliminary tests, phase separation was observed in the final materials for lignin contents above 5 mol% (**Figure 4.3.11**).This issue, likely ascribed to the rapid evaporation of acetone during processing, was effectively resolved by replacing acetone with dimethyl sulfoxide (DMSO). To confirm that the high-boiling solvent DMSO is not present anymore in the final material after curing, possibly affecting the gel content or the mechanical properties of the material, the sample was weighed before and after the curing. The total mass of the components without solvent was taken before and after curing (m_i and m_f, respectively). The difference between the two values was Δm = -10 mg, showing no mass increase due to solvent left inside the material. The small difference in mass is within the error range of the measurement (m_i = 344 mg), probably due to small material losses while transferring the sample.

Figure 4.3.11 – Left: thermoset with 15 mol% of lignin, cured with acetone as solvent. Phase separation is clearly visible in the final material. Right: thermoset with 15 mol% of lignin cured in DMSO. No sign of phase separation is observed.

In **Figure 4.3.12**, exemplary IR spectra of the resins are shown, along with a reference spectrum of **ESBO**. After curing, notable spectral changes can be observed: the characteristic stretching band of the oxirane ring, clearly visible in the **ESBO** spectrum, is not observed in either resin spectra, indicating that the epoxy groups have successfully reacted. In addition, an increase in the broad

O−H stretching region is evident (3600 – 3100 cm^{-1}), consistent with the formation of β-hydroxy ester groups resulting from the epoxy-acid curing reaction. Additionally, the carbonyl stretching vibration of the resins displays a small shoulder at 1710 cm^{-1}, which may correspond to unreacted carboxylic acid groups.

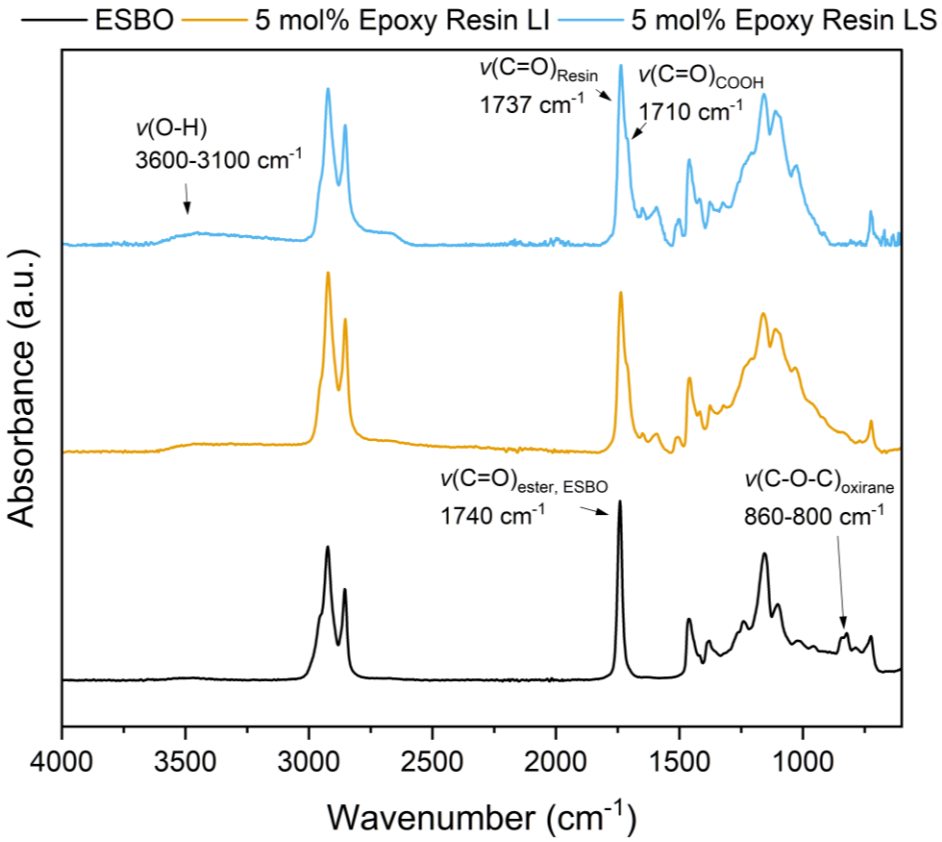

Figure 4.3.12 – Stacked IR spectra of ESBO (black curve), the epoxy resin with 5 mol% of Lignin Itaconate (orange curve), and epoxy resin with 5 mol% of Lignin Succinate (blue curve).

A small amount of DBU (0.5 wt% in respect to the total resin mass) was necessary as catalyst in order to achieve faster crosslinking. The IR spectra of the resins without and with 0.5 wt% of DBU as catalyst are shown in **Figure 4.3.13**.

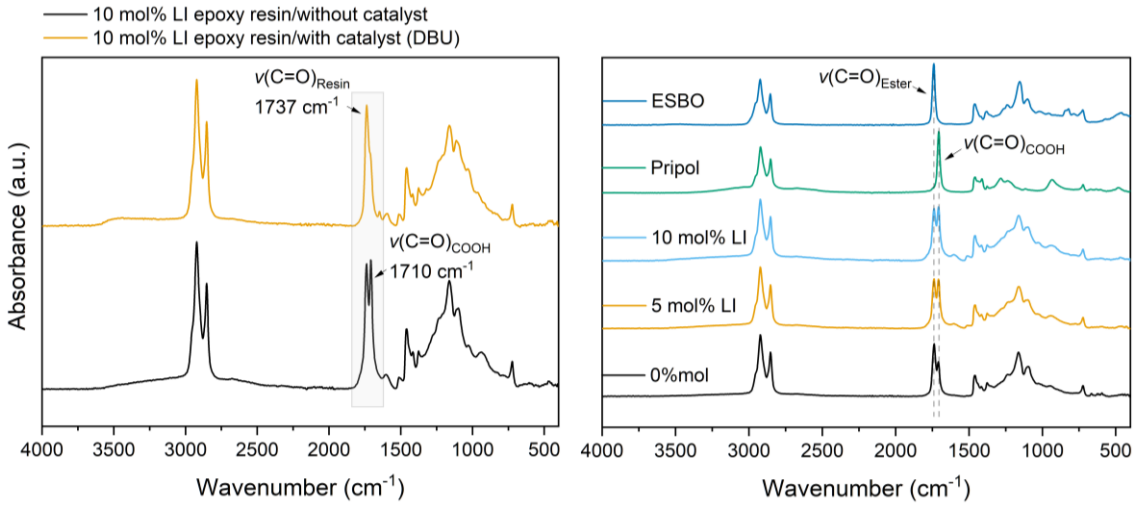

Figure 4.3.13 – Left: IR overlay of the resins with 10 mol% LI without catalyst (black) and with – DBU (blue), under the same curing conditions. Right: Overlay of the starting materials (ESBO and Pripol) and three formulations of the resins with different mol percentages of LI without DBU as catalyst. All the presented data are related to LI as lignin component.

If the catalyst was not present in the formulation, the cured resins presented a splitting in the carbonyl region, where the signal at ~1750 cm^{-1} is ascribed to the carbonyl stretching vibration for the ester groups of **ESBO**, while the other peak (~1710 cm^{-1}) is attributed instead to the carbonyl stretching vibration of free unreacted -COOH. It can be seen that under the same curing conditions, the reaction in the presence of the catalyst proceeded significantly faster.

Real-time IR spectroscopy was employed to monitor the curing of the resins over time. Two formulations containing 5 mol% of **LI** were analyzed, with and without DBU, as shown in **Figure 4.3.14**. As a comparison, the curing behavior of the resin containing 5 mol% of **LS** was also monitored and is reported in **Figure 4.3.15**.

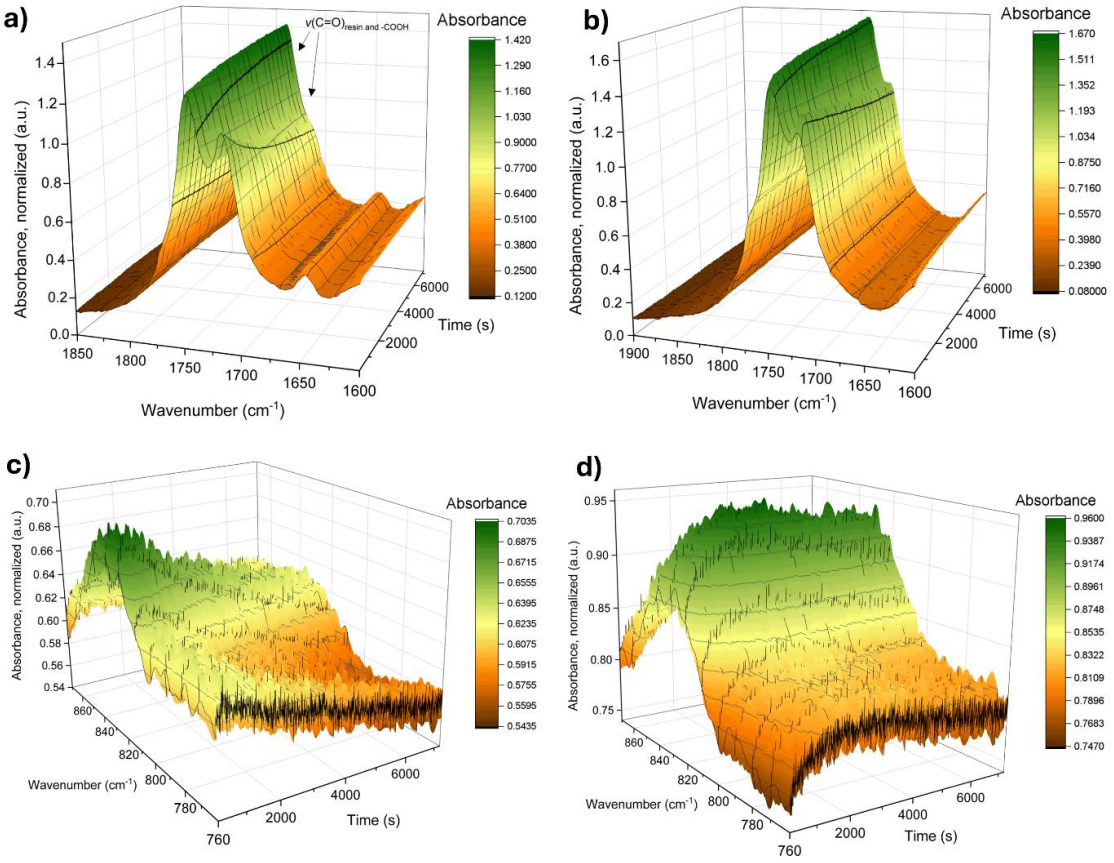

Figure 4.3.14 – Realtime IR curves of the 5 mol% lignin formulations, with (a,c) and without DBU (b,d). For both cases, a zoom in the region of the carbonyl area (a,b, 1600 – 1850 cm^{-1}) and the epoxy region (c,d, 760 – 860 cm^{-1}) is presented over time.

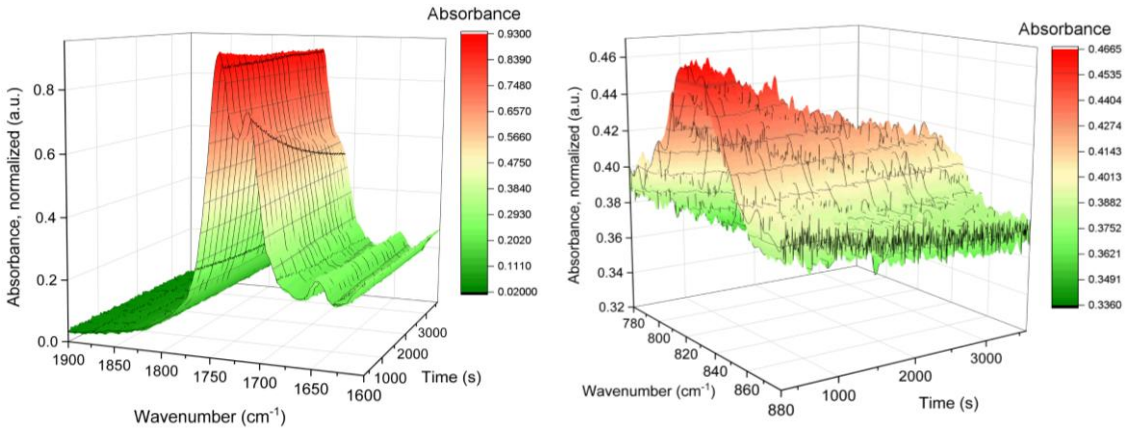

Figure 4.3.15 – Real-time curing followed *via* RT- FTIR of a 5 mol% LS epoxy resin in the presence of catalyst.

A closer inspection of the carbonyl region reveals that the shoulder peak at ~1700 cm^{-1}, attributed to free −COOH groups, decreases progressively in both systems, indicating ongoing esterification. In the presence of DBU as catalyst, this shoulder becomes significantly less prominent within the observed time of ~3000 s, suggesting a more complete consumption of carboxylic acid groups. Simultaneously, a clear decrease in the intensity of the epoxy absorption band is observed, particularly in the catalyzed formulation, confirming accelerated reaction rate.

To assess the evolution of the absorbance peak area associated with free −COOH groups over time, a peak deconvolution analysis was performed on the carbonyl region. The area of the signal compared to its initial value is plotted over time shown in **Figure 4.3.16**. A comparison was made to evaluate the catalyst presence (**Figure 4.3.16**, left) and the lignin type (**Figure 4.3.16**, right). Details of the deconvolution procedure are provided in the Exp. Section (**paragraph 6.6.4.3**).

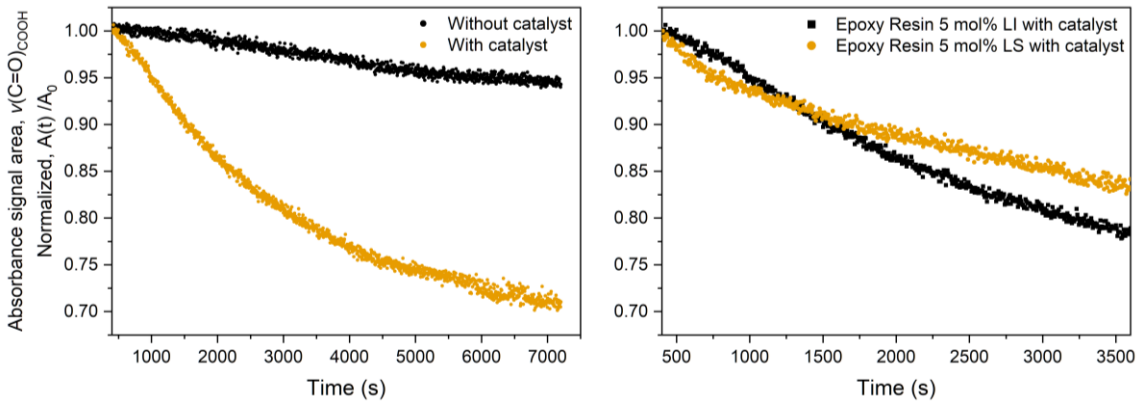

Figure 4.3.16 – Normalized absorbance signal area of the free -COOH groups over time. Left: an epoxy resin formulation with 5 mol% LI, with and without catalytic amounts of DBU. Right: two epoxy resin formulations with 5 mol% of LI or LS, both in the presence of catalytic amounts of DBU. The time range differs between the graphs (7000 s for LI and 3500 s for LS) due to practical time constraints.

As depicted from **Figure 4.3.16**, left, the normalized absorbance signal area for −COOH groups decreases at a much faster rate in the presence of DBU as catalyst, confirming that its presence is necessary for a faster and efficient curing

procedure. On the right, the normalized absorbance signal area corresponding to the −COOH groups is plotted over time for the resins containing 5 mol% of **LI** or **LS**, both cured under identical conditions and in the presence of DBU. Since the initial comparison on the left indicated that the curing reaction rate significantly decreased after approximately 4000 s, the acquisition time for the comparative experiment between the two lignin derivatives was limited to 3500 s, which was sufficient to evaluate potential differences in the curing kinetics between the two systems. The results suggest that the curing behavior of resin with **LI** proceeds slightly faster than the one with **LS**. However, considering the small lignin content in both resins (5 mol%), the overall curing kinetics are likely dominated by **Pripol^{TM}** matrix. Moreover, the final extent of −COOH consumption is similar for both systems, indicating comparable overall reactivity.

Different stoichiometric ratios were tested, and from their respective IR spectra it was possible to compare the relative amounts of free carboxylic acid compared to the ester carbonyl groups through a peak deconvolution method. The results show that with an excess of epoxy groups, more free carboxylic acids are converted and crosslinked within the network. In particular, going from 1:1 to 1:1.5 COOH:Epoxy ratio decreased the free fatty acids percentage ratio from 33 to 24 % (**Figure 4.3.17** and **Table 4.3.4**).

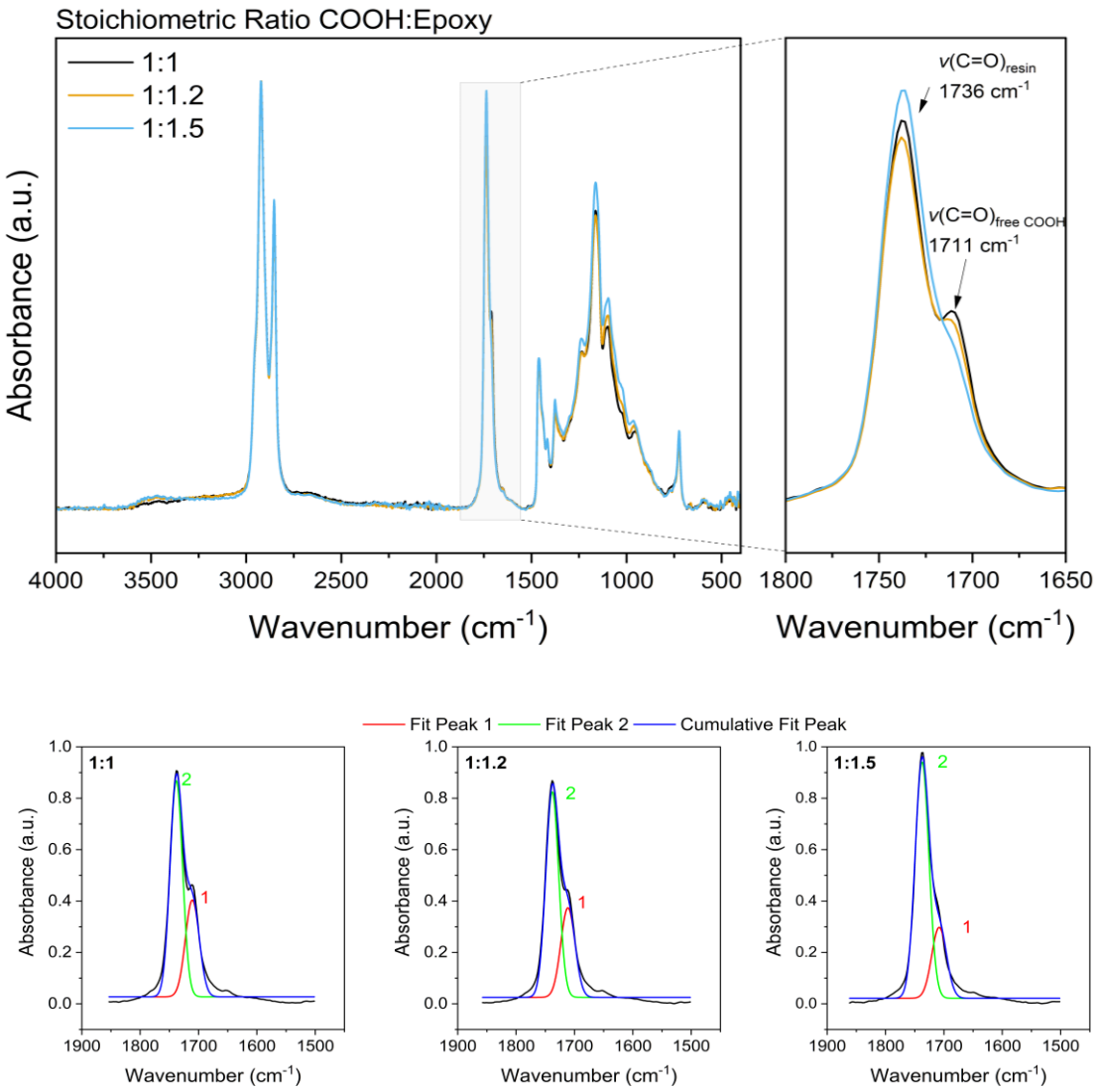

Figure 4.3.17 – Above: Overlay of IR spectra for three different stoichiometric ratios (1:1, 1:1.2, 1:1.5 COOH:Epoxy), normalized at the C-H stretching signal (ν(C-H), 2920 cm^{-1}). Below, the fitting of the deconvoluted peaks ascribed to the free carboxylic acid carbonyl stretching vibration (1) and ester carbonyl stretching vibration (2).

Table 4.3.4 – Results of the peak deconvolution method giving the area of the two peaks (1 = free carboxylic acids and 2 = ester groups), as well as their percentage ratios and R-square.

Ratio COOH:Epoxy	Area (a.u.)		Free carboxylic acid (%)	Ester (%)	R-square
	Peak 1	Peak 2			
1:1	11.19	22.58	33	67	0.9888
1:1.2	10.59	22.20	32	68	0.9879
1:1.5	8.78	27.35	24	76	0.9938

The same range of lignin mol% compositions and optimized conditions (**Table 6.6.7,** Exp. Section) established for the **LI**-based resins were extended to the **LS** formulations. The gel contents of 78–92 % for all thermosets (see **Table 4.3.5**) confirm a successful network formation within the resins for both lignin macromonomers. The gel contents for **LS** are slightly higher than the ones for the resins obtained with **LI**, which can be attributed to higher −COOH functionalities of **LS** (1.79 mmol·g^{-1} −COOH) compared to **LI** (1.39 mmol·g^{-1} −COOH), thus increasing the crosslinking density. The relatively low gel content values of the resins could be influenced by several factors. Firstly, the internal epoxy groups of **ESBO** are intrinsically less reactive than terminal epoxy groups of established monomers such as DGEBA, showing lower crosslinking densities compared to other compounds bearing terminal epoxies.[398] Moreover, the structure of **Pripol^{TM}**, with its long aliphatic chain and bulky structure, could likely lead to reduced crosslinking density and lower reactivity compared to smaller, more rigid carboxylic crosslinkers such as linear aliphatic diacids, owing to steric effects, as also discussed in the work from Matharu *et al*.[399] In line with this, additional experiments were designed using shorter difunctional renewable acids (azelaic, C_9 and adipic, C_6) for resins containing 30 mol% of **LI** under identical curing conditions. The aim was to investigate the influence of **Pripol^{TM}** on the gel content, compared to shorter chain diacids. This indeed resulted in higher gel contents (92 and 95 %, for azelaic and adipic, respectively) compared to the **Pripol**-based system (86 %), but simultaneously resulted in very poor mechanical properties (the materials were glassy and very brittle), which rendered their handling and further analysis particularly challenging. Finally, **Pripol™** provided a suitable compromise between successful network formation and favorable mechanical properties, slightly reducing the gel content, but still maintaining satisfactory values.

Table 4.3.5 – Gel contents of the epoxy resins developed with varying contents of different lignin macromonomers LI and LS.

Lignin Content (mol%)	GC Lignin Itaconate (%)	GC Lignin Succinate (%)
0	78	78
5	84	90
10	83	90
15	81	85
25	81	92
35	83	91

4.3.5.2.1 Thermal Properties of the Epoxy Resins

Thermal analyses of the thermosets were performed using Differential Scanning Calorimetry (DSC) and Thermal gravimetric Analysis (TGA) measurements. All formulations exhibited relatively low glass transition temperatures (T_g) around -30 °C, consistent with the high flexibility observed at room temperature (DSC curves are reported in the Exp. Section (**Figure 6.6.34**). No clear correlation between lignin content and T_g values was identified for either functionalized lignin, suggesting that the highly aliphatic nature of the polymer matrix predominantly governs the thermal behavior. However, a slight increase in T_g was observed for higher lignin contents in the **LS**-based epoxy resins, indicating that the more rigid lignin structure may contribute to a modest restriction of chain mobility and thus a higher T_g.

The TGA curves (**Figure 6.6.35**, Exp. Section) show that all the thermosets present increased thermal stability compared to the starting materials of modified lignin, which present lower $T_{d,5\%}$ (213 and 230 °C, for **LI** and **LS**, respectively) compared to the thermosets (with the lowest $T_{d,5\%}$ of 282 °C) (**Table 4.3.6**). The materials present single-step degradation curves, with the $T_{d,5\%}$ values decreasing with increased lignin content (from 347 °C for 0 mol% lignin to 282 and 294 °C for 35 mol% of **LI** and **LS**, respectively). This is likely due to the lower thermal stability brought by the starting lignin macromonomers. Residues are

increasing as well with lignin content, which was expected because lignin contributes to char formation. The lower residues for the **LS**-type resins can be explained by a lower wt% of the lignin in the final materials, as the **LS** presented higher functionalization. An overview of the data is presented in **Table 4.3.6**.

Table 4.3.6 – Overview of the thermal data for the set of epoxy resins with LI and LS, as well as the starting lignin derivatives.

mol% lignin	T_g (°C)	$T_{d,5\%}$ (°C)	$T_{d,50\%}$ (°C)	Residues (%)	Lignin Content (wt%)
0	-36	347	427	1	-
5 - LI	-32	348	429	4	6
10 - LI	-33	345	432	5	12
15 - LI	-32	331	434	12	18
25 - LI	-33	290	428	22	28
35 - LI	-31	282	436	27	36
5 - LS	-29	323	417	5	5
10 - LS	-30	321	416	7	10
15 - LS	-32	305	417	8	14
25 - LS	-24	310	415	9	23
35 - LS	-23	294	414	15	31
LI	140	213	441	36	-
LS	104	230	423	35	-

4.3.5.2.2 Rheology and DMA Experiments

Amplitude sweep and frequency sweep tests on the formulations containing 0, 5 and 10 mol% of **LI** (higher lignin contents were too brittle to be characterized mechanically) were investigated. The amplitude sweep tests were carried out to identify the linear viscoelastic region (LVER) and the behavior of the material within the LVER. All formulations presented a dominant elastic component with the storage modulus G' > G'', and a clear solid-like behavior, as depicted in **Figure 4.3.18**. Increasing the lignin content influences the LVER, making the materials more resistant to deformation and increasing the shear strain that can be applied to the materials before they start to undergo irreversible changes in their structure. This indicates that the incorporation of lignin itaconate into the thermoset matrix reinforces the network, likely due to the rigid, multifunctional nature of lignin, which increases crosslink density and restricts chain mobility. In the thermoset with the highest lignin content tested (10 mol%) the LVER ended at 13 %, versus a 1.2 % shear strain for the thermoset without lignin, suggesting that the presence of the lignin itaconate in the thermoset matrix strongly contributes to the viscoelastic behavior of the materials. A frequency sweep (**Figure 6.6.36**, Exp. Section) between 0.01 and 10 Hz also revealed a dominant storage modulus and a viscoelastic solid behavior in all the materials, confirming the results of the amplitude sweep.

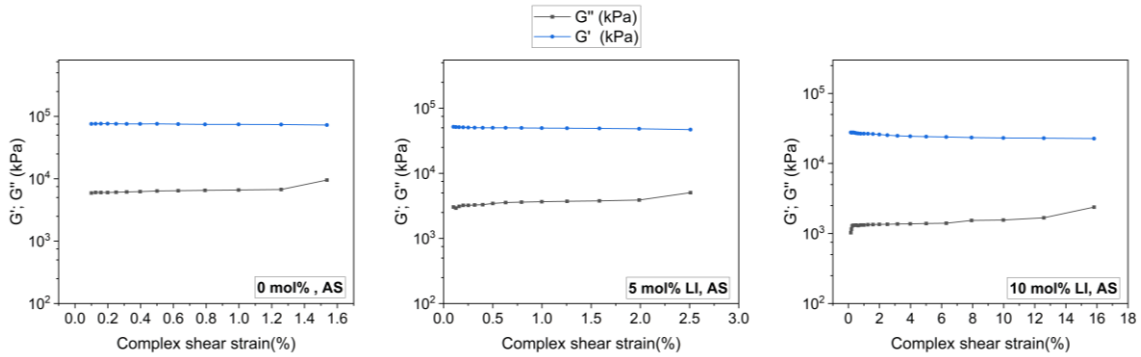

Figure 4.3.18 – Amplitude sweep experiments for LI epoxy resins with lignin contents of 0, 5, and 10 mol%.

Dynamic Mechanical Analysis (DMA) experiments were performed on the formulations with the lowest lignin contents to gain observations into the mechanical behavior of the materials. Specifically, resins containing 0 mol%, 5 mol% and 10 mol% of LI or LS were investigated. **Figure 4.3.19 (a)** presents the overlaid DMA curves. For each formulation, three to five replicates were analyzed to ensure reproducibility. All samples exhibited a sharp decrease in storage modulus (E′, **Table 4.3.7**) at the glass transition temperature (T_g, or T_α, corresponding to the α-relaxation). This pronounced drop, particularly near the instrument transducer's sensitivity limit, can introduce experimental challenges, as reflected in some of the curve resolutions. In particular, the thermoset containing 10 mol% **LI** approached the detector limit, making data above the onset unreliable for quantitative interpretation. Despite these limitations, the thermosets displayed comparable maximum storage moduli in the glassy and rubbery region, suggesting similar crosslinking densities (ν_e). In particular, the crosslinking densities were calculated according to the theory of rubber elasticity (Exp. section, **paragraph 6.2**). The results show a general trend of increasing crosslink density with higher lignin content, as expected from the incorporation of the polyfunctional macromonomer (**Table 4.3.7**). This finding highlights how lignin incorporation can be used to tailor the network architecture and, consequently, the mechanical and viscoelastic properties of the thermosets. The relatively large standard deviations observed in some cases can be attributed to the intrinsic heterogeneity of the networks and the structural irregularities of the lignin derivatives. This can be regarded as a future challenge in lignin chemistry, as such deviations limit real world applications. As the materials transit through the glass transition region, their elasticity changes, leading to a minimum in storage modulus. **Figure 4.3.19 (b)**, shows that the T_g values determined by DMA (from the onset of E′) correlated well with those obtained by DSC. The T_g values derived from the maximum tanδ—higher than the onset ones—provide an indication of the glass transition region relevant for potential application conditions.

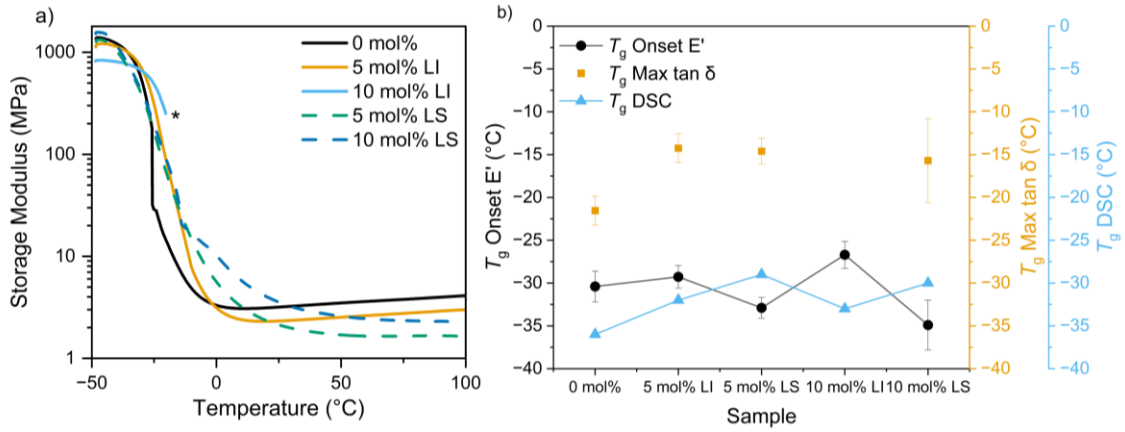

Figure 4.3.19 – a) representative DMA curves for the formulation tested. *: n.a. due to experimental difficulties (see Exp. Section, **Figure 6.6.37** and Figure **6.6.38**). b) Comparison of the T_g values obtained from DMA and DSC methods.

Table 4.3.7 – Overview of the most significant data obtained from DMA experiments.

Sample	$E'_{-50°C}$ (MPa)	$E'_{25°C}$ (MPa)	T_g (°C) Onset E´	T_g (°C) Max tan δ	ν_e (x10^3 mol/m^3)
0 mol%	1242 ± 110	2.78 ± 0.38	-30.4 ± 1.8	-21.54 ± 1.70	0.501 ± 0.12
5 mol% LI	1352 ± 192	3.52 ± 1.04	-29.28 ± 1.31	-14.25 ± 1.68	0.76 ± 0.34
5 mol% LS	1138 ± 212	2.12 ± 0.004	-32.9 ± 1.2	-14.6 ± 1.5	0.572 ± 0.03
10 mol% LI	850 ± 85	-*	-26.70 ± 1.57	-*	-*
10 mol% LS	1311 ± 202	3.42 ± 0.17	-34.9 ± 2.9	-15.7 ± 4.9	1.128 ± 0.04

*: n.a. due to experimental difficulties (see Exp. Section**, Figure 6.6.37**)

4.3.5.2.3 Tensile Strength Measurements of the Resins

The investigation of mechanical properties provided further understanding of the behavior of the thermosets. **Figure 4.3.20 (a)** shows representative stress-strain curves for the different formulations. Thermosets prepared with **LI** exhibited higher elastic moduli compared to the other formulations, suggesting that the incorporation of itaconate moieties contributes to increased rigidity and stiffness, as can be expected in comparison to succinic moieties. These formulations also showed lower strain at break, indicating a more brittle behavior with a higher likelihood of structural defects. Conversely, thermosets prepared with **LS** displayed lower elastic moduli—even compared to the 0 mol% formulation—along with higher elongation at break, consistent with the introduction of more flexible succinate moieties into the network. In contrast to the thermal analysis results, the mechanical performance appears to be strongly influenced by both the lignin content and its chemical nature, indicating that the type and amount of lignin play a major role in defining the overall mechanical response of the otherwise aliphatic matrix. In **Figure 4.3.20 (b)**, an overview of the important parameters obtained from the stress-strain curves is presented. **Table 4.3.8** summarizes the key results obtained from the DMA and tensile strength measurements. Once again, the large standard deviations observed in some cases confirm the heterogeneous nature of the materials, particularly for the formulation containing 10 mol% **LI**. For this sample, five replicates were tested to ensure reproducibility. Such variability is typical for systems with high lignin contents.[400,401]

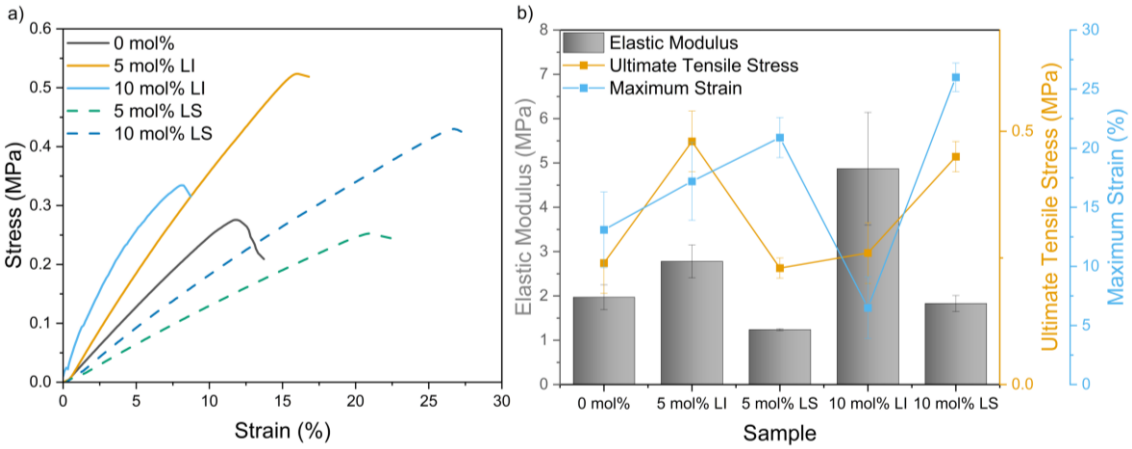

Figure 4.3.20 – a) representative stress-strain curves of the tested formulations. b) overview of the most significant parameters (elastic modulus, ultimate tensile stress and maximum strain) obtained from stress-strain curves of the formulations. For all the samples, 3 to 5 replicates were tested for each measurement, see Exp. Section, **Figure 6.6.39** and **Figure 6.6.40**).

Table 4.3.8 – Overview of the most significant data obtained from tensile strength measurements.

Sample	Elastic Modulus (MPa)	Ultimate Stress (MPa)	Strain (%)
0 mol%	1.97 ± 0.28	0.24 ± 0.06	13.1 ± 3.2
5 mol% LI	2.78 ± 0.37	0.48 ± 0.06	17.2 ± 3.3
5 mol% LS	1.24 ± 0.02	0.23 ± 0.02	20.9 ± 1.7
10 mol% LI	4.87 ± 1.27	0.26 ± 0.06	6.5 ± 2.6
10 mol% LS	1.83 ± 0.18	0.45 ± 0.03	26.0 ± 1.2

4.3.5.2.4 Degradation of the Resins

Due to the presence of hydrolyzable ester bonds in the structure of the thermosets, it was investigated if the materials could be degraded *via* hydrolysis. These include esters formed between the lignin backbone and the itaconate moieties, as well as esters resulting from the reaction of carboxylic acid groups (both from LI and Pripol™) with the epoxy groups of ESBO and the ester groups of ESBO itself. The degradation behavior was exemplarily studied on a 10 mol% **LI** epoxy resin. Both alkaline and acidic conditions were tested for the hydrolysis of the resin. A determined amount of 10 mol% **LI** epoxy resin was submerged in either an alkaline or acidic solution and stirred for 4 days at 80 °C. The outcome of the degradation was analyzed *via* IR spectroscopy and ^{31}P NMR.

Acidic conditions were investigated, as in principle they represent a more sustainable option; in contrast to alkaline hydrolysis, they do not require a subsequent neutralization step to recover the product, which generates additional waste. Under acidic conditions in fact, the lignin fraction is expected to precipitate following the breakdown of the thermoset matrix. Two different acidic media were tested: a 1 M HCl solution and a 1 M citric acid (CA) solution, alongside a 0.6 M NaOH solution for the alkaline conditions, adapted from literature conditions.[373] The degradation conditions were kept identical for all treatments (4 days, 80 °C, for detailed experimental procedures see Exp. Section, **paragraph 6.6.4.7**). In both acidic cases, a brown, powdery precipitate was obtained after the reaction (see **Figure 4.3.21b**).

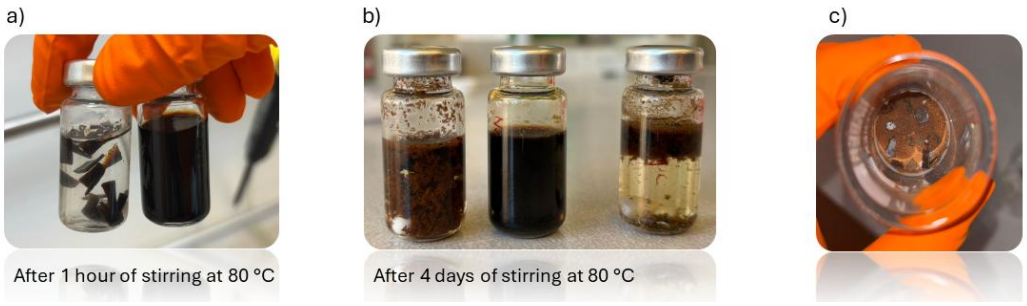

Figure 4.3.21 – a) Comparison between acidic hydrolysis in HCl (left) and alkaline (right) after 1 hour of stirring at 80 °C. The thermoset under alkaline conditions completely dissolved forming

a homogeneous solution. b) Left: hydrolysis with HCl solution, middle: hydrolysis with NaOH solution, right: hydrolysis with citric acid solution. the picture was taken 4 days after stirring at 80 °C. c) Recovered solids after hydrolysis with citric acid. The bigger pieces are undegraded thermoset. *Pictures are taken by the author*.

This precipitate was filtered, collected, and dried. Only partially degraded resin fragments were visually detected, even after four days of reaction, indicating that degradation under acidic hydrolysis proceeded only partially (**Figure 4.3.21c**). For clarity, in **Scheme 4.3.6** the degradation procedures are illustrated.

Scheme 4.3.6 – Illustrative scheme for the degradation procedure of thermoset 10 mol% - LI under alkaline or acidic conditions.

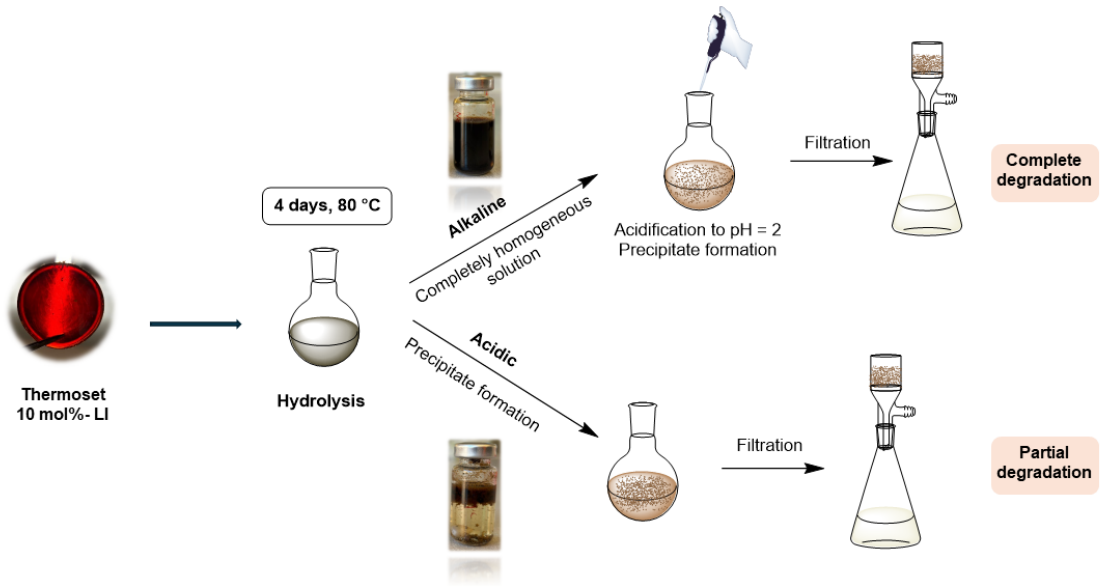

To separate the remaining undegraded material, the solids were suspended in acetone, and the insoluble resin fragments were removed by hot filtration. This procedure yielded two distinct fractions: an undissolved portion corresponding to the remaining thermoset pieces, and a dissolved portion, which was subsequently recovered by precipitation in acidic water. For the sake of comparability between methods, the product from alkaline hydrolysis was also subjected to dissolution in acetone and reprecipitation; however, in this case, complete dissolution in the solvent was observed, indicating a successful and complete breakdown of the resin matrix. An overview of all collected fractions is provided in **Table 4.3.9**. Nevertheless, degradation under alkaline conditions proved highly effective, as confirmed by IR spectroscopy (**Figure 4.3.22**, in

black), which showed the complete disappearance of the ester carbonyl stretching band, leaving only the characteristic carbonyl signal of the carboxylic acid groups stretching. The IR spectrum of the dissolved fraction obtained from citric acid hydrolysis (**Figure 4.3.22**, in blue) still displayed characteristic ester carbonyl stretching vibration signals, indicating that the degradation process was incomplete.

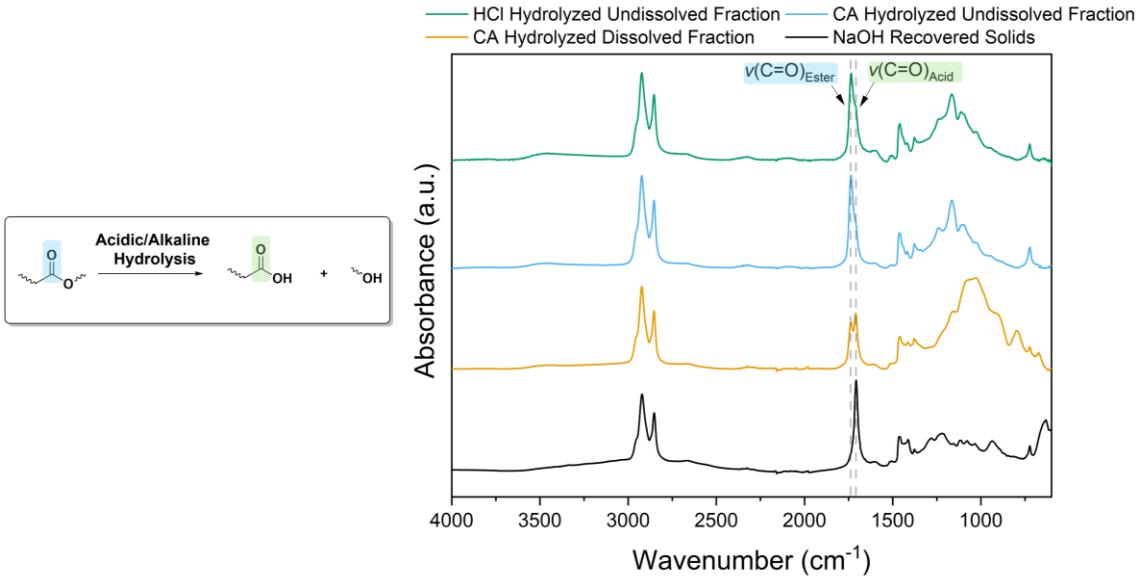

Figure 4.3.22 – IR spectra overlay of the different collected hydrolysis fractions. The IR of the solids collected after alkaline hydrolysis (black spectrum) shows a complete disappearance of the stretching vibration signals for the ester carbonyl, sign that the degradation proceeded successfully. After acidic hydrolysis with citric acid (blue spectrum) there is a splitting in the carbonyl region, sign that the degradation progressed only partially. The IRs of the undissolved fractions after acidic hydrolysis (red and green) show a spectrum very similar to the initial thermosets, sign that the degradation was minimal.

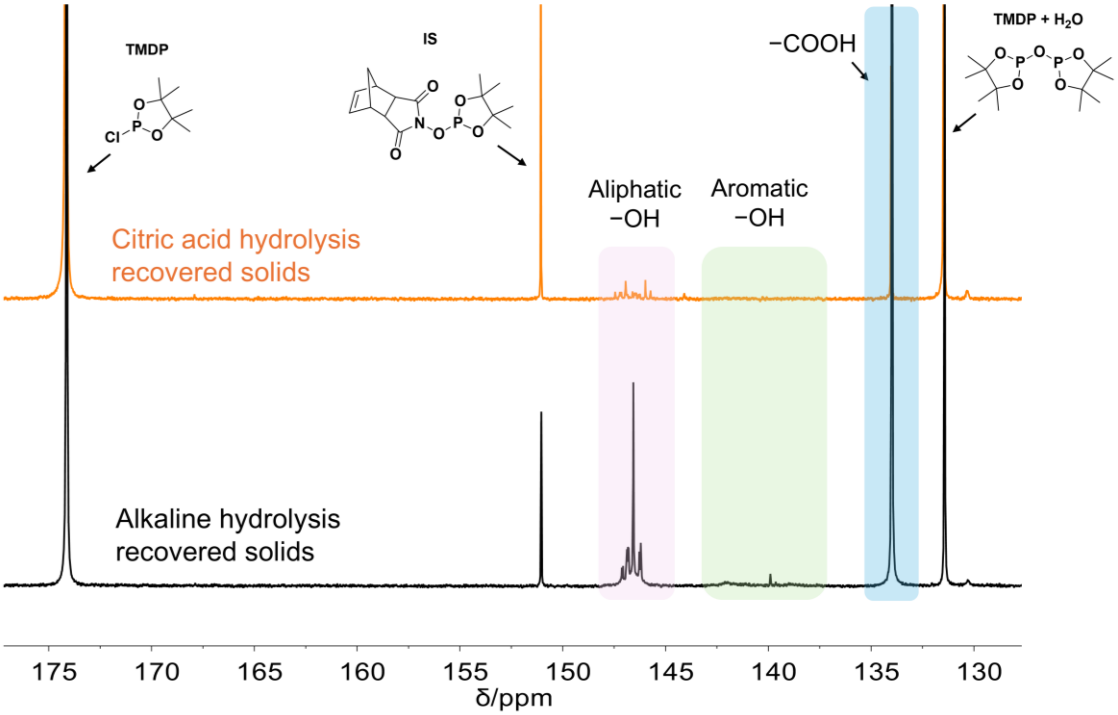

Figure 4.3.23 – ^{31}P NMR of the recovered solids after alkaline hydrolysis (black) and after acid hydrolysis with citric acid (orange). In both cases, aromatic hydroxyl groups are not present (or in very low quantity), while there are strong signals in the aliphatic and carboxylic acid regions, as would be expected after hydrolysis of the aliphatic thermoset matrix.

The ^{31}P NMR spectra of the recovered fractions (**Figure 4.3.23**) revealed a strong presence of aliphatic and carboxylic acid (–COOH) groups, with minimal to no signals corresponding to aromatic hydroxyl groups typically associated with lignin. These results confirm that probably only a limited amount of lignin was recovered in these fractions, however it is necessary to consider that the lignin content within the sample was low compared to the fatty acid content. In fact, even additional purification steps *via* dissolution and reprecipitation were not successful to isolate it, and the lignin fraction could not be recovered.

Overall, an efficient hydrolysis pathway for the resins was established, leading to complete degradation under alkaline conditions, but only partial degradation under acidic ones. These findings highlight the potential of such thermosetting

materials for applications where controlled degradability under hot alkaline conditions is desirable, such as in packaging adhesives or removable labels.

Table 4.3.9 – Overview of the collected weights of the fractions after hydrolysis both under alkaline and acidic conditions. In the parentheses are indicated the percentages in respect of their starting weight.

Hydrolysis Solution	Starting Weight (mg)	Total recovered weight (not purified) (mg)[a]	Dissolved Fraction (mg)[a]	Undissolved Fraction (mg)[a]
NaOH	503	454 (90%)	263 (52%)	n.a.
HCl	503	483 (96%)	28 (6%)	388 (77%)
CA	503	496 (98%)	44 (9%)	399 (79%)

n.a. : non applicable because the entirety of the sample was soluble in acetone. [a]: Values in parentheses indicate the percentage of recovered sample relative to the initial starting weight.

As shown in **Table 4.3.9**, the total unpurified recovered weight correlates very well with the starting weight. For the alkaline conditions, in order to recover the solids and neutralize the mixture, a precipitation step in acidic water was necessary, and this would explain the slightly lower value of the recovered weight (90 %) compared to the other conditions, where this step was not necessary. Afterwards, all the recovered solids were subjected to a first round of dissolution in acetone and reprecipitation in acidic water, as this could help with purification. As can be seen, after this purification step for the alkaline conditions the entire sample dissolved in acetone, with no undissolved fraction visually detected. However, only 52 % of the initial sample weight was recovered after reprecipitation (58 % compared to the previous step), indicating that some small molecules generated during degradation were soluble in both acetone and water and were therefore lost during filtration. In contrast, under acidic hydrolysis conditions, a large fraction remained insoluble in acetone (77 % and 79 % for HCl and citric acid, respectively), indicating that degradation was only partial. The dissolved solids recovered via subsequent precipitation were also minimal, and in the case of the HCl-treated sample, the amount was insufficient for further characterization.

4.3.5.2.5 Conclusions

In this part, a novel route for lignin functionalization with itaconic anhydride was developed and optimized. The influence of key reaction parameters—anhydride equivalents, catalyst, temperature, and reaction time—was systematically investigated. Under the applied conditions, isomerization of itaconic to citraconic anhydride occurred, consistent with literature reports and without affecting the introduced functional groups. The process was successfully scaled up, yielding comparable conversion and product characteristics. The precipitation medium could be reused up to three times, and solvent recovery of 75 % reduced the synthetic E-factor from 6.9 to 2.7. The resulting lignin derivatives were incorporated as multifunctional crosslinkers in fully biobased epoxy resins alongside epoxidized soybean oil and **Pripol™ 1009** and subsequently compared to analogous lignin succinate derivatives.

The thermosets exhibited high gel contents, thermal stability up to 280 °C, and low glass transition temperatures (ranging from -36 to -23 °C), consistent with their flexible and ductile behavior. Notably, resins based on lignin itaconate showed higher elastic moduli and lower strains at break compared to lignin succinate resins, indicating enhanced stiffness from itaconate incorporation. Finally, degradation studies demonstrated complete hydrolysis under alkaline conditions and partial degradation under acidic media, highlighting the potential of these materials as alkaline cleavable, biobased epoxy networks for sustainable applications. Their combination of high biobased content, flexibility and alkaline-hydrolyzable ester linkages suggests potential in applications where high stiffness is not required, but removability, elasticity and end-of-life degradability are advantageous.

4.3.5.3 Thia-Michael Thermosets

As a proof of concept, the reactivity of the Michael system was investigated as well. The activated double bonds of **LI**, that are most likely in the isomerized form (citraconate) as discussed in **paragraph 4.3.3**, were employed, together with a thiol-crosslinker, to achieve thia-Michael thermosets. Thia-Michael addition can proceed effectively also under uncatalyzed conditions.[402] It was furthermore recently demonstrated by Subbotina and Olsén *et al*.[388] that the thiol crosslinker pentaerythritol tetrakis(3-mercaptopropionate), PTEMP, could be employed to achieve crosslinked networks together with maleated lignin derivatives.

Scheme 4.3.7 – General scheme of the Thia-Michael thermosets through the reaction of LI and PETMP, showing also the possible isomers.

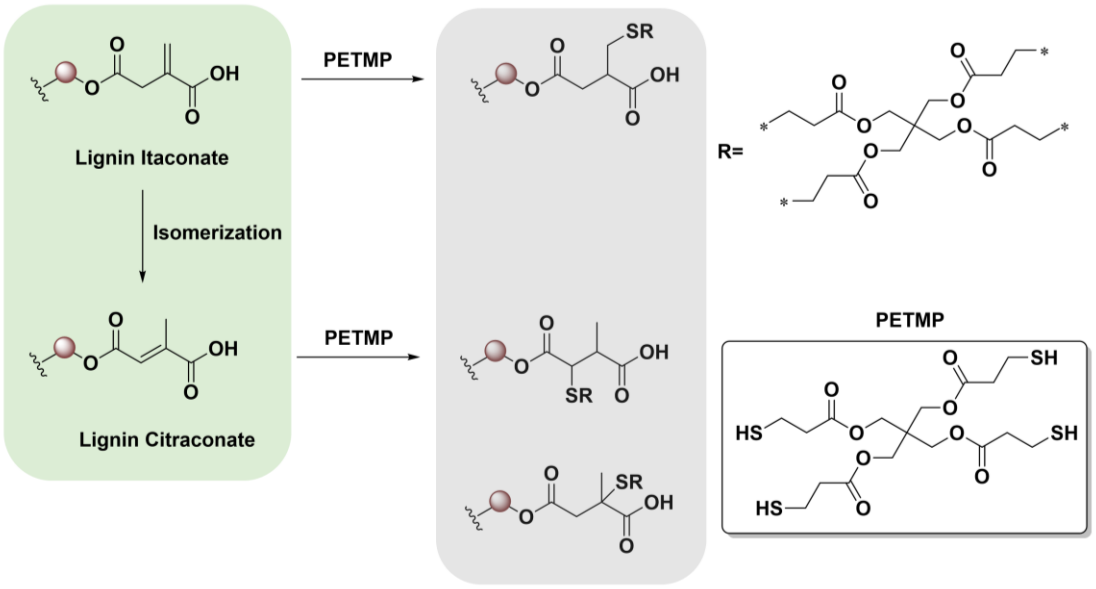

In this proof-of-concept, curing of the thermosets was carried out by mixing the starting materials in the presence of a minimal amount of THF, using a stoichiometric SH-to-double bond ratio of 1:1. The solvent was then allowed to evaporate at room temperature, followed by thermal curing in an oven at 140 °C for 72 h (details on the curing procedure are provided in **Chapter 6.6.5**). Afterwards, the sample was allowed to cool and the gel content was examined. The thermoset appeared as a glassy, brown and very brittle material, with an

optimal gel content of 99 %. From the IR spectra, signals ascribed to a successful curing can be identified (**Figure 4.3.24**). In particular, the signal associated with the stretching vibration of S-H groups in the crosslinker (2656 cm^{-1}) is no longer present in the cured thermoset. Moreover, the stretching vibration signal of the C=C groups (1650 cm^{-1}), albeit weak, completely disappears in the spectrum of the cured thermoset, demonstrating a successful reaction between the thiol groups and the double bonds of the Michael system, as confirmed by the high gel content.

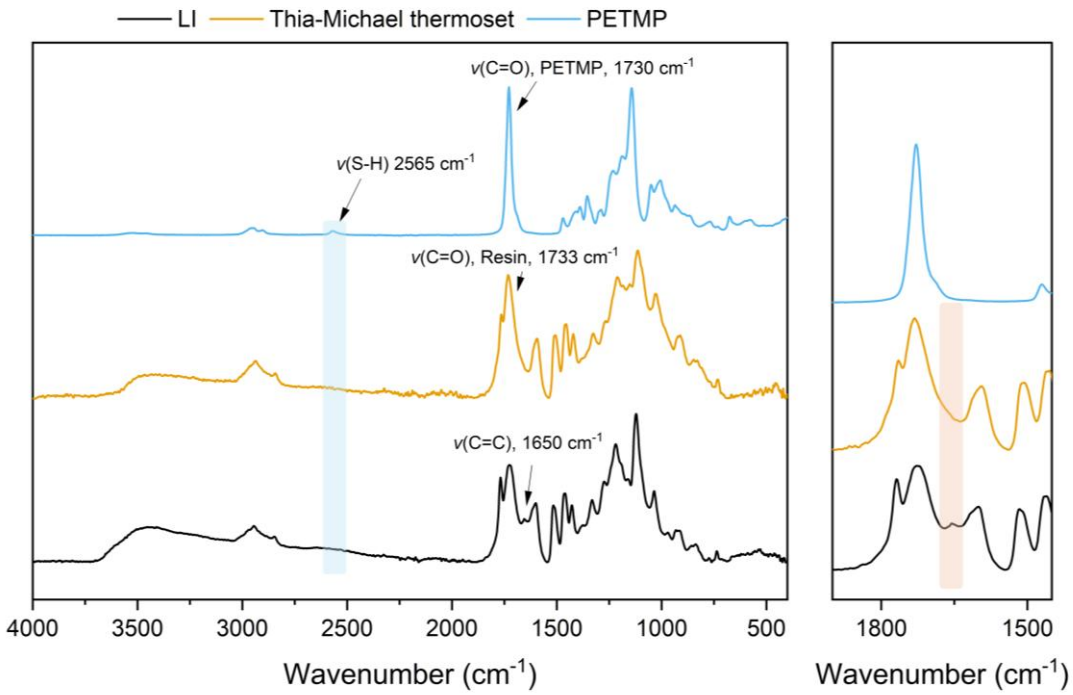

Figure 4.3.24 – IR spectra overlay of the starting material LI (black), the cured Thia-Michael thermoset (orange), and the crosslinker PETMP (light blue). On the right, a zoom in the region 1900-1450 cm^{-1} highlights the disappearing signal associated with the stretching vibration of C=C groups, following the curing.

This proof of concept demonstrates that the **LI** macromonomer can also effectively act as a crosslinker through Michael-type reactivity, in addition to its carboxylic acid functionality. The high gel content obtained indicates an efficient curing process and effective network formation, which are key parameters in the design of thermoset materials, and provides a solid basis for future optimization, which, with appropriate fine-tuning, could lead to the development of promising materials.

4.3.6 Conclusions and Outlook

In this chapter, lignin was successfully functionalized with itaconic anhydride, yielding a well-defined macromonomer that was thoroughly characterized *via* IR, ^{31}P NMR, HSQC, SEC, DSC, and TGA. The introduction of itaconate functionalities enabled the effective use of the modified lignin as a multifunctional crosslinker in different thermosetting systems. In particular, its applicability was demonstrated in Passerini-based networks and epoxy resins, while Thia–Michael reactions were explored as a proof of concept. These results highlight the versatility of itaconate-functionalized lignin as a renewable building block for thermoset various materials and provide a solid foundation for further optimization of network architectures and material properties in future studies.

5 Conclusions

This doctoral thesis investigated the use of functionalized lignins as macromonomers for the development of renewable polymeric materials. The theoretical background outlined the state of the art in sustainable lignin modification, highlighting both recent advances and the persistent challenges associated with the intrinsic heterogeneity and limited reproducibility of this biopolymer. In particular, despite the increasing attention to sustainability, many literature protocols for lignin modification still rely on toxic and/or carcinogenic reagents or their precursors, often in contrast with the principles of Green Chemistry. Within this context, the predominant aim of this work was to modify and employ lignin as a macromonomer for different polymer applications, especially thermosets, while simultaneously developing more sustainable and environmentally benign synthetic strategies.

In the first part of this work, lignin was investigated as a polyol for the synthesis of lignin-derived polycarbonates using dimethyl carbonate as a cross-linker. Several reaction parameters and synthetic strategies were systematically explored. Despite successful lignin modification, no successful route to the targeted polycarbonates could be identified.

A subsequent approach involving the pre-functionalization of lignin with DMC to yield the intermediate “pre-functionalized lignin”, to enable self-condensation, was a successful step within the workflow. This generated a derivative with complete methylation of the aromatic hydroxyl groups and partial reactivity of the aliphatic hydroxyl groups. However, the self-condensation of this derivative did not yield the expected outcome. A subsequent approach involving the use of an additional diol (1,12-dodecanediol) to promote condensation, was also unsuccessful despite extensive optimization efforts. As a result, this project was discontinued. Nevertheless, these studies provided valuable insight into the reactivity limitations of lignin in carbonate-forming systems and identified aspects that could be addressed in future work.

A successful outcome of this thesis was the improvement of an environmentally friendly two-step modification protocol to introduce cyclic carbonate moieties onto lignin, enabling its use as a sustainable alternative to toxic and hazardous isocyanates in polyurethane production. Lignin-based non-isocyanate polyurethane (NIPU) thermosets were synthesized using cyclic carbonate–functionalized lignin in combination with a novel high-oleic sunflower oil–based polyamine. The synthesis and optimization of this renewable polyamine were investigated under both batch and continuous-flow conditions. The lignin content in the final materials was tuned through the addition of erythritol bis-cyclic carbonate, allowing the preparation of ductile thermosets. The curing behavior was studied in detail by IR spectroscopy, and the resulting materials were comprehensively characterized in terms of their thermal, mechanical, and network properties, including gel content.

In the final project, a novel and efficient functionalization of lignin using renewable itaconic anhydride was successfully achieved and thoroughly characterized by ^{31}P NMR, 2D NMR, IR, DSC, and TGA. The same modification strategy was applied to succinic anhydride, yielding an analogous lignin derivative that enabled a direct comparison in terms of structure–property relationships. The reactivity of both macromonomers was initially evaluated in Passerini-based thermosets by varying the diisocyanide chain length and lignin content. A library of thermosets was prepared and characterized using IR spectroscopy, DSC, TGA, and gel content analysis. Although successful network formation was achieved, challenges remain in balancing gel content and mechanical performance, indicating the need for further optimization.

In addition, the lignin derivatives were successfully employed in the synthesis of fully renewable epoxy resin thermosets in combination with epoxidized soybean oil and Pripol™. These materials, prepared with varying lignin contents, were extensively characterized, and their curing behavior was monitored by real-time FTIR spectroscopy. Degradation studies demonstrated complete degradation of

the epoxy thermosets under alkaline conditions, highlighting their potential for more sustainable end-of-life scenarios.

Finally, as a proof of concept, the Michael system reactivity of the functionalized lignin derivatives was explored in thia-Michael thermoset systems. A gel content of 99 % was achieved, confirming efficient network formation, which was further supported by IR spectroscopic analysis.

Overall, this thesis presents different strategies for the modification and utilization of lignin derivatives as macromonomers. Although not all of them led to materials with application relevant properties, it could be shown that lignin can effectively be used as a platform macromonomer for different materials. This outcome reflects the intrinsic complexity and challenges associated with lignin chemistry, which continues to limit its widespread application. Nevertheless, the successful approaches developed herein provide a solid foundation and valuable reference for future research aimed at advancing sustainable lignin-based polymer materials.

6 Experimental Section

6.1 Solvents and Reagents

Table 6.1.1 – Summary of the used solvents and reagents with details on purity, supplier and additional notes.

Chemical	Purity / grade	Supplier	Notes
1,3,5-Trioxane	≥ 99%	Sigma-Aldrich	—
1,4-Dioxane	99.5%	Fluka Chemicals	—
1,6-Hexamethylenediamine	> 99.5%	Fisher Chemicals	—
1,8-Diazabicyclo(5.4.0)undec-7-ene (DBU)	> 98%	Fluorochem	—
1,12-Dodecanediamine	98%	Sigma-Aldrich	—
1,12-Dodecanediol	99%	Sigma-Aldrich	—
1,1,3,3-Tetramethylguanidine (TMG)	> 99%	TCI	—
1,5,7-Triazabicyclo(4.4.0)dec-5-ene (TBD)	> 98%	TCI Chemicals	—
2,2-Dimethoxy-2-phenylacetophenone (DMAP)	99%	Thermo Scientific	—
2-Chloro-4,4,5,5-tetramethyl-1,3,2-dioxaphospholane (TMDP)	95%	Sigma-Aldrich	—
3,4,5-Trichloropyridine	97%	Chem-Pur	—
Acetone	≥ 99.5%	Sigma-Aldrich	Dried and stored over molecular sieves
Azelaic acid	98%	Sigma-Aldrich	—
Cesium carbonate	99.5%	Fisher Chemicals	—

Chloroform	≥ 99.8%	Fisher Chemicals	—
Chromium(III) acetylacetonate	99.99% (trace metal basis)	Sigma-Aldrich	—
Cyrene™	98%	Sigma-Aldrich	—
Dichloromethane (DCM)	≥ 99%	Fisher Chemicals	—
Dimethyl carbonate	Anhydrous, > 99%	Sigma-Aldrich	—
Dimethyl sulfoxide (DMSO)	> 99.7%	Acros Organics	Dried and stored over molecular sieves
Ethanol	> 99.8%	Fisher Chemicals	—
Ethyl formate	98%	Fisher Chemicals	—
ESBO (Vikoflex® 7170)	—	Cargill	—
Glycerol carbonate (4-(hydroxymethyl)-1,3-dioxolan-2-one)	90%	BLDpharm	—
High oleic sunflower oil	Food grade	Rapunzel; Alnatura	—
Itaconic anhydride	97%	Fisher Scientific	—
Mesaconic acid	99%	Sigma-Aldrich	—
meso-Erythritol	99%	Alfa Aesar	—
n-Dodecylamine	98%	Fisher Chemicals	—
N,N-Dimethylacetamide (DMAc)	99.5%, anhydrous	Thermo Scientific	Dried over molecular sieves
N-Hydroxy-5-norbornene-2,3-dicarboxylic acid imide (NHND)	97%	Alfa Aesar	—
N,N′-Bis(3,5-bis(trifluoromethyl)phenyl)thiourea (Schreiner's thiourea)	> 98%	TCI Chemicals	—
Nonanal	95%	Sigma-Aldrich	—
Organosolv beech wood lignin	—	Fraunhofer CBP (Leuna, germany)	Dried at 60 °C under vacuum for 24 h

Potassium carbonate (K_2CO_3)	> 99%, anhydrous	Fisher Scientific	—
p-Toluenesulfonyl chloride (p-TsCl)	> 99%	Sigma-Aldrich	—
Pripol™ 1009	Acid value 196 mg KOH g^{-1}	Cargill	—
Propan-2-ol	> 99.5%	Fisher Chemical	—
Pyridine	≥ 99%	Sigma-Aldrich	—
Sebacic acid	99%	Sigma-Aldrich	—
Succinic anhydride	> 95%	TCI	—
Deuterated solvents (DMSO-d_6, $CDCl_3$)	—	EurisoTop	—

6.2 Instrumentation and Laboratory Equipment

Infrared (IR) Spectroscopy

Infrared spectra were recorded using a Bruker ALPHA attenuated total reflection (ATR) IR spectrometer or PerkinElmer Spectrum 100 instrument with an attenuated total reflection (ATR) unit on a diamond crystal and a temperature-controlled stage (Specac, high Temperature ATR golden gate accessory). 16 scans in the range of ν = 4000 – 400 cm^{-1} or ν = 4000 – 600 cm^{-1} at ambient temperature were recorded at a resolution of 4 cm^{-1}. Real-time FTIR measurements were conducted at 140 °C, with spectra collected at 6 min intervals. All spectra were baseline-corrected and normalized to the aromatic C=C stretching vibration at 1505 cm^{-1} using Spectrum software.

Column Chromatography

Performed with silica gel F254 (SIGMA-ALDRICH) and solvents purchased in HPLC grade.

Nuclear Magnetic Resonance (NMR) Spectroscopy

^{1}H NMR spectra were recorded using a Bruker Ascend 400 MHz or a Bruker Avance DRX 500 MHz spectrometer, with 16 to 128 scans, a delay time d_1 ranging from 1 to 5 s, at 298 K. The chemical shift was reported in parts per million (ppm) and referenced to characteristic signals of deuterated solvents, e.g. DMSO-d_6 at 2.50 ppm or chloroform-d_1 at 7.26 ppm. ^{13}C NMR spectra were recorded using a Bruker Avance DRX spectrometer at 126 MHz with 1024 to 32768 scans, with delay time d_1 of 1 to 4 s at 298 K. The chemical shift was reported in parts per million (ppm) and referenced to characteristic signals of deuterated solvents, e.g. DMSO-d_6 at 39.52 ppm or chloroform-d_1 at 77.16 ppm. Peak deconvolution was performed applying the GSD (Global Spectrum Deconvolution) method with refinement level 3 (10 fitting cycles) and 10 improvement cycles.

Quantitative ^{31}P NMR

For quantitative determination of hydroxyl values, an exact amount of 28-32 mg of lignin sample (previously dried under vacuum at 70 °C) was weighed. Subsequently, 100 µL of a solution of chromium(III) acetylacetonate (5 mg/mL) as relaxation agent and the internal standard (IS) endo-*N*-hydroxy-5-norbornene-2,3-dicarboximide (NHND, 18 mg/mL) in $CDCl_3$:pyridine (1 : 1.6 v/v) are added to the lignin sample, and 450 µL of solvent mixture $CDCl_3$:pyridine (1 : 1.6 v/v) are added to aid solubilization. After a homogeneous solution was obtained, 2-chloro-4,4,5,5-tetramethyl-1,2,3-dioxaphospholane (TMDP, 70 µL) was added and the solution was stirred for an additional 15 minutes. Afterwards, it was transferred into a NMR tube for subsequent measurement using a Bruker Ascend instrument at 162 MHz with 512 scans and a delay time d_1 of 10 seconds at 298 K and a spectral width of 100 ppm (190–90 ppm).[403,404]

The chemical shifts are reported relative to the reaction product of 2-chloro-4,4,5,5-tetramethyl-1,2,3-dioxaphospholane with water, at 132.2 ppm. Integrals are assigned to the functional groups as followed: δ = 152.5 – 151.7 (NHND), 149.5 – 145 (aliphatic hydroxyl groups), 145 - 141.2 (syringyl hydroxyl groups), 140.8 – 137.7 (guaiacyl hydroxyl groups), 135.7 – 134 (carboxylic acids).

Calculations were performed by first determining the mole quantity of IS in the IS solution:

$$NHND\ in\ IS\ solution\ (mmol) = \frac{mass\ of\ NHND\ added\ to\ the\ IS\ solution\ (g)}{M_w\ of\ NHND\ (179.17\frac{g}{mol})} * purity\ of\ NHND\ (\%) * 1000 \quad \text{Eq. S1}$$

Afterwards, the mole quantity of IS (NHND) in the NMR sample was calculated:

$$NHND\ in\ NMR\ sample\ (mmol) = \frac{NHND\ in\ IS\ solution\ (mmol)}{total\ mass\ of\ IS\ solution\ (g)} * mass\ of\ 0.1\ mL\ of\ IS\ solution\ (g) \quad \text{Eq. S2}$$

I_{ratio} between the spectral region of interest (I_{OH}) over the IS integration peak (I_{NHND}) is determined:

$$I_{ratio} = \frac{integral\ of\ the\ region\ of\ interest}{integral\ of\ IS\ peak} = \frac{I_{OH}}{I_{NHND}} \quad \text{Eq. S3}$$

Finally, to calculate the amount of different hydroxyl groups in lignin, *i.e.* OH / g lignin:

$$mmol\ of\ \ OH\ groups\ per\ g\ of\ lignin = \frac{I_{ratio} * mmol\ of\ NHND\ in\ NMR\ sample}{dry\ weight\ of\ lignin} \quad \text{Eq. S4}$$

Quantitative ^{13}C NMR

Quantitative ^{13}C analysis was performed according to the procedure described from Meier and Over.[247] A weighed, dry lignin sample (95.0 mg) was dissolved in 500 µL DMSO-d_6. 100 µL of a solution of the internal standard (**IS**) 1,3,5-trioxane (65 mg/mL) and chromium(III) acetylacetonate (24.9 mg/mL) as relaxation agent in DMSO-d_6 were added. Measurements were performed with inverse gated decoupling, 32768 scans, delay time d_1 of 4 s at 298 K.

Calculations were performed by first determining the mole quantity of IS in the IS solution:

$$trioxane\ in\ IS\ solution\ (mmol) = \frac{mass\ of\ trioxane\ added\ to\ the\ IS\ solution\ (g)}{M\ of\ trioxane\ \left(90.08 \frac{g}{mol}\right)} * purity\ of\ trioxane\ (\%) * 1000 \quad \text{Eq. S5}$$

Afterwards, the mole quantity of the IS (trioxane) in the NMR sample was calculated:

$$trioxane\ in\ NMR\ sample\ (mmol) = \frac{trioxane\ in\ IS\ solution\ (mmol)}{total\ mass\ of\ IS\ solution\ (g)} * mass\ of\ 0.1\ mL\ of\ IS\ solution\ (g) \quad \text{Eq. S6}$$

The integral ratio (I_{ratio}) between the spectral region of interest and the IS integration peak ($I_{Trioxane}$) is determined:

$$I_{ratio} = \frac{integral\ of\ the\ region\ of\ interest}{integral\ of\ IS\ peak} = \frac{I_{OH}}{I_{trioxane}} \quad \text{Eq. S7}$$

Finally, to calculate the amount of carbonyl groups in lignin, which is expressed in mmol·g^{-1} carbonyl:

$$mmol\ of\ carbonyl\ groups\ per\ g\ of\ lignin = \frac{I_{ratio} * mmol\ of\ trioxane\ in\ NMR\ sample}{dry\ weight\ of\ lignin} \quad \text{Eq. S8}$$

Size Exclusion Chromatography

For samples of **Chapter 4.1**, SEC measurements were performed on a Shimadzu SEC system equipped with a Shimadzu isocratic pump (LCYCLO20AD), a Shimadzu refractive index detector (24 °C, RID-20A), a Shimadzu autosampler (SIL-20A) and a Varian column oven (model 510, 50 °C). For separation, a three-column setup was used with one SDV 3 µm, 8 x 50 mm precolumn and two SDV 3 µm, 100 Å, 3 x 300 mm columns supplied by PSS, Germany. Anhydrous tetrahydrofuran stabilized with 250 ppm butylated hydroxytoluene (≥ 99.9%) supplied by SIGMA-ALDRICH was used at a flow rate of 1.0 mL min-1. For calibration, linear poly(methyl methacrylate) (PMMA) standards (Agilent) with M_p ranging from 875 Da to 1.678× 10^6 Da were used. SEC measurements of **Chapters 4.2** and **4.3**, were performed on an Agilent Technologies 1260 Infinity II system equipped with a Mixed-C and Mixed-E Agilent column, and a differential refractive index detector. The used eluent was DMAc containing 0.034 wt% LiBr. The number average molar mass (M_n), the weight average molar mass (M_w), and the dispersity ($Đ = M_w/M_n$) of the samples were determined using a calibration of polystyrene (PS) standards with M_p ranging from 370 to 2.52 × 10^6 Da. The samples were dissolved in the eluent at a concentration of 2 mg/mL and filtered over a 0.2 µL filter.

Mass Spectrometry (MS)

Electrospray ionization (ESI) experiments were recorded on a Q-Exactive (Orbitrap) mass spectrometer (Thermo Fisher Scientific) equipped with a HESI II probe to record high resolution. The spectra were evaluated by molecular signals $(M + H)^+$ and indicated with their mass-to-charge ratio (m/z).

Differential Scanning Calorimetry (DSC)

DSC measurements were performed on a Mettler Toledo DSC 3 STARe system. Aluminum crucibles (40 µL) were used to weigh a precise amount of each sample, between 3 and 7 mg. The samples were measured in two heating cycles to remove any thermal history: from 25 to 200, 200 to −50, and −50 to 200 °C. DSC curves presented are relative to the second heating cycle. A heating or cooling rate of 10 – 30 K min^{-1} was applied. For the **Chapter 4.3**, DSC thermograms were obtained using a DSC-1 instrument (Mettler Toledo). Approximately 5 mg of sample was sealed in a 40 µL aluminum crucible with a pierced lid. The samples were measured in two heating cycles to remove any thermal history. For lignin samples: from 25 to 170, 170 to -50, and -50 to 170 °C. For thermoset samples: from 25 to 180, 180 to −90, and −90 to 180 °C. DSC curves presented are relative to the second heating cycle. A heating or cooling rate of 10 K min^{-1} was applied. glass transition temperatures (T_g) were determined as the midpoint of the second heating cycle.

Thermogravimetric Analysis (TGA)

Thermogravimetric measurements were performed using a TGA Q5500 instrument from TA Instruments. The samples were dried under vacuum (10 mbar) at 70 °C overnight before measurement. The samples (5 – 6 mg) were heated in a Pt crucible from 25 to 600 °C under a nitrogen atmosphere at a heating rate of 10 K min^{-1}. $T_{d,5\%}$ is defined as the temperature at which 5 % weight loss of the sample occurred, while $T_{d,50\%}$ is defined as the temperature at which 50 % of the weight loss of the sample occurred. Residue (%) is defined as the weight percentage of residual mass at the end of the analysis. For **Chapter 4.3**, TGA was performed using a TGA/DSC-1 instrument (Mettler Toledo).

Approximately 10 mg of sample was placed in a 70 µL alumina crucible and heated from 25 °C (10 min isothermal) to 600 °C at 10 K min⁻¹ under nitrogen (50 mL min⁻¹). The temperatures corresponding to 5 % ($T_{d,5\%}$) and 50 % ($T_{d,50\%}$) weight loss were determined as well as the residues.

DMA and Tensile Strength Measurements

For **Chapter 4.2**, a Discovery DMA 850 from TA instruments was used to modulate from -50 °C to 200 °C at a heating rate of 3 K min^{-1}. The measurements were performed with tensile geometry at a frequency of 1 Hz, an initial force of 0.1 N and a strain sweep of 0.02%. Analyses were carried out in triplicate to ensure sample homogeneity and reproducibility. For **Chapter 4.3**, thermomechanical properties were measured using a DMA Q800 instrument equipped with an ACS-3 cooling accessory (TA Instruments) in tension film mode. Samples were tested under a 0.1% oscillatory strain at a frequency of 1 Hz, with a pre-load force of 0.01 N. Samples were cooled to -50 °C, equilibrated for 5 min, and subsequently heated to 100°C at 3 °C min⁻¹. Three replicates were tested for every sample. The crosslinking densities (ν_e) of the thermosets were calculated from the storage modulus in the rubbery state, according to the theory of rubber elasticity, with the following equation:

$$\nu_e = \frac{E_e^{'}}{3RT} \qquad \text{Eq. S9}$$

where:

$E_e^{'}$ is the storage modulus in the rubbery plateau region (Pa); R is the universal gas constant (J mol^{-1} K^{-1}); T is the absolute temperature (K) at which $E_e^{'}$ was measured, corresponding to T_g + 20 °C. Tensile measurements were performed on the same instrument in tension film mode, with a strain ramp. An

initial strain of 0.01% was applied, then increased to 100% with an increase of 10% min^{-1} strain at a temperature of 25 °C, with a pre-load force of 0.001 N.

Rheometer

Rheological analyses were conducted using a Discovery Hybrid Rheometer 2 (DHR-2, TA Instruments) equipped with a peltier plate temperature-control system. Responses were evaluated in a 20 mm stainless steel plate–plate geometry. Amplitude-sweep experiments were performed at a constant frequency (ω) of 1 Hz and temperature of 25 °C, strain (γ) was increased until deviation from linear range were detected. Frequency-sweep experiments were performed at the maximum strain detected in the LVER at a constant temperature of 25 °C and frequency range between 10 and 0.01 Hz.

Water Contact Angle (WCA)

Contact angle measurements were performed with a DSA25S contact angle goniometer (Krüss) using the sessile drop technique. A water droplet with a size of 5 µL was slowly added onto the thermoset samples by a micrometer syringe and contact angles between the surface of the thermoset against the water droplet were measured. The average value of five measurements was calculated for each sample with a standard deviation of less than 5°.

Gel Content Determination

Weighed bar samples of the cured thermosets were immersed in THF for 24 hours. Afterwards, the swollen samples were dried gently between paper sheets and weighed again. Then, the samples were dried at 60 °C for 24 h, and their final weight was recorded.

The swelling percentage is defined as:

$$Swelling\ (\%) = \frac{m_{sw} - m_d}{m_d} \cdot 100\% \qquad \text{Eq. S10}$$

And the gel content of the samples is defined as:

$$Gel\ content\ (\%) = \frac{m_d}{m_i} \cdot 100\% \qquad \text{Eq. S11}$$

where:

m_{sw} is the final weight of the sample after gently drying between paper sheets

m_d is the final weight of the sample after drying at 60 °C for 24 hours

m_i is the initial weight of the sample

6.3 Organosolv Lignin Characterization

Characterization was performed *via* ^{31}P NMR, ^{1}H NMR, ^{13}C NMR, SEC (DMAc and THF), FTIR, DSC, TGA. Data are reported in **Table 6.3.1**.

Table 6.3.1 – Characterization data of Organosolv lignin (OL).

$OH_{Aliphatic}$ (mmol·g^{-1})[a]	$OH_{Aromatic}$ (mmol·g^{-1})[a]	COOH (mmol·g^{-1})[a]	OH_{Total} (mmol·g^{-1})[a]	M_n (g·mol^{-1})[b]	$Đ$
2.42 ± 0.05	1.83 ± 0.04	0.100 ± 0.005	4.35 ± 0.08	5000	2.6

[a]: Determined via ^{31}P NMR. Measurements were performed in triplicates. [b]: SEC-DMAc (PS standards).

SEC-THF (PMMA standards): M_n = 800 g·mol^{-1}; $Đ$ = 1.6

IR (ATR platinum diamond): $\tilde{\nu}$ / cm^{-1} = 3443, 2937, 2841, 1722, 1594, 1512, 1456, 1423, 1325, 1216, 1115, 1031.

^{1}H NMR (400 MHz, DMSO-d$_6$) δ_H / ppm = 7.50 – 6.25 (m, C**H**$_{aryl}$); 4.0 – 3.50 (s, OC**H$_3$**, O**H**); 1.40 – 0-70 (m, C**H**$_{alkyl}$).

^{13}C NMR (126 MHz, DMSO-d$_6$) δ_C / ppm = 152.61, 147.81, 135.32, 115.88, 107.52, 104.08, 93.38, 60.08, 56.38, 15.74.

T_g = 140 °C; $T_{d,5\%}$ = 267 °C

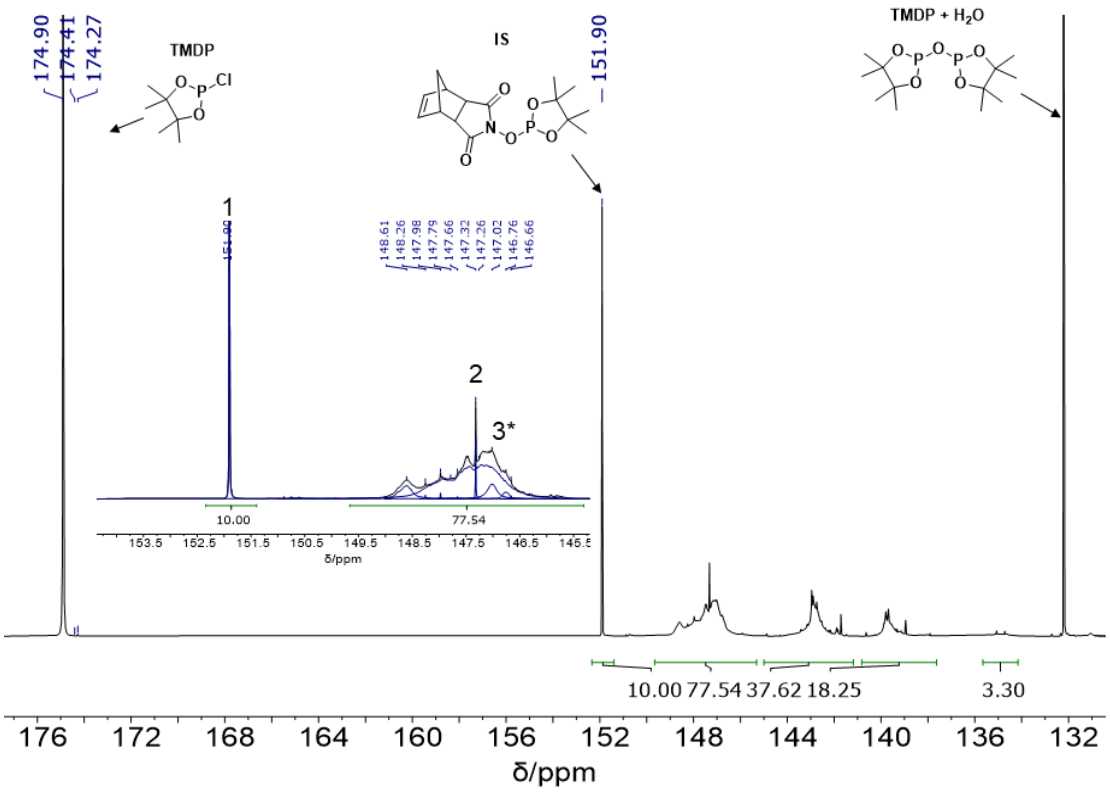

Figure 6.3.1 – ^{31}P NMR of pristine Organosolv lignin. Residual ethanol (sharp signal at 147.32 ppm) could not be fully removed, even after drying at 60 °C under vacuum (10 mbar) for 5 days, as also reported from Jääskeläinen et al.[405] To obtain more accurate results, peak deconvolution was performed and is shown in the expanded view (blue lines in **Figure 6.3.1**) and in **Table 6.3.2.**

Table 6.3.2 – Peak deconvolution data for OL.

Signal	*δ* (ppm)	Area (arb. unit)
1	151.90	199877
2	147.32	20596
3*	149.7-145.3	1549857

*: Area of the integral between 149.7 – 145.3 ppm.

6.3.1 Theoretical Yield Calculations for Lignin Modification

A simplified theoretical yield was calculated, assuming 100% conversion of the reactive sites toward the main reaction, following **Eq. S12**:

$$m_f = m_i \left(1 + \Delta M_{graft} \left(reactive\ sites\ in \frac{mol}{g}\right)\right) \qquad \text{Eq. S12}$$

where:

m_f = final mass of the modified lignin (g)

m_i = initial mass of pristine lignin (g)

ΔM_{graft}= increase in the molecular weight caused by the modification (g/mol)

$reactive\ sites$ = number of moieties participating in the reaction (depending on the reaction type) in mol/g.

6.4 Experimental Procedures for Chapter 4.1 – Lignin Carbonates

6.4.1 First Approach-DMC as Limiting Reagent

6.4.1.1 General Procedure for the Self-Condensation of OL with Stoichiometric Amounts of DMC:

Scheme 6.4.1 – General reaction scheme for the self-condensation of lignin with stoichiometric amounts of DMC.

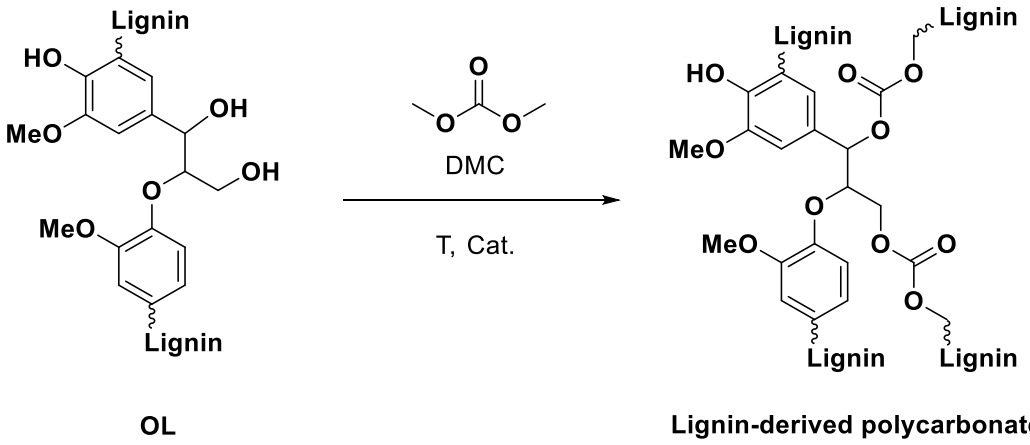

OL **Lignin-derived polycarbonates**

In a pressure vial, dried OL (1.00 g, 4.35 mmol -OH g^{-1}, 4.35 mmol -OH, dried previously for 24 h at 70 °C and 10 mbar) is added and dissolved in dry DMSO, with a concentration of 5 wt%. Afterwards, anhydrous DMC (anhydrous, 4.35 mmol, 392 mg, 366 µL, 1.00 equiv.) and the base (DBU, TBD or TBAB, 4.35 mmol, 1.00 equiv.) are added to the vial, the vial is closed with a septum pierced with a needle. The reaction is carried out at 90 °C for 24–72 h. After the desired time, the reaction mixture is precipitated in aqueous acidic condition (pH < 2, acidified with HCl 1 M), stirred for 30 minutes and filtrated on a fritted frit (porosity: P-4). The recovered solids were washed three times with deionized water (50 mL) and dried under vacuum at 70 °C for at least 24 h prior to analysis. The reaction was followed *via* IR spectroscopy and ^{31}P NMR, and the relative data are presented and discussed in **Chapter 4.1.3**.

The desired product was not successfully isolated.

6.4.2 Second Approach—Intermediate Route

6.4.2.1 General Procedure for the Synthesis of the Intermediate:

Scheme 6.4.2 – General reaction scheme for the pre-functionalized lignin intermediate synthesis.

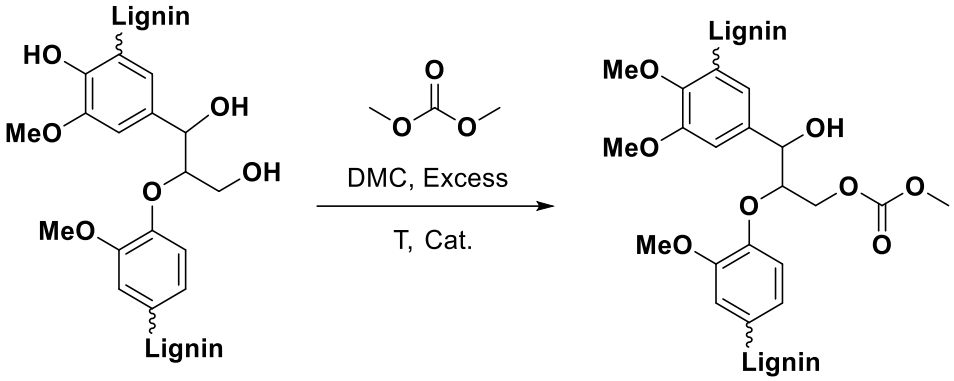

OL **Pre-functionalized lignin**

General procedure for the synthesis of pre-functionalized lignin intermediate in a 0.5 g scale:

In a pressure vial, dried OL (0.50 g, 4.35 mmol -OH g^{-1}, 2.18 mmol -OH, dried previously for 24 h at 70 °C and 10 mbar) is suspended in anhydrous DMC (21.8 mmol, 1.96 g, 1.80 mL, 10.0 equiv.). TBAB (4.35 mmol, 1.40 g, 2.00 equiv.) is added and the reaction mixture is stirred at 90 °C under Ar atmosphere for 5 h. After the desired time, the reaction mixture was precipitated in aqueous acidic condition (pH < 2, acidified with HCl 1 M), stirred for 30 minutes and filtrated on a fritted frit (porosity: P-4). The recovered solids were washed three times with deionized water (50 mL) and dried under vacuum at 70 °C for at least 24 h prior to analysis.

General procedure for the synthesis of pre-functionalized lignin intermediate in a 6 g scale:

In a round-bottom flask dried OL, (10 g, 4.35 mmol -OH g^{-1}, 43.5 mmol -OH, dried previously for 24 h at 70 °C and 10 mbar) was suspended in DMC (anhydrous, 435 mmol, 39.2 g, 37 mL, 10 equiv.). An additional 15 mL of DMC (total: 14.0 equiv.) were needed to fully solubilize OL and to ensure a homogeneous solution and stirring. Tetrabutylammonium bromide (TBAB, 87 mmol, 28.1 g,

2.00 equiv.) is added and the reaction mixture is flushed with Ar and vigorously stirred under reflux of DMC, for 6 hours (9.88 g, 85% theoretical yield). Theoretical yield was calculated taking into account the different reactivities of lignin reactive sites, assuming a full conversion of aromatic -OH and carboxylic acid groups to their methylated analogs, and a full conversion of the aliphatic -OH to carboxymethylated derivatives, according to **Eq. S12**.

Work-up with recovery of TBAB:

The phase-transfer catalyst was recycled according to the previously reported procedure from our group. After the reaction mixture was cooled down to r.t., cold, distilled water (600 mL) was used as precipitation medium. Dark brown solids precipitated and they were filtrated on a fritted frit (porosity: P-4) and washed with additional deionized water (100 mL). Afterwards, the filtrates aqueous phase was evaporated under reduced pressure (80 mbar, 60 °C) to recover TBAB as a viscous yellowish liquid, that crystalized after cooling. (25.5 g, 91% recovery). The purity of recovered TBAB was verified *via* ^{1}H NMR, and the spectrum looks identical to commercial TBAB (**Figure 4.1.10**).

6.4.2.2 Pre-functionalized Lignin Characterization

Characterization was performed *via* ^{31}P NMR, ^{1}H NMR, ^{13}C NMR, SEC-THF, FTIR. Data are reported in **Table 6.4.1**.

Table 6.4.1 – Characterization data of pre-functionalized lignin (intermediate).

$OH_{Aliphatic}$ (mmol·g^{-1})[a]	$OH_{Aromatic}$ (mmol·g^{-1})[a]	COOH (mmol·g^{-1})[a]	OH_{Total} (mmol·g^{-1})[a]	M_n (g·mol^{-1})[b]	*Đ*
1.495	0	0	1.495	1100	3.1

[a]: Determined via ^{31}P NMR. [b]: SEC-THF.

IR (ATR platinum diamond): $\tilde{\nu}$ / cm^{-1} = 3485, 2939, 2836, 1744, 1587, 1505, 1456, 1419, 1328, 1260, 1123, 1024.

^{1}H NMR (400 MHz, DMSO-d$_6$) δ_H / ppm = 7.55 – 6.10 ppm (m, C**H**$_{aryl}$); 4.09 – 2.93 (s, OC**H$_3$**, O**H**); 1.53 – 0.72 (m, C**H**$_{alkyl}$).

^{13}C NMR (126 MHz, DMSO-d$_6$) δ_C / ppm = 155.00, 152.90, 148.76, 136.62, 119.37, 111.55, 103.87, 72.35, 59.99, 55.85, 15.13.

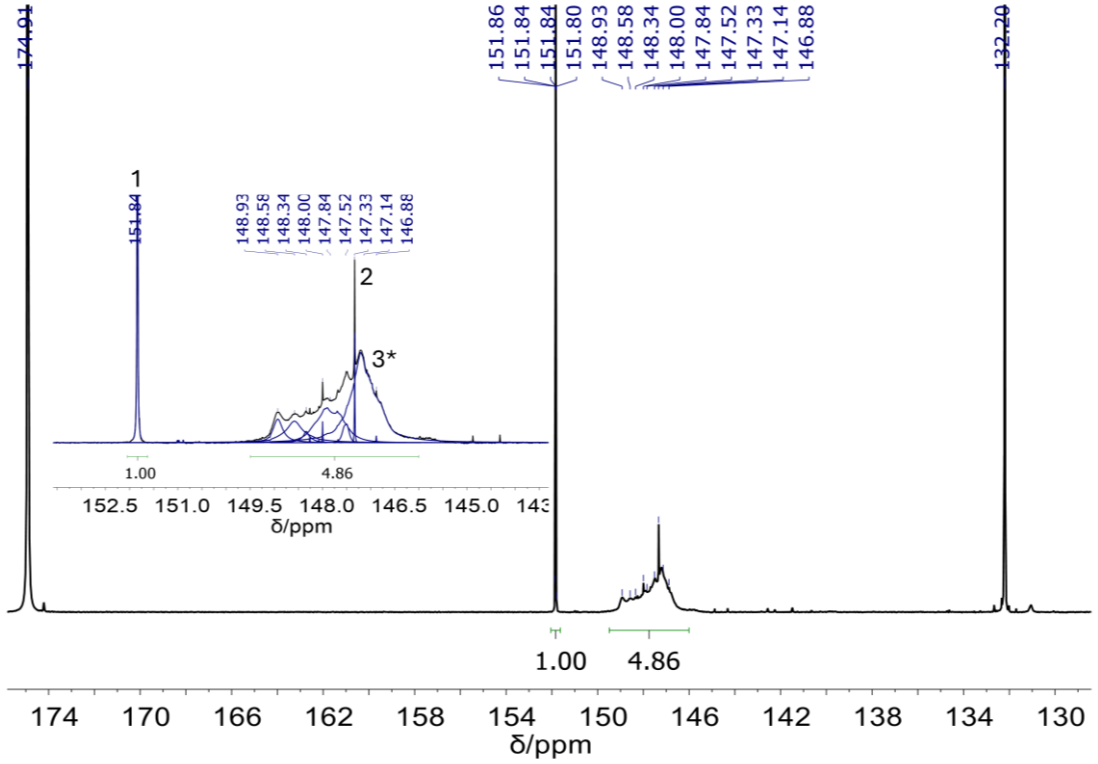

Figure 6.4.1 – ^{31}P NMR spectrum of pre-functionalized lignin. Residual ethanol (sharp signal at 147.33 ppm) could not be removed, even after drying at 60 °C under vacuum (10 mbar) for 5 days, as also reported from Jääskeläinen et al.[405] To obtain more accurate results, peak deconvolution was performed and is shown in the expanded view (blue lines).

Table 6.4.2 – Peak deconvolution data for pre-functionalized lignin (intermediate).

Signal	*δ* (ppm)	Area (arb.unit)
1	151.84	211799
2	147.32	13508
3*	149.5-146.1	1024002

*: Area of the integral between 149.5 – 146.1 ppm.

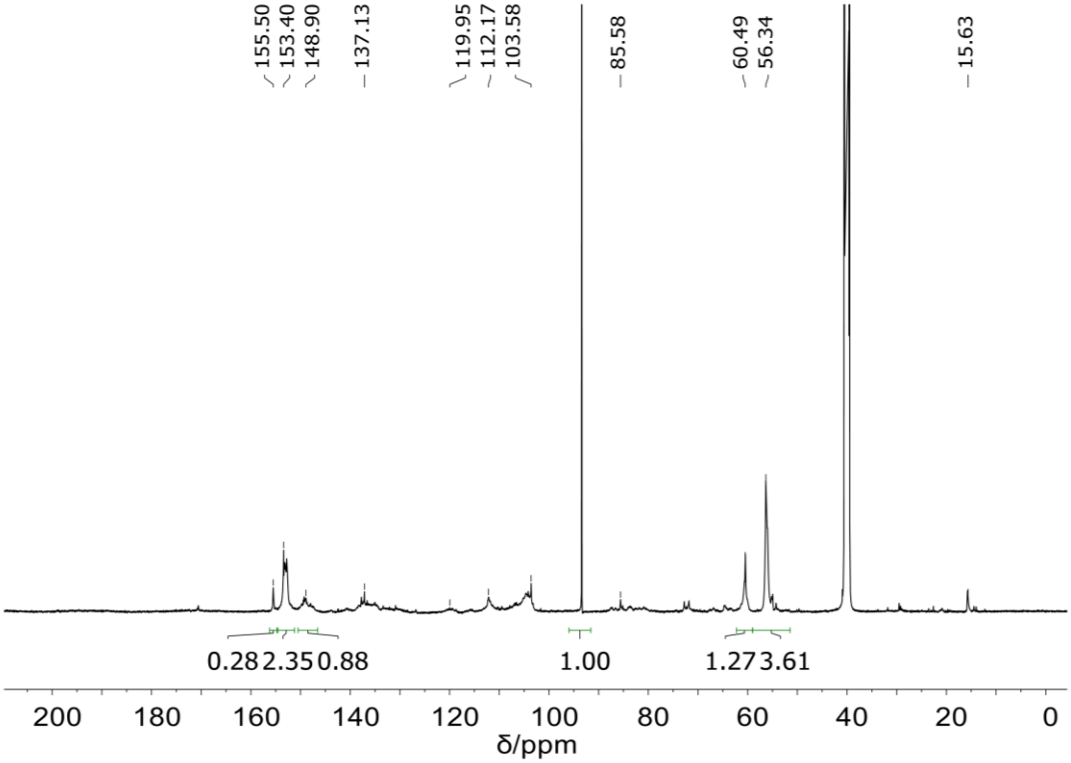

Figure 6.4.2 – ^{13}C NMR of pre-functionalized lignin.

Table 6.4.3 – Quantitative ^{13}C NMR data for pre-functionalized lignin (intermediate).

mmol IS in the sample (mmol)	**I_{ratio} Carbonyl signal**	**Carbonyl content (mmol·g^{-1})**
0.06295	0.28	0.19

6.4.2.3 General Procedure for the Self-condensation of the Intermediate

Scheme 6.4.3 – General reaction scheme for the self-condensation of the pre-functionalized lignin with itself.

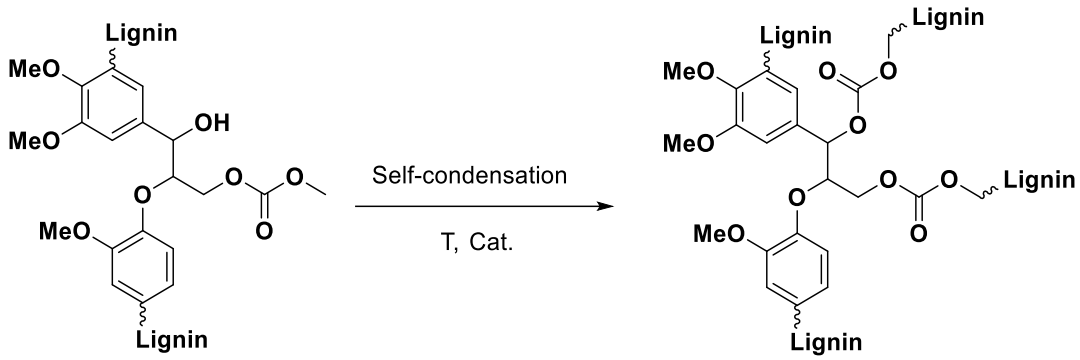

Pre-functionalized lignin **Lignin-derived polycarbonates**

Pre-functionalized lignin (1.00 g, 1.495 mmol -OH g^{-1}, 1.495 mmol -OH, dried previously for 24 h at 70 °C and 10 mbar) is dissolved in a solvent (Cyrene™ or DMAc, both anhydrous) with a concentration of 150 mg/mL in a pressure vial. DBU (0.30 mmol, 45.5 mg, 44.6 µL, 0.20 equiv.) is added. The vial is closed with a septum pierced with a needle. The reaction is carried out at 90 °C for 3-48 h. Aliquots are taken over 3, 24 and 48 h for both conditions and followed *via* SEC and ^{31}P NMR. After the desired time, the aliquot of reaction mixture is precipitated in aqueous acidic condition (pH < 2, acidified with HCl 1 M), stirred for 30 minutes and filtrated on a fritted frit (porosity: P-4). The recovered solids were washed three times with deionized water (50 mL) and dried under vacuum at 70 °C for at least 24 h prior to analysis. The relative SEC and ^{31}P NMR data are presented and discussed in **Chapter 4.1.4**.

The desired product was not successfully isolated.

6.4.2.4 Self-Condensation with 1,12- Dodecanediol

Scheme 6.4.4 – General reaction scheme for the condensation of pre-functionalized lignin with 1,12-dodecanediol.

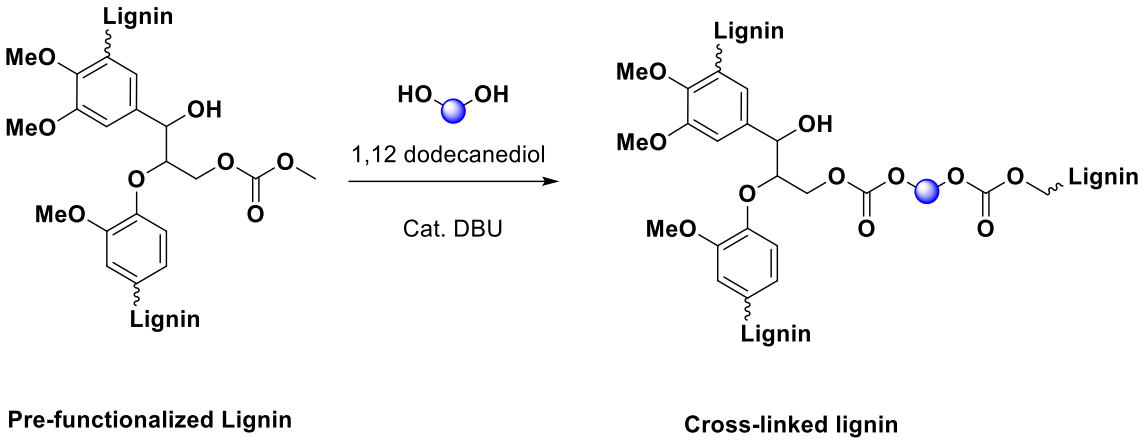

Pre-functionalized Lignin **Cross-linked lignin**

Pre-functionalized lignin (1.00 g, 0.28 mmol carbonate g^{-1}, 0.28 mmol carbonate, calculated from quantitative ^{13}C NMR, 1.495 mmol -OH g^{-1}, 1.495 mmol -OH, dried previously for 24 h at 70 °C and 10 mbar) is dissolved in a suitable solvent (DMAc or Cyrene™, anhydrous) with a concentration of 150 mg/mL in a pressure vial and DBU (1.78 mmol -OH, 54.0 mg, 53.0 µL, 0.20 equiv. in respect to the total -OH groups, both from lignin and 1,12-dodecanediol) is added. 1,12 dodecanediol (0.28 mmol -OH, 2 functionalities, 0.14 mmol dodecanediol, 28.3 mg, 1.00 equiv. in respect of the carbonate groups) is added. The vial is closed with a septum pierced with a needle. The reaction is carried out at 90 °C for 3-48 h. Aliquots are taken over 3, 24 and 48 h for both conditions and followed *via* SEC. The aliquot of reaction mixture is precipitated in aqueous acidic condition (pH < 2, acidified with HCl 1 M), stirred for 30 minutes and filtrated on a fritted frit (porosity: P-4). The recovered solids were washed three times with deionized water (50 mL) and dried under vacuum at 70 °C for at least 24 h prior to analysis.

SEC traces are presented and discussed in **Chapter 4.1.4**.

The desired product was not successfully isolated.

6.5 Experimental Procedure for Chapter 4.2 – Lignin-NIPUs *via* HOSO-derived Polyamine

6.5.1 UV-systems and Reaction Setups

System 1) A UV lamp of 365 nm of 45 W was used. Details of the distances between lamp and sample are shown in the figures below (**Figure 6.5.1**).

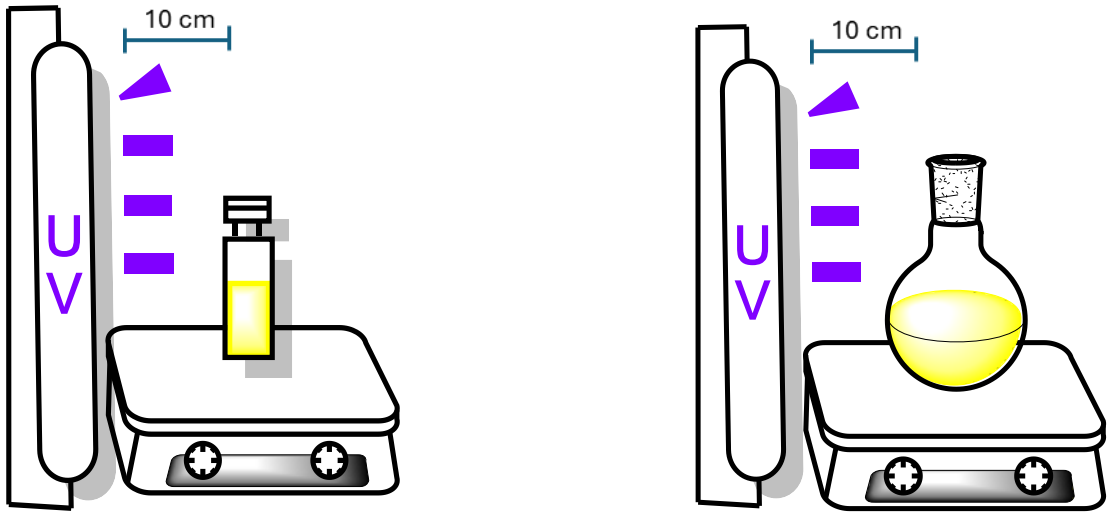

Figure 6.5.1− UV system (lamp 365 nm, 45 W) for small-scale reactions (left) and for larger-scale reactions (right).

System 2) A system consisting of five LEDs (1 cm x 1 cm) placed in a circle and installed on a metallic plate was used. Typically, the vial containing the reaction mixture was placed directly on one LED. (**Figure 6.5.2**).

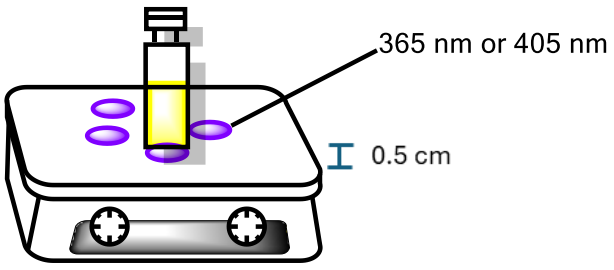

Figure 6.5.2 − LEDs system (365 nm, 2W).

System 3) A UV lamp of 365 nm of 45 W and a UV lamp of 365 nm of 12 W were used. Details of the distances between lamps and sample are shown in the figures below (**Figure 6.5.3**).

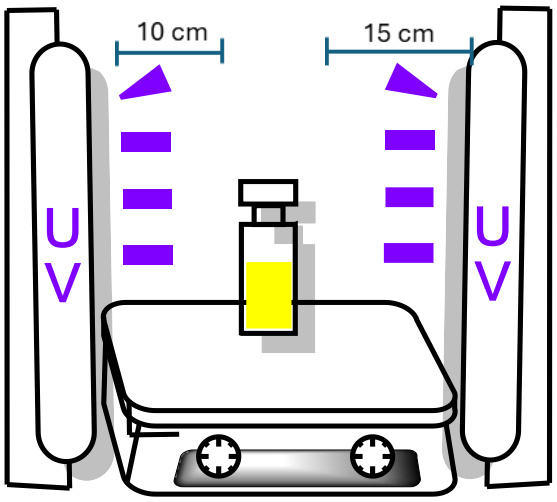

Figure 6.5.3− Both-side irradiation system. UV lamp 365 nm 45 W (left side), UV lamp 365 nm 12 W (right side).

Continuous Flow reactor

Photoreactions in flow were conducted using an E-series flow reactor from Vapourtec with photochem equipment. As irradiation source, a 365 nm LED with 16 W power was used. The inner volume of the reactor capillary is 10 mL. A flow rate ranging from 1 to 9 mL/min was applied. Total irradiation time was up until 6 hours.

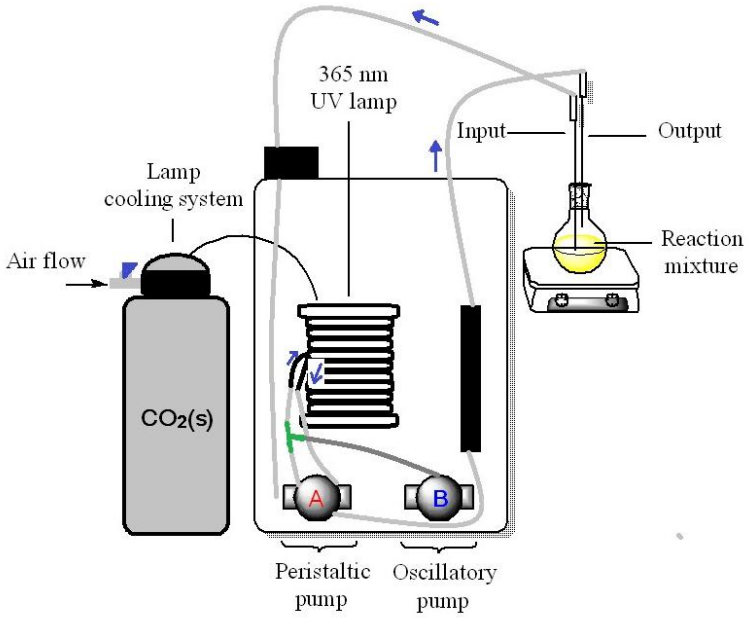

Figure 6.5.4 − Flow reactor setup (closed-loop system).

6.5.2 Triglyceride Modification

6.5.2.1 Calculation of Triglycerides Unsaturation by ^{1}H NMR

Equations system:[406]

$$\text{Vinylic hydrogens integral} = 2A + 4B + 6C$$

$$\text{Linoleic bisallylic hydrogens integral} = 2B$$

$$\text{Linolenic bisallylic hydrogens integral} = 4C$$

$$A + B + C + D = 3$$

A = oleic chain (monounsaturated)

B = linoleic chain (diiunsaturated)

C = linolenic chain (triunsaturated)

D = saturated chain

High oleic sunflower oil (Alnatura)

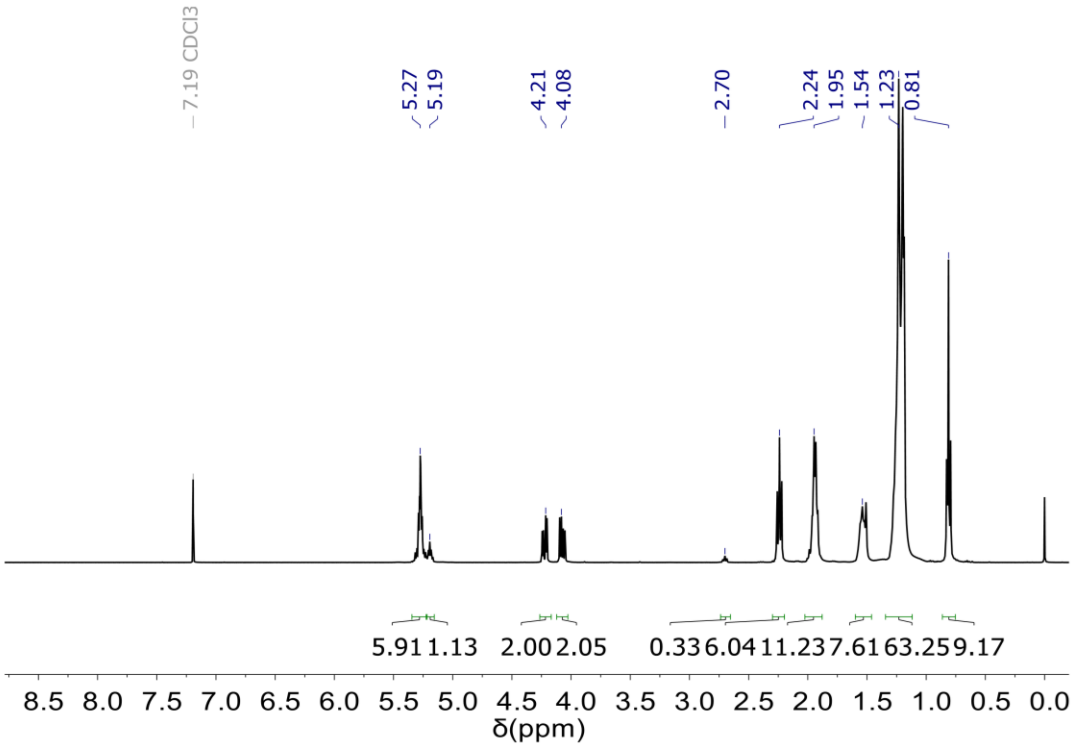

Figure 6.5.5 – ^{1}H NMR of the employed HOSO during experiments in $CDCl_3$.

In general, once normalised to integral = 2, the peaks of the glycerol -CH_2-CH-CH_2- unit (4.21 ppm), the integrals of the vinylic hydrogen (5.27 ppm), linoleic bisallylic hydrogens (2.70 ppm) and linoleic bisallylic hydrogen (2.80 ppm) were evaluated according to the above shown equation system. In the specific case of this HOSO sample, no tri-unsaturated chains were present (no 2.80 ppm peak, see **Figure 6.5.5**).

$$5.91 = 2A + 4B + 6C$$
$$0.33 = 2B$$
$$0 = 4C$$
$$A + B + C + D = 3$$

This equation resulted in: A = 2.625, B = 0.165, C = 0, D = 0.21. Total = 3.

Table 6.5.1 – Percentage distribution of double bond types of the employed HOSO used for the experiments.

Peak	Percentage
A = monounsatured, oleic chain	88 %
B = diunsatured, linoleic chain	5.5 %
C = triunsatured	0.0 %
D = saturated	7.0 %

The average double bond per triglyceride is the weighted average of double bonds per chain = 0.985, which was approximated to 1 double bond per chain or approximately 3 per triglyceride.

6.5.2.2 Synthesis of High Oleic Sunflower Oil (HOSO)–derived Polyamine (PA) – *Batch with DMPA*

Scheme 6.5.1 – General reaction scheme for the synthesis of HOSO-derived polyamine (PA).

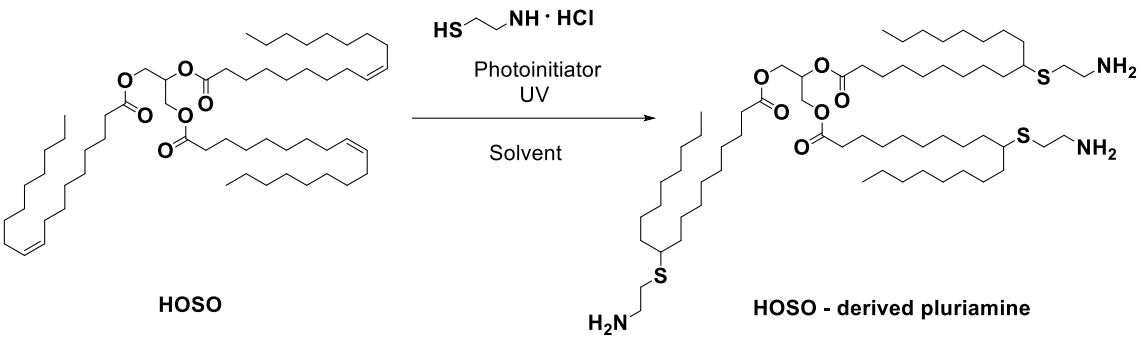

The procedure was adapted and modified from Stemmelen *et al*.:[407] 500 mg (0.56 mmol) of high Oleic Sunflower oil (**HOSO**, 88 % of monounsaturated fatty acid chains, average 3 double bonds per triglyceride, calculated by ^{1}H NMR as shown above, from Alnatura)[406] were placed in a glass vial, together with cysteamine hydrochloride (**CAHC**, 5.08 mmol, 577.14 mg, 3 equiv. per double bond) and the correct amount of the solvent mixture chosen (depending on the concentration, see **Table 4.2.1**). The mixture was stirred for 30 min. Afterwards, 0.3 equivalents of 2,2-dimethoxy-2-phenylacetophenone (DMPA, 0.169 mmol, 43.42 mg, 0.1 equiv. per double bond) were added. The reaction was stirred for the chosen time at room temperature and irradiated by UV light (see different setups in **Figure 6.5.1**, **Figure 6.5.2**, **Figure 6.5.3**). At the end of the reaction, the solvent was removed using a rotary evaporator. Subsequently, 20 mL of chloroform were added to the dried crude. The organic phase was therefore washed with saturated sodium carbonate solution and multiple times with distilled water until neutral pH was observed. Afterwards, the residual traces of water were removed with anhydrous sodium sulfate. After filtration of the Na_2SO_4, the solvent was removed using a rotary evaporator. The product appeared as a slightly yellow oil. Double bond conversion: 84%, yield: 98%.

6.5.2.3 Synthesis of High Oleic Sunflower Oil (HOSO)–derived Polyamine (PA) – Batch, Aliquots Addition

The procedure was adapted and modified from Rios *et al.*:[320] Briefly, 1 g of High Oleic Sunflower oil (**HOSO**, 88% of oleic fatty acid chains, average 3 double bonds per triglyceride, calculated from ^{1}H NMR, from Alnatura) was placed in a glass vial, together with the necessary amount of 2,2-dimethoxy-2-phenylacetophenone (**DMPA**, 0.339 mmol, 87 mg, 0.1 equiv. per double bond) and 4.5 mL of iPrOH. The mixture was stirred until homogeneous. Cysteamine hydrochloride (**CAHC**, 10.16 mmol, 1.15 g, 3 equiv. per db) was added in three aliquots, according to **Table 6.5.2**. The reaction was stirred for 24 h at room temperature and irradiated with 365 nm UV-light (45 W + 12 W lamps, see **Figure 6.5.3**). At the end of the reaction, the solvent was removed using a rotary evaporator. Subsequently, 20 mL of chloroform were added to the dried crude. The organic phase was washed with saturated sodium carbonate solution and multiple times with distilled water until neutral pH was observed. Afterwards, the residual traces of water were removed with anhydrous sodium sulfate. After filtration of the Na_2SO_4, the solvent was removed using rotary evaporator. The product resulted was obtained as slight yellow oil. Double bond conversion: 98%, yield: 98%.

Table 6.5.2 – Multistep addition of CAHC, aliquot weights and distribution.

CAHC aliquot	1	2	3
Weight (g)	0.575	0.2875	0.2875
Time (h)[a]	0	1.5	4

[a]: Time from the start of the reaction.

6.5.2.4 Synthesis of High Oleic Sunflower Oil (HOSO)–derived Polyamine (PA) – Continuous Flow

2 g of High Oleic Sunflower oil (**HOSO**, 88% of monounsaturated fatty acid chains, average 3 double bonds per triglyceride, calculated from ^{1}H NMR, from Alnatura) and 2.31 g (20.3 mmol, 9 equiv.) of **CAHC** were dissolved in 12 mL isopropanol and stirred for 30 min. Subsequently, 2,2-dimethoxy-2-phenylacetophenone **DMPA** (174 mg, 0.3 equiv.) and more isopropanol (2 mL) were added. The reaction mixture (under stirring) was fed to the flow reactor in a closed-loop mode. A scheme of the flow reactor is represented above (**Figure 6.5.4**).

6.5.2.5 Characterization of High Oleic Sunflower Oil (HOSO)–derived Polyamine (PA)

^{1}H NMR (400 MHz, $CDCl_3$) δ_H / ppm = 5.37 (m, -C**H** from unreacted double bonds), 5.25 (q, -C**H** from glycerol backbone), 4.08 – 4.34 (m, -C**H$_2$** from glycerol backbone), 2.77 – 2.92 (t, -C**H$_2$**NH_2), 2.47–2.71 (m, - C**H**SC**H$_2$**), 2.22 – 2.38 (t, - COC**H$_2$**), 1.65 – 1.83 (s, -N**H$_2$**), 1.08 – 1.65 (m, -C**H$_2$** from fatty acid chains), 0.87 (t, -C**H$_3$**).

^{13}C NMR (101 MHz, $CDCl_3$) δ_C / ppm = 173.37, 69.01, 62.22, 46.03, 41.84, 35.19, 34.14, 32.03, 29.79, 29.74, 29.44, 29.23, 26.97, 24.96, 22.80, 14.25.

IR (ATR platinum diamond): $\tilde{\nu}$ / cm^{-1} = 2923, 2853, 1740, 1650, 1604, 1462, 1275, 1158, 755.

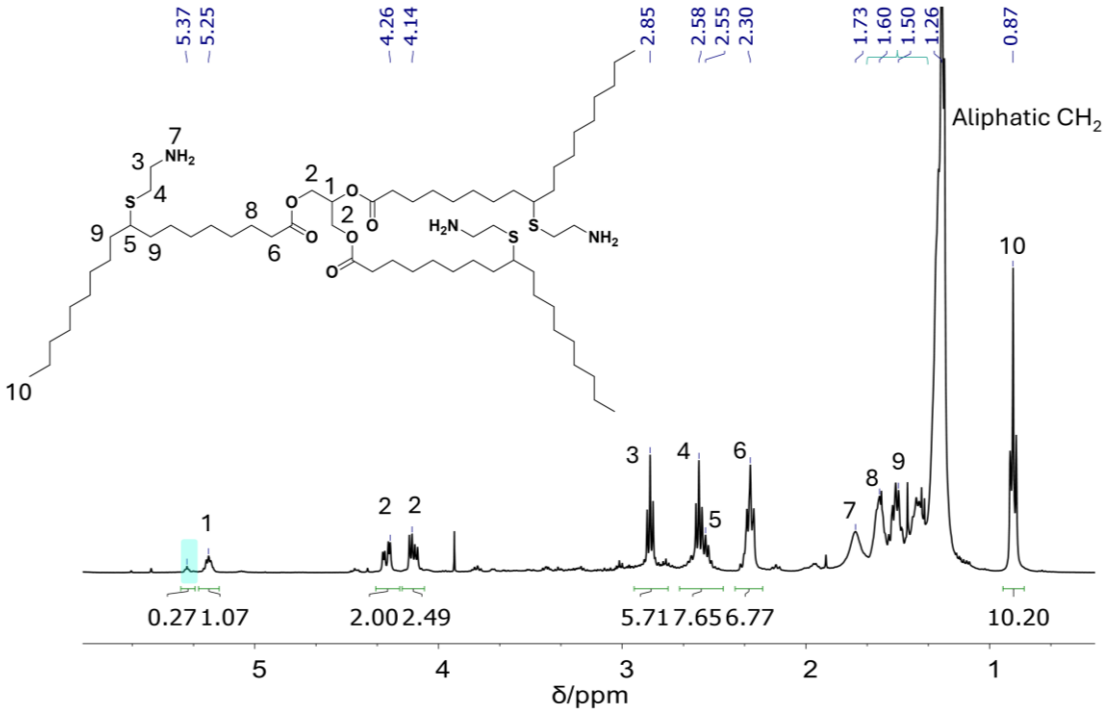

Figure 6.5.6 – ^{1}H NMR in $CDCl_3$ spectrum of **PA** with a conversion of 95 %. Signal assignation was performed via 2D – NMR spectroscopy techniques (HMBC, HSQC, COSY), DEPT – 135 and according to literature values.

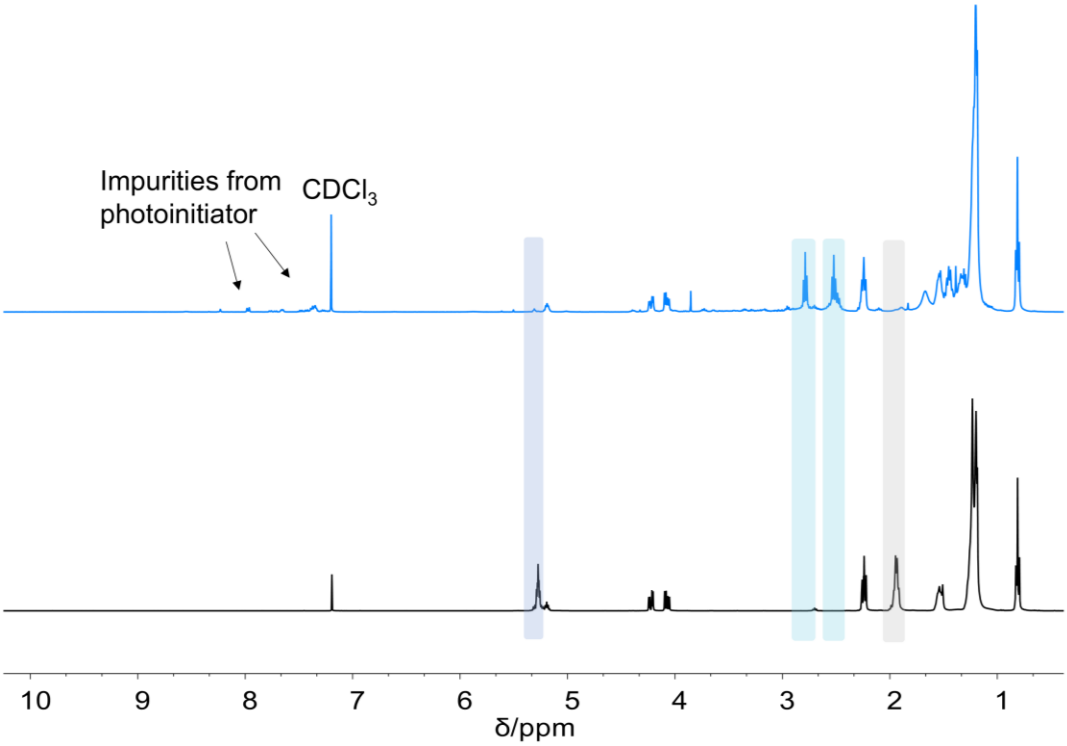

Figure 6.5.7 – Overlay of ^{1}H NMR spectra for pristine HOSO (black, bottom) and **PA** (top, blue). The disappearance of the signal attributed to the -CH protons of the double bonds (vinylic protons, highlighted in violet) indicates a high conversion (95%), confirming the successful reaction. In the spectrum of the aminated HOSO, two new signals (highlighted in light blue) appear, corresponding to the CH_2 protons directly attached to the $-NH_2$ and -S groups, respectively. Additionally, the signal for the allylic $-CH_2$ protons disappears in **PA**.

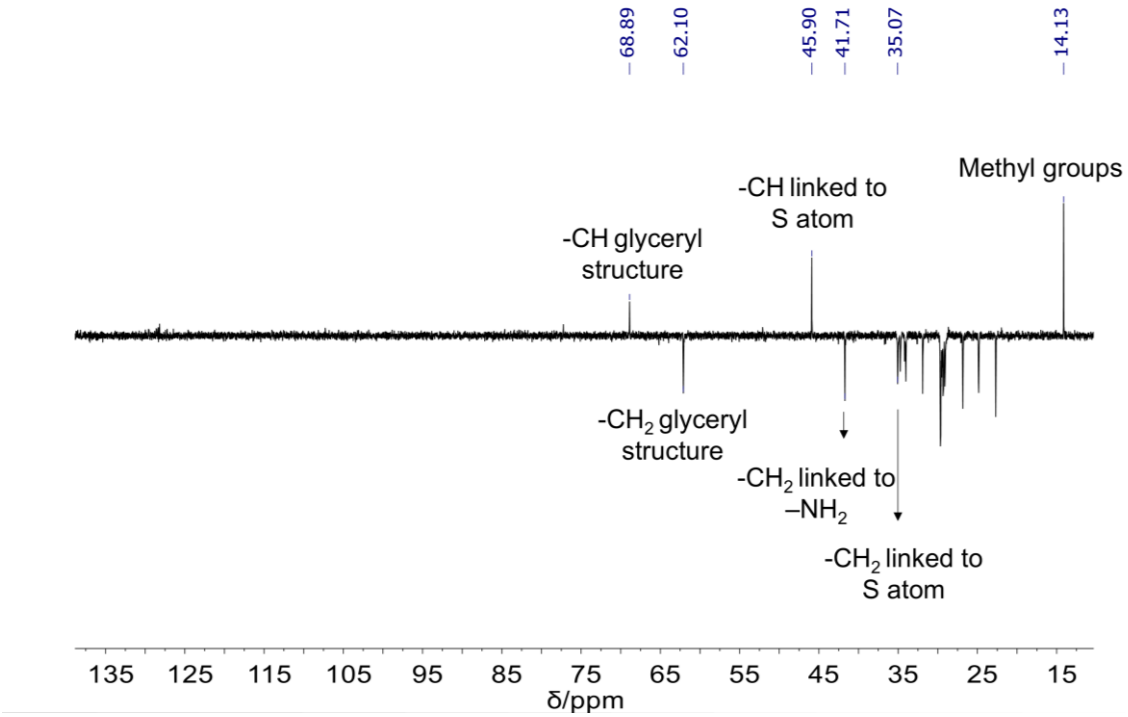

Figure 6.5.8 – DEPT – 135 spectrum of **PA** with a double bond conversion of 95 % in $CDCl_3$. CH and CH_3 groups are shown as positive, while CH_2 are negative.

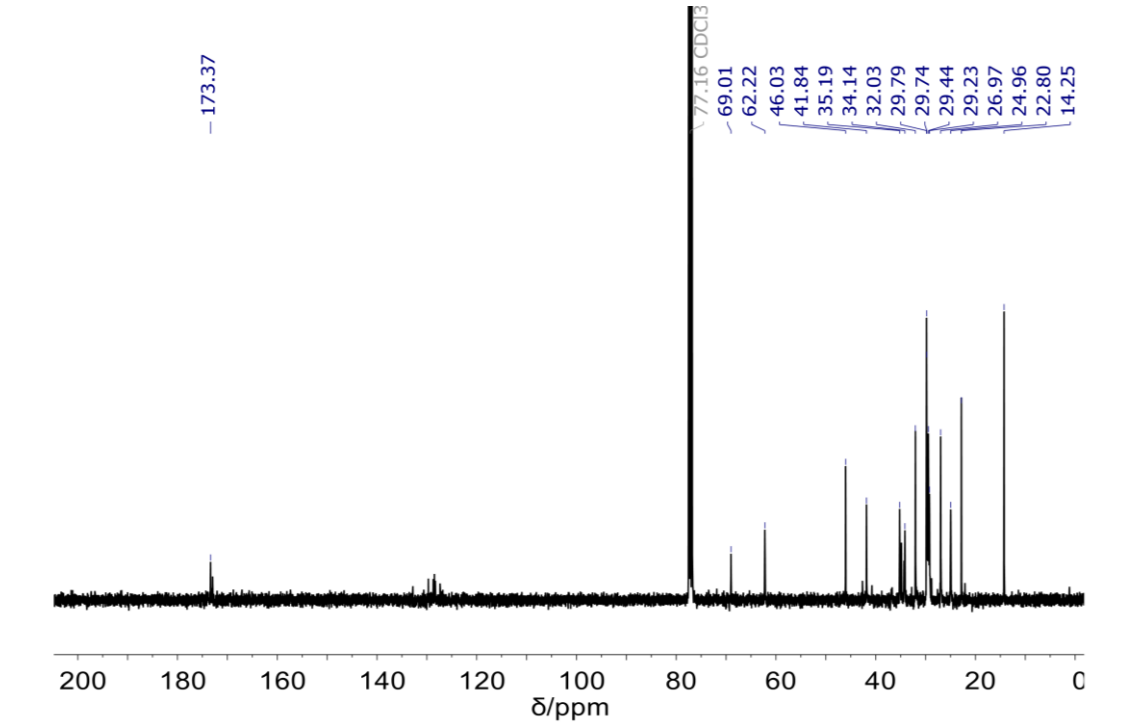

Figure 6.5.9 – ^{13}C NMR of PA in $CDCl_3$ with a double bond conversion of 95 %.

Conversion calculation:

Conversion of the double bonds was calculated based on the normalized integral of the signal ascribed to the double bond protons, both in the pristine HOSO (5.27 ppm, *I* = 5.91) and in the aminated HOSO (5.37 ppm).

$$Conversion\ (\%) = \frac{I_{CH=CH\ HOSO} - I_{CH=CH\ aminated\ HOSO}}{I_{CH=CH\ HOSO}} \times 100 \qquad \text{Eq. S13}$$

Amine functionality calculation:

Introduced functionalities (f) equals to the functional groups of cysteamine introduced to the aminated HOSO per trigyceride. The theoretical maximum equals to 3 (if all three double bonds of HOSO have reacted), which corresponds to 100 % conversion. Functionalities are therefore calculated based on the conversion reached, according to the equation:

$$f = \frac{Conversion\ (\%)}{100\ \%} \times 3 \qquad \text{Eq. S14}$$

Molecular weight calculation:

$$MW\ final = MW(HOSO) + (f \times 77.137) \qquad \text{Eq. S15}$$

Yield calculation:

To calculate the yield of the product, the theoretical mass has to be calculated first, with the final MW obtained in the calculation above. The yield of the product can then be calculated as follows:

$$Yield = \frac{Obtained\ weight\ of\ product}{Theoretical\ mass} \times 100\% \qquad \text{Eq. S16}$$

6.5.2.6 Conversion Monitoring in Flow Reactions

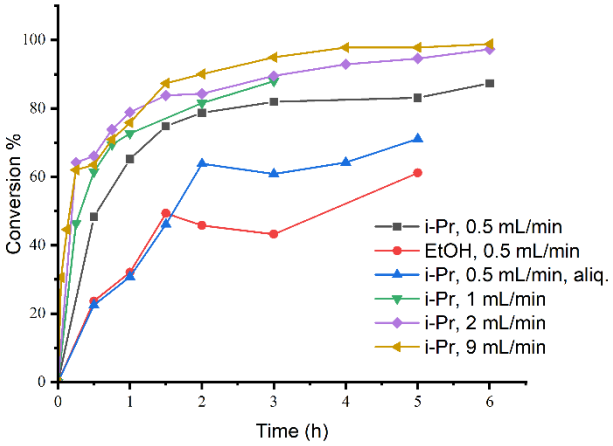

Figure 6.5.10 – Comparison of reaction conversions for flow experiments. To evaluate the conversion, a 100 µL sample was taken at different reaction times and ^{1}H NMR was recorded. Different flow rates and different solvents were evaluated.

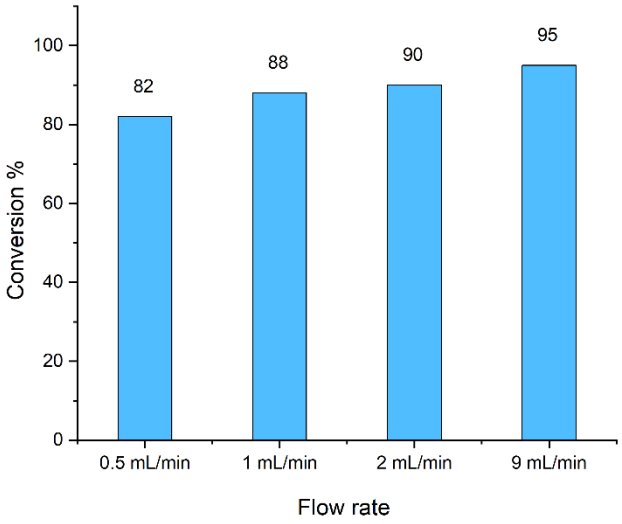

Figure 6.5.11 – Conversion after 3 h of reaction time in flow experiments.

6.5.3 Lignin Modification

6.5.3.1 General Procedure for the Synthesis of Hydroxyalkylated Lignin (HAL) with Glycerol Carbonate

Characterization was performed *via* ^{31}P NMR, ^{1}H NMR, ^{13}C NMR, SEC-DMAc, FT-IR, DSC, TGA. Data are reported in **Table 6.5.3**.

Table 6.5.3 – Characterization data of HAL.

$OH_{Aliphatic}$ (mmol·g^{-1})[a]	$OH_{Aromatic}$ (mmol·g^{-1})[a]	COOH (mmol·g^{-1})[a]	OH_{Total} (mmol·g^{-1})[a]	M_n (g·mol^{-1})[b]	*Đ*
4.66	0	0	4.66	13800	4.8

[a]: Determined via ^{31}P NMR. [b]: SEC-DMAc.

Scheme 6.5.2 – General reaction scheme for the synthesis of Hydroxyalkylated lignin. Only isomers of the etherification pathway with GC are shown, leading to 1,2-diols and 1,3-diols structures. For a comprehensive overview of all the possible structures, see **Scheme 4.2.2** and **Scheme 4.2.3**.

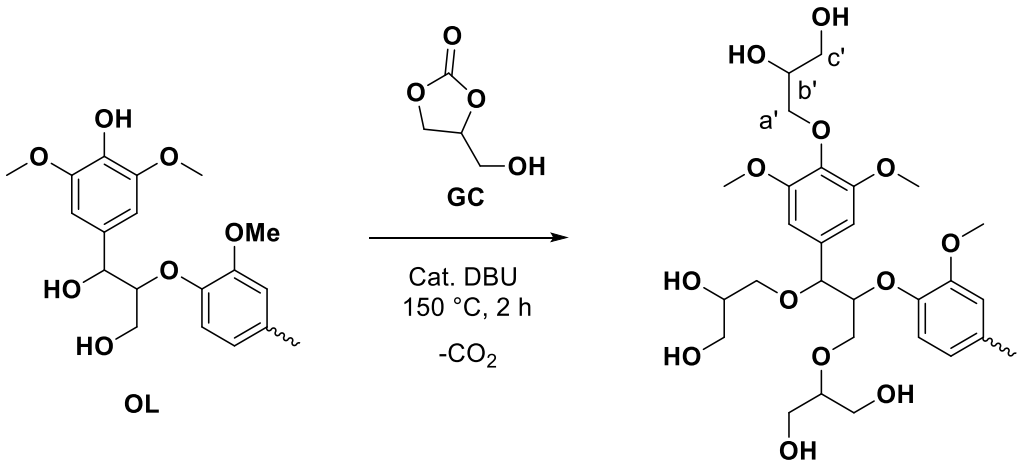

10.0 g of lignin (OL: 4.35 mmol OH g^{-1} dry lignin) were suspended in glycerol carbonate (435 mmol, 51.3 g, 36.7 mL, 10.0 equiv.) and DBU (4.35 mmol, 0.66 g, 0.65 mL, 0.10 equiv.) was added. The reaction mixture was allowed to react at 150 °C for 2 hours under Argon flow. After reaching 100 °C, strong evolution of CO_2 was observed. After completion of the reaction, the crude product was

dissolved in a minimum amount of DMSO and the product was recovered by precipitation in a tenfold amount of acidified deionized water (pH < 2, acidified with HCl 1 M). After filtration on a fritted frit (porosity: P-4) and washing with water (5 x 50 mL), the isolated product was dried at 60 °C under vacuum. Yield: 11.0 g, 83% theoretical yield, calculated according to **Eq. S12**.

^{1}H NMR (400 MHz, DMSO-d$_6$) δ_H / ppm = 7.50 – 6.25 ppm (m, C**H**$_{aryl}$); 5.30 - 4.10 (m, C**H**$_{a,b,c}$); 4.0 – 3.50 (s, OC**H**$_3$, O**H**); 1.40 – 0-70 (m, C**H**$_{alkyl}$).

^{13}C NMR (126 MHz, DMSO-d$_6$) δ_C / ppm = 154.97, 152.14, 92.90, 75.58, 72.94, 70.51, 68.59, 66.01, 63.09, 60.01, 55.84, 15.29.

IR (ATR platinum diamond): $\tilde{\nu}$ / cm^{-1} = 3425, 2933, 2871, 1790, 1590, 1504, 1456, 1417, 1327, 1224, 1121, 1031, 843.

T_g = 99 °C; $T_{d,5\%}$ = 267 °C

Hydroxyl content: 4.66 mmol OH g^{-1} dry sample, calculated from ^{31}P NMR.

Degree of substitution (DS) calculations:

DS phenolic hydroxyl groups: 1 (^{31}P NMR shows no aromatic hydroxyl groups left after the reaction; therefore, the DS is set to one for complete substitution).

DS aliphatic hydroxyl groups: 0.75, determined from ^{13}C NMR, according to the procedure established by Lehnen *et al.*[256] Signal of the installed hydroxyl terminated carbon (b') is correlated to the total amount of aliphatic carbon atoms next to hydroxyls (60.01 ppm) according to **Eq. S17**:

$$DS_{aliphatic} = \frac{I_{b'}}{I_{b'} + I_{C-OH}} \qquad \text{Eq. S17}$$

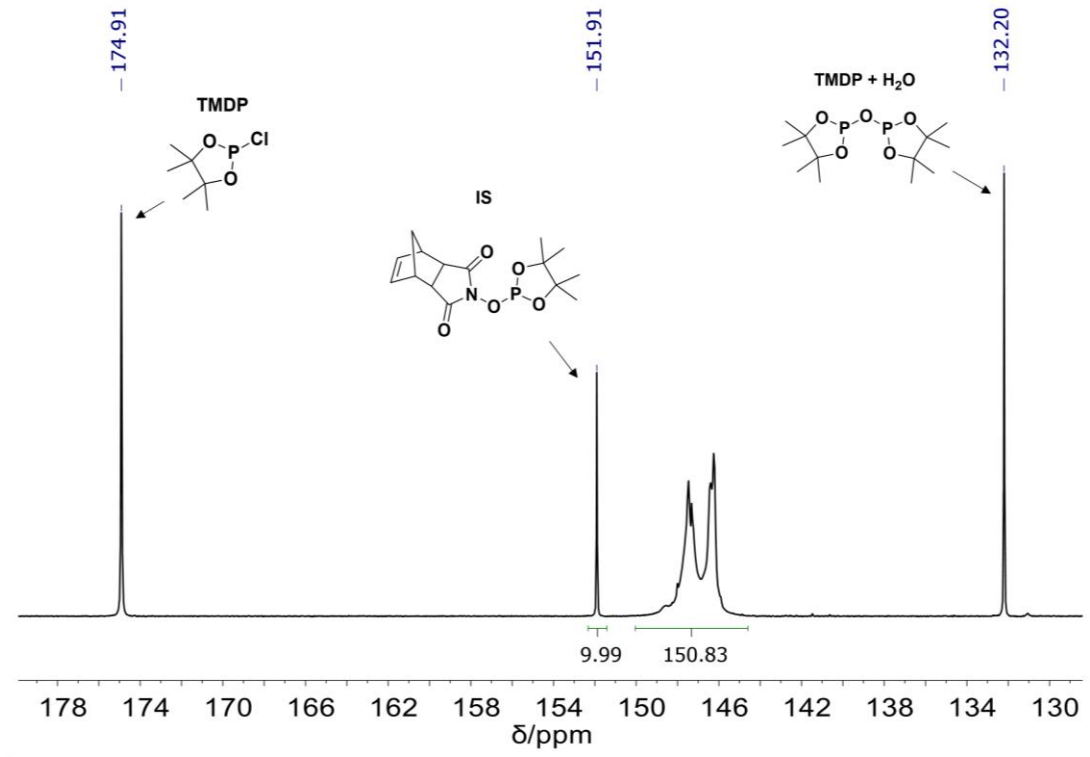

Figure 6.5.12 – ^{31}P NMR of HAL.

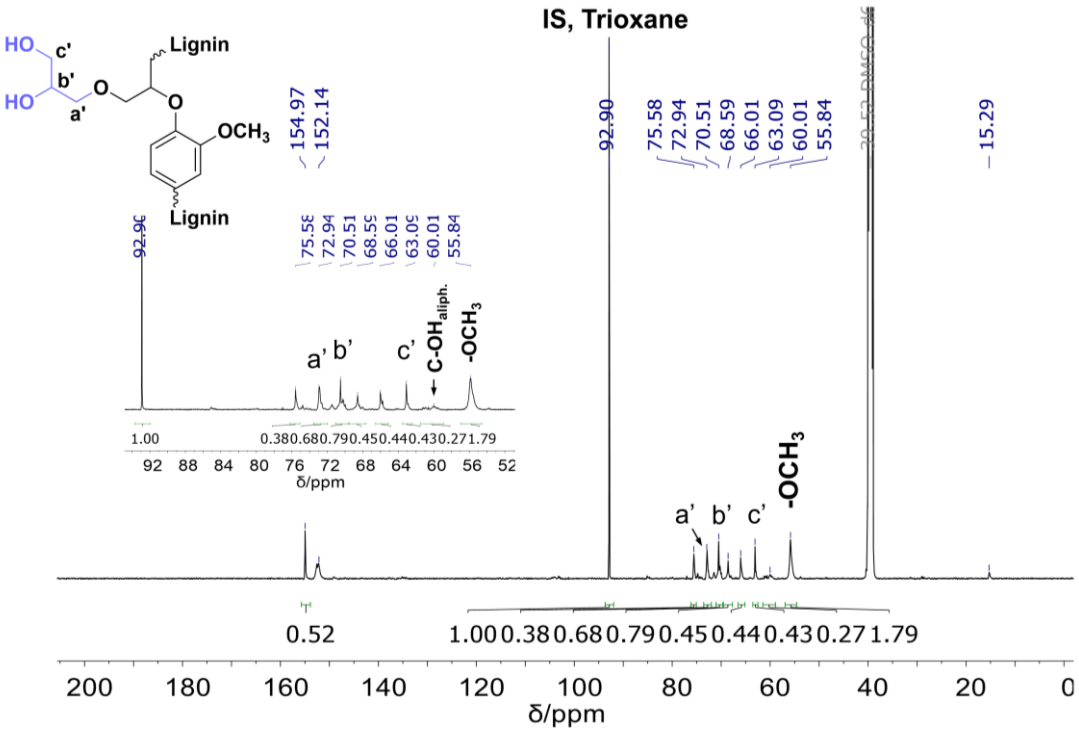

Figure 6.5.13 – ^{13}C NMR of HAL, signal assignment was conducted based on literature data.[271]

Table 6.5.4 – Quantitative ^{13}C NMR data for HAL.

mmol IS in the sample (mmol)	I_{ratio} Carbonyl signal	Carbonyl content (mmol·g^{-1})
0.06169	0.52	0.34

6.5.3.2 General Procedure for the Synthesis of Cyclic Carbonate Functionalized Lignin with Dimethyl Carbonate

Characterization was performed *via* ^{31}P NMR, ^{1}H NMR, ^{13}C NMR, SEC-DMAc, FT-IR, DSC, TGA. Data are reported in **Table 6.5.5**.

Table 6.5.5 – Characterization data of CCFL.

$OH_{Aliphatic}$ (mmol·g^{-1})[a]	$OH_{Aromatic}$ (mmol·g^{-1})[a]	COOH (mmol·g^{-1})[a]	OH_{Total} (mmol·g^{-1})[a]	M_n (g·mol^{-1})[b]	*Đ*
1.64	0	0	1.64	12600	3.9

[a]: Determined via ^{31}P NMR. [b]: SEC-DMAc.

Scheme 6.5.3 – General reaction scheme for the synthesis of cyclic carbonate functionalized lignin. The main reaction leading to the formation of cyclic carbonate structures is shown, as well as the formation of linear carbonates due to the reaction of hydroxyl groups with only one side of DMC. Both possible isomers deriving from etherification with GC are shown (forming 1,2-diols and 1,3-diols).

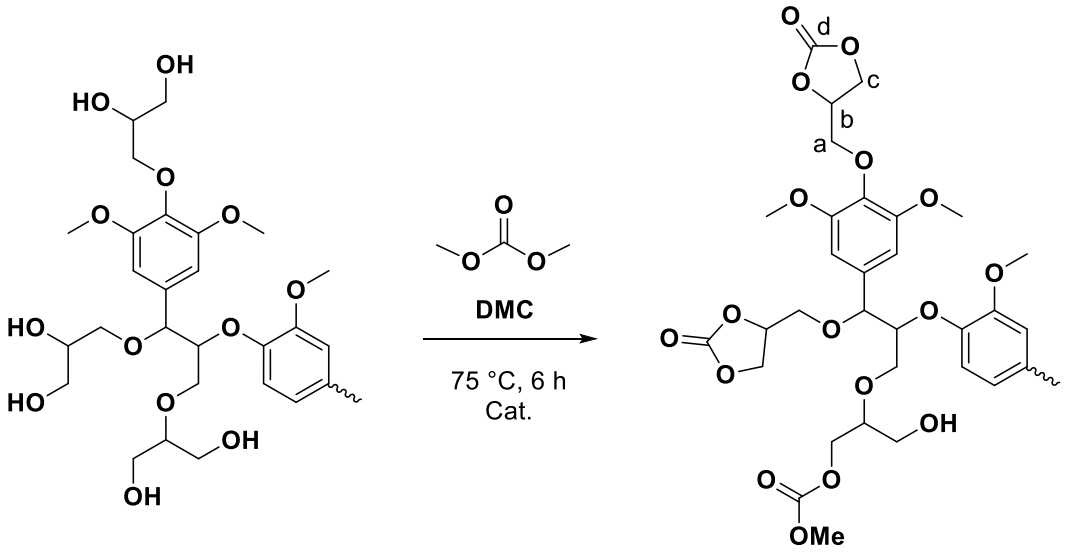

Solventless procedure:

In a crimp vial, 1.00 g of previously synthesized hydroxyalkylated lignin (4.66 mmol OH g^{-1} dry lignin) was suspended in DMC (anhydrous, 23.3 mmol, 2.09 g, 2.00 mL, 5.00 equiv.). The catalyst DBU (1.86 mmol, 284 mg, 278 µL, 0.40 equiv.) was added to the reaction vessel, and this was flushed with a gentle Argon flow for 5 to 10 minutes. Afterwards, the desired temperature was applied, and the reaction was stirred for 6 h at 75 °C. After completion of the reaction, the crude product was recovered by precipitation in a tenfold amount of acidified deionized water (pH < 2, acidified with HCl 1 M). After filtration on a fritted frit (porosity: P-4) and washing with water (5 x 50 mL), the isolated product was dried at 60 °C under vacuum (10 mbar). hydroxyl content: 1.68 mmol OH per g, calculated from ^{31}P NMR.

Procedure with solvent:

6.00 g of previously synthesized hydroxyalkylated lignin (4.66 mmol OH g^{-1} dry lignin) were dissolved in DMAc (anhydrous, 15 mL) with gentle heating. Afterwards, anhydrous DMC was added (140 mmol, 12.6 g, 11.8 mL, 5.00 equiv.) as well as the catalyst TBD (11.2 mmol, 1.56 g, 0.40 equiv.), and the vessel was flushed with a gentle Argon flow for 5 to 10 minutes. Afterwards, the desired temperature was applied, and the reaction was stirred for 6 h at 75 °C. After completion of the reaction, the crude product is recovered by precipitation in a tenfold amount of acidified deionized water (pH < 2, acidified with HCl 1 M). After filtration and washing with water (5 x 50 mL), the isolated product was dried at 60 °C under vacuum (10 mbar). Yield: 5.83 g, 86% theoretical yield, calculated according to **Eq. S12**.

^{1}H NMR (400 MHz, DMSO-d_6) δ_H / ppm = 7.6 – 5.9 ppm (m, C**H**$_{aryl}$); 5.3 – 4 (m, C**H**$_{a,b,c}$); 4.0 – 3.4 (s, OC**H$_3$**, O**H**); 1.40 – 0-70 (m, C**H**$_{alkyl}$).

^{13}C NMR (126 MHz, DMSO-d_6) δ_C / ppm = 155.43, 153.03, 149.54, 135.63, 103.37, 93.36, 76.04, 73.33, 71.92, 70.70, 66.46, 63.55, 60.39, 56.25, 55.10, 15.69.

IR (ATR platinum diamond): $\tilde{\nu}$ / cm^{-1} = 3493, 2937, 1792, 1748, 1592, 1506, 1456, 1329, 1267, 1125, 1051, 847, 771.

T_g = 117 °C; $T_{d,5\%}$ = 222 °C.

Hydroxyl content: 1.64 mmol OH g^{-1}, calculated from ^{31}P NMR.

Carbonyl content: 0.91 mmol g^{-1}, calculated from ^{13}C NMR.

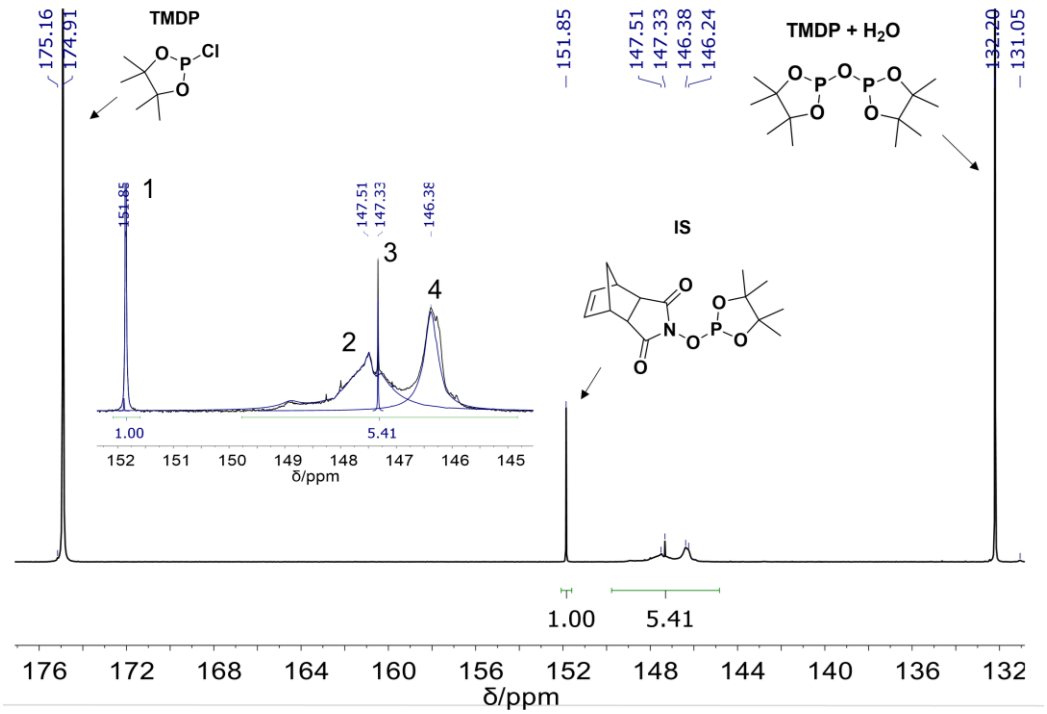

Figure 6.5.14 – ^{31}P NMR of CCFL. Residual ethanol (sharp signal at 147.32 ppm) could not be removed, even after drying at 60 °C under vacuum (10 mbar) for 5 days, as also reported from Jääskeläinen *et al*.[405] To obtain more accurate results, peak deconvolution was performed and is shown in the expanded view (blue lines).

Table 6.5.6 – Peak deconvolution data for the ^{31}P NMR of CCFL.

Signal	*δ* (ppm)	Area (arb.unit)
1	151.85	47648669
2	147.51	169196204
3	147.33	4115611
4	146.38	120457654

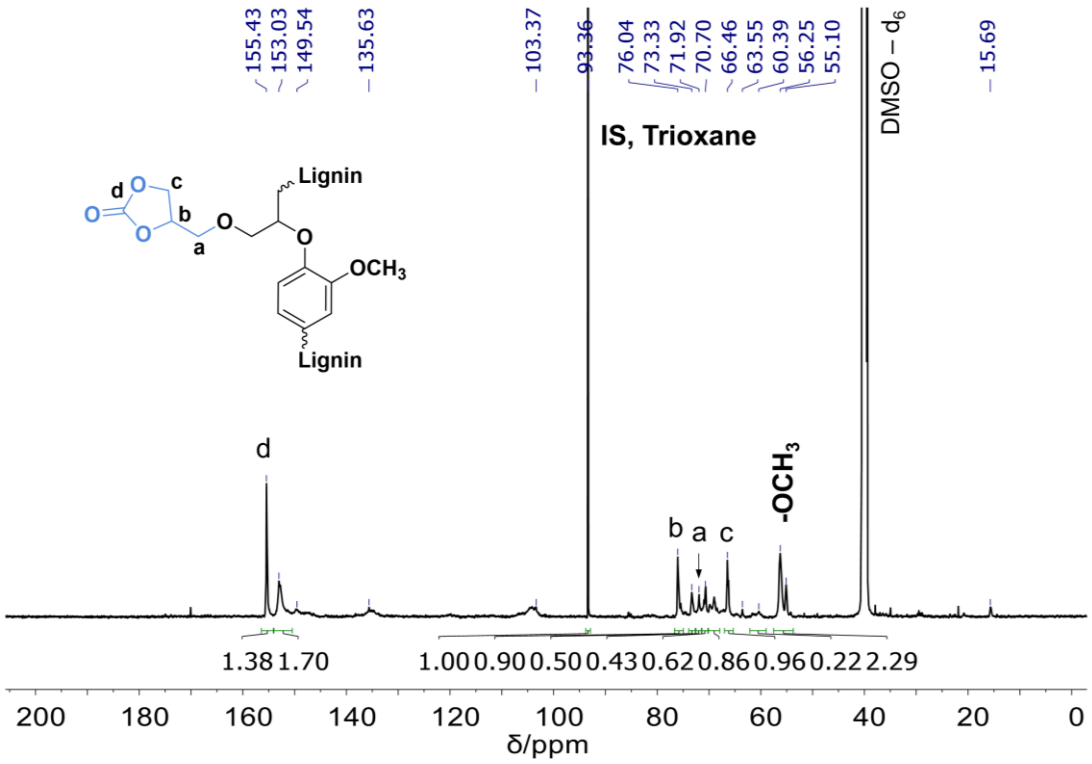

Figure 6.5.15 – ^{13}C NMR of CCFL, signal assignment was conducted based on literature data.[271]

Table 6.5.7 − Quantitative ^{13}C NMR data for CCFL.

mmol IS in the sample	I_{ratio} Carbonyl signal	Carbonyl content (mmol g^{-1})
0.06289	1.38	0.91

6.5.3.3 Thermal Properties of HAL and CCFL

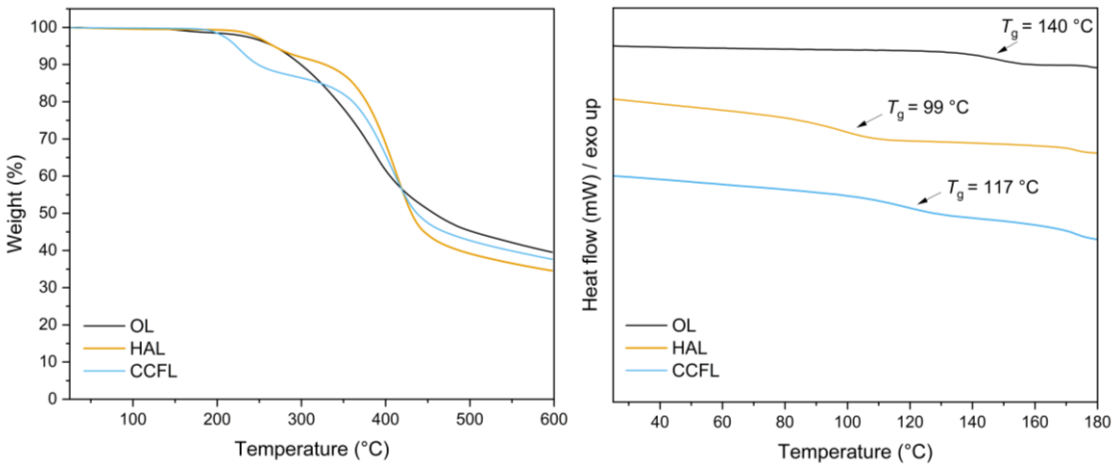

Figure 6.5.16 – TGA (left) and DSC (right) thermograms of organosolv lignin (black), hydroxyalkylated lignin (red) and cyclic carbonate functionalized lignin (blue). Values are shown in **Table 6.5.8**.

Table 6.5.8 – Values obtained from thermal analyses TGA and DSC for unmodified OL, HAL, and CCFL.

Sample	$T_{d,5\%}$ (°C)	$T_{d,30\%}$ (°C)	Residues (%)	T_g (°C)
OL	267	376	45	140
HAL	267	398	35	99
CCFL	222	391	38	117

6.5.4 Thermosets

6.5.4.1 Synthesis of Erythritol bis-cyclic Carbonate (EBC)

Scheme 6.5.4 – General reaction scheme for the synthesis of erythritol bis-cyclic carbonate.

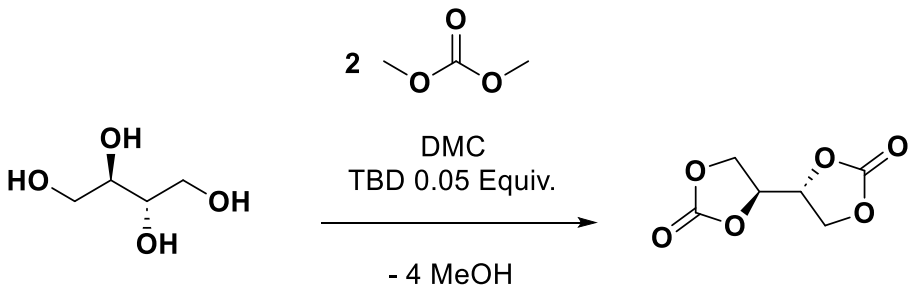

Procedure:

A procedure described in previous work from Meier *et al*.[338] was applied: In particular, in a 100 mL flask, erythritol (2.00 g, 16.4 mmol, 1.00 equiv.) and TBD (114 mg, 0.820 mmol, 0.05 equiv.) were dispersed in 41 mL of DMC (43.9 g, 0.49 mol, solvent and reactant) and heated to 60 °C for 40 min at the rotary evaporator at 320 mbar. The crystalline erythritol dissolved completely after 35 min and after 45 min, a white precipitate was formed. The product was filtered off after the mixture was cooled to room temperature and washed with fresh DMC yielding a white powder (Yield: 2.53 g, 90%).

^{1}H NMR (400 MHz, DMSO-d$_6$) δ_H / ppm = 5.22 – 5.06 (m, 2H), 4.71 – 4.54 (m, 2H, diastereotopic signals), 4.49 – 4.32 (m, 2H, diastereotopic signals).

^{13}C NMR (101 MHz, DMSO-d$_6$) δ_C / ppm = 154.62, 75.38, 65.16.

IR (ATR platinum diamond): $\tilde{\nu}$ / cm^{-1} = 1804, 1781, 1545, 1485, 1382, 1300, 1205, 1146, 1072, 1031, 983, 896, 773, 740, 719.

HRMS (ESI-MS, (M+H)$^+$, $C_6H_7O_6$) calcd. 175.0237, found 175.0237.

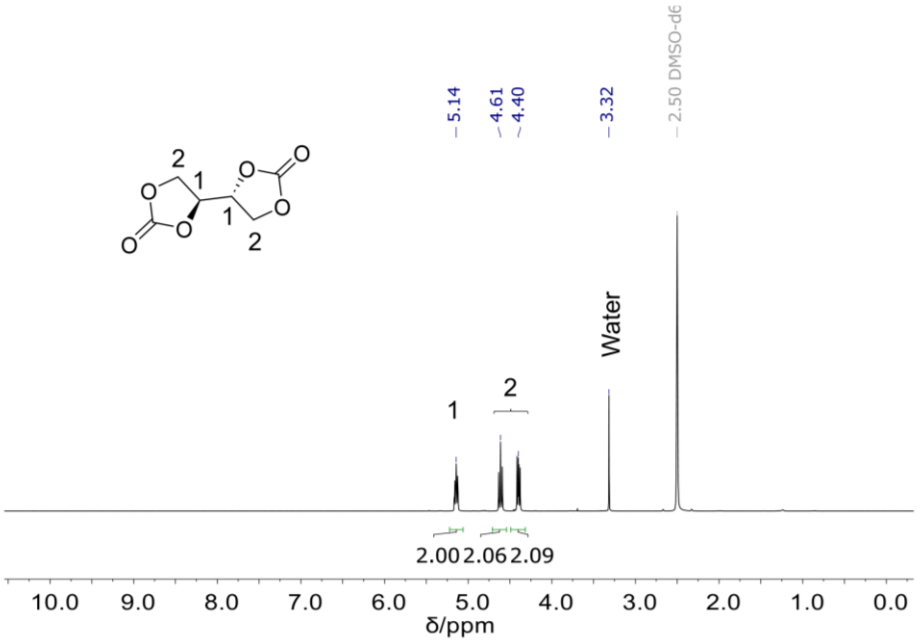

Figure 6.5.17 – ^{1}H NMR spectrum of erythritol bis-cyclic carbonate in DMSO-d_6.

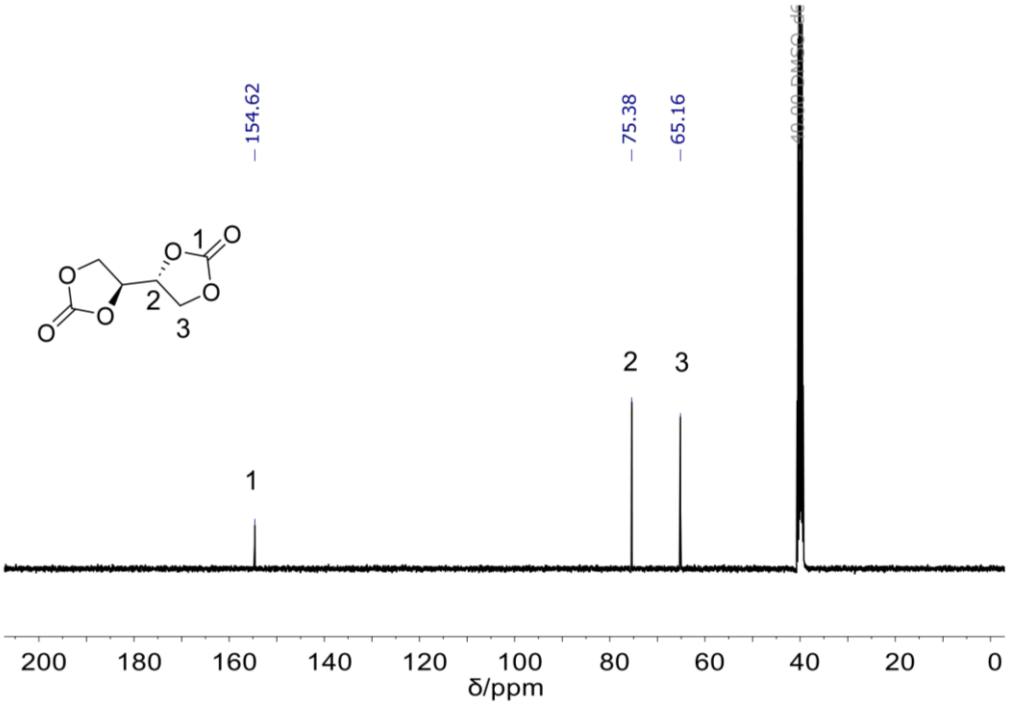

Figure 6.5.18 – ^{13}C NMR spectrum of erythritol bis-cyclic carbonate in DMSO-d_6.

6.5.4.2 General Procedure for the Synthesis of Lignin-based NIPU Thermoset with EBC as a Third Component

In a 10 mL scintillation vial, the necessary amount of previously synthesized PA was weighed. Then, EBC, CCFL and TBD were weighed and added to the vial. DMSO (typically 1 mL for 125 mg CCFL) was added and the solution was vortexed until completely homogeneous (typically 15 to 20 minutes). If necessary, gentle heating was applied to aid the dissolution of all components. The homogeneous solutions were poured into pre-heated teflon molds (40×10×15 mm) at 50 °C. The curing was performed by heating gradually in the oven until the desired temperature (150 °C) was reached. The samples were cured at 150 °C for 2.5 days. Curing performance was followed by IR spectroscopy, monitoring the disappearance of the signal at 1792 cm^{-1} ascribed to the stretching band of carbonyls from cyclic carbonate moieties.

6.5.4.3 DMA Analyses

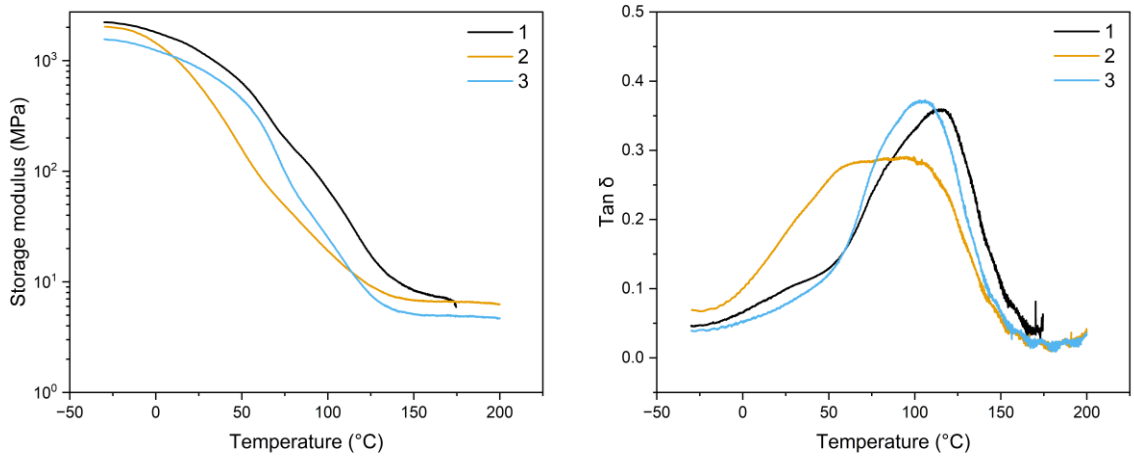

Figure 6.5.19 – DMA curves for the thermoset with 38 wt% of lignin. Measurements were performed in triplicates.

Table 6.5.9 – Overview of the values of the storage modulus in MPa, E', at different temperatures, and the T_g values calculated on the onset of E' and at the peak of tan δ for the sample with 38 wt% lignin content. Measurements were performed in triplicates and results for the three entries are shown.

Entry	$E'_{-30°C}$ (MPa)	$E'_{25°C}$ (MPa)	$E'_{150°C}$ (MPa)	T_g Onset E' (°C)	T_g Max tanδ (°C)
1	2000	1260	7.30	56.9	99.8
2	2340	1420	6.91	56.3	92.6
3	1570	980	2.94	52.5	99.5

6.6 Experimental Procedures for Chapter 4.3 – Functionalization of Lignin with Cyclic Anhydrides

6.6.1 Lignin Functionalization

6.6.1.1 Calculations of Conversions for Lignin

For the determination of the consumed aliphatic and aromatic hydroxyl groups—and consequently the calculation of conversion percentages—it is essential to account for the molecular weight increase resulting from the modification with the cyclic anhydride, relative to the starting material (Organosolv lignin, acetone-fractionated). The consumption of aliphatic and phenolic hydroxyl groups was quantified using **Eq. S18** and **S19**, while the corresponding percentage conversions were calculated according to **Eq. S20** and **S21**.

$$OH_{aliph,\ consumed} = \frac{OH_{aliph,\ starting\ lignin} - OH_{aliph,\ modified\ lignin}}{\left(1 + \left(\frac{Mw_{Itaconic\ anhydride}}{1000} \times OH_{aliph,\ modified\ lignin}\right)\right)} \quad \text{Eq. S18}$$

$$OH_{arom,\ consumed} = \frac{OH_{arom,\ starting\ lignin} - OH_{arom,\ modified\ lignin}}{\left(1 + \left(\frac{Mw_{Itaconic\ anhydride}}{1000} \times OH_{arom,\ modified\ lignin}\right)\right)} \quad \text{Eq. S19}$$

$$XOH_{aliph} = \frac{OH_{aliphatic,\ consumed}}{OH_{aliph,\ starting\ lignin}} \quad \text{Eq. S20}$$

$$XOH_{arom} = \frac{OH_{arom,\ consumed}}{OH_{arom,\ starting\ lignin}} \quad \text{Eq. S21}$$

6.6.1.2 General Procedure for the Fractionation of Lignin with Acetone

Scheme 6.6.1 – Visual representation of the fractionation of Organosolv lignin.

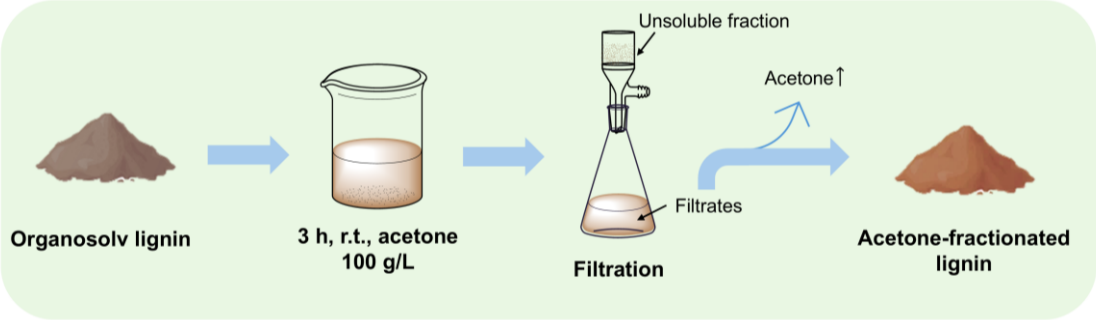

OL (previously dried at 70 °C under 10 mbar vacuum) was suspended in acetone with a concentration of 100 g/L. The suspension was stirred at r.t. for 3 hours, afterwards it was filtrated on a Buchner filter equipped with grade 5 filter paper. The filtrates were collected, and the solvent was evaporated under reduced pressure. The residue was collected with a minimal amount of clean acetone and precipitated in a tenfold amount of acidified deionized water (pH < 2, acidified with HCl 1 M).The solids were filtrated on a fritted filter (porosity P-4), washed with cleaned deionized water, and dried under vacuum (10 mbar, 70 °C) for at least 48 hours prior to analysis.

Fractionation was performed on a 15 g scale and a 50 g scale, with yields of 62% and 67%, respectively (gravimetric yield of fractionation, based on starting weight). The 15 g scale acetone lignin fractionation will be indicated hereon with OL Acetone (1), while the 50 g scale acetone lignin fractionation will be indicated with OL Acetone (2). Characterization of both lignin is reported in **Table 6.6.1**.

OL Acetone (3) was performed on a 60 g scale with a 67% yield and used as starting material to synthesize succynilated (LS-BB-TMG) and itaconated lignin (LI-BB-TMG) with TMG as catalyst.

Table 6.6.1 – Characterization of pristine lignin (OL) and both batches after acetone fractionation.

Entry	$OH_{Aliphatic}$ (mmol·g^{-1})[a]	$OH_{Aromatic}$ (mmol·g^{-1})[a]	COOH (mmol·g^{-1})[a]	OH_{Total} (mmol·g^{-1})[a]	M_n (g·mol^{-1})[b]	*Đ*
OL	2.42 ± 0.05	1.83 ± 0.04	0.100 ± 0.004	4.35 ± 0.08	3000	3.7
OL Acetone (1)	2.52 ± 0.03	2.42 ± 0.04	0.060 ± 0.005	5.01 ± 0.07	2900	2.7
OL Acetone (2)	2.24 ± 0.03	2.03 ± 0.02	0.070 ± 0.004	4.34 ± 0.05	2800	2.6
OL Acetone (3)	2.26 ± 0.02	2.12 ± 0.07	0.080 ± 0.002	4.42 ± 0.05	2500	2.5

[a]: Determined via ^{31}P NMR. Measurements were performed in triplicate.[b]: SEC-DMAc.

For the optimization of the reaction conditions between fractionated lignin and IAn, the first fractionation in a 15 g batch (**OL Acetone (1)**) was utilized. For the upscaling of the functionalization reaction of lignin with itaconic anhydride with DBU as catalyst (LI-BB-DBU), the 50 g fractionation batch (**OL Acetone (2)**) was utilized. **OL Acetone (3)** was used in the final part of the project to synthesize two upscaled batches of succinylated and itaconated lignin with TMG.

OL Acetone (2): T_g = 125 °C; $T_{d,5\%}$ = 252 °C

OL Acetone (3): T_g = 127 °C; $T_{d,5\%}$ = 252 °C

6.6.1.3 General Procedure for the Functionalization of Lignin with Itaconic Anhydride (0.5 g Batch Scale)

The experimental synthesis described in this section was carried out by Gianluca Giuseppe Rizzo as part of his chemistry thesis ("Vertiefungspraktikum") and by Aaron Seider, who contributed to the synthetic work in his role as a student research assistant; both were co-supervised by the author.

Scheme 6.6.2 – General scheme of the reaction between Acetone-frationated OL and IAn with DBU as catalyst.

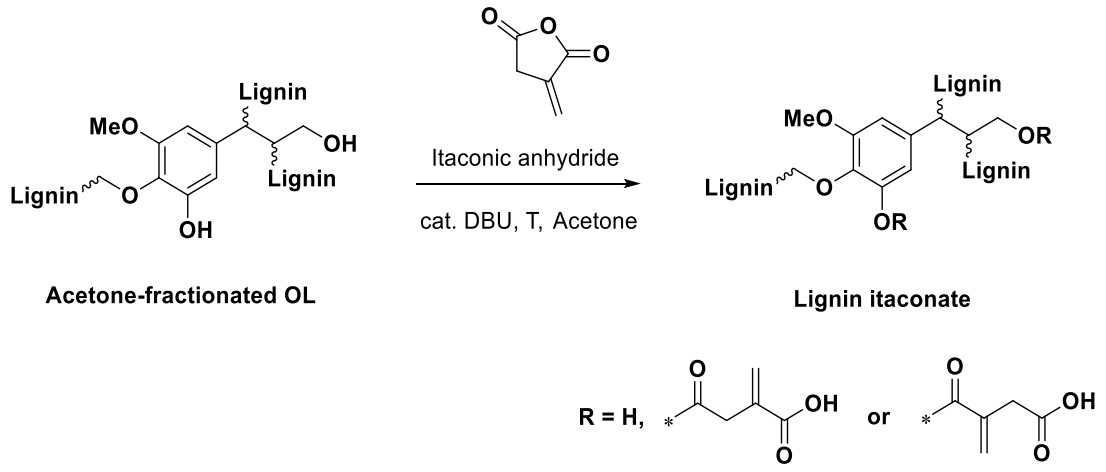

0.50 g of OL Acetone (1) (5.01 mmol OH g^{-1} dry lignin) were dissolved in 5 mL of dry acetone. Afterwards, the desired amount of itaconic anhydride (1.20 – 4.20 equiv.) was added to the reaction mixture, as well as the catalyst. The reaction vessel was flushed with argon and heated to the desired temperature. At the end of the reaction time, the vessel was allowed to cool down, and the reaction mixture was precipitated in a tenfold amount of aqueous acidic condition (pH < 2, acidified with HCl 1 M). Afterwards, solids were recovered *via* filtration on a P-4 fritted filter, washed with cleaned deionized water, and dried under vacuum (10 mbar, 70 °C) for at least 24 hours prior to analysis. If needed, the process of redissolution in acetone and reprecipitation in aqueous acidic condition (pH < 2, acidified with HCl 1 M) was repeated to remove impurities. For specific parameters tested, see **Chapter 4.3**.

6.6.1.4 General Procedure for the Functionalization of Lignin with Itaconic Anhydride (15 g Batch – DBU)

15.0 g of OL Acetone (2) (4.34 mmol OH g^{-1} dry lignin) were dissolved in dry acetone (150 mL) in a 500 mL round bottom flask. Afterwards, IAn (30.7 g, 4.20 equiv. related to the total of OH groups) and the catalyst DBU (595 mg, 583 µL, 6 mol% related to the total of OH groups) were added. The flask was equipped with an air condenser. The system was flushed with argon for a few minutes. After reaching the desired temperature, the reaction was stirred for 24 h at 45 °C. At the end of the reaction time, the vessel was allowed to cool down, and the reaction mixture was precipitated in a tenfold amount of acidified deionized water (pH < 2, acidified with HCl 1 M) and stirred for one hour. Afterwards, solids were recovered *via* filtration on a P-4 fritted filter, washed with cleaned deionized water until filtrates were neutral, and dried under vacuum (10 mbar, 70 °C) for 72 hours prior to analysis. The procedure of dissolution in minimal amount of acetone and precipitation in aqueous acidic condition (pH < 2, acidified with HCl 1 M) was repeated three times to eliminate impurities. Yield: 22.3 g, 93% theoretical yield, calculated according to **Eq. S12**.

^{1}H NMR (400 MHz, DMSO-d_6) δ_H / ppm = 13.2 – 11.9 (s, -COO**H**); 7.8 – 5.8 ppm (m, C$\mathbf{H}_{aryl}$); 5.1– 3.2 (s, OC$\mathbf{H_3}$, O**H**); 2.2 – 0.5 (m, C$\mathbf{H}_{alkyl}$).

^{13}C NMR (126 MHz, DMSO-d_6) δ_C / ppm = 174.46, 173.89, 172.92, 168.38, 165.93, 162.77, 152.31, 147.95, 144.79, 142.49, 141.07, 138.88, 134.89, 120.25, 115.61, 108.20, 103.64, 71.29, 64.20, 60.11, 59.47, 56.28, 55.92, 55.92, 51.13, 45.15, 30.72, 25.60, 17.26, 15.28, 11.64, 10.39, 9.41.

IR (ATR platinum diamond): $\tilde{\nu}$ / cm^{-1} = 3450, 2933, 2842, 1764, 1723, 1649, 1594, 1505, 1454, 1427, 1330, 1267, 1215, 1116, 1030, 911, 730.

T_g = 140 °C; $T_{d,5\%}$ = 212 °C.

Table 6.6.2 – Characterization data of the synthesized upscale batch of LI-BB-DBU.

Entry	$OH_{aliphatic}$ (mmol·g^{-1})[a]	$OH_{aromatic}$ (mmol·g^{-1})[a]	COOH (mmol·g^{-1})[a]	OH_{total} (mmol·g^{-1})[a]	M_n (g·mol^{-1})[b]	*Đ*
LI (DBU)	0.900 ± 0.004	1.26 ± 0.02	1.39 ± 0.02	3.55 ± 0.02	5200	7.2

[a]: Determined *via* ^{31}P NMR. Measurements performed in triplicate. [b]: SEC-DMAc.

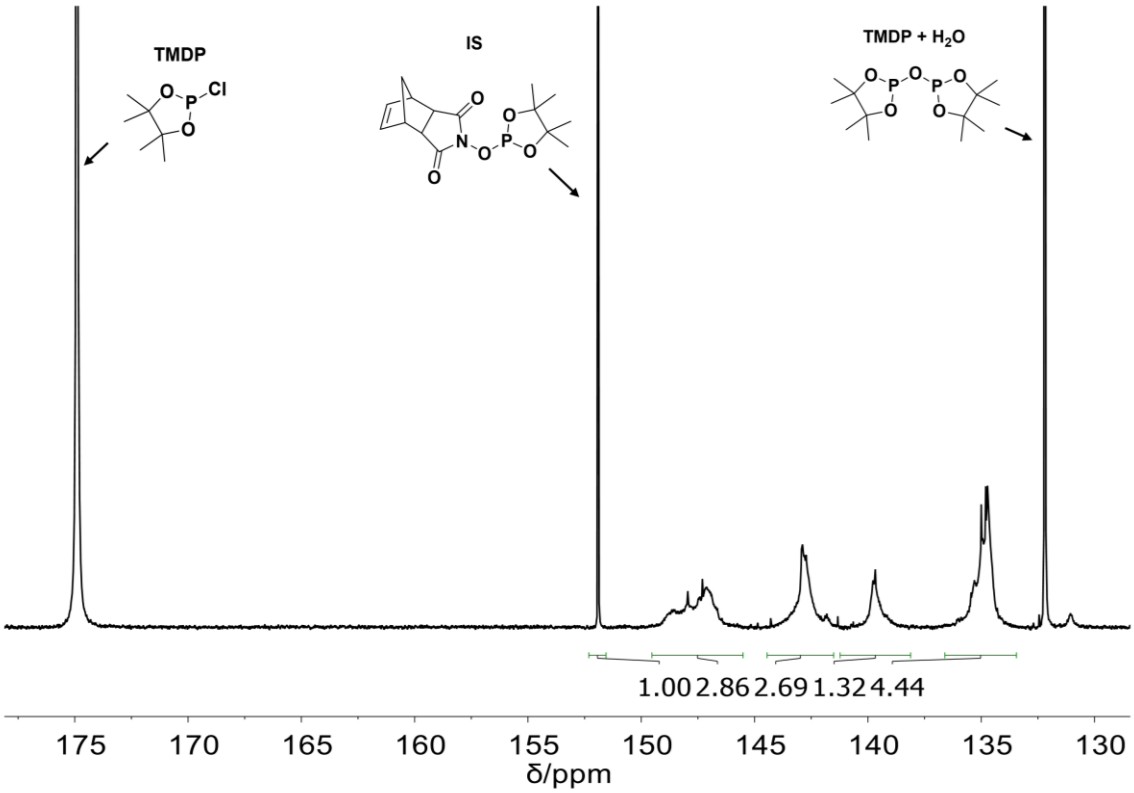

Figure 6.6.1 – ^{31}P NMR of the synthesized upscale batch of LI-BB-DBU.

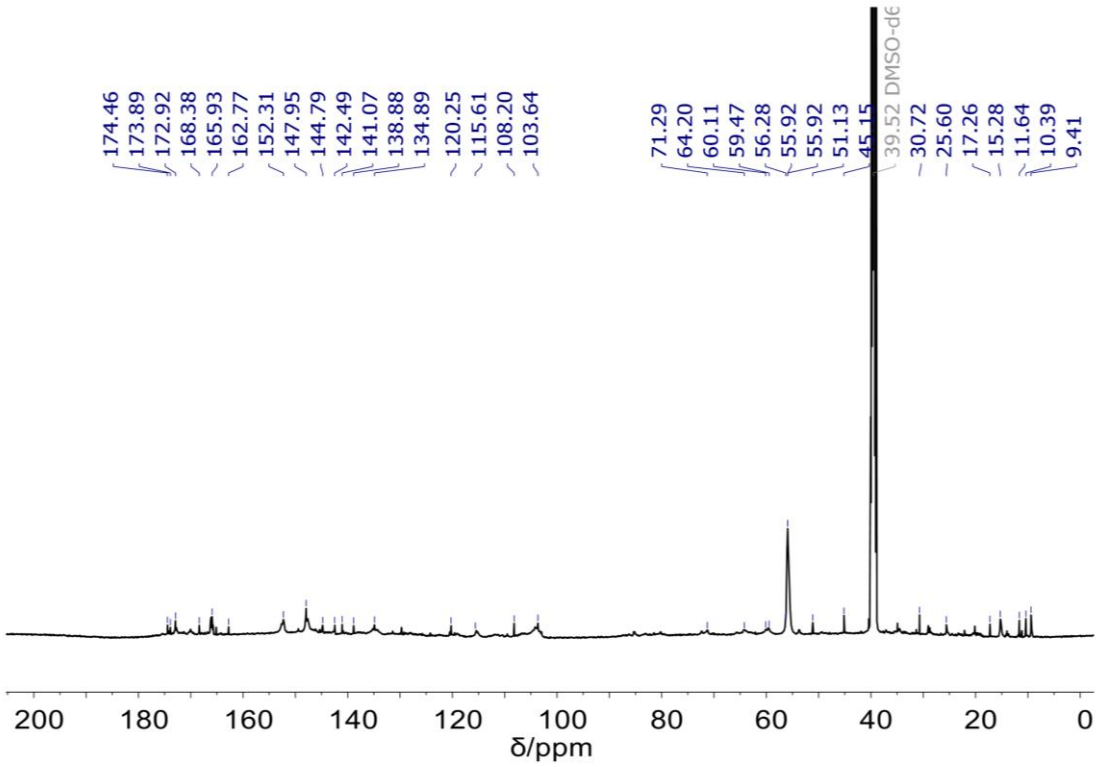

Figure 6.6.2 – ^{13}C NMR of the synthesized upscale batch of LI-BB-DBU.

6.6.1.5 General Procedure for the Functionalization of Lignin with Itaconic Anhydride (15 g Batch – TMG)

Scheme 6.6.3 – General scheme of the reaction between Acetone-fractionated OL and IAn with TMG as catalyst.

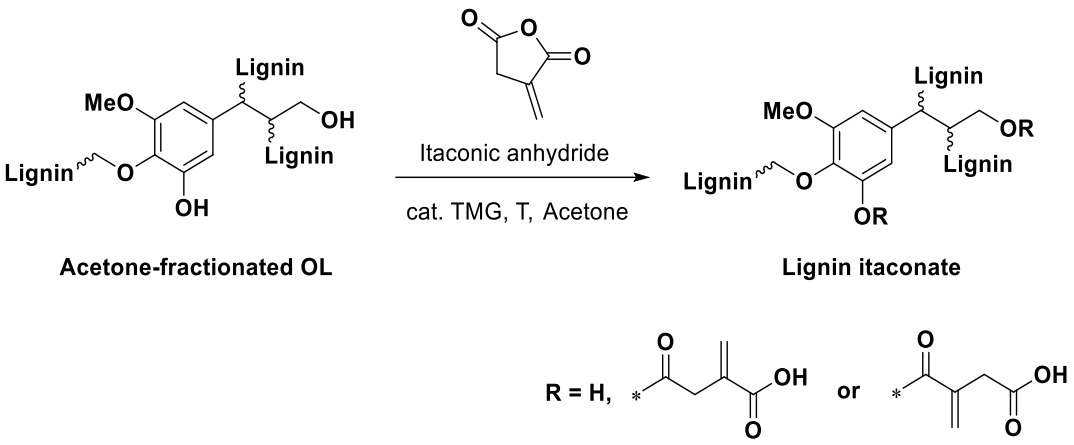

15.0 g of OL Acetone (3) (4.42 mmol OH g^{-1} dry lignin) were dissolved in dry acetone (150 mL) in a 500 mL round bottom flask. Afterwards, itaconic anhydride (30.7 g, 4.20 equiv. related to the total of OH groups) and the catalyst TMG (458 mg, 499 µL, 6 mol% related to the total of OH groups) were added the flask, equipped with an air condenser. The system was flushed with argon for a few minutes. After reaching the desired temperature, the reaction was stirred for 24 h at 45 °C.

At the end of the reaction time, the vessel was allowed to cool down, and the reaction mixture was precipitated in a tenfold amount of acidified deionized water (pH < 2, acidified with HCl 1 M) and stirred for one hour. Afterwards, solids were recovered *via* filtration on a P-4 frit, washed with cleaned deionized water until filtrates were neutral, and dried under vacuum (10 mbar, 70 °C) for 72 hours prior to analysis. The procedure of dissolution in minimal amount of acetone and precipitation in aqueous acidic condition (pH < 2, acidified with HCl 1 M) was repeated three times to eliminate impurities. Yield: 20.7 g, 92% theoretical yield, calculated according to **Eq. S12**.

^{1}H NMR (400 MHz, DMSO-d$_6$) δ_H / ppm = 13.4 – 12.2 (s, -COO**H**); 7.9 – 5.9 ppm (m, C**H**$_{aryl}$); 5.5 – 3.2 (s, OC**H$_3$**, O**H**); 2.4 – 0.5 (m, C**H**$_{alkyl}$).

IR (ATR platinum diamond): $\tilde{\nu}$ / cm^{-1} = 3443, 2933, 2859, 1762, 1729, 1602, 1513, 1462, 1421, 1324, 1273, 1215, 1158, 1114, 1032, 929, 835, 730.

T_g = 149 °C; $T_{d,5\%}$ = 209 °C.

Table 6.6.3 – Characterization of the synthesized upscale batch of LI-BB-TMG.

Entry	$OH_{Aliphatic}$ (mmol·g^{-1})[a]	$OH_{Aromatic}$ (mmol·g^{-1})[a]	COOH (mmol·g^{-1})[a]	OH_{Total} (mmol·g^{-1})[a]	M_n (g·mol^{-1})[b]	$Đ$
LI (TMG)	0.68 ± 0.02	1.20 ± 0.02	1.62 ± 0.02	3.50 ± 0.06	5100	11

[a]: Determined via ^{31}P NMR. Measurements performed in triplicate. [b]: SEC-DMAc.

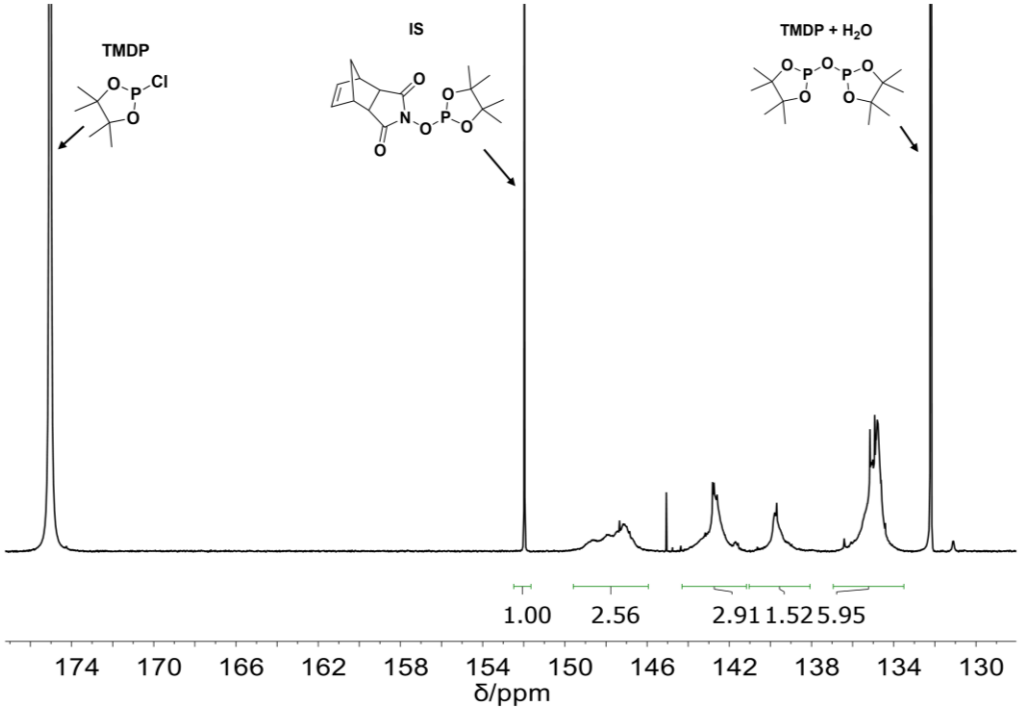

Figure 6.6.3 – ^{31}P NMR of the synthesized upscale batch of LI-BB-TMG.

6.6.1.6 General Procedure for the Functionalization of Lignin with Succinic Anhydride (0.5 g Batch Scale)

The experimental synthesis described in this section was conducted by Sophia Abou El Mirate within the framework of her training ("Ausbildung") in chemistry, under the co-supervision of the author.

Scheme 6.6.4 – General scheme of the reaction between Acetone-frationated OL and SAn with TMG as catalyst.

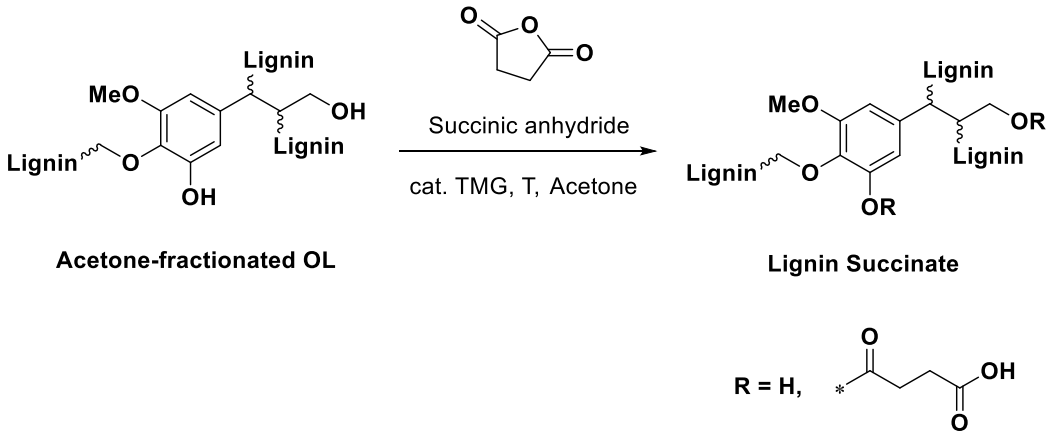

Acetone-fractionated OL **Lignin Succinate**

0.50 g of OL Acetone (2) (4.34 mmol OH g^{-1} dry lignin) were dissolved in 5 mL of dry acetone. Afterwards, the desired amount of succinic anhydride (912 mg, 4.20 equiv.) was added to the reaction mixture, as well as the catalyst TMG (15 mg, 16 µL, 6 mol%). The reaction vessel was flushed with argon and heated to the desired temperature (45 °C, 24 h).

At the end of the reaction time, the vessel was allowed to cool down, and the reaction mixture was precipitated in a tenfold amount of acidified deionized water (pH < 2, acidified with HCl 1 M). Afterwards, solids were recovered *via* filtration on a P-4 fritted filter, washed with cleaned deionized water, and dried under vacuum (10 mbar, 70 °C) for at least 24 hours prior to analysis. If needed, the process of redissolution in acetone and reprecipitation in aqueous acidic condition (pH < 2, acidified with HCl 1 M) was repeated to remove impurities.

6.6.1.7 General Procedure for the Functionalization of Lignin with Succinic Anhydride (15 g Batch – TMG)

The experimental synthesis described in this section was conducted by Sophia Abou El Mirate within the framework of her training ("Ausbildung") in chemistry, under the co-supervision of the author.

15.0 g of OL Acetone (3) (4.42 mmol OH g^{-1} dry lignin) were dissolved in dry acetone (150 mL) in a 500 mL round bottom flask. Afterwards, succinic anhydride (27.9 g, 4.20 equiv. related to the total of OH groups) and the catalyst TMG (458 mg, 499 µL, 6 mol% related to the total of OH groups) were added the flask, equipped with an air condenser. The system was flushed with argon for a few minutes. After reaching the desired temperature, the reaction was stirred for 24 h at 45 °C. At the end of the reaction time, the vessel was allowed to cool down, and the reaction mixture was precipitated in a tenfold amount of acidified deionized water (pH < 2, acidified with HCl 1 M) and stirred for one hour. Afterwards, solids were recovered *via* filtration on a P-4 fritted filter, washed with cleaned deionized water until filtrates were neutral, and dried under vacuum (10 mbar, 70 °C) for 72 hours prior to analysis. The procedure of dissolution in minimal amount of acetone and precipitation in aqueous acidic condition (pH < 2, acidified with HCl 1 M) was repeated twice to eliminate impurities. Yield: 15.3 g, 71% theoretical yield, calculated according to **Eq. S12**.

^{1}H NMR (400 MHz, DMSO-d_6) δ_H / ppm = 12.5 – 11.8 (s, -COO**H**); 7.6 – 5.8 ppm (m, C$\mathbf{H}_{aryl}$); 5.6 – 3.1 (s, OC$\mathbf{H_3}$, O**H**); 1.5 – 0.5 (m, C$\mathbf{H}_{alkyl}$).

IR (ATR platinum diamond): $\tilde{\nu}$ / cm^{-1} = 3293, 2933, 2828, 1731, 1711, 1594, 1505, 1458, 1417, 1328, 1205, 1125, 1030, 824.

T_g = 104 °C; $T_{d,5\%}$ = 229 °C.

Table 6.6.4 – Characterization data of the synthesized upscale batch of LS-BB-TMG.

Entry	$OH_{Aliphatic}$ (mmol·g^{-1})[a]	$OH_{Aromatic}$ (mmol·g^{-1})[a]	COOH (mmol·g^{-1})[a]	OH_{Total} (mmol·g^{-1})[a]	M_n (g·mol^{-1})[b]	*Đ*
LS (TMG)	0.46 ± 0.01	1.47 ± 0.04	1.79 ± 0.02	3.72 ± 0.05	3700	2.7

[a]: Determined via ^{31}P NMR. Measurements performed in triplicate. [b]: SEC-DMAc.

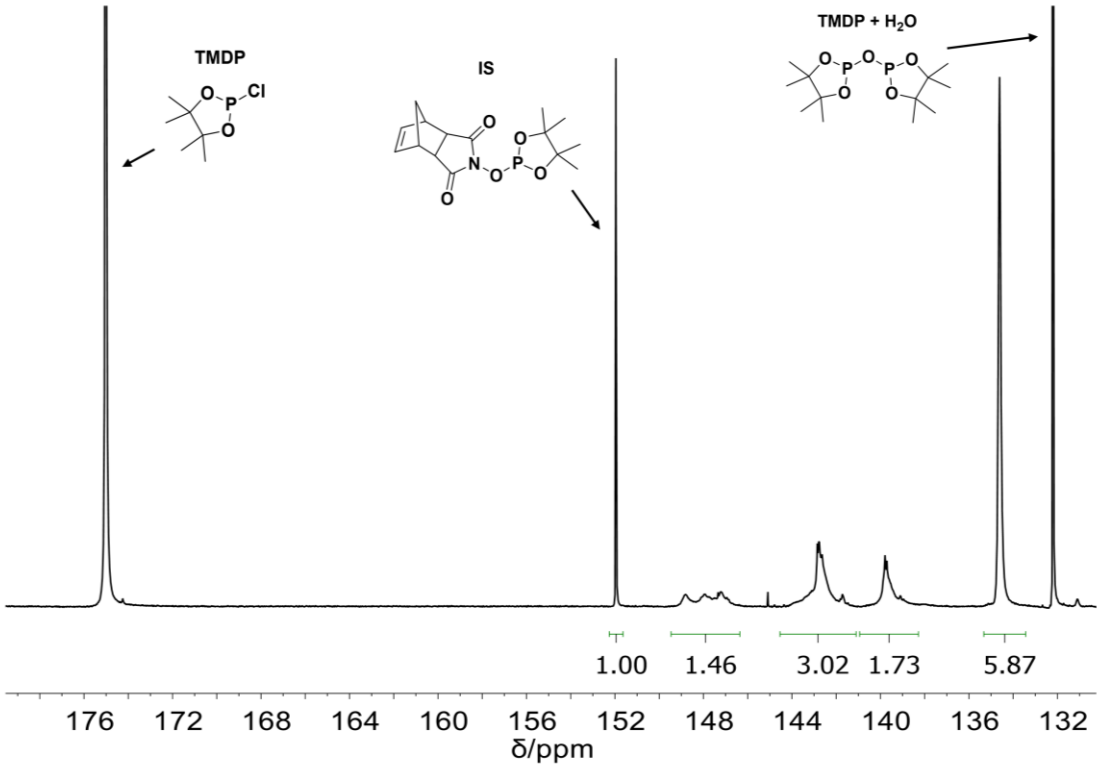

Figure 6.6.4 – ^{31}P NMR of the synthesized upscale batch of LS-BB-TMG.

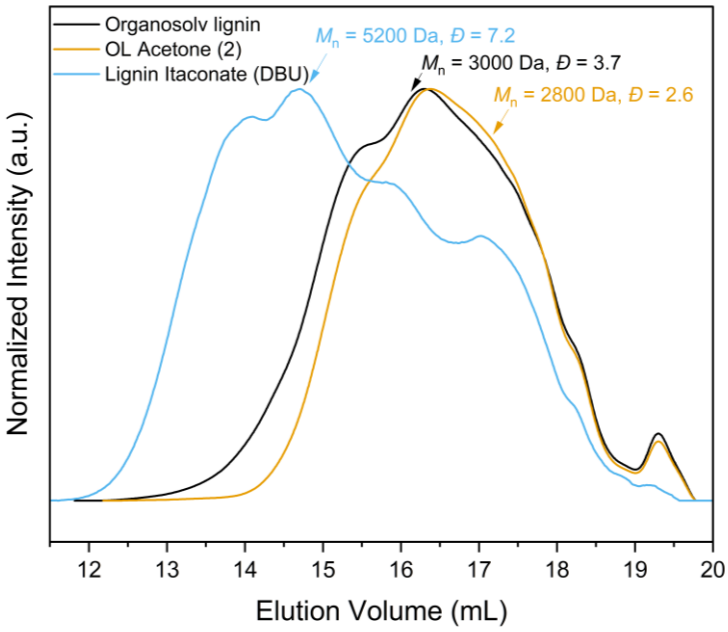

Figure 6.6.5 – SEC traces of pristine organosolv lignin (black), fractionated in acetone (OL Acetone 2, orange), and modified lignin itaconate (15 g scale, DBU as catalyst, blue trace) in DMAc−LiBr.

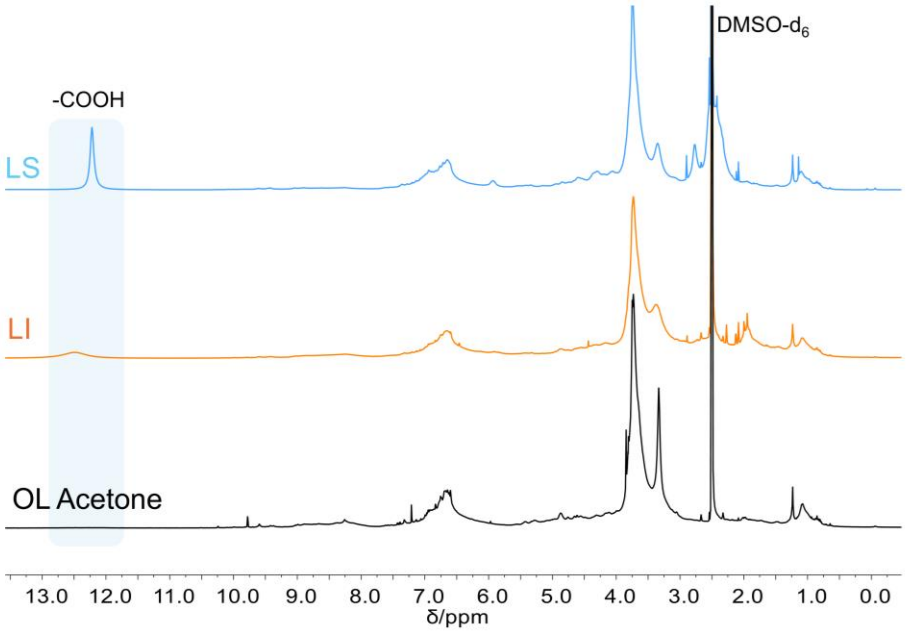

Figure 6.6.6 – Exemplary ^{1}H NMR spectra in DMSO-d_6 of lignin fractionated in acetone (OL acetone, black), lignin itaconate (orange) and lignin succinate (blue). highlighted in blue the region where the signal ascribed to the carboxylic acid is visible.

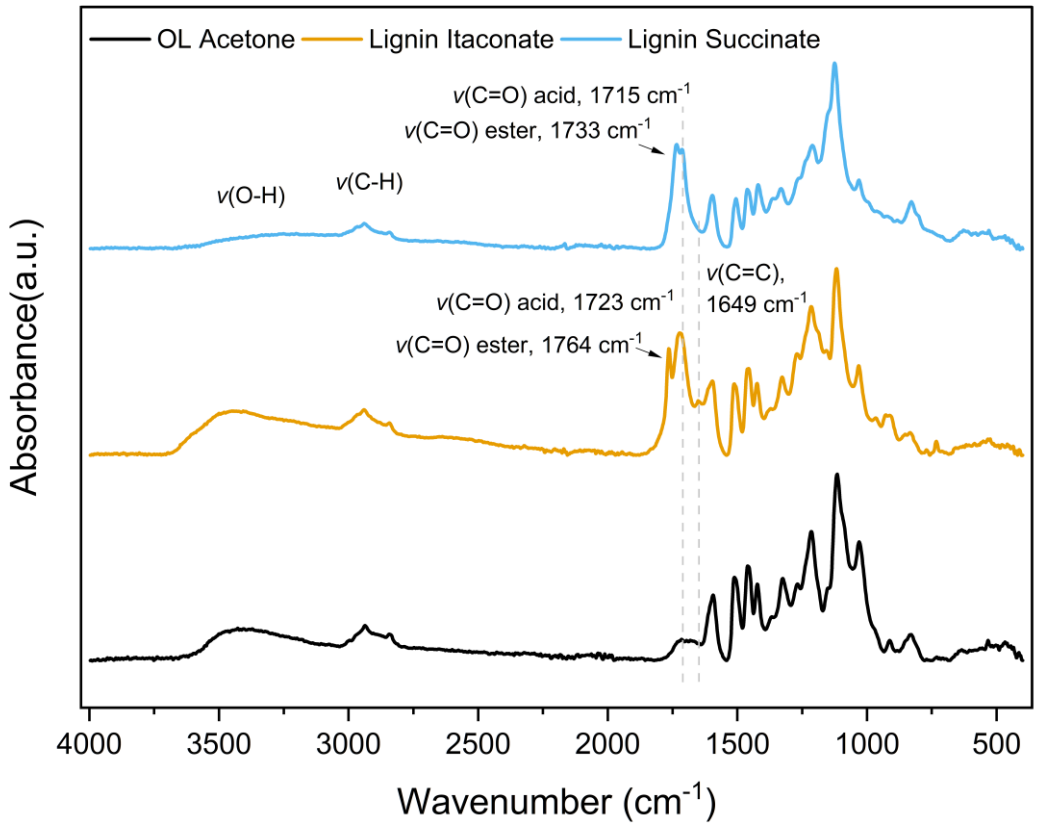

Figure 6.6.7 – Overlay of IR spectra for both the starting material (OL acetone, black) and the lignin derivative modified with itaconic anhydride, lignin itaconate (orange), as well as the derivative modified with succinic anhydride, lignin succinate (blue). Typical signals associated with the functionalization are shown.

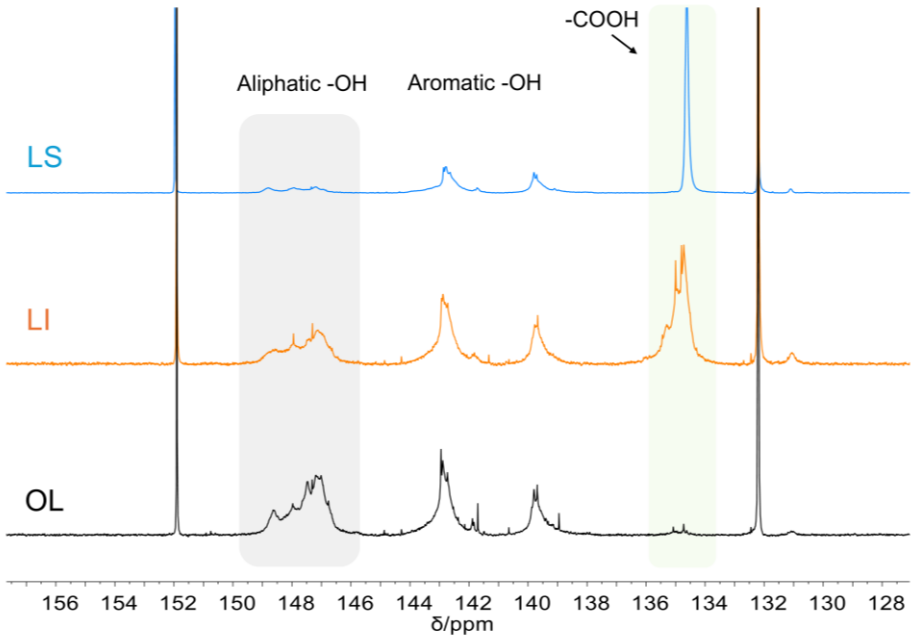

Figure 6.6.8 – Exemplary ^{31}P NMR spectra of lignin fractionated in acetone (OL acetone, black), lignin itaconate (orange) and lignin succinate (blue).Highlighted in green the aliphatic -OH region and in yellow the -COOH region.

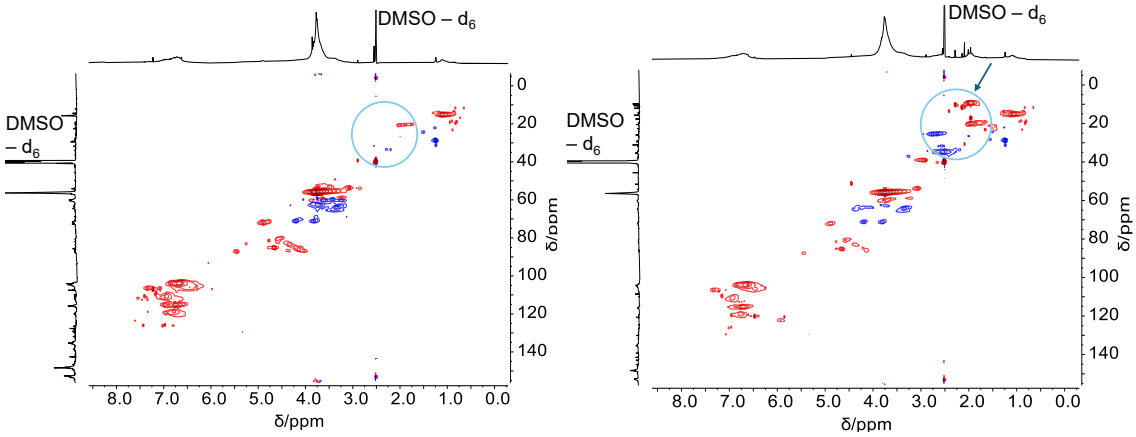

Figure 6.6.9 – Complete HSQC traces for OL acetone (left) and lignin itaconate (right) in DMSO-d_6. In the circled area, new signals appear after the modification. In particular, a new methyl signal (indicated with the arrow) could be associated with the methyl group of the citraconate moieties.

6.6.2 E-factor Calculations and Recovered Solvent Characterization

The solvent recovery described in this section was conducted by Gianluca Giuseppe Rizzo within the framework of his thesis ("Vertiefungspraktikum") in chemistry, under the co-supervision of the author.

After lignin functionalization in a 15 g scale with itaconic anhydride, the same workup procedure as described above was applied. After precipitation and filtration of the desired product, the acetone was then recovered from the remaining mixture *via* vacuum distillation. However, efficient separation proved challenging, due to the low acetone concentration in the mixture (~0.1 mL acetone per mL precipitation medium) and the elevated volume of the mixture to distill. Nevertheless, a total of 75 % of the initial acetone was recovered and dried over 3 Å molecular sieves for 72 hours. Spectroscopic analysis reveals that the recovered solvent is clean, however water impurities remain present (19 %, as calculated from ^{1}H NMR).

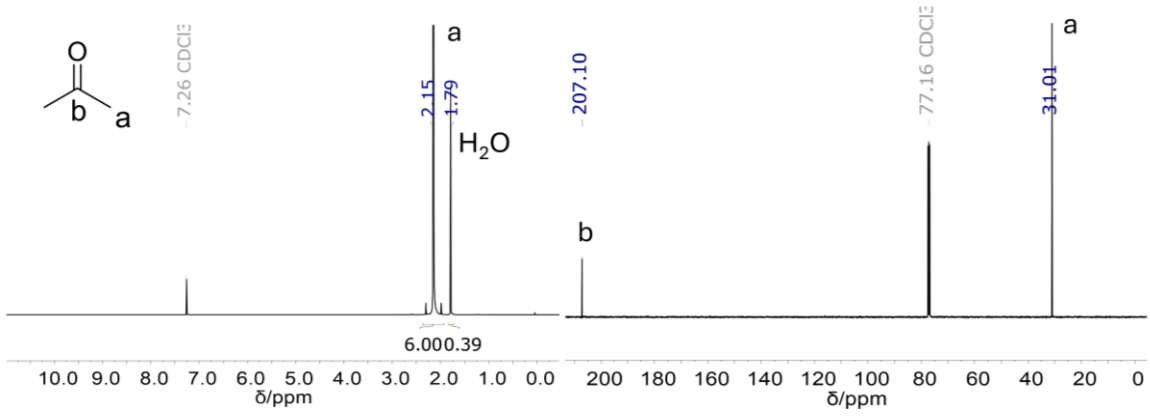

Figure 6.6.10 – ^{1}H NMR (left) and ^{13}C NMR (right) of the recovered solvent in $CDCl_3$.

6.6.2.1 Information Concerning E-factor Calculations

The E-factor values reported in this chapter are intended as a simplified metric to illustrate the solvent contribution and its impact on the synthetic procedures. These calculations do not account for the lignin pretreatment (fractionation) or for the aqueous medium used during the work-up. This choice was made to remain consistent with Sheldon's original work on the E-factor, in which water is excluded to avoid misleading or non-comparable results,[24] and to ensure comparability with a previous work,[93] where synthetic E-factors for lignin modifications were also calculated without including the water used in precipitation or purification steps.[93] Despite this simplification, the presented E-factor values should be regarded as a useful comparative parameter for assessing solvent influence and comparing with literature data. For the E-factor calculations the following general formula was used:

$$E - factor = \frac{Mass\ of\ raw\ material - Mass\ of\ desired\ product}{Mass\ of\ derided\ product} \qquad \text{Eq. S22}$$

For the E-factor calculations and definition of the solvent contribution, two cases are defined:

No recycling of solvent

Weight of raw materials: Organosolv Lignin (acetone fractionated): 15.00 g; DBU: 0.630 g; IAn: 30.65 g; Acetone: 116.9 g; Total: 163.2 g

Weight of desired product: 20.70 g

$$E - factor = \frac{163.2 - 20.70}{20.70} = 6.9$$

With recycling of solvent

Weight of raw materials: Organosolv lignin (acetone fractionated): 15.00 g; DBU: 0.630 g; IAn: 30.65 g; Acetone: 116.9 g; Total: 163.2 g

Weight of desired product: 20.70 g

Weight of recovered solvent: 87.23 g

$$E - factor = \frac{163.2 - 20.70 - 87.23}{20.70} = 2.7$$

6.6.3 General Passerini Thermosets Formulation

200 mg of LI (1.39 mmol·g^{-1} COOH, 0.28 mmol COOH, 0.35 equiv., previously dried at 70 °C under 10 mbar vacuum for 24 h) was weighted. Pripol™ 1009 (147 mg, 0.52 mmol COOH, 0.65 equiv.) or another (poly)carboxylic acid, was weighted in a vial and dissolved with 1 mL of acetone. Nonanal (113 mg, 0.80 mmol, 1.00 equiv.) and the desired bis-isocyanide (0.40 mmol, 0.50 equiv.) were weighed together in a vial. Afterwads, LI and the Pripol™ solution were transferred to the vial with the aldehyde and the bis-isocyanide component, and 1 mL of acetone was again added. The solution was vortexed at r.t. for 20 minutes (or until everything dissolved) and was subsequently transferred to a Teflon mold. The thermosets were left to evaporate under a fumehood covered with a Petri dish overnight. The next day, the curing was conducted in an oven pre-heated at 75 °C for 4 h, followed by a post-curing at 100 °C for 8 h.

Table 6.6.5 – Overview of the stoichiometric ratio for two exemplary Passerini thermosets with 35 mol% LI and 100 mol% LI and Pripol™ as additional carboxylic acid component.

Entry	Carboxylic acid component (Equiv.)			Isocyanide component	Aldehyde component	Lignin content (mol%)[a]
	Pripol™	LI	Total equiv.	1,6 or 1,12-bis (Equiv.)	Nonanal (Equiv.)	
1	0.65	0.35	1	0.5	1	35
2	0	1	1	0.5	1	100

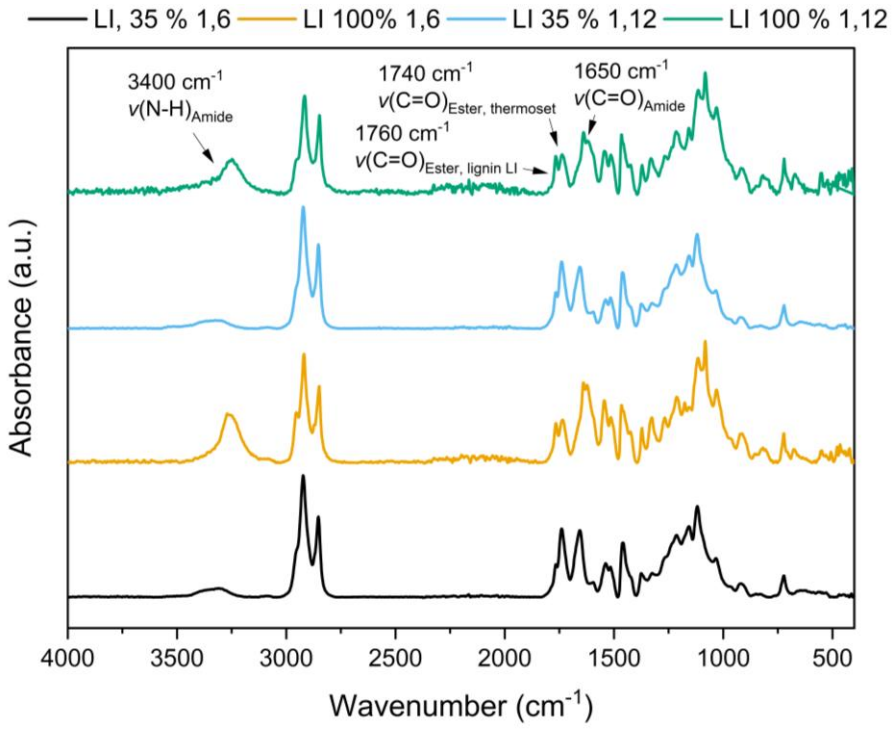

Figure 6.6.11 – IR spectra of the different Passerini thermosets with 35 and 100 mol% LI.

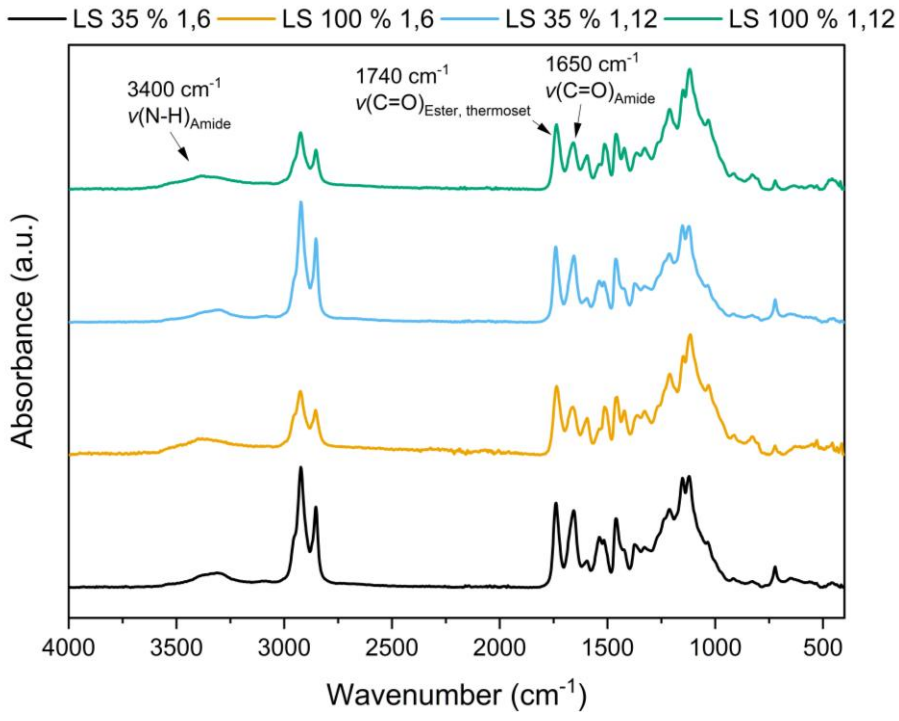

Figure 6.6.12 – IR spectra of the different Passerini thermosets with 35 and 100 mol% LS.

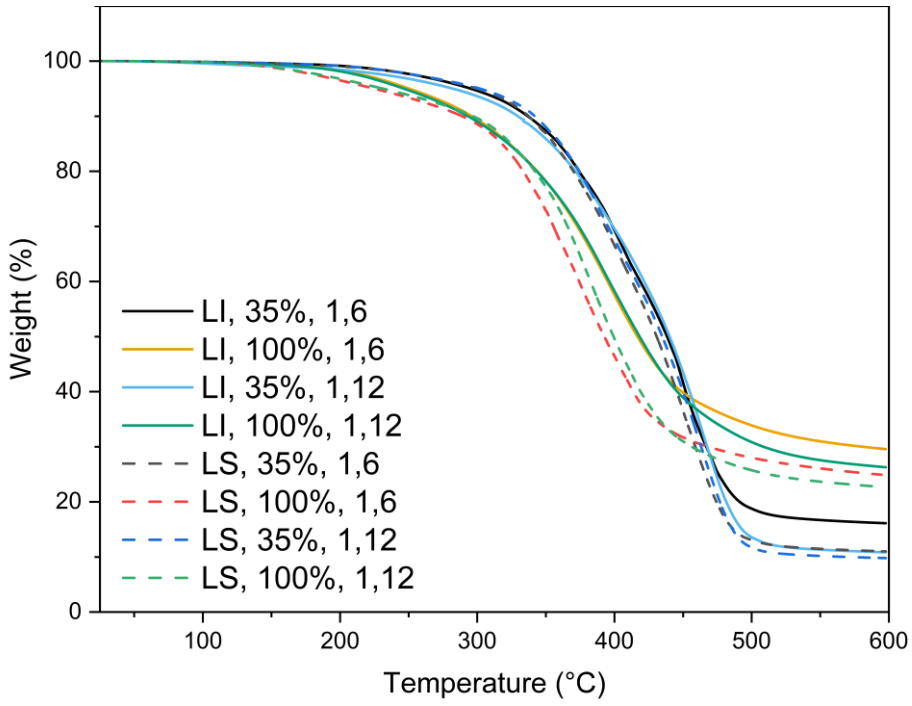

Figure 6.6.13 – TGA curves of the Passerini thermosets with both LI and LS with 35 and 100 mol%, with 1,6- or 1,12-bis(isocyanides).

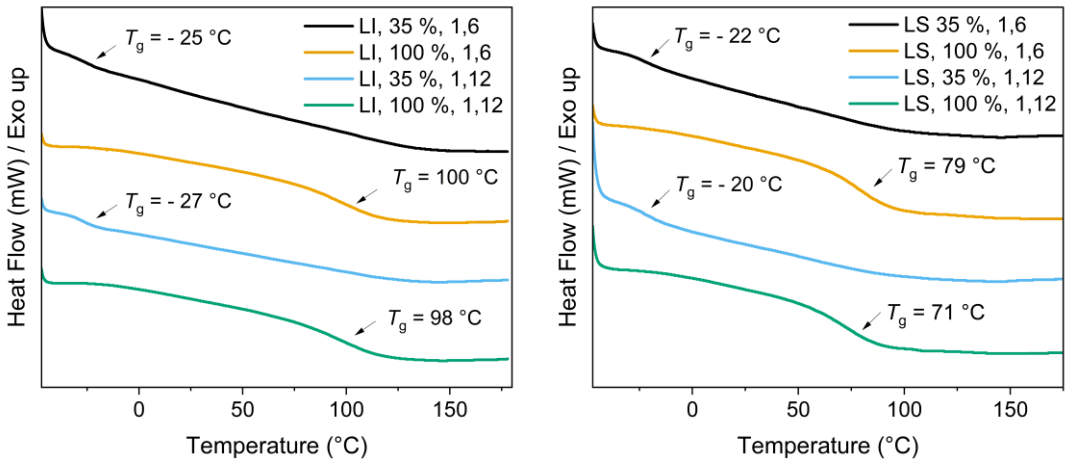

Figure 6.6.14 – DSC curves of the Passerini thermosets with both LI and LS with 35 and 100 mol%, with 1,6- or 1,12-bis(isocyanides).

6.6.3.1 Synthesis of Starting Materials

6.6.3.1.1 Formamides and Isocyanides

All isocyanides were synthesized according to the procedure published by Meier *et al*.[408]

n-*Dodecylformamide*

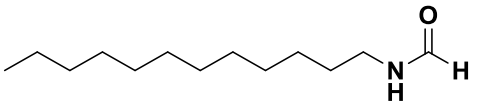

Chemical Formula: $C_{13}H_{27}NO$
Molecular Weight: 213,37

Dodecylamine (4.63 g, 25.0 mmol, 1.00 equiv.) and ethyl formate (20.2 mL, 18.5 g, 0.250 mol, 10.0 equiv.) were stirred under reflux for 16 h. Afterwards, the remaining ethyl formate and ethanol were removed under reduced pressure and the crude product (5.10 g, 23.9 mmol, 89%) was used without further purification.

^{1}H NMR (400 MHz, DMSO-d$_6$) δ_H / ppm = 8.00 – 7.92 (m, 2H), 3.05 (q, J = 6.6 Hz, 2H), 1.38 (p, J = 6.8 Hz, 2H), 1.26 – 1.22 (m, 19H), 0.84 (t, 3H).

^{13}C NMR (126 MHz, DMSO-d$_6$) δ_C / ppm = 164.42, 160.82, 37.02, 31.30, 29.04, 28.99, 28.71, 26.34, 22.10, 13.96.

IR (ATR platinum diamond): $\tilde{\nu}$ / cm^{-1} = 3289, 3031, 2954, 2929, 2886, 2865, 2849, 1643, 1534, 1465, 1378, 1216, 778, 722, 666.

HRMS (ESI-MS, (M+H)$^+$, $C_{13}H_{28}NO$) calcd.: 214.2165; found:.214.2162.

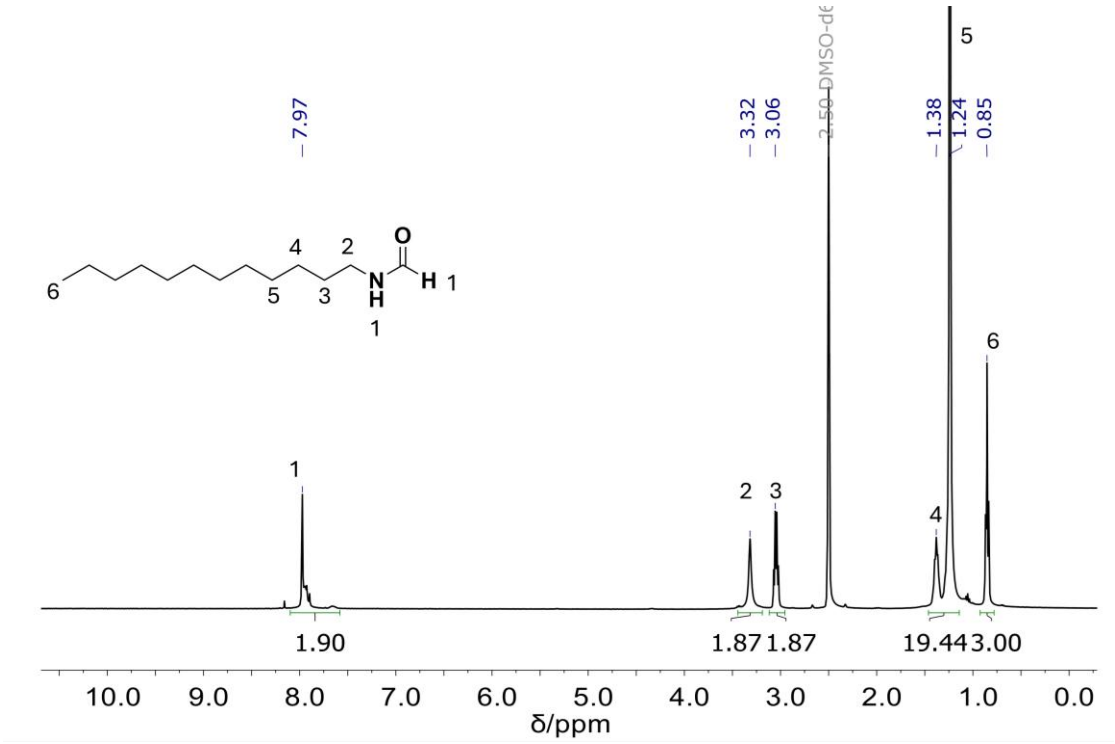

Figure 6.6.15 – ^{1}H NMR spectrum of the synthesized *n*-dodecylformamide.

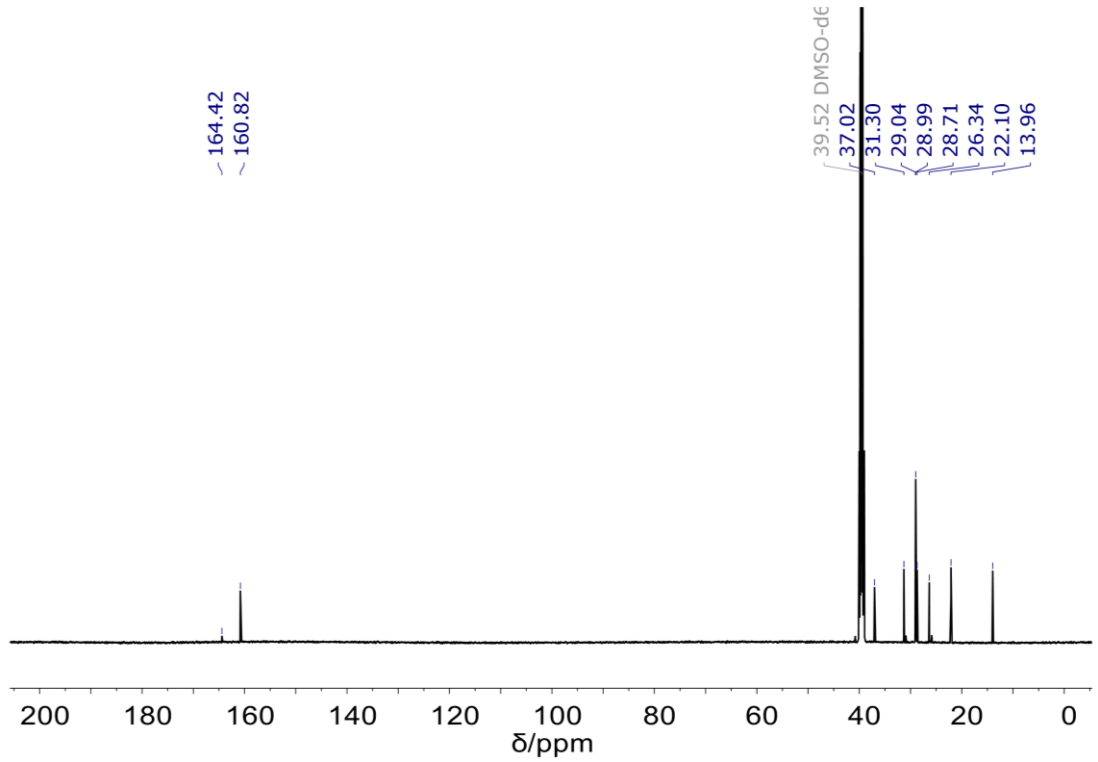

Figure 6.6.16 – ^{13}C NMR spectrum of the synthesized *n*-dodecylformamide.

n-*Dodecylisocyanide*

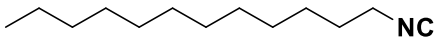

Chemical Formula: $C_{13}H_{25}N$
Molecular Weight: 195,35

n-Dodecylformamide (2.00 g, 9.38 mmol, 1.00 equiv.) is dissolved in 18.8 mL of DCM (c(formamide) = 0.5 mol/L) and pyridine (2.23 g, 2.27 mL, 28.2 mmol, 3.00 equiv.) was added. Subsequently, *p*-toluenesulfonyl chloride (2.70 g, 14.1 mmol, 1.50 equiv.) was added under cooling the reaction mixture with a water bath. The mixture was stirred at room temperature until full conversion of the formamide was reached (monitoring *via* TLC). The mixture was cooled down to 0°C and a saturated sodium carbonate solution was added (in a volume equal to DCM) and it was stirred for 30 minutes. Afterwards, water and DCM were added (in a double amount of the original volume of DCM each) and the phases were separated. The aqueous phase was extracted 3x with fresh DCM and the combined extracts were washed 3x with water and 1x with brine. The washed organic phase was dried over sodium sulfate and the solvent was removed under reduced pressure. The crude product was purified *via* flash column chromatography (cyclohexane:ethyl acetate = 2:1) to obtain the desired compound (1.55 g, 7.88 mmol, 84%).

R_f = 0.94 (cyclohexane/ethyl acetate, 7:3).

^{1}H NMR (500 MHz, $CDCl_3$) δ_H / ppm = 3.37 (tt, *J* = 6.7, 2.0 Hz, 2H), 1.72 – 1.62 (m, 2H), 1.42 (q, *J* = 11.9, 7.1 Hz, 2H), 1.28 – 1.24 (m, 17H), 0.88 (t, *J* = 6.9 Hz, 3H).

^{13}C NMR (126 MHz, $CDCl_3$) δ_C / ppm = 155.7 (t), 41.7 (t), 32.03, 29.72, 29.63, 29.49, 29.46, 29.24, 28.83, 26.44, 22.81, 14.09.

IR (ATR platinum diamond): $\tilde{\nu}$ / cm^{-1} = 2923, 2853, 2145, 1465, 722.

HRMS (ESI-MS, $(M+H)^+$, $C_{13}H_{26}N_2$) calcd.: 196.2060; found: 196.2058.

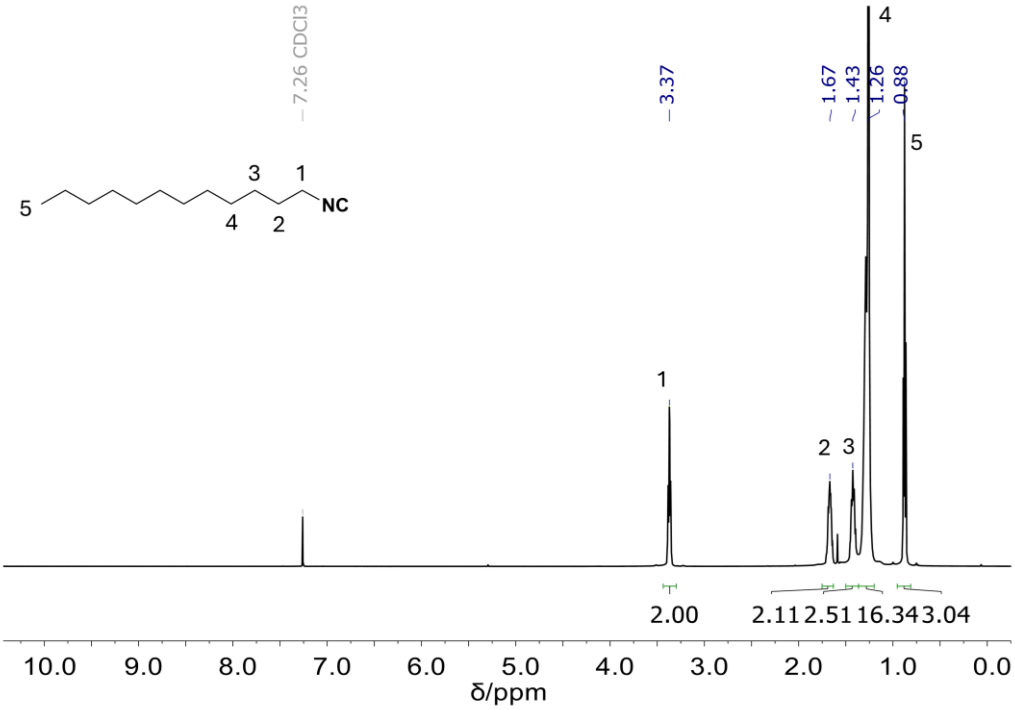

Figure 6.6.17 – ^{1}H NMR spectrum of the synthesized *n*-dodecylisocyanide.

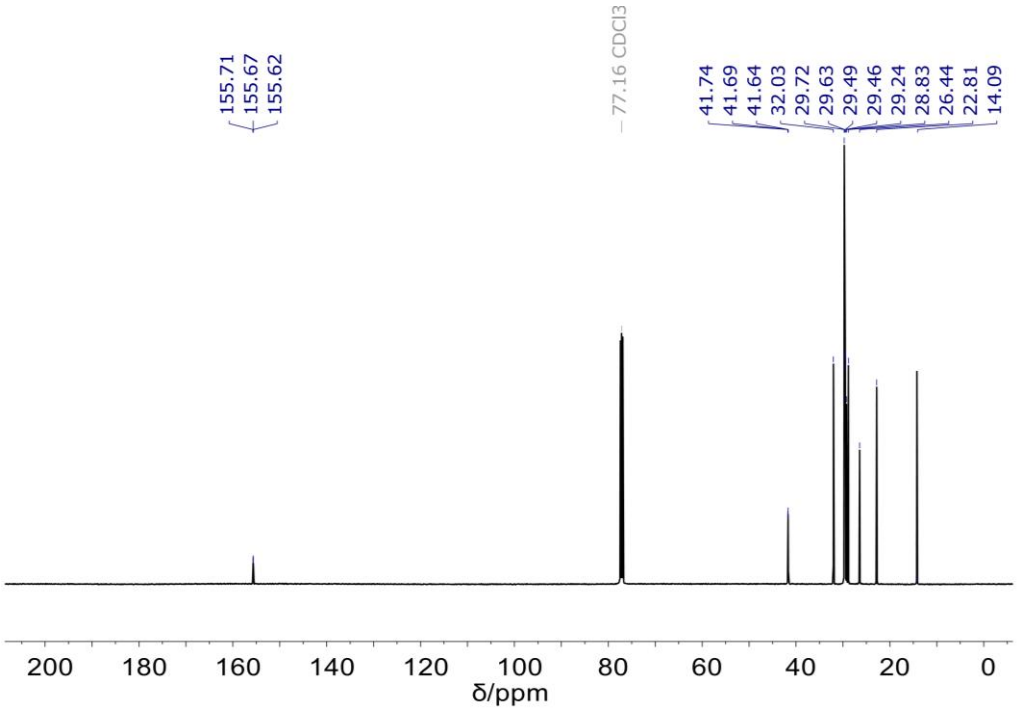

Figure 6.6.18 – ^{13}C NMR spectrum of the synthesized *n*-dodecylisocyanide.

1,12–bis(formamido)dodecane

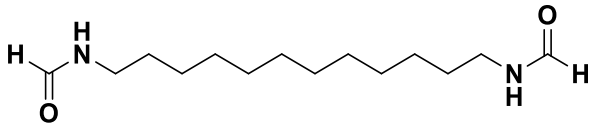

Chemical Formula: $C_{14}H_{28}N_2O_2$
Molecular Weight: 256,39

1,12-Bis(diamino)dodecane (5.00 g, 25.0 mmol, 1.00 equiv.) and ethyl formate (20.2 mL, 18.5 g, 0.250 mol, 10.0 equiv.) were stirred under reflux for 16 h. Afterwards, the remaining ethyl formate and ethanol were removed under reduced pressure and the crude product (6.09 g, 23.8 mmol, 95%) was used without further purification.

^{1}H NMR (500 MHz, DMSO-d$_6$) δ_H / ppm = 7.99 – 7.86 (m, 3H), 3.05 (q, J = 6.6 Hz, 4H), 1.37 (p, J = 6.8 Hz, 4H), 1.24 (s, 16H).

^{13}C NMR (126 MHz, DMSO-d$_6$) δ_C / ppm = 164.43, 160.84, 40.81, 37.03, 30.89, 28.68, 26.34, 25.86.

IR (ATR platinum diamond): $\tilde{\nu}$ / cm^{-1} = 3283, 3031, 2939, 2923, 2886, 2849, 1629, 1528, 1471, 1462, 1378, 1306, 1257, 1222, 1195, 780, 738, 699.

HRMS (ESI-MS, $(M+H)^+$, $C_{14}H_{29}N_2O_2$) calcd.: 257.2224 ; found: 257.2219.

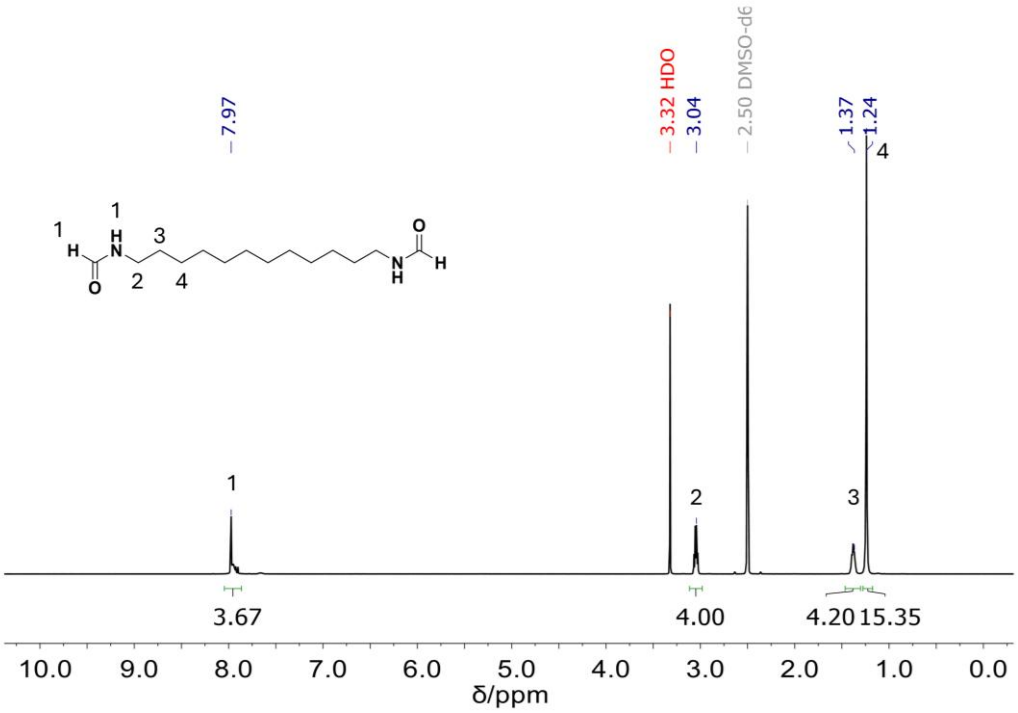

Figure 6.6.19 – ^{1}H NMR spectrum of the synthesized 1,12–bis(formamido)dodecane.

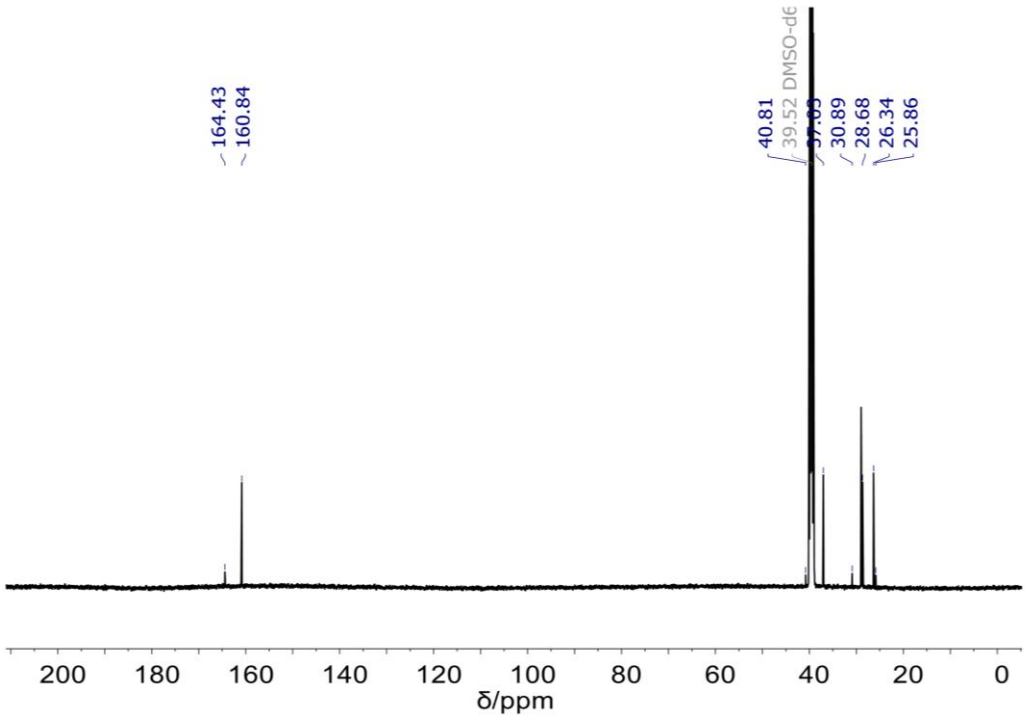

Figure 6.6.20 – ^{13}C NMR spectrum of the synthesized 1,12–bis(formamido)dodecane.

1,12–bis(isocyano)dodecane

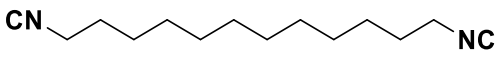

Chemical Formula: $C_{14}H_{24}N_2$
Molecular Weight: 220,36

1,12-Bis(formamido)dodecane (5.00 g, 19.5 mmol, 1.00 equiv.) is dissolved in 39 mL of DCM (c(formamide) = 0.5 mol/L) and pyridine (9.25 g, 9.44 mL, 117 mmol, 6.00 equiv.) was added. Subsequently, *p*-toluenesulfonyl chloride (11.2 g, 58.5 mmol, 3.00 equiv.) was added under cooling the reaction mixture with a water bath. The mixture was stirred at room temperature until full conversion of the formamide was reached (monitoring *via* TLC). The mixture was cooled down to 0°C and a saturated sodium carbonate solution was added (in a volume equal to DCM) and it was stirred for 30 minutes. Afterwards, water and DCM were added (in a double amount of the original volume of DCM each) and the phases were separated. The aqueous phase was extracted 3x with fresh DCM and the combined extracts were washed 3x with water and 1x with brine. The washed organic phase was dried over sodium sulfate and the solvent was removed under reduced pressure. The crude product was purified *via* flash column chromatography (cyclohexane:ethyl acetate = 2:1) to obtain the desired compound (3.18 g, 14.4 mmol, 74%).

R_f = 0.53 (*n*-hexane/ethyl acetate, 5:1).

^{1}H NMR (400 MHz, $CDCl_3$) δ_H / ppm = 3.37 (tt, J = 6.7, 2.0 Hz, 4H), 1.72 – 1.60 (m, 4H), 1.42 (p, J = 6.9 Hz, 4H), 1.34 – 1.26 (m, 13H).

^{13}C NMR (101 MHz, $CDCl_3$) δ_C / ppm = 155.7 (t), 41.65 (t), 29.48, 29.39, 29.17, 28.75, 26.38.

IR (ATR platinum diamond): $\tilde{\nu}$ / cm^{-1} = 2925, 2855, 2145, 1454, 1351, 722.

HRMS (ESI-MS, $(M+H)^+$, $C_{14}H_{25}N_2$) calcd.: 221.2012 ; found: 221.2010.

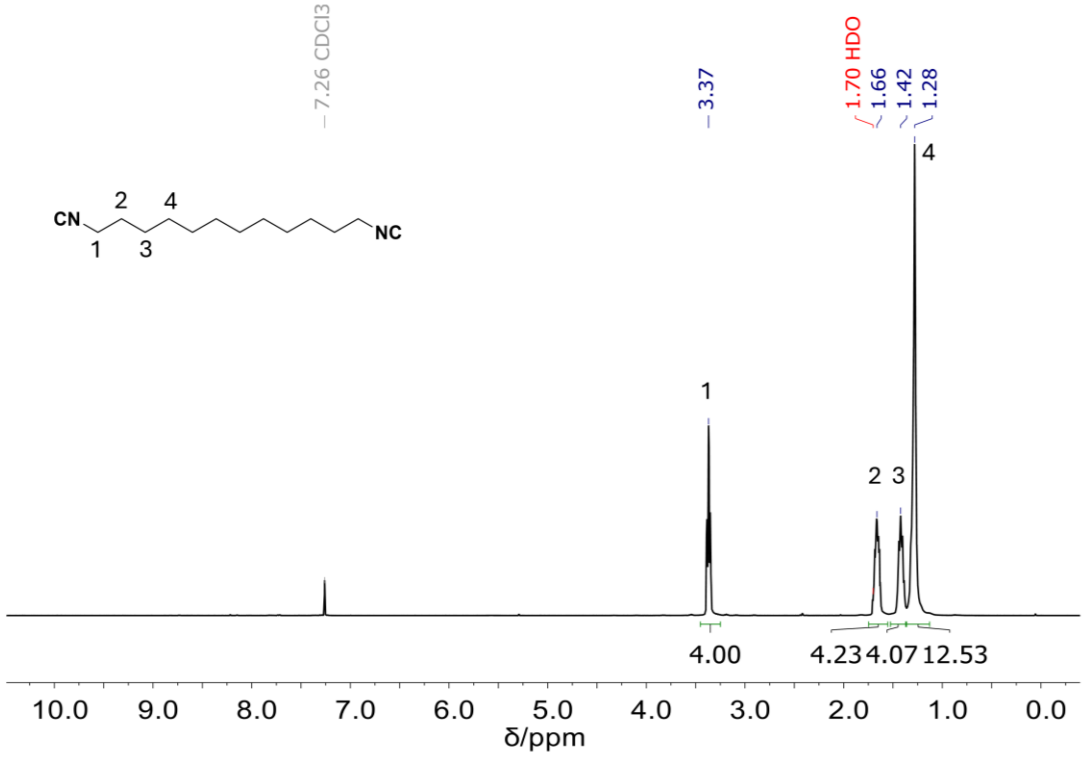

Figure 6.6.21 – ^{1}H NMR spectrum of the synthesized 1,12–bis(isocyano)dodecane.

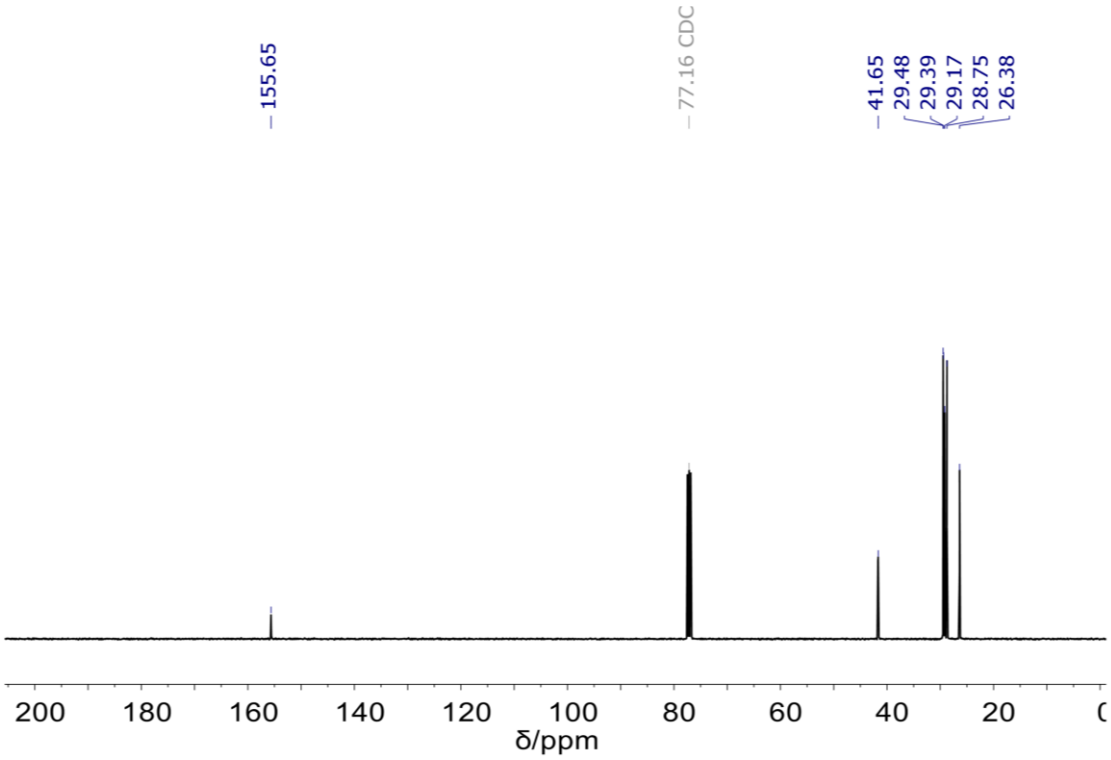

Figure 6.6.22 – ^{13}C NMR spectrum of the synthesized 1,12–bis(isocyano)dodecane.

1,6–bis(formamido)hexane

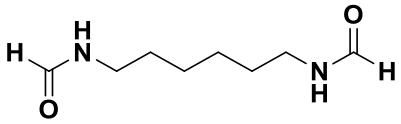

Chemical Formula: $C_8H_{16}N_2O_2$
Molecular Weight: 172,23

1,6-Bis(diamino)hexane (5.00 g, 43.0 mmol, 1.00 equiv.) and ethyl formate (34.7 mL, 31.9 g, 0.430 mol, 10.0 equiv.) were stirred under reflux for 16 h. Afterwards, the remaining ethyl formate and ethanol were removed under reduced pressure and the crude product (7.26 g, 42.1 mmol, 98%) was used without further purification.

^{1}H NMR (400 MHz, DMSO-d$_6$) δ_H / ppm = 8.14 – 7.61 (m, 2H), 3.05 (q, J = 6.6 Hz, 2H), 1.38 (p, J = 6.8 Hz, 2H), 1.26 (s, 2H).

^{13}C NMR (101 MHz, DMSO-d$_6$) δ_C / ppm = 164.47, 160.89, 40.77, 37.00, 30.85, 28.96, 26.01, 25.53.

IR (ATR platinum diamond): $\tilde{\nu}$ / cm^{-1} = 3275, 3030, 2943, 2913, 2888, 2865, 2853, 1627, 1528, 1475, 1460, 1442, 1386, 1306, 1236, 1212, 1082, 778, 740, 706, 461.

HRMS (ESI-MS, (M+H)$^+$, $C_8H_{17}N_2O_2$) calcd.: 173.1285; found: 173.1281.

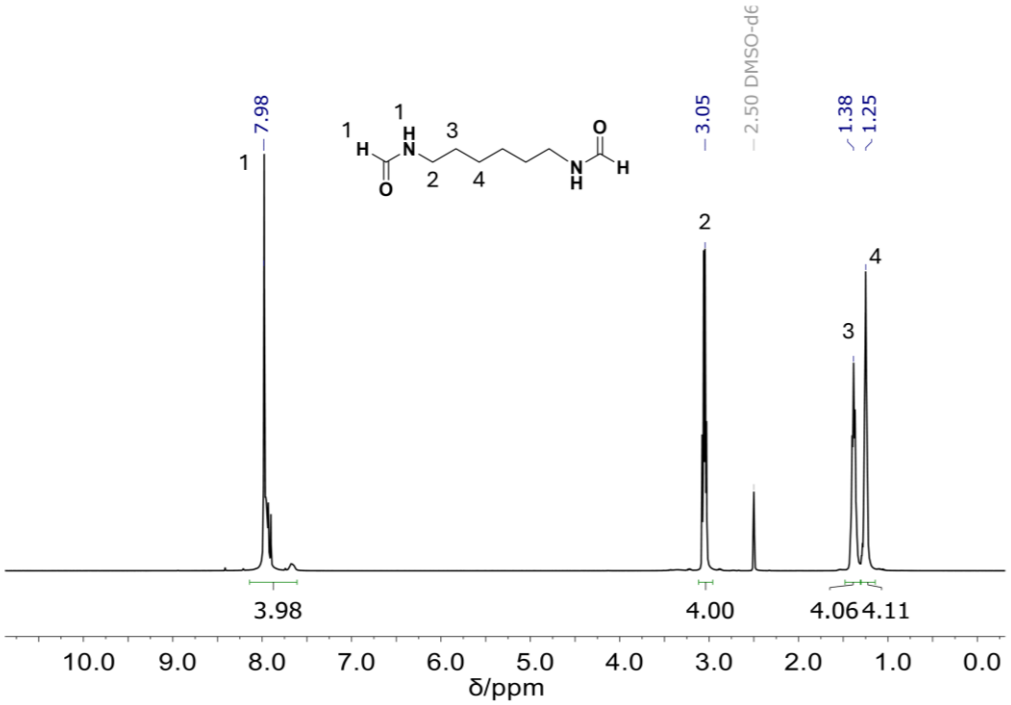

Figure 6.6.23 – ^{1}H NMR spectrum of the synthesized 1,6–bis(formamido)hexane.

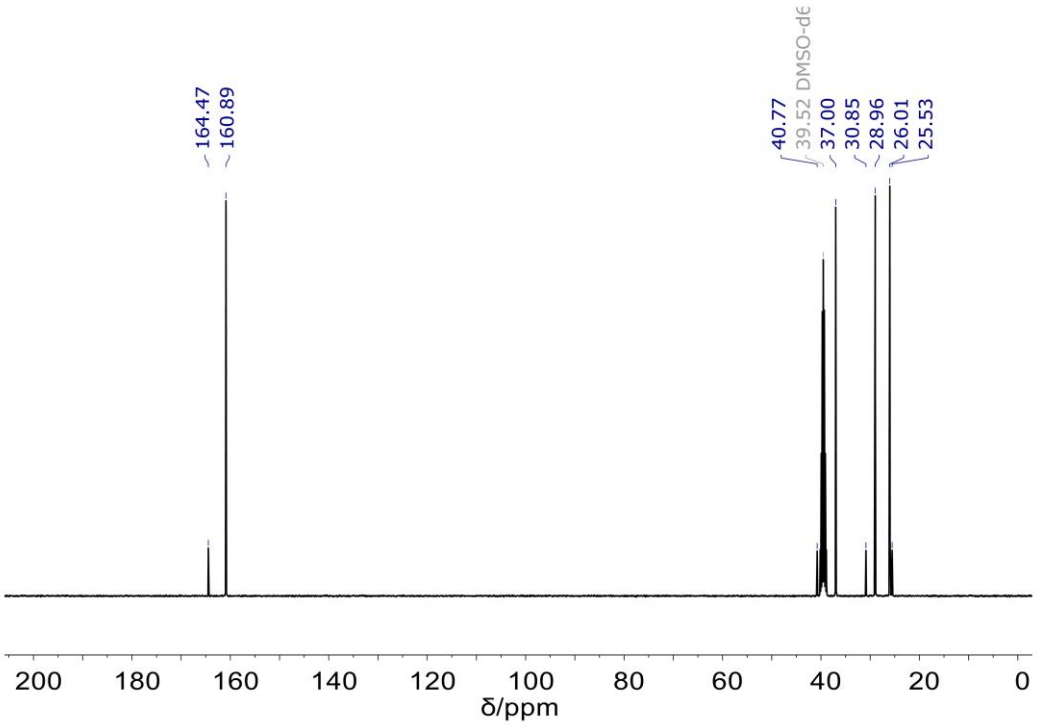

Figure 6.6.24 – ^{13}C NMR spectrum of the synthesized 1,6–bis(formamido)hexane.

1,6–bis(isocyano)hexane

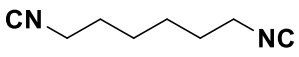

Chemical Formula: $C_8H_{12}N_2$
Molecular Weight: 136,20

1,6-Bis(formamido)hexane (5.00 g, 29.0 mmol, 1.00 equiv.) is dissolved in 58 mL of DCM (c(formamide) = 0.5 mol/L) and pyridine (13.8 g, 14.1 mL, 174 mmol, 6.00 equiv.) was added. Subsequently, *p*-toluenesulfonyl chloride (16.6 g, 87.0 mmol, 3.00 equiv.) was added under cooling the reaction mixture with a water bath. The mixture was stirred at room temperature until full conversion of the formamide was reached (monitoring *via* TLC). The mixture was cooled down to 0°C and a saturated sodium carbonate solution was added (in a volume equal to DCM) and it was stirred for 30 minutes. Afterwards, water and DCM were added (in a double amount of the original volume of DCM each) and the phases were separated. The aqueous phase was extracted 3x with fresh DCM and the combined extracts were washed 3x with water and 1x with brine. The washed organic phase was dried over sodium sulfate and the solvent was removed under reduced pressure. The crude product was purified *via* flash column chromatography (cyclohexane:ethyl acetate = 2:1) to obtain the desired compound (2.81 g, 20.6 mmol, 71%).

R_f = 0.36 (cyclohexane/ethyl acetate, 2:1).

^{1}H NMR (500 MHz, $CDCl_3$) δ_H / ppm = 3.39 (tt, J = 8.8, 5.4, 2.1 Hz, 4H), 1.72 – 1.64 (m, 4H), 1.51 – 1.42 (m, 4H).

^{13}C NMR (126 MHz, $CDCl_3$) δ_C / ppm = 155.76 (t), 41.18 (t), 28.55, 25.27.

IR (ATR platinum diamond): $\tilde{\nu}$ / cm^{-1} = 2943, 2863, 2147, 1454, 1351, 956.

HRMS (ESI-MS, $(M+H)^+$, $C_8H_{13}N_2$) calcd.: 137.1073; found: 137.1072.

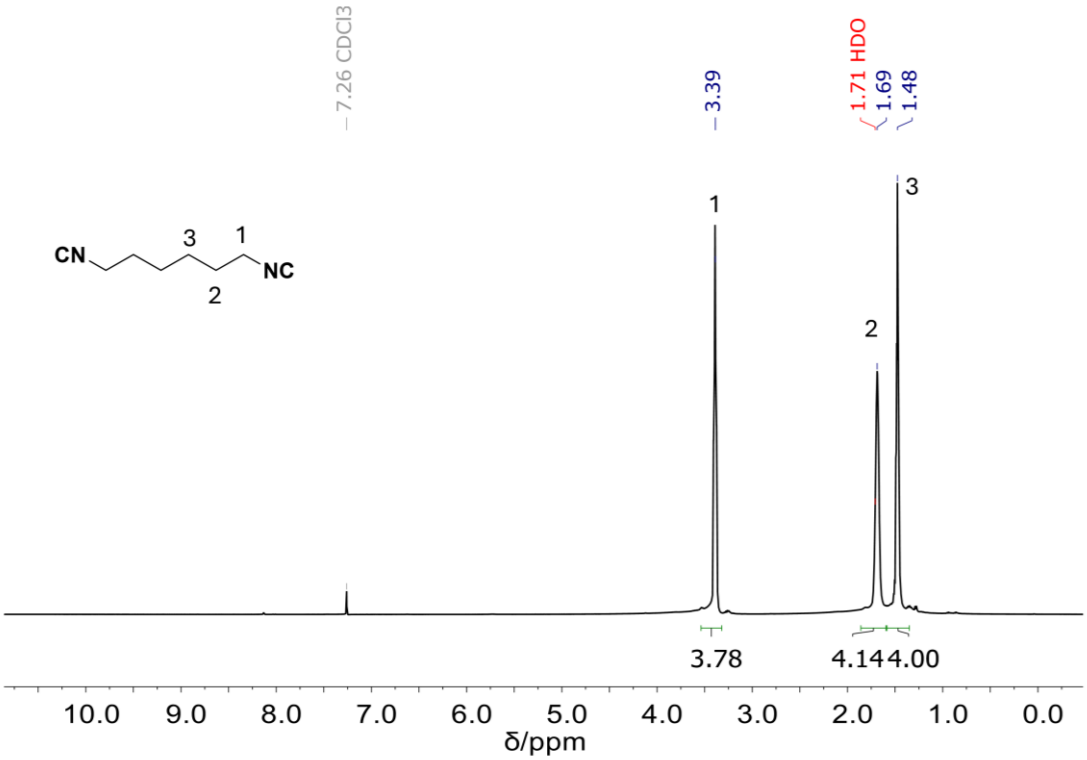

Figure 6.6.25 – ^{1}H NMR spectrum of the synthesized 1,6–bis(isocyano)hexane.

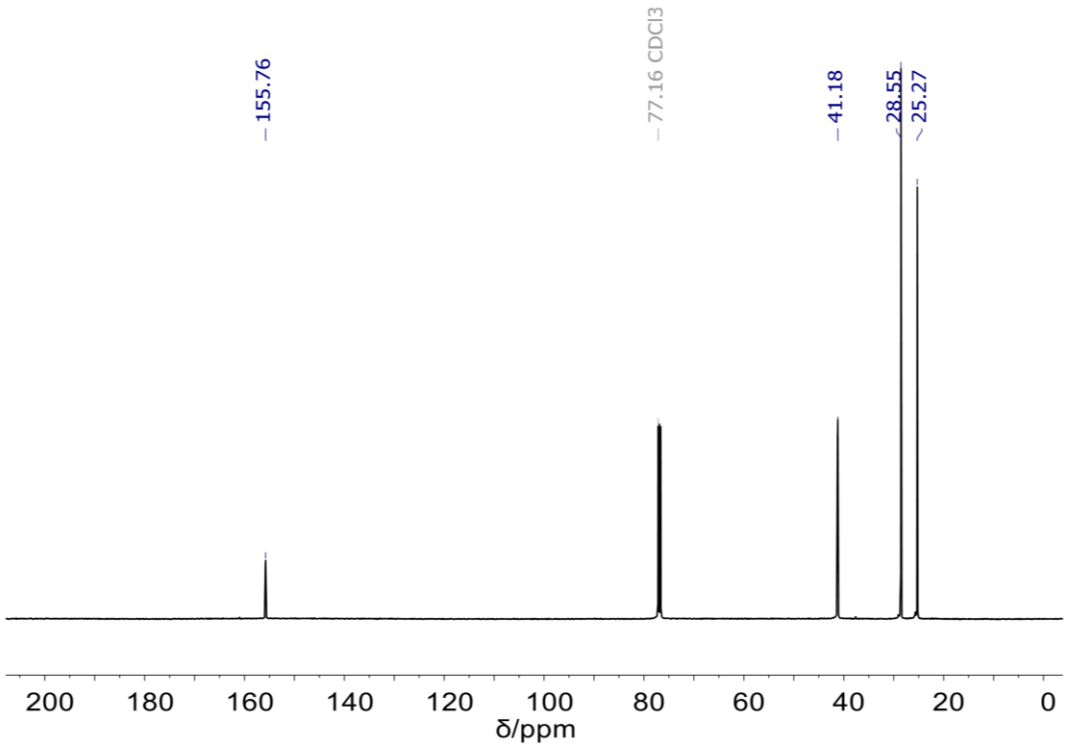

Figure 6.6.26 – ^{13}C NMR spectrum of the synthesized 1,6–bis(isocyano)hexane.

6.6.3.1.2 Passerini Model Reactions

The experimental synthesis described in this section was conducted by Sophia Abou El Mirate within the framework of her training ("Ausbildung") in chemistry, under the co-supervision of the author.

As previously described in **Section 4.3.5.1**, a model Passerini reaction was carried out to evaluate the influence of the solvent (acetone) on the formation of the desired product. Mesaconic acid, the isomeric analogue of itaconic acid, was reacted with nonanal and *n*-dodecyl isocyanide under identical reaction conditions, using either THF or acetone as the solvent.

Scheme 6.6.5 – General reaction scheme of the model reaction with mesaconic acid, nonanal and *n*-dodecylisocyanide, both in acetone or THF. Both possible adducts are shown, but the Acetone adduct can form only when acetone is used as solvent.

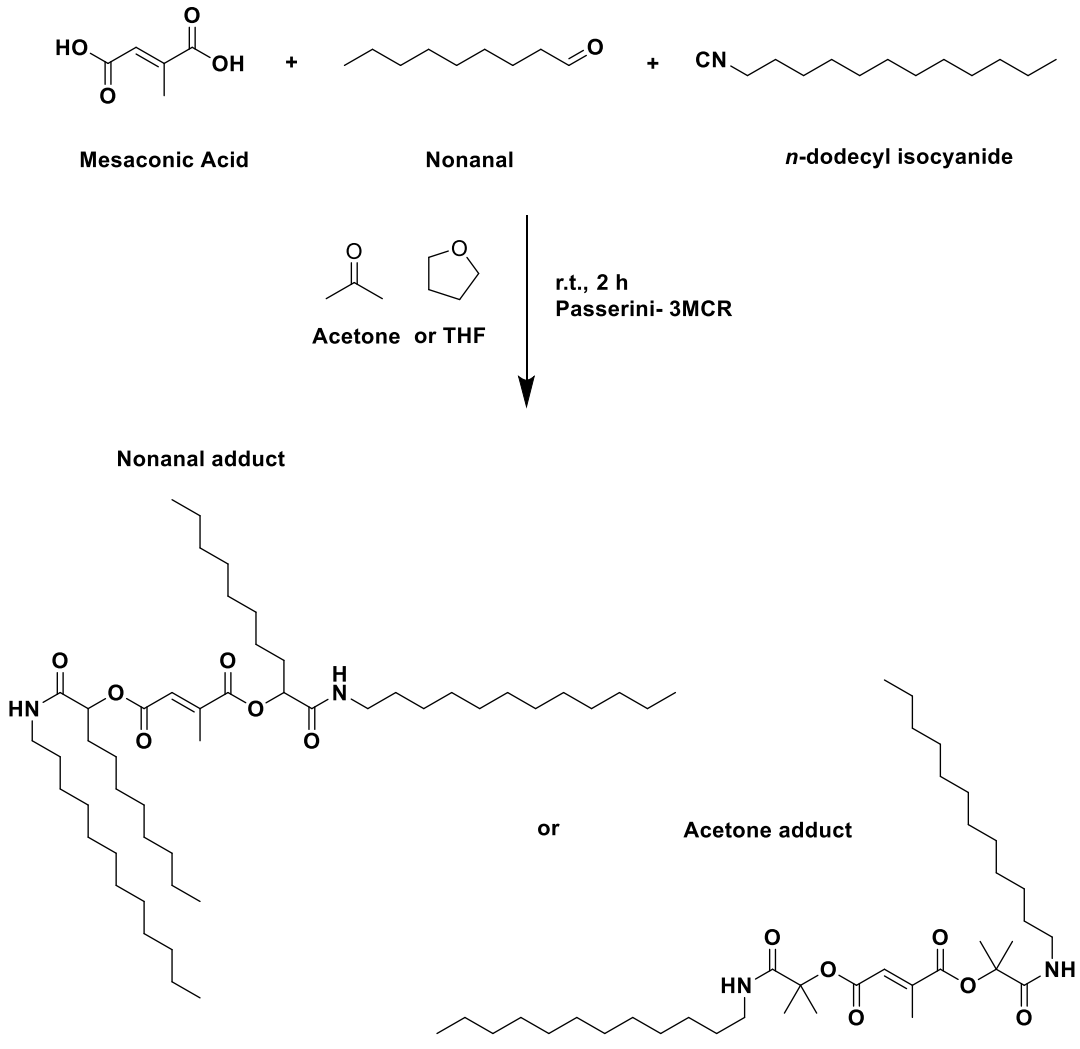

6.6.3.1.2.1 General Procedure for the Synthesis of the Passerini Model Compound to Evaluate the Influence of the Solvent

Mesaconic acid (75.0 mg, 0.576 mmol, 1.00 equiv.), nonanal (95% purity, 296 µL, 259 mg, 1.73 mmol, 3.00 equiv., 1.50 equiv. per -COOH), and n-dodecyl isocyanide (338 mg, 1.73 mmol, 3.00 equiv., 1.50 equiv. per -COOH) were weighed and introduced into a screw-cap vial. The selected anhydrous solvent (acetone or THF) was added (2 mL), and the reaction mixture was stirred at room temperature.

Workup for the reaction conducted in acetone:

After approximately 1 h, the gradual formation of a white precipitate was observed. To prevent clogging and ensure continuous stirring, additional portions of acetone were added (1.5 mL after 1 h and a further 2 mL after 2 h). The reaction mixture was then allowed to stir at room temperature for a total reaction time of 24 h. The resulting precipitate was collected by filtration through a fritted glass funnel (porosity P-4), washed with cold acetone, and dried under reduced pressure overnight to afford a white powder (yield: 258 mg, 0.320 mmol, 56%).

Workup for the reaction conducted in THF:

After a total reaction time of 24 h, the solvent was then removed under reduced pressure, and the residue was treated with cold acetone to induce precipitation. The resulting white solid was isolated by filtration through a fritted glass funnel (porosity P-4), washed with cold acetone, and dried under reduced pressure overnight to give a white powder (yield: 234 mg, 0.291 mmol, 51%).

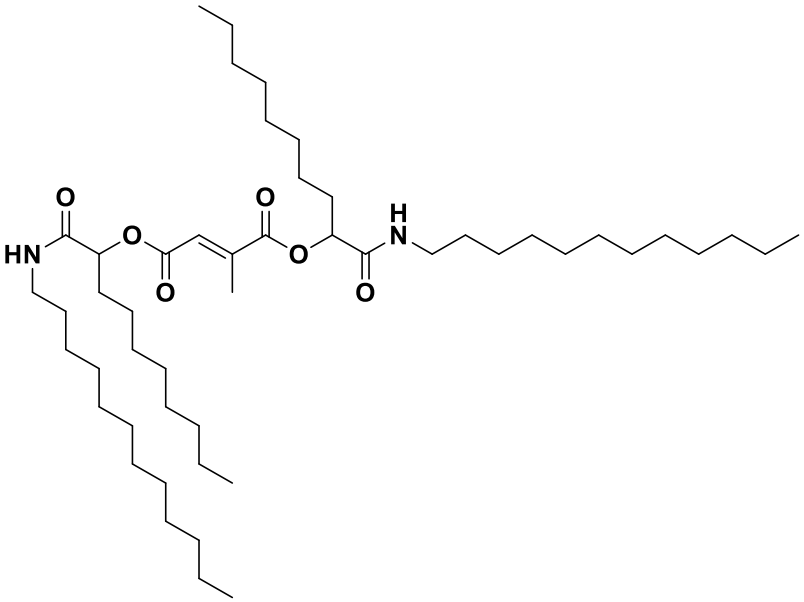

Nonanal adduct

Chemical Formula: $C_{49}H_{92}N_2O_6$
Molecular Weight: 805,28

Model compound obtained from the reaction in acetone

R_f = 0.66 (cyclohexane/ethyl acetate, 2:1).

^{1}H NMR (400 MHz, $CDCl_3$) δ_H / ppm = 6.89 (s, 1H), 5.97 (t, *J* = 5.6 Hz, 1H), 5.85 (t, *J* = 5.8, 3.4 Hz, 1H), 5.27 – 5.11 (m, 2H), 3.37 – 3.16 (m, 4H), 2.35 (s, 3H), 1.98 – 1.79 (m, 4H), 1.51 (p, *J* = 7.1 Hz, 4H), 1.42 – 1.11 (m, 63H), 0.87 (t, *J* = 6.9, 2.2 Hz, 13H).

^{13}C NMR (101 MHz, $CDCl_3$) δ_C / ppm = 169.74, 169.51, 166.35, 164.67, 145.15, 127.00, 76.03, 75.08, 39.80, 32.26, 30.09, 29.64, 27.29, 25.24, 23.14, 15.07, 14.57.

IR (ATR platinum diamond): $\tilde{\nu}$ / cm^{-1} = 3295, 2956, 2919, 2871, 2851, 1732, 1658, 1559, 1467, 1356, 1244, 1193, 1113, 1090, 901, 773, 720, 693, 677, 666.

HRMS (ESI, $(M+H)^+$, $C_{49}H_{93}N_2O_6$) calcd.: 805.7028; found: 805.7048.

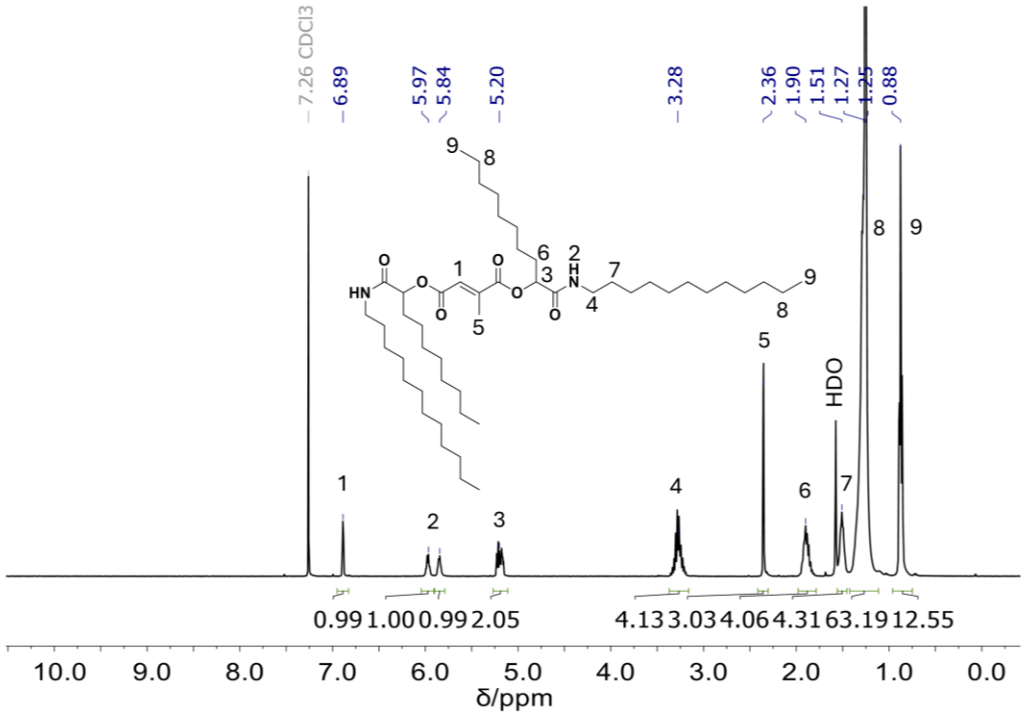

Figure 6.6.27 – ^{1}H NMR of the isolated Passerini model compound after reaction in acetone.

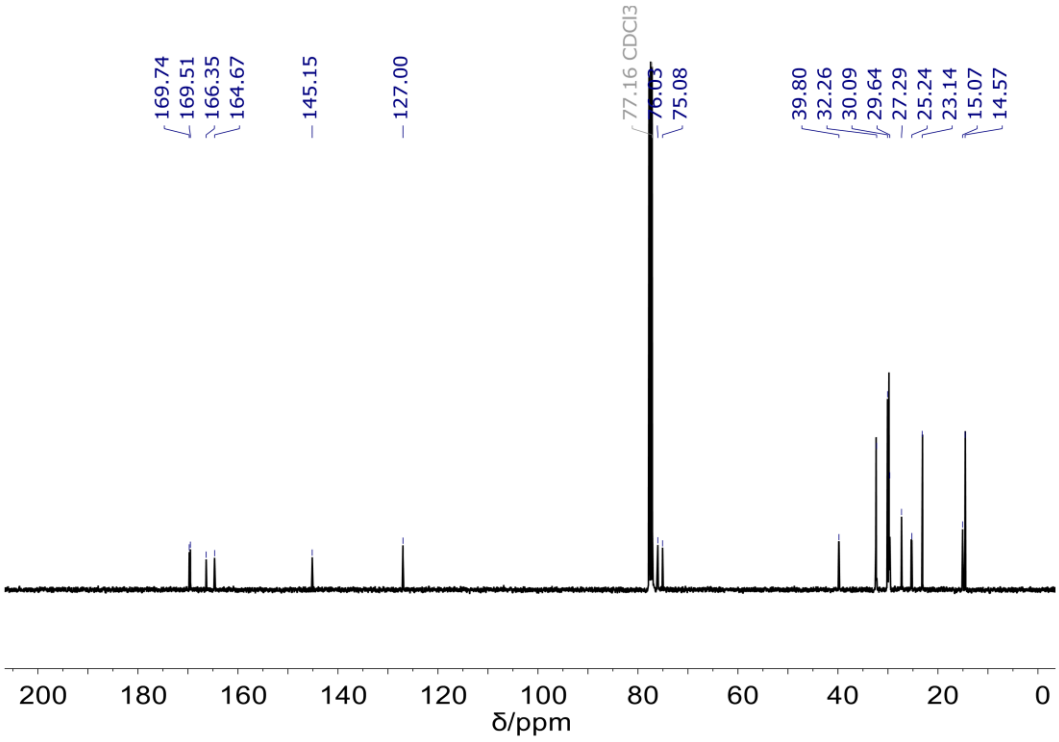

Figure 6.6.28 – ^{13}C NMR of the isolated Passerini model compound after reaction in acetone.

Model compound obtained from the reaction in THF

R_f = 0.66 (cyclohexane/ethyl acetate, 2:1).

^{1}H NMR (400 MHz, $CDCl_3$) δ_H / ppm = 6.89 (s, 1H), 5.96 (t, J = 5.7 Hz, 1H), 5.83 (t, J = 6.4 Hz, 1H), 5.28 – 5.14 (m, 2H), 3.38 – 3.16 (m, 4H), 2.36 (s, 3H), 2.01 – 1.75 (m, 4H), 1.50 (p, J = 7.0 Hz, 4H), 1.41 – 1.14 (m, 64H), 0.88 (t, 12H).

^{13}C NMR (101 MHz, $CDCl_3$) δ_C / ppm = 169.42, 169.19, 166.04, 164.36, 144.83, 126.68, 75.71, 74.76, 39.54, 32.05, 29.78, 29.40, 26.97, 25.04, 22.78, 14.75, 14.23.

IR (ATR platinum diamond): $\tilde{\nu}$ / cm^{-1} = 3297, 2956, 2919, 2849, 1732, 1658, 1559, 1467, 1456, 1356, 1247, 1195, 1113, 1092, 773, 720, 693.

HRMS (ESI, $(M+H)^+$, $C_{49}H_{93}N_2O_6$): calcd. 805.7028; found: 805.7039.

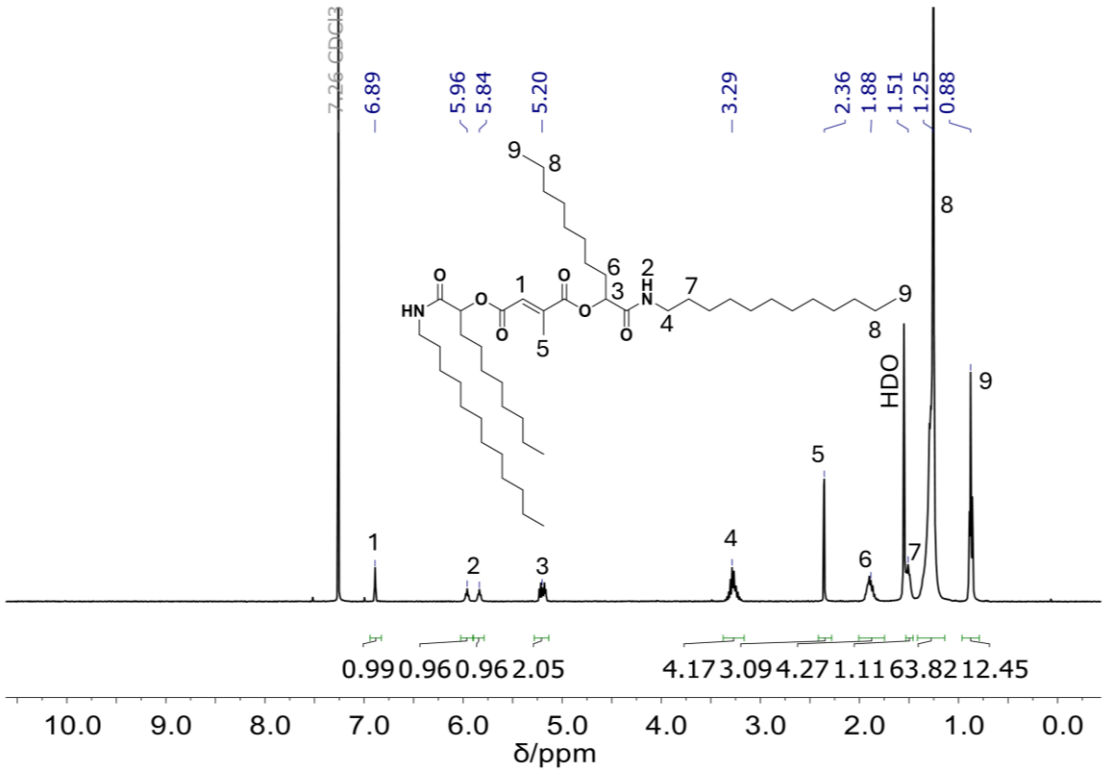

Figure 6.6.29 – ^{1}H NMR of the isolated Passerini model compound after reaction in THF.

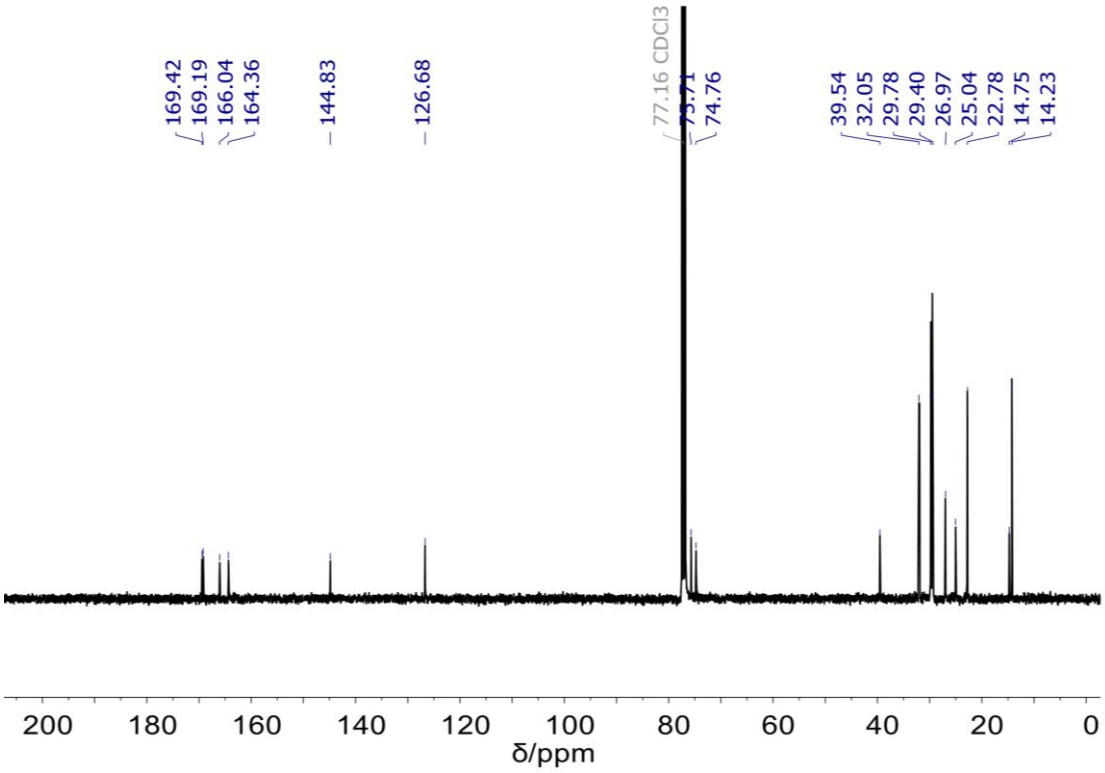

Figure 6.6.30 – ^{13}C NMR of the isolated Passerini model compound after reaction in THF.

6.6.4 Epoxy Thermosets

6.6.4.1 Characterization of Epoxidized Soybean Oil (ESBO)

For quantifying the epoxide groups of ESBO, a quantitative ^{1}H NMR spectrum was conducted with 3,4,5-trichloropyridine as internal standard (IS). The resulting spectrum is reported in **Figure 6.6.31**.

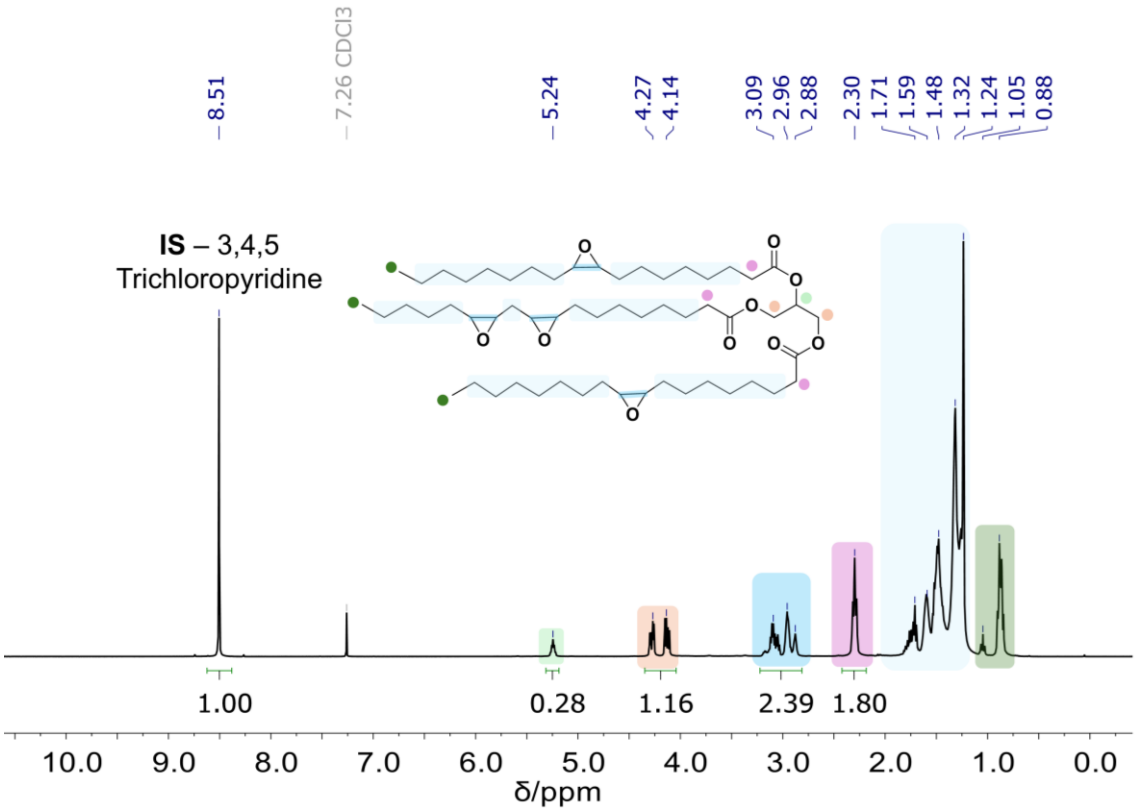

Figure 6.6.31 – ^{1}H NMR of ESBO in $CDCl_3$ with the IS 3,4,5-trichloropyridine and peak assignment.

The following calculations (**Eq. S23**) were followed to calculate the value of epoxy groups in mmol·g^{-1}:

$$mmol \cdot g^{-1}\ of\ epoxy\ groups\ in\ ESBO = \frac{\frac{\int epoxy\ region * H_{IS}}{\int IS * H_{epoxy}} * mmol\ of\ IS}{mass\ of\ ESBO\ (g)} \qquad \text{Eq. S23}$$

Where:

- *Integral of epoxy region* corresponds to the integral of the area between 3.25 – 2.75 ppm;
- *Integral of IS* is the integral value of the internal standard
- H_{IS} equals to 2;
- H_{epoxy} equals to 2;
- *Mass of ESBO* is the mass of the unknown sample to analyze in grams

For the calculation of the mmol of IS added to the sample the **Eq. S24** was used:

$$mmol\ of\ IS\ added\ to\ the\ sample = \frac{mass\ of\ IS\ (mg)}{M_w\ of\ IS\ \left(\frac{mg}{mmol}\right)} * Purity\ of\ IS \qquad \text{Eq. S24}$$

Where:

- *Purity of IS* is 97%;
- *Mass of IS* is the mass of internal standard used in the test in mg;
- M_w *of IS* is the molecular weight of the internal standard.

Internal standard: 3,4,5-Trichloropyridine (Purity: 97%)

Table 6.6.6 – Values of the masses of ESBO and IS taken for the triplicate tests, as well as the calculated values of mmol·g^{-1} of epoxides.

Test #	ESBO (mg)	IS (mg)	Epoxides (mmol·g^{-1})
1	33.8	12.6	4.74
2	33.0	12.6	4.75
3	34.1	12.6	4.77

The test was performed in triplicate giving an average value of (**4.753 ± 0.015**) mmol epoxy·g^{-1}.

6.6.4.2 General Epoxy Resin Formulation

For the preparation and curing of the epoxy resins, 125 mg of lignin derivative (LI, 1.39 mmol·g^{-1} COOH, 0.173 mmol COOH or LS, 1.79 mmol·g^{-1} COOH, 0.220 mmol COOH, previously dried at 70 °C under 10 mbar vacuum for 24 h) were weighed into a 10 mL scintillation vial together with predetermined amounts of Pripol™ and ESBO. The total stoichiometric ratio of COOH to epoxy groups was maintained at 1:1.2. A minimal amount of anhydrous DMSO (as much as needed to solubilize the mixture, typically 1.5 mL for lignin contents ≥ 15 mol% to 2 mL for lignin contents ≤ 10 mol%) was added to ensure homogeneity, and the mixture was vortexed at room temperature for 5 min. The samples were then sonicated for 30 min, after which 0.5 wt% of DBU catalyst (relative to the total weight of the components, excluding solvent) was added. The mixture was vortexed again for 5 min and then transferred with a pipette into circular Teflon molds. Curing was carried out in two stages: initially, the samples were equilibrated overnight at 80 °C covered by a Petri dish, followed by a gradual temperature increase (20 °C/h) to 140 °C. Afterwards, the curing was then continued at 140 °C for 2 days, and subsequently under vacuum (10 mbar) at 140 °C for an additional day.

Table 6.6.7 − Overview of the molar composition for the synthesized epoxy thermosets, with varying lignin contents.

Lignin content (mol%)[a]	Carboxylic Acid component (equiv.)			Epoxy component
	Pripol™ 1009	LI or LS	Total −COOH (equiv.)	ESBO (equiv.)
0	1	0	1	1.2
5	0.95	0.05	1	1.2
10	0.9	0.1	1	1.2
15	0.85	0.15	1	1.2
25	0.75	0.25	1	1.2
35	0.65	0.35	1	1.2

[a]: molar content of Lignin LI or LS (in percent) with respect to the total moles of carboxylic acid component.

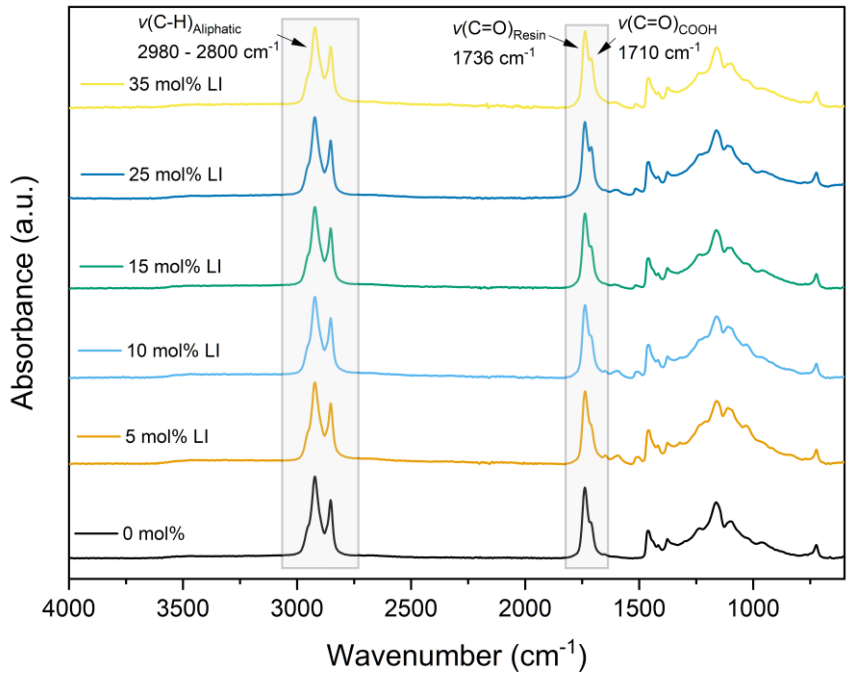

Figure 6.6.32 – Overlay of IR spectra with different lignin contents (ranging from 0 to 35 mol%) for the epoxy resins obtained with LI as lignin component.

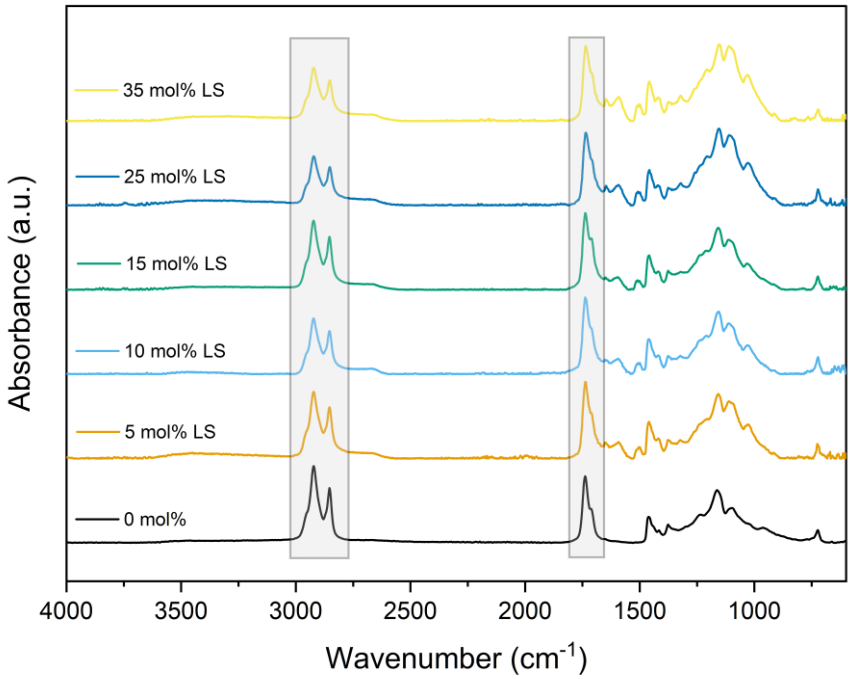

Figure 6.6.33 – Overlay of IR spectra with different lignin contents (ranging from 0 to 35 mol%) for the epoxy resins obtained with LS as lignin component.

6.6.4.3 Peak Deconvolution Methods

6.6.4.3.1 Peak Deconvolution of Single Spectra

For the calculation of the percentage ratio between free carboxylic acid and ester groups in the resins, the overlapping signals were deconvoluted to ensure reliable quantification. These deconvolutional calculations were performed using the software OriginPro 2023, applying a gauss-amplitude function. For the fitting procedure, the peak centers (xc) were fixed at 1711 cm^{-1} (Fit 1) and 1738 cm^{-1} (Fit 2), corresponding to the free −COOH and ester carbonyl groups, respectively. The peak widths (w), defined as w = FWHM/√ln4, were not fixed during the fitting process. The final ranges obtained for w from the fitting output were 11.48–13.13 for w_1 and 10.57–12.00 for w_2.

6.6.4.3.2 Peak Deconvolution Over Time

To quantify the evolution of the signal at 1715 cm^{-1} over time, a peak-fitting procedure was applied to resolve the overlapping bands corresponding to the ester groups (1738 cm^{-1}) and the free −COOH groups (1715 cm^{-1}). A gaussian amplitude function was employed for the deconvolution. For the fitting of the two peaks, the following constraints were applied: 1700 < $x\mathrm{c}_1$ < 1720 and 1730 < $x\mathrm{c}_2$ < 1745, where xc represents the peak center; and 8 < (w_1, w_2) < 15, where w denotes the peak width (w = FWHM/√ln4). These parameters were previously determined through single-spectrum deconvolution. The area of the absorbance peak attributed to free −COOH groups was normalized to its initial value and plotted as a function of time. The deconvolution was performed starting from time values greater than 400 s, as initially the presence of solvent hindered the visibility of the resin peaks.

6.6.4.4 Thermal Properties

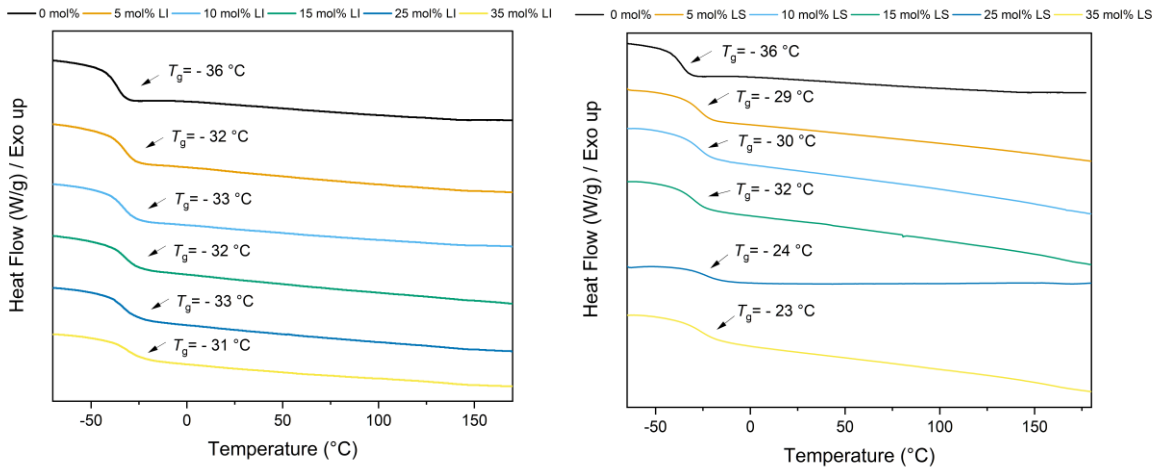

Figure 6.6.34 – DSC Traces of the resin formulation with LI and LS, with different lignin contents.

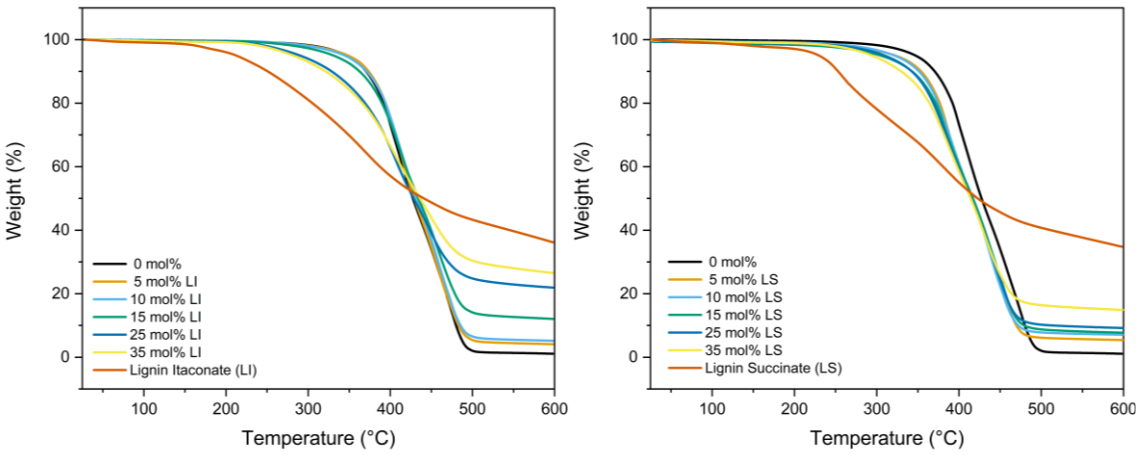

Figure 6.6.35 – TGA curves of LI and LS epoxy resins with different lignin contents as well as the pristine starting materials LI and LS for comparison.

6.6.4.5 Rheology and DMA Analyses

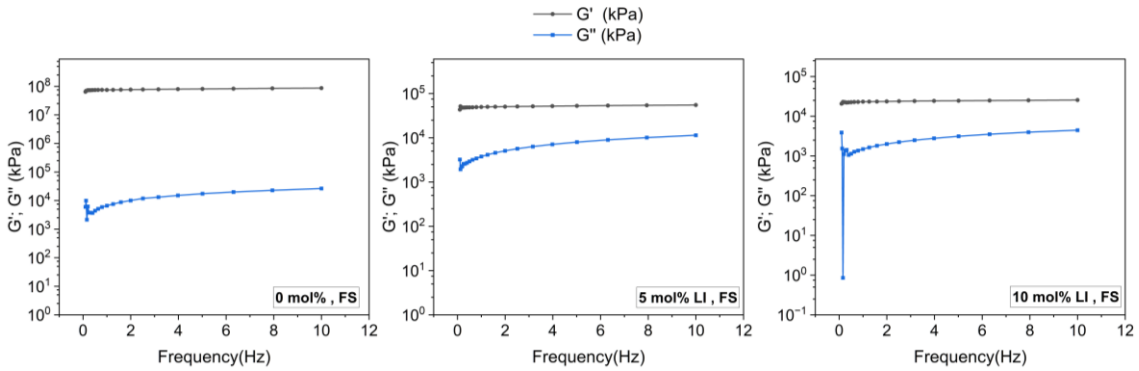

Figure 6.6.36 – Frequency sweep experiments for LI epoxy resins with lignin contents of 0, 5, and 10 mol%.

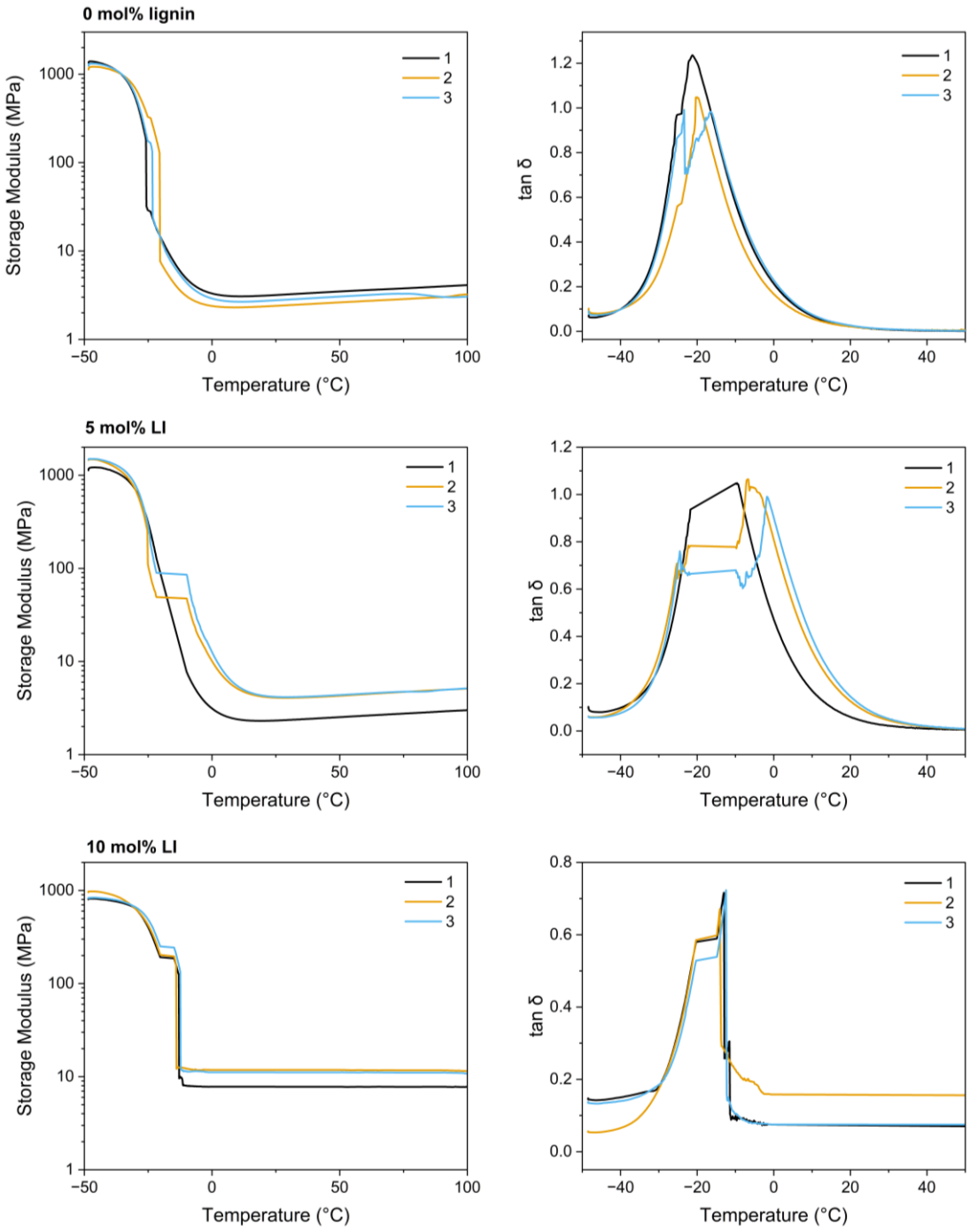

Figure 6.6.37 – Triplicate measurements of the DMA analyses for the sample with 0 mol% lignin and LI epoxy resins. For the sample with 10 mol% LI, only the onset could be determined.

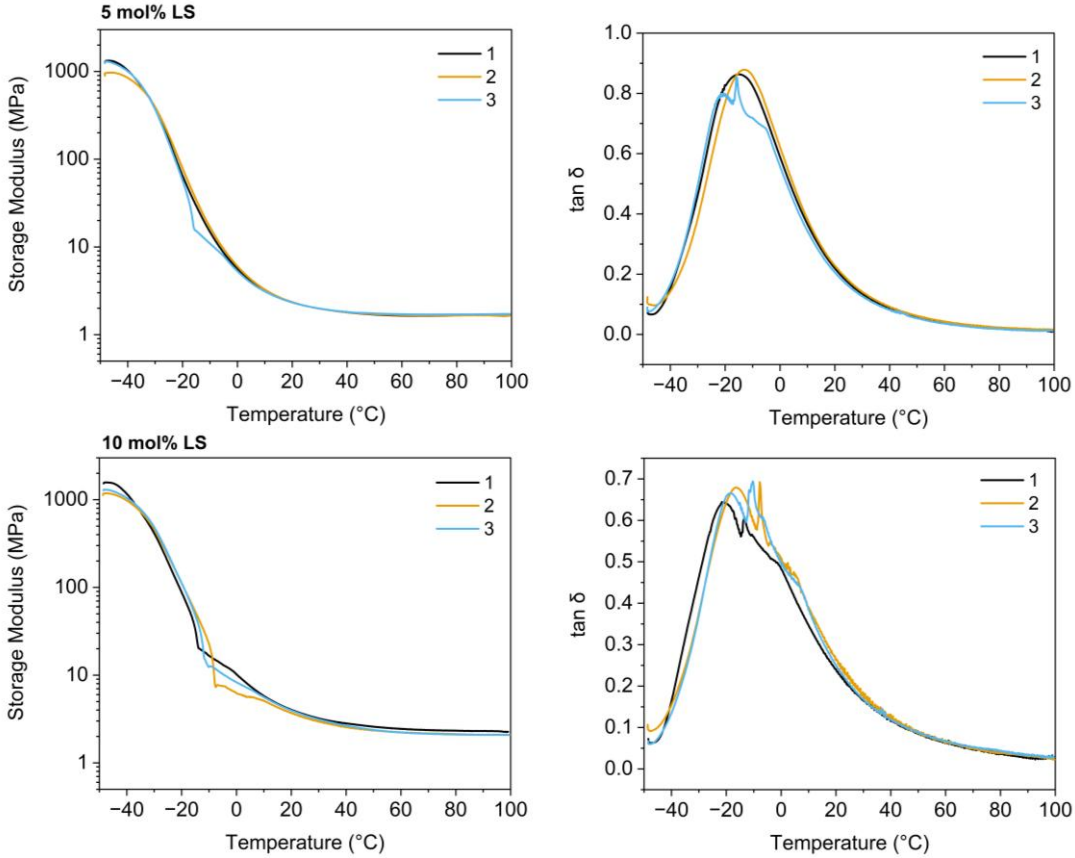

Figure 6.6.38 – Triplicate measurements of the DMA analyses for the LS epoxy resins. It can be seen how in some cases the rapid drop in the storage modulus very close to the resolution of the transducer of the instrument, leading to experimental difficulties.

6.6.4.6 Tensile Strength Measurements

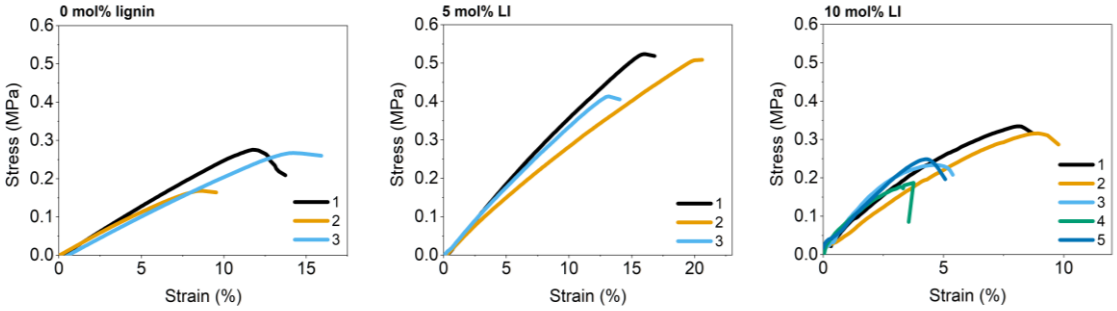

Figure 6.6.39 – Overview of the tensile strength measurements for the sample with 0 mol% lignin and LI epoxy resins. In the case of sample containing 10 mol% LI, the measurements were repeated five times because of its lower reproducibility.

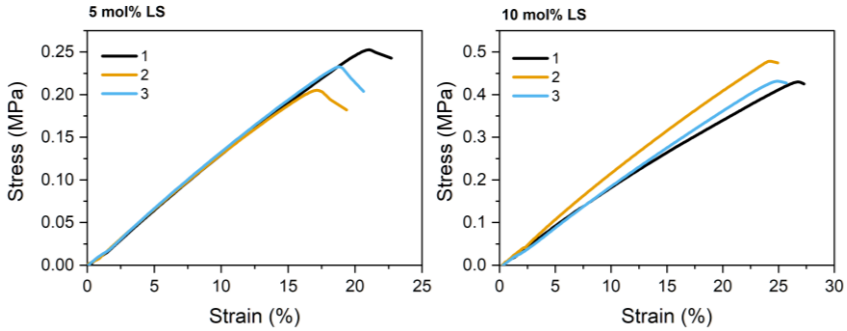

Figure 6.6.40 – Overview of the triplicates of the tensile strength measurements for LS epoxy resins.

6.6.4.7 Epoxy Resins Degradability Tests

For the degradation tests, ca. 500 mg of thermoset were cut into pieces and their exact weight was recorded. Afterwards, they were transferred into a crimp vial and suspended in either a solution of 0.6 M sodium hydroxide (NaOH), 1 M hydrochloric acid (HCl), or 1 M citric acid (CA). The solutions were heated to 80 °C for 4 days. For the alkaline hydrolysis, the resulting solution was acidified with HCl to a pH of 2 and the precipitate was collected *via* filtration and washed with distilled water. For further purification, the filtrates were again dissolved in acetone, reprecipitated in acidic aqueous medium (pH = 2) and recollected *via* filtration. For the acidic hydrolysis, some thermoset pieces did not degrade after 4 days of stirring at 80 °C. Therefore, the collected solids after acidic hydrolysis were suspended in acetone, leading to an undissolved fraction (likely the undegraded thermosets, separated *via* hot filtration) and a dissolved fraction, that was collected *via* precipitation in acidic aqueous medium (pH = 2, acidified with HCl 1 M) and subsequent filtration.

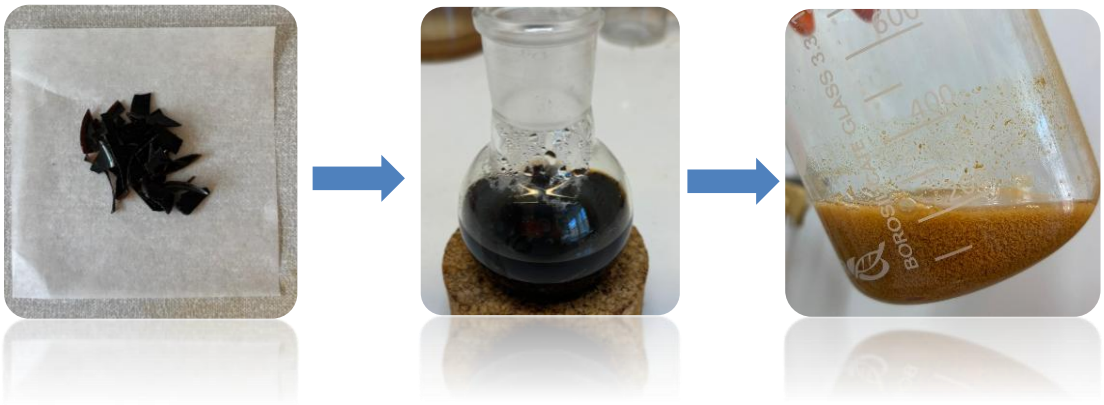

Figure 6.6.41 – Left: thermoset containing 10 mol% LI, cut into pieces. Middle: homogeneous brown solution obtained after alkaline hydrolysis. Right: solution after acidification to pH = 2, with visible precipitate formation.

6.6.5 Thia-Michael Thermosets

200 mg of LI (1.39 mmol·g^{-1} COOH, 0.280 mmol COOH, equivalent to the mmol of double bonds, previously dried at 70 °C under 10 mbar vacuum for 24 h), were weighed into a 10 mL scintillation vial together with PTEMP (34 mg, 0.280 mmol -SH, four functionalities) and 1 mL of THF was added to solubilize the mixture. The total stoichiometric ratio of double bond to -SH was maintained at 1:1. The mixture was vortexed at room temperature for 10 minutes, then was transferred with a pipette into a rectangular Teflon mold. The solvent was allowed to evaporate under the fumehood at room temperature, covered with a Petri dish for 5 h. Afterwards it was transferred to a pre-heated oven at 75 °C and left at this temperature overnight. Subsequently, the curing was conducted at 140 °C for 72 h.

IR data are presented and discussed in **Chapter 4.3.5.3**.

Gel content (THF): 99 %

7 Appendix

7.1 Calculations of the E-factor Values of Chapter 2.2.1

General information

The E-factor calculations presented herein consider the synthetic E-factors, without considering any pretreatment/solubilization done to the lignin prior to the synthesis. E_{simple} is defined as the simple E-factor, where no solvents are included in the calculation; $E_{complex}$ on the other hand also includes the solvent contribution to the E-factor. If no final, isolated weight of lignin was reported in the respective manuscripts, a theoretical yield was calculated following **Eq. S12**, assuming 100 % conversion of the reactive sites toward the main reaction, thus assuming the lowest possible E-factor for the respective literature described reaction.

7.2 E-Factor Calculations for Amino Group Functionalized Lignin

Calculated E-factors for amination procedures are summarized in **Table 7.2.1**. Below the table, all calculations are listed to ensure reproducibility.

Table 7.2.1 - E factors for amination procedures.

Work	Modification	Functionalizing agent	E_{simple}	$E_{complex}$	$E_{solvent}$ (%)
She[143]	Amination (Mannich)	Dimethylamine, Ethylenediamine and Diethylenetriamine	4.15[a]	12.66[a]	67
Li[144]	Amination (Mannich)	Dimethylamine	5.51[a]	20.62[a]	73
Jameel[142]	Amination (Mannich)	Dimethylamine, Diethylamine	2.98	13.74	78
Biesalski[148]	Amination (Mannich)	Diethylenetriamine, 1,3-Propylenediamine, Ethylenediamine, Ammonia	1.91-5.04	12.93-26.59	81-90
Kim[153]	Amination	2-Chloroethylamine hydrochloride	12.27	142	91
Renneckar[157]	Amination	2-Oxazolidinone	3.10	–	–

[a]: no final weight of isolated product was reported, therefore final weight of the product was calculated based on theoretical yield.

Jiao, g.-J.; Peng, P.; Sun, S.-L.; Geng, Z.-C.; She, D. “Amination of Biorefinery Technical Lignin by Mannich Reaction for Preparing highly Efficient Nitrogen Fertilizer”. *Int. J. Biol*. Macromol. **2019**, 127, 544–554.

Starting materials: 5.00 g phenolated lignin (7.79 mmol per g lignin reactive sites, 0.13 mmol per g lignin AlOH, 5.84 mmol per g lignin ArOH), 20.0 g formaldehyde (666 mmol in 37% aq. solution, 54 g total weight considering water), 15 g ethylenediamine (250 mmol, in 40% aq. solution, 37.5 g total weight considering water), 0.16 g sodium hydroxide (4 mmol, 0.4 mol/L, 10.02 g total weight considering water).

Desired product: 7.81 g (theoretical yield)

$$m_f = m_i \left(1 + \Delta M_{graft} \left(reactive\ sites\ in \frac{mol}{g}\right)\right) = 5\ g\ (1 + 72.1 \frac{g}{mol}\left(7.79 \times 10^{-3} \frac{mol}{g}\right) = 7.81\ g$$

$$E_{simple} = \frac{\sum starting\ materials - desired\ product}{desired\ product} = \frac{40.16 - 7.81}{7.81} = 4.14$$

$$E_{complex} = \frac{\sum starting\ materials\ (+solvents) - desired\ product}{desired\ product} = \frac{106.52 - 7.81}{7.81} = 12.64$$

$$Solvent\ contribution = \frac{weight\ of\ solvent}{\sum starting\ materials\ (+solvent) - desired\ product} = \frac{66.36}{98.72} = 0.672 = \mathbf{67.2}\%$$

Du, X.; Li, J.; Lindström, M. E. “Modification of Industrial Softwood Kraft Lignin Using Mannich Reaction with and without Phenolation Pretreatment”. *Ind. Crops Prod*. **2014**, 52, 729–735

Starting materials: 0.10 g LignoBoost lignin from spruce kraft black liquor (1.96 mmol per g lignin reactive sites, 1.60 mmol per g lignin AlOH, 0.45 mmol per g lignin COOH, 3.59 mmol per g lignin ArOH), 0.165 g formaldehyde (5.5 mmol, in 37% aq. solution, 0.446 g total weight considering water), 0.248 g dimethylamine (5.5 mmol, in 40% aq. solution, 0.62 g total weight considering water), 0.21 g acetic acid (3.5 mmol), 1.024 g (80% solution of 1,4-dioxane in water).

Desired product: 0.111 g (theoretical yield)

$$m_f = m_i \left(1 + \Delta M_{graft} \left(reactive\ sites\ in \frac{mol}{g}\right)\right) = 0.1\ g\ (1 + 57.06 \frac{g}{mol}\left(1.96 \times 10^{-3} \frac{mol}{g}\right) = 0.111\ g$$

$$E_{simple} = \frac{\sum starting\ materials - desired\ product}{desired\ product} = \frac{0.723 - 0.111}{0.111} = 5.51$$

$$E_{complex} = \frac{\sum starting\ materials\ (+solvents) - desired\ product}{desired\ product} = \frac{2.4 - 0.111}{0.111} = 20.62$$

$$Solvent\ contribution = \frac{weight\ of\ solvent}{\sum starting\ materials\ (+solvent) - desired\ product} = \frac{1.677}{2.29} = 0.732 = \mathbf{73.2}\%$$

Kollman, M.; Jiang, X.; Thompson, S. J.; Mante, O.; Dayton, D. C.; Chang, H.; Jameel, H. "Improved Understanding of Technical Lignin Functionalization through Comprehensive Structural Characterization of Fractionated Pine Kraft Lignins Modified by the Mannich Reaction". G*reen Chem*. **2021**, 23 (18), 7122–7136

Starting materials: 0.10 g BioChoice® lignin, 0.150 g formaldehyde (5 mmol in 37% aq. solution, 0.406 g total weight considering water), 0.2254 g dimethylamine (5 mmol), 1.03 g 1,4-dioxane. Volume of 0.5 M NaOH solution used to adjust the pH is not reported.

Desired product: 0.1192 g (isolated yield)

$$E_{simple} = \frac{\sum starting\ materials - desired\ product}{desired\ product} = \frac{0.475 - 0.1192}{0.1192} = 2.98$$

$$E_{complex} = \frac{\sum starting\ materials\ (+solvents) - desired\ product}{desired\ product} = \frac{1.76 - 0.1192}{0.1192} = 13.78$$

$$Solvent\ contribution = \frac{weight\ of\ solvent}{\sum starting\ materials\ (+solvent) - desired\ product} = \frac{1.286}{1.64} = 0.783 = \mathbf{78.3}\%$$

Ott, M. W.; Dietz, C.; Trosien, S.; Mehlhase, S.; Bitsch, M. J.; Nau, M.; Meckel, T.; Geissler, A.; Siegert, G.; Huong, J.; Hertel, B.; Stark, R. W.; Biesalski, M. "Co-Curing of Epoxy Resins with Aminated Lignins: Insights into the Role of

Lignin Homo Crosslinking during Lignin Amination on the Elastic Properties". *Holzforschung,* **2021**, 75 (4), 390–398

Starting materials: 40.0 g Softwood kraft lignin, 3.20 g sodium hydroxide (80.0 mmol, 404 g of total solution considering water), 18.6 g formaldehyde (620 mmol, in 35% aq. solution, 53.2 g total weight considering water), 64.0 g diethylene triamine (DETA, 620 mmol); or 45.9 g of 1,3-propylenediamine (PDA, 619 mmol); or 60.1 g of ethylenediamine (EDA, 1000 mmol); or 17.5 g of ammonia (1028 mmol, in 25% aq. solution, 70 g total weight considering water).

Desired product(s):

diethylenetriamine-functionalized lignin KL-DETA: 40.3 g (isolated yield)

1,3-propylenediamine-functionalized lignin KL-PDA: 37.0 g (isolated yield)

ethylenediamine-functionalized lignin KL-EDA: 20.2 g (isolated yield)

ammonia-functionalized lignin KL-NH3: 25.0 g (isolated yield)

Desired product	**Raw materials (total weight in g without solvent)**	**Raw materials (total weight in g with solvent)**	**Desired product (g)**	**E_{simple}**	**$E_{complex}$**	**Solvent contribution to the E-factor (%)**
KL-DETA	125.8	561.2	40.3	2.12	12.93	84
KL-PDA	107.7	543.1	37.0	1.91	13.68	86
KL-EDA	121.9	557.3	20.2	5.04	26.59	81
KL-NH3	79.32	567.2	25.0	2.17	21.69	90

Chen, J.; An, L.; Bae, J. H.; Heo, J. W.; Han, S. Y.; Kim, Y. S. “Green and Facile Synthesis of Aminated Lignin-Silver Complex and Its Antibacterial Activity”. *Ind. Crops Prod*. **2021**, 173, 114102

Starting materials: 1.00 g kraft lignin, 3.22 g 2-chloroethylamine hydrochloride (27.76 mmol), 6.00 g sodium hydroxide (150 mmol, 106 g of total solution considering water).

Desired product: 0.77 g (isolated yield)

$$E_{simple} = \frac{\sum starting\ materials - desired\ product}{desired\ product} = \frac{10.22 - 0.77}{0.77} = 12.27$$

$$E_{complex} = \frac{\sum starting\ materials\ (+solvents) - desired\ product}{desired\ product} = \frac{110.22 - 0.77}{0.77}$$

$$= 142.14$$

$$Solvent\ contribution = \frac{weight\ of\ solvent}{\sum starting\ materials\ (+solvent) - desired\ product} = \frac{100}{109.45} = 0.914 =$$

$\mathbf{91.4}\%$

Liu, L.; Wan, X.; Chen, S.; Boonthamrongkit, P.; Sipponen, M.; Renneckar, S. “Solventless Amination of Lignin and Natural Phenolics Using 2-Oxazolidinone”. *ChemSusChem*, **2023**, 16 (15), e202300276.

Starting materials: 2.00 g softwood kraft lignin (5.90 mmol reactive sites per g lignin, total sum of ArOH and COOH groups), 6.16 g 2-oxazolidinone (70.8 mmol, 6.00 equiv. in respect to the sum of ArOH and COOH groups), 0.12 g sodium hydroxide (2.95 mmol, 0.25 equiv.)

Desired product: 2.02 g (isolated yield)

$$E_{simple} = \frac{\sum starting\ materials - desired\ product}{desired\ product} = \frac{8.28 - 2.02}{2.02} = 3.10$$

$E_{complex} = E_{simple}$ because no additional solvents are used.

7.3 E-Factor Calculations for Epoxide Functionalized Lignin

Calculated E-factors for epoxidation procedures are summarized below. **Table 7.3.1** provides an overview and all calculations are listed below to ensure reproducibility.

Table 7.3.1 - E-factors for epoxidation procedures.

Work	Modification	Functionalizing agent	E_{simple}	$E_{complex}$	$E_{solvent}$ (%)	$E_{sequence}$
Meier[160]	Glycidylation	Epichlorohydrin	6.35	–	–	–
Zhang[161]	Glycidylation	Epichlorohydrin	4.24[a]	4.50[a]	5.7	–
Sun[162]	Glycidylation	Epichlorohydrin	0.73[a]	57.0[a]	99	–
Sasaki[167]	Glycidylation	Epichlorohydrin	14.0	16.2	14	–
Zhang[168]	Glycidylation	Epichlorohydrin	6.23	16.2	62	–
Daugaard[175]	1. Epoxidation	Hydrogen peroxide	1.05	4.78	78	38.0
	2. Esterification	Epoxidized fatty acids	4.29	22.7	81	
Avérous[179]	1. Chlorination	Oxalyl chloride	0.78[a]	7.13[a]	89	14.2
	2. Esterification	Oleyl chloride	0.57	–	–	
	3. Epoxidation	Peracetic acid	0.21[a]	7.39[a]	97	
Renneckar[182]	1. Hydroxyethylation	Ethylene carbonate	2.19	–	–	5.80
	2. Esterification	Oleic Acid	2.15	–	–	
Vásquez-Garay[185]	1. Allylation	Allyl bromide	2.58[a]	31.4[a]	92	82.8
	2. Epoxidation	Hydrogen peroxide, Enzyme	1.45	51.5	97	

[a]: no final weight of isolated product was reported, therefore final weight of the product was calculated based on theoretical yield.

Over, L. C.; Grau, E.; Grelier, S.; Meier, M. A. R.; Cramail, H. “Synthesis and Characterization of Epoxy Thermosetting Polymers from Glycidylated Organosolv Lignin and Bisphenol A”. *Macromol. Chem. Phys*. **2017**, 218, 1600411.

Starting materials: 25.0 g organosolv lignin (6.08 mmol OH per g lignin), 118 g epichlorohydrin (1.28 mol, 8.41 equiv.), 9.5 g tetrabutylammonium bromide (19.7 mmol, 13.0 mol%), 29.9 g potassium hydroxide (533 mmol, 3.51 equiv.).

Desired product: 24.8 g (isolated yield)

$$E_{simple} = \frac{\sum starting\ materials - desired\ product}{desired\ product} = \frac{182.4 - 24.8}{24.8} = 6.35$$

$E_{complex} = E_{simple}$ because no additional solvents are used.

Wang, X.; Leng, W.; Nayanathara, R. M. O.; Caldona, E. B.; Liu, L.; Chen, L.; Advincula, R. C.; Zhang, Z.; Zhang, X. “Anticorrosive Epoxy Coatings from Direct Epoxidation of Bioethanol Fractionated Lignin”. *Int. J. Biol. Macromol*. **2022**, 221, 268-277.

Starting materials: 10.0 g bioethanol fractionated lignin (6.20 mmol reactive sites per g lignin: 1.59 mmol AlOH per g lignin, 3.24 mmol ArOH per g lignin, 1.37 mmol COOH per g lignin), 59.7 g epichlorohydrin (645 mmol, 10.4 equiv.), 0.1 g tetramethylammonium chloride (91.0 µmol, 1.47 mol%), 4.30 g sodium hydroxide (20 wt% aqueous NaOH solution, 21.5 mmol, 0.347 equiv.).

Desired product: 13.48 g (theoretical yield)

$$m_f = m_i \left(1 + \Delta M_{graft} \left(reactive\ sites\ in \frac{mol}{g}\right)\right)$$

$$m_f = 10.0\ g\ \left(1 + 56.064 \frac{g}{mol}\ \ (6.20 \times 10^{-3}\ \frac{mol}{g})\right) = 13.48\ g$$

$$E_{simple} = \frac{\sum starting\ materials - desired\ product}{desired\ product} = \frac{70.66 - 13.48}{13.48} = 4.24$$

$$E_{complex} = \frac{\sum starting\ materials\ (+solvents) - desired\ product}{desired\ product} = \frac{74.1 - 13.48}{13.48} = 4.50$$

$$Solvent\ contribution = \frac{weight\ of\ solvent}{\sum starting\ materials\ (+solvent) - desired\ product} = \frac{3.44}{60.62}$$
$$= 0.057 = \mathbf{5.7}\%$$

Li, X.-Y.; Xiao, L.-P.; Zou, S.-L.; Xu, Q.; Wang, Q.; Lv, Y.-H.; Sun, R.-C. "Preparation and Characterization of Bisphenol A-Based Thermosetting Epoxies Based on Modified Lignin". *ACS Appl. Polym. Mater*. **2023**, 5, 3611-3621.

Starting materials: 2.00 g lignin (0.94 mmol reactive sites per g lignin: 0.36 mmol AlOH per g lignin, 0.42 mmol ArOH per g lignin, 0.16 mmol COOH per g lignin), 1.55 g epichlorohydrin (16. 8 mmol, 8.91 equiv.), 0.10 g sodium hydroxide (2.50 mmol ,1.33 equiv.), 118.65 g acetone (150 mL).

Desired product: 2.11 g (theoretical yield)

$$m_f = m_i \left(1 + \Delta M_{graft} \left(reactive\ sites\ in \frac{mol}{g}\right)\right)$$

$$m_f = 2.00\ g\ \left(1 + 56.064\ \frac{g}{mol}(0.94 \times 10^{-3}\ \frac{mol}{g})\right) = 2.11\ g$$

$$E_{simple} = \frac{\sum starting\ materials - desired\ product}{desired\ product} = \frac{3.65 - 2.11}{2.11} = 0.73$$

$$E_{complex} = \frac{\sum starting\ materials\ (+solvents) - desired\ product}{desired\ product} = \frac{122.3 - 2.11}{2.11}$$
$$= 56.96$$

$$Solvent\ contribution = \frac{weight\ of\ solvent}{\sum starting\ materials\ (+solvent) - desired\ product} = \frac{118.65}{120.19} = 0.987 = \mathbf{98.7}\%$$

Sasaki, C.; Wanaka, M.; Takagi, H.; Tamura, S.; Asada, C.; Nakamura, Y. "Evaluation of Epoxy Resins synthesized from Steam-exploded Bamboo Lignin". *Ind. Crops Prod.* **2013**, 43, 757-761.

Starting materials: 10.0 g bamboo lignin (8.30 mmol OH per g lignin), 160 g epichlorohydrin (1.73 mol, 20.8 equiv.), 7.00 g tetrabutylammonium bromide (14.5 mmol, 17.5 mol%), 50.0 g sodium hydroxide (50 wt% aqueous NaOH solution, 625 mmol, 7.53 equiv.), 5.5 g dimethyl sulfoxide (5 mL).

Desired product: 13.5 g (isolated yield)

$$E_{simple} = \frac{\sum starting\ materials - desired\ product}{desired\ product} = \frac{202 - 13.5}{13.5} = 13.96$$

$$E_{complex} = \frac{\sum starting\ materials\ (+solvents) - desired\ product}{desired\ product} = \frac{232.5 - 13.5}{13.5} = 16.22$$

$$Solvent\ contribution = \frac{weight\ of\ solvent}{\sum starting\ materials\ (+solvent) - desired\ product} = \frac{30.5}{219} = 0.139 = \mathbf{13.9}\%$$

Xin, J.; Li, M.; Li, R.; Wolcott, M. P.; Zhang, J. "Green Epoxy Resin System Based on Lignin and Tung Oil and Its Application in Epoxy Asphalt". *ACS Sustainable Chem. Eng.* **2016**, 4, 2754-2761.

Starting materials: 5.00 g partially depolymerized lignin (4.70 mmol reactive sites per g lignin: 0.700 mmol AlOH per g lignin, 3.70 mmol ArOH per g lignin, 0.3 mmol COOH per g lignin), 30.0 g epichlorohydrin (314 mmol, 13.4 equiv.), 75 mg benzyltriethylammonium chloride (329 µmol, 1.40 mol%), 1.23 g sodium hydroxide (30.8 mmol, 1.31 equiv.), 50 g dimethyl sulfoxide.

Desired product: 5.02 g (isolated yield)

$$E_{simple} = \frac{\sum starting\ materials - desired\ product}{desired\ product} = \frac{36.31 - 5.02}{5.02} = 6.23$$

$$E_{complex} = \frac{\sum starting\ materials\ (+solvents) - desired\ product}{desired\ product} = \frac{86.31 - 5.02}{5.02}$$
$$= 16.19$$

$$Solvent\ contribution = \frac{weight\ of\ solvent}{\sum starting\ materials\ (+solvent) - desired\ product} = \frac{50}{81.29}$$
$$= 0.615 = \mathbf{61.5}\%$$

Silau, H.; Garcia, A. G.; Woodley, J. M.; Dam-Johansen, K.; Daugaard, A. E. "Bio-Based Epoxy Binders from Lignin Derivatized with Epoxidized Rapeseed Fatty Acids in Bimodal Coating Systems". *ACS Appl. Polym. Mater*. **2022**, 4, 444-451.

Epoxidation of rapeseed oil fatty acid mixture

Starting materials: 50 g biodiesel fatty acids (238 mmol vinyl groups), 27.3 g formic acid (594 mmol, 2.00 equiv.), 67.3 g hydrogen peroxide (30 wt%, 594 mmol, 2.00 equiv.), 129.75 g toluene (150 mL).

Desired product: 47.5 g (isolated yield)

$$E_{simple} = \frac{\sum starting\ materials - desired\ product}{desired\ product} = \frac{97.532 - 47.5}{47.5} = 1.05$$

$$E_{complex} = \frac{\sum starting\ materials\ (+solvents) - desired\ product}{desired\ product} = \frac{274.42 - 47.5}{47.5}$$
$$= 4.78$$

$$Solvent\ contribution = \frac{weight\ of\ solvent}{\sum starting\ materials\ (+solvent) - desired\ product} = \frac{176.89}{226.92}$$
$$= 0.780 = \mathbf{78.0}\%$$

Steglich esterification

Starting materials: 10.0 g kraft lignin (6.40 mmol OH per g lignin), 0.78 g 4-dimethylaminopyridine (6.40 mmol, 10 mol%), 38.5 g epoxidized fatty acid (128 mmol, 2.00 equiv.), 14.52 g dicyclohexylcarbodiimide (70.4 mmol, 1.10 equiv.), 222.25 g tetrahydrofuran (250 mL).

Desired product: 12.05 g (isolated yield)

$$E_{simple} = \frac{\sum starting\ materials - desired\ product}{desired\ product} = \frac{63.8 - 12.05}{12.05} = 4.29$$

$$E_{complex} = \frac{\sum starting\ materials\ (+solvents) - desired\ product}{desired\ product} = \frac{286.05 - 12.05}{12.05}$$
$$= 22.74$$

$$Solvent\ contribution = \frac{weight\ of\ solvent}{\sum starting\ materials\ (+solvent) - desired\ product} = \frac{222.25}{274}$$
$$= 0.811 = \mathbf{81.1}\%$$

E-factor of complete sequence

Reaction 1: A (fatty acids) + Reagents→ B (epoxidized Fatty Acids(eFA))

Reaction 2: B (eFA) + C (lignin) + Reagents→ D (lignin epoxide)

Reaction 1: $E_{complex}$: 4.78 $\frac{\text{kg waste}}{\text{kg eFA}}$

Reaction 2: $E_{complex}$: 22.74 $\frac{\text{kg waste}}{\text{kg lignin epoxide}}$; **Multiplier Reaction 1:** $\frac{\text{kg eFA}}{\text{kg lignin epoxide}} = \frac{38.5}{12.05} = 3.20$

$E_{sequence}$: 22.74 $\frac{\text{kg waste}}{\text{kg lignin epoxide}}$ (**Reaction 2**)

+ 4.78 $\frac{\text{kg waste}}{\text{kg eFA}}$ × 3.20 $\frac{\text{kg eFA}}{\text{kg lignin epoxide}}$ (**Reaction 1**)

= 38.00 $\frac{\text{kg waste}}{\text{kg lignin epoxide}}$

Laurichesse, S.; Huillet, C.; Avérous, L. “Original Polyols based on Organosolv Lignin and Fatty Acids: New Bio-based Building Blocks for Segmented Polyurethane Synthesis”. *Green Chem*. **2014**, 16, 3958-3970.

Chlorination of oleic acid

Starting materials: 40.0 g oleic acid (142 mmol), 35.95 g oxalyl chloride (283 mmol, 2.00 equiv.), 270.6 g ethyl acetate (300 mL)

Desired product: 42.6 g (142 mmol, theoretical yield)

$$E_{simple} = \frac{\sum starting\ materials - desired\ product}{desired\ product} = \frac{75.95 - 42.6}{42.6} = 0.78$$

$$E_{complex} = \frac{\sum starting\ materials\ (+solvents) - desired\ product}{desired\ product} = \frac{346.55 - 42.6}{42.6} = 7.13$$

$$Solvent\ contribution = \frac{weight\ of\ solvent}{\sum starting\ materials\ (+solvent) - desired\ product} = \frac{270.6}{304.02} = 0.890 = \mathbf{89.0}\%$$

Esterification of organosolv lignin with oleyl chloride

Starting materials: 30 g organosolv lignin (2.26 mmol OH per g lignin), 40.7 g oleyl chloride (135 mmol, 2.00 equiv.).

Desired product: 45.0 g (isolated yield)

$$E_{simple} = \frac{\sum starting\ materials - desired\ product}{desired\ product} = \frac{70.7 - 45.0}{45.0} = 0.57$$

$E_{complex} = E_{simple}$ because no additional solvents are used.

Epoxidation of oleic acid lignin ester

Starting materials: 45 g esterified lignin (1.6 mmol double bonds per g lignin), 10.95 g peracetic acid (144 mmol, 2.00 equiv.), 331.25 g dichloromethane (250 mL).

Desired product: 46.15 g (theoretical yield)

$$m_f = m_i \left(1 + \Delta M_{graft} \left(reactive\ sites\ in \frac{mol}{g}\right)\right)$$

$$m_f = 45.0\ g\ \left(1 + 15.999\ \frac{g}{mol}(1.60 \times 10^{-3}\ \frac{mol}{g})\right) = 46.15\ g$$

$$E_{simple} = \frac{\sum starting\ materials - desired\ product}{desired\ product} = \frac{55.95 - 46.15}{46.15} = 0.21$$

$$E_{complex} = \frac{\sum starting\ materials\ (+solvents) - desired\ product}{desired\ product} = \frac{387.2 - 46.15}{46.15}$$

$$= 7.39$$

$$Solvent\ contribution = \frac{weight\ of\ solvent}{\sum starting\ materials\ (+solvent) - desired\ product} = \frac{331.25}{341.05}$$

$$= 0.971 = \mathbf{97.1}\%$$

E-factor of complete sequence

Reaction 1: A (oleic acid) + Reagents → B (oleyl chloride)

Reaction 2: B (oleyl Chloride) + C (lignin) + Reagents→ D (lignin ester)

Reaction 3: D (lignin ester) + Reagents → E (lignin epoxide)

Reaction 1: $E_{complex}$: 7.13 $\frac{\text{kg waste}}{\text{kg oleyl chloride}}$

Reaction 2: $E_{complex}$: 0.57 $\frac{\text{kg waste}}{\text{kg lignin ester}}$; **Multiplier Reaction 1:** $\frac{\text{kg oleyl chloride}}{\text{kg lignin ester}} = \frac{40.7}{45.0} = 0.904$

Reaction 3: $E_{complex}$: 7.39 $\frac{\text{kg waste}}{\text{kg lignin epoxide}}$; **Multiplier Reaction 2:** $\frac{\text{kg lignin ester}}{\text{kg lignin epoxide}} = \frac{45.0}{46.15} = 0.975$

$E_{sequence}$: 7.39 $\frac{\text{kg waste}}{\text{kg lignin epoxide}}$ (**Reaction 3**)

+ 0.57 $\frac{\text{kg waste}}{\text{kg lignin ester}}$ × 0.975 $\frac{\text{kg lignin ester}}{\text{kg lignin epoxide}}$ (**Reaction 2**)

+ 7.13 $\frac{\text{kg waste}}{\text{kg oleyl chloride}}$ × 0.904 $\frac{\text{kg oleyl chloride}}{\text{kg lignin ester}}$ × 0.975 $\frac{\text{kg lignin ester}}{\text{kg lignin epoxide}}$ (**Reaction 1**)

= 14.24

Liu, L.-Y.; Hua, Q.; Renneckar, S. "A Simple Route to synthesize Esterified Lignin Derivatives". *Green Chem*. **2019**, 21, 3682-3692.

Hydroxyethylation of organosolv lignin

Starting materials: 30 g organosolv lignin (6.36 mmol reactive sites per g lignin: 1.97 mmol AlOH per g lignin, 4.07 mmol ArOH per g lignin, 0.32 mmol COOH per g lignin), 64.51 g ethylene carbonate (733 mmol, 6.00 equiv. of ArOH), 1.29 g sodium carbonate (12.2 mmol, 0.100 equiv. of ArOH).

Desired product: 30 g (isolated yield; 4.30 mmol AlOH and 0.41 mmol ArOH per g lignin, 0.02 mmol COOH per g lignin**,** 91% AlOH)

$$E_{simple} = \frac{\sum starting\ materials - desired\ product}{desired\ product} = \frac{95.80 - 30.0}{30.0} = 2.19$$

$E_{complex} = E_{simple}$ because no additional solvents are used.

Esterification of hydroxyethylated lignin with oleic acid

Starting materials: 5 g hydroxyethylated lignin (4.71 mmol reactive sites per g lignin: 4.30 mmol AlOH per g lignin, 0.41 mmol ArOH per g lignin, 0.02 COOH per g lignin), 44.5 g oleic acid (50 mL, 158 mmol, 6.66 equiv.).

Recycled starting materials: 40.05 g oleic acid (90%)

Desired product: 3 g (isolated yield)

$$E_{simple} = \frac{\sum starting\ materials - desired\ product - recycled\ oleic\ acid}{desired\ product}$$

$$= \frac{49.5 - 3.0 - 40.05}{3.0}$$

$$E_{simple} = \frac{49.5 - 3.00 - 40.05}{3.00} = 2.15$$

$E_{complex} = E_{simple}$ because no additional solvents are used.

E-factor of complete sequence

Reaction 1: A (lignin) + Reagents→ B (hydroxyethylated lignin (HEL))

Reaction 2: B (HEL) + Reagents→ C (lignin ester)

Reaction 1: $E_{complex}$: 2.19 $\frac{\text{kg waste}}{\text{kg hEL}}$

Reaction 2: $E_{complex}$: 2.15 $\frac{\text{kg waste}}{\text{kg lignin ester}}$; **Multiplier Reaction 1:** $\frac{\text{kg hEL}}{\text{kg lignin ester}} = \frac{5}{3} = 1.667$

$E_{sequence}$: 2.15 $\frac{\text{kg waste}}{\text{kg lignin ester}}$ (**Reaction 2**)

+ 2.19 $\frac{\text{kg waste}}{\text{kg hEL}}$ × 1.667 $\frac{\text{kg hEL}}{\text{kg lignin ester}}$ (**Reaction 1**)

= 5.80

Vásquez-Garay, F.; Teixeira Mendonça, R.; Peretti, S. W. “Chemoenzymatic Lignin Valorization: Production of Epoxidized Pre-polymers using Candida Antarctica Lipase B. Enzyme”. *Microb. Technol*. **2018**, 112, 6-13.

Allylation of organosolv lignin

Starting materials: 3.0 g organosolv lignin (2.29 mmol OH per g lignin), 4.7 g potassium carbonate (34.0 mmol, 4.95 equiv.), 4.05 g allyl bromide (97 wt%, 32.5 mmol, 4.73 equiv.), 94.4 g dimethylformamide (100 mL).

Desired product: 3.28 g (theoretical yield)

$$m_f = m_i \left(1 + \Delta M_{graft}\left(reactive\ sites\ in \frac{mol}{g}\right)\right)$$

$$m_f = 3.0\ g\ \left(1 + 40.065\ \frac{g}{mol}\left(2.29 \times 10^{-3}\ \frac{mol}{g}\right)\right) = 3.28\ g$$

$$E_{simple} = \frac{\sum starting\ materials - desired\ product}{desired\ product} = \frac{11.75 - 3.28}{3.28} = 2.58$$

$$E_{complex} = \frac{\sum starting\ materials\ (+solvents) - desired\ product}{desired\ product} = \frac{106.15 - 3.28}{3.28} = 31.36$$

$$Solvent\ contribution = \frac{weight\ of\ solvent}{\sum starting\ materials\ (+solvent) - desired\ product} = \frac{94.4}{102.87} = 0.918 = \mathbf{91.8}\%$$

Epoxidation of allylated lignin

Starting materials: 3 g allylated lignin (2.09 mmol double bonds per g lignin), 2.46 g caprylic acid (17.1 mmol, 2.72 equiv.), 0.6 g immobilized lipase, 4.27 g hydrogen peroxide (30 wt%, 37.7 mmol, 6.00 equiv.), 147.05 g toluene (170 mL).

Desired product: 3.0 g (isolated yield)

$$E_{simple} = \frac{\sum starting\ materials - desired\ product}{desired\ product} = \frac{7.34 - 3.0}{3.0} = 1.45$$

$$E_{complex} = \frac{\sum starting\ materials\ (+solvents) - desired\ product}{desired\ product} = \frac{157.38 - 3.0}{3.0}$$

$$= 51.46$$

$$Solvent\ contribution = \frac{weight\ of\ solvent}{\sum starting\ materials\ (+solvent) - desired\ product} = \frac{147.05}{154.38} = 0.972 =$$

$\mathbf{97.2}\%$

E-factor of complete sequence

Reaction 1: A (lignin) + Reagents→ B (allylated lignin)

Reaction 2: B (allylated lignin) + Reagents→ C (lignin epoxide)

Reaction 1: $E_{complex}$: 31.36 $\frac{\text{kg waste}}{\text{kg allylated lignin}}$

Reaction 2: $E_{complex}$: 51.46 $\frac{\text{kg waste}}{\text{kg lignin epoxide}}$; **Multiplier Reaction 1:** $\frac{\text{kg allylated lignin}}{\text{kg lignin epoxide}} = 1.0$

$E_{sequence}$: 51.46 $\frac{\text{kg waste}}{\text{kg lignin epoxide}}$ (**Reaction 2**)

+ 31.36 $\frac{\text{kg waste}}{\text{kg allylated lignin}}$ × 1.0 $\frac{\text{kg allylated lignin}}{\text{kg lignin epoxide}}$ (**Reaction 1**)

= 82.82

7.4 E-Factor Calculations for Carboxylic Acid Functionalized Lignin

Hirose, S.; Hatakeyama, T.; Hatakeyama, H. “Synthesis and Thermal Properties of Epoxy Resins from Ester-Carboxylic Acid Derivative of Alcoholysis Lignin”. *Macromolecular Symposia*. **2003**, 197, 157-170.

Starting materials: 50 g alcoholysis lignin, 50 g ethylene glycol (806 mmol), 196 g succinic anhydride (1.96 mol), 2.69 g dimethylbenzylamine (19.9 mmol).

Desired product: 298.69 g (“ALEGPA”, theoretical yield)

$$E_{complex} = \frac{\sum starting\ materials\ (+solvents) - desired\ product}{desired\ product} = \frac{298.69 - 289.69}{298.69} = 0$$

$$Lignin\ \text{wt\%}\ \text{in ALEGPA} = \frac{50}{298.69} = 0.167 = \mathbf{16.7}\%$$

Exemplary wt% calculation of lignin in epoxy resin with 100% and 80% ALEGPA (acid/epoxy = 1.0)

Carboxylic acid content (ALEGPA) = 6.62 mmol × g^{-1}

Carboxylic acid content (ethylene glycol polyacid, EGPA) = 7.63 mmol × g^{-1}

Epoxy content (EGDGE) = 7.70 mmol × g^{-1}

$$\text{Lignin wt\% in 100\% ALEGPA Resin} = \frac{\text{m(ALEGPA)}}{\text{m(ALEGPA)} + \text{m(EGDGE)}} \times \text{wt\% lignin in ALEGPA}$$

$$= \frac{\frac{1}{6.62}}{\frac{1}{6.62} + \frac{1}{7.70}} \times 16.7\ wt\% = 8.98\ wt\%$$

$$\text{Lignin wt\% in 80\% ALEGPA, 20\% EGPA Resin} =$$

$$\frac{\text{m(ALEGPA)}}{\text{m(ALEGPA)+m(EGPA)+m(EGDGE)}} \times \text{wt\% lignin in ALEGPA} = \frac{0.8}{0.8+0.2+\frac{(0.8\times 6.62+0.2\times 7.63)}{7.70}} \times 16.7\ \text{wt\%}$$

$$= 7.08\ \text{wt\%}$$

7.5 E-Factor Calculations for Ester Group Functionalized Lignin

Calculated E-factors for esterification procedures are summarized in **Table 7.5.1**. Below the table, all calculations are listed to ensure reproducibility.

Table 7.5.1 - E-factors for esterification procedures.

Work	Modification	Functionalizing agent	E_{simple}	$E_{complex}$	$E_{solvent}$ (%)	$E_{sequence}$
Koivu[210]	Esterification	1. Acetyl chloride	1.02	6.65	85	–
		2. Octanoyl chloride	1.63	7.25	78	–
		3. Lauroyl chloride	2.03	7.66	73	–
		4. Palmitoyl chloride	2.44	8.07	70	–
Dubois[212]	Esterification	Oleyl chloride	0.08[a]	–	–	–
	1.Chlorination	Oxalyl chloride	0.86	2.01	57	1.25
	2.Esterification	10-Undecenoyl chloride	0.10[a]	–	–	
Avérous[179]	Chlorination	Oxalyl chloride	0.78[a]	7.13[a]	89	–
Wool[194]	Esterification	1. Acetic anhydride	2.05	–	–	–
		2. Propionic anhydride	2.05	–	–	–
		3. Butyric anhydride	2.05	–	–	–
		4. Methacrylic anhydride	6.36	10.5	39	10.5
Luo[214]	Esterification	1. Crotonic anhydride	1.75	–	–	–
		2. Butyric anhydride	1.59	–	–	–
Renneckar[182,224]	1.Hydroxyethylation	Ethylene carbonate[182]	2.19	–	–	–
	2.Esterification	1a. Propionic acid[224]	9.93	–	–	12.1
		1b. Propionic acid with recycling[182]	0.99	–	–	3.18
		2. Valeric acid[182]	0.94	–	–	3.13
		3. Octanoic acid[182]	0.91	–	–	3.10
		4. Oleic acid[182]	2.15	–	–	5.80
Verge[225]	Esterification	3-(4-Hydroxyphenyl) propanoic acid	1.19	–	–	–

[a]: no final weight of isolated product was reported, therefore final weight of the product was calculated based on theoretical yield.

Koivu, K. A. Y.; Sadeghifar, H.; Nousiainen, P. A.; Argyropoulos, D. S.; Sipilä, J. “Effect of Fatty Acid Esterification on the Thermal Properties of Softwood Kraft Lignin”. *ACS Sustainable Chem. Eng*. **2016**, 4, 5238-5247.

Starting materials: 5.0 g softwood kraft lignin (6.70 mmol reactive groups per g lignin: 2.30 mmol AlOH per g lignin, 4.40 mmol ArOH per g lignin), 3.72 g pyridine (47.0 mmol, 1.40 equiv.), 26.67 g tetrahydrofuran (30 mL), 7.08 g dimethylformamide (7.5 mL), and 3.40 g acetyl chloride (43.4 mmol, 1.30 equiv.); or 7.05 g octanoyl chloride (43.4 mmol, 1.30 equiv.); or 9.48 g lauroyl chloride (43.4 mmol, 1.30 equiv.); or 11.92 g palmitoyl chloride (43.4 mmol, 1.30 equiv.).

Desired product: 6 g for all modifications (isolated yield)

Desired product	**Raw materials (total weight in g without solvent)**	**Raw materials (total weight in g with solvent)**	**Desired product (g)**	**E_{simple}**	**$E_{complex}$**	**$E_{solvent}$ (%)**
Lignin acetate	12.12	45.87	6	1.02	6.65	84.7
Lignin octanoate	15.77	49.52	6	1.63	7.25	77.6
Lignin laurate	18.20	51.95	6	2.03	7.66	73.4
Lignin palmitate	20.64	54.39	6	2.44	8.07	69.7

Xing, Q.; Ruch, D.; Dubois, P.; Wu, L.; Wang, W.-J. “Biodegradable and high-Performance Poly(butylene adipate-co-terephthalate)–Lignin UV-Blocking Films”. *ACS Sustainable Chem. Eng*. **2017**, 5, 10342-10351.

Chlorination of 10-undecenoic acid

Starting materials: 25 g 10-undecenoic acid (136 mmol), 26.25 g oxalyl chloride (204 mmol, 1.50 equiv.), 31.57 g ethyl acetate.

Desired product: 27.5 g (isolated yield, 95%)

$$E_{simple} = \frac{\sum starting\ materials - desired\ product}{desired\ product} = \frac{51.25 - 27.5}{27.5} = 0.86$$

$$E_{complex} = \frac{\sum starting\ materials\ (+solvents) - desired\ product}{desired\ product} = \frac{82.82 - 27.5}{27.5} = 2.01$$

$$Solvent\ contribution = \frac{weight\ of\ solvent}{\sum starting\ materials\ (+solvent) - desired\ product} = \frac{31.57}{55.32}$$
$$= 0.571 = \mathbf{57.1}\%$$

Esterification of soda lignin with 10-undecenoyl chloride and oleyl chloride

Starting materials: 40 g soda lignin (5.20 mmol OH per g lignin), and 62.59 g oleyl chloride (208 mmol, 1.00 equiv.) or 42.17 g 10-undecenoyl chloride (208 mmol, 1.00 equiv.).

Desired products:

Oleyl lignin: 95.0 g (theoretical yield, ΔM_{graft} = 264.453 g mol^{-1})

10-Undecenoyl lignin: 74.58 g (theoretical yield, ΔM_{graft} = 166.264 g mol^{-1})

Desired product	Raw materials (total weight in g without solvent)	Raw materials (total weight in g with solvent)	Desired product (g)	E_{simple}	$E_{complex}$	$E_{solvent}$ (%)
Oleyl lignin	102.59	102.59	95.0	0.08	–	–
10-Undecenoyl lignin	82.17	82.17	74.58	0.10	–	–

E-factor of esterification sequence

Reaction 1: A (10-undecenoic acid) + Reagents→ B (10-undecenoyl chloride)

Reaction 2: B (10-undecenoyl chloride) + Reagents→ C (lignin ester)

Reaction 1: $E_{complex}$: 2.01 $\frac{\text{kg waste}}{\text{kg undecenoyl chloride}}$

Reaction 2: $E_{complex}$: 0.10 $\frac{\text{kg waste}}{\text{kg lignin ester}}$; **Multiplier Reaction 1:**

$\frac{\text{kg undecenoyl chloride}}{\text{kg lignin ester}} = \frac{42.17}{74.58} = 0.57$

$E_{sequence}$: 0.10 $\frac{\text{kg waste}}{\text{kg lignin ester}}$ (**Reaction 2**)

+ 2.01 $\frac{\text{kg waste}}{\text{kg undecenoyl chloride}}$ × 0.57 $\frac{\text{kg undecenoyl chloride}}{\text{kg lignin ester}}$ (**Reaction 1**)

= 1.25

Laurichesse, S.; Huillet, C.; Avérous, L. “Original Polyols Based on Organosolv Lignin and Fatty Acids: New Bio-based Building Blocks for Segmented Polyurethane Synthesis”. *Green Chem*. **2014**, 16, 3958-3970.

Chlorination of oleic acid

Starting materials: 40.0 g oleic acid (142 mmol), 35.95 g oxalyl chloride (283 mmol, 2.00 equiv.), 270.6 g ethyl acetate (300 mL)

Desired product: 42.6 g (142 mmol, theoretical yield)

$$E_{simple} = \frac{\sum starting\ materials - desired\ product}{desired\ product} = \frac{75.95 - 42.6}{42.6} = 0.78$$

$$E_{complex} = \frac{\sum starting\ materials\ (+solvents) - desired\ product}{desired\ product}$$

$$= \frac{346.55 - 42.6}{42.6} = 7.13$$

$$Solvent\ contribution = \frac{weight\ of\ solvent}{\sum starting\ materials\ (+solvent) - desired\ product} = \frac{270.6}{304.02} = 0.890$$

$$= \mathbf{89.0}\%$$

Thielemans, W.; Wool, R. P. “Lignin Esters for Use in Unsaturated Thermosets: Lignin Modification and Solubility Modeling”. *Biomacromolecules*. **2005**, 6, 1895-1905.

Starting materials: 1 g kraft lignin, 50.0 mg 1-methylimidazole (609 µmol), and 2.00 g acetic anhydride (19.6 mmol) or 2.00 g propionic anhydride (15.4 mmol) or 2.00 g butyric anhydride (12.6 mmol) or 6.31 g methacrylic anhydride (40.9 mmol) and 4.14 g dioxane (4 mL).

Desired product: 1 g for all modifications (isolated yield)

Desired product	Raw materials (total weight in g without solvent)	Raw materials (total weight in g with solvent)	Desired product (g)	E_{simple}	$E_{complex}$	$E_{solvent}$ (%)
Lignin acetate	3.05	3.05	1	2.05	–	–
Lignin propionate	3.05	3.05	1	2.05	–	–
Lignin butyrate	3.05	3.05	1	2.05	–	–
Lignin methacrylate	7.36	11.5	1	6.36	10.5	39.4

Luo, S.; Cao, J.; McDonald, A. G. “Cross-linking of Technical Lignin via Esterification and Thermally Initiated Free Radical Reaction”. *Ind. Crops Prod*. **2018**, 121, 169-179.

Starting materials: 10 g kraft lignin (5.10 mmol OH per g lignin), 1.03 g 1-methylimidazole (12.5 mmol, 25.0 mol%), and 26.0 g crotonic anhydride (167 mmol, 3.31 equiv.) or 24.18 g butyric anhydride (153 mmol, 3.00 equiv.).

Desired products:

Lignin crotonate: 13.47 g (theoretical yield, ΔM_{graft} = 68.075 g mol^{-1})

Lignin butyrate: 13.57 g (theoretical yield, ΔM_{graft} = 70.091 g mol^{-1})

Desired product	Raw materials (total weight in g without solvent)	Raw materials (total weight in g with solvent)	Desired product (g)	E_{simple}	$E_{complex}$	$E_{solvent}$ (%)
Lignin crotonate	37.03	37.03	13.47	1.75	–	–
Lignin butyrate	35.21	35.21	13.57	1.59	–	–

Liu, L.-Y.; Cho, M.; Sathitsuksanoh, N.; Chowdhury, S.; Renneckar, S. “Uniform Chemical Functionality of Technical Lignin Using Ethylene Carbonate for Hydroxyethylation and Subsequent Greener Esterification”. *ACS Sustainable Chem. Eng*. **2018**, 6, 12251-12260.

Hydroxyethylation of organosolv lignin

Note: Calculation is performed from other reference of same authors to allow sequence calculation[7]

Starting materials: 30 g organosolv lignin (6.36 mmol reactive sites per g lignin: 1.97 mmol AlOH per g lignin, 4.07 mmol ArOH per g lignin, 0.32 mmol COOH per g lignin), 64.51 g ethylene carbonate (733 mmol, 6.00 equiv. of ArOH), 1.29 g sodium carbonate (12.2 mmol, 0.100 equiv. of ArOH).

Desired product: 30 g (isolated yield; 4.30 mmol AlOH and 0.41 mmol ArOH per g lignin, 0.02 mmol COOH per g lignin**, 91% AlOH**)

$$E_{simple} = \frac{\sum starting\ materials - desired\ product}{desired\ product} = \frac{95.80 - 30.0}{30.0} = 2.19$$

$E_{complex} = E_{simple}$ because no additional solvents are used.

Esterification of hydroxyethylated lignin with propionic acid (no recycling)

Starting materials: 1 g hydroxyethylated lignin, 9.93 g propionic acid (10 mL).

Desired product: 1 g (isolated yield)

$$E_{simple} = \frac{\sum starting\ materials - desired\ product}{desired\ product} = \frac{10.93 - 1.0}{1.0} = 9.93$$

$E_{complex} = E_{simple}$ because no additional solvents are used.

E-factor of sequence: hydroxyethylation and esterification with propionic acid (no recycling)

Reaction 1: A (lignin) + Reagents→ B (hydroxyethylated lignin (HEL))

Reaction 2: B (HEL) + Reagents→ C (lignin ester)

Reaction 1: $E_{complex}$: 2.19 $\frac{\text{kg waste}}{\text{kg hEL}}$

Reaction 2: $E_{complex}$: 9.93 $\frac{\text{kg waste}}{\text{kg lignin ester}}$; **Multiplier Reaction 1:** $\frac{\text{kg hEL}}{\text{kg lignin ester}} = \frac{1}{1} = 1.0$

$E_{sequence}$: 9.93 $\frac{\text{kg waste}}{\text{kg lignin ester}}$ (**Reaction 2**)

+ 2.19 $\frac{\text{kg waste}}{\text{kg hEL}}$ × 1.0 $\frac{\text{kg hEL}}{\text{kg lignin ester}}$ (**Reaction 1**)

= 12.12

Liu, L.-Y.; Hua, Q.; Renneckar, S. “A simple Route to synthesize Esterified Lignin Derivatives”. *Green Chem.* **2019**, 21, 3682-3692.

Hydroxyethylation of organosolv lignin

Starting materials: 30 g organosolv lignin (6.36 mmol reactive sites per g lignin: 1.97 mmol AlOH per g lignin, 4.07 mmol ArOH per g lignin, 0.32 mmol CO_2H per g lignin), 64.51 g ethylene carbonate (733 mmol, 6.00 equiv. of ArOH), 1.29 g sodium carbonate (12.2 mmol, 0.100 equiv. of ArOH).

Desired product: 30 g (isolated yield; 4.30 mmol AlOH and 0.41 mmol ArOH per g lignin, 0.02 mmol CO_2H per g lignin, **91% AlOH**)

$$E_{simple} = \frac{\sum starting\ materials - desired\ product}{desired\ product} = \frac{95.80 - 30.0}{30.0} = 2.19$$

$E_{complex} = E_{simple}$ because no additional solvents are used.

Esterification of hydroxyethylated lignin with propionic acid (recycling)

Starting materials: 5 g hydroxyethylated lignin (4.71 mmol reactive sites per g lignin: 4.30 mmol AlOH per g lignin, 0.41 mmol ArOH per g lignin, 0.02 mmol COOH per g lignin), 49.65 g propionic acid (50 mL, 670 mmol, 28.5 equiv.).

Recycled starting materials: 44.69 g propionic acid (90%)

Desired product: 5 g (isolated yield)

$$E_{simple} = \frac{\sum starting\ materials - desired\ product - recycled\ propionic\ acid}{desired\ product}$$

$$E_{simple} = \frac{54.65 - 5.00 - 44.69}{5.00} = 0.99$$

$E_{complex} = E_{simple}$ because no additional solvents are used.

E-factor of sequence: hydroxyethylation and esterification with propionic acid (recycling)

Reaction 1: A (lignin) + Reagents→ B (hydroxyethylated lignin (HEL))

Reaction 2: B (HEL) + Reagents→ C (lignin ester)

Reaction 1: $E_{complex}$: 2.19 $\frac{\text{kg waste}}{\text{kg hEL}}$

Reaction 2: $E_{complex}$: 0.99 $\frac{\text{kg waste}}{\text{kg lignin ester}}$; **Multiplier Reaction 1:** $\frac{\text{kg hEL}}{\text{kg lignin ester}} = \frac{5}{5} = 1.00$

$E_{sequence}$: 0.99 $\frac{\text{kg waste}}{\text{kg lignin ester}}$ (**Reaction 2**)

+ 2.19 $\frac{\text{kg waste}}{\text{kg hEL}}$ × 1.00 $\frac{\text{kg hEL}}{\text{kg lignin ester}}$ (**Reaction 1**)

= 3.18

Esterification of hydroxyethylated lignin with valeric acid (recycling)

Starting materials: 5 g hydroxyethylated lignin (4.71 mmol reactive sites per g lignin: 4.30 mmol AlOH per g lignin, 0.41 mmol ArOH per g lignin, 0.02 mmol COOH per g lignin), 46.95 g valeric acid (50 mL, 460 mmol, 19.5 equiv.).

Recycled starting materials: 42.26 g valeric acid (90%)

Desired product: 5 g (isolated yield)

$$E_{simple} = \frac{\sum starting\ materials - desired\ product - recycled\ valeric\ acid}{desired\ product}$$

$$E_{simple} = \frac{51.95 - 5.00 - 42.26}{5.00} = 0.94$$

$E_{complex} = E_{simple}$ because no additional solvents are used.

E-factor of sequence: hydroxyethylation and esterification with valeric acid (recycling)

Reaction 1: A (lignin) + Reagents→ B (hydroxyethylated lignin (HEL))

Reaction 2: B (HEL) + Reagents→ C (lignin ester)

Reaction 1: $E_{complex}$: 2.19 $\frac{\text{kg waste}}{\text{kg hEL}}$

Reaction 2: $E_{complex}$: 0.94 $\frac{\text{kg waste}}{\text{kg lignin ester}}$; **Multiplier Reaction 1:** $\frac{\text{kg hEL}}{\text{kg lignin ester}} = \frac{5}{5} = 1.00$

$E_{sequence}$: 0.94 $\frac{\text{kg waste}}{\text{kg lignin ester}}$ (**Reaction 2**)

+ 2.19 $\frac{\text{kg waste}}{\text{kg hEL}}$ × 1.00 $\frac{\text{kg hEL}}{\text{kg lignin ester}}$ (**Reaction 1**)

= 3.13

Esterification of hydroxyethylated lignin with octanoic acid (recycling)

Starting materials: 5 g hydroxyethylated lignin (**4**.71 mmol reactive sites per g lignin: 4.30 mmol AlOH per g lignin, 0.41 mmol ArOH per g lignin, 0.02 mmol COOH per g lignin), 45.5 g octanoic acid (50 mL, 316 mmol, 13.4 equiv.).

Recycled starting materials: 40.95 g octanoic acid (90%)

Desired product: 5 g (isolated yield)

$$E_{simple} = \frac{\sum starting\ materials - desired\ product - recycled\ octanoic\ acid}{desired\ product}$$

$$E_{simple} = \frac{50.5 - 5.00 - 40.95}{5.00} = 0.91$$

$E_{complex} = E_{simple}$ because no additional solvents are used.

E-factor of sequence: hydroxyethylation and esterification with octanoic acid (recycling)

Reaction 1: A (lignin) + Reagents→ B (hydroxyethylated lignin (HEL))

Reaction 2: B (HEL) + Reagents→ C (lignin ester)

Reaction 1: $E_{complex}$: 2.19 $\frac{\text{kg waste}}{\text{kg hEL}}$

Reaction 2: $E_{complex}$: 0.91 $\frac{\text{kg waste}}{\text{kg lignin ester}}$; **Multiplier Reaction 1:** $\frac{\text{kg hEL}}{\text{kg lignin ester}} = \frac{5}{5} = 1.00$

$E_{sequence}$: 0.91 $\frac{\text{kg waste}}{\text{kg lignin ester}}$ (**Reaction 2**)

+ 2.19 $\frac{\text{kg waste}}{\text{kg hEL}}$ × 1.00 $\frac{\text{kg hEL}}{\text{kg lignin ester}}$ (**Reaction 1**)

= 3.10

Esterification of hydroxyethylated lignin with oleic acid (recycling)

Starting materials: 5 g hydroxyethylated lignin (**4**.71 mmol reactive sites per g lignin: 4.30 mmol AlOH per g lignin, 0.41 mmol ArOH per g lignin, 0.02 COOH per g lignin), 44.5 g oleic acid (50 mL, 158 mmol, 6.66 equiv.).

Recycled starting materials: 40.05 g oleic acid (90%)

Desired product: 3 g (isolated yield)

$$E_{simple} = \frac{\sum starting\ materials - desired\ product - recycled\ oleic\ acid}{desired\ product}$$

$$= \frac{49.5 - 3.0 - 40.05}{3.0}$$

$$E_{simple} = \frac{49.5 - 3.00 - 40.05}{3.00} = 2.15$$

$E_{complex} = E_{simple}$ because no additional solvents are used.

E-factor of sequence: hydroxyethylation and esterification with oleic acid (recycling)

Reaction 1: A (lignin) + Reagents→ B (hydroxyethylated lignin (HEL))

Reaction 2: B (HEL) + Reagents→ C (lignin ester)

Reaction 1: $E_{complex}$: 2.19 $\frac{\text{kg waste}}{\text{kg hEL}}$

Reaction 2: $E_{complex}$: 2.15 $\frac{\text{kg waste}}{\text{kg lignin ester}}$; **Multiplier Reaction 1:** $\frac{\text{kg hEL}}{\text{kg lignin ester}} = \frac{5}{3} =$ 1.667

$E_{sequence}$: $2.15\ \frac{\text{kg waste}}{\text{kg lignin ester}}$ (**Reaction 2**)

$+ 2.19\ \frac{\text{kg waste}}{\text{kg hEL}} \times 1.667\ \frac{\text{kg hEL}}{\text{kg lignin ester}}$ (**Reaction 1**)

$= 5.80$

Adjaoud, A.; Dieden, R.; Verge, P. "Sustainable Esterification of a Soda Lignin with Phloretic Acid". *Polymers*. **2021**, 13, 637.

Starting materials: 2 g soda lignin (2.00 mmol reactive sites per g lignin: 2.00 mmol AlOH per g lignin, 3.94 mmol ArOH per g lignin, 0.78 mmol CO_2H per g lignin), 3.32 g phloretic acid (20.0 mmol, 5.00 equiv.), 500 mg *para*-toluene sulfonic acid (2.90 mmol, 72.6 mol%).

Desired product: 2.66 g (theoretical yield)

$$m_f = m_i \left(1 + \Delta M_{graft} \left(reactive\ sites\ in \frac{mol}{g}\right)\right)$$

$$m_f = 2.0\ g\ \left(1 + 165.168\ \frac{g}{mol}(2.00 \times 10^{-3}\ \frac{mol}{g})\right) = 2.66\ g$$

$$E_{simple} = \frac{\sum starting\ materials - desired\ product}{desired\ product} = \frac{5.82 - 2.66}{2.66} = 1.19$$

$E_{complex} = E_{simple}$ because no additional solvents are used.

7.6 E-Factor Calculations for Multiple Bond Functionalized Lignin

Calculated E-factors for multiple bond insertion procedures are summarized in **Table 7.6.1**, all calculations are listed to ensure reproducibility.

Table 7.6.1 - Calculated E-factors for multiple bond insertion.

Work	Modification	Functionalizing agent	E_{simple}	$E_{complex}$	$E_{sequence}$
Renneckar[236]	Hydroxyethylation	Ethylene carbonate	4.80	–	7.76
	Esterification	Acrylic acid	3.07		
Meier and Over[247]	Allylation	Diallyl carbonate	5.42 - 9.43	–	–
Meier et al.[248]	Allylation	Diallylcarbonate	1.87[a]	–	–
Johansson[249]	Allylation	Diallyl carbonate	2.09[a]	–	–
Avérous[337]	Vinylation	Vinyl ethylene carbonate	6.01	–	–

[a]: no final weight of isolated product was reported, therefore final weight of the product was calculated based on theoretical yield.

Qi Hua, Li-Yang Liu, Mijung Cho, Muzaffer A. Karaaslan, Huaiyu Zhang, Chang Soo Kim, and Scott Renneckar “Functional Lignin Building Blocks: Reactive Vinyl Esters with Acrylic Acid”. *Biomacromolecules,* **2023**, 24, 2, 592–603.

Hydroxyethylation of softwood kraft lignin

10.0 g softwood kraft lignin (3.90 mmol ArOH per g lignin), 50 g ethylene carbonate (568 mmol, 14.5 equiv. in respect of the total of ArOH), 0.8 g Na_2CO_3 (7.55 mmol, 0.20 equiv.).

Desired product: 10.5 g (isolated yield)

$$E_{simple}\ hydroxyethylation = \frac{\sum starting\ materials\ step\ 1 - desired\ product\ 1}{desired\ product\ 1} = \frac{60.8-10.5}{10.5} = 4.8$$

Esterification of hydroxyethylated lignin with acrylic acid

1.00 g hydroxyethylated lignin (4.30 mmol AlOH per g lignin, 0.38 mmol ArOH per g lignin, 0.11 mmol COOH per g lignin), 3.15 g acrylic acid (43.7 mmol, 3 mL, d=1.05 g/mL)

Desired product: 1.02 g (isolated yield)

$$E_{simple}\ esterification = \frac{\sum starting\ materials\ step\ 2 - desired\ product\ 2}{desired\ product\ 2} = \frac{4.15-1.02}{1.02} = 3.07$$

E-factor of whole sequence

Reaction 1: A (lignin) + Reagents→ B (hydroxyethylated lignin(HEL))

Reaction 2: B (hydroxyethylated lignin) + Reagents→ C (final product)

Reaction 1: $E_{complex}$: 4.8 $\frac{\text{kg waste}}{\text{kg hEL}}$

Reaction 2: $E_{complex}$: 3.07 $\frac{\text{kg waste}}{\text{kg final product}}$; **Multiplier Reaction 1:** $\frac{\text{kg hEL}}{\text{kg final product}} = \frac{1}{1.02} = 0.978$

$E_{sequence}$: 3.07 $\frac{\text{kg waste}}{\text{kg final product}}$ (**Reaction 2**)

+ 4.8 $\frac{\text{kg waste}}{\text{kg hEL}}$ × 0.978 $\frac{\text{kg hEL}}{\text{kg final prouct}}$ (**Reaction 1**)

= 7.76 $\frac{\text{kg waste}}{\text{kg final product}}$

Over, L. C.; Meier, M. A. R. “Sustainable Allylation of Organosolv Lignin with Diallyl Carbonate and Detailed Structural Characterization of Modified Lignin”. *Green Chem*. **2016**, 18 (1), 197–207.

Starting materials: 0.15 g organosolv lignin (6.10 mmol reactive sites per g lignin), 1.30 g diallyl carbonate (9.15 mmol DAC, 10.0 equiv.), 0.295 g tetrabutylammonium bromide (0.915 mmol TBAB, 1.00 equiv.)

Procedure for recovery of TBAB: obtained allylated lignin 0.140 g, recovered TBAB: 0.285 g (97%)

Procedure for recovery of DAC: obtained allylated lignin 0.146 g, DAC recovered: 0.807 g (62%)

$$E_{simple}(TBAB\ recov.) = \frac{\sum starting\ materials - desired\ product}{desired\ product} = \frac{1.46 - 0.14}{0.14} = 9.43$$

$$E_{simple}(DAC\ recov.) = \frac{\sum starting\ materials - desired\ product}{desired\ product} = \frac{0.938 - 0.146}{0.146} = 5.42$$

$E_{complex} = E_{simple}$ because no additional solvents are used.

Over, L. C.; Hergert, M.; Meier, M. A. R. “Metathesis Curing of Allylated Lignin and Different Plant Oils for the Preparation of Thermosetting Polymer Films with Tunable Mechanical Properties”. *Macromol. Chem. Phys*. **2017**, 218 (16), 1700177.

Starting materials: 30.0 g organosolv lignin (6.1 mmol reactive sites per g lignin), 76.0 g diallyl carbonate (535 mmol DAC, 3.00 equiv.), 11.9 g tetrabutylammonium bromide (37.0 mmol TBAB, 0.20 equiv.)

Recovery of TBAB: 10.9 g (92%)

Desired product: 37.3 g (theoretical yield)

$$m_f = m_i \left(1 + \Delta M_{graft} \left(reactive\ sites\ in \frac{mol}{g}\right)\right) = 30\ g\ (1 + 40.032 \frac{g}{mol}\left(6.1 \times 10^{-3} \frac{mol}{g}\right) = 37.3\ g$$

$$E_{simple}(TBAB\ recov.) = \frac{\sum starting\ materials - desired\ product}{desired\ product} = \frac{107 - 37.3}{37.3} = 1.87$$

$E_{complex} = E_{simple}$ because no additional solvents are used.

Ribca, I.; Sochor, B.; Betker, M.; Roth, S. V.; Lawoko, M.; Sevastyanova, O.; Meier, M. A. R.; Johansson, M. “Impact of Lignin Source on the Performance of Thermoset Resins”. *Eur. Polym. J. 2023*, 194, 112141.

Starting materials: 1.00 g hardwood lignin (6.00 mmol g^{-1} reactive sites per g lignin, 6.00 mmol per g lignin of various OH groups), 2.60 g diallyl carbonate (18.3 mmol DAC, 3.00 equiv.), 1.90 g tetrabutylammonium bromide (5.90 mmol TBAB, 1.00 equiv.)

Recovery of TBAB: 1.672 g (88%)

Desired product: 1.24 g (theoretical yield)

$$m_f = m_i \left(1 + \Delta M_{graft} \left(reactive\ sites\ in \frac{mol}{g}\right)\right) = 1\ g\ (1 + 40.032 \frac{g}{mol}\left(6 \times 10^{-3} \frac{mol}{g}\right) = 1.24\ g$$

$$E_{simple}(TBAB\ recov.) = \frac{\sum starting\ materials - desired\ product}{desired\ product} = \frac{3.828 - 1.24}{1.24} = 2.09$$

$E_{complex} = E_{simple}$ because no additional solvents are used.

Duval, A.; Avérous, L. “Cyclic Carbonates as Safe and Versatile Etherifying Reagents for the Functionalization of Lignins and Tannins”. *ACS Sustain. Chem. Eng*. 2017, 5 (8), 7334–7343.

Starting materials: 10 g Soda lignin (5.8 mmol g^{-1} reactive sites, 1.76 mmol AlOH per g lignin, 4.04 mmol COOH groups per g lignin), 66.17 g vinyl ethylene carbonate (580 mmol VEC, 10 equiv.), 0.8 g potassium carbonate (5.8 mmol K_2CO_3, 0.1 equiv.).

Desired product: 10.97 g (isolated yield, 78% of theoretical yield)

Theoretical yield:

$$m_f = m_i \left(1 + \Delta M_{graft} \left(reactive\ sites\ in \frac{mol}{g}\right)\right) = 10\ g\ (1 + 70 \frac{g}{mol}\left(5.8 \times 10^{-3} \frac{mol}{g}\right) = 14.06\ g$$

Isolated yield = 78%, 10.97 g

$$E_{simple} = \frac{\sum starting\ materials - desired\ product}{desired\ product} = \frac{76.97 - 10.97}{10.97} = 6.01$$

$E_{complex} = E_{simple}$ because no additional solvents are used.

7.7 E-Factor Calculations for Hydroxyl Group Functionalized Lignin

Table 7.7.1 – Summary of E-factor for hydroxyalkylation procedures*

Work	Modification	Functionalizing agent	E_{simple}	$E_{sequence}$
Lehnen et al.[256]	Hydroxyalkylation	Ethylene carbonate Propylene carbonate Butylene carbonate Glycerol carbonate	3.59[a] 3.89[a] 4.16[a] 4.19[a]	–
Avérous et al.[257]	Hydroxyalkylation	Ethylene carbonate Propylene carbonate Vinyl ethylene carbonate Glycerol carbonate	4.94 6.17 6.02 6.02	–
Avérous et al.[259]	Hydroxyalkylation	Ethylene carbonate (PEG)	0	–
Lehnen et al.[271]	Hydroxyalkylation Transesterification	Glycerol carbonate Dimethyl carbonate	4.19[a] 5.04[a]	9.06

* : no solvents have been used, therefore $E_{complex}$ is not reported. [a]: no final weight of isolated product was reported, therefore final weight of the product was calculated based on theoretical yield.

Kühnel, I.; Saake, B.; Lehnen, R. “Comparison of Different Cyclic Organic Carbonates in the Oxyalkylation of Various Types of Lignin”. *React. Funct. Polym*. **2017**, 120, 83–91.

Starting materials: 1.00 g organosolv lignin (5.17 mmol OH per g lignin), 4.55 g ethylene carbonate (EC, 51.7 mmol, 10.0 equiv.), or 5.28 g propylene carbonate (PC, 51.7 mmol, 10.0 equiv.), or 6.00 g butylene carbonate (BC, 51.7 mmol, 10.0 equiv.), or 6.10 g glycerol carbonate (GC, 51.7 mmol, 10.0 equiv.), 79 mg DBU (0.517 mmol, 0.10 equiv.).

Desired product: (theoretical yield, calculated for 5.17 x 10^{-3} mol g^{-1} reactive sites)

$$m_f = m_i \left(1 + \Delta M_{graft} \left(reactive\ sites\ in \frac{mol}{g}\right)\right)$$

Functionalizing agent	Raw materials (Total weight in g)	Desired product (Theoretical yield, g)	E_{simple}	$E_{complex}$	$E_{solvent}$ (%)
EC	5.63	1.23	3.59	–	–
PC	6.36	1.30	3.89	–	–
BC	7.08	1.37	4.16	–	–
GC	7.18	1.38	4.19	–	–

EC: $m_f = 1.00\ g\ (1 + 44.032\ \mathrm{g\ mol^{-1}} \times 5.17\ \times 10^{-3}\ mol\ \mathrm{g^{-1}}) = 1.23\ g$

PC: $m_f = 1.00\ g\ (1 + 58.048\ \mathrm{g\ mol^{-1}} \times 5.17\ \times 10^{-3}\ mol\ \mathrm{g^{-1}}) = 1.30\ g$

BC: $m_f = 1.00\ g\ (1 + 72.064\ g\ \mathrm{mol^{-1}} \times 5.17\ \times 10^{-3}\ mol\ \mathrm{g^{-1}}) = 1.37\ g$

GC: $m_f = 1.00\ g\ (1 + 74.048\ g\ \mathrm{mol^{-1}} \times 5.17\ \times 10^{-3}\ mol\ \mathrm{g^{-1}}) = 1.38\ g$

$E_{complex} = E_{simple}$ because no additional solvents are used.

Duval, A.; Avérous, L. “Cyclic Carbonates as Safe and Versatile Etherifying Reagents for the Functionalization of Lignins and Tannins”. *ACS Sustain. Chem. Eng.* **2017**, 5 (8), 7334–7343.

Starting materials: 10 g soda lignin (5.80 mmol OH per g lignin), 51.07 g ethylene carbonate (58.0 mmol, 10.0 equiv.), or 59.21 g propylene carbonate (58.0 mmol, 10.0 equiv.), or 66.18 g vinyl ethylene carbonate (VEC, 58.0 mmol, 10.0 equiv.), or 68.44 g glycerol carbonate (58.0 mmol, 10.0 equiv.), 0.8 g potassium carbonate (5.8 mmol, 0.1 equiv.).

$$m_f = m_i \left(1 + \Delta M_{graft}\left(reactive\ sites\ in \frac{mol}{g}\right)\right)$$

Functionalizing agent	**Raw materials (Total weight in g)**	**Theoretical yield, (g)[a]**	**Desired product Yield (%,g)**	**E_{simple}**	**$E_{complex}$**	**$E_{solvent}$ (%)**
EC	61.87	12.55	83%, 10.42	4.94	–	–
PC	70.01	13.37	73%, 9.76	6.17	–	–
VEC	76.98	14.06	78%, 10.97	6.02	–	–
GC	79.24	14.30	79%, 11.29	6.02	–	–

[a]: theoretical yield calculated for 5.8 x 10^{-3} mol g^{-1} reactive sites

EC: $m_f = 10.00\ g\ (1 + 44.032\ \mathrm{g\ mol^{-1}} \times 5.8\ \times 10^{-3}\ mol\ \mathrm{g^{-1}}) = 12.55\ g$

PC: $m_f = 10.00\ g\ (1 + 58.048\ \mathrm{g\ mol^{-1}} \times 5.8\ \times 10^{-3}\ mol\ \mathrm{g^{-1}}) = 13.37\ g$

VEC: $m_f = 10.00\ g\ (1 + 70.056\ g\ \mathrm{mol^{-1}} \times 5.8\ \times 10^{-3}\ mol\ \mathrm{g^{-1}}) = 14.06\ g$

GC: $m_f = 10.00\ g\ (1 + 74.048\ g\ \mathrm{mol^{-1}} \times 5.8\ \times 10^{-3}\ mol\ \mathrm{g^{-1}}) = 14.30\ g$

$E_{complex} = E_{simple}$ because no additional solvents are used.

Duval, A.; Vidal, D.; Sarbu, A.; René, W.; Avérous, L. “Scalable Single-Step Synthesis of Lignin-Based Liquid Polyols with Ethylene Carbonate for Polyurethane Foams”. *Mater. Today Chem*. **2022**, 24, 100793.

Starting materials: 40-60 g organosolv lignin (1.89 AlOH, 3.58 ArOH, and 0.06 COOH groups, mmol per g lignin), 160 – 140 g PEG (of average molar mass 200, 300 and 400 g/mol; 3.62, 2.41, 1.81 equiv. with respect to total OH groups in lignin, considering 40 g of lignin), EC 38.96 g (0.44 mol, 2 equiv. with respect to total OH groups in lignin, considering 40 g of lignin), 6.114 g K_2CO_3 (0.044 mol, 0.1 equiv. to EC).

The obtained homogeneous liquid polyols were used without further purification for the foam preparation, therefore no waste is generated.

$E_{simple} = 0$

Kühnel, I.; Saake, B.; Lehnen, R. “A New Environmentally Friendly Approach to Lignin-Based Cyclic Carbonates”. *Macromol. Chem. Phys*. **2018**, 219 (7), 1700613.

Oxyalkylation of organosolv lignin with glycerol carbonate

1 g organosolv lignin (5.17 mmol OH per g lignin), 6.10 g glycerol carbonate (51.7 mmol, 10 equiv. in respect of the total of OH in lignin), 79 mg DBU (0.517 mmol, 0.1 equiv. in respect of the total of OH in lignin).

Desired product 1: 1.38 g (theoretical yield)

$$m_f = 1.00\ g\ \left(1 + 74.048\ \frac{g}{mol}(5.17\ \times 10^{-3}\ \frac{mol}{g})\right) = 1.38\ g$$

$$E_{simple}\ oxyalkylation = \frac{\sum starting\ materials\ step\ 1 - desired\ product\ 1}{desired\ product\ 1} = \frac{7.18-1.38}{1.38} = 4.19$$

Transesterification of organosolv lignin with dimethyl carbonate

0.2 g oxyalkylated lignin (5.05 mmol AlOH per g lignin), 0.455 g dimethyl carbonate (5.05 mmol, 5 equiv. in respect of the total of OH in lignin), 0.55 g DMSO (0.5 mL), 0.056 g K_2CO_3 (0.404 mmol, 0.4 equiv. in respect of the total of OH in lignin).

Desired product 2: 0.209 g (98% theoretical yield)

$$m_f = 0.200\ g\ (1 + 25.984\ g\ \mathrm{mol}^{-1} \times 2.525\ \times 10^{-3}\ mol\ \mathrm{g}^{-1}) = 0.213\ g$$

$$E_{simple}\ transesterification = \frac{\sum starting\ materials\ step\ 2 - desired\ product\ 2}{desired\ product\ 2} = \frac{1.26-0.209}{0.209} = 5.04$$

E-factor of whole sequence

Reaction 1: A (lignin) + Reagents→ B (oxyalkylated lignin(OL))

Reaction 2: B (oxyalkylated lignin) + Reagents→ C (final product)

Reaction 1: $E_{complex}$: 4.19 $\frac{\text{kg waste}}{\text{kg OL}}$

Reaction 2: $E_{complex}$: 5.04 $\frac{\text{kg waste}}{\text{kg final product}}$; **Multiplier Reaction 1:** $\frac{\text{kg OL}}{\text{kg final product}} = \frac{0.2}{0.2087} = 0.958$

$E_{sequence}$: 5.04 $\frac{\text{kg waste}}{\text{kg final product}}$ (**Reaction 2**)

+ 4.19 $\frac{\text{kg waste}}{\text{kg OL}}$ × 0.958 $\frac{\text{kg OL}}{\text{kg final prouct}}$ (**Reaction 1**)

= 9.055 $\frac{\text{kg waste}}{\text{kg final product}}$

8 Publication List

Publications are arranged in ascending chronological order. First authorship applies to all entries.

1. Cellulose Functionalization with Methyl Ferulate in a Switchable Solvent System, **Celeste Libretti** and Michael A. R. Meier. *Macromolecules,* 2023, 56, 18, 7532–7542.

2. From Waste to Resource: Advancements in Sustainable Lignin Modification, **Celeste Libretti**, Luis Santos Correa and Michael A. R. Meier. *Green Chemistry*, 2024, 26, 4358 – 4386.

3. Optimized Synthesis of a High Oleic Sunflower Oil Derived Polyamine and its Lignin-based NIPUs, Francesca Chiara Destaso, **Celeste Libretti**, Cédric Le Coz, Etienne Grau, Henri Cramail and Michael A. R. Meier. *Green Chemistry*, 2025, 27, 1440-1450.

4. Biobased Epoxy Resins from Itaconic Anhydride–Functionalized Lignin: Insights and Comparison with Succinic Analogues. **Celeste Libretti**, Gianluca Giuseppe Rizzo, Sophia Abou El Mirate, Mats Johansson and Michael A. R. Meier. *RSC Sustainability, accepted.*

9 Conference Contributions

APME (Advanced Polymers via Macromolecular Engineering) 2023, Paris, France | 23rd-27th April 2023. *Poster Contribution* - Cellulose functionalization with methyl ferulate in a switchable solvent system.

EWLP 2024, Turku, Finland | 26th - 30th August 2024. *Poster Contribution* - Fully bio-based lignin containing non-isocyanate polyurethanes.

Makro 2024 Polymers for a Sustainable Future - Biennial Meeting of the Macromolecular Division of the GDCh, Dresden, Germany | 16th-18th September 2024. *Poster Contribution* - Fully bio-based lignin containing non-isocyanate polyurethanes.

WWSC International Conference, Stockholm, Sweden | 15th-18th June 2025. *Oral contribution* - Optimized synthesis of a high oleic sunflower oil derived polyamine and its lignin-based NIPUs.

10 CV

Celeste Libretti

Industrial and Polymer Chemist

Information

Date of birth	31/08/1997
City	Karlsruhe
Nationality	Italian

Profile

Polymer chemist with a strong background in natural polymers and biomaterials. Experienced in analysing complex technical information and critically comparing material performance across different systems. Skilled in interpreting scientific literature and communicating technical findings in a clear, structured and evidence-based manner.

Key skills

- Polymer processing & material applications (fibers, biopolymers, pulp & paper applications,)
- Sustainability assessments and green metrics
- Supervision of thesis students/Azubis/Practical courses
- Cross-functional collaboration (R&D, packaging, suppliers)
- Data analysis (experience with GC, FTIR, DSC, TGA, GPC/SEC, NMR, DMA, Rheology, Tensile strength) & practical problem-solving
- Communication, presentations & knowledge transfer

Professional Experience

Karlsruhe Institute of Technology (KIT), Karlsruhe, DE
Group of Prof. Dr. Michael A.R. Meier

PhD in Polymer Chemistry | 03/2023 - 05/2026

Chemical modification of lignin to enhance its compatibility in advanced resin systems (such as NIPUs, epoxy resins, thiol-ene thermosets).

KTH Royal Intitute of Technology, Stockholm, SE
Group of Prof. Mats Johansson

Visiting PhD Researcher | 06/2025 - 09/2025

Completed a project involving different modified lignin structures for fully biobased epoxy resins and compared structure-property relationships.

Research Fellowship | 08/2022 - 02/2023

Investigated non-toxic cellulose derivatives with antioxidant properties for skincare applications.

Sacmi Imola S.C., Imola, IT
Internship | 07/2021 - 02/2022

Developed and scaled up a cellulose fiber hydrophobization system as a sustainable alternative to HDPE caps for Tetra Pak cartons, moving from lab-scale synthesis to industrial prototype. Gained expertise in process additives and non-toxic paper formulation (retention aids, strength agents, sizing agents).

Achievements and Awards

Presented three posters and one oral contribution at international conferences around Europe. First author of four publications.
Awarded scolarships: "Toso Montanari" Fellowship for Research and Advanced Studies Abroad (2022); KHYS (Karlsruhe House of Young Scientists) Research Travel grant (2025)

Certificates and Trainings

Introduction to Python for Data Science, 2023
Effective Visual Communication, The Seyens Method™, 2023

Education

Alma Mater Studiorum - University of Bologna
M.Sc. Industrial Chemistry, 2019 - 2022

- Summa cum laude

Alma Mater Studiorum - University of Bologna
B.Sc. Environmental and material chemistry and Technology, 2016 - 2019

Languages

Italian (Mothertongue)
English (Fluent professional knowledge)
German (Intermediate knowledge - ongoing learning)

11 Abbreviation List

AAF	Aldehyde-Assisted Fractionation
AE	Atom Economy
BADGE / BPADGE	Bisphenol-A diglycidyl ether
BOD	Biochemical Oxygen Demand
BPA	Bisphenol A
CA	Citric Acid
CAHC	Cysteamine hydrochloride salt
cEF	Complex E-factor
ClAn	Citraconic anhydride
CMR	Carcinogenic, Mutagenic, Reprotoxic
CNSL	Cashew Nutshell Liquid
COD	Chemical Oxygen Demand
DAC	Diallyl carbonate
DBU	1,8-diazabicyclo(5.4.0)undec-7-ene
DDT	1,1,1-trichloro-2,2-bis(4-chlorophenyl)ethane
DESs	Deep Eutectic Solvents
DMA	Dynamic Mechanical Analysis
DMAc	Dimethylacetamide
DMAP	4-(Dimethylamino)pyridine
DMC	Dimethyl carbonate
DMPA	2,2-Dimethoxy-2-phenylacetophenone
DMSO	Dimethyl sulfoxide
DSC	Differential Scanning Calorimetry
Đ	Dispersity Index
EBC	Erythritol-bis cyclic carbonate
ECH	Epichlorohydrin
EPA	Environmental Protection Agency
ESBO	Epoxidized Soybean Oil
EtOH	Ethanol
GC	Glycerol carbonate
GHGs	Greenhouse Gases
GTE	Glycerol-to-epichlorohydrin
GWP	Global Warming Potential

HAL	Hydroxyalkylated Lignin
HOSO	High Oleic Sunflower Oil
HSQC	Heteronuclear Single Quantum Correlation
IAn	Itaconic anhydride
ILs	Ionic Liquids
IPCC-AR6	Intergovernmental Panel on Climate Change, Sixth Assessment Report
iPrOH	Isopropanol
LC	Lignin Carbonate
LCA	Life Cycle Assessment
LD	Lethal Dose
LED	Light-Emitting Diode
LI	Lignin Itaconate
LS	Lignin Succinate
MCR	Multicomponent Reaction
MeOH	Methanol
M_n	Number-average molecular weight
M_w	Weight-average molecular weight
MXDA	m-Xylylenediamine
NaOH	Sodium hydroxide
NIPU	Non-isocyanate Polyurethanes
NMR	Nuclear Magnetic Resonance
OL	Organosolv Lignin
PA	Polyamine
PF	Phenol–formaldehyde resin
PHU	Polyhydroxyurethane
PMI	Process Mass Intensity
PTEMP	Pentaerythritol tetrakis(3-mercaptopropionate)
PU / PUs	Polyurethane(s)
r.t.	Room temperature
SAn	Succinic anhydride
sEF	Simple E-factor
SDGs	Sustainable Development Goals
SEC	Size Exclusion Chromatography
SFDR	Sustainable Finance Disclosure Regulation

TBAB	Tetrabutylammonium bromide
TBD	1,5,7-Triazabicyclo(4.4.0)dec-5-ene
TCDD	2,3,7,8-Tetrachlorodibenzo-p-dioxin
T_g	Glass transition temperature
TGA	Thermogravimetric Analysis
THF	Tetrahydrofuran
TMG	1,1,3,3-Tetramethylguanidine
UV	Ultraviolet
WCA	Water Contact Angle

12 Bibliography

(1) Calvin, K.; Dasgupta, D.; Krinner, G.; Mukherji, A.; Thorne, P. W.; Trisos, C.; Romero, J.; Aldunce, P.; Barrett, K.; Blanco, G.; Cheung, W. W. L.; Connors, S.; Denton, F.; Diongue-Niang, A.; Dodman, D.; Garschagen, M.; Geden, O.; Hayward, B.; Jones, C.; Jotzo, F.; Krug, T.; Lasco, R.; Lee, Y.-Y.; Masson-Delmotte, V.; Meinshausen, M.; Mintenbeck, K.; Mokssit, A.; Otto, F. E. L.; Pathak, M.; Pirani, A.; Poloczanska, E.; Pörtner, H.-O.; Revi, A.; Roberts, D. C.; Roy, J.; Ruane, A. C.; Skea, J.; Shukla, P. R.; Slade, R.; Slangen, A.; Sokona, Y.; Sörensson, A. A.; Tignor, M.; Van Vuuren, D.; Wei, Y.-M.; Winkler, H.; Zhai, P.; Zommers, Z.; Hourcade, J.-C.; Johnson, F. X.; Pachauri, S.; Simpson, N. P.; Singh, C.; Thomas, A.; Totin, E.; Arias, P.; Bustamante, M.; Elgizouli, I.; Flato, G.; Howden, M.; Méndez-Vallejo, C.; Pereira, J. J.; Pichs-Madruga, R.; Rose, S. K.; Saheb, Y.; Sánchez Rodríguez, R.; Ürge-Vorsatz, D.; Xiao, C.; Yassaa, N.; Alegría, A.; Armour, K.; Bednar-Friedl, B.; Blok, K.; Cissé, G.; Dentener, F.; Eriksen, S.; Fischer, E.; Garner, G.; Guivarch, C.; Haasnoot, M.; Hansen, G.; Hauser, M.; Hawkins, E.; Hermans, T.; Kopp, R.; Leprince-Ringuet, N.; Lewis, J.; Ley, D.; Ludden, C.; Niamir, L.; Nicholls, Z.; Some, S.; Szopa, S.; Trewin, B.; Van Der Wijst, K.-I.; Winter, G.; Witting, M.; Birt, A.; Ha, M.; Romero, J.; Kim, J.; Haites, E. F.; Jung, Y.; Stavins, R.; Birt, A.; Ha, M.; Orendain, D. J. A.; Ignon, L.; Park, S.; Park, Y.; Reisinger, A.; Cammaramo, D.; Fischlin, A.; Fuglestvedt, J. S.; Hansen, G.; Ludden, C.; Masson-Delmotte, V.; Matthews, J. B. R.; Mintenbeck, K.; Pirani, A.; Poloczanska, E.; Leprince-Ringuet, N.; Péan, C. *IPCC, 2023: Climate Change 2023: Synthesis Report. Contribution of Working Groups I, II and III to the Sixth Assessment Report of the Intergovernmental Panel on Climate Change [Core Writing Team, H. Lee and J. Romero (Eds.)]. IPCC, Geneva, Switzerland.*, First.; Intergovernmental Panel on Climate Change (IPCC), 2023. https://doi.org/10.59327/IPCC/AR6-9789291691647.

(2) United Nations Environment Programme. *Emissions Gap Report 2025: Off Target - Continued Collective Inaction Puts Global Temperature Goal at Risk*; United Nations Environment Programme, 2025. https://doi.org/10.59117/20.500.11822/48854.

(3) Krause, M. The World Is Likely to Exceed a Key Global Warming Target Soon. Now What?, 2025. https://www.unep.org/news-and-stories/story/world-likely-exceed-key-global-warming-target-soon-now-what (accessed 2026-02-12).

(4) Mann, M. E.; Bradley, R. S.; Hughes, M. K. Northern Hemisphere Temperatures during the Past Millennium: Inferences, Uncertainties, and

Limitations. *Geophysical Research Letters* **1999**, *26* (6), 759–762. https://doi.org/10.1029/1999GL900070.

(5) Brumfiel, G. Academy Affirms Hockey-Stick Graph. *Nature* **2006**, *441* (7097), 1032–1033. https://doi.org/10.1038/4411032a.

(6) PAGES2k Consortium; Emile-Geay, J.; McKay, N. P.; Kaufman, D. S.; Von Gunten, L.; Wang, J.; Anchukaitis, K. J.; Abram, N. J.; Addison, J. A.; Curran, M. A. J.; Evans, M. N.; Henley, B. J.; Hao, Z.; Martrat, B.; McGregor, H. V.; Neukom, R.; Pederson, G. T.; Stenni, B.; Thirumalai, K.; Werner, J. P.; Xu, C.; Divine, D. V.; Dixon, B. C.; Gergis, J.; Mundo, I. A.; Nakatsuka, T.; Phipps, S. J.; Routson, C. C.; Steig, E. J.; Tierney, J. E.; Tyler, J. J.; Allen, K. J.; Bertler, N. A. N.; Björklund, J.; Chase, B. M.; Chen, M.-T.; Cook, E.; De Jong, R.; DeLong, K. L.; Dixon, D. A.; Ekaykin, A. A.; Ersek, V.; Filipsson, H. L.; Francus, P.; Freund, M. B.; Frezzotti, M.; Gaire, N. P.; Gajewski, K.; Ge, Q.; Goosse, H.; Gornostaeva, A.; Grosjean, M.; Horiuchi, K.; Hormes, A.; Husum, K.; Isaksson, E.; Kandasamy, S.; Kawamura, K.; Kilbourne, K. H.; Koç, N.; Leduc, G.; Linderholm, H. W.; Lorrey, A. M.; Mikhalenko, V.; Mortyn, P. G.; Motoyama, H.; Moy, A. D.; Mulvaney, R.; Munz, P. M.; Nash, D. J.; Oerter, H.; Opel, T.; Orsi, A. J.; Ovchinnikov, D. V.; Porter, T. J.; Roop, H. A.; Saenger, C.; Sano, M.; Sauchyn, D.; Saunders, K. M.; Seidenkrantz, M.-S.; Severi, M.; Shao, X.; Sicre, M.-A.; Sigl, M.; Sinclair, K.; St. George, S.; St. Jacques, J.-M.; Thamban, M.; Kuwar Thapa, U.; Thomas, E. R.; Turney, C.; Uemura, R.; Viau, A. E.; Vladimirova, D. O.; Wahl, E. R.; White, J. W. C.; Yu, Z.; Zinke, J. A Global Multiproxy Database for Temperature Reconstructions of the Common Era. *Sci Data* **2017**, *4* (1), 170088. https://doi.org/10.1038/sdata.2017.88.

(7) Wahl, E. R.; Ammann, C. M. Robustness of the Mann, Bradley, Hughes Reconstruction of Northern Hemisphere Surface Temperatures: Examination of Criticisms Based on the Nature and Processing of Proxy Climate Evidence. *Climatic Change* **2007**, *85* (1–2), 33–69. https://doi.org/10.1007/s10584-006-9105-7.

(8) Kaufman, H.; Zhu, X.; Diedrich, C.; Doherty, J. *Plastics - Exposing Their Climate Impacts*; Plastics and Climate Project, 2025.

(9) *Plastics – fueling oil demand, climate change and pollution*. United Nations. https://www.un.org/en/climatechange/science/climate-issues/plastics (accessed 2026-02-12).

(10) Roy, D.; Dey, A. K.; Mandal, A.; Kamila, B. A Comprehensive Review on the Sustainable Approach of Fossil-Based Polymers toward Bio-Based

Polymers. *Polym. Bull.* **2025**, *82* (17), 11625–11696. https://doi.org/10.1007/s00289-025-06006-9.

(11) *Sustainability*. United Nations. https://www.un.org/en/academic-impact/sustainability (accessed 2026-01-26).

(12) Purvis, B.; Mao, Y.; Robinson, D. Three Pillars of Sustainability: In Search of Conceptual Origins. *Sustain Sci* **2019**, *14* (3), 681–695. https://doi.org/10.1007/s11625-018-0627-5.

(13) *Sustainable Development Goals*. United Nations. https://www.un.org/sustainabledevelopment/ (accessed 2026-01-26).

(14) Carson, R. *Silent Spring*, 50. anniversary ed., 1. Mariner Books ed.; Mariner Books, Houghton Mifflin Harcourt: Boston, 2002.

(15) *DDT - A Brief History and Status*. epa.gov. https://www.epa.gov/ingredients-used-pesticide-products/ddt-brief-history-and-status (accessed 2026-01-26).

(16) Kleiman, Dr. J. *Love Canal: A Brief History*. Geneseo New York's Public Honors College. https://www.geneseo.edu/history/love_canal_history/ (accessed 2026-01-26).

(17) Eskenazi, B.; Warner, M.; Brambilla, P.; Signorini, S.; Ames, J.; Mocarelli, P. The Seveso Accident: A Look at 40 Years of Health Research and Beyond. *Environment International* **2018**, *121*, 71–84. https://doi.org/10.1016/j.envint.2018.08.051.

(18) Anastas, P. T.; Warner, J. C. *Green Chemistry: Theory and Practice*; Oxford University Press: Oxford, 1998.

(19) *Presidential Green Chemistry Challenge: 2011 Small Business Award - BioAmber, Inc*. epa.gov. https://www.epa.gov/greenchemistry/presidential-

green-chemistry-challenge-2011-small-business-award (accessed 2026-01-26).

(20) Bomgardner, M. M. No Buyer for Succinic Acid Maker BioAmber. *C&EN* **2018**.

(21) McCoy, M. Succinic Acid, Once a Biobased Chemical Star, Is Barely Being Made. *C&EN* **2019**.

(22) Trost, B. M. Atom Economy—A Challenge for Organic Synthesis: Homogeneous Catalysis Leads the Way. *Angew. Chem. Int. Ed. Engl.* **1995**, *34* (3), 259–281. https://doi.org/10.1002/anie.199502591.

(23) Pandey, J.; Singh, S.; Dubey, R. Atom Economy Green Synthesis in Organic Chemistry. *J Chem Pharm Res.* **2025**, *17* (1). https://doi.org/DOI:10.37532/0975-7384.2025.17(1).233.

(24) Sheldon, R. A. Organic Synthesis; Past, Present and Future. *Chem. Ind.* **1992**, 903–906.

(25) Sheldon, R. A. The E Factor 25 Years on: The Rise of Green Chemistry and Sustainability. *Green Chem.* **2017**, *19* (1), 18–43. https://doi.org/10.1039/C6GC02157C.

(26) Roschangar, F.; Sheldon, R. A.; Senanayake, C. H. Overcoming Barriers to Green Chemistry in the Pharmaceutical Industry – the Green Aspiration Level™ Concept. *Green Chem.* **2015**, *17* (2), 752–768. https://doi.org/10.1039/C4GC01563K.

(27) Sheldon, R. A.; Bode, M. L.; Akakios, S. G. Metrics of Green Chemistry: Waste Minimization. *Current Opinion in Green and Sustainable Chemistry* **2022**, *33*, 100569. https://doi.org/10.1016/j.cogsc.2021.100569.

(28) Sheldon, R. A. The E Factor at 30: A Passion for Pollution Prevention. *Green Chem.* **2023**, *25* (5), 1704–1728. https://doi.org/10.1039/D2GC04747K.

(29) Monteith, E. R.; Mampuys, P.; Summerton, L.; Clark, J. H.; Maes, B. U. W.; McElroy, C. R. Why We Might Be Misusing Process Mass Intensity (PMI) and a Methodology to Apply It Effectively as a Discovery Level Metric. *Green Chem.* **2020**, *22* (1), 123–135. https://doi.org/10.1039/C9GC01537J.

(30) *Critical review of life cycle assessments according to ISO*. Fraunhofer IBP. https://www.ibp.fraunhofer.de/en/expertise/life-cycle-engineering/review-of-life-cycle-assessments-according-to-iso.html (accessed 2026-01-28).

(31) Liu, M.; Zhu, G.; Tian, Y. The Historical Evolution and Research Trends of Life Cycle Assessment. *Green Carbon* **2024**, *2* (4), 425–437. https://doi.org/10.1016/j.greenca.2024.08.003.

(32) Mudersbach, M.; Jürgens, M.; Pohler, M.; Spierling, S.; Venkatachalam, V.; Endres, H.; Barner, L. Life Cycle Assessment in a Nutshell—Best Practices

and Status Quo for the Plastic Sector. *Macromol. Rapid Commun.* **2025**, *46* (8), 2300466. https://doi.org/10.1002/marc.202300466.

(33) Wu, W.; Chang, J.-S. Integrated Algal Biorefineries from Process Systems Engineering Aspects: A Review. *Bioresource Technology* **2019**, *291*, 121939. https://doi.org/10.1016/j.biortech.2019.121939.

(34) Kokare, S.; Oliveira, J. P.; Godina, R. Life Cycle Assessment of Additive Manufacturing Processes: A Review. *Journal of Manufacturing Systems* **2023**, *68*, 536–559. https://doi.org/10.1016/j.jmsy.2023.05.007.

(35) Voorthuis, J.; Gijbels, C. A Fair Accord: Cradle to Cradle as a Design Theory Measured against John Rawls' Theory of Justice and Immanuel Kant's Categorical Imperative. *Sustainability* **2010**, *2* (1), 371–382. https://doi.org/10.3390/su2010371.

(36) McDonough, W.; Braungart, M. *Cradle to Cradle: Remaking the Way We Make Things*, 1st ed.; North Point Press: New York, 2002.

(37) Dömling, A.; Wang, W.; Wang, K. Chemistry and Biology Of Multicomponent Reactions. *Chem. Rev.* **2012**, *112* (6), 3083–3135. https://doi.org/10.1021/cr100233r.

(38) Cioc, R. C.; Ruijter, E.; Orru, R. V. A. Multicomponent Reactions: Advanced Tools for Sustainable Organic Synthesis. *Green Chem.* **2014**, *16* (6), 2958–2975. https://doi.org/10.1039/C4GC00013G.

(39) Strecker, A. Ueber Die Künstliche Bildung Der Milchsäure Und Einen Neuen, Dem Glycocoll Homologen Körper. *Ann. Chem. Pharm.* **1850**, *75* (1), 27–45. https://doi.org/Ueber die künstliche Bildung der Milchsäure und einen neuen, dem Glycocoll homologen Körper.

(40) Tao, L.; Zhu, C.; Wei, Y.; Zhao, Y. Biginelli Multicomponent Reactions in Polymer Science. In *Multi-Component and Sequential Reactions in Polymer Synthesis*; Theato, P., Ed.; Advances in Polymer Science; Springer International Publishing: Cham, 2014; Vol. 269, pp 43–59. https://doi.org/10.1007/12_2014_301.

(41) Anjos, J. V. D.; Srivastava, R. M.; Costa-Silva, J. H.; Scotti, L.; Scotti, M. T.; Wanderley, A. G.; Leite, E. S.; Melo, S. J. D.; Junior, F. J. B. M. Comparative Computational Studies of 3,4-Dihydro-2,6-Diaryl-4-Oxo-Pyrimidine-5-Carbonitrile Derivatives as Potential Antinociceptive Agents. *Molecules* **2012**, *17* (1), 809–819. https://doi.org/10.3390/molecules17010809.

(42) Matos, L. H. S.; Masson, F. T.; Simeoni, L. A.; Homem-de-Mello, M. Biological Activity of Dihydropyrimidinone (DHPM) Derivatives: A Systematic Review. *European Journal of Medicinal Chemistry* **2018**, *143*, 1779–1789. https://doi.org/10.1016/j.ejmech.2017.10.073.

(43) Pu, M.-X.; Guo, H.-Y.; Quan, Z.-S.; Li, X.; Shen, Q.-K. Application of the Mannich Reaction in the Structural Modification of Natural Products.

Journal of Enzyme Inhibition and Medicinal Chemistry **2023**, *38* (1), 2235095. https://doi.org/10.1080/14756366.2023.2235095.

(44) Wu, H.; Wang, Z.; Tao, L. The Hantzsch Reaction in Polymer Chemistry: Synthesis and Tentative Application. *Polym. Chem.* **2017**, *8* (47), 7290–7296. https://doi.org/10.1039/C7PY01718A.

(45) Ramozzi, R.; Morokuma, K. Revisiting the Passerini Reaction Mechanism: Existence of the Nitrilium, Organocatalysis of Its Formation, and Solvent Effect. *J. Org. Chem.* **2015**, *80* (11), 5652–5657. https://doi.org/10.1021/acs.joc.5b00594.

(46) Oelmann, S.; Meier, M. A. R. Synthesis and Unimolecular Micellar Behavior of Amphiphilic Star-Shaped Block Copolymers Obtained via the Passerini Three Component Reaction. *RSC Adv.* **2017**, *7* (71), 45195–45199. https://doi.org/10.1039/C7RA08982A.

(47) Oelmann, S.; Solleder, S. C.; Meier, M. A. R. Controlling Molecular Weight and Polymer Architecture during the Passerini Three Component Step-Growth Polymerization. *Polym. Chem.* **2016**, *7* (10), 1857–1860. https://doi.org/10.1039/C5PY02030A.

(48) Sehlinger, A.; Schneider, R.; Meier, M. A. R. Passerini Addition Polymerization of an AB-Type Monomer – A Convenient Route to Versatile Polyesters. *European Polymer Journal* **2014**, *50*, 150–157. https://doi.org/10.1016/j.eurpolymj.2013.10.019.

(49) Sehlinger, A.; Meier, M. A. R. Passerini and Ugi Multicomponent Reactions in Polymer Science. In *Multi-Component and Sequential Reactions in Polymer Synthesis*; Theato, P., Ed.; Advances in Polymer Science; Springer International Publishing: Cham, 2014; Vol. 269, pp 61–86. https://doi.org/10.1007/12_2014_298.

(50) Kumar, S.; Arora, A.; Kumar, S.; Kumar, R.; Maity, J.; Singh, B. K. Passerini Reaction: Synthesis and Applications in Polymer Chemistry. *European Polymer Journal* **2023**, *190*, 112004. https://doi.org/10.1016/j.eurpolymj.2023.112004.

(51) Kreye, O.; Tóth, T.; Meier, M. A. R. Introducing Multicomponent Reactions to Polymer Science: Passerini Reactions of Renewable Monomers. *J. Am. Chem. Soc.* **2011**, *133* (6), 1790–1792. https://doi.org/10.1021/ja1113003.

(52) Zhang, J.; Wu, Y.-H.; Wang, J.-C.; Du, F.-S.; Li, Z.-C. Functional Poly(Ester–Amide)s with Tertiary Ester Linkages via the Passerini Multicomponent Polymerization of a Dicarboxylic Acid and a Diisocyanide with Different Electron-Deficient Ketones. *Macromolecules* **2018**, *51* (15), 5842–5851. https://doi.org/10.1021/acs.macromol.8b01168.

(53) Sehlinger, A.; Bartnick, N.; Gunkel, I.; Meier, M. A. R.; Montero De Espinosa, L. Phase Segregation in Supramolecular Polymers Based on Telechelics Synthesized via Multicomponent Reactions. *Macro Chemistry*

& Physics **2017**, *218* (22), 1700302. https://doi.org/10.1002/macp.201700302.

(54) Pettignano, A.; Daunay, A.; Moreau, C.; Cathala, B.; Charlot, A.; Fleury, E. Sustainable Modification of Carboxymethyl Cellulose by Passerini Three-Component Reaction and Subsequent Adsorption onto Cellulosic Substrates. *ACS Sustainable Chem. Eng.* **2019**, *7* (17), 14685–14696. https://doi.org/10.1021/acssuschemeng.9b02634.

(55) Söyler, Z.; Onwukamike, K. N.; Grelier, S.; Grau, E.; Cramail, H.; Meier, M. A. R. Sustainable Succinylation of Cellulose in a CO_2 -Based Switchable Solvent and Subsequent Passerini 3-CR and Ugi 4-CR Modification. *Green Chem.* **2018**, *20* (1), 214–224. https://doi.org/10.1039/C7GC02577G.

(56) Luleburgaz, S.; Hizal, G.; Durmaz, H.; Tunca, U. Modification of Electron Deficient Polyester via Huisgen/Passerini Sequence. *Polymer* **2017**, *127*, 45–51. https://doi.org/10.1016/j.polymer.2017.08.055.

(57) Kolb, H. C.; Finn, M. G.; Sharpless, K. B. Click Chemistry: Diverse Chemical Function from a Few Good Reactions. *Angew. Chem. Int. Ed.* **2001**, *40* (11), 2004–2021. https://doi.org/10.1002/1521-3773(20010601)40:11<2004::AID-ANIE2004>3.0.CO;2-5.

(58) Devaraj, N. K.; Finn, M. G. Introduction: Click Chemistry. *Chem. Rev.* **2021**, *121* (12), 6697–6698. https://doi.org/10.1021/acs.chemrev.1c00469.

(59) Castro, V.; Rodríguez, H.; Albericio, F. CuAAC: An Efficient Click Chemistry Reaction on Solid Phase. *ACS Comb. Sci.* **2016**, *18* (1), 1–14. https://doi.org/10.1021/acscombsci.5b00087.

(60) Tasdelen, M. A. Diels–Alder “Click” Reactions: Recent Applications in Polymer and Material Science. *Polym. Chem.* **2011**, *2* (10), 2133. https://doi.org/10.1039/c1py00041a.

(61) Campos, L. M.; Killops, K. L.; Sakai, R.; Paulusse, J. M. J.; Damiron, D.; Drockenmuller, E.; Messmore, B. W.; Hawker, C. J. Development of Thermal and Photochemical Strategies for Thiol−Ene Click Polymer Functionalization. *Macromolecules* **2008**, *41* (19), 7063–7070. https://doi.org/10.1021/ma801630n.

(62) Killops, K. L.; Campos, L. M.; Hawker, C. J. Robust, Efficient, and Orthogonal Synthesis of Dendrimers via Thiol-Ene “Click” Chemistry. *J. Am. Chem. Soc.* **2008**, *130* (15), 5062–5064. https://doi.org/10.1021/ja8006325.

(63) Ahangarpour, M.; Kavianinia, I.; Brimble, M. A. Thia-Michael Addition: The Route to Promising Opportunities for Fast and Cysteine-Specific Modification. *Org. Biomol. Chem.* **2023**, *21* (15), 3057–3072. https://doi.org/10.1039/D2OB02262A.

(64) Brown, J. S.; Ruttinger, A. W.; Vaidya, A. J.; Alabi, C. A.; Clancy, P. Decomplexation as a Rate Limitation in the Thiol-Michael Addition of *N* -

Acrylamides. *Org. Biomol. Chem.* **2020**, *18* (32), 6364–6377. https://doi.org/10.1039/D0OB00726A.

(65) Gennari, A.; Wedgwood, J.; Lallana, E.; Francini, N.; Tirelli, N. Thiol-Based Michael-Type Addition. A Systematic Evaluation of Its Controlling Factors. *Tetrahedron* **2020**, *76* (47), 131637. https://doi.org/10.1016/j.tet.2020.131637.

(66) Emori, E.; Arai, T.; Sasai, H.; Shibasaki, M. A Catalytic Michael Addition of Thiols to α,β-Unsaturated Carbonyl Compounds: Asymmetric Michael Additions and Asymmetric Protonations. *J. Am. Chem. Soc.* **1998**, *120* (16), 4043–4044. https://doi.org/10.1021/ja980397v.

(67) Belbekhouche, S.; Guerrouache, M.; Carbonnier, B. Thiol-Maleimide Michael Addition Click Reaction: A New Route to Surface Modification of Porous Polymeric Monolith. *Macromol. Chem. Phys.* **2016**, *217* (8), 997–1006. https://doi.org/10.1002/macp.201500427.

(68) Chatani, S.; Nair, D. P.; Bowman, C. N. Relative Reactivity and Selectivity of Vinyl Sulfones and Acrylates towards the Thiol–Michael Addition Reaction and Polymerization. *Polym. Chem.* **2013**, *4* (4), 1048–1055. https://doi.org/10.1039/C2PY20826A.

(69) Nair, D. P.; Podgórski, M.; Chatani, S.; Gong, T.; Xi, W.; Fenoli, C. R.; Bowman, C. N. The Thiol-Michael Addition Click Reaction: A Powerful and Widely Used Tool in Materials Chemistry. *Chem. Mater.* **2014**, *26* (1), 724–744. https://doi.org/10.1021/cm402180t.

(70) Northrop, B. H.; Frayne, S. H.; Choudhary, U. Thiol–Maleimide "Click" Chemistry: Evaluating the Influence of Solvent, Initiator, and Thiol on the Reaction Mechanism, Kinetics, and Selectivity. *Polym. Chem.* **2015**, *6* (18), 3415–3430. https://doi.org/10.1039/C5PY00168D.

(71) Sutherland, B. P.; El-Zaatari, B. M.; Halaszynski, N. I.; French, J. M.; Bai, S.; Kloxin, C. J. On-Resin Macrocyclization of Peptides Using Vinyl Sulfonamides as a Thiol-Michael "Click" Acceptor. *Bioconjugate Chem.* **2018**, *29* (12), 3987–3992. https://doi.org/10.1021/acs.bioconjchem.8b00751.

(72) Zhang, B.; Chakma, P.; Shulman, M. P.; Ke, J.; Digby, Z. A.; Konkolewicz, D. Probing the Mechanism of Thermally Driven Thiol-Michael Dynamic Covalent Chemistry. *Org. Biomol. Chem.* **2018**, *16* (15), 2725–2734. https://doi.org/10.1039/C8OB00397A.

(73) Chakma, P.; Rodrigues Possarle, L. H.; Digby, Z. A.; Zhang, B.; Sparks, J. L.; Konkolewicz, D. Dual Stimuli Responsive Self-Healing and Malleable Materials Based on Dynamic Thiol-Michael Chemistry. *Polym. Chem.* **2017**, *8* (42), 6534–6543. https://doi.org/10.1039/C7PY01356F.

(74) Crolais, A. E.; Dolinski, N. D.; Boynton, N. R.; Radhakrishnan, J. M.; Snyder, S. A.; Rowan, S. J. Enhancing the Equilibrium of Dynamic Thia-

Michael Reactions through Heterocyclic Design. *J. Am. Chem. Soc.* **2023**, *145* (26), 14427–14434. https://doi.org/10.1021/jacs.3c03643.

(75) Hoyle, C. E.; Lee, T. Y.; Roper, T. Thiol–Enes: Chemistry of the Past with Promise for the Future. *J. Polym. Sci. A Polym. Chem.* **2004**, *42* (21), 5301–5338. https://doi.org/10.1002/pola.20366.

(76) Lowe, A. B. Thiol-Ene "Click" Reactions and Recent Applications in Polymer and Materials Synthesis. *Polym. Chem.* **2010**, *1* (1), 17–36. https://doi.org/10.1039/B9PY00216B.

(77) Hoyle, C. E.; Bowman, C. N. Thiol-Ene Click Chemistry. *Angewandte Chemie International Edition* **2010**, *49* (9), 1540–1573. https://doi.org/10.1002/anie.200903924.

(78) Morgan, C. R.; Magnotta, F.; Ketley, A. D. Thiol/Ene Photocurable Polymers. *J. Polym. Sci. Polym. Chem. Ed.* **1977**, *15* (3), 627–645. https://doi.org/10.1002/pol.1977.170150311.

(79) Walling, C.; Helmreich, W. Reactivity and Reversibility in the Reaction of Thiyl Radicals with Olefins[1]. *J. Am. Chem. Soc.* **1959**, *81* (5), 1144–1148. https://doi.org/10.1021/ja01514a032.

(80) Segers, B.; Nimmegeers, P.; Spiller, M.; Tofani, G.; Jasiukaitytė-Grojzdek, E.; Dace, E.; Kikas, T.; Marchetti, J. M.; Rajić, M.; Yildiz, G.; Billen, P. Lignocellulosic Biomass Valorisation: A Review of Feedstocks, Processes and Potential Value Chains and Their Implications for the Decision-Making Process. *RSC Sustainability* **2024**, *2* (12), 3730–3749. https://doi.org/10.1039/D4SU00342J.

(81) Naik, S. N.; Goud, V. V.; Rout, P. K.; Dalai, A. K. Production of First and Second Generation Biofuels: A Comprehensive Review. *Renewable and Sustainable Energy Reviews* **2010**, *14* (2), 578–597. https://doi.org/10.1016/j.rser.2009.10.003.

(82) Sulis, D. B.; Lavoine, N.; Sederoff, H.; Jiang, X.; Marques, B. M.; Lan, K.; Cofre-Vega, C.; Barrangou, R.; Wang, J. P. Advances in Lignocellulosic Feedstocks for Bioenergy and Bioproducts. *Nat Commun* **2025**, *16* (1), 1244. https://doi.org/10.1038/s41467-025-56472-y.

(83) Bachmann, M.; Kätelhön, A.; Winter, B.; Meys, R.; Müller, L. J.; Bardow, A. Renewable Carbon Feedstock for Polymers: Environmental Benefits from

Synergistic Use of Biomass and CO_2. *Faraday Discuss.* **2021**, *230*, 227–246. https://doi.org/10.1039/D0FD00134A.

(84) *Plastics the Fast Facts 2025*; Plasticseurope. https://plasticseurope.org/knowledge-hub/plastics-the-fast-facts-2025/ (accessed 2026-01-31).

(85) Babu, R. P.; O'Connor, K.; Seeram, R. Current Progress on Bio-Based Polymers and Their Future Trends. *Prog Biomater* **2013**, *2* (1), 8. https://doi.org/10.1186/2194-0517-2-8.

(86) Suri, S.; Singh, A. Modification of Starch by Novel and Traditional Ways: Influence on the Structure and Functional Properties. *Sustainable Food Technol.* **2023**, *1* (3), 348–362. https://doi.org/10.1039/D2FB00043A.

(87) Mou, L.; Li, J.; Lu, Y.; Li, G.; Li, J. Polylactic Acid: A Future Universal Biobased Polymer with Multifunctional Performance—from Monomer Synthesis, and Processing to Applications: A Review. *Journal of Hazardous Materials Advances* **2025**, *18*, 100757. https://doi.org/10.1016/j.hazadv.2025.100757.

(88) Barletta, M.; Aversa, C.; Ayyoob, M.; Gisario, A.; Hamad, K.; Mehrpouya, M.; Vahabi, H. Poly(Butylene Succinate) (PBS): Materials, Processing, and Industrial Applications. *Progress in Polymer Science* **2022**, *132*, 101579. https://doi.org/10.1016/j.progpolymsci.2022.101579.

(89) Zytner, P.; Kumar, D.; Elsayed, A.; Mohanty, A.; Ramarao, B. V.; Misra, M. A Review on Polyhydroxyalkanoate (PHA) Production through the Use of Lignocellulosic Biomass. *RSC Sustainability* **2023**, *1* (9), 2120–2134. https://doi.org/10.1039/D3SU00126A.

(90) Gibson, L. J. The Hierarchical Structure and Mechanics of Plant Materials. *J. R. Soc. Interface.* **2012**, *9* (76), 2749–2766. https://doi.org/10.1098/rsif.2012.0341.

(91) Kamdem Tamo, A.; Doench, I.; Deffo, G.; Zambou Jiokeng, S. L.; Doungmo, G.; Fotsop, C. G.; Tonleu Temgoua, R. C.; Montembault, A.; Serghei, A.; Njanja, E.; Kenfack Tonle, I.; Osorio-Madrazo, A. Lignocellulosic Biomass and Its Main Structural Polymers as Sustainable Materials for (Bio)Sensing Applications. *J. Mater. Chem. A* **2025**, *13* (30), 24185–24253. https://doi.org/10.1039/D5TA02900G.

(92) Hindi, S. S. Z.; Abohassan, R. A. Cellulosic Microfibril and Its Embedding Matrix within Plant Cell Wall. *IJIRSET* **2016**, *5* (3), 2727–2734. https://doi.org/DOI:10.15680/IJIRSET.2016.0503004.

(93) Libretti, C.; Santos Correa, L.; Meier, M. A. R. From Waste to Resource: Advancements in Sustainable Lignin Modification. *Green Chem.* **2024**, *26* (8), 4358–4386. https://doi.org/10.1039/D4GC00745J.

(94) Feofilova, E. P.; Mysyakina, I. S. Lignin: Chemical Structure, Biodegradation, and Practical Application (a Review). *Appl Biochem*

Microbiol **2016**, *52* (6), 573–581. https://doi.org/10.1134/S0003683816060053.

(95) Bertella, S.; Luterbacher, J. S. Simultaneous Extraction and Controlled Chemical Functionalization of Hardwood Lignin for Improved Phenolation. *Green Chem.* **2021**, *23* (9), 3459–3467. https://doi.org/10.1039/D1GC00358E.

(96) Guadix-Montero, S.; Sankar, M. Review on Catalytic Cleavage of C–C Inter-Unit Linkages in Lignin Model Compounds: Towards Lignin Depolymerisation. *Top Catal* **2018**, *61* (3–4), 183–198. https://doi.org/10.1007/s11244-018-0909-2.

(97) Dorrestijn, E.; Laarhoven, L. J. J.; Arends, I. W. C. E.; Mulder, P. The Occurrence and Reactivity of Phenoxyl Linkages in Lignin and Low Rank Coal. *Journal of Analytical and Applied Pyrolysis* **2000**, *54* (1–2), 153–192. https://doi.org/10.1016/S0165-2370(99)00082-0.

(98) Wang, C.; Kelley, S. S.; Venditti, R. A. Lignin-Based Thermoplastic Materials. *ChemSusChem* **2016**, *9* (8), 770–783. https://doi.org/10.1002/cssc.201501531.

(99) Karagoz, P.; Khiawjan, S.; Marques, M. P. C.; Santzouk, S.; Bugg, T. D. H.; Lye, G. J. Pharmaceutical Applications of Lignin-Derived Chemicals and Lignin-Based Materials: Linking Lignin Source and Processing with Clinical Indication. *Biomass Conv. Bioref.* **2023**. https://doi.org/10.1007/s13399-023-03745-5.

(100) Inwood, J. P. W.; Pakzad, L.; Fatehi, P. Production of Sulfur Containing Kraft Lignin Products. *BioResources* **2017**, *13* (1), 53–70. https://doi.org/10.15376/biores.13.1.53-70.

(101) Glasser, W. G. Lignin-Based Polymers. In *Encyclopedia of Materials: Science and Technology*; Elsevier, 2001; pp 1–4. https://doi.org/10.1016/B0-08-043152-6/00788-9.

(102) Chen, H. Lignocellulose Biorefinery Feedstock Engineering. In *Lignocellulose Biorefinery Engineering*; Elsevier, 2015; pp 37–86. https://doi.org/10.1016/B978-0-08-100135-6.00003-X.

(103) Liu, J.; Li, X.; Li, M.; Zheng, Y. Lignin Biorefinery: Lignin Source, Isolation, Characterization, and Bioconversion. In *Advances in Bioenergy*; Elsevier, 2022; Vol. 7, pp 211–270. https://doi.org/10.1016/bs.aibe.2022.05.004.

(104) Giannakopoulou, A.; Tsapara, G.; Troganis, A. N.; Koralli, P.; Chochos, C. L.; Polydera, A. C.; Katapodis, P.; Barkoula, N.-M.; Stamatis, H. Development of a Multi-Enzymatic Approach for the Modification of

Biopolymers with Ferulic Acid. *Biomolecules* **2022**, *12* (7), 992. https://doi.org/10.3390/biom12070992.

(105) Windeisen, E.; Wegener, G. Lignin as Building Unit for Polymers. In *Polymer Science: A Comprehensive Reference*; Elsevier, 2012; pp 255–265. https://doi.org/10.1016/B978-0-444-53349-4.00263-6.

(106) The Environmental Impact of Kraft Pulping. https://paper-pulper.com/the-environmental-impact-of-kraft-pulping/.

(107) Gavrilescu, D.; Puitel, A. C.; Dutuc, G.; Craciun, G. ENVIRONMENTAL IMPACT OF PULP AND PAPER MILLS. *Environ. Eng. Manag. J.* **2012**, *11* (1), 81–85. https://doi.org/10.30638/eemj.2012.012.

(108) Cybulska, I.; Brudecki, G.; Rosentrater, K.; Julson, J. L.; Lei, H. Comparative Study of Organosolv Lignin Extracted from Prairie Cordgrass, Switchgrass and Corn Stover. *Bioresource Technology* **2012**, *118*, 30–36. https://doi.org/10.1016/j.biortech.2012.05.073.

(109) Melikoglu, M. Organosolv Lignin: A Comprehensive Review of Pretreatment Advancements and Biorefinery Integration. *Next Materials* **2025**, *9*, 101136. https://doi.org/10.1016/j.nxmate.2025.101136.

(110) Da Silva, A. R. G.; Errico, M.; Rong, B.-G. Solvent Recycle and Impurity Purge Evaluation for Organosolv Pretreatment Method for Bioethanol Production from Lignocellulosic Biomass. In *Computer Aided Chemical Engineering*; Elsevier, 2017; Vol. 40, pp 1141–1146. https://doi.org/10.1016/B978-0-444-63965-3.50192-6.

(111) *Organosolv Lignin Market Summary*. Reports and Data. https://www.reportsanddata.com/report-detail/organosolv-lignin-market (accessed 2026-01-22).

(112) Kumar, A.; Anushree; Kumar, J.; Bhaskar, T. Utilization of Lignin: A Sustainable and Eco-Friendly Approach. *Journal of the Energy Institute* **2020**, *93* (1), 235–271. https://doi.org/10.1016/j.joei.2019.03.005.

(113) Yadav, P.; Athanassiadis, D.; Antonopoulou, I.; Rova, U.; Christakopoulos, P.; Tysklind, M.; Matsakas, L. Environmental Impact and Cost Assessment of a Novel Lignin Production Method. *Journal of Cleaner Production* **2021**, *279*, 123515. https://doi.org/10.1016/j.jclepro.2020.123515.

(114) Bernier, E.; Lavigne, C.; Robidoux, P. Y. Life Cycle Assessment of Kraft Lignin for Polymer Applications. *Int J Life Cycle Assess* **2013**, *18* (2), 520–528. https://doi.org/10.1007/s11367-012-0503-y.

(115) Hoang, A. T.; Nguyen, X. P.; Duong, X. Q.; Ağbulut, Ü.; Len, C.; Nguyen, P. Q. P.; Kchaou, M.; Chen, W.-H. Steam Explosion as Sustainable Biomass Pretreatment Technique for Biofuel Production: Characteristics

and Challenges. *Bioresource Technology* **2023**, *385*, 129398. https://doi.org/10.1016/j.biortech.2023.129398.

(116) Mahmood, N.; Yuan, Z.; Schmidt, J.; Xu, C. (Charles). Hydrolytic Depolymerization of Hydrolysis Lignin: Effects of Catalysts and Solvents. *Bioresource Technology* **2015**, *190*, 416–419. https://doi.org/10.1016/j.biortech.2015.04.074.

(117) Pienihäkkinen, E.; Lindfors, C.; Ohra-aho, T.; Lehtonen, J.; Granström, T.; Yamamoto, M.; Oasmaa, A. Fast Pyrolysis of Hydrolysis Lignin in Fluidized Bed Reactors. *Energy Fuels* **2021**, *35* (18), 14758–14769. https://doi.org/10.1021/acs.energyfuels.1c01719.

(118) Lu, X.; Gu, X. A Review on Lignin Pyrolysis: Pyrolytic Behavior, Mechanism, and Relevant Upgrading for Improving Process Efficiency. *Biotechnol Biofuels* **2022**, *15* (1), 106. https://doi.org/10.1186/s13068-022-02203-0.

(119) Figueirêdo, M. B.; Hita, I.; Deuss, P. J.; Venderbosch, R. H.; Heeres, H. J. Pyrolytic Lignin: A Promising Biorefinery Feedstock for the Production of Fuels and Valuable Chemicals. *Green Chem.* **2022**, *24* (12), 4680–4702. https://doi.org/10.1039/D2GC00302C.

(120) Figueirêdo, M. B.; Deuss, P. J.; Venderbosch, R. H.; Heeres, H. J. Catalytic Hydrotreatment of Pyrolytic Lignins from Different Sources to Biobased Chemicals: Identification of Feed-Product Relations. *Biomass and Bioenergy* **2020**, *134*, 105484. https://doi.org/10.1016/j.biombioe.2020.105484.

(121) Talebi Amiri, M.; Dick, G. R.; Questell-Santiago, Y. M.; Luterbacher, J. S. Fractionation of Lignocellulosic Biomass to Produce Uncondensed Aldehyde-Stabilized Lignin. *Nat Protoc* **2019**, *14* (3), 921–954. https://doi.org/10.1038/s41596-018-0121-7.

(122) Behaghel De Bueren, J.; Héroguel, F.; Wegmann, C.; Dick, G. R.; Buser, R.; Luterbacher, J. S. Aldehyde-Assisted Fractionation Enhances Lignin Valorization in Endocarp Waste Biomass. *ACS Sustainable Chem. Eng.* **2020**, *8* (45), 16737–16745. https://doi.org/10.1021/acssuschemeng.0c03360.

(123) Vendamme, R.; Behaghel De Bueren, J.; Gracia-Vitoria, J.; Isnard, F.; Mulunda, M. M.; Ortiz, P.; Wadekar, M.; Vanbroekhoven, K.; Wegmann, C.; Buser, R.; Héroguel, F.; Luterbacher, J. S.; Eevers, W. Aldehyde-Assisted Lignocellulose Fractionation Provides Unique Lignin Oligomers for the Design of Tunable Polyurethane Bioresins. *Biomacromolecules* **2020**, *21* (10), 4135–4148. https://doi.org/10.1021/acs.biomac.0c00927.

(124) Bertella, S.; Bernardes Figueirêdo, M.; De Angelis, G.; Mourez, M.; Bourmaud, C.; Amstad, E.; Luterbacher, J. S. Extraction and Surfactant

Properties of Glyoxylic Acid-Functionalized Lignin. *ChemSusChem* **2022**, *15* (15), e202200270. https://doi.org/10.1002/cssc.202200270.

(125) George, A.; Brandt, A.; Tran, K.; Zahari, S. M. S. N. S.; Klein-Marcuschamer, D.; Sun, N.; Sathitsuksanoh, N.; Shi, J.; Stavila, V.; Parthasarathi, R.; Singh, S.; Holmes, B. M.; Welton, T.; Simmons, B. A.; Hallett, J. P. Design of Low-Cost Ionic Liquids for Lignocellulosic Biomass Pretreatment. *Green Chem.* **2015**, *17* (3), 1728–1734. https://doi.org/10.1039/C4GC01208A.

(126) Ovejero-Pérez, A.; Rigual, V.; Domínguez, J. C.; Alonso, M. V.; Oliet, M.; Rodriguez, F. Organosolv and Ionosolv Processes for Autohydrolyzed Poplar Fractionation: Lignin Recovery and Characterization. *International Journal of Biological Macromolecules* **2022**, *197*, 131–140. https://doi.org/10.1016/j.ijbiomac.2021.12.079.

(127) Ovejero-Pérez, A.; Rigual, V.; Domínguez, J. C.; Alonso, M. V.; Oliet, M.; Rodriguez, F. Effect of Autohydrolysis and Ionosolv Treatments on Eucalyptus Fractionation and Recovered Lignin Properties. *RSC Adv.* **2023**, *13* (15), 10338–10348. https://doi.org/10.1039/D2RA08013C.

(128) Chen, Z.; Ragauskas, A.; Wan, C. Lignin Extraction and Upgrading Using Deep Eutectic Solvents. *Industrial Crops and Products* **2020**, *147*, 112241. https://doi.org/10.1016/j.indcrop.2020.112241.

(129) Zhou, M.; Fakayode, O. A.; Ren, M.; Li, H.; Liang, J.; Zhou, C. Green and Sustainable Extraction of Lignin by Deep Eutectic Solvent, Its Antioxidant Activity, and Applications in the Food Industry. *Critical Reviews in Food Science and Nutrition* **2023**, 1–19. https://doi.org/10.1080/10408398.2023.2181762.

(130) Beaucamp, A.; Muddasar, M.; Amiinu, I. S.; Moraes Leite, M.; Culebras, M.; Latha, K.; Gutiérrez, M. C.; Rodriguez-Padron, D.; Del Monte, F.; Kennedy, T.; Ryan, K. M.; Luque, R.; Titirici, M.-M.; Collins, M. N. Lignin for Energy Applications – State of the Art, Life Cycle, Technoeconomic Analysis and Future Trends. *Green Chem.* **2022**, *24* (21), 8193–8226. https://doi.org/10.1039/D2GC02724K.

(131) Liu, Y.; Deak, N.; Wang, Z.; Yu, H.; Hameleers, L.; Jurak, E.; Deuss, P. J.; Barta, K. Tunable and Functional Deep Eutectic Solvents for Lignocellulose Valorization. *Nat Commun* **2021**, *12* (1), 5424. https://doi.org/10.1038/s41467-021-25117-1.

(132) Rico-García, D.; Ruiz-Rubio, L.; Pérez-Alvarez, L.; Hernández-Olmos, S. L.; Guerrero-Ramírez, G. L.; Vilas-Vilela, J. L. Lignin-Based Hydrogels: Synthesis and Applications. *Polymers* **2020**, *12* (1), 81. https://doi.org/10.3390/polym12010081.

(133) Gan, M. J.; Niu, Y. Q.; Qu, X. J.; Zhou, C. H. Lignin to Value-Added Chemicals and Advanced Materials: Extraction, Degradation, and

Functionalization. *Green Chem.* **2022**, *24* (20), 7705–7750. https://doi.org/10.1039/D2GC00092J.

(134) Figueiredo, P.; Lintinen, K.; Hirvonen, J. T.; Kostiainen, M. A.; Santos, H. A. Properties and Chemical Modifications of Lignin: Towards Lignin-Based Nanomaterials for Biomedical Applications. *Progress in Materials Science* **2018**, *93*, 233–269. https://doi.org/10.1016/j.pmatsci.2017.12.001.

(135) Lang, J. M.; Shrestha, U. M.; Dadmun, M. The Effect of Plant Source on the Properties of Lignin-Based Polyurethanes. *Front. Energy Res.* **2018**, *6*, 4. https://doi.org/10.3389/fenrg.2018.00004.

(136) Jiao, G.-J.; Xu, Q.; Cao, S.-L.; Peng, P.; She, D. Controlled-Release Fertilizer with Lignin Used to Trap Urea/Hydroxymethylurea/ Urea-Formaldehyde Polymers. *BioResources* **2018**, *13* (1), 1711–1728. https://doi.org/10.15376/biores.13.1.1711-1728.

(137) Klinger, K. M.; Liebner, F.; Hosoya, T.; Potthast, A.; Rosenau, T. Ammoxidation of Lignocellulosic Materials: Formation of Nonheterocyclic Nitrogenous Compounds from Monosaccharides. *J. Agric. Food Chem.* **2013**, *61* (38), 9015–9026. https://doi.org/10.1021/jf401960m.

(138) Meier, D.; Zúñiga-Partida, V.; Ramírez-Cano, F.; Hahn, N.-C.; Faix, O. Conversion of Technical Lignins into Slow-Release Nitrogenous Fertilizers by Ammoxidation in Liquid Phase. *Bioresource Technology* **1994**, *49* (2), 121–128. https://doi.org/10.1016/0960-8524(94)90075-2.

(139) Jiao, Y. Synthesis and Application of the Cationic Lignin Amine Flocculant. *Tenside Surfactants Detergents* **2010**, *47* (6), 381–384. https://doi.org/10.3139/113.110090.

(140) Kazzaz, A. E.; Fatehi, P. Reusable Porous Amphoteric Lignin for Water Desalination. *Journal of Environmental Chemical Engineering* **2021**, *9* (4), 105339. https://doi.org/10.1016/j.jece.2021.105339.

(141) Meng, X.; Scheidemantle, B.; Li, M.; Wang, Y.; Zhao, X.; Toro-González, M.; Singh, P.; Pu, Y.; Wyman, C. E.; Ozcan, S.; Cai, C. M.; Ragauskas, A. J. Synthesis, Characterization, and Utilization of a Lignin-Based Adsorbent for Effective Removal of Azo Dye from Aqueous Solution. *ACS Omega* **2020**, *5* (6), 2865–2877. https://doi.org/10.1021/acsomega.9b03717.

(142) Kollman, M.; Jiang, X.; Thompson, S. J.; Mante, O.; Dayton, D. C.; Chang, H.; Jameel, H. Improved Understanding of Technical Lignin Functionalization through Comprehensive Structural Characterization of Fractionated Pine Kraft Lignins Modified by the Mannich Reaction. *Green Chem.* **2021**, *23* (18), 7122–7136. https://doi.org/10.1039/D1GC01842F.

(143) Jiao, G.-J.; Peng, P.; Sun, S.-L.; Geng, Z.-C.; She, D. Amination of Biorefinery Technical Lignin by Mannich Reaction for Preparing Highly Efficient Nitrogen Fertilizer. *International Journal of Biological*

Macromolecules **2019**, *127*, 544–554. https://doi.org/10.1016/j.ijbiomac.2019.01.076.

(144) Du, X.; Li, J.; Lindström, M. E. Modification of Industrial Softwood Kraft Lignin Using Mannich Reaction with and without Phenolation Pretreatment. *Industrial Crops and Products* **2014**, *52*, 729–735. https://doi.org/10.1016/j.indcrop.2013.11.035.

(145) Jiang, X.; Liu, J.; Du, X.; Hu, Z.; Chang, H.; Jameel, H. Phenolation to Improve Lignin Reactivity toward Thermosets Application. *ACS Sustainable Chem. Eng.* **2018**, *6* (4), 5504–5512. https://doi.org/10.1021/acssuschemeng.8b00369.

(146) Podschun, J.; Saake, B.; Lehnen, R. Reactivity Enhancement of Organosolv Lignin by Phenolation for Improved Bio-Based Thermosets. *European Polymer Journal* **2015**, *67*, 1–11. https://doi.org/10.1016/j.eurpolymj.2015.03.029.

(147) 1,4-Dioxane; MSDS No. 296309 [Online]; Sigma-Aldrich Chemie GmbH, Taufkirchen, DE, 2023. https://www.sigmaaldrich.com/DE/en/sds/sial/296309?userType=anonymous (accessed 2023-12-17).

(148) Ott, M. W.; Dietz, C.; Trosien, S.; Mehlhase, S.; Bitsch, M. J.; Nau, M.; Meckel, T.; Geissler, A.; Siegert, G.; Huong, J.; Hertel, B.; Stark, R. W.; Biesalski, M. Co-Curing of Epoxy Resins with Aminated Lignins: Insights into the Role of Lignin Homo Crosslinking during Lignin Amination on the Elastic Properties. *Holzforschung* **2021**, *75* (4), 390–398. https://doi.org/10.1515/hf-2020-0060.

(149) Abarro, G. J.; Podschun, J.; Diaz, L. J.; Ohashi, S.; Saake, B.; Lehnen, R.; Ishida, H. Benzoxazines with Enhanced Thermal Stability from Phenolated Organosolv Lignin. *RSC Adv.* **2016**, *6* (109), 107689–107698. https://doi.org/10.1039/C6RA22334F.

(150) Phalak, G. A.; Patil, D. M.; Mhaske, S. T. Synthesis and Characterization of Thermally Curable Guaiacol Based Poly(Benzoxazine-Urethane) Coating for Corrosion Protection on Mild Steel. *European Polymer Journal* **2017**, *88*, 93–108. https://doi.org/10.1016/j.eurpolymj.2016.12.030.

(151) Zhang, Y.; Liu, X.; McHale, C.; Li, R.; Zhang, L.; Wu, Y.; Ye, X.; Yang, X.; Ding, S. Bone Marrow Injury Induced via Oxidative Stress in Mice by Inhalation Exposure to Formaldehyde. *PLoS ONE* **2013**, *8* (9), e74974. https://doi.org/10.1371/journal.pone.0074974.

(152) Suresh, S.; Bandosz, T. J. Removal of Formaldehyde on Carbon -Based Materials: A Review of the Recent Approaches and Findings. *Carbon* **2018**, *137*, 207–221. https://doi.org/10.1016/j.carbon.2018.05.023.

(153) Chen, J.; An, L.; Bae, J. H.; Heo, J. W.; Han, S. Y.; Kim, Y. S. Green and Facile Synthesis of Aminated Lignin-Silver Complex and Its Antibacterial

Activity. *Industrial Crops and Products* **2021**, *173*, 114102. https://doi.org/10.1016/j.indcrop.2021.114102.

(154) 2-Chloroethylamine Hydrochloride; MSDS No. C40200 [Online]; Sigma-Aldrich Chemie GmbH, Taufkirchen, DE, 2023. https://www.sigmaaldrich.com/DE/en/sds/aldrich/c40200?userType=anonymous (accessed 2023-12-17).

(155) Ruijten, D.; Narmon, T.; De Weer, H.; Van Der Zweep, R.; Poleunis, C.; Debecker, D. P.; Maes, B. U. W.; Sels, B. F. Hydrogen Borrowing: Towards Aliphatic Tertiary Amines from Lignin Model Compounds Using a Supported Copper Catalyst. *ChemSusChem* **2022**, *15* (19), e202200868. https://doi.org/10.1002/cssc.202200868.

(156) Jacobs, B.; Yao, Y.; Van Nieuwenhove, I.; Sharma, D.; Graulus, G.-J.; Bernaerts, K.; Verberckmoes, A. Sustainable Lignin Modifications and Processing Methods: Green Chemistry as the Way Forward. *Green Chem.* **2023**, *25* (6), 2042–2086. https://doi.org/10.1039/D2GC04699G.

(157) Liu, L.; Wan, X.; Chen, S.; Boonthamrongkit, P.; Sipponen, M.; Renneckar, S. Solventless Amination of Lignin and Natural Phenolics Using 2-Oxazolidinone. *ChemSusChem* **2023**, *16* (15), e202300276. https://doi.org/10.1002/cssc.202300276.

(158) 2-Oxazolidinone; MSDS No. O9409 [Online]; Sigma-Aldrich Chemie GmbH, Taufkirchen, DE, 2023. https://www.sigmaaldrich.com/DE/en/sds/aldrich/o9409?userType=anonymous (accessed 2023-12-17).

(159) Yang, X.; Xu, L.; Zhu, Y.; Zhang, S.; Jia, G.; Du, J. Efficient Fabrication of Oxazolidinones for the Carboxylative Cyclization with Carbon Dioxide. *Journal of CO2 Utilization* **2023**, *74*, 102531. https://doi.org/10.1016/j.jcou.2023.102531.

(160) Over, L. C.; Grau, E.; Grelier, S.; Meier, M. A. R.; Cramail, H. Synthesis and Characterization of Epoxy Thermosetting Polymers from Glycidylated Organosolv Lignin and Bisphenol A. *Macromol. Chem. Phys.* **2017**, *218* (4), 1600411. https://doi.org/10.1002/macp.201600411.

(161) Wang, X.; Leng, W.; Nayanathara, R. M. O.; Caldona, E. B.; Liu, L.; Chen, L.; Advincula, R. C.; Zhang, Z.; Zhang, X. Anticorrosive Epoxy Coatings from Direct Epoxidation of Bioethanol Fractionated Lignin. *International Journal of Biological Macromolecules* **2022**, *221*, 268–277. https://doi.org/10.1016/j.ijbiomac.2022.08.177.

(162) Li, X.-Y.; Xiao, L.-P.; Zou, S.-L.; Xu, Q.; Wang, Q.; Lv, Y.-H.; Sun, R.-C. Preparation and Characterization of Bisphenol A-Based Thermosetting

Epoxies Based on Modified Lignin. *ACS Appl. Polym. Mater.* **2023**, *5* (5), 3611–3621. https://doi.org/10.1021/acsapm.3c00262.

(163) Behr, A.; Eilting, J.; Irawadi, K.; Leschinski, J.; Lindner, F. Improved Utilisation of Renewable Resources: New Important Derivatives of Glycerol. *Green Chem.* **2008**, *10* (1), 13–30. https://doi.org/10.1039/B710561D.

(164) Krafft, P.; Gilbeau, P.; Gosselin, B.; Claessens, S. Process for Producing Dichloropropanol from Glycerol. EP1760060B1, 2007.

(165) Lithner, D.; Larsson, Å.; Dave, G. Environmental and Health Hazard Ranking and Assessment of Plastic Polymers Based on Chemical Composition. *Science of The Total Environment* **2011**, *409* (18), 3309–3324. https://doi.org/10.1016/j.scitotenv.2011.04.038.

(166) (±)-Epichlorohydrin; MSDS No. 45340 [Online]; Sigma-Aldrich Chemie GmbH, Taufkirchen, DE, 2023. https://www.sigmaaldrich.com/DE/en/sds/sial/45340?userType=anonymous (accessed 2024-01-29).

(167) Sasaki, C.; Wanaka, M.; Takagi, H.; Tamura, S.; Asada, C.; Nakamura, Y. Evaluation of Epoxy Resins Synthesized from Steam-Exploded Bamboo Lignin. *Industrial Crops and Products* **2013**, *43*, 757–761. https://doi.org/10.1016/j.indcrop.2012.08.018.

(168) Xin, J.; Li, M.; Li, R.; Wolcott, M. P.; Zhang, J. Green Epoxy Resin System Based on Lignin and Tung Oil and Its Application in Epoxy Asphalt. *ACS Sustainable Chem. Eng.* **2016**, *4* (5), 2754–2761. https://doi.org/10.1021/acssuschemeng.6b00256.

(169) Møller, L.; Leck Fotel, F.; Bo Larsen, P. Survey of Bisphenol A and Bisphenol-Adiglycidylether Polymer, 2012. https://www2.mst.dk/udgiv/publications/2013/04/978-87-93026-14-8.pdf (accessed 2024-12-12).

(170) Garcia, F. G.; Soares, B. G.; Pita, V. J. R. R.; Sánchez, R.; Rieumont, J. Mechanical Properties of Epoxy Networks Based on DGEBA and Aliphatic Amines. *J of Applied Polymer Sci* **2007**, *106* (3), 2047–2055. https://doi.org/10.1002/app.24895.

(171) Alexander, H. C.; Dill, D. C.; Smith, L. W.; Guiney, P. D.; Dorn, P. Bisphenol a: Acute Aquatic Toxicity. *Enviro Toxic and Chemistry* **1988**, *7* (1), 19–26. https://doi.org/10.1002/etc.5620070104.

(172) Rochester, J. R. Bisphenol A and Human Health: A Review of the Literature. *Reproductive Toxicology* **2013**, *42*, 132–155. https://doi.org/10.1016/j.reprotox.2013.08.008.

(173) Bisphenol A; MSDS No. 239658 [Online]; Sigma-Aldrich Chemie GmbH, Taufkirchen, DE, 2023.

https://www.sigmaaldrich.com/DE/en/sds/aldrich/239658?userType=anonymous (accessed 2023-12-29).

(174) Gioia, C.; Lo Re, G.; Lawoko, M.; Berglund, L. Tunable Thermosetting Epoxies Based on Fractionated and Well-Characterized Lignins. *J. Am. Chem. Soc.* **2018**, *140* (11), 4054–4061. https://doi.org/10.1021/jacs.7b13620.

(175) Silau, H.; Garcia, A. G.; Woodley, J. M.; Dam-Johansen, K.; Daugaard, A. E. Bio-Based Epoxy Binders from Lignin Derivatized with Epoxidized Rapeseed Fatty Acids in Bimodal Coating Systems. *ACS Appl. Polym. Mater.* **2022**, *4* (1), 444–451. https://doi.org/10.1021/acsapm.1c01351.

(176) Neises, B.; Steglich, W. Simple Method for the Esterification of Carboxylic Acids. *Angew. Chem. Int. Ed. Engl.* **1978**, *17* (7), 522–524. https://doi.org/10.1002/anie.197805221.

(177) Höfle, G.; Steglich, W.; Vorbrüggen, H. 4-Dialkylaminopyridines as Highly Active Acylation Catalysts. [New Synthetic Method (25)]. *Angew. Chem. Int. Ed. Engl.* **1978**, *17* (8), 569–583. https://doi.org/10.1002/anie.197805691.

(178) DCC; MSDS No. D80002 [Online]; Sigma-Aldrich Chemie GmbH, Taufkirchen, DE, 2023. https://www.sigmaaldrich.com/DE/en/sds/aldrich/d80002?userType=anonymous (accessed 2023-12-20).

(179) Laurichesse, S.; Huillet, C.; Avérous, L. Original Polyols Based on Organosolv Lignin and Fatty Acids: New Bio-Based Building Blocks for Segmented Polyurethane Synthesis. *Green Chem.* **2014**, *16* (8), 3958–3970. https://doi.org/10.1039/C4GC00596A.

(180) Chua, S.-C.; Xu, X.; Guo, Z. Emerging Sustainable Technology for Epoxidation Directed toward Plant Oil-Based Plasticizers. *Process Biochemistry* **2012**, *47* (10), 1439–1451. https://doi.org/10.1016/j.procbio.2012.05.025.

(181) Biermann, U.; Friedt, W.; Lang, S.; Lühs, W.; Machmüller, G.; Metzger, J. O.; Rüsch Gen. Klaas, M.; Schäfer, H. J.; Schneider, M. P. New Syntheses with Oils and Fats as Renewable Raw Materials for the Chemical Industry. *Angew. Chem. Int. Ed.* **2000**, *39* (13), 2206–2224.

https://doi.org/10.1002/1521-3773(20000703)39:13<2206::AID-ANIE2206>3.0.CO;2-P.

(182) Liu, L.-Y.; Hua, Q.; Renneckar, S. A Simple Route to Synthesize Esterified Lignin Derivatives. *Green Chem.* **2019**, *21* (13), 3682–3692. https://doi.org/10.1039/C9GC00844F.

(183) Clements, J. H. Reactive Applications of Cyclic Alkylene Carbonates. *Ind. Eng. Chem. Res.* **2003**, *42* (4), 663–674. https://doi.org/10.1021/ie020678i.

(184) Ethylene Oxide; MSDS No. 387614 [Online]; Sigma-Aldrich Chemie GmbH, Taufkirchen, DE, 2023. https://www.sigmaaldrich.com/DE/en/sds/aldrich/387614?userType=anonymous (accessed 2024-01-05).

(185) Vásquez-Garay, F.; Teixeira Mendonça, R.; Peretti, S. W. Chemoenzymatic Lignin Valorization: Production of Epoxidized Pre-Polymers Using Candida Antarctica Lipase B. *Enzyme and Microbial Technology* **2018**, *112*, 6–13. https://doi.org/10.1016/j.enzmictec.2018.01.007.

(186) Allyl Bromide; MSDS No. 337528 [Online]; Sigma-Aldrich Chemie GmbH, Taufkirchen, DE, 2023. https://www.sigmaaldrich.com/DE/en/sds/aldrich/337528?userType=anonymous (accessed 2024-01-03).

(187) Hirose, S.; Hatakeyama, T.; Hatakeyama, H. Synthesis and Thermal Properties of Epoxy Resins from Ester-carboxylic Acid Derivative of Alcoholysis Lignin. *Macromolecular Symposia* **2003**, *197* (1), 157–170. https://doi.org/10.1002/masy.200350715.

(188) Hirose, S.; Hatakeyama, T.; Hatakeyama, H. Glass Transition and Thermal Decomposition of Epoxy Resins from the Carboxylic Acid System Consisting of Ester-Carboxylic Acid Derivatives of Alcoholysis Lignin and Ethylene Glycol with Various Dicarboxylic Acids. *Thermochimica Acta* **2005**, *431* (1–2), 76–80. https://doi.org/10.1016/j.tca.2005.01.043.

(189) Ismail, T. N. M. T.; Hassan, H. A.; Hirose, S.; Taguchi, Y.; Hatakeyama, T.; Hatakeyama, H. Synthesis and Thermal Properties of Ester-type Crosslinked Epoxy Resins Derived from Lignosulfonate and Glycerol. *Polymer International* **2010**, *59* (2), 181–186. https://doi.org/10.1002/pi.2705.

(190) Monteil-Rivera, F.; Paquet, L. Solvent-Free Catalyst-Free Microwave-Assisted Acylation of Lignin. *Industrial Crops and Products* **2015**, *65*, 446–453. https://doi.org/10.1016/j.indcrop.2014.10.060.

(191) Scarica, C.; Suriano, R.; Levi, M.; Turri, S.; Griffini, G. Lignin Functionalized with Succinic Anhydride as Building Block for Biobased

Thermosetting Polyester Coatings. *ACS Sustainable Chem. Eng.* **2018**, *6* (3), 3392–3401. https://doi.org/10.1021/acssuschemeng.7b03583.

(192) Sun, J.; Wang, C.; Stubbs, L. P.; He, C. Carboxylated Lignin as an Effective Cohardener for Enhancing Strength and Toughness of Epoxy. *Macro Materials & Eng* **2017**, *302* (12), 1700341. https://doi.org/10.1002/mame.201700341.

(193) Zhang, Y.; Wang, H.; Eberhardt, T. L.; Gu, Q.; Pan, H. Preparation of Carboxylated Lignin-Based Epoxy Resin with Excellent Mechanical Properties. *European Polymer Journal* **2021**, *150*, 110389. https://doi.org/10.1016/j.eurpolymj.2021.110389.

(194) Thielemans, W.; Wool, R. P. Lignin Esters for Use in Unsaturated Thermosets: Lignin Modification and Solubility Modeling. *Biomacromolecules* **2005**, *6* (4), 1895–1905. https://doi.org/10.1021/bm0500345.

(195) Zhou, S.; Huang, K.; Xu, X.; Wang, B.; Zhang, W.; Su, Y.; Hu, K.; Zhang, C.; Zhu, J.; Weng, G.; Ma, S. Rigid-and-Flexible, Degradable, Fully Biobased Thermosets from Lignin and Soybean Oil: Synthesis and Properties. *ACS Sustainable Chem. Eng.* **2023**, *11* (8), 3466–3473. https://doi.org/10.1021/acssuschemeng.2c06990.

(196) Liu, W.; Zhou, R.; Goh, H. L. S.; Huang, S.; Lu, X. From Waste to Functional Additive: Toughening Epoxy Resin with Lignin. *ACS Appl. Mater. Interfaces* **2014**, *6* (8), 5810–5817. https://doi.org/10.1021/am500642n.

(197) Zhang, Y.; Li, J.; Wu, X.; Wang, D.; Zhou, S.; Han, S.; Wang, H.; Sun, F. Simultaneously Reinforcing and Toughening of Shape-Memory Epoxy Resin with Carboxylated Lignosulfonate: Facile Preparation and Effect Mechanism. *International Journal of Biological Macromolecules* **2022**, *217*, 243–254. https://doi.org/10.1016/j.ijbiomac.2022.07.047.

(198) Lohbeck, K.; Haferkorn, H.; Fuhrmann, W.; Fedtke, N. Maleic and Fumaric Acids. In *Ullmann's Encyclopedia of Industrial Chemistry*; Wiley-VCH, Ed.; Wiley, 2000. https://doi.org/10.1002/14356007.a16_053.

(199) Cornils, B.; Lappe, P.; By Staff, U. Dicarboxylic Acids, Aliphatic. In *Ullmann's Encyclopedia of Industrial Chemistry*; Wiley-VCH Verlag GmbH & Co. KGaA, Ed.; Wiley-VCH Verlag GmbH & Co. KGaA: Weinheim, Germany, 2014; pp 1–18. https://doi.org/10.1002/14356007.a08_523.pub3.

(200) Isikgor, F. H.; Becer, C. R. Lignocellulosic Biomass: A Sustainable Platform for the Production of Bio-Based Chemicals and Polymers. *Polym. Chem.* **2015**, *6* (25), 4497–4559. https://doi.org/10.1039/C5PY00263J.

(201) Bechthold, I.; Bretz, K.; Kabasci, S.; Kopitzky, R.; Springer, A. Succinic Acid: A New Platform Chemical for Biobased Polymers from Renewable

Resources. *Chem Eng & Technol* **2008**, *31* (5), 647–654. https://doi.org/10.1002/ceat.200800063.

(202) Boarino, A.; Charmillot, J.; Figueirêdo, M. B.; Le, T. T. H.; Carrara, N.; Klok, H.-A. Ductile, High-Lignin-Content Thermoset Films and Coatings. *ACS Sustainable Chem. Eng.* **2023**, *11* (46), 16442–16452. https://doi.org/10.1021/acssuschemeng.3c03030.

(203) Dick, G. R.; Komarova, A. O.; Luterbacher, J. S. Controlling Lignin Solubility and Hydrogenolysis Selectivity by Acetal-Mediated Functionalization. *Green Chem.* **2022**, *24* (3), 1285–1293. https://doi.org/10.1039/D1GC02575A.

(204) Alder, C. M.; Hayler, J. D.; Henderson, R. K.; Redman, A. M.; Shukla, L.; Shuster, L. E.; Sneddon, H. F. Updating and Further Expanding GSK's Solvent Sustainability Guide. *Green Chem.* **2016**, *18* (13), 3879–3890. https://doi.org/10.1039/C6GC00611F.

(205) *Avantium,Volta Technology*. https://www.avantium.com/technologies/volta/ (accessed 2024-01-22).

(206) Kaczur, J. J.; Lakkaraju, P.; Teamey, K. Method and System for Electrochemical Reduction of Carbon Dioxide Employing a Gas Diffusion Electrode. US10329676B2, 2019.

(207) Shuai, L.; Amiri, M. T.; Questell-Santiago, Y. M.; Héroguel, F.; Li, Y.; Kim, H.; Meilan, R.; Chapple, C.; Ralph, J.; Luterbacher, J. S. Formaldehyde Stabilization Facilitates Lignin Monomer Production during Biomass Depolymerization. *Science* **2016**, *354* (6310), 329–333. https://doi.org/10.1126/science.aaf7810.

(208) Sen, S.; Patil, S.; Argyropoulos, D. S. Thermal Properties of Lignin in Copolymers, Blends, and Composites: A Review. *Green Chem.* **2015**, *17* (11), 4862–4887. https://doi.org/10.1039/C5GC01066G.

(209) Taher, M. A.; Wang, X.; Faridul Hasan, K. M.; Miah, M. R.; Zhu, J.; Chen, J. Lignin Modification for Enhanced Performance of Polymer Composites. *ACS Appl. Bio Mater.* **2023**, *6* (12), 5169–5192. https://doi.org/10.1021/acsabm.3c00783.

(210) Koivu, K. A. Y.; Sadeghifar, H.; Nousiainen, P. A.; Argyropoulos, D. S.; Sipilä, J. Effect of Fatty Acid Esterification on the Thermal Properties of Softwood Kraft Lignin. *ACS Sustainable Chem. Eng.* **2016**, *4* (10), 5238–5247. https://doi.org/10.1021/acssuschemeng.6b01048.

(211) Van der Steen, M.; Stevens, C. V. Undecylenic Acid: A Valuable and Physiologically Active Renewable Building Block from Castor Oil. *ChemSusChem* **2009**, *2* (8), 692–713. https://doi.org/10.1002/cssc.200900075.

(212) Xing, Q.; Ruch, D.; Dubois, P.; Wu, L.; Wang, W.-J. Biodegradable and High-Performance Poly(Butylene Adipate- *Co* -Terephthalate)–Lignin UV-

Blocking Films. *ACS Sustainable Chem. Eng.* **2017**, *5* (11), 10342–10351. https://doi.org/10.1021/acssuschemeng.7b02370.

(213) Améduri, B.; Boutevin, B.; Czub, P.; Penczek, P.; Pielichowski, J.; Rodríguez-Pérez, M. A.; Taguet, A.; Abe, A.; Dusˇek, K.; Kobayashi, S. *Crosslinking in Materials Science: Technical Applications*; Advances in Polymer Science; Springer Berlin Heidelberg, 2005.

(214) Luo, S.; Cao, J.; McDonald, A. G. Cross-Linking of Technical Lignin via Esterification and Thermally Initiated Free Radical Reaction. *Industrial Crops and Products* **2018**, *121*, 169–179. https://doi.org/10.1016/j.indcrop.2018.05.007.

(215) Thiebaud, S.; Borredon, M. E. Solvent-Free Wood Esterification with Fatty Acid Chlorides. *Bioresource Technology* **1995**, *52* (2), 169–173. https://doi.org/10.1016/0960-8524(95)00018-A.

(216) Henderson, R. K.; Hill, A. P.; Redman, A. M.; Sneddon, H. F. Development of GSK's Acid and Base Selection Guides. *Green Chem.* **2015**, *17* (2), 945–949. https://doi.org/10.1039/C4GC01481B.

(217) 1-Methylimidazole for Synthesis; MSDS No. 8.05852 [Online]; Sigma-Aldrich Chemie GmbH, Taufkirchen, DE, 2023. https://www.sigmaaldrich.com/DE/en/sds/mm/8.05852?userType=anonymous (accessed 2024-01-23).

(218) Oxalyl Chloride, ReagentPlus®, ≥99%; MSDS No.221015 [Online]; Sigma-Aldrich Chemie GmbH, Taufkirchen, DE, 2024. https://www.sigmaaldrich.com/DE/en/sds/aldrich/221015?userType=anonymous (accessed 2024-01-01).

(219) Pfoertner, K.; Oppenländer, T. Photochemistry. In *Ullmann's Encyclopedia of Industrial Chemistry*; Wiley-VCH, Ed.; Wiley, 2012. https://doi.org/10.1002/14356007.a19_573.pub2.

(220) Held, H.; Rengstl, A.; Mayer, D. Acetic Anhydride and Mixed Fatty Acid Anhydrides. In *Ullmann's Encyclopedia of Industrial Chemistry*; Wiley-VCH, Ed.; Wiley, 2000. https://doi.org/10.1002/14356007.a01_065.

(221) Samel, U.; Kohler, W.; Gamer, A. O.; Keuser, U.; Yang, S.; Jin, Y.; Lin, M.; Wang, Z.; Teles, J. H. Propionic Acid and Derivatives. In *Ullmann's Encyclopedia of Industrial Chemistry*; Wiley-VCH, Ed.; Wiley, 2018; pp 1–20. https://doi.org/10.1002/14356007.a22_223.pub4.

(222) Kubitschke, J.; Lange, H.; Strutz, H. Carboxylic Acids, Aliphatic. In *Ullmann's Encyclopedia of Industrial Chemistry*; Wiley-VCH Verlag GmbH & Co. KGaA, Ed.; Wiley-VCH Verlag GmbH & Co. KGaA: Weinheim, Germany, 2014; pp 1–18. https://doi.org/10.1002/14356007.a05_235.pub2.

(223) Luo, S.; Cao, J.; McDonald, A. G. Esterification of Industrial Lignin and Its Effect on the Resulting Poly(3-Hydroxybutyrate-Co-3-Hydroxyvalerate) or

Polypropylene Blends. *Industrial Crops and Products* **2017**, *97*, 281–291. https://doi.org/10.1016/j.indcrop.2016.12.024.

(224) Liu, L.-Y.; Cho, M.; Sathitsuksanoh, N.; Chowdhury, S.; Renneckar, S. Uniform Chemical Functionality of Technical Lignin Using Ethylene Carbonate for Hydroxyethylation and Subsequent Greener Esterification. *ACS Sustainable Chem. Eng.* **2018**, *6* (9), 12251–12260. https://doi.org/10.1021/acssuschemeng.8b02649.

(225) Adjaoud, A.; Dieden, R.; Verge, P. Sustainable Esterification of a Soda Lignin with Phloretic Acid. *Polymers* **2021**, *13* (4), 637. https://doi.org/10.3390/polym13040637.

(226) Liu, L.-Y.; Chen, S.; Ji, L.; Jang, S.-K.; Renneckar, S. One-Pot Route to Convert Technical Lignin into Versatile Lignin Esters for Tailored Bioplastics and Sustainable Materials. *Green Chem.* **2021**, *23* (12), 4567–4579. https://doi.org/10.1039/D1GC01033F.

(227) Trejo-Machin, A.; Verge, P.; Puchot, L.; Quintana, R. Phloretic Acid as an Alternative to the Phenolation of Aliphatic Hydroxyls for the Elaboration of Polybenzoxazine. *Green Chem.* **2017**, *19* (21), 5065–5073. https://doi.org/10.1039/C7GC02348K.

(228) Liu, H.; Chung, H. Visible-Light Induced Thiol–Ene Reaction on Natural Lignin. *ACS Sustainable Chem. Eng.* **2017**, *5* (10), 9160–9168. https://doi.org/10.1021/acssuschemeng.7b02065.

(229) DMAP 4-(Dimethylamino)Pyridine Novabiochem®; MSDS No. 8.51055 [Online]; Sigma-Aldrich Chemie GmbH, Taufkirchen, DE, 2023. https://www.sigmaaldrich.com/DE/en/sds/mm/8.51055?userType=anonymous (accessed 2023-12-20).

(230) N,N-Dimethylformamide; MSDS No. 227056 [Online]; Sigma-Aldrich Chemie GmbH, Taufkirchen, DE, 2023. https://www.sigmaaldrich.com/DE/en/sds/sial/227056?userType=anonymous (accessed 2023-12-20).

(231) Yuan, L.; Zhang, Y.; Wang, Z.; Han, Y.; Tang, C. Plant Oil and Lignin-Derived Elastomers via Thermal Azide–Alkyne Cycloaddition Click Chemistry. *ACS Sustainable Chem. Eng.* **2019**, *7* (2), 2593–2601. https://doi.org/10.1021/acssuschemeng.8b05617.

(232) Han, Y.; Yuan, L.; Li, G.; Huang, L.; Qin, T.; Chu, F.; Tang, C. Renewable Polymers from Lignin via Copper-Free Thermal Click Chemistry. *Polymer* **2016**, *83*, 92–100. https://doi.org/10.1016/j.polymer.2015.12.010.

(233) Tetrahydrofuran, MSDS No. 401757 [Online]; Sigma-Aldrich Chemie GmbH, Taufkirchen, DE, 2023.

https://www.sigmaaldrich.com/DE/en/sds/sial/401757?userType=anonymous (accessed 2023-12-20).

(234) Propargyl Bromide; MSDS No. 81831 [Online]; Sigma-Aldrich Chemie GmbH, Taufkirchen, DE, 2023. https://www.sigmaaldrich.com/DE/en/sds/sial/81831?userType=anonymous (accessed 2023-12-21).

(235) Trimethylacetic Anhydride; MSDS No. 143502 [Online]; Sigma-Aldrich Chemie GmbH, Taufkirchen, DE, 2023. https://www.sigmaaldrich.com/DE/en/sds/aldrich/143502?userType=anonymous (accessed 2023-12-21).

(236) Hua, Q.; Liu, L.-Y.; Cho, M.; Karaaslan, M. A.; Zhang, H.; Kim, C. S.; Renneckar, S. Functional Lignin Building Blocks: Reactive Vinyl Esters with Acrylic Acid. *Biomacromolecules* **2023**, *24* (2), 592–603. https://doi.org/10.1021/acs.biomac.2c00806.

(237) Acrylic Acid; MSDS No. 147230 [Online]; Sigma-Aldrich Chemie GmbH, Taufkirchen, DE, 2023. https://www.sigmaaldrich.com/DE/en/sds/aldrich/147230?userType=undefined (accessed 2023-12-21).

(238) Jawerth, M.; Johansson, M.; Lundmark, S.; Gioia, C.; Lawoko, M. Renewable Thiol–Ene Thermosets Based on Refined and Selectively Allylated Industrial Lignin. *ACS Sustainable Chem. Eng.* **2017**, *5* (11), 10918–10925. https://doi.org/10.1021/acssuschemeng.7b02822.

(239) Allyl Chloride; MSDS No. A30702 [Online]; Sigma-Aldrich Chemie GmbH, Taufkirchen, DE, 2023. https://www.sigmaaldrich.com/DE/en/sds/aldrich/a30702?userType=anonymous (accessed 2023-12-21).

(240) Llevot, A.; Monney, B.; Sehlinger, A.; Behrens, S.; Meier, M. A. R. Highly Efficient Tsuji–Trost Allylation in Water Catalyzed by Pd-Nanoparticles. *Chem. Commun.* **2017**, *53* (37), 5175–5178. https://doi.org/10.1039/C7CC02380D.

(241) Truong, C. C.; Mishra, D. K.; Mishra, V. Organic Carbonate as a Green Solvent for Biocatalysis. In *Green Sustainable Process for Chemical and*

Environmental Engineering and Science; Elsevier, 2021; pp 253–275. https://doi.org/10.1016/B978-0-12-819721-9.00010-8.

(242) Sen, S.; Patil, S.; Argyropoulos, D. S. Methylation of Softwood Kraft Lignin with Dimethyl Carbonate. *Green Chem.* **2015**, *17* (2), 1077–1087. https://doi.org/10.1039/C4GC01759E.

(243) Li, Y.; Sarkanen, S. Alkylated Kraft Lignin-Based Thermoplastic Blends with Aliphatic Polyesters. *Macromolecules* **2002**, *35* (26), 9707–9715. https://doi.org/10.1021/ma021124u.

(244) Li, Y.; Sarkanen, S. Miscible Blends of Kraft Lignin Derivatives with Low-T_g Polymers. *Macromolecules* **2005**, *38* (6), 2296–2306. https://doi.org/10.1021/ma047546g.

(245) Sadeghifar, H.; Cui, C.; Argyropoulos, D. S. Toward Thermoplastic Lignin Polymers. Part 1. Selective Masking of Phenolic Hydroxyl Groups in Kraft Lignins via Methylation and Oxypropylation Chemistries. *Ind. Eng. Chem. Res.* **2012**, *51* (51), 16713–16720. https://doi.org/10.1021/ie301848j.

(246) Duval, A.; Avérous, L. Mild and Controlled Lignin Methylation with Trimethyl Phosphate: Towards a Precise Control of Lignin Functionality. *Green Chem.* **2020**, *22* (5), 1671–1680. https://doi.org/10.1039/C9GC03890F.

(247) Over, L. C.; Meier, M. A. R. Sustainable Allylation of Organosolv Lignin with Diallyl Carbonate and Detailed Structural Characterization of Modified Lignin. *Green Chem.* **2016**, *18* (1), 197–207. https://doi.org/10.1039/C5GC01882J.

(248) Over, L. C.; Hergert, M.; Meier, M. A. R. Metathesis Curing of Allylated Lignin and Different Plant Oils for the Preparation of Thermosetting Polymer Films with Tunable Mechanical Properties. *Macromol. Chem. Phys.* **2017**, *218* (16), 1700177. https://doi.org/10.1002/macp.201700177.

(249) Ribca, I.; Sochor, B.; Betker, M.; Roth, S. V.; Lawoko, M.; Sevastyanova, O.; Meier, M. A. R.; Johansson, M. Impact of Lignin Source on the Performance of Thermoset Resins. *European Polymer Journal* **2023**, *194*, 112141. https://doi.org/10.1016/j.eurpolymj.2023.112141.

(250) Tabanelli, T.; Monti, E.; Cavani, F.; Selva, M. The Design of Efficient Carbonate Interchange Reactions with Catechol Carbonate. *Green Chem.* **2017**, *19* (6), 1519–1528. https://doi.org/10.1039/C6GC03466G.

(251) Filippi, L.; Meier, M. A. R. Fully Renewable Non-Isocyanate Polyurethanes via the Lossen Rearrangement. *Macromol. Rapid Commun.* **2021**, *42* (3), 2000440. https://doi.org/10.1002/marc.202000440.

(252) Allyl Alcohol; MSDS No. 240532 [Online]; Sigma-Aldrich Chemie GmbH, Taufkirchen, DE, 2023.

https://www.sigmaaldrich.com/DE/en/sds/aldrich/240532?userType=anonymous (accessed 2023-12-28).

(253) Fairbairn, A.; Cheney, H.; Cherniavsky, A. Commercial Scale Manufacture of Allyl Chloride and Allyl Alcohol from Propylene. *Chemical Engineering Progress* **1947**, *43* (6), 280–290.

(254) Zulay Silva Vargas, K. Upscaling Allyl Alcohol Synthesis from Glycerol. PhD dissertation, Centrale Lille Institut, 2020.

(255) Aliahmadi, M.; Nemati Kharat, A.; Janczak, J. Catalytic Deoxydehydration of Glycerol to Allyl Alcohol in the Presence of Mono-Oxygenated Rhenium Diphosphine Complexes. *Polyhedron* **2024**, *248*, 116734. https://doi.org/10.1016/j.poly.2023.116734.

(256) Kühnel, I.; Saake, B.; Lehnen, R. Comparison of Different Cyclic Organic Carbonates in the Oxyalkylation of Various Types of Lignin. *Reactive and Functional Polymers* **2017**, *120*, 83–91. https://doi.org/10.1016/j.reactfunctpolym.2017.09.011.

(257) Duval, A.; Avérous, L. Cyclic Carbonates as Safe and Versatile Etherifying Reagents for the Functionalization of Lignins and Tannins. *ACS Sustainable Chem. Eng.* **2017**, *5* (8), 7334–7343. https://doi.org/10.1021/acssuschemeng.7b01502.

(258) Kühnel, I.; Saake, B.; Lehnen, R. Oxyalkylation of Lignin with Propylene Carbonate: Influence of Reaction Parameters on the Ensuing Bio-Based Polyols. *Industrial Crops and Products* **2017**, *101*, 75–83. https://doi.org/10.1016/j.indcrop.2017.03.002.

(259) Duval, A.; Vidal, D.; Sarbu, A.; René, W.; Avérous, L. Scalable Single-Step Synthesis of Lignin-Based Liquid Polyols with Ethylene Carbonate for Polyurethane Foams. *Materials Today Chemistry* **2022**, *24*, 100793. https://doi.org/10.1016/j.mtchem.2022.100793.

(260) 4-Vinyl-1,3-Dioxolan-2-One; MSDS No. 496820 [Online]; Sigma-Aldrich Chemie GmbH, Taufkirchen, DE, 2022. https://www.sigmaaldrich.com/DE/en/sds/aldrich/496820?userType=anonymous (accessed 2024-01-02).

(261) Glasser, W. G.; Leitheiser, R. H. Engineering Plastics from Lignin: 11. Hydroxypropyl Lignins as Components of Fire Resistant Foams. *Polymer Bulletin* **1984**, *12* (1), 1–5. https://doi.org/10.1007/BF00258264.

(262) Li, Y.; Ragauskas, A. J. Kraft Lignin-Based Rigid Polyurethane Foam. *Journal of Wood Chemistry and Technology* **2012**, *32* (3), 210–224. https://doi.org/10.1080/02773813.2011.652795.

(263) Kurańska, M.; Pinto, J. A.; Salach, K.; Barreiro, M. F.; Prociak, A. Synthesis of Thermal Insulating Polyurethane Foams from Lignin and Rapeseed Based Polyols: A Comparative Study. *Industrial Crops and*

Products **2020**, *143*, 111882. https://doi.org/10.1016/j.indcrop.2019.111882.

(264) Cateto, C. A.; Barreiro, M. F.; Rodrigues, A. E.; Belgacem, M. N. Optimization Study of Lignin Oxypropylation in View of the Preparation of Polyurethane Rigid Foams. *Ind. Eng. Chem. Res.* **2009**, *48* (5), 2583–2589. https://doi.org/10.1021/ie801251r.

(265) Perez-Arce, J.; Centeno-Pedrazo, A.; Labidi, J.; Ochoa-Gómez, J. R.; Garcia-Suarez, E. J. A Novel and Efficient Approach to Obtain Lignin-Based Polyols with Potential Industrial Applications. *Polym. Chem.* **2020**, *11* (46), 7362–7369. https://doi.org/10.1039/D0PY01142H.

(266) Nadji, H.; Bruzzèse, C.; Belgacem, M. N.; Benaboura, A.; Gandini, A. Oxypropylation of Lignins and Preparation of Rigid Polyurethane Foams from the Ensuing Polyols. *Macro Materials & Eng* **2005**, *290* (10), 1009–1016. https://doi.org/10.1002/mame.200500200.

(267) (±)-Propylene Oxide; MSDS No. 82320 [Online]; Sigma-Aldrich Chemie GmbH, Taufkirchen, DE, 2024. https://www.sigmaaldrich.com/DE/en/sds/aldrich/82320?userType=anonymous (accessed 2024-01-22).

(268) Du, Q.; Liang, H.; Zhang, Q. Hazards of Propylene Oxide Aerosols in the Secondary Explosion. *Combustion Science and Technology* **2023**, *195* (1), 153–168. https://doi.org/10.1080/00102202.2021.1939320.

(269) Duval, A.; Avérous, L. Oxyalkylation of Condensed Tannin with Propylene Carbonate as an Alternative to Propylene Oxide. *ACS Sustainable Chem. Eng.* **2016**, *4* (6), 3103–3112. https://doi.org/10.1021/acssuschemeng.6b00081.

(270) Pescarmona, P. P. Cyclic Carbonates Synthesised from CO2: Applications, Challenges and Recent Research Trends. *Current Opinion in Green and Sustainable Chemistry* **2021**, *29*, 100457. https://doi.org/10.1016/j.cogsc.2021.100457.

(271) Kühnel, I.; Saake, B.; Lehnen, R. A New Environmentally Friendly Approach to Lignin-Based Cyclic Carbonates. *Macromol. Chem. Phys.* **2018**, *219* (7), 1700613. https://doi.org/10.1002/macp.201700613.

(272) De La Cruz-Martínez, F.; Castro-Osma, J. A.; Lara-Sánchez, A. Catalytic Synthesis of Bio-Sourced Organic Carbonates and Sustainable Hybrid Materials from CO2. In *Advances in Catalysis*; Elsevier, 2022; Vol. 70, pp 189–236. https://doi.org/10.1016/bs.acat.2022.07.003.

(273) Chen, Q.; Gao, K.; Peng, C.; Xie, H.; Zhao, Z. K.; Bao, M. Preparation of Lignin/Glycerol-Based Bis(Cyclic Carbonate) for the Synthesis of

Polyurethanes. *Green Chem.* **2015**, *17* (9), 4546–4551. https://doi.org/10.1039/C5GC01340B.

(274) Salanti, A.; Zoia, L.; Orlandi, M. Chemical Modifications of Lignin for the Preparation of Macromers Containing Cyclic Carbonates. *Green Chem.* **2016**, *18* (14), 4063–4072. https://doi.org/10.1039/C6GC01028H.

(275) Sternberg, J.; Pilla, S. Materials for the Biorefinery: High Bio-Content, Shape Memory Kraft Lignin-Derived Non-Isocyanate Polyurethane Foams Using a Non-Toxic Protocol. *Green Chem.* **2020**, *22* (20), 6922–6935. https://doi.org/10.1039/D0GC01659D.

(276) Sternberg, J.; Pilla, S. Chemical Recycling of a Lignin-Based Non-Isocyanate Polyurethane Foam. *Nat Sustain* **2023**, *6* (3), 316–324. https://doi.org/10.1038/s41893-022-01022-3.

(277) Vanniappan, G.; Naebe, M.; Haque, A. N. M. A.; Panda, T. K.; Bhattacharyya, D. Recent Progress in Lignin Recovery and Functionalization: Toward Sustainable Material Application. *Sustainable Materials and Technologies* **2025**, *45*, e01554. https://doi.org/10.1016/j.susmat.2025.e01554.

(278) Yan, L.; Huertas-Alonso, A. J.; Liu, H.; Dai, L.; Si, C.; Sipponen, M. H. Lignin Polymerization: Towards High-Performance Materials. *Chem. Soc. Rev.* **2025**, *54* (14), 6634–6651. https://doi.org/10.1039/D4CS01044B.

(279) Kapuge Dona, N. L.; Smith, R. C. Tailoring Polymer Properties Through Lignin Addition: A Recent Perspective on Lignin-Derived Polymer Modifications. *Molecules* **2025**, *30* (11), 2455. https://doi.org/10.3390/molecules30112455.

(280) Truncali, A.; Laxminarayan, T.; Rajagopalan, N.; Weinell, C. E.; Kiil, S.; Johansson, M. Epoxidized Technical Kraft Lignin as a Particulate Resin Component for High-Performance Anticorrosive Coatings. *J Coat Technol Res* **2024**, *21* (6), 1875–1891. https://doi.org/10.1007/s11998-023-00899-9.

(281) Ribca, I.; Jawerth, M. E.; Brett, C. J.; Lawoko, M.; Schwartzkopf, M.; Chumakov, A.; Roth, S. V.; Johansson, M. Exploring the Effects of Different Cross-Linkers on Lignin-Based Thermoset Properties and Morphologies. *ACS Sustainable Chem. Eng.* **2021**, *9* (4), 1692–1702. https://doi.org/10.1021/acssuschemeng.0c07580.

(282) Zou, S.-L.; Xiao, L.-P.; Li, X.-Y.; Yin, W.-Z.; Sun, R.-C. Lignin-Based Composites with Enhanced Mechanical Properties by Acetone Fractionation and Epoxidation Modification. *iScience* **2023**, *26* (3), 106187. https://doi.org/10.1016/j.isci.2023.106187.

(283) Jawerth, M. E.; Brett, C. J.; Terrier, C.; Larsson, P. T.; Lawoko, M.; Roth, S. V.; Lundmark, S.; Johansson, M. Mechanical and Morphological

Properties of Lignin-Based Thermosets. *ACS Appl. Polym. Mater.* **2020**, *2* (2), 668–676. https://doi.org/10.1021/acsapm.9b01007.

(284) Wang, H.; Xu, F.; Zhang, Z.; Feng, M.; Jiang, M.; Zhang, S. Bio-Based Polycarbonates: Progress and Prospects. *RSC Sustainability* **2023**, *1* (9), 2162–2179. https://doi.org/10.1039/D3SU00248A.

(285) Chen, Q.; Huang, W.; Chen, P.; Peng, C.; Xie, H.; Zhao, Z. K.; Sohail, M.; Bao, M. Synthesis of Lignin-Derived Bisphenols Catalyzed by Lignosulfonic Acid in Water for Polycarbonate Synthesis. *ChemCatChem* **2015**, *7* (7), 1083–1089. https://doi.org/10.1002/cctc.201500010.

(286) Koelewijn, S.-F.; Van Den Bosch, S.; Renders, T.; Schutyser, W.; Lagrain, B.; Smet, M.; Thomas, J.; Dehaen, W.; Van Puyvelde, P.; Witters, H.; Sels, B. F. Sustainable Bisphenols from Renewable Softwood Lignin Feedstock for Polycarbonates and Cyanate Ester Resins. *Green Chem.* **2017**, *19* (11), 2561–2570. https://doi.org/10.1039/C7GC00776K.

(287) Meylemans, H. A.; Groshens, T. J.; Harvey, B. G. Synthesis of Renewable Bisphenols from Creosol. *ChemSusChem* **2012**, *5* (1), 206–210. https://doi.org/10.1002/cssc.201100402.

(288) Trita, A. S.; Over, L. C.; Pollini, J.; Baader, S.; Riegsinger, S.; Meier, M. A. R.; Gooßen, L. J. Synthesis of Potential Bisphenol A Substitutes by Isomerising Metathesis of Renewable Raw Materials. *Green Chem.* **2017**, *19* (13), 3051–3060. https://doi.org/10.1039/C7GC00553A.

(289) Acquah, E. K.; Holmes, D.; Dunne, K.; Bher, A.; Sadrabadi, S. A.; Joodaky, A.; Auras, R.; Nejad, M. Synthesis and Characterization of Lignin-Based Polycarbonate Polyols for Flexible Polyurethane Foam Application. *ChemSusChem* **2026**, *19* (2), e202502528. https://doi.org/10.1002/cssc.202502528.

(290) *Clariant launches 100% bio-based surfactants range driving the transition towards renewable carbon*. https://www.clariant.com/en/Corporate/News/2022/02/Clariant-launches-100-biobased-surfactants-range-driving-the-transition-towards-renewable-carbon#_ftnref1 (accessed 2026-02-01).

(291) Fiorani, G.; Perosa, A.; Selva, M. Dimethyl Carbonate: A Versatile Reagent for a Sustainable Valorization of Renewables. *Green Chem.* **2018**, *20* (2), 288–322. https://doi.org/10.1039/C7GC02118F.

(292) Tundo, P.; Selva, M. The Chemistry of Dimethyl Carbonate. *Acc. Chem. Res.* **2002**, *35* (9), 706–716. https://doi.org/10.1021/ar010076f.

(293) Rosamilia, A. E.; Aricò, F.; Tundo, P. Reaction of the Ambident Electrophile Dimethyl Carbonate with the Ambident Nucleophile

Phenylhydrazine. *J. Org. Chem.* **2008**, *73* (4), 1559–1562. https://doi.org/10.1021/jo701818d.

(294) Pearson, R. G. Hard and Soft Acids and Bases. *J. Am. Chem. Soc.* **1963**, *85* (22), 3533–3539. https://doi.org/10.1021/ja00905a001.

(295) Tundo, P.; Rossi, L.; Loris, A. Dimethyl Carbonate as an Ambident Electrophile. *J. Org. Chem.* **2005**, *70* (6), 2219–2224. https://doi.org/10.1021/jo048532b.

(296) Argyropoulos, D. S. 31P NMR in Wood Chemistry: A Review of Recent Progress. *Res. Chem. Intermed.* **1995**, *21* (3–5), 373–395. https://doi.org/10.1007/BF03052265.

(297) Meng, X.; Crestini, C.; Ben, H.; Hao, N.; Pu, Y.; Ragauskas, A. J.; Argyropoulos, D. S. Determination of Hydroxyl Groups in Biorefinery Resources via Quantitative 31P NMR Spectroscopy. *Nat Protoc* **2019**, *14* (9), 2627–2647. https://doi.org/10.1038/s41596-019-0191-1.

(298) Stanley, J. N. G.; Selva, M.; Masters, A. F.; Maschmeyer, T.; Perosa, A. Reactions of P-Coumaryl Alcohol Model Compounds with Dimethyl Carbonate. Towards the Upgrading of Lignin Building Blocks. *Green Chem.* **2013**, *15* (11), 3195. https://doi.org/10.1039/c3gc40334c.

(299) Fritz-Langhals, E. Unique Superbase TBD (1,5,7-Triazabicyclo[4.4.0]Dec-5-Ene): From Catalytic Activity and One-Pot Synthesis to Broader Application in Industrial Chemistry. *Org. Process Res. Dev.* **2022**, *26* (11), 3015–3023. https://doi.org/10.1021/acs.oprd.2c00248.

(300) Flores, I.; Demarteau, J.; Müller, A. J.; Etxeberria, A.; Irusta, L.; Bergman, F.; Koning, C.; Sardon, H. Screening of Different Organocatalysts for the Sustainable Synthesis of PET. *European Polymer Journal* **2018**, *104*, 170–176. https://doi.org/10.1016/j.eurpolymj.2018.04.040.

(301) Shieh, W.-C.; Dell, S.; Repič, O. 1,8-Diazabicyclo[5.4.0]Undec-7-Ene (DBU) and Microwave-Accelerated Green Chemistry in Methylation of Phenols, Indoles, and Benzimidazoles with Dimethyl Carbonate. *Org. Lett.* **2001**, *3* (26), 4279–4281. https://doi.org/10.1021/ol016949n.

(302) Dong, W.; Yoshida, Y.; Endo, T. Synthesis of Poly(Hydroxyurethane) from 5-membered Cyclic Carbonate under Mild Conditions in the Presence of Bicyclic Guanidine and Their Reaction Process. *Journal of Polymer Science* **2021**, *59* (6), 502–509. https://doi.org/10.1002/pol.20200825.

(303) Ouk, S.; Thiébaud, S.; Borredon, E.; Le Gars, P. High Performance Method for O-Methylation of Phenol with Dimethyl Carbonate. *Applied*

Catalysis A: General **2003**, *241* (1–2), 227–233. https://doi.org/10.1016/S0926-860X(02)00467-2.

(304) Sen, S.; Patil, S.; Argyropoulos, D. S. Methylation of Softwood Kraft Lignin with Dimethyl Carbonate. *Green Chem.* **2015**, *17* (2), 1077–1087. https://doi.org/10.1039/C4GC01759E.

(305) Destaso, F. C.; Libretti, C.; Le Coz, C.; Grau, E.; Cramail, H.; Meier, M. A. R. Optimized Synthesis of a High Oleic Sunflower Oil Derived Polyamine and Its Lignin-Based NIPUs. *Green Chem.* **2025**, *27* (5), 1440–1450. https://doi.org/10.1039/D4GC05645K.

(306) Statista Research Department. *Market volume of polyurethane worldwide from 2015 to 2022, with a forecast for 2023 to 2030*. Statista. https://www.statista.com/statistics/720341/global-polyurethane-market-size-forecast (accessed 2024-07-02).

(307) Das, A.; Mahanwar, P. A Brief Discussion on Advances in Polyurethane Applications. *Advanced Industrial and Engineering Polymer Research* **2020**, *3* (3), 93–101. https://doi.org/10.1016/j.aiepr.2020.07.002.

(308) Brito, A. How Polyurethane Can Be Used in Today's Manufacturing Industry. *Reinforced Plastics* **2020**, *64* (5), 268–270. https://doi.org/10.1016/j.repl.2020.06.001.

(309) Bello, D.; Herrick, C. A.; Smith, T. J.; Woskie, S. R.; Streicher, R. P.; Cullen, M. R.; Liu, Y.; Redlich, C. A. Skin Exposure to Isocyanates: Reasons for Concern. *Environmental Health Perspectives* **2007**, *115* (3), 328–335. https://doi.org/10.1289/ehp.9557.

(310) Karol, M. H.; Kramarik, J. A. Phenyl Isocyanate Is a Potent Chemical Sensitizer. *Toxicology Letters* **1996**, *89* (2), 139–146. https://doi.org/10.1016/S0378-4274(96)03798-8.

(311) PHOSGENE. In *National Research Council (US) Committee on Toxicology. Emergency and Continuous Exposure Limits for Selected Airborne Contaminants: Volume 2.*; National Academies Press (US): Washington (DC), 1984.

(312) *Isocyanates*. Occupational Safety and Health Administration (OSHA). https://www.osha.gov/isocyanates (accessed 2024-07-02).

(313) Mundo, F.; Caillol, S.; Ladmiral, V.; Meier, M. A. R. On Sustainability Aspects of the Synthesis of Five-Membered Cyclic Carbonates. *ACS Sustainable Chem. Eng.* **2024**, *12* (17), 6452–6466. https://doi.org/10.1021/acssuschemeng.4c01274.

(314) Rother, D.; Schlüter, U. Occupational Exposure to Diisocyanates in the European Union. *Annals of Work Exposures and Health* **2021**, *65* (8), 893–907. https://doi.org/10.1093/annweh/wxab021.

(315) *ANNEX XVII TO REACH – Conditions of restriction - Restrictions on the manufacture, placing on the market and use of certain dangerous substances, mixtures and articles*.

https://echa.europa.eu/documents/10162/503ac424-3bcb-137b-9247-09e41eb6dd5a (accessed 2024-07-03).

(316) PDF.Pdf. https://eur-lex.europa.eu/legal-content/EN/TXT/PDF/?uri=CELEX:32020R1149 (accessed 2024-07-18).

(317) Gomez-Lopez, A.; Elizalde, F.; Calvo, I.; Sardon, H. Trends in Non-Isocyanate Polyurethane (NIPU) Development. *Chem. Commun.* **2021**, *57* (92), 12254–12265. https://doi.org/10.1039/D1CC05009E.

(318) Scheelje, F. C. M.; Meier, M. A. R. Non-Isocyanate Polyurethanes Synthesized from Terpenes Using Thiourea Organocatalysis and Thiol-Ene-Chemistry. *Commun Chem* **2023**, *6* (1), 239. https://doi.org/10.1038/s42004-023-01041-x.

(319) Scheelje, F. C. M.; Destaso, F. C.; Cramail, H.; Meier, M. A. R. Nitrogen-Containing Polymers Derived from Terpenes: Possibilities and Limitations. *Macro Chemistry & Physics* **2023**, *224* (3), 2200403. https://doi.org/10.1002/macp.202200403.

(320) Echeverri, D. A.; Inciarte, H. C.; Cortés, N.; Estenoz, D. A.; Polo, M. L.; Rios, L. A. Synthesis of a Renewable Polyamine from Canola Oil by Photocatalyzed Thiol-ene Addition of Cysteamine under Green Conditions. *J of Applied Polymer Sci* **2023**, *140* (28), e54036. https://doi.org/10.1002/app.54036.

(321) Stemmelen, M.; Lapinte, V.; Habas, J.-P.; Robin, J.-J. Plant Oil-Based Epoxy Resins from Fatty Diamines and Epoxidized Vegetable Oil. *European Polymer Journal* **2015**, *68*, 536–545. https://doi.org/10.1016/j.eurpolymj.2015.03.062.

(322) Javni, I.; Hong, D. P.; Petrović, Z. S. Soy-based Polyurethanes by Nonisocyanate Route. *J of Applied Polymer Sci* **2008**, *108* (6), 3867–3875. https://doi.org/10.1002/app.27995.

(323) Meier, M. A. R. Plant-Oil-Based Polyamides and Polyurethanes: Toward Sustainable Nitrogen-Containing Thermoplastic Materials. *Macromol. Rapid Commun.* **2019**, *40* (1), 1800524. https://doi.org/10.1002/marc.201800524.

(324) Evstigneyev, E. I.; Shevchenko, S. M. Lignin Valorization and Cleavage of Arylether Bonds in Chemical Processing of Wood: A Mini-Review. *Wood Sci Technol* **2020**, *54* (4), 787–820. https://doi.org/10.1007/s00226-020-01183-4.

(325) Salanti, A.; Zoia, L.; Mauri, M.; Orlandi, M. Utilization of Cyclocarbonated Lignin as a Bio-Based Cross-Linker for the Preparation of Poly(Hydroxy Urethane)s. *RSC Adv.* **2017**, *7* (40), 25054–25065. https://doi.org/10.1039/C7RA03416D.

(326) Sternberg, J.; Pilla, S. Materials for the Biorefinery: High Bio-Content, Shape Memory Kraft Lignin-Derived Non-Isocyanate Polyurethane Foams

Using a Non-Toxic Protocol. *Green Chem.* **2020**, *22* (20), 6922–6935. https://doi.org/10.1039/D0GC01659D.

(327) *Global vegetable oil production 2023/24*. Statista. https://www.statista.com/statistics/263978/global-vegetable-oil-production-since-2000-2001/ (accessed 2024-07-18).

(328) Biermann, U.; Bornscheuer, U. T.; Feussner, I.; Meier, M. A. R.; Metzger, J. O. Fatty Acids and Their Derivatives as Renewable Platform Molecules for the Chemical Industry. *Angew Chem Int Ed* **2021**, *60* (37), 20144–20165. https://doi.org/10.1002/anie.202100778.

(329) Ionescu, M.; Radojčić, D.; Wan, X.; Petrović, Z. S.; Upshaw, T. A. Functionalized Vegetable Oils as Precursors for Polymers by Thiol-Ene Reaction. *European Polymer Journal* **2015**, *67*, 439–448. https://doi.org/10.1016/j.eurpolymj.2014.12.037.

(330) Myriam, D.; Rémi, A.; Bernard, B.; Sylvain, C. Synthesis of Bio-Based Building Blocks from Vegetable Oils: A Platform Chemicals Approach.

(331) Vu, N. D.; Bah, S.; Deruer, E.; Duguet, N.; Lemaire, M. Robust Organocatalysts for the Cleavage of Vegetable Oil Derivatives to Aldehydes through Retrobenzoin Condensation. *Chemistry – A European Journal* **2018**, *24* (32), 8141–8150. https://doi.org/10.1002/chem.201800091.

(332) Cramail, H.; Maisonneuve, L.; Grau, E.; Alfos, C.; Wirotius, A. Fatty Acid-Based (Bis) 6-Membered Cyclic Carbonates as Efficient Isocyanate Free Poly(Hydroxyurethane) Precursors. *Polym. Chem.* **2014**, *5*. https://doi.org/10.1039/C4PY00922C.

(333) Miloslavskiy, D.; Gotlib, E.; Figovsky, O.; Pashin, D. Cyclic Carbonates Based on Vegetable Oils. *International Letters of Chemistry, Physics and Astronomy* **2014**, *27*, 20–29. https://doi.org/10.18052/www.scipress.com/ILCPA.27.20.

(334) Stemmelen, M.; Pessel, F.; Lapinte, V.; Caillol, S.; Habas, J.-P.; Robin, J.-J. A Fully Biobased Epoxy Resin from Vegetable Oils: From the Synthesis of the Precursors by Thiol-Ene Reaction to the Study of the Final Material: A Fully Biobased Epoxy Resin. *J. Polym. Sci. A Polym. Chem.* **2011**, *49* (11), 2434–2444. https://doi.org/10.1002/pola.24674.

(335) Stemmelen, M.; Pessel, F.; Lapinte, V.; Caillol, S.; Habas, J. -P.; Robin, J. -J. A Fully Biobased Epoxy Resin from Vegetable Oils: From the Synthesis of the Precursors by Thiol-ene Reaction to the Study of the Final Material. *J. Polym. Sci. A Polym. Chem.* **2011**, *49* (11), 2434–2444. https://doi.org/10.1002/pola.24674.

(336) Echeverri, D. A.; Inciarte, H. C.; Cortés, N.; Estenoz, D. A.; Polo, M. L.; Rios, L. A. Synthesis of a Renewable Polyamine from Canola Oil by Photocatalyzed Thiol-Ene Addition of Cysteamine under Green Conditions.

Journal of Applied Polymer Science **2023**, *140* (28), e54036. https://doi.org/10.1002/app.54036.

(337) Duval, A.; Avérous, L. Cyclic Carbonates as Safe and Versatile Etherifying Reagents for the Functionalization of Lignins and Tannins. *ACS Sustainable Chem. Eng.* **2017**, *5* (8), 7334–7343. https://doi.org/10.1021/acssuschemeng.7b01502.

(338) Dannecker, P.-K.; Meier, M. A. R. Facile and Sustainable Synthesis of Erythritol Bis(Carbonate), a Valuable Monomer for Non-Isocyanate Polyurethanes (NIPUs). *Sci Rep* **2019**, *9* (1), 9858. https://doi.org/10.1038/s41598-019-46314-5.

(339) Zhang, N.; Tao, P.; Lu, Y.; Nie, S. Effect of Lignin on the Thermal Stability of Cellulose Nanofibrils Produced from Bagasse Pulp. *Cellulose* **2019**, *26* (13–14), 7823–7835. https://doi.org/10.1007/s10570-019-02657-w.

(340) Hasan, G.; Musajan, D.; Hou, G.; He, M.; Li, Y.; Yimit, M. Role of Different Lignin Systems in Polymers: Mechanical Properties and Thermal Stability. *Polish Journal of Chemical Technology* **2020**, *22* (4), 10–16. https://doi.org/10.2478/pjct-2020-0032.

(341) Xu, Y.; Odelius, K.; Hakkarainen, M. One-Pot Synthesis of Lignin Thermosets Exhibiting Widely Tunable Mechanical Properties and Shape Memory Behavior. *ACS Sustainable Chem. Eng.* **2019**, *7* (15), 13456–13463. https://doi.org/10.1021/acssuschemeng.9b02921.

(342) Lisý, A.; Ház, A.; Nadányi, R.; Jablonský, M.; Šurina, I. About Hydrophobicity of Lignin: A Review of Selected Chemical Methods for Lignin Valorisation in Biopolymer Production. *Energies* **2022**, *15* (17), 6213. https://doi.org/10.3390/en15176213.

(343) Elniski, A.; Dongre, P.; Bujanovic, B. M. Lignin Use in Enhancing the Properties of Willow Pellets. *Forests* **2023**, *14* (10), 2041. https://doi.org/10.3390/f14102041.

(344) Tryznowski, M.; Izdebska-Podsiadły, J.; Żołek-Tryznowska, Z. Wettability and Surface Free Energy of NIPU Coatings Based on Bis(2,3-Dihydroxypropyl)Ether Dicarbonate. *Progress in Organic Coatings* **2017**, *109*, 55–60. https://doi.org/10.1016/j.porgcoat.2017.04.011.

(345) Panchireddy, S.; Grignard, B.; Thomassin, J.-M.; Jerome, C.; Detrembleur, C. Bio-Based Poly(Hydroxyurethane) Glues for Metal Substrates. *Polym. Chem.* **2018**, *9* (19), 2650–2659. https://doi.org/10.1039/C8PY00281A.

(346) Libretti, C.; Rizzo, G.; Abou El Mirate, S.; Johansson, M.; Meier, M. A. R. Biobased Epoxy Resins from Itaconic Anhydride Functionalized Lignin:

Insights and Comparison with Succinic Analogues. *RSC Sustainability* **2026**, Accepted Manuscript. https://doi.org/10.1039/D6SU00045B.

(347) Fazeli, M.; Mukherjee, S.; Baniasadi, H.; Abidnejad, R.; Mujtaba, M.; Lipponen, J.; Seppälä, J.; Rojas, O. J. Lignin beyond the *Status Quo* : Recent and Emerging Composite Applications. *Green Chem.* **2024**, *26* (2), 593–630. https://doi.org/10.1039/D3GC03154C.

(348) Bellinetto, E.; Fumagalli, N.; Astorri, M.; Turri, S.; Griffini, G. Elucidating the Role of Lignin Type and Functionality in the Development of High-Performance Biobased Phenolic Thermoset Resins. *ACS Appl. Polym. Mater.* **2024**, *6* (2), 1191–1203. https://doi.org/10.1021/acsapm.3c02136.

(349) Wang, Y.-Y.; Wyman, C. E.; Cai, C. M.; Ragauskas, A. J. Lignin-Based Polyurethanes from Unmodified Kraft Lignin Fractionated by Sequential Precipitation. *ACS Appl. Polym. Mater.* **2019**, *1* (7), 1672–1679. https://doi.org/10.1021/acsapm.9b00228.

(350) Arefmanesh, M.; Nikafshar, S.; Master, E. R.; Nejad, M. From Acetone Fractionation to Lignin-Based Phenolic and Polyurethane Resins. *Industrial Crops and Products* **2022**, *178*, 114604. https://doi.org/10.1016/j.indcrop.2022.114604.

(351) Zou, S.-L.; Xiao, L.-P.; Li, X.-Y.; Yin, W.-Z.; Sun, R.-C. Lignin-Based Composites with Enhanced Mechanical Properties by Acetone Fractionation and Epoxidation Modification. *iScience* **2023**, *26* (3), 106187. https://doi.org/10.1016/j.isci.2023.106187.

(352) Over, L. C.; Grau, E.; Grelier, S.; Meier, M. A. R.; Cramail, H. Synthesis and Characterization of Epoxy Thermosetting Polymers from Glycidylated Organosolv Lignin and Bisphenol A. *Macromol. Chem. Phys.* **2017**, *218* (4), 1600411. https://doi.org/10.1002/macp.201600411.

(353) Shundo, A.; Yamamoto, S.; Tanaka, K. Network Formation and Physical Properties of Epoxy Resins for Future Practical Applications. *JACS Au* **2022**, *2* (7), 1522–1542. https://doi.org/10.1021/jacsau.2c00120.

(354) Yang, C.; Topuz, F.; Park, S.-H.; Szekely, G. Biobased Thin-Film Composite Membranes Comprising Priamine–Genipin Selective Layer on Nanofibrous Biodegradable Polylactic Acid Support for Oil and Solvent-Resistant Nanofiltration. *Green Chem.* **2022**, *24* (13), 5291–5303. https://doi.org/10.1039/D2GC01476A.

(355) Lisiecka, M. Z. Biological Effects of Epoxy Resins on the Human Body: Toxicity and Allergic Reactions. *Drug and Chemical Toxicology* **2025**, 1–11. https://doi.org/10.1080/01480545.2025.2557405.

(356) Park, J.; Lee, S. Biodegradable Epoxy Thermosets Prepared by Mixing Diglycidyl Ether of Bisphenol A and Epoxidized Soybean Oil and Their

Electrical and Mechanical Properties. *J of Applied Polymer Sci* **2025**, *142* (15), e56739. https://doi.org/10.1002/app.56739.

(357) Yang, X.; Li, J.; Wang, Y.; Tan, L.; Han, L.; Lu, J.; Li, M.; Fang, D.; Huang, X.; Xu, Y.; Zhang, C. Synthesis and Characterization of Fully Biobased Epoxy Elastomers Prepared from Different Plant Oils. *ACS Sustainable Chem. Eng.* **2023**, *11* (38), 13950–13961. https://doi.org/10.1021/acssuschemeng.3c02634.

(358) Caillol, S. Cardanol: A Promising Building Block for Biobased Polymers and Additives. *Current Opinion in Green and Sustainable Chemistry* **2018**, *14*, 26–32. https://doi.org/10.1016/j.cogsc.2018.05.002.

(359) Zhou, X.; Yu, Z.; Fang, Y.; Hu, H.; Cheng, S.; Tang, Z.; Liu, Y. High-Performance Fully Bio-Based Dynamic Covalent Supramolecular Epoxy Resin: Synthesis and Properties. *Green Chem.* **2025**, *27* (12), 3248–3260. https://doi.org/10.1039/D4GC06425A.

(360) Nabipour, H.; Wang, X.; Song, L.; Hu, Y. A High Performance Fully Bio-Based Epoxy Thermoset from a Syringaldehyde-Derived Epoxy Monomer Cured by Furan-Derived Amine. *Green Chem.* **2021**, *23* (1), 501–510. https://doi.org/10.1039/D0GC03451G.

(361) Song, Z.; Liu, L.; Zhang, P.; Xue, K.; Hua, Z.; You, T.; Wu, Y.; Cui, H.; Hu, Z.; Huang, Y. Fully Bio-Based Acetal Diepoxy Monomer with High Modulus, Good Thermal Stability and Readily Degradability. *Polym. Chem.* **2024**, *15* (47), 4824–4834. https://doi.org/10.1039/D4PY01038H.

(362) Epichlorohydrin in Drinking-Water, Background Document for Development of WHO Guidelines for Drinking-Water Quality, 2004. https://cdn.who.int/media/docs/default-source/wash-documents/wash-chemicals/epichlorohydrin-bd.pdf?sfvrsn=4dd62bab_4 (accessed 2025-09-30).

(363) Ohshima, S.; Shibata, T.; Sasaki, N.; Okuda, H.; Nishizawa, H.; Ohsawa, M.; Matsumoto, M.; Nakayama, E. [Subacute toxicity of an amine-curing agent for epoxy resin]. *Sangyo Igaku* **1984**, *26* (3), 197–204.

(364) Lisiecka, M. Z. Biological Effects of Epoxy Resins on the Human Body: Toxicity and Allergic Reactions. *Drug and Chemical Toxicology* **2025**, 1–11. https://doi.org/10.1080/01480545.2025.2557405.

(365) Shao, X.; Zhao, P.; Tian, Z.; Zhang, N.; Wang, H.; Li, X.; Cui, X.; Hou, X.; Deng, T. A Novel Bio-Based Anhydride Curing Agent for the Synthesis of

High-Performance Epoxy Resin. *Polymer Degradation and Stability* **2024**, *229*, 110979. https://doi.org/10.1016/j.polymdegradstab.2024.110979.

(366) Jaillet, F.; Desroches, M.; Auvergne, R.; Boutevin, B.; Caillol, S. New Biobased Carboxylic Acid Hardeners for Epoxy Resins. *Euro J Lipid Sci & Tech* **2013**, *115* (6), 698–708. https://doi.org/10.1002/ejlt.201200363.

(367) Andriani, F.; Karlsson, M.; Elder, T.; Lawoko, M. Lignin Carboxymethylation: Probing Fundamental Insights into Structure–Reactivity Relationships. *ACS Sustainable Chem. Eng.* **2024**, *12* (4), 1705–1713. https://doi.org/10.1021/acssuschemeng.3c07385.

(368) Andriani, F.; Lawoko, M. Oxidative Carboxylation of Lignin: Exploring Reactivity of Different Lignin Types. *Biomacromolecules* **2024**, *25* (7), 4246–4254. https://doi.org/10.1021/acs.biomac.4c00326.

(369) Zhen, X.; Cui, X.; Al-Haimi, A. A. N. M.; Wang, X.; Liang, H.; Xu, Z.; Wang, Z. Fully Bio-Based Epoxy Resins from Lignin and Epoxidized Soybean Oil: Rigid-Flexible, Tunable Properties and High Lignin Content. *International Journal of Biological Macromolecules* **2024**, *254*, 127760. https://doi.org/10.1016/j.ijbiomac.2023.127760.

(370) Zhou, S.; Huang, K.; Xu, X.; Wang, B.; Zhang, W.; Su, Y.; Hu, K.; Zhang, C.; Zhu, J.; Weng, G.; Ma, S. Rigid-and-Flexible, Degradable, Fully Biobased Thermosets from Lignin and Soybean Oil: Synthesis and Properties. *ACS Sustainable Chem. Eng.* **2023**, *11* (8), 3466–3473. https://doi.org/10.1021/acssuschemeng.2c06990.

(371) Resende, G.; Azevedo, G. D.; Souto, F.; Calado, V. Chemical Modification of Softwood Kraft Lignin with Succinic Acid. *ACS Omega* **2024**, *9* (52), 50945–50956. https://doi.org/10.1021/acsomega.4c03127.

(372) Scarica, C.; Suriano, R.; Levi, M.; Turri, S.; Griffini, G. Lignin Functionalized with Succinic Anhydride as Building Block for Biobased Thermosetting Polyester Coatings. *ACS Sustainable Chem. Eng.* **2018**, *6* (3), 3392–3401. https://doi.org/10.1021/acssuschemeng.7b03583.

(373) Subbotina, E.; Olsén, P.; Lawoko, M.; Berglund, L. A. Maleated Technical Lignin Thermosets and Biocomposites Designed for Degradation.

(374) Hashim, B.; Khan, W. U.; Hantoko, D.; Nasser, G. A.; Sanhoob, M. A.; Bakare, A. I.; Govender, N. S.; Ali, S. A.; Hossain, M. M. *N* -Butane Oxidation to Maleic Anhydride: Reaction Mechanism and Kinetics Over VPO Catalyst. *Ind. Eng. Chem. Res.* **2024**, *63* (14), 5987–6002. https://doi.org/10.1021/acs.iecr.3c04371.

(375) Kanzow, A.; Hartwig, B.; Buschmann, P.; Lengsfeld, K. G.; Höhne, C. M.; Hoke, J. S.; Knüppe, F.; Köster, F.; Van Spronsen, J. K.; Grabow, J.-U.; McNaughton, D.; Obenchain, D. A. Tautomer Identification Troubles: The Molecular Structure of Itaconic and Citraconic Anhydride Revealed by

Rotational Spectroscopy. *Phys. Chem. Chem. Phys.* **2025**, *27* (18), 9491–9503. https://doi.org/10.1039/D5CP00389J.

(376) Maleic Anhydride; MSDS No. 63200 [Online]; Sigma-Aldrich Chemie GmbH, Taufkirchen, DE. https://www.sigmaaldrich.com/DE/en/sds/sial/63200?userType=undefined.

(377) Itaconic Anhydride; MSDS No. 259926 [Online]; Sigma-Aldrich Chemie GmbH, Taufkirchen, DE. https://www.sigmaaldrich.com/DE/en/sds/aldrich/259926?userType=anonymous.

(378) Robert, T.; Friebel, S. Itaconic Acid – a Versatile Building Block for Renewable Polyesters with Enhanced Functionality. *Green Chem.* **2016**, *18* (10), 2922–2934. https://doi.org/10.1039/C6GC00605A.

(379) Willke, Th.; Vorlop, K.-D. Biotechnological Production of Itaconic Acid. *Applied Microbiology and Biotechnology* **2001**, *56* (3–4), 289–295. https://doi.org/10.1007/s002530100685.

(380) Biermann, U.; Bornscheuer, U. T.; Feussner, I.; Meier, M. A. R.; Metzger, J. O. Fatty Acids and Their Derivatives as Renewable Platform Molecules for the Chemical Industry. *Angew Chem Int Ed* **2021**, *60* (37), 20144–20165. https://doi.org/10.1002/anie.202100778.

(381) Leonard, E. C. Polymerization-dimer Acids. *J Americ Oil Chem Soc* **1979**, *56* (11Part2). https://doi.org/10.1007/BF02667445.

(382) Pettignano, A.; Daunay, A.; Moreau, C.; Cathala, B.; Charlot, A.; Fleury, E. Sustainable Modification of Carboxymethyl Cellulose by Passerini Three-Component Reaction and Subsequent Adsorption onto Cellulosic Substrates. *ACS Sustainable Chem. Eng.* **2019**, *7* (17), 14685–14696. https://doi.org/10.1021/acssuschemeng.9b02634.

(383) Söyler, Z.; Onwukamike, K. N.; Grelier, S.; Grau, E.; Cramail, H.; Meier, M. A. R. Sustainable Succinylation of Cellulose in a CO_2 -Based Switchable Solvent and Subsequent Passerini 3-CR and Ugi 4-CR Modification. *Green Chem.* **2018**, *20* (1), 214–224. https://doi.org/10.1039/C7GC02577G.

(384) Santos Correa, L.; Leidenheimer, S.; Meier, M. A. R. Sunflower Oil-Based Thermosets *via* the Passerini Three-Component Reaction. *Polym. Chem.* **2025**, *16* (7), 821–832. https://doi.org/10.1039/D4PY01358A.

(385) Henderson, R. K.; Jiménez-González, C.; Constable, D. J. C.; Alston, S. R.; Inglis, G. G. A.; Fisher, G.; Sherwood, J.; Binks, S. P.; Curzons, A. D. Expanding GSK's Solvent Selection Guide – Embedding Sustainability into Solvent Selection Starting at Medicinal Chemistry. *Green Chem.* **2011**, *13* (4), 854. https://doi.org/10.1039/c0gc00918k.

(386) 1,1,3,3-Tetramethylguanidine; MSDS No. 241768 [Online]; Sigma-Aldrich Chemie GmbH, Taufkirchen, DE, 2025.

https://www.sigmaaldrich.com/DE/en/sds/aldrich/241768?userType=anonymous (accessed 2025-02-19).

(387) 1,8-Diazabicyclo[5.4.0]Undec-7-Ene; MSDS No. 139009 [Online]; Sigma-Aldrich Chemie GmbH, Taufkirchen, DE, 2023. https://www.sigmaaldrich.com/DE/en/sds/aldrich/139009?userType=anonymous (accessed 2025-02-19).

(388) Subbotina, E.; Olsén, P.; Lawoko, M.; Berglund, L. A. Maleated Technical Lignin Thermosets and Biocomposites Designed for Degradation. *ACS Sustainable Chem. Eng.* **2024**, *12* (9), 3632–3642. https://doi.org/10.1021/acssuschemeng.3c06741.

(389) Barb, W. G. Interconversions of Itaconic and Citraconic Anhydride in Amine Solutions. *J. Chem. Soc.* **1955**, 1647. https://doi.org/10.1039/jr9550001647.

(390) Galanti, M. C.; Galanti, A. V. Kinetic Study of the Isomerization of Itaconic Anhydride to Citraconic Anhydride. *J. Org. Chem.* **1981**, *47* (8), 1572–1574.

(391) Long, K. F.; Wang, H.; Dimos, T. T.; Bowman, C. N. Effects of Thiol Substitution on the Kinetics and Efficiency of Thiol-Michael Reactions and Polymerizations. *Macromolecules* **2021**, *54* (7), 3093–3100. https://doi.org/10.1021/acs.macromol.0c02677.

(392) Connor, Ralph.; McClellan, Wm. R. The Michael Condensation. V*. The Influence of the Experimental Conditions and the Structure of the Acceptor Upon the Condensation. *J. Org. Chem.* **1939**, *3* (6), 570–577. https://doi.org/10.1021/jo01223a005.

(393) Banfi, L.; Basso, A.; Lambruschini, C.; Moni, L.; Riva, R. The 100 Facets of the Passerini Reaction. *Chem. Sci.* **2021**, *12* (47), 15445–15472. https://doi.org/10.1039/D1SC03810A.

(394) Mustata, F.; Tudorachi, N. Curing Kinetics and Thermal Characterization of Epoxy Resin Cured with Amidodicarboxylic Acids. *Applied Thermal Engineering* **2017**, *125*, 285–296. https://doi.org/10.1016/j.applthermaleng.2017.07.037.

(395) Rothenhäusler, F.; Kettenbach, M.; Ruckdaeschel, H. Influence of the Stoichiometric Ratio on the Curing Kinetics and Mechanical Properties of Epoxy Resin Cured with a Rosin-Based Anhydride. *Macro Materials & Eng* **2023**, *308* (11), 2300122. https://doi.org/10.1002/mame.202300122.

(396) Jing, F.; Zhao, R.; Li, C.; Xi, Z.; Wang, Q.; Xie, H. Influence of the Epoxy/Acid Stoichiometry on the Cure Behavior and Mechanical Properties

of Epoxy Vitrimers. *Molecules* **2022**, *27* (19), 6335. https://doi.org/10.3390/molecules27196335.

(397) Couture, G.; Granado, L.; Fanget, F.; Boutevin, B.; Caillol, S. Limonene-Based Epoxy: Anhydride Thermoset Reaction Study. *Molecules* **2018**, *23* (11), 2739. https://doi.org/10.3390/molecules23112739.

(398) Huang, K.; Zhang, P.; Zhang, J.; Li, S.; Li, M.; Xia, J.; Zhou, Y. Preparation of Biobased Epoxies Using Tung Oil Fatty Acid-Derived C21 Diacid and C22 Triacid and Study of Epoxy Properties. *Green Chem.* **2013**, *15* (9), 2466. https://doi.org/10.1039/c3gc40622a.

(399) Ding, C.; Shuttleworth, P. S.; Makin, S.; Clark, J. H.; Matharu, A. S. New Insights into the Curing of Epoxidized Linseed Oil with Dicarboxylic Acids. *Green Chem.* **2015**, *17* (7), 4000–4008. https://doi.org/10.1039/C5GC00912J.

(400) Duval, A.; Benali, W.; Avérous, L. Turning Lignin into a Recyclable Bioresource: Transesterification Vitrimers from Lignins Modified with Ethylene Carbonate. *Green Chem.* **2024**, *26* (14), 8414–8427. https://doi.org/10.1039/D4GC00567H.

(401) Duval, A.; Benali, W.; Avérous, L. Exploiting Lignin Structure and Reactivity to Design Vitrimers with Controlled Ratio of Dynamic to Non-Dynamic Bonds. *ChemSusChem* **2025**, *18* (3), e202401480. https://doi.org/10.1002/cssc.202401480.

(402) Berne, D.; Lemouzy, S.; Guiffrey, P.; Caillol, S.; Ladmiral, V.; Manoury, E.; Poli, R.; Leclerc, E. Catalyst-Free Thia-Michael Addition to α-Trifluoromethylacrylates for 3D Network Synthesis. *Chemistry A European J* **2023**, *29* (20), e202203712. https://doi.org/10.1002/chem.202203712.

(403) Granata, A.; Argyropoulos, D. S. 2-Chloro-4,4,5,5-Tetramethyl-1,3,2-Dioxaphospholane, a Reagent for the Accurate Determination of the Uncondensed and Condensed Phenolic Moieties in Lignins. *J. Agric. Food Chem.* **1995**, *43* (6), 1538–1544. https://doi.org/10.1021/jf00054a023.

(404) King, A. W. T.; Jalomäki, J.; Granström, M.; Argyropoulos, D. S.; Heikkinen, S.; Kilpeläinen, I. A New Method for Rapid Degree of Substitution and Purity Determination of Chloroform-Soluble Cellulose Esters, Using 31P NMR. *Anal. Methods* **2010**, *2* (10), 1499. https://doi.org/10.1039/c0ay00336k.

(405) Domínguez-Robles, J.; Tamminen, T.; Liitiä, T.; Peresin, M. S.; Rodríguez, A.; Jääskeläinen, A.-S. Aqueous Acetone Fractionation of Kraft, Organosolv and Soda Lignins. *International Journal of Biological Macromolecules* **2018**, *106*, 979–987. https://doi.org/10.1016/j.ijbiomac.2017.08.102.

(406) Vela, P.; Vázquez-Tato, M.; Seijas, J.; Sainz, M. J.; Mansilla, J.; Feás, X.; Salinero, C. *NMR Analysis of the Triglyceride Composition of Cold Pressed*

Oil from Camellia Reticulata and Camellia Japonica; 2011. https://doi.org/10.3390/ecsoc-15-00754.

(407) Mattar, N.; Langlois, V.; Renard, E.; Rademacker, T.; Hübner, F.; Demleitner, M.; Altstädt, V.; Ruckdäschel, H.; Rios de Anda, A. Fully Bio-Based Epoxy-Amine Thermosets Reinforced with Recycled Carbon Fibers as a Low Carbon-Footprint Composite Alternative. *ACS Appl. Polym. Mater.* **2021**, *3* (1), 426–435. https://doi.org/10.1021/acsapm.0c01187.

(408) Waibel, K. A.; Nickisch, R.; Möhl, N.; Seim, R.; Meier, M. A. R. A More Sustainable and Highly Practicable Synthesis of Aliphatic Isocyanides. *Green Chem.* **2020**, *22* (3), 933–941. https://doi.org/10.1039/C9GC04070F.